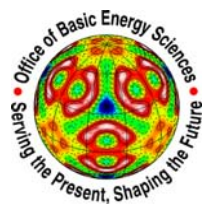


2005 Atomic, Molecular and Optical Sciences

Research Meeting



**Airlie Conference Center
Warrenton, Virginia
September 11-15, 2005**



**Sponsored by:
U.S. Department of Energy
Office of Basic Energy Sciences
Chemical Sciences, Geosciences & Biosciences Division**

Cover Art Courtesy of Airlie Conference Center

Foreword

This volume summarizes the 2005 Research Meeting of the Atomic, Molecular and Optical Sciences (AMOS) Program sponsored by the U. S. Department of Energy (DOE), Office of Basic Energy Sciences (BES), and comprises descriptions of all of the current research sponsored by the AMOS program. The research meeting is held annually for the DOE laboratory and university principal investigators within the BES AMOS Program in order to facilitate scientific interchange among the PIs and to promote a sense of program identity.

In addition to presentations by our principal investigators, we have continued our tradition of inviting distinguished plenary speakers. This year, we are delighted that Peter Weber from Brown University agreed to join us to present his work on ultrafast molecular dynamics with ultrashort electron pulses. We gratefully acknowledge the contributions of all of this year's speakers.

Despite perennial budget uncertainty, the BES/AMOS program continues to be vibrant and forward moving, thanks to our scientists and the outstanding research they perform. We were pleased to be able to initiate five new grants in the past year, three to theorists and two to experimentalists, enhancing the program in areas of ultracold atoms and molecules and in high-field physics. We also launched new ultrafast laboratories at Lawrence Berkeley and at Stanford, and many of our principle investigators have been involved in planning research for the Linac Coherent Light Source. We are indebted to all of the members of the scientific community who have contributed valuable time toward the review of colleagues' proposals, either by mail review of grant applications or on-site reviews of multi-PI programs. These thorough and thoughtful reviews have been central to the continued vitality the AMOS Program.

Thanks also to the staff of the Oak Ridge Institute of Science and Education, in particular Sophia Kitts, and Kellye Sliger, and to the Airlie Conference Center for assisting with logistical aspects of the meeting. Last but not least we thank our colleagues in the Chemical Sciences, Biosciences, and Geosciences Division - Diane Marceau, Robin Felder, and Michaelena Kyler-King - for their indispensable behind-the-scenes efforts in support of the BES/AMOS program.

Michael P. Casassa
Richard Hilderbrandt
Eric A. Rohlfing
Chemical Sciences, Geosciences and Biosciences Division
Office of Basic Energy Sciences
Department of Energy

Agenda

2005 Meeting of the Atomic, Molecular and Optical Sciences Program
Office of Basic Energy Sciences
U. S. Department of Energy
Airlie Center, Warrenton, Virginia, September 11-14, 2005
Draft Agenda (8/11/05)

Sunday, September 11

3:00-6:00 pm **** Registration ****
6:00 pm **** Reception (Pub, No Host) ****
7:00 pm **** Dinner ****

Monday, September 12

7:00 am **** Breakfast ****

8:00 am *Welcome and Introductory Remarks*
Michael Casassa BES/DOE

Session I Chair: Margaret Murnane
8:15 am **** Plenary Talk ****
Ultrafast Molecular Dynamics with Ultrashort Electron Pulses
Peter Weber, Brown University

9:15 am *Attosecond Science: Generation, Metrology and Application*
Louis DiMauro, Ohio State University

9:45 am *Development and Utilization of Bright Tabletop Sources of Coherent
Soft X-ray Radiation*
Jorge Rocca, Colorado State University

10:15 am **** Break ****

10:45 am *The Kansas Light Source: From a Femtosecond to an Attosecond Facility*
Zenghu Chang, Kansas State University

11:15 am *Structure and Dynamics of Atoms, Ions, Molecules and Surfaces:
Strong-Field Molecular Physics*
Igor Litvinyuk, Kansas State University

11:45 am *High Intensity Laser Driven Explosions of Homo-Nuclear and Hetero-
Nuclear Molecular Clusters*
Todd Ditmire, University of Texas

12:15 pm **** Lunch ****

Session II Chair: Vince McKoy
5:00 pm *Molecular Structure and Electron-Driven Dissociation and Ionization*
Kurt Becker, Stevens Institute of Technology
5:30 pm *Electron-Atom and Electron-Molecule Collision Processes*
Tom Rescigno, Lawrence Berkeley National Laboratory
6:00 pm ***** Reception (Roof Terrace, No Host) *****
6:30 pm ***** Dinner *****

Session III Chair: Lew Cocke
7:30 pm *The Multicharged Ion Research Facility Upgrade Project*
Fred Meyer, Oak Ridge National Laboratory
8:00 pm *Electron-Molecular Ion Interactions*
Randy Vane, Oak Ridge National Laboratory
8:30 pm *Analysis of Structure in Low-Energy Ion-Atom Collisions*
Joe Macek, University of Tennessee

Tuesday, September 13

7:00 am ***** Breakfast *****

Session IV Chair: Phil Bucksbaum
8:00 am *Using Intense Short Laser Pulses to Manipulate and View Molecular Dynamics*
Robert Jones, University of Virginia
8:30 am *Atomic and Molecular Physics in Strong Fields*
Shih-I Chu, University of Kansas
9:00 am *Control of Molecular Dynamics: Algorithms for Design and Implementation*
Herschel Rabitz, Princeton University
9:30 am *Coherent Control of Multiphoton Transitions in the Gas and Condensed Phases with Ultrashort Shaped Pulses*
Marcos Dantus, Michigan State University

10:00 am ***** Break *****

10:30 am *Theory and Simulations of Ultrafast Nonlinear X-Ray Spectroscopy of Molecules*
Shaul Mukamel, University of California, Irvine
11:00 am *Nonlinear Photoacoustic Spectroscopies Probed by Ultrafast EUV Light*
Keith Nelson, Massachusetts Institute of Technology
11:30 am *Femtosecond X-ray Beamline for Studies of Structural Dynamics*
Robert Schoenlein, Lawrence Berkeley National Laboratory

Noon ***** Lunch *****

- Session V** Chair: Thom Orlando
- 4:30 pm *Electronic Excitations in Carbon Nanotubes Induced by Femtosecond Pump-Probe LASER Pulses*
Pat Richard, Kansas State University
- 5:00 pm *Structure and Dynamics of Atoms, Ions, Molecules and Surfaces: Atomic Physics with Ion Beams, Lasers and Synchrotron Radiation*
Uwe Thumm, Kansas State University
- 5:30 pm *High-*n* Rydberg Atoms and Tailored Pulses: A Laboratory for Wavefunction Engineering, Nonlinear Dynamics and Decoherence*
Carlos Reinhold, Oak Ridge National Laboratory
- 6:00 pm ***** Reception (Roof Terrace, No Host) *****
- 7:00 pm ***** Banquet (Pavilion) *****

Wednesday, September 14

- 7:00 am ***** Breakfast *****
- Session VI** Chair: Nora Berrah
- 8:00 am *Mode-Specific Polyatomic Photoionization*
Robert Lucchese, Texas A&M University
- 8:30 am *An X-ray Microprobe of Laser-Ionized Atoms*
Elliot Kanter, Argonne National Laboratory
- 9:00 am *Nondipolar Photoelectron Angular Distributions: A Spectroscopic Tool to Study Quadrupole Resonances*
Bertold Krässig, Argonne National Laboratory
- 9:30 am *Inner-Shell Photoionization of Atoms and Small Molecules*
Ali Belkacem, Lawrence Berkeley National Laboratory
- 10:00 am ***** Break *****
- 10:30 am *Reaction and Fragmentation Interferometry*
James Feagin, California State University, Fullerton
- 11:00 am *A Dual Bose-Einstein Condensate: Towards the Formation of Heteronuclear Molecules*
Chandra Raman, Georgia Institute of Technology
- 11:30 am *Atomic Physics Based Simulations of Ultra-Cold Plasmas*
Francis Robicheaux, Auburn University
- Noon *Closing Remarks*
Michael Casassa BES/DOE
- 12:10 pm ***** Lunch *****

Table of Contents

Invited Presentations (Ordered by Agenda)

<i>Ultrafast Molecular Dynamics with Ultrashort Electron Pulse</i> Peter Weber	1
<i>Attosecond Science: Generation, Metrology & Application</i> Louis F. DiMauro	2
<i>Development and Utilization of Bright Tabletop Sources of Coherent Soft X-Ray Radiation</i> Jorge J. Rocca	6
<i>The Kansas Light Source: From a Femtosecond to an Attosecond Facility</i> Zenghu Chang	10
<i>Structure and Dynamics of Atoms, Ions, Molecules and Surfaces: Strong-Field Molecular Physics</i> I. V. Litvinyuk	14
<i>High Intensity Laser Driven Explosions of Homo-Nuclear and Hetero-Nuclear Molecular Clusters</i> Todd Ditmire	18
<i>Molecular Structure and Electron-Driven Dissociation and Ionization</i> Kurt H. Becker	22
<i>Electron-Atom and Electron-Molecule Collision Processes</i> Thomas N. Rescigno	26
<i>The ORNL Multicharged Ion Research Facility Upgrade Project</i> Fred Meyer	30
<i>Electron-Molecular Ion Interactions</i> Randy Vane	32
<i>Analysis of Structure in Low-Energy Ion-Atom Collisions</i> Joe Macek	35
<i>Using Intense Short Laser Pulses to Manipulate and View Molecular Dynamics</i> Robert R. Jones	40
<i>Atomic and Molecular Physics in Strong Fields</i> Shih-I Chu	44
<i>Control of Molecular Dynamics: Algorithms for Design and Implementation</i> Herschel Rabitz	48

<i>Coherent Control of Multiphoton Transitions in the Gas and Condensed Phases with Ultrashort Shaped Pulses</i>	
Marcos Dantus	52
<i>Theory and Simulations of Nonlinear X-Ray Spectroscopy of Molecules</i>	
Shaul Mukamel	56
<i>Nonlinear Photoacoustic Spectroscopies Probed by Ultrafast EUV Light</i>	
Keith A. Nelson	60
<i>Femtosecond X-Ray Beamline for Studies of Structural Dynamics</i>	
Robert W. Schoenlein	64
<i>Electronic Excitations in Carbon Nanotubes Induced by Femtosecond Pump-Probe LASER Pulses</i>	
Pat Richard	68
<i>Structure and Dynamics of Atoms, Ions, Molecules and Surfaces: Atomic Physics with Ion Beams, Lasers and Synchrotron Radiation</i>	
Uwe Thumm	72
<i>High-n Rydberg Atoms and Tailored Pulses: A Laboratory for Wavefunction Engineering, Nonlinear Dynamics and Decoherence.</i>	
Carlos O. Reinhold	76
<i>Mode-Specific Polyatomic Photoionization</i>	
Robert R. Lucchese	79
<i>An X-ray Microprobe of Laser-Ionized Atoms</i>	
Elliot P. Kanter	82
<i>Nondipolar Photoelectron Angular Distributions: A Spectroscopic Tool to Study Quadrupole Resonances</i>	
Bertold Krässig	83
<i>Inner-Shell Photoionization of Atoms and Small Molecules</i>	
Ali Belkacem	84
<i>Reaction and Fragmentation Interferometry</i>	
James M. Feagin	88
<i>A Dual Bose-Einstein Condensate: Towards the Formation of Heteronuclear Molecules</i>	
Chandra Raman	92

<i>Atomic Physics Based Simulations of Ultra-Cold Plasmas</i> Francis Robicheaux	96
--	-----------

Laboratory Research Summaries (by Institution)

AMO Physics at Argonne National Laboratory	100
---	------------

<i>X-Ray Microprobe of Optical Strong-Field Processes</i> Linda Young	100
---	------------

<i>Nondipole Interactions in Photoelectron Angular Distributions</i> Steve Southworth	103
---	------------

<i>Double K-Photoionization of Heavy Atoms</i> Elliot Kanter	104
--	------------

<i>Two Photon Decay and Inner-Shell Vacancy Cascades</i> Robert Dunford	104
---	------------

<i>Gerade and Ungerade Photo-Double Ionization Correlation Functions in Helium at 100 eV and 450 eV Above Threshold</i> Bertold Krässig	105
---	------------

Overview of J. R. Macdonald Laboratory Program for Atomic, Molecular, and Optical Physics	108
--	------------

<i>Structure and Dynamics of Atoms, Ions, Molecules, and Surfaces: Molecular Dynamics with Ion and Laser Beams</i> Itzik Ben-Itzhak	109
---	------------

<i>Structure and Dynamics of Atoms, Ions, Molecules and Surfaces: Atomic Physics with Ion Beams, Lasers and Synchrotron Radiation</i> C.L.Cocke	112
---	------------

<i>Population Dynamics in Coherent Excitation of Cold Atoms</i> Bret D. DePaola	116
---	------------

<i>Time-Dependent Treatment of Three-Body Systems in Intense Laser Fields</i> Bret D. Esry	120
--	------------

<i>Theoretical Studies of Interactions of Atoms, Molecules and Surfaces</i> Chii Dong Lin	123
---	------------

Atomic, Molecular and Optical Sciences at LBNL	127
<i>Atomic, Molecular, and Optical Science: Fractional-Cycle Excitation of Bound State Transitions</i>	
Harvey Gould	128
Atomic, Molecular and Optical Science at LANL	132
<i>Multiparticle Processes and Interfacial Interactions in Nanoscale Systems Built from Nanocrystal Quantum Dots</i>	
Victor Klimov	132
Atomic and Molecular Physics Research at Oak Ridge National Laboratory.....	136
<i>The MIRF High Voltage Platform; In-Situ Electron Cyclotron Resonance (ECR) Plasma Potential Determination Using Emissive and Langmuir Probes; Low-Energy Ion-Surface Interactions</i>	
Fred W. Meyer	136
<i>Angular Distribution Studies of Ions Guided Through a Nanocapillary Array</i>	
H. F. Krause.....	139
<i>Electron-Molecular Ion Interactions</i>	
M. E. Bannister	140
<i>Near-Thermal Collisions of Multicharged Ions with H and Multi-Electron Targets</i>	
C. C. Havener	142
<i>High-n Rydberg Atoms and Tailored Pulses: A Laboratory for Wavefunction Engineering, Non-Linear Dynamics and Decoherence</i>	
C. O. Reinhold.....	143
<i>Analysis of Structure in Low-Energy Ion-Atom Collisions</i>	
J. H. Macek.....	144
 University Research Summaries (by PI)	
<i>Properties of Transition Metal Atoms and Ions</i>	
Donald R. Beck.....	150

<i>Probing Complexity Using the Advanced Light Source</i> Nora Berrah	154
<i>Bose-Fermi Mixtures Near an Interspecies Feshbach Resonance</i> John L. Bohn	158
<i>Exploiting Universality in Atoms with Large Scattering Lengths</i> Eric Braaten	161
<i>Ultrafast X-Ray Coherent Control</i> Philip H. Bucksbaum	162
<i>Formation of Ultracold Molecules</i> Robin Côté	166
<i>Optical Two-Dimensional Fourier-Transform Spectroscopy of Semiconductors</i> Steven T. Cundiff	167
<i>Theoretical Investigations of Atomic Collision Physics</i> Alexander Dalgarno	171
<i>Interactions of Ultracold Molecules: Collisions, Reactions, and Dipolar Effects</i> David DeMille	175
<i>Ultracold Molecules: Physics in the Quantum Regime</i> John Doyle	177
<i>Atomic Electrons in Strong Radiation Fields</i> Joseph H. Eberly	181
<i>Studies of Autoionizing States Relevant to Dielectronic Recombination</i> Thomas F. Gallagher	185
<i>Experiments in Ultracold Collisions</i> Phillip L. Gould	189
<i>Physics of Correlated Systems</i> Chris H. Greene	192
<i>Chemistry with Ultracold Molecules</i> Dudley Herschbach	196
<i>Resonant Interactions in Quantum Degenerate Bose and Fermi Gases</i> Murray Holland	199

<i>Exploring Quantum Degenerate Bose-Fermi Mixtures</i> Deborah Jin	203
<i>Ultrafast Atomic and Molecular Optics at Short Wavelengths</i> Henry C. Kapteyn	207
<i>Physics of Low-Dimensional Bose-Einstein Condensates</i> Eugene B. Kolomeisky	211
<i>Ion/Excited-Atom Collision Studies with a Rydberg Target and a CO₂ Laser</i> Stephen R. Lundeen	215
<i>Photoabsorption by Atoms and Ions</i> Steven T. Manson	219
<i>Electron-Driven Processes in Polyatomic Molecules</i> Vincent McKoy	223
<i>Electron/Photon Interactions with Atoms/Ions</i> Alfred Z. Msezane	228
<i>Single Molecule Absorption and Fluorescence in Inhomogeneous Environments</i> Lukas Novotny	232
<i>Electron-Driven Excitation and Dissociation of Molecules</i> Ann E. Orel	236
<i>Low-Energy Electron Interactions with Complex Targets</i> Thomas M. Orlando	240
<i>Energetic Photon and Electron Interactions with Positive Ions</i> Ronald A. Phaneuf	244
<i>Cold Rydberg Atom Gases and Plasmas in Strong Magnetic Fields</i> Georg Raithel	248
<i>Development and Characterization of Replicable Tabletop Ultrashort Pulse X-ray Sources for Chemical Dynamics Research</i> Christian Reich	251
<i>New Directions in Intense-Laser Alignment</i> Tamar Seideman	255
<i>Measurement of Electron Impact Excitation Cross Sections of Highly Ionized Ions</i> Augustine J. Smith	259

<i>Dynamics of Few-Body Processes</i> Anthony F. Starace	262
<i>Femtosecond and Attosecond Laser-Pulse Energy Transformation and Concentration in Nanostructured Systems</i> Mark I. Stockman	266
<i>Quantum Dynamics of Optically-Trapped Fermi Gases</i> John E. Thomas	270
<i>Inner-Shell Electron Spectroscopy and Chemical Properties of Atoms and Small Molecules</i> T. Darrah Thomas	274
<i>Laser-Produced Coherent X-Ray Sources</i> Donald Umstadter	278
<i>Towards Ultra-Cold Molecules – Laser Cooling and Magnetic Trapping of Neutral, Ground-State, Polar Molecules for Collision Studies</i> Jun Ye	282

Invited Presentations
(ordered by agenda)

Ultrafast molecular dynamics with ultrashort electron pulses

Peter Weber

Department of Chemistry

Brown University

324 Brook Street

Providence, RI 02912

The talk explores different approaches to study transient molecular structures using electron scattering. We show that electron energies ranging from only several eV, to the range of traditional high-energy electron diffraction (20 - 40 keV), all the way to the relativistic MeV range can be employed, with each electron energy regime offering unique advantages. As a model system we use tertiary amines, which are excited to either the 3p or the 3s Rydberg states by excitation with an ultrashort laser pulse. The ensuing dynamics is probed with electrons. In the low electron energy regime, Rydberg fingerprint spectroscopy is shown to provide a tool for time-dependent structure characterization. True time-dependent molecular structures are revealed by medium energy (20 keV) regime, pump-probe electron diffraction. Finally, the potential of ultrafast-pulsed relativistic (5 MeV) electron diffraction to solve molecular dynamics problems is highlighted. The potential benefits and advantages of the different electron energy regimes are contrasted and discussed.

ATTOSECOND SCIENCE: GENERATION, METROLOGY & APPLICATION

LOUIS F. DIMAURO
The Ohio State University
Department of Physics
Columbus, OH 43210
dimauro@mps.ohio-state.edu

1. PROGRAM SCOPE

The primary objective of the “Attosecond Science: Generation, Metrology & Application” grant at The Ohio State University (OSU) is the exploration of the physics that could result in the production of *light pulses with both the time-scale and the length-scale each approaching atomic dimension*. In other words, the formation of kilovolt x-rays bursts with attosecond (10^{-18} s) duration.

The strategy is to utilize the frequency scaling of the strong-field phenomenon of high harmonic generation for producing a broadband frequency comb of short wavelength radiation. In the frequency domain the harmonic comb is a powerful laboratory source of short wavelength coherent light. In the time-domain, proper synthesis of the frequency comb will yield a train of pulses or a single pulse with attosecond (10^{-18} s) durations. The scientific importance of breaking the femtosecond barrier is obvious: the time-scale necessary for probing the motion of an electron(s) in the ground state is attoseconds (atomic unit of time $\equiv 24$ as). The availability of such attosecond pulses would allow, for the first time, the study of the time-dependent dynamics of correlated electron systems by freezing the electronic motion, in essence exploring the structure with ultra-fast snapshots, then following the subsequent evolution using pump-probe techniques. The explicit dynamics of excited states of atoms could be followed characterizing, for example, processes like autoionization or non-adiabatic transitions during atomic collisions. These pulses also would allow investigations of the dynamics of bond breaking and formation during chemical reactions. Such studies would lead ultimately to developing new more fundamental methods for the complete quantum control of electron dynamics. All of these areas of science are well centered in the scientific scope of DOE Basic Energy Sciences (BES).

2. RECENT PROGRESS

The efforts in FY05 focused on building both the experimental and theoretical tools needed to perform the work outlined in the proposal. The progress included:

1. Building the infrastructure in the DiMauro laboratories in the newly constructed Physics Research Building (PRB) at The Ohio State University.
2. Reestablish the functionality of the laboratory apparatus moved from Brookhaven National Laboratory (BNL) to OSU.
3. Develop theoretical methods for testing and guiding the attosecond experiments.

The PI and the majority of the group (3 Stony Brook physics graduate students and one post-doctoral research associate) moved to OSU from BNL in October 2004. The new laboratories in PRB were scheduled for completion at that time but an unanticipated failure in the buildings mechanical systems delayed the completion of the construction for several months. The PRB did not receive occupational safety certification until February 2005. Nonetheless the DiMauro group was given special dispensation by the University Architectural Office to begin establishing some of the laboratories infrastructure prior to this date although with significant constraints. At the time of this writing, the basic infrastructure (HVAC, processed chilled water, computer networking, cable trays, electrical and safety systems) needed for laboratory operation is ready. The group is now in the process of rebuilding the laser and vacuum systems.

The laboratory space consists of three rooms totaling 3,000 ft². The rooms are configured to allow optical access from the main laser clean room area (1,800 ft²) to the adjacent target rooms (600 ft² each) where the experiments are conducted. As seen in Fig. 1, the main laser room consists of four optical bench setups totaling 325 ft² of vibrationally damped table space. Each table set supports a laser systems and associated diagnostics that will provide one of the three colors (0.8 μm, 2 μm and 4 μm) of intense ultra-short pulses needed for this project. All the laser systems operate at a minimum of one kilohertz repetition rate. The 2 μm and 4 μm laser systems were functional at BNL but as these lasers are being rebuilt at OSU a number of improvements are being implemented either to enhance laser performance or reliability.

In the photograph to the far left the blue semi-transparent curtains surround each table set for environmental control and laser safety. The back table set houses the 4 μm laser system which consists of a synchronized titanium sapphire and Nd:YLF amplified laser systems, the 4 μm light is derived as the difference frequency between these two colors. The new additions to this systems include a new Nd:YLF oscillator (Time-Bandwidth Lasers) for more stable performance and shorter pulse, 80 fs, titanium sapphire operation (the BNL system was 2 ps) and a multi-pass titanium sapphire amplifier for improved energy output. At the time of this writing both the titanium sapphire and Nd:YLF sections are operational and production of the 4 μm light is underway. It is anticipated that the 4 μm system will be functional by early August 2005.

Also shown in the same figure is the 2 μm laser system on the near left table set. A number of improvements have been added to this system and are operational. The 100 fs titanium sapphire oscillator has been replaced with a new 8 fs oscillator (Nanolayers Venteon broadband oscillator). The CPA has been redesigned and constructed with a band-pass for 25 fs amplified operation. Currently a multi-pass titanium sapphire power amplifier is being added to the system for 6 mJ pulse operation. The 2 μm pulses are generated using a commercial optical parametric amplifier (Quantronix Topas OPA visible in lower left-hand corner of figure) purchased as part of this contract. This system should be operational by September 2005.



Figure 1: From left to right the photos are the main laser clean room, attosecond target room and scaled interaction target room in the new Physics Research Building at OSU.

In the same figure the near right optical table set will house the commercial (Femtolaser Produktions) titanium sapphire amplifier laser system with carrier-envelope phase stabilized output. At the time of this writing the system has been installed but the performance did not meet specifications. Prof. DiMauro is working with the vendor to rectify this problem.

Parallel construction of the experimental rooms is progressing. The middle photograph in Fig. 1 shows the attosecond target room. A harmonic test-stand is under construction for characterizing the frequency comb of the high harmonic light interacting with a long wavelength (2 μm and 4 μm) fundamental field. The vacuum box with the Plexiglas covered flange is a 0.7 m Hettrick x-ray imaging spectrometer on loan from the AMOP group (L. Young-group leader) at Argonne National Laboratory. The vacuum chamber on the optical table is the harmonic source chamber. It is anticipated that the harmonic test-stand will become operational in September 2005. A separate vacuum apparatus for

performing applications with attosecond pulses is being designed under the supervision of Prof. Agostini. The apparatus will consist of a harmonic source chamber, a transport section with XUV focusing optics and an experimental science chamber for conducting attosecond experiments. The science chamber will incorporate a COLTRIMS design for both electron and ion detection. An end of year schedule for completion of the attosecond application apparatus is expected.

The photograph of the scaled interaction target room is shown on the right in Fig. 1. The apparatus in this room will be used to continue the scaled interactions of alkali atoms with an intense long wavelength fundamental field started at BNL. The required apparatus needed for the first set of experiments (pictured on the optical table) is nearly complete. We anticipate that this apparatus will start producing data by the end of September using the 4 μm source.

In order to investigate the validity of the classical scaling of harmonic and attosecond generation discussed in our original proposal we have initiated a 3-D quantum mechanical treatment of the problem. Our analysis is capable of studying various inert gas atoms at different wavelengths. The calculations are based on numerical solutions of the time-dependent Schrödinger equation using a single active electron (SAE) approximation. We calculate both the photoelectron energy distribution and the high harmonic spectral and phase distributions. The CPU intensive calculations are being performed with time allocations at the Ohio Supercomputing Center. The post-doctoral research associate, Dr. Jennifer Tate, supported on this contract is conducting this work.

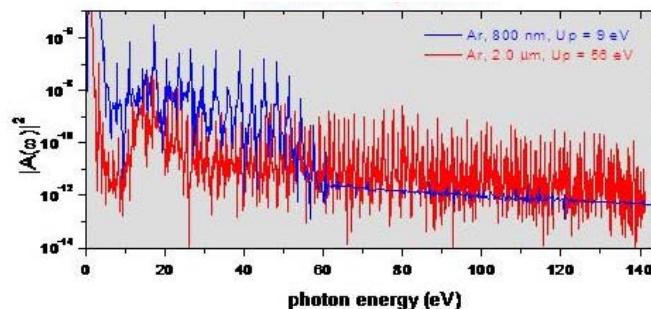


Figure 2: Quantum mechanical TDSE calculation using a SAE approximation of argon harmonic emission at 0.2 PW/cm^2 with 0.8 μm (blue) and 2 μm (red) fundamental driver fields. The 2 μm cutoff energy is 180 eV.

Figure 2 shows some of our results for argon high harmonic emission excited by both an 8-cycle 0.8 μm and 2 μm fundamental field. The 0.8 μm calculation (blue line) is in agreement with the experimentally measured harmonic plateau seen for argon, which has a cutoff at approximately 50 eV. However, argon atom exposed to a 2 μm fundamental field at the same intensity shows a plateau with similar strength that extends well beyond the 140 eV limit of the plot. In fact the harmonic cutoff is at 180 eV, not shown in the figure. Thus the quantum calculation agrees with the semi-classical analysis and verifies the viability of our strategy for producing shorter wavelength harmonic emission. Furthermore, the expected λ^2 decrease in harmonic emission due to the wave packet spread is not as severe as predicted analytically since the classical analysis does not account for the higher-order trajectories. Our harmonic test-stand apparatus will be invaluable in providing a direct quantitative comparison between experiment and theory, which has been for the most part overlooked.

Less obvious but equally compelling in the long wavelength scaling strategy proposed by the Ohio State group is the ability to create shorter attosecond pulses. As presented in our original proposal, quasi-classical analysis show that by virtue of the longer wavelength drive field a more effective synchronization of the classical trajectories can result in a shorter attosecond burst. The improvement in optimum pulse duration scales classically as $\lambda^{-3/2}$. For example, the 2 μm and 4 μm fundamental driver should yield attosecond pulses that are at least 4-times and 10-times shorter, respectively, than currently

possible with titanium sapphire. We are focusing our numerical efforts for investigating this classical prediction.

3. FUTURE PLANS

The future aim of the program can be categorized as:

1. Utilize the scaled interactions approach to test fundamental concepts of attosecond generation and metrology.
2. Realize novel arrangements using the scaled interaction approach for advancing the development of high harmonic and attosecond generation.
3. Utilize the wavelength scaling of strong-field interactions to push high harmonic generation into kilovolt photon energies (x-rays) while defining new limits on attosecond pulse durations. The goal is the unprecedented development of light pulses that can achieve both the *atomic time* and *length scales*.
4. Develop advance metrology for short wavelength pulse characterization and provide fundamental tests of known metrology against direct measurements utilizing the scaled interaction approach.
5. Initiate a program in attophysics: applications of attosecond light pulses.
6. Establish and maintain a working attosecond source at OSU based on a carrier envelope phase (CEP) stabilized few-cycle near infrared laser system.
7. Advance the optical technology needed for the routine production of attosecond x-rays.

4. DOE SPONSORED PUBLICATIONS

1. “*Scaled Intense Laser-Atom Physics: The Long Wavelength Regime*”, T. O. Clatterbuck, C. Lynga, P. Colosimo, J. D. D. Martin, B. Sheehy, L. F. DiMauro, P. Agostini and K. C. Kulander, *J. Mod. Optics* **50**, 441-450 (2003).
2. “*Observation of a Transition in the Dynamics of Strong-Field Double Ionization*”, J. L. Chaloupka, J. Rudati, L. F. DiMauro, P. Agostini and K. C. Kulander, *Phys. Rev. Lett.* **90**, 033002-1-4 (2003).
3. “*First Ultraviolet High-Gain Harmonic-Generation Free Electron Laser*”, L. H. Yu *et al.*, *Phys. Rev. Lett.* **91**, 074801-1-4 (2003).
4. “*First SASE and seeded FEL lasing of the NSLS DUV-FEL at 266 and 400 nm*”, L. F. DiMauro *et al.*, *Nucl. Instr. and Meth. A* **507**, 15-18 (2003).
5. “*Yield and Temporal Characterization of High Order Harmonics from a Tightly Focused Geometry: Intense Mid-Infrared Excitation of a Cesium Vapor*”, T. O. Clatterbuck, P. M. Paul, C. Lynga, B. Sheehy, L. F. DiMauro, P. Agostini, K. C. Kulander and I. A. Walmsley, *Phys. Rev. A* **69** 033807-1-5 (2004).
6. “*Characterization of Attosecond Electromagnetic Pulses*”, E. Kosik, E. Cormier, C. Dorrer, I. A. Walmsley and L. F. DiMauro, in *Ultrafast Optics*, eds. F. Krausz, G. Korn, P. Corkum, I. A. Walmsley, (Springer, New York, 2004).
7. “*The Physics of Attosecond Pulses*”, P. Agostini and L. F. DiMauro, *Reports on Progress in Physics* **67**, 813-855 (2004).
8. “*Multiphoton Double Ionization via Field-Independent Resonant Excitation*”, J. Rudati, J. L. Chaloupka, P. Agostini, K. C. Kulander and L. F. DiMauro, *Phys. Rev. Lett.* **92**, 203001 (2004).
9. “*Self-referencing, spectrally or spatially encoded spectral interferometry for the characterization of attosecond electromagnetic pulses*”, E. Cormier, I. A. Walmsley, E. M. Kosik, L. Corner and L. F. DiMauro, *Phys. Rev. Lett.* **94**, 033905 (2005).
10. “*Enhanced High Harmonic Generation from a Prepared Excited State*”, P. M. Paul, C. Lynga, T. O. Clatterbuck, P. Colosimo, L. F. DiMauro, P. Agostini and K. C. Kulander, *Phys. Rev. Lett.* **94**, 113906 (2005).

Development and utilization of bright tabletop sources of coherent soft x-ray radiation

Jorge J. Rocca,

Electrical and Computer Eng Department, Colorado State University, Fort Collins, CO 80523-1373
rocca@engr.colostate.edu

Henry C. Kapteyn

JILA/Physics Department, University of Colorado, Boulder, CO 80309-0440
kapteyn@jila.colorado.edu

Program Description

We are investigating aspects of the development and use of compact coherent soft x-ray sources based on fast capillary discharges and high order harmonic up-conversion, and soft x-ray laser amplification. These sources are very compact, yet can generate soft x-ray radiation with peak spectral brightness several orders of magnitude larger than a synchrotron beam line. In relation to source development, we are exploring the generation of high harmonics in a *pre-ionized* medium created by a capillary discharge. The use of pre-ionized nonlinear media may make it possible to generate coherent light at > 1 KeV photon energy, by reducing ionization-induced defocusing of the incident laser. Other recent results includes the successful development of a 10 Hz repetition rate desk-top size 46.9 nm wavelength laser for photochemistry applications. This new laser source is currently routinely used as a single photon ionization source in nanocluster spectroscopy experiments.

Discharge-created plasma waveguides for high harmonic generation from ions

We are investigating the generation and quasi-phase-matched generation of high harmonics of femtosecond Ti:Sa laser pulses ($\lambda = 800$ nm) in a plasma waveguide created using an electrical capillary discharge plasma columns with a selected degree of ionization. Such pre-ionized nonlinear media may

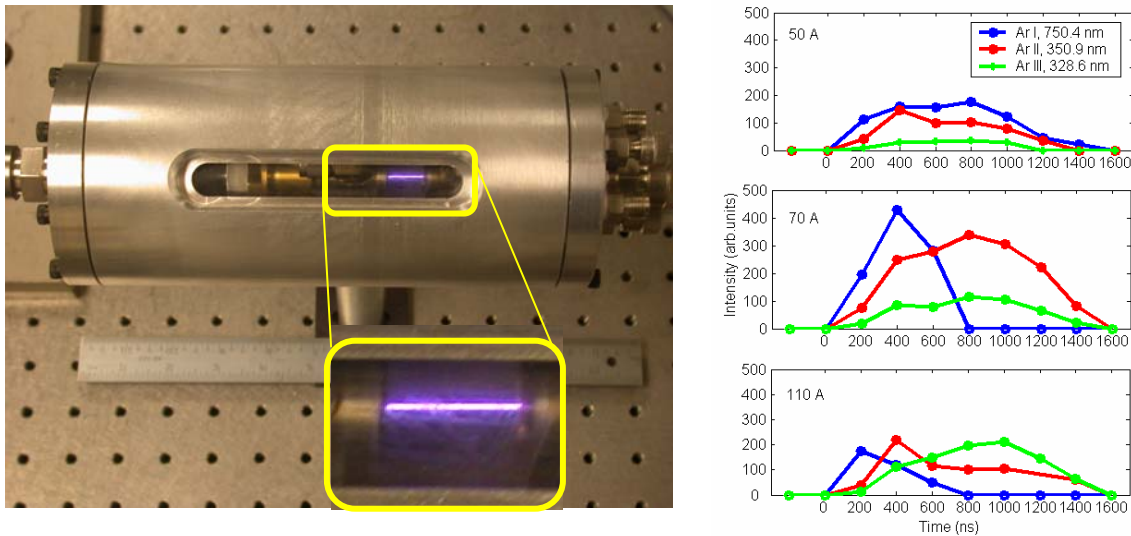


Figure 1. (left) photograph of the capillary discharge plasma waveguide device operating in argon gas. The capillary has a diameter of 200 micrometers and a length of 5 cm. (right) Spectra of the plasma showing the temporal evolution of the intensity of Ar I, Ar II and Ar III lines in a 200 um diameter capillary discharge plasma for three different discharge currents. The data shows the degree of ionization can be selected by adjusting the discharge current.

lead to the generation of coherent light at photon energies > 1 KeV. In this scheme, an electrical discharge creates a totally ionized medium, which the degree of ionization is selected by the choosing the amplitude of the discharge current through the capillary in which the high-harmonic driving laser will propagate. This provides access to significantly larger ionization potential values than those of neutral atoms, contributing to the generation of shorter wavelengths. The driver laser intensity can be significantly increased before tunnel ionization again becomes an important loss. This should result in an increase in the cutoff energy and also significantly reduce the driver laser energy loss due to optically-induced ionization and correspondingly higher high harmonic generation (HHG) generation efficiency. Finally, the radial distribution of the electron density profile in the capillary plasma is concave, generating an index guide. This allows for a reduced laser intensity at the walls of the capillary, making it possible to guide pulses at the higher intensities required for shorter wavelength HHG, without damage to the walls.

With this objective we have developed and characterized a discharge-ionized gas-filled capillary channel in which both the degree of ionization and the electron density profile can be tailored for propagation of an intense ultrashort laser pulse. A photograph of the compact discharge is shown at the left of figure 1. Using a two-temperature one-dimensional Lagrangian hydrodynamic/atomic code developed at CSU we have predicted the characteristics of the capillary plasmas and the discharge parameters that are required to optimize the degree of ionization and the guiding for HHG generation. Current pulses of about $1 \mu\text{s}$ duration and 10-150 A amplitude were used to create plasma channels in 200-250 μm diameter capillary tubes. In this discharges the dynamics of the plasma is dominated by ohmic heating and heat conduction losses. Shortly after the initiation of the current pulse the plasma expands as a result of the larger temperature increase in the axial region of the plasma due to ohmic heating. The outer region of the plasma remains colder due to heat conduction to the capillary walls. This generates a radial electron temperature profile with maximum on axis and minimum at the capillary wall. This concave electron density profile gives origin to an index of refraction distribution with maximum on axis, that guides the laser light. Figure 1 (right) shows the relative intensity of lines from Ar I, Ar II and Ar III spectra as a function of capillary discharge current for discharge currents of 50, 70 and 100 A. The data shows it is possible to select the degree of ionization by controlling the discharge current. This plasma waveguide can reliably operate at repetitions rates up to 100 Hz, which is unprecedented for a discharge designed for laser guiding.

Plasma guiding results

We have studied the propagation of a 800 nm wavelength laser beam in plasma channels generated by pulse-discharge excitation into a 5 cm long quartz capillary 200 micrometers in diameter filled with Ar pressures between 5 and 10 Torr. The plasmas were excited by current pulses of about $1 \mu\text{s}$ duration and amplitudes ranging from 10 A to 100 A. The laser pulses were generated by a Ti:sapphire laser and had an energy of a few millijoules and a duration of about 50 fs. The blue trace in figure 2 (top) shows the current pulse with an amplitude of about 55 A used to generate the plasma. The same figure shows the variation of the measured laser beam transmission thorough the capillary hannel. With the discharge off about 30 percent of the laser beam energy is guided thought the 5 cm long capillary tube. When the discharge is turned on and the plasma waveguide is formed the fraction of the beam energy guided through the channel increases to about 60 percent and remains at that level for the duration of the current pulse.

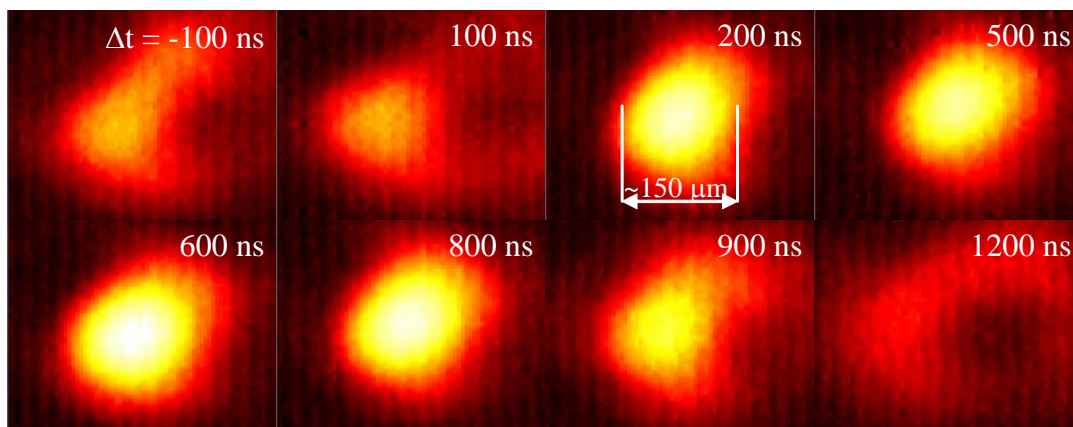
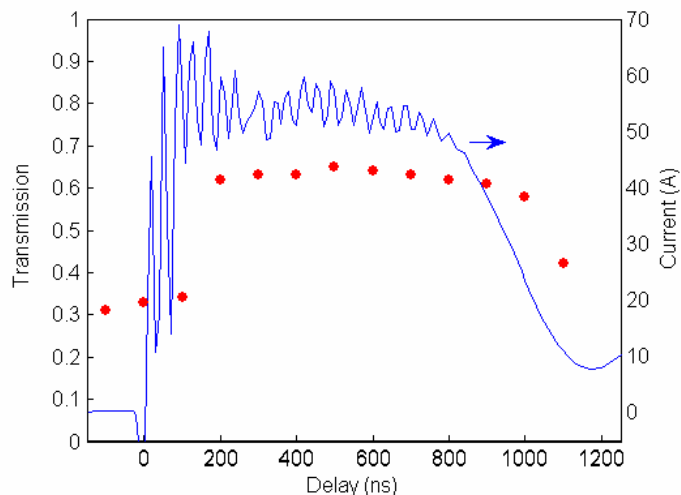


Figure 2. (top). The dots represent the fraction of the energy of the laser pulse that is guided through the 5 cm long capillary. When the discharge current (blue curve) is turned on, the intensity of the transmitted light increases to 60 percent. (bottom) near field images of the guided beam. The pattern of the guided beam improves greatly in presence of the discharge created plasma waveguide.

Figure 2 (bottom) shows a sequence of near field pattern of the laser pulse exiting the waveguide as a function of delay between the beginning the current pulse and the injection of the laser pulse. Prior to the formation of the discharge-crated plasma channel the beam pattern of the transmitted beam changes significantly from one shot to another, and does not present a well defined mode. In contrast, about 200 ns after the initiation of the discharge the guided beam displays a near Gaussian distribution with a beam diameter of about 150 μm . This beam profile, which corresponds to the fundamental mode of the guide, remains constant as a function of delay until the end of the current pulse. These measurements demonstrate that there is a temporal window of duration similar to that of the current pulse during which the plasma constitutes an excellent plasma guide for laser beams.

Desk-top size soft x-ray laser as single-photon ionization source for the study of nanoclusters

In a separate development a desk-size capillary discharge laser emitting at $\lambda = 46.9 \text{ nm}$ (26.5 eV), which first prototype had been previously developed as part of this program, was installed in a photochemistry laboratory at CSU to be used as single photon ionization source for the study of the electronic structure of nanoclusters. Laser pulses with energy $\sim 10 \text{ uJ}$ are generated at up to 12 Hz repetition rate by single pass

amplification in a 21 cm long Ne-like Ar capillary discharge plasma column. The capillary lifetime was measured to be $2\text{-}3 \cdot 10^4$ shots. This new type of portable laser is of interest for numerous applications requiring a compact intense source of short wavelength laser light. In the past several months this compact laser has been routinely used in mass spectroscopy studies. Molecules studied include ammonia, water and methanol nanoclusters. The use of 46.9 nm photoionization allowed the observation of methanol/water clusters not seen with VUV laser ionization. Through single photon ionization the reactivity and catalytic behavior of these molecules will also be studied.

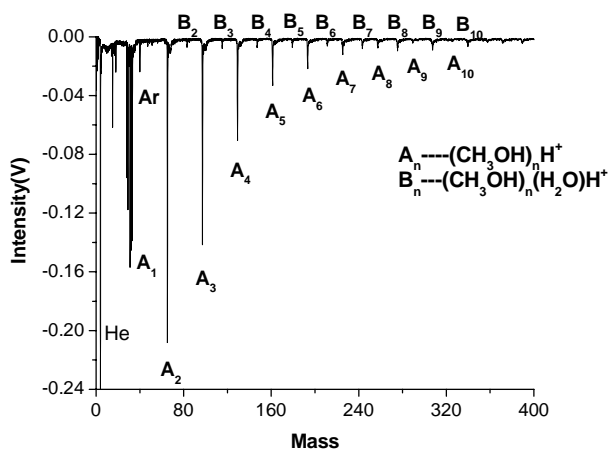


Figure 3. (left) desk-top size 46.5 nm capillary discharge laser and (right) mass spectrum of methanol clusters produced by single photon ionization using this laser (spectrum by S. Heinbuch, F. Dong and E. Bernstein)

Future plans During the next year of the project we will explore the generation of high harmonic from ions in these discharge-created plasma waveguides. Methods for quasi-phase matching will be developed.

Journal publications from DOE sponsored research 2002-05

1. S. Heinbuch, M. Grisham, D. Martz, and J.J. Rocca, "Demonstration of a desk-top size high repetition rate soft x-ray laser", *Optics Express*, **13**, 4050, (2005).
2. Y. Wang, B.M. Luther, M. Berrill, M. Marconi, J.J. Rocca, "Capillary discharge-driven metal vapor plasma waveguides", *Physical Review E*, In press (2005).
3. B.M. Luther, Y. Wang, M. Berrill, D. Alessi, M.C. Marconi, M.A. Larotonda, and J.J. Rocca, "Highly ionized Ar plasma waveguides generated by a fast capillary discharge", *IEEE Transactions on Plasma Science*, **33**, 582, (2005).
4. Y. Wang, B.M. Luther, F. Pedacci, M. Berrill, F. Brizuela, M. Marconi, M.A. Larotonda, V.N. Shlyaptsev, and J.J. Rocca, "Dense Capillary Discharge Plasma Waveguide Containing Ag Ions", *IEEE Transactions on Plasma Science*, **33**, 584, (2005).
5. M. Grisham, G. Vaschenko, C.S. Menoni, J.J. Rocca, Yu.P. Pershyn, E.N. Zubarev, D.L. Voronov, V.A. Sevryukova, V.V. Kondratenko, A.V. Vinogradov, and I.A. Artioukov, "Damage of Extreme Ultraviolet Sc/Si Multilayer Mirrors Exposed to Intense 46.9 nm Laser Pulses", *Optics Letters* **29**, 620, (2004).
6. S. Le Pape, Ph. Zeitoun, M. Idir, P. Dhez, J.J. Rocca, and M. François, "Electromagnetic field distribution measurements in the soft x-ray range: full characterization of a soft x-ray laser beam", *Physical Review Letters*, **88**, 183901 (2002).

The Kansas Light Source: From a femtosecond to an attosecond facility

Zenghu Chang

J. R. Macdonald Laboratory, Department of Physics,
Kansas State University, Manhattan, KS 66506, chang@phys.ksu.edu

The goals of this aspect of the JRML program are (1) to generate few-cycle laser pulses for attosecond generation, (2) to study attosecond x-ray sources based on the polarization gating of high-order harmonic generation, and (3) to improve the resolution of ultrafast x-ray streak cameras.

1. High energy 6.2 fs pulses for attosecond pulse generation, Ghimire Shambhu, Chris Nakamura, Bing Shan, Chun Wang and Zenghu Chang.

The Kansas Light Source (KLS) at the J. R. Macdonald laboratory is an ultrafast laser facility for AMO studies [1-9]. For attosecond pulse generation and other applications, we investigated a novel method to increase the energy of the sub-10 fs pulses with the KLS [1]. The hollow-core fiber/chirped mirror compressor is one of the most effective ways to generate few-cycle laser pulses. It is believed that multiphoton ionization and self-focusing are the two dominating factors that limit the maximum input energy before the spatial mode of the output beam breaks. On one hand, the ionized gas causes the laser beam to defocus in the region close to the entry of the fiber and inside the fiber. On the other hand, the self-focusing transfers the energy of the pulse from the fundamental fiber mode to the higher order modes. The interplay between plasma defocusing and self-focusing makes the process even more complicated. Both multiphoton ionization and self-focusing (optical-Kerr effect) are nonlinear processes. For the same laser energy, the electric field strength is less for circular light than that of linear light. The nonlinear processes are weaker when the input pulses are circularly polarized due to reduction in the field strength. Because of the reduction in the field strength, both nonlinear processes are weaker when the input pulses are circular polarized. Thus, we expected the fiber could work at a higher input energy level. The experiment was done with input energies up to 1.6 mJ from the *Kansas Light Source*, which operates at a repetition rate of 1 kHz at a central wave length of 790 nm. The FWHM of the measured pulse was 33 fs. The setup is shown in the top portion of figure 1.

The well characterized linearly polarized pulses passed through a zero-order quarter wave plate in order to vary the polarization state of the beam. The laser beam was focused by a plano-convex lens with a one meter focal length. The inner diameter of the hollow-core fiber is 400 μm and the length is 90 cm. The fiber was placed on a v-grooved aluminium rod kept in a pressurized chamber filled with Ar gas. The throughput of the fiber was 65-70% for both circular and linear polarization of the input. When the gas was pumped out, the output energy increased linearly as the input energy increased for both the circular and linear inputs. The spatial profiles of the output beam were identical for the circular and the linear input. When the gas pressure was 0.5 bar, the output energy was the same for the two polarization states at very low input energy (0.5 mJ).

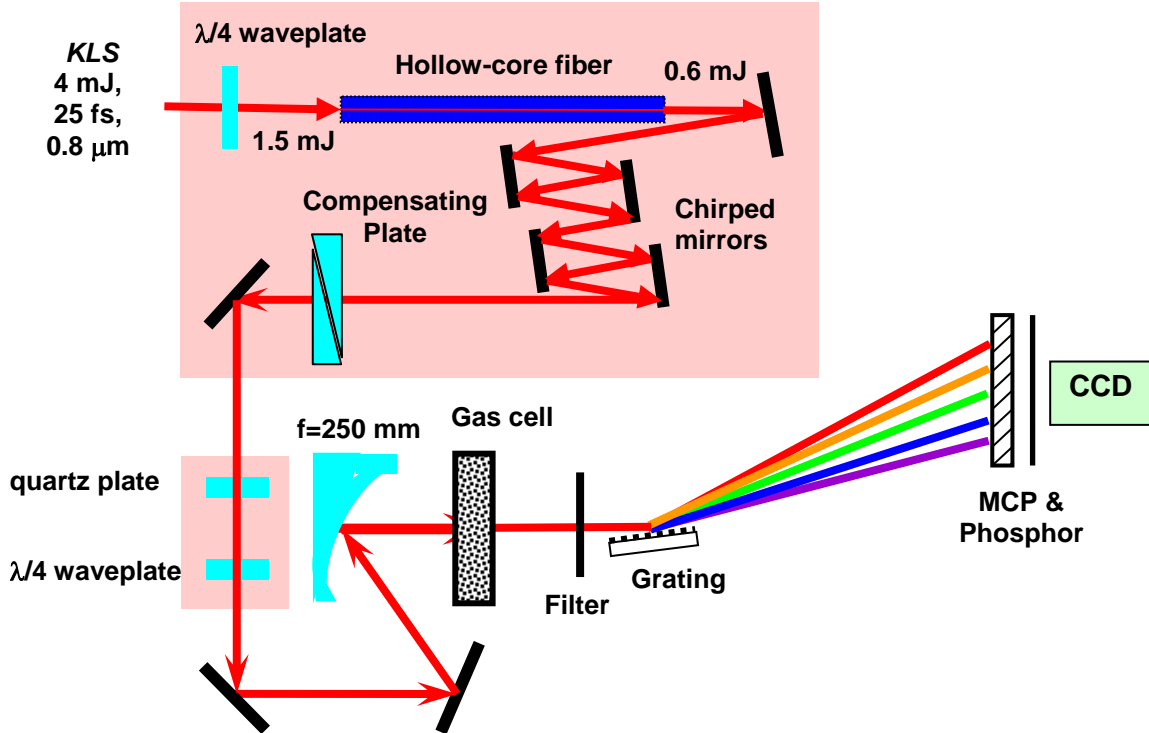


Figure 1. The generation of energetic 6 fs lasers pulses (top portion) and its application on the generation of XUV supercontinuum by a polarization gating (bottom portion).

The output energy did not increase linearly with the input energy for both polarization states. However, the deviation started at a lower input energy for the linear polarization than that for the circular polarization. The decrease of throughput with the increase of the input energy was accompanied by the degradation of the spatial profile. The spatial profile of the output beam started to degrade at a much lower input energy for the linear polarization than that for the circular polarization. For attosecond pulse generation, it is beneficial to use the lowest order spatial mode. However, the maximum output energy that still preserve the good spatial mode for the circular input was 0.79 mJ which is 1.5 time higher than that for the linear input. Moreover, the spectra of the output pulses were comparable for the two polarization states. The increase of the pulse energy by using circularly polarized input can be attributed to the suppression of ionization. The spectrum broadening in the fiber is caused mainly by self-phase modulation. Since self-phase modulation and self-focusing are from the same nonlinear effect (optical-Kerr effect), one can not reduce the self-focusing but maintain the self-phase modulation unchanged to obtain the required bandwidth. The order of nonlinearity of multiphoton ionization is higher than the third order optical-Kerr effect, thus it can be reduced more effectively when the field is changed from linear to circular polarization.

The spectrally broadened pulses emerging from the fiber were compressed by using chirped mirrors. When the input beam was circularly polarized, the pulse energy after the chirped mirrors and the collimation mirrors was 0.6 mJ. The energy of the 6.2 fs pulses is the highest energy achieved in argon with pulses duration less than 7 fs.

2. Towards single shot measurement of the attosecond XUV supercontinuum generated by a polarization gating, *Mahendra Shakya, Steve Gilbertson, Bing Shan, Ghimire Shambhu, and Zenghu Chang*

It has been demonstrated by the PI's group experimentally that a supercontinuum covering the plateau and cutoff region is generated when the driving laser pulse with a time-dependent ellipticity is composed by few-cycle pulses [10]. When polarization gating of high harmonic generation is done using sub-10 fs lasers, the harmonic spectrum is sensitive to the carrier-envelope phase (CE phase) of the lasers [11, 12]. If the harmonic spectra intensity is strong enough, it is possible to measure the CE phase of each laser pulse by observing the shot to shot variation of the harmonic spectra. We have worked on improving the yield of the attosecond supercontinuum and the detection sensitivity in order to measure the single shot spectrum.

The experimental setup for generating attosecond supercontinuum is shown in the bottom portion of figure 1. The circularly polarized laser pulse from the fiber was overcompensated for dispersion by using the chirp mirrors to give an estimated pulse of ~8 fs duration with 0.6 mJ energy onto the Ar gas target. A quartz plate with 0.5 mm thickness splits the circularly polarized pulse into two orthogonal, linearly polarized pulses delayed with each other by 15 fs, due to the different group velocities along and perpendicular to the optic axis. An achromatic quarter wave plate is placed after the quartz plate with its optic axis oriented 45 degree from that of the quartz plate. The wave plate combines the two linear pulses and converts them into a pulse with a time dependent ellipticity, i.e., the leading and trailing edge of the pulse is circularly polarized while the middle portion is linearly polarized. The portion with ellipticity less than 0.2 lasts only one half of a laser cycle, which is responsible to generate the high harmonic field. When the high harmonic spectra are measured with a spectrometer, phase offset between the carrier and the envelope of the pulse becomes an important factor. Our goal is to measure the carrier envelope phase of each laser pulse by measuring the polarization gated harmonic spectra. This method should be useful to the experiments that use lasers whose CE phase is not locked. A new XUV spectrometer that uses a toroidal grating was used to measure the spectrum, as shown in the figure. To further increase the signal of XUV spectrum we tuned the gas density at the interacting region in a gas cell to reach the phase matching condition. The measured harmonic spectrum integrated indicates that it is strong enough for a single shot measurement. We are also working on measuring the attosecond pulse duration [13].

3. Calibration of an accumulative x-ray streak camera with high harmonic pulses, *Mahendra Shakya and Zenghu Chang*

A streak camera with 280 fs resolution has been developed by our group [14, 15] for applications at the third and the fourth generation x-ray sources [16]. The resolution was measured with pulses centered at 260nm, i.e., the 3rd harmonics of the Kansas Light Source. The response time of the camera for x-ray/XUV can be different from that for UV, thus we plan to use the zero-order diffraction of the XUV grating in the attosecond pulse generation for the calibration of the streak camera.

PUBLICATIONS

1. S. Ghimire, B. Shan, C. Wang, and Z. Chang, “*High-Energy 6.2-fs Pulses for Attosecond Pulse Generation*,” *Laser Physics*, **15**, No. 6, 838-842(2005).
2. A. S. Alnaser, C. M. Maharjan, X. M. Tong, B. Ulrich, P. Ranitovic, B. Shan, Z. Chang, C.D. Lin, C. L. Cocke, and I. V. Litvinyuk, “*Effects of orbital symmetries in dissociative ionization of molecules by few-cycle laser pulses*,” *Phys. Rev. A* **71**, 031403(R) (2005).
3. M. Zamkov, N. Woody, B. Shan, Z. Chang, P. Richard, “*Lifetime of charge carriers in multiwalled nanotubes*,” *Phys. Rev. Lett.*, **94**, 056803 (2005).
4. A. S. Alnaser, X.-M. Tong, T. Osipov, S. Voss, C.M. Maharjan, P. Ranitovic, B. Ulrich, B. Shan, Z. Chang, C. D. Lin, and C. L. Cocke, “*Routes to control of H₂ Coulomb explosion in few-cycle laser pulses*,” *Phys. Rev. Lett.*, **93**, 183202 (2004).
5. A. S. Alnaser, X. M. Tong, T. Osipov, S. Voss, C. M. Maharjan, B. Shan, Z. Chang, and C. L. Cocke, “*Laser-peak-intensity calibration using recoil-ion momentum imaging*,” *Phys. Rev. A* **70**, 023413 (2004).
6. M. Zamkov, N. Woody, S. Bing, H.S. Chakraborty, Z. Chang, U. Thumm, and P. Richard, “*Time-resolved photoimaging of image-potential states in carbon nanotubes*,” *Phys. Rev. Lett.*, **93**, 156803 (2004).
7. A.S. Alnaser, S. Voss, X.-M. Tong, C.M. Maharjan, P. Ranitovic, B. Ulrich, T. Osipov, B. Shan, Z. Chang and C. L. Cocke, “*Effects of molecular structure on ion disintegration patterns in ionization of O₂ and N₂ by short laser pulses*,” *Phys. Rev. Lett.*, **93**, 113003 (2004).
8. Richard Bredy, Howard A. Camp, and Hai Nguyen, Takaaki Awata, Bing Shan, Zenghu Chang, and B. D. DePaola, “*Three-dimensional spatial imaging in multiphoton ionization rate measurements*,” *J. Opt. Soc. Am. B* **21**, 2221 (2004).
9. K. Kulkarni, Z. Chang, and S. Lei, 2004, “*Surface Micro/Nanostructuring of Cutting Tool Materials by Femtosecond Laser Micromachining*,” *Transactions of the North American Manufacturing Research Institution of SME* **32**, 25 (2004).
10. Bing Shan, Shambhu Ghimire, and Zenghu Chang, “*Generation of attosecond XUV supercontinuum by polarization gating*,” *Journal of Modern Optics*, **52**, 277 (2005).
11. Zenghu Chang, “*Single attosecond pulse and xuv supercontinuum in the high-order harmonic plateau*,” *Phys. Rev. A*, *Phys. Rev. A*, **70**, 043802 (2004).
12. Zenghu Chang, “*Chirp of the attosecond pulses generated by a polarization gating*,” *Phys. Rev. A*, **71**, 023813 (2005).
13. Z. X. Zhao, Zenghu Chang, X. M. Tong, and C. D. Lin, “*Circularly-polarized laser-assisted photoionization spectra of argon for attosecond pulse measurements*,” *Optics express*, **13**, 1966 (2005).
14. Mahendra Man Shakya and Zenghu Chang, “*Achieving 280 fs resolution with a streak camera by reducing the deflection dispersion*,” *Appl. Phys. Lett.* **87**, 041103 (2005).
15. M. M. Shakya, Z. Chang, "An accumulative x-ray streak camera with 280-fs resolution", *Proceedings of SPIE*, Vol. **5534**, pp125-131 (2004).
16. S. L. Johnson, P. A. Heimann, A. G. MacPhee, A. M. Lindenberg, O. R. Monteiro, Z. Chang, R. W. Lee, and R. W. Falcone, “*Bonding in liquid carbon studied by time-resolved x-ray absorption spectroscopy*,” *Phys. Rev. Lett.*, **94**, 057407 (2005).

Structure and Dynamics of Atoms, Ions, Molecules and Surfaces: Strong-Field Molecular Physics

I. V. Litvinyuk, Physics Department, J.R. Macdonald Laboratory, Kansas State University,
Manhattan, KS 66506, ivl@phys.ksu.edu

The goal of this aspect of the JRML program is to study interactions of molecules with intense ($>10^{13}$ W/cm²) ultrashort (5 – 100 fs) laser pulses. That includes molecular alignment, high harmonic generation, single and multiple ionization, laser-induced rearrangement (isomerization), and Coulomb explosion of molecules. Our objective is to understand the detailed mechanisms of field-molecule interactions and, ultimately, to be able to control molecular processes using strong laser fields.

Recent progress and future plans:

1) Studying mechanisms of strong-field ionization of molecules

A. S. Alnaser, M. Zamkov, X. M. Tong, C.M. Maharjan, P. Ranitovic, S. Bing, C. D. Lin, Z. Chang, L. Cocks and I.V. Litvinyuk

The purpose of this project is to understand detailed mechanisms and pathways of molecular ionization by intense laser pulses. We achieve this by analyzing charged reaction fragments (ions and electrons) using the “reaction microscope” (COLTRIMS apparatus). We conduct our experiments in the regime where the first ionization step is almost always tunneling. The mechanisms of further electron removal still remain very poorly understood, particularly in the case of molecules. Possible pathways include simple sequential tunneling mechanism, electron re-collision, enhanced ionization at critical distance, multi-photon excitation, shake-up/shake-off. Depending on pulse parameters (peak intensity, duration, frequency chirp) and particular molecule, various mechanisms can be operational, sometimes simultaneously, requiring various experimental approaches to disentangle them. The following are some examples of the studies we completed:

- Effects of orbital symmetries in dissociative ionization of molecules by few-cycle laser pulses

We have measured angular distributions of ion fragments produced in dissociative double ionization of CO, CO₂, and C₂H₂ by intense ultrashort laser pulses. We found that for sub-10-fs pulses of sufficiently low intensity the fragments’ angular distributions for all studied molecules are determined by angular dependence of the first ionization step. Those experimental angular distributions were in good agreement with angular dependent ionization probabilities calculated with the molecular tunneling ionization theory. The measured angular distributions directly reflect the symmetry of the corresponding molecular orbitals. For higher laser intensities and longer pulse durations, dynamic alignment and post-ionization alignment start to affect the angular distributions and ion fragments are preferentially ejected along the laser-polarization direction.

- Resonant excitation during strong field dissociative ionization

We studied dissociative ionization of oxygen by intense femtosecond laser pulses with central wavelengths between 550 nm and 1800 nm, by measuring kinetic energy release spectra and angular distributions of fragments resulting from symmetric dissociation of doubly charged molecular ions (O₂²⁺ → O⁺ + O⁺ channel). Ability to vary the laser wavelength, utilizing our new optical parametric

amplifier (OPA), is important for elucidating resonant pathways, which are frequency dependent. We identify the dication excited state ($B^3\Pi_g$) whose production depends resonantly on the laser wavelength. This presents unambiguous evidence in support of importance of the resonant excitation channels in strong field ionization of molecules (see Figure 1)

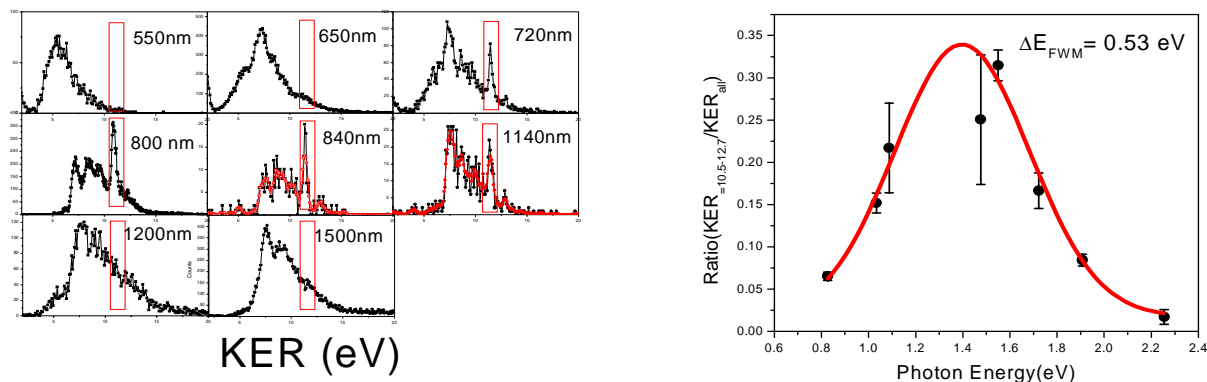


Figure 1. (Left) KER spectra of correlated O^+ fragments for different laser frequencies ($B^3\Pi_g$ state band is highlighted). (Right) Relative yield of $B^3\Pi_g$ dication as function of photon energy.

- Multi-photon resonant effects during single ionization in tunneling regime: Origin of the “dip” in longitudinal momentum distributions

This study addresses the origin of recently observed structures in longitudinal ion recoil momentum distributions for single ionization in tunneling regime. It deals with an issue of more general interest (importance of multi-photon resonances in tunneling ionization) and was done not with molecules but with noble gas atoms (Ne and Ar). Since its recent observation, the origin of the “dip” at zero momentum in longitudinal recoil momentum distributions for Ne^+ (and later for He^+) was a matter of some debate. Originally attributed to electron re-collision, it was also ascribed to influence of Coulomb potential of the ion on outgoing electron trajectories, and to a “discrete photon absorption mechanism in the tunnel regime”. To clarify the issue, we studied ionization of neon and argon by intense linearly polarized femtosecond laser pulses of different wavelengths (400 nm, 800 nm and 1800 nm) and peak intensities, by measuring momentum distributions of singly charged positive ions in the direction parallel to laser polarization. For Ne the momentum distributions exhibited a characteristic dip at zero momentum at 800 nm, a complex multi-peak structure at 400 nm and no structure at 1800 nm. Similarly, for Ar the momentum distributions evolved from complex multi-peak structure (400 nm) to a smooth distribution characteristic of pure tunneling ionization (800 nm high intensities and 1800 nm). In the intermediate regime (800 nm, medium to low intensities), for both molecules we observed recoil ion momentum distributions modulated by quasi-periodic structures usually seen in the photoelectron energy spectra in multi-photon regime (ATI spectra). Based on our results, we conclude that the central minimum, observed in Ne momentum distributions, should not be attributed to effects of electron re-collision, as was suggested earlier, but instead is due to multi-photon contribution to ionization, in agreement with recent interpretation by Faisal and Schlegel.

In the future, we are planning to measure complete 3D electron momentum distributions for single and double ionization of molecules in different ionization regimes. We will also study dependence of molecular ionization on carrier-envelope phase (CAP) of few-cycle pulses, taking advantage of future KLS CAP-stabilization/-determination capabilities.

2) Studying mechanisms and dynamics of laser-induced Coulomb explosion of molecules

A. S. Alnaser, I. Bocharova, D. Ray, C .M. Maharjan, P. Ranitovic, Z. Chang, C. L. Cocke and I.V. Litvinyuk

The purpose of this project is to understand detailed mechanisms and dynamics of Coulomb explosion of multiply charged molecular ions produced by intense ultra-short laser pulses. Our ultimate goal is development of time-resolved Coulomb explosion imaging, which would allow us to directly follow evolving molecular structure in real time. Towards that goal we work on developing and refining laser pump-probe techniques with ultra-short (< 8 fs) pulses. Part of this effort, dealing with H_2/D_2 is covered by C.L. Cocke in his abstract (see his “Two-electron removal from small molecules by short intense laser pulses” and Figure 1). In a similar way we studied Coulomb explosion of highly charged N_2 and O_2 molecular ions using pump-probe technique. We observed ultra-fast dynamics for different dissociation channels of the two molecules. Similar to H_2 , dissociating and oscillating branches are seen in the same experiment. We are planning to extend these studies to tri-atomic (CO_2) and four-atomic (C_2H_2) molecules.

3) Strong-field experiments on dynamically aligned molecules

A. S. Alnaser, I. Bocharova, D. Ray, C .M. Maharjan, P. Ranitovic, Z. Chang, C. L. Cocke and I.V. Litvinyuk

In this project, we take advantage of our ability to control molecular alignment using rotational wavepackets to study field-molecule interactions in molecular frame. Here we also use pump-probe technique. The pump pulse creates a coherent rotational wavepacket. At a proper delay, when molecules are optimally aligned, the probe pulse interrogates them. Depending on parameters of the probe pulse, we could study high harmonic generation, ionization or dissociation of aligned molecules. In this respect, this project is closely related and overlaps with 1) and 2), as the main goal remains to better understand molecular behavior in strong laser field. In one study we measured transverse electron momentum distributions for single ionization of oxygen molecules aligned perpendicularly to the field. We observed that for aligned molecules transverse electron momentum is no longer radially symmetric around the polarization direction, as is the case for atoms and isotropic molecular ensembles. The momentum distribution is narrower in the direction of molecular axis, reflecting the original shape of the tunneling electron wavepacket (see Figure 2). Thus we observe a signature of molecular structure in the ionized electron momentum. In the future, we are planning to measure in detail full 3D electron momentum distributions for oxygen and nitrogen aligned parallel and perpendicular to the laser polarization.

Publications appearing in 2004-2005

1. “*Laser Coulomb explosion imaging of small molecules*” F. Légaré, Kevin F. Lee, I.V. Litvinyuk, P.W. Dooley, S.S. Wesolowski, P.R. Bunker, P. Dombi, F. Krausz, A.D. Bandrauk, D.M. Villeneuve and P.B. Corkum, *Phys. Rev. A* **71**, 013415 (2005)
2. “*Shake-up excitation during intense field tunnel ionization*” I. Litvinyuk, F. Legare, P. W. Dooley, D. M. Villeneuve, P. B. Corkum, J. Zanghellini, A. Pegarkov, C. Fabian, and T. Brabec, *Phys. Rev. Lett.* **94**, 033003 (2005)

3. "Effects of orbital symmetries in dissociative ionization of molecules by few-cycle laser pulses", A.S. Alnaser, C. M. Maharjan, X.-M. Tong, B. Ulrich, P. Ranitovic, B. Shan, Z. Chang, C. D. Lin, C. L. Cocke and I.V. Litvinyuk, Phys. Rev. A 71, 031403R (2005)
4. "Laser-induced interference, focusing, and diffraction of rescattering molecular photoelectrons", S. N. Yurchenko, S. Patchkovskii, I. V. Litvinyuk, P. B. Corkum and G. L. Yudin, Phys. Rev. Lett. 93, 223003 (2004)
5. "Two-pulse alignment of molecules", Kevin F Lee, I. V. Litvinyuk, P. W. Dooley, Michael Spanner, D. M. Villeneuve and P. B. Corkum, J. Phys. B 37, L43-L48 (2004)

Electron momentum distributions

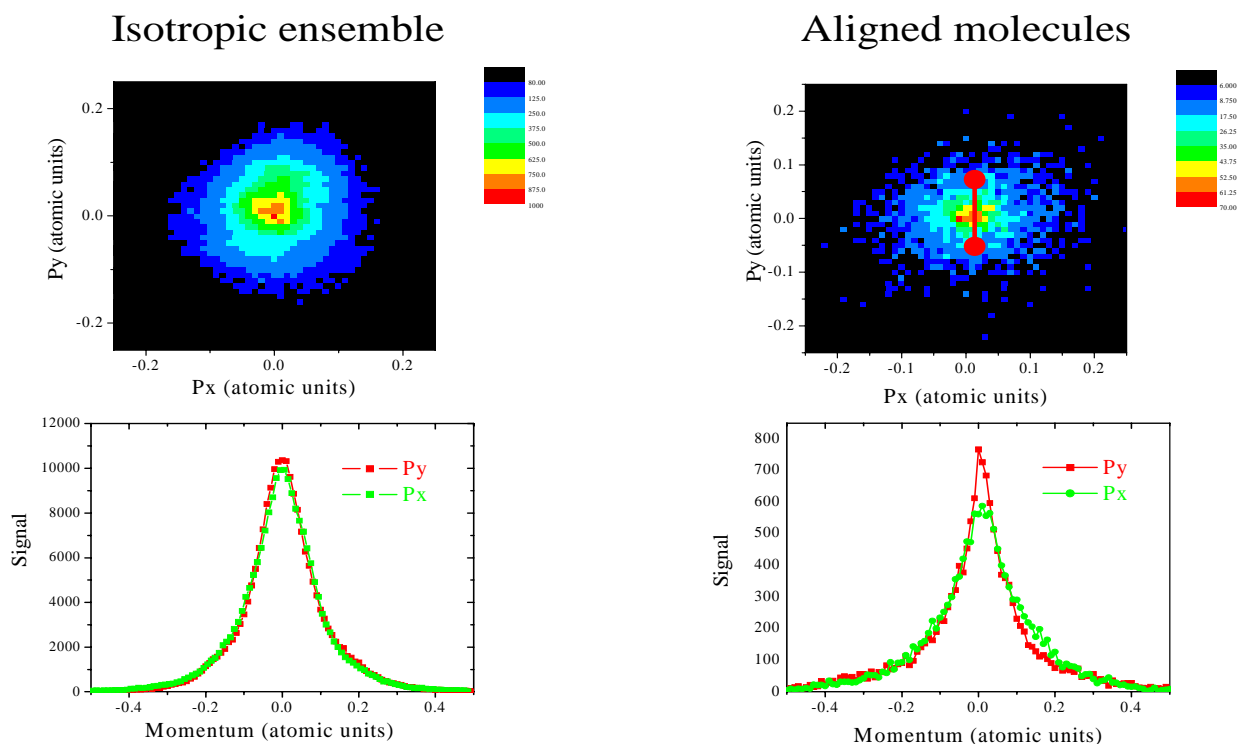


Figure 2. Transverse electron momentum distributions for isotropic (left) and aligned (right) oxygen molecules. Upper panels show 2D electron momentum in the plane perpendicular to laser polarization (alignment axis is indicated). Lower panels present projections of the same distributions on the two axes in the plane.

High Intensity Laser Driven Explosions of Homo-nuclear and Hetero-nuclear Molecular Clusters

Project DE-FG02-03ER15406

Abstract (Summer 2005)

Principal Investigator:

Todd Ditmire

Department of Physics

University of Texas at Austin, MS C1600, Austin, TX 78712

Phone: 512-471-3296

e-mail: tditmire@physics.utexas.edu

Program Scope:

The nature of the interactions between high intensity, ultrafast laser pulses and atomic clusters of a few hundred to a few thousand atoms has come under study by a number of groups world wide. Such studies have found some rather unexpected results, including the striking finding that these interactions appear to be more energetic than interactions with either single atoms or solid density plasmas and that clusters explode with substantial energy when irradiated by an intense laser. It is now well established that the explosions of low-Z molecular clusters such as hydrogen or deuterium clusters explode mainly by a Coulomb explosion. Our program under the last three year cycle studied the interplay between a traditional Coulomb explosion description of the cluster disassembly and a plasma-like hydrodynamic explosion, particularly for small to medium sized clusters (<1000 atoms) and clusters composed of low-Z atoms. In this program we have started to extend these studies, particularly with an eye toward the optimization of cluster explosions for use in a high flux, laser driven neutron source. We are examining the details of the Coulomb explosion of molecular clusters and we are studying the temporal dynamics of the electron ejection and ion expansion through pump probe techniques. We have also started studying in detail the dynamics of explosions of mixed species clusters, such as methane (and deuterated methane) where it is now conjectured that dynamic effects play an important role in the ejection of the lighter ions. We are looking at a number of diagnostics but mainly have been concerned with examining ion energy spectra and fusion neutron yield in deuterated cluster plasmas. In the past year, our experiments have focused primarily on studies of explosions of methane and deuterated methane clusters with the hope of isolating the predicted dynamic acceleration effect expected of the lighter ion species. We have also begun to implement plans to perform experiments on the irradiation of clusters with XUV pulses.

Progress During the Past Year

We have an ongoing campaign to study high intensity laser interactions with exploding clusters (ie intensity $\geq 10^{17}$ W/cm²). During the past year, with support from this BES grant, we have performed two activities in this area: we have studied the explosion of heteronuclear clusters and we have begun the construction of an experiment that will allow us to irradiate clusters with intense short wavelength (100-10 nm) femtosecond pulses generated by the laser. This second activity is in the early construction phases and will be detailed in the report next year. However, we have had good success in study of exploding mixed species clusters. These experiments follow on fusion experiments which we have performed in previous years and are motivated by the desire to find clusters which produce higher energy deuterons (which lead to higher fusion yields).

Our work has been motivated by a series of results published in recent years. Over the last several years, there has been much activity in studying high intensity, ultrashort laser pulse interactions with atomic clusters. The most dramatic consequence of this unique interaction has been the observation of high charge states and very fast ions [1-3]. The ejection of ions with many keV of energy from exploding clusters can

be exploited to drive nuclear fusion [4-7], and we have studied this phenomena quite extensively over the past few years under funding from this grant. In the early stages of the present three year grant period (year 1) we performed initial work with CD_4 clusters in the context of the fusion experiment.

At high enough intensity, particularly in smaller, low- Z clusters, an ultrashort laser pulse can quickly strip the cluster of most of its electrons resulting in a pure Coulomb explosion. The ions expand by mutual repulsion in the fully ionized cluster sphere. In this simple picture, the ion kinetic energies are simply related to their initial potential energy at their equilibrium position in the cluster. This model has been very successful in explaining the ion energies observed in a number of experiments with low to mid- Z clusters [2,8].

When we proposed this grant we asked the question of whether mixed species, heteronuclear clusters like CD_4 , will behave in the same manner as single species clusters under intense ultrafast laser irradiation. Theoretical results suggest that explosions of clusters with mixed atomic species may be more complicated and exhibit some interesting differences [9,10]. The motivation for studying Coulomb explosions of mixed species clusters has been advanced recently through molecular dynamic simulations by Last and Jortner which indicate that the energies of lighter deuterons from exploding heteronuclear clusters, like D_2O or CD_4 , could be increased through a dynamical effect [9,10]. In general, if the kinematic parameter for species $A = q_A m_B / q_B m_A$, is greater than 1 (where q and m are the charge and mass of the light ion A and heavy ion B), then the light ions will outrun the heavier ions, exploding in an outer shell with a higher average energy beyond what would be expected from the naïve estimate of ion energy based on initial potential energy as in the simple Coulomb explosion picture.

In our work this year, we performed an experimental confirmation of this dynamic enhancement of light ion energies from exploding heteronuclear clusters using methane (CH_4) and fully deuterated methane (CD_4). At the intensities used here ($\geq 10^{17} \text{W/cm}^2$) the C atoms in the cluster can be stripped to $4+$ [10]. In this case $A = 1.5$ for CD_4 clusters whereas $A = 3$ for CH_4 . Considering only the initial potential energy, the deuterons and protons from the same sized CH_4 and CD_4 clusters would acquire the same explosion energy upon irradiation. However, if the predicted kinematic enhancement of the light ion energies occurs, then the effect should be stronger in the case of CH_4 compared to CD_4 and be detectable through a study of these two molecular clusters under identical cluster formation and irradiation conditions. By comparing ion energy spectra we indeed observe a clear enhancement in the explosion energy of protons compared to deuterons.

In our experiment, pictured in figure 1, a pulsed supersonic gas jet directed through a skimmer produced a low density cluster beam. The energies of the ions created by the laser cluster interaction were determined by measuring the time of flight (TOF) of the ions in a field free drift tube. A microchannel plate (MCP) detected ions in a small angular cone from the focus. In our experiments we estimate that the mean CH_4 cluster size is 3 nm. To irradiate the clusters we utilized the THOR laser at UT which delivers pulses with duration 35 fs and energy up to 700 mJ, though only 50 mJ were utilized in these experiments. The laser was focused using an $f/4.9$ refractive graded index yielding intensity of $\sim 3 \times 10^{17} \text{W/cm}^2$.

This year we have also performed a series of particle simulations to elucidate the physics in our experiment. Simulations of the dynamics of a driven electron cloud inside a cluster suggest that a cluster will be fully stripped of electrons by the laser field, if the ponderomotive potential is comparable to or larger than the surface potential of the charged cluster.

Figure 2 shows kinetic energy spectra at different laser intensities, normalized using the original TOF traces, comparing CH_4 and CD_4 data. The low energy components of the spectra are not shown so the curves do not intersect. The energy ranges that we attribute solely to the lighter ion species are marked with dotted lines. Clearly the hydrogen energies always exceed the measured deuterium energies in the range presented here. This appears to confirm the validity of the theory predicting kinetic energy enhancement. Unexpected is the increase of maximum ion energy with laser intensity since a pure Coulomb explosion is driven solely by ion repulsion forces and the laser conditions beyond the saturation intensity are irrelevant. This behavior could also be a consequence of a cluster size distribution since at the lower intensities the

larger clusters may not be fully stripped of their electrons. We are investigating this anomaly presently and hope to derive some information about these dynamics through a set of pump probe experiments we are beginning this year.

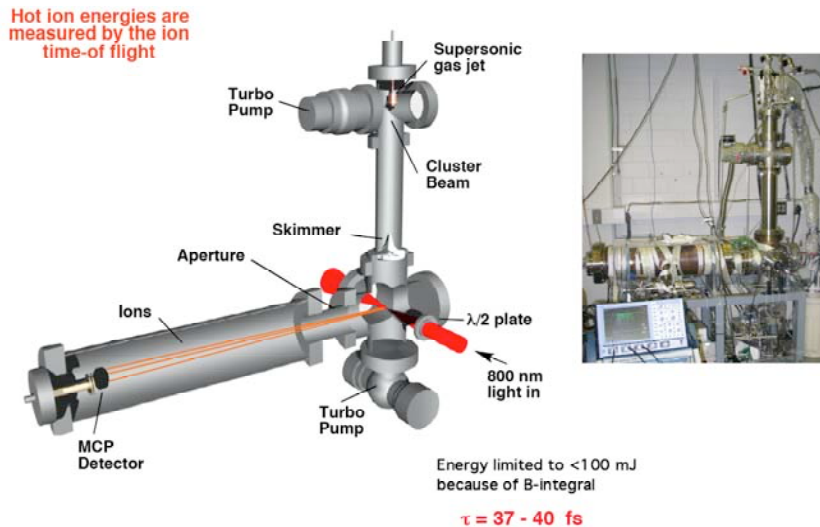


Figure 1: Carton illustrating our Time of Flight apparatus on the THOR laser at UT. A picture of this chamber is at the right.

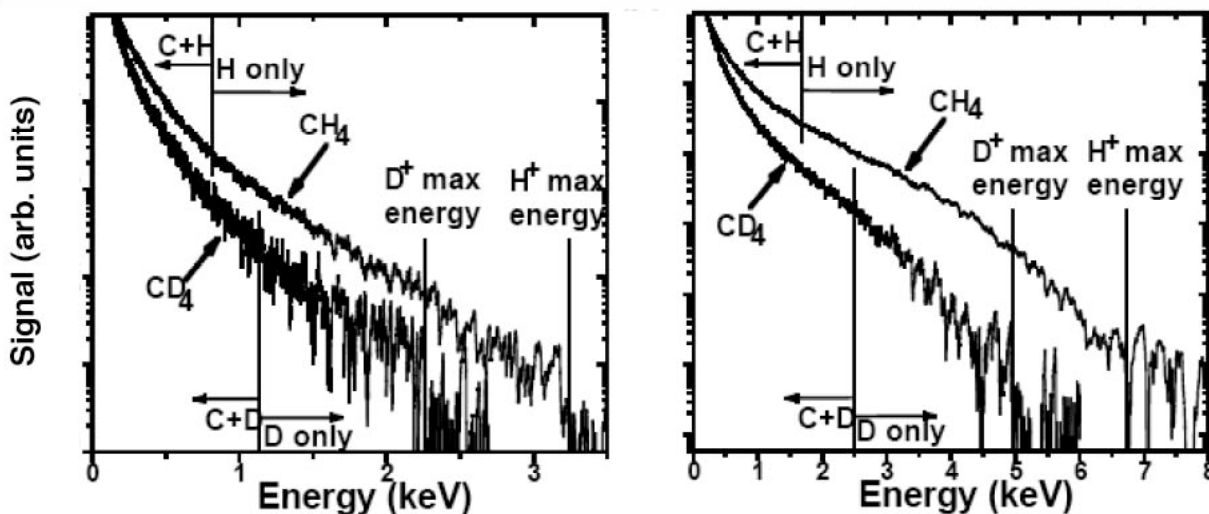


Figure 2: Energy spectra from CH_4 and CD_4 clusters at a laser intensity of (left) $1.2 \times 10^{17} \text{ W/cm}^2$ and (right) $3.2 \times 10^{17} \text{ W/cm}^2$. Dotted lines indicate the regions where the signals are assumed to be solely due to the light ion species, H^+ or D^+ .

Future Research Plans

Our future plans are oriented along two principal directions

1) Continue fusion neutron yield measurements in exploding CD₄ clusters. In particular, we would like to examine, and manipulate the effects of laser propagation effects in the gas jet on the plasma production and ultimate neutron production. One idea that we will explore will be to use the second, compressed beam to “clean away” absorbing cluster gas in the leading edge of the gas jet. This should allow us to penetrate more deeply into the jet and reach higher density, where we expect a high fusion rate and higher yield.

2) Begin studies of XUV pulse interactions with clusters. During this year we have begun construction of a separate beamline and chamber on the THOR laser which will allow us to generate high order harmonics with the full 0.7 J of laser energy and focus these harmonics into a cluster jet with an XUV mirror. The beamline will be completed in one month (Sept.) and we will focus pulses of up to 1 μJ of energy in the 40 – 15 nm range into a low density jet of clusters. We have arranged this to allow studies both with rare gas clusters and metal clusters. This will allow us to tune the excitation wavelength to near the giant dipole resonance of the cluster microplasma. Such experiments will lead the way to future experiments on the LCLS.

References for Abstract

1. T. Ditmire *et al.*, Nature (London) **386**, 54-56 (1997).
2. M. Lezius *et al.*, Phys. Rev. Lett. **80**, 261-264 (1998).
3. V. Kumarappan, M. Krishnamurthy, and D. Mathur, Phys. Rev. Lett. **87**, 085005 (2001).
4. T. Ditmire *et al.* Nature (London) **398**, 489-492 (1999).
5. J. Zweiback *et al.*, Phys. Plasmas **9**, 3108-3120 (2002).
6. G. Grillon *et al.*, Phys. Rev. Lett. **89**, 065005 (2002).
7. K. W. Madison *et al.*, Phys. Plasmas **11**, 270-277 (2004).
8. S. Sakabe *et al.*, Phys. Rev. A **69**, 023203 (2004).
9. I. Last and J. Jortner, Phys. Rev. Lett. **87**, 033401 (2001).
10. I. Last and J. Jortner, J. Phys. Chem. A. **106**, 10877-10885 (2002).

Papers published on work supported by this grant and the preceding grant (2002-2005):

- *1) M. Hohenberger, D. R. Symes, K. W. Madison, A. Sumeruk, and T. Ditmire, “Dynamic Acceleration Effects in Explosions of Laser Irradiated Heteronuclear Clusters”, *Phys. Rev. Lett.* Submitted.
- 2) F. Buergens, K. W. Madison, D. R. Symes, R. Hartke, J. Osterhoff, W. Grigsby, G. Dyer and T. Ditmire, “Angular distribution of neutrons from deuterated cluster explosions driven by fs-laser pulses”, *Phys. Rev. E*, Submitted
- 3) R. Hartke, D. R. Symes, F. Buergens, L. Ruggles, J. L. Porter, T. Ditmire, “Neutron Detector Calibration using a table-top laser heated plasma neutron source” *Nuc. Inst. And Methods A* **540**, 464 (2005).
- 4) K. W. Madison, R. Fitzpatrick, P. K. Patel, D. Price, T. Ditmire, “The role of laser pulse duration in Coulomb explosions of deuterium cluster targets” *Phys. Rev. A* **70**, 053201 (2004).
- 5) K. W. Madison, P. K. Patel, D. Price, A. Edens, M. Allen, T. E. Cowan, J. Zweiback, and T. Ditmire, “Fusion neutron and ion emission from laser induced explosions of deuterium and deuterated methane clusters” *Phys. Plas.* **11**, 270 (2004).
- 6) T. Ditmire, S. Bless, G. Dyer, A. Edens, W. Grigsby, G. Hays, K. Madison, A. Maltsev, J. Colvin, M. J. Edwards, R. W. Lee, P. Patel, D. Price, B. A. Remington, R. Sheppherd, A. Wootton, J. Zweiback, E. Liang and K. A. Kiely, “Overview of future directions in high energy-density and high-field science using ultra-intense lasers” *Rad. Phys. And Chem.* **70**, 535 (2004).
- 7) K. W. Madison, P. K. Patel, M. Allen, D. Price, T. Ditmire, “An investigation of fusion yield from exploding deuterium cluster plasmas produced by 100 TW laser pulses” *J. Opt. Soc. Am. B* **20**, 113 (2003).
- 8) J. W. G. Tisch, N. Hay, K. J. Mendham, E. Springate, D. R. Symes, A. J. Comley, M. B. Mason, E. T. Gumbrell, T. Ditmire, R. A. Smith, J. P. Marangos, M. H. R. Hutchinson, “Interaction of intense laser pulses with atomic clusters: Measurements of ion emission, simulations and applications” *Nuc. Inst. Meth. B – Beam Interacts with Materials and Atoms* **205**, 310 (2003).
- 9) J. Zweiback, T.E. Cowan, R. A. Smith, J. H. Hartley, R. Howell, G. Hays, K. B. Wharton, J. K. Crane, V. P. Yanovsky and T. Ditmire “Detailed Study of Nuclear Fusion From Femtosecond Laser-Driven Explosions of Deuterium Clusters” *Phys. Plas.* **9**, 3108 (2002).

Molecular Structure and Electron-Driven Dissociation and Ionization

Kurt H. Becker and Vladimir Tarnovsky

Department of Physics and Engineering Physics and Center for Environmental Systems,
Stevens Institute of Technology, Hoboken, NJ 07030
phone: (201) 216-5671; fax: (201) 216-5638; kbecker@stevens.edu

Program Scope:

This program is aimed at investigating the molecular structure and the collisional dissociation and ionization of selected molecules and free radicals. The focus areas are (1) ionization studies of selected molecules and free radicals and (2) the study of electron-impact induced neutral molecular dissociation processes. Targets of choice for ionization studies include WF_6 , SiCl_4 and BCl_3 and their radicals, the molecular halogens Cl_2 , Br_2 , and F_2 and the radicals SF , SF_2 , and SF_4 . Targets of choice for the neutral molecular dissociation studies include SiCl_4 , BCl_3 , NO_2 , and N_2O . The fragments to be probed include $\text{Si}(^1\text{S})$, $\text{Si}(^1\text{D})$, $\text{Si}(^3\text{P})$, $\text{BCl}(X\ ^1\Sigma)$, $\text{B}(^2\text{P}^0)$, and $\text{NO}(X\ ^2\Pi)$. This choice is motivated on one hand by the relevance of these species in specific technological applications involving low-temperature processing plasmas and, on the other hand, by basic collision physics aspects (WF_6 is similar in its structure to SF_6 , SiCl_x and BCl_x are similar to TiCl_x and SiF_x).

The scientific objectives of the research program can be summarized as follows:

- (1) to provide the atomic and molecular data that are required in efforts to understand the properties of low-temperature processing plasmas on a microscopic scale
- (2) to identify the key species that determine the dominant plasma chemical reaction pathways
- (3) to measure cross sections and reaction rates for the formation of these key species and to attempt to deduce predictive scaling laws
- (4) to establish a broad collisional and spectroscopic data base which serves as input to modeling codes and CAD tools for the description and modeling of existing processes and reactors and for the development and design of novel processes and reactors
- (5) to provide data that are necessary to develop novel plasma diagnostics tools and to analyze more quantitatively the data provided by existing diagnostics techniques

Specific Recent Progress:

SF₃⁺ Ionization Cross Section Shape: While most partial ionization cross sections for the formation of positive fragment ions from SF_6 exhibit the smooth energy dependence, which is typical for ionization cross section curves, the SF_3^+ partial ionization cross section function displays a pronounced structure around 40 eV. This structure might indicate that several processes with different threshold energies contribute to the measured SF_3^+ partial ionization cross section. We carried out a detailed study of the formation of SF_3^+ fragment ions produced by electron impact on SF_6 using the mass-analyzed ion kinetic energy (MIKE) scan technique. The use of this technique allowed us to identify a contribution to the measured SF_3^+ signal arising from the Coloumb explosion of doubly positively charged SF_4^{2+} ions into two singly charged ions, SF_3^+ and F^+ , with a threshold energy of about 43 eV. The direct dissociative ionization of SF_6 leading to the formation of SF_3^+ fragment ions has a threshold of about 22 eV.

Ionization of Cl₂: We measured absolute partial cross sections for the formation of Cl_2^+ , Cl_2^{++} , Cl^+ , and Cl^{++} ions following electron impact on molecular chlorine (Cl_2) from threshold to 900 eV using a time-of-flight mass spectrometer. The ion spectrum at all impact energies is

dominated by the singly charged fragment ions with maximum cross section values of $4.6 \times 10^{-16} \text{ cm}^2$ for Cl_2^+ at 32 eV and $4.0 \times 10^{-16} \text{ cm}^2$ for Cl^+ at 70 eV. The cross sections for the formation of the doubly charged ions are more than one order of magnitude lower. Double ionization processes account for about 6% of the total ion yield at 70 eV. The absolute total ionization cross section of Cl_2 was obtained as the sum of all measured partial ionization cross sections.

Ionization of Uracil: Even though we did not propose to study any biologically important molecules in our original proposal, we seized the opportunity to carry out a measurement of partial cross sections for the formation of selected positive and negative ions resulting from electron interactions with the RNA base uracil ($\text{C}_4\text{H}_4\text{N}_2\text{O}_2$) and put them on an absolute scale. Absolute calibration of the measured partial cross sections for the formation of the three most intense positive ions, the parent $\text{C}_4\text{H}_4\text{N}_2\text{O}_2^+$ ion and the $\text{C}_3\text{H}_3\text{NO}^+$ and OCN^+ fragment ions, was achieved by normalization of the total single uracil ionization cross section (obtained as the sum of all measured partial single ionization cross sections) to a calculated cross section based on the semi-classical Deutsch-Märk (DM) formalism at 100 eV. Subsequently, we used the OCN^+ cross section in conjunction with the known sensitivity ratio for positive and negative ion detection in our apparatus (obtained from the well-known cross sections for SF_4^+ and SF_4^- formation from SF_6) to determine the dissociative attachment cross section for OCN^- formation from uracil. This cross section was found to be roughly an order of magnitude smaller, about $5 \times 10^{-22} \text{ m}^2$ at 6.5 eV, compared to previously reported preliminary value. We attribute this discrepancy to the difficult determination of the uracil target density in the earlier work. Using a reliably calculated cross section for normalization purposes avoids this complication.

Ionization of SiCl_4 : SiCl_4 has a similar structure to fluorinated and hydrogenated targets that we studied in the past (SiF_4 , SiH_4). No ionization cross section data are available for the molecule. Perhaps most importantly, the SiCl_4 molecule is a candidate for electron-impact ionization studies on thin deposited SiCl_4 films (T. Orlando, private communication, 2002). This affords a unique opportunity to explore how the ionization properties of a molecule change from the gas phase to the condensed phase. We measured absolute partial cross sections for the formation of the SiCl_x^+ ($x=1-4$), Si^+ , and Cl^+ singly charged as well as the SiCl_x^{++} ($x=1-4$) and Si^{++} doubly charged positive ions following electron impact on SiCl_4 . Dissociative ionization was found to be the dominant process. The SiCl_3^+ fragment ion has the largest partial ionization cross section with a maximum value of slightly above $6 \times 10^{-20} \text{ m}^2$ at about 100 eV. The cross sections for the formation of SiCl_4^+ , SiCl^+ , and Cl^+ have maximum values around $4 \times 10^{-20} \text{ m}^2$. Some of the cross section curves exhibit an unusual energy dependence with a pronounced low-energy maximum at an energy around 30 eV followed by a broad second maximum at around 100 eV. This is similar to what has been observed earlier for other Cl-containing molecules of similar structure (TiCl_4 and CCl_4) as well as for the Cl_2^+ partial ionization cross section from Cl_2 . The structure is most likely due to the presence of indirect ionization channels that compete with direct ionization. The maximum cross section values for the formation of the doubly charged ions, with the exception of SiCl_3^{++} , are $0.05 \times 10^{-20} \text{ m}^2$ or less. The experimentally determined total single ionization cross section of SiCl_4 is compared with results of semi-empirical calculations and good agreement is found in terms of the absolute cross section value, but minor discrepancies exist in the cross section shape.

Ionization Cross Section Calculations. All experimental ionization studies were also supported by our continuing effort to extend and refine our semi-classical approach to the calculation of total single ionisation cross sections for molecules and free radicals. In particular, we have now incorporated the correct “quantum mechanical $\ln(E)/E$ high-energy dependence into the DM

formalism. We now have a level of agreement between calculation and experiment of better than 20% (often better than 10%). This level of agreement gives us confidence as to the predictive capabilities of our approach for molecules for which no experimental data are available.

Neutral Molecular Dissociation Studies. We completed the cross-comparison of neutral dissociation cross sections for SiH₄, SiF₄, and several Si-organic compounds (TMS, HMDSO, TEOS) with particular emphasis on the determination of final-state specific cross sections for the formation of Si(¹S) and Si(¹D) atoms. In the case of the formation of Si(¹S) atoms from SiH₄ and SiF₄ we found cross sections of about $5 \times 10^{-17} \text{ cm}^2$ (SiH₄) and $2.8 \times 10^{-17} \text{ cm}^2$ (SiF₄) at 60 eV. The Si(¹S) cross sections from SiH₄ and SiF₄ have distinctly different energy dependences.

Ongoing studies and future work - Ionization

SiCl_x Radicals: We are in the process of carrying out a comprehensive series of absolute partial ionization cross section measurements for the SiCl_x (x=1-3) radicals using our fast-beam apparatus. The experimental results will be complemented by semi-classical calculations of the total single ionization cross sections.

Ionization of other Organic and Biologically Relevant Molecules: Polycyclic aromatic hydrocarbons (PAHs) are important in environmental applications because of their toxicity in conjunction with their appearance as by-products in the combustion of organics. Two PAH compounds, coronene (C₂₄H₁₂) and corannulene (C₂₀H₁₀) are of special interest. They represent prototypical bowl-shaped (corannulene) and planar PAHs (coronene) structures. Coronene, a very stable compound, consists of 7 benzene rings. Corannulene has a curved-surface structure and is often referred to as a “buckybowl” molecule as it represent the “polar cap” or 1/3 of a C₆₀ fullerene or “buckeyball” molecule. Nevertheless, there remains a rather large uncertainty in the ionization energies that have been reported for these two prototypical PAH compounds. We are in the process of measuring the ionization energies of singly and multiply charged ions produced by electron ionization of coronene and corannulene under controlled experimental conditions.

BCl₃ and the BCl_x Radicals: There is some information in the literature on the formation of positive and negative ions formed by electron impact on BCl₃ and on the spectroscopy of BCl₃ and the BCl free radical, which is widely used in optical diagnostics studies of BCl₃-containing plasmas. There have also been some recent calculations of electron collisions with BCl₃. We are in the process of measuring a complete set of absolute partial ionization cross sections for BCl₃ and for the BCl radical with special emphasis on the low-energy, near-threshold region using the fast-beam technique. Based on some preliminary studies we will be using pure BCl₃ or a defined mixture of BCl₃ and Ar to produce the primary ions.

Ionization cross section calculations: Specific emphasis for the cross section calculations is on targets such as positive molecular ions (e.g. C₂H₂⁺), Na Rydberg atoms, and the lanthanides.

Ongoing studies and future work – Neutral Dissociation

SiCl₄: This molecule is a natural choice as a target for the neutral dissociation studies leading to final-state specific Si cross sections as it extends the sequence of SiH₄ and SiF₄ to the chlorine-containing compound. Moreover, similar to SiH₄ and SiF₄, we also measure ionization and dissociative ionization cross sections for SiCl₄, so that this becomes another molecule for which we will have a broad data base of collisional data on ionization and dissociation.

The work on SiCl₄ will conclude our neutral dissociation work using the apparatus described above. Persistent problems with the laser render it ineffective to devote further resources (students, funds) to this effort at the present time

Publications Acknowledging DOE Support (since 2003)

1. H. Deutsch, K. Becker, P. Defrance, U. Onthong, M. Probst, S. Matt, P. Scheier, and T.D. Märk, "Calculated Absolute Cross Sections for the Electron-Impact Ionization of Simple Molecular Ions", *Int. J. Mass Spectrom.* 223/224, 639-45 (2003)
2. R. Basner, M. Schmidt, and K. Becker, "Absolute Total and Partial Electron-Impact Ionization Cross Sections for B₂H₆", *J. Chem. Phys.* 118, 2153 (2003)
3. H. Deutsch, P. Scheier, K. Becker, and T.D. Märk, "Revised High-Energy Behavior of the DM Formula for the Calculation of Electron Impact Ionization Cross Sections of Atoms", *Int. J. Mass Spectrom.* 233, 13-7 (2004)
4. H. Deutsch, P. Scheier, K. Becker, and T.D. Märk, "Calculated Cross Sections for the Electron-Impact Detachment from Negative Ions Using the DM Formalism", *Chem. Phys. Lett.* 382, 26-31 (2003)
5. R. Basner, M. Schmidt, and K. Becker, "Measurement of Absolute Partial and Total Electron Ionization Cross Sections of Tungsten Hexafluoride", *Int. J. Mass Spectrom.* 233, 25-31 (2004)
6. W.Huo, V. Tarnovsky, and K. Becker, "Electron Impact Ionization Cross Sections of SF₅ and SF₃", *Int. J. Mass Spectrom.* 233, 111-6 (2004)
7. S. Feil, K. Gluch, P. Scheier, K. Becker, and T.D. Märk, "The Anomalous Shape of the Cross Section for the Formation of SF₃⁺ Fragment Ions Produced by Electron Impact on SF₆ Revisited", *J. Chem. Phys.* 120, 11465-8 (2004)
8. H. Deutsch, , K. Becker, A.N. Grum-Grzhimailo, K. Bartschat, H. Summers, M. Probst, S. Matt-Leubner, and T.D. Märk, "Calculated Cross Sections for the Electron Impact Ionization of Excited Ar Atoms Using the DM Formalism, *Int. J. Mass Spectrom.* 233, 39-43 (2004)
9. S. Feil, K. Gluch, S. Matt-Leubner, P. Scheier, J. Limtrakul, M. Probst. H. Deutsch, A. Stamatovic, K. Becker, and T.D. Märk,, "Absolute Partial and Total Cross Sections for Positive and Negative Ion Formation Following Electron Impact on Uracil", *J. Phys. B* 37, 3013-20 (2004)
10. B.C. Garrett, D.A. Dixon, D.M. Camaioni, D. M. Chipman, M.A. Johnson, C.D. Jonah, G.A. Kimmel, J.H. Miller, T. N. Rescigno, P. J. Rossky, S.S. Xantheas, S.D. Colson, A.H. Laufer, D. Ray, P.F. Barbara, D. M. Bartels, K.H. Becker, K.H. Bowen. S.E. Bradford, I. Carmichael, J.V. Coe, L.E. Corrales, J.P. Cowin, M. Dupuis, K.B. Eisenthal, J.A. Franz, M.S. Gutowski, K.D. Jordan, B.D. Kay, J.A. LaVerne, S. V. Lymar, T. E. Madey, C.W. McCurdy, D. Meisel, S. Mukamel, A.R. Nilsson, T.M. Orlando N. G.Petrik, S. M. Pimblott, J. R. Rustad, G. K. Schenter, S. J. Singer, A.Tokmakoff, L.-W. Wang C. Wittig, and T.S. Zwier, "The Role of Water on Electron-Initiated Processes and Radical Chemistry: Issues and Scientific Advances, *Chem. Reviews* 105, 355-89 (2005),
11. S. Matt-Leubner, S. Feil, K. Gluch, J. Fedor, A. Stamatovic, O. Echt, P. Scheier, K. Becker, and T.D. Märk "Energetics, Kinetics, and Dynamics of Decaying Metastable Ions Studied with a High Resolution Three-Sector-Field Mass Spectrometer", *Plasma Sources Sci. Techn.* 14, 26-30 (2005)
12. H. Deutsch, P. Scheier, S. Matt-Leubner, K. Becker, and T.D. Märk "A Detailed Comparison of Calculated and Measured Electron-Impact Ionization Cross Sections of Atoms Using the Deutsch-Märk (DM) Formalism", *Int. J. Mass Spectrom.* 243, 215-21 (2005)
13. H. Deutsch, K. Becker, A.N. Grum-Grzhimailo, M. Probst, S. Matt-Leubner, and T.D. Märk, "Calculated Electron Impact Ionization Cross Sections of Excited Ne Atoms Using the DM Formalism", *Contr. Plasma Phys.* (2005), in press,
14. K. Becker and V. Tarnovsky, "Electron Impact Ionization of Molecules and Free Radicals", "Atomic and Plasma-Material Interaction Data for Fusion (APID), IAEA Reports (2005), in press
15. K. Becker, N. Masoud, K. Martus, and K.H. Schoenbach, "Electron-Driven Processes in High-Pressure Plasmas", *Europ. Phys. J. D* (2005), in press, Invited Topical Review
16. R. Basner, M. Gutkin, J. Mahoney, V. Tarnovsky, H. Deutsch, and K. Becker, "Electron Impact Ionization of Silicon Tetrachloride", *J. Chem. Phys.* (2005), in press

Electron-Atom and Electron-Molecule Collision Processes

C. W. McCurdy and T. N. Rescigno

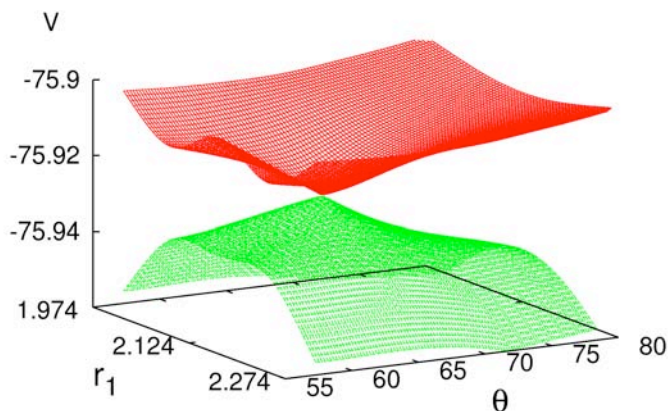
Chemical Sciences, Lawrence Berkeley National Laboratory, Berkeley, CA 94720
cwmccurdy@lbl.gov, tnrescigno@lbl.gov

Program Scope: This project seeks to develop theoretical and computational methods for treating electron collision processes that are important in electron-driven chemistry and physics and that are currently beyond the grasp of first principles methods, either because of the complexity of the targets or the intrinsic complexity of the processes themselves. New methods are being developed and applied for treating low-energy electron collisions with polyatomic molecules and clusters. A state-of-the-art approach is used to treat multidimensional nuclear dynamics in polyatomic systems during resonant electron collisions and predict channeling of electronic energy into vibrational excitation and dissociation. A second focus is the development of new methods for solving multiple photoionization and electron-impact ionization of atoms and molecules. Preliminary results on molecular double photoionization and novel methods promise a complete treatment of recent experiments at the ALS on multiple ionization of oriented molecules.

Recent Progress and Future Plans: We report progress in three distinct areas covered under this project, namely electron-polyatomic molecule collisions, double photoionization and electron impact ionization.

1. Electron-Molecule Collisions

We have continued our work on dissociative electron attachment (DEA) to water. Low-energy dissociative attachment in water proceeds via formation of negative ion, Feshbach resonances and is governed by complex nuclear and electronic resonance dynamics. The first phase of our study, DEA through the 2B_1 resonance, has been completed. To complete our benchmark study of this system, we are examining DEA through the 2A_1 and 2B_2 resonances. The topology of the water anion surfaces, which we have detailed in paper that will soon appear in *Phys. Rev. A*, is complicated. In linear geometry, the 2B_1 and 2A_1 states become degenerate and are strongly coupled by Renner-Teller effects. There is also a conical intersection between the 2A_1 and 2B_2 surfaces which significantly influences the dynamics that leads to production of O^- . In 2B_2 symmetry, we find avoided crossings between the Feshbach resonance and a broader shape resonance of the same symmetry, as well as additional crossings in 2B_1 and 2A_1 symmetry in the exit wells of their potential surfaces associated with charge transfer between the H^- and O^- channels. The final series of wavepacket calculations that will determine the DEA cross sections and branching ratios will require a diabaticization of the complex 2A_1 and 2B_2 surfaces along the conical intersection and the inclusion of Renner-Teller coupling between the 2B_1 and 2A_1 surfaces in the resonance nuclear dynamics. This benchmark study of DEA will be the first to treat, from first principles, all aspects of an electron polyatomic collision, including not only the determination of the fixed-nuclei electronic cross sections, but also a treatment of the nuclear dynamics in full dimensionality.



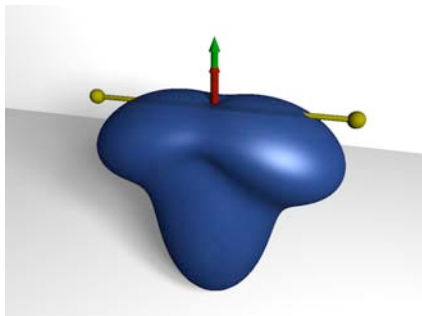
A conical intersection between the 2A_1 and 2B_2 surfaces of the water anion lies on a line close to the plane of C_{2v} symmetry and strongly influences the dynamics of O^- production.

Our initial study of the dynamics of resonant vibrational excitation of NO, which used the complex Kohn method to characterize the resonance curves along with a local complex potential model for the nuclear dynamics, has been extended to include non-local effects in the excitation dynamics, which are critically important near threshold, and to predict cross sections for dissociative electron attachment. This work, carried out in collaboration with Prof. A.E. Orel of UC Davis, gave vibrational excitation cross sections in excellent agreement with the most recent experiments and was recently published in Phys. Rev. A. We have extended this approach to carry out a similar study of resonant excitation of the CF radical, which is produced in the plasma excitation of C_2F_4 . This work, which will be submitted to Phys. Rev. A, has revealed serious inconsistencies in the only other theoretical study of the this problem to date.

2. Double Photoionization

We have successfully applied the exterior complex scaling (ECS) method, which has formed the basis of our approach to collision problems involving two or more unbound electrons in the final state, to carry out the first fully *ab initio* non-perturbative study of double photoionization of a molecular target, namely H_2 . Our initial efforts, which use complex-scaled B-splines and single-center expansions, have produced the total *and* single differential cross sections for randomly oriented molecules and were published as a Rapid Communication in Phys Rev A. We have now extended this work to include a full study of the triply differential double ionization cross sections for oriented H_2 molecules, with a view towards providing a complete analysis of the COLTRIMS experiments which were performed at the ALS and reported in Phys. Rev. Letters and Nature in 2004.

Currently under development is a modification of the single-center approach which will replace the B-splines with a more efficient discrete variable representation (DVR). While this approach will make it easier to obtain fully converged results for the double photoionization of D_2 or H_2 , it would be difficult to generalize to heavier systems, since single-center expansions are known to converge slowly when the nuclear charges are greater than one. We are therefore also working on a hybrid approach that combines the use of molecular Gaussian basis sets with finite-element/DVR grid-based methods and ECS. Such an approach avoids the use of single-center expansions, simplifies the computation of two-electron integrals and will pave the way for studies of double photoionization of more complex molecules.



Triple differential cross section for double photoionization of aligned H₂. One ejected electron, with 90% of the available energy, is fixed along the polarization direction (green arrow), which is perpendicular to the molecular axis (yellow figure). Figure shows the distribution of probability for the second ejected electron.

3. Electron-Impact Ionization

With a powerful approach combining the finite element method with the discrete variable representation (FEM-DVR) and ECS, we have made major progress on breakup problems with three active electrons: We have studied electron impact ionization of helium in the S-wave model using a time-dependent version of the FEM-DVR approach. This work, published in *Phys. Rev. A*, was the first *ab initio* study of a true Coulomb 4-body problem that did not invoke a frozen-core model for the target atom. We also published the first *non-perturbative* study of excitation-autoionization (exciting an autoionizing state by electron impact) and showed the signature it leaves on the singly differential ionization cross section. The results have been published as a Rapid Communication in *Phys. Rev. A*. These studies demonstrate the viability of the ECS approach to problems with 3 active electrons. A complete solution to the electron-helium problem, beyond the S-wave model, would couple individual 3-D angular momentum channels in an iterative approach that is now within the reach of supercomputers.

Publications (2003-2005):

1. T. N. Rescigno and C. W. McCurdy, "Collisional Breakup in Coulomb Systems", in *Many-Particle Quantum Dynamics in Atoms and Molecules*, edited by V. Shevelko and J. Ullrich (Springer-Verlag, Heidelberg, 2003).
2. C. W. McCurdy, W. A. Isaacs, H.-D. Meyer and T. N. Rescigno, "Resonant Vibrational Excitation of CO₂ by Electron Impact: Nuclear Dynamics on the Coupled Components of the $^2\Pi_u$ resonance", *Phys. Rev. A* **67**, 042708 (2003).
3. T. N. Rescigno, M. Baertschy and C. W. McCurdy, "Resolution of phase ambiguities in electron-impact ionization amplitudes", *Phys. Rev. A* **68**, 020701 (R) (2003).
4. C. Trevisan, A. E. Orel and T. N. Rescigno, "Ab Initio Study of Low-Energy Electron Collisions with Ethylene", *Phys. Rev. A* **68**, 062707 (2003)
5. W. Vanroose, C. W. McCurdy and T. N. Rescigno, "Scattering of Slow Electrons by Polar Molecules: Application of Effective-Range Potential Theory to HCl", *Phys. Rev. A* **68**, 052713 (2003)
6. W. Vanroose, Z. Zhang, C. W. McCurdy and T. N. Rescigno, "Threshold Vibrational Excitation of CO₂ by Slow Electrons", *Phys. Rev. Letts.* **92**, 053201 (2004).

7. C. W. McCurdy and F. Martin, “Implementation of Exterior Complex Scaling in B-Splines to Solve Atomic and Molecular Collision Problems”, *J. Phys. B* **37**, 917 (2004).
8. C. W. McCurdy, D. A. Horner, T. N. Rescigno and F. Martin, “Theoretical Treatment of Double Photoionization of Helium Using a B-spline Implementation of Exterior Complex Scaling”, *Phys. Rev. A* **69**, 032707 (2004).
9. Z. Zhang, W. Vanroose, C. W. McCurdy, A. E. Orel and T. N. Rescigno, “Low-energy Electron Scattering by NO: Ab Initio Analysis of the $^3\Sigma^-$, $^1\Delta$ and $^1\Sigma^+$ shape resonances in the local complex potential model”, *Phys. Rev. A* **69**, 062711 (2004).
10. D. J. Haxton, Z. Zhang, C. W. McCurdy and T. N. Rescigno, “Complex Potential Surface for the 2B_1 Metastable State of the Water Anion”, *Phys. Rev. A* **69**, 062713 (2004).
11. D. J. Haxton, Z. Zhang, H.-D. Meyer, T. N. Rescigno and C. W. McCurdy, “Dynamics of Dissociative Attachment of Electrons to Water Through the 2B_1 Metastable State of the Anion”, *Phys. Rev. A* **69**, 062714 (2004).
12. C. S. Trevisan, A. E. Orel and T. N. Rescigno, “Ab initio study of Low-Energy Electron Collisions with tetrafluoroethene, C₂F₄”, *Phys. Rev. A* **70**, 012704 (2004).
13. C. W. McCurdy, M. Baertschy and T. N. Rescigno, “Solving the Three-Body Coulomb Breakup Problem Using Exterior Complex Scaling”, *J. Phys. B* **37**, R137 (2004).
14. D. A. Horner, J. Colgan, F. Martin, C. W. McCurdy, M. S. Pindzola and T. N. Rescigno, “Symmetrized Complex Amplitudes for He Double Photoionization from the Time-Dependent Close Coupling and Exterior Complex Scaling Methods”, *Phys. Rev. A* **70**, 064701 (2004).
15. D. A. Horner, C. W. McCurdy and T. N. Rescigno, “Electron-Helium Scattering in the S-wave Model Using Exterior Complex Scaling”, *Phys. Rev. A* **71**, 012701 (2005).
16. W. Vanroose, F. Martin, T. N. Rescigno and C. W. McCurdy, “Nonperturbative Theory of Double Photoionization of the Hydrogen Molecule”, *Phys. Rev. A* **70**, 050703 (R) (2004).
17. D. A. Horner, C. W. McCurdy and T. N. Rescigno, “Electron Impact Excitation-Ionization of Helium in the S-Wave Limit”, *Phys. Rev. A* **71**, 010701 (2005).
18. C. S. Trevisan, K. Houfek, Z. Zhang, A. E. Orel, C. W. McCurdy and T. N. Rescigno, “A Nonlocal, Ab Initio Model of Dissociative Electron Attachment and Vibrational Excitation of NO”, *Phys. Rev. A* **71**, 052714 (2005).
19. D.J. Haxton, T. N. Rescigno and C. W. McCurdy, “Topology of the Adiabatic Potential Energy Surfaces for the Resonance States of the Water Anion”, *Phys. Rev. A* (*accepted*).

The ORNL MIRF Upgrade Project

F. W. Meyer, M. E. Bannister, J. W. Hale, and H. J. You¹

A new 250 kV high voltage platform² has been installed at the ORNL Multicharged Ion Research Facility (MIRF) to extend the energy range of multicharged ions available for experimental investigations of their collisional interactions with electrons, atoms, molecules, and solid surfaces. In late January of 2005, this first, and most challenging, phase of a major upgrade project at the MIRF was completed, and routine operation started.

The second phase of the facility upgrade entails relocation of the present CAPRICE ECR ion source within MIRF, and installation of a floating beamline, to extend the availability of very low energy multicharged or molecular ion beams. In this new configuration, keV-energy beams will be transported with high efficiency to end stations and then decelerated there to a few eV \times q (where q is the charge state of the ion of interest), using efficient ion optics already developed for the MIRF floating ion-surface interaction experiment. With these two ECR sources, an energy range of almost five orders of magnitude will be available to the various experiments, a significant improvement over the 1-25 keV/q energy range capability of the present MIRF source configuration.

The current upgrade project is the most far-ranging in the facility's history. It involved the new design, fabrication, and installation of a 250 kV high voltage platform and ECR ion source together with associated beamlines, and major relocations and upgrades of end stations. Concurrent with this effort, an active research program was maintained with the present CAPRICE ECR source. In addition to expanding the capabilities of present on-line experiments, access to higher energy beams makes possible new investigations as well, such as studies of dissociative recombination of molecular ions beyond the mass limit of current magnetic storage rings.

The new all-permanent magnet ECR ion source³, built at CEA Grenoble, operates in the frequency range 12.75 – 14.5 GHz at power levels up to 750W, and is capable of producing up to 0.5 mA of Ar⁸⁺. Its magnetic field structure is achieved using compact NdFeB permanent magnet assemblies for both radial hexapolar and axial solenoidal fields, both of which have peak values in the excess of 1 T, and thus requires no high current power supplies. The performance of the new source exceeds that of the MIRF's present 10 GHz CAPRICE source by up to factors of 2 to 3 in the case of the highest charge state Xe ions.

To achieve the wide 20 – 270 \times q keV design energy range with maximum beam transmission, a number of specific features were incorporated into the design of the beam transport system². All effective optic element apertures on the platform and those up to, and including, the first 65 degree spherical deflector beam switcher were designed for 100% beam transport for beams having an unnormalized emittance of 160 π -mm-mrad at 20 \times q keV. This large acceptance was achieved for the electrostatic beam switcher by the use of two interchangeable sets of deflection electrodes, the first with a 2.5 inch gap to handle beams up to about 150 \times q keV, and the second set with a 1.5 inch gap to handle the lower divergence-angle beams at energies beyond this value. In addition, two einzel lenses were added on either side of the acceleration column to permit refocusing of the beam at the entrance waist of the tandem quadrupole triplet section for low platform voltages where the focusing of the acceleration column itself is weak or non-existent. Finally, large 2-inch-acceptance-aperture quadrupole lenses were used in a tandem configuration before the first beam switcher to achieve both high transmission at low energies and sufficient focusing power with \pm 20 kV electrode potentials at high energies.

Monitoring and control functions on the HV platform⁴ as well as the beamlines leading to the various end stations are achieved via Allen-Bradley ControlLogix programmable logic controllers (PLC's) in three separate chassis linked by Ethernet-bridge-driven fiber-optic cables and controlled by a single Logix5555 processor in the ground potential chassis. Several devices employ serial protocols over RS-232 or GPIB communication channels. All devices are integrated into a Linux-hosted, EPICS-based distributed control system which provides device independent, uniform access to all hardware via a distributed real-time database

Total power required by platform components in the present configuration is a little over 20 kW, and is supplied by an efficient 250 kV mineral-oil-filled isolation transformer capable of providing up to 30 kW of three-phase 208V power, leaving almost 10 kW available for future expansion.

In parallel with the above upgrade activities, measurements were carried out to more fully characterize the plasmas of the facility's ECR sources. In order to accurately determine energies of beams decelerated to eV-range energies, and very low relative collision velocities in merged beams configurations, it is

important to know the plasma potentials of the ion sources used to produce the ion beams, since they define the birth potential of the extracted ions. To this end, real-time, in-situ, plasma potential measurements⁵ have been carried out for the CAPRICE ECR ion source and correlated with extracted beam characteristics. The measurements were carried out using both active and passive Langmuir probes, which were inserted perpendicularly from the plasma chamber wall at the mid-plane of the ECR zone between one of the six radial loss cones of the magnetic field structure, where their perturbation of the main ECR plasma is small. The probes were inserted from the extraction side of the ECR source in order to avoid perturbation of the coaxial microwave injection. Ion beam extraction and measurement were not affected by the presence of the probes. In addition to plasma potential information, the measurements permitted estimates to be made of ECR plasma electron density and temperature, and provided insights into the evolution of these plasma parameters as conditions for multicharged ion production were optimized.

¹PhD student, Hanyang University, Seoul, Korea; partial support from the Korean Science and Engineering Foundation (KOSEF).

²F. W. Meyer, M. E. Bannister, D. Dowling, J. W. Hale, C. C. Havener, J. W. Johnson, R. C. Juras, H. F. Krause, A. J. Mendez, J. Sinclair, A. Tatum, C. R. Vane, E. Bahati Musafiri, M. Fogle, R. Rejoub, L. Vergara, "The ORNL Multicharged Ion Research Facility Upgrade project," to be published in *Nucl. Instrum. Methods Phys. Res. B.* (2005).

³F. W. Meyer, M. E. Bannister, J. W. Hale, J. W. Johnson, and D. Hitz, "The ORNL Multicharged Ion Research Facility (MIRF) High Voltage Platform project", 2005 Particle Accelerator Conference, Knoxville, TN, May 16 – 20, 2005, to be published, *IEEE Conference Proceedings* (2005).

⁴M. E. Bannister, F. W. Meyer, J. Sinclair, "Control System for the ORNL Multicharged Ion Research Facility High Voltage Platform", 2005 Particle Accelerator Conference, Knoxville, TN, May 16 – 20, 2005, to be published, *IEEE Conference Proceedings* (2005).

⁵H. J. You, Y. Liu, and F. W. Meyer, "In-situ Electron Cyclotron Resonance (ECR) Plasma Potential Determination Using An Emissive Probe," 2005 Particle Accelerator Conference, Knoxville, TN, May 16 – 20, 2005, to be published, *IEEE Conference Proceedings* (2005).

Electron-Molecular Ion Interactions.

C. R. Vane

Physics Division, Oak Ridge National Laboratory, Oak Ridge, TN 37831

Fundamental interactions of electrons with molecular ions involve an array of processes of recombination, dissociation, excitation, and ionization, which are important in determining the structure, dynamics, and evolution of charge, energy, and constituent components of all low to moderate temperature plasmas where populations of molecules and molecular ions may be significant. Principal examples of areas in which inelastic electron-molecular ion collisions are important include plasma processing, such as used in the semiconductor industry for etching, deposition, and implantation, and fusion energy research, which has recently focused attention on the cool, dense plasma regimes of present and future devices. In plasma processing, for example, knowledge of electron—molecular ion collision processes is key to modeling and optimizing the complex plasma and surface chemistry used to modify and create the desired material properties or integrated circuit structures. Similar electron-impact processes are important in fusion reactors because molecules, molecular ions, and electrons are abundant in the cool, dense edge and divertor regions and are intrinsically involved in plasma-wall erosion and edge plasma charge, momentum, and energy balance. In addition, electron—molecular ion collisions are of interest in gas laser and lighting development programs, in studies of planetary atmospheres and astrophysical environments, and, owing to fundamental interest, in the few-body atomic-scale re-arrangement problem.

In particular, among the open, challenging questions posed to both theoretical and experimental investigations are:

- how electronic and nuclear motions and energies are coupled in fragmenting complex systems,
- how electrons induce excitation or ionization of molecular ions that leads to fragmentation,
- how the number and constituents of the fragments are determined,
- how the kinetic energy released in the dissociation is partitioned among the products,
- how fragmentation depends on the initial electronic and rovibronic states, and
- what electronic and ro-vibronic states result from the breakup, i.e., how the available energy is distributed among the internal degrees of freedom?

The ORNL Multicharged Ion Research Facility (MIRF) offers experimental facilities enabling a variety of electron-molecular ion measurements and the MIRF is currently being upgraded and enhanced to extensively broaden the precision and scope of these studies. The completed project will provide unique capabilities and synergies with other research that will present several novel opportunities to directly address many of the above fundamental questions. Specifically, the MIRF electron-ion crossed beams apparatus is currently used for measurements of cross sections for direct ionization, dissociative excitation (DE), and dissociative ionization (DI) for a variety of internally “warm” molecular ions obtained from the Caprice ECR ion source and a separate electron impact Colutron ion source. We have concentrated on relatively simple tri-atomic molecular ions, particularly hydrocarbons and others important to fusion applications, and especially those systems for which we are also studying dissociative recombination processes at the CRYRING heavy ion storage ring in Stockholm.

For example, in the last year at MIRF we have begun investigations of dissociation of N_2H^+ ions, experiments complementary to dissociative recombination (DR) studies of N_2H^+ undertaken by our collaborators at CRYRING.¹ The preliminary DE and DI cross sections for 30-100 eV collisions leading to NH^+ fragments are relatively energy insensitive at $\sim 3\text{-}4 \times 10^{-17} \text{ cm}^2$, but indicate some peaked structure near 20 eV. Studies have also been continued this year for CH_3^+ ions, and cross section measurements have been completed for the 3–100 eV range for the CH^+ and C^+ fragment channels. We have also made measurements at MIRF for dissociation of DCO^+ ions producing CO^+ ions² with the measured cross sections

showing resonance structures near 15 eV, similar to results previously obtained for the production of CH^+ from the dissociation of CH_2^+ .³

Electron-molecular ion studies at the ORNL MIRF have been limited primarily to experiments dealing with electron impact dissociative excitation and ionization. With the high voltage platform upgrade, another fundamentally important reaction channel can be explored utilizing the merged electron-ion beams energy loss (MEIBEL) apparatus modified to handle higher energy ions and to permit post-merged beam analysis of ionic and neutral fragments, namely dissociative recombination. DR has now been studied at storage rings for a wide array of molecular ions with cross section results that sometimes differ substantially from flowing-afterglow methods. Single-pass, merged-beams experiments that we will carry out at MEIBEL can provide new complementary measurements, which will be focused on plasma processing and fusion relevant species, especially more complex, heavier species, as well as some lying beyond the capability of present storage rings.

Additionally, higher beam energies provided by the new MIRF high-voltage platform will enable related studies of molecular ion dissociation through electron capture from atomic and molecular neutral beams. These studies will be performed using a COLTRIMS endstation apparatus, which has been designed to carry out high-resolution analysis and detection, including multi-hit imaging, of charged and neutral products arising from electron transfer reactions. The COLTRIMS technique will be employed to make high-resolution momentum transfer measurements to identify the specific states involved in the dissociative electron capture processes.

Studies at CRYRING of dissociative recombination of relatively simple three-body molecular ions are also continuing in our ongoing collaboration with Prof. Mats Larsson and colleagues at the Manne Siegbahn Laboratory (MSL), Stockholm University. Absolute cross sections, branching fractions, and measurements of the dissociation kinematics, especially of the three-body breakup channel, are being investigated at zero relative energy for a variety of light and heavy vibrationally-cold triatomic di-hydrides and other molecular ions with three-body channels. This research is being carried out using the MSL CRYRING heavy ion storage ring, which is expected to continue to be available for our electron-molecular ion measurements at least into calendar year 2007, after which research will shift to development of experiments in a new cold, all electrostatic, double storage ring (DESIREE) being constructed at Stockholm University. The main advantage of using the storage ring technique is that the excess internal energy of the molecular ions from the ion source is allowed to radiatively cool to the vibrational ground state during storage prior to measurements with merged electrons. The initial internal state population of the molecular ions being studied is therefore relatively well-defined, making interpretation and comparison with theory more relevant. The stored merged beams geometry also facilitates recombination measurements at very low relative energies where the DR process dominates.

We have now completed analysis of CRYRING CH_2^+ , and NH_2^+ three-body DR measurements and those results have been compared with our previous H_2O^+ data in a recent publication.⁴ We have similarly recently completed initial measurements and analyses for DR of PD_2^+ and SD_2^+ ions, and preliminary results have been presented.⁵⁻⁶ We have also initiated DR studies at CRYRING of two new systems, D_5O_2^+ and O_3^+ , as a continuation of previous measurements concerning the DR of similar molecules, such as H_2O^+ , NH_2^+ , CH_2^+ , and SD_2^+ that have all revealed three-body break-up as the dominant reaction channel. In order to study the three body break-up dynamics in detail, a high-resolution imaging technique is used to measure the displacements of the fragments from the center of mass of the molecule. The displacement is related to the kinetic energy of the fragment and therefore contains information about the dynamics involved in the process, i.e., the internal state distribution of the fragments. These event-by-event measurements yield information about how the kinetic energy is distributed between the two light fragments and the angular distribution of the dissociating molecules. In all of the triatomic di-hydride systems previously studied, the branching fractions showed very roughly (7:2:1) ratios for ($\text{X} + \text{H} + \text{H}$; $\text{XH} + \text{H}$; $\text{X} + \text{H}_2$), while the observed energy sharing and angular distributions of the three-body breakup product channel could depend heavily on the structure, bonding and charge centre of the parent molecular ion. In contrast to these previously-studied di-hydride systems, D_5O_2^+ provides an excellent opportunity for investigating the role played by internal states of fragments in the DR process. The preliminary branching results indicate that the $\text{D}_2\text{O} + \text{D} + \text{D}_2\text{O}$ channel contributes more than 90% of the DR. The energy available to the products is

approximately 5 eV; for ground state fragments this would mean 5 eV of kinetic energy, mostly given to the single D atom. Preliminary analysis of the imaging measurements, however, suggests that this is not the case, but instead that a significant portion of the available energy is used in internal excitation of the D₂O fragment molecules. A more detailed analysis of the imaging data is in progress. For the O₃⁺ system, preliminary branching fractions show that more than 60% of DR events lead to three separate O atoms, consistent with the dominance of the three-body channels observed in DR of di-hydride ions. This finding would have a significant impact on models of atmospheric chemistry where DR plays a crucial role by producing excited O atoms. Analysis of the imaging data for the O₃⁺ system has just commenced. Absolute DR cross sections have also been measured in the 0-1 eV range for both D₅O₂⁺ and O₃⁺.

As noted above, measurements of DE and DI at MIRF have previously concentrated on using the cross beams apparatus and on ions from the Caprice ECR ion source, and limited to collision energies > 3 eV and to detection of only heavy ionic fragments. These limitations are being addressed by the addition of another cross-beams apparatus to the MIRF facility, formerly located at JILA⁷, which has been specifically designed to permit analysis of the light ion dissociation fragments. Similarly, the upgrade of the MIRF includes development and implementation of a number of different molecular ion sources, based primarily on designs using supersonic expansion cooling of ions in a helium or other carrier gas. Similar sources⁸ have been employed successfully at CRYRING and other laboratories for electron-molecular ion measurements using ground-state rovibrational molecular ions, with results that indicate the importance of initial states especially to the DR process. These cold ion sources will be mounted at the MIRF on both the new high voltage platform for measurements with the MEIBEL and COLTRIMS endstations, and on the light fragment JILA crossed beams apparatus, permitting studies of dissociation processes with controlled initial state molecular ions. Using both warm and cold sources will allow us to controllably study the effects of initial internal states on the various dissociation processes.

The availability of different sources, variation of source operating parameters, and comparison with ion-storage-ring results for DE, will enable near-threshold studies that probe the dependence of DE, DI, DR and dissociative electron capture on the initial excited states of the molecular ions. Such work is an important foundation for comparison with theoretical results computed for given initial rovibronic and electronic state composition, as well as being crucial for efforts to understand real-world plasmas which exist in very different temperature regimes (e.g., ground-state molecular ions of fundamental interest for benchmarking theory or in cold astrophysical plasmas, or molecular ions present in warmer plasmas such as in plasma processing devices where a range of excited states will be present).

1. W.D. Geppert, R. Thomas, J. Semaniak, A. Ehlerding, T.J. Millar, F. Österdahl, M. af Ugglas, N. Djuric, A. Paál, and M. Larsson, "Dissociative Recombination of N₂H⁺: Evidence for Fracture of the N-N Bond," *Astrophys. J.* **609**, 459 (2004).
2. E. M. Bahati, R. D. Thomas, C. R. Vane, and M. E. Bannister, "Electron-impact dissociation of D¹³CO⁺ molecular ions to ¹³CO⁺ ions," *J. Phys. B* **38**, 1645 (2005).
3. C. R. Vane, M. E. Bannister, and R. Thomas, "Electron-Impact Dissociation of CH₂⁺ Producing CH⁺ Fragments," XXIII ICPEAC Abstracts, Stockholm, Sweden (2003).
4. R. Thomas et al., "Three-Body Fragmentation Dynamics of Amidogen and Methylene Radicals via Dissociative Recombination," *Phys. Rev. A* **71**, 032711 (2005).
5. V. Zhaunerchyk et al, "Dissociative recombination study of PD₂⁺ at CRYRING: absolute cross sections, chemical branching ratios and three-body-fragmentation," to be published, *Molecular Physics* (2005).
6. F. Hellberg et al., "Investigating the breakup dynamics of dihydrogen sulfide ions recombining with electrons," *J. Chem. Phys.* **122**, 224314 (2005).
7. N. Djuric, S. Zhou, G.H. Dunn, and M. Bannister, "Electron-impact dissociative excitation of CD_n⁺ (n= 2-5): Detection of light fragment ions D⁺ and D₂⁺," *Phys. Rev A* **58**, 304 (1998).
8. B. J. McCall et al., "An Enhanced Cosmic-Ray Flux towards Zeta-Persei Inferred from a Laboratory Study of the H₃⁺-e⁻ Recombination Rate," *Nature* **422**, 500 (2003).

Analysis of Structure in Low-Energy Ion-Atom Collisions

J. H. Macek

*Department of Physics and Astronomy,
University of Tennessee, Knoxville, Tennessee and
Oak Ridge National Laboratory, Oak Ridge, Tennessee
email:jmacek@utk.edu*

1 Program scope

Structure in atomic cross sections relate to specific mechanisms of atomic processes initiated by particle impact. Such structure occurs most prominently in the low-energy domain, since the wave properties of particle motion are most important when the wavelength $\lambda = \hbar/\sqrt{2mE}$ is large. One part of our project involves modelling this structure theoretically.

The hidden crossing theory has proved to be a valuable framework for modelling ion-atom collisions when the semiclassical representation holds. To apply this theory at energies where the wave properties become important, it is necessary to formulate the theory without invoking the semiclassical approximation. At the fundamental level, this reformulation requires that the usual Born-Oppenheimer separation of variables is replaced by the hyperspherical adiabatic representation. Computations of potential energy curves and adiabatic energy eigenvalues are more difficult in this representation thus one part of our project concentrates on modifications of the semiclassical theory that can be employed with the wave representation.

The projects listed in this abstract are sponsored by the Department of Energy, Division of Chemical Sciences, through a grant to the University of Tennessee. The research is carried out in cooperation with Oak Ridge National Laboratory under the ORNL-UT Distinguished Scientist program.

2 Recent progress

A wave version of the hidden crossing theory has also been developed to treat collisions with energies below 1 keV. The theory has been applied to collisions of anti-protons with atomic hydrogen [7]. No unusual structures in

cross sections are found. Our simple analytic representation is well adapted to modeling of protonium formation for applications involving slow protons in dilute backgrounds of atomic hydrogen.

Calculations of rearrangement collisions at energies below a few eV must employ a completely wave treatment. We have recently made very accurate calculations of spin exchange in proton-hydrogen collisions in the 10^{-4} - 10 eV energy range for benchmark purposes [8]. The integral cross sections, *i. e.* the cross sections integrated over scattering angles show much structure. One purpose of these benchmark calculations is to classify all of the structure. We identify features that correspond to conventional shape resonances and zero angle glory oscillations. In addition, we find structures that cannot be identified with these two well-understood features.

To analyze these features we separate a part of the cross section that has semiclassical glory oscillations from a part that relates explicitly to quantum mechanics. This separation is accomplished by employing a relatively unknown technique of Mulholland and employed by Vogt and Wannier. They show that any partial wave sum \mathcal{S}

$$\mathcal{S} = \frac{2\pi}{k_i^2} \sum_{L=0}^{\infty} f(L + 1/2)(L + 1/2) \quad (1)$$

may be written as the sum of three rather different terms:

$$\begin{aligned} \mathcal{S} = & \frac{2\pi}{k_i^2} \int_0^{\infty} f(\lambda)\lambda d\lambda - \text{Re} \left\{ \int_0^{i\infty} \frac{2\pi f(\lambda)/k_i^2}{1 + \exp[-i2\pi\lambda]} \lambda d\lambda \right\} \\ & - \frac{2\pi}{k_i^2} \text{Re} \left\{ \sum_m \frac{f_r(\lambda_m)\lambda_m}{1 + \exp[i2\pi\lambda_m]} \right\} \end{aligned} \quad (2)$$

where λ_m are the poles of $f(\lambda)$ in the upper right quadrant of the complex λ plane, and $f_r(\lambda_m)$ are the residues of $f(\lambda)$ at the poles. These poles are commonly referred to as Regge poles and have been extensively used to analyze angular distributions. The Sommerfeld-Watson transformation used in the analysis of Regge, however, does not apply to integral cross sections, but Eq. (2) does.

The Mulholland identity, of Eq. (2) separates the sum into a smooth part, given by the first two terms in Eq. (2), from the pole contributions, given by the last term. The first term is recognized as a semiclassical, impact parameter-type, contribution. Zero-angle glory oscillations associated with a point of stationary phase originate with this term, thus Eq. (2) provides

a natural way to separate oscillations that are unrelated to extrema of the phase shift from those that are related.

The second term involving an integration along the imaginary axis is a correction that is small in almost all applications. The third term, namely a sum over pole contributions is associated with the low energy oscillations. Narrow shape resonances also appear in this term, but they are readily separated from the broad peaks, except perhaps for relatively broad shape resonances that occur at low angular momenta and therefore low energy (below 0.03 eV).

This leads to an identification of the oscillations with Regge trajectories and allows us to classify the “Regge oscillations”. Since this analysis originates with the work of Vogt and Wannier, the oscillations are more appropriately termed “Vogt-Wannier oscillations”. In any event, the Mulholland identity serves to separate a semiclassical contribution from resonance and other quantal contributions to any partial wave sum.

The sum over pole terms is often difficult to evaluate owing to the need to compute the positions of the poles rather accurately. We have shown that these pole terms $\lambda_m(E)$ are Sturmian eigenvalues of the radial Schrödinger equation, and have developed a WKB type approximation to compute them. These eigenvalues are then used to compute the third term in Eq. (2) for elastic scattering and charge exchange in $H^+ + H$ scattering. This term is shown to oscillate in the low energy region.

In addition to zero-angle glory and Vogt-Wannier oscillations, cross sections may also show more conventional Rosenthal and Stueckleberg oscillations. Our computations of the total cross section for the reaction



where M is a generally complex molecule, *e. g.* C_{60} , show Rosenthal oscillations owing to the energy separation of the $P_{1/2}$ and $P_{3/2}$ levels of Xe. Similar oscillations are seen in total cross section measurements, and these oscillations help confirm our model for this counter-intuitive process.

Stueckleberg oscillations usually average out in total cross sections. We have shown that an exception occurs for the prototypical three-boson reaction



at the threshold for the breakup process. Only one final three-body channel dominates as the total energy approaches 0, thus Stueckleberg oscillations do

not average out for this process. An analytic expression for the threshold breakup cross section has been derived.

3 Future plans

We will continue our study of the "Vogt-Wannier" oscillations in cross sections for atomic process. There is some evidence that these oscillations are related to Cooper minima in photoabsorption processes. For that reason we will examine Regge trajectories for the Thomas Fermi potential applicable generally to a wide variety of atomic processes to see if the Regge oscillations show up in integral electrons scattering cross sections, and in photoabsorption processes.

Our two-center Sturmian calculations of total ionization cross sections for one electron species involves a routine, but rather time consuming, step that greatly reduces the efficiency of the method. We will examine techniques to make this step more efficient. At present there is a 20% discrepancy between benchmark LTDSE ionization cross sections, experiment, and our two-center Sturmian results for proton-hydrogen collisions. This discrepancy may be due to differing estimates of the population of states with $n > 4$ in the different calculations. We will adapt the two-center Sturmian theory to the computation of such high Rydberg states to see if this is indeed the source of the discrepancy. It is important to resolve this issue since cross sections with accuracies in the 1% range are needed for diagnostic purposes.

We will continue our study of three particle interactions at the threshold for application to both boson and fermion species. Of particular interest is the parameter region where loosely bound three-body states occur. We will investigate this prospect using multi-channel zero-range potential models to include Feshbach resonances in three-body interactions.

4 References to DOE sponsored research that appeared in 2003-2005

1. Exact electron spectra in collisions of two zero-range potentials with non-zero impact parameters, S.Yu. Ovchinnikov, D.B. Khrebtukov, and J.H. Macek, *Phys. Rev. A* **65**, 032722 (2002).

2. Electron Emission in $H^- - He, H_2$ Collisions, G. N. Ogurtsov, S. Yu. Ovchinnikov, and V. M. Mikoushkin, in (23rd International Conference on Photonic Electronic and Atomic Collisions, invited talks, July 2003 Stockholm, Sweden), *Physica Scripta* **T110**, 370 (2004).
3. Ionization of atoms by antiproton impact, J. H. Macek in *Electron Scattering From Atoms, Molecules, Nuclei and Bulk Matter*, Ed. by C. Whelan, (Kluwer Scientific 2002).
4. Annihilation of Low Energy Antiprotons in Hydrogen, S. Yu. Ovchinnikov and J.H. Macek, in (17th International Conference on the Application of Accelerators in Research and Industry, November 2002, Denton TX), *AIP Conference Proceedings*, **680** (2003).
5. Ionization Dynamics in Atomic Collisions, S. Yu. Ovchinnikov, J. H. Macek, Yu. S. Gordeev, and G. N. Ogurtsov, in *Atomic Processes* Ed. by S. Shevel'ko, (Springer, 2003), Ch. 25.
6. Dynamics of Ionization in Atomic Collisions, J. H. Macek, Yu. S. Gordeev, and G. N. Ogurtsov, *Physics Reports*, **389**, 119-159 (2004).
7. Energy and angular distributions of electrons ejected from atomic hydrogen by low energy proton impact, J. H. Macek and S. Yu. Ovchinnikov, *Phys. Rev. A*, accepted for publication.
8. Computations of elastic scattering and spin exchange in $H^+ + H$ collisions for impact energies between 10^{-4} and 10 eV, Predrag Krstić, J. H. Macek, and S. Yu. Ovchinnikov, *Phys. Rev. A*, accepted for publication.

Using Intense Short Laser Pulses to Manipulate and View Molecular Dynamics

Robert R. Jones, Physics Department, University of Virginia,
382 McCormick Road, P.O. Box 400714, Charlottesville, VA 22904-4714
rrj3c@virginia.edu

I. Program Scope

Our primary focus is the exploration and control of phenomena associated with non-perturbative laser/molecule interactions. Intense non-resonant laser pulses can radically affect molecular motion, both in internal and external degrees of freedom. By monitoring the electrons, ions, and/or photons emitted from irradiated molecules, one can obtain information regarding the molecules' dynamical response to the laser field. Moreover, by tailoring the time-dependent laser field, ionization, fragmentation, and/or high harmonic generation yields can be altered or controlled. Not surprisingly, the molecule's alignment with respect to the laser polarization is a critical parameter in determining the effect of the field. Furthermore, while the angular distribution of electrons, ions, or photons emitted relative to a molecule fixed axis contains key information relevant to the strong-field interaction, this information may only be interpretable if the molecular axis has a well-defined direction in the laboratory frame. Consequently, the random alignment/orientation of molecules in typical gaseous samples poses a significant obstacle to understanding and controlling strong-field molecular dynamics. Thus, much of our current research relies on the use of short laser pulses to coherently prepare aligned and/or oriented molecular targets for use in subsequent experiments.

II. Recent Progress and Results

We have used intense short laser pulses to transiently align diatomic molecules for strong field ionization and high harmonic generation experiments. In the experiments, an alignment pulse (or pulses) drives a sequence of Raman transitions within each molecule, producing a rotational wavepacket whose evolution is characterized by periodic molecular alignment [1]. After a time-delay, the molecules are exposed to a second, more intense "signal" laser pulse, resulting in molecular ionization, fragmentation, and/or the emission of high harmonics. By selecting the appropriate time-delay and/or polarization angle between the alignment and signal lasers, we can systematically explore the efficiency of these strong-field processes as a function of the angle between the signal laser polarization and the molecular axis. In practice, the non-zero rotational temperature of the molecular sample, and the restriction on the maximum alignment laser intensity set by the molecular ionization threshold, limits the achievable degree of alignment. Thus, we work with preferentially, not perfectly, aligned ensembles.

We have used 100 fsec and 30 fsec 780 nm laser pulses to transiently align room temperature N₂, O₂, and CO. In all cases, we find that the degree of alignment is significantly enhanced by using two alignment pulses that are temporally separated by a half- or integer-multiple of the rotational period. We characterize the time-dependent alignment using Coulomb explosion initiated by a very intense, time-delayed circularly polarized 30 fsec 780 nm probe. The explosion pulse rapidly removes multiple electrons from the neutral molecules so that they explode due to the Coulomb repulsion of the remaining positive ions [2]. There is no preferential molecular orientation for the multiple-ionization event in the circular polarization plane of the explosion pulse. Thus, the Coulomb explosion maps the initial angular distribution of the target molecules onto the angular distribution of the outgoing ion fragments. Ions originating from molecules that are preferentially aligned along the axis of the spectrometer arrive at the detector at different times and produce a bi-modal peak in the TOF spectrum. Ion fragments from molecules that are aligned perpendicular to the spectrometer axis strike the detector at the same time, resulting in a single peak in the TOF spectrum. Thus, in a

single laser shot, we can obtain a qualitative measure of alignment directly from the ion TOF spectrum. Alternatively, we can quantitatively measure the degree of alignment using a multi-hit, event mode detector. A wire-grid anode enables our determination of the transverse position and time of flight for each detected fragment. We record the vector momenta of up to 15 ion fragments per laser shot to reconstruct the molecular angular distribution at the instant of the Coulomb explosion.

A) Ionization of Transiently Aligned molecules

Processes such as high harmonic generation and non-sequential multiple ionization in atoms and molecules are mediated by electrons that are first tunnel-ionized and then driven back into their parent ions by an intense laser field. However, in molecules, accurate rates for the critical ionization step are extremely difficult to calculate, and discrepancies between theory and experiment persist. Direct comparisons between theory and experiment are complicated by the random alignment of molecules in experiments, uncertainties in the degree to which molecules align during the ionizing pulse, and the lack of experimental data on ionization rate anisotropies for molecules aligned at different angles relative to the ionizing field. These issues can be eliminated or significantly reduced by using transiently aligned molecular targets.

Previously, we found that the tunneling ionization rate from an unaligned sample of CO molecules is suppressed, by roughly a factor of two, relative to its ‘companion atom’ Kr which has a nearly identical ionization potential. We have now measured the CO:Kr ionization rate ratio as a function of the alignment of the CO molecular axis with respect to the ionizing laser polarization. We find that below ionization saturation, molecular alignment is an important parameter in determining the ionization rate. We measure an ionization rate ratio, $R_{\parallel}:R_{\perp} = 1.9 \pm 0.6$, for molecules aligned parallel vs. perpendicular to the ionizing laser field. Our measurements are in qualitative agreement with theoretical results based on molecular orbital ADK (MO-ADK) calculations [3]. A manuscript describing the experiment and results has been accepted for publication in Physical Review A. Interestingly, analogous measurements on aligned N_2 (a molecule which is slightly easier to ionize than its companion atom Ar) indicate a larger $R_{\parallel}:R_{\perp} = 3.5 \pm 0.5$, ionization rate anisotropy [2]. We intend to exploit transient alignment to explore the source of differences between ionization rates of other molecules and their companion atoms.

B. High Harmonic Generation from Transiently Aligned Molecules

One expects that the energy and angular distribution of electrons and HHG photons emitted during an intense laser pulse will depend on both electronic structure and the spatial distribution of nuclei within an irradiated molecule. This dependence might be exploited i) to control ionization or HHG via intense laser manipulation of molecular structure; or conversely, ii) to use HHG or electron emission as probes of molecular structure and dynamics with sub-Angstrom spatial and femtosecond temporal resolution [4]. Of course, the ability to study aligned rather than randomly oriented molecules is critical for achieving this control or interpreting emission yields for imaging applications. Accordingly, we and several other groups have begun to explore HHG using transiently aligned molecules [5]. Rather than use a more common gas-jet-based source, we have constructed a hollow-core waveguide HHG apparatus [6]. This geometry might be advantageous for future applications of transient alignment for quasi-phase matching with counter propagating alignment and signal beams.

We have observed harmonic generation in Ar and N_2 and have characterized the role of phase-matching in the emission into different harmonic orders as a function of gas pressure and laser intensity. For the alignment experiments, we use a Michelson interferometer to couple two time-

delayed 30 fsec, 780 nm laser pulses into a single fiber. The first pulse which is slightly chirped due to the interferometer beamsplitter, creates a rotational wavepacket in N_2 while producing negligible harmonics. The transient alignment of this wavepacket results in significant variations (as large as a factor of 3) in the harmonic yield from the second pulse, as a function of the relative delay between the two pulses. In general, significantly higher harmonic emission is observed from molecules aligned parallel rather than perpendicular to the intense laser field. This variation is presumably due to one or more of the following: i) the ionization rate anisotropy for molecules aligned parallel vs. perpendicular to the laser field; ii) the anisotropy in the probability that a tunnel ionized electron will recollide with its parent ion; iii) the anisotropy in the probability that a recolliding electron will recombine with its parent ion and emit a high energy photon; or iv) a macroscopic effect due to phase-matching or birefringence in the anisotropic molecular medium.

Our characterization of room temperature alignment and previous measurements of the ionization anisotropy in N_2 indicate that the ionization rates in our sample vary by only a few percent between times of maximal parallel and perpendicular alignment. In addition, measurements using elliptically polarized beams, which make it possible to translate the recolliding electron relative to the transverse location of the parent ion, show negligible dependence of the recollision probability on molecular alignment. Thus, in the absence of phase-matching effects, the large alignment dependence of the harmonic yields can be attributed to the anisotropic recombination cross-section of the returning electron [5]. However, we find that phase-matching can indeed have a dramatic dependence on the alignment dependence of the harmonic yield. By slightly changing the spatial coupling of the two beams into the fiber, we sometimes observe a reversal of the enhancement of some harmonics, but not others. This reversal results in maximum harmonic signal for perpendicular rather than parallel alignment, precisely the opposite of the single molecule response. The precise origin of this effect is not completely understood, but a manuscript detailing our observations is nearly ready for submission.

C. Closed-Loop Optimization of Transient Alignment of Room Temperature Molecules

A key aspect of our program is the development of improved methods to transiently align molecular targets. As mentioned above, in our ionization anisotropy measurements, we obtain better alignment with reduced ionization background by kicking our molecules with two, time-delayed alignment pulses. However, even more sophisticated pulse shapes have been suggested for optimizing the alignment [7]. Accordingly, we are exploring the use of a laser pulse-shaper in conjunction with a genetic learning algorithm in a closed-loop optimal control scheme to search for the best laser pulse “shape” for achieving maximal alignment of our room temperature samples at specific target times [8]. The qualitative single-shot alignment characterization technique described previously provides the critical rapid feedback for these optimization experiments.

To date, we have not found any pulse shapes that align molecules better than single unshaped pulses do (technical limitations on the maximum temporal separation between shaped pulse features prevent us from finding the known, “two-kicks separated by the rotational revival period” solution that is described above). However, we do find solutions that perform as well as unshaped pulses. More interestingly, our numerical rigid-rotor simulation code predicts that many of these should not be effective at aligning the molecules. Potential reasons for this apparent disagreement between experiment and theory include the distribution of alignment pulse intensities throughout the experimental volume and the approximation of intensity-independent molecular polarizabilities in the rigid rotor simulation. These experiments and our analysis are continuing.

III. Future Plans

As noted in preceding sections, we intend to continue i) our measurements of ionization rate anisotropies for aligned molecules and ii) our experiments and analysis of closed-loop control of transient alignment through laser pulse-shaping. In addition, we have recently begun to study the polarization of harmonics emitted by aligned molecules. Recent theoretical work predicts a dramatic dependence of the VUV polarization angle and helicity on the relative alignment of the molecule and the fundamental laser field [10]. In principle, aligned molecules could be used to produce coherent VUV radiation with well-defined, non-linear polarizations. Alternatively, this polarization dependence could be exploited as a more sensitive time-resolved probe of molecular structure.

We are also attempting to demonstrate field-free orientation of polar molecules by subjecting them to sub-picosecond half-cycle electric field pulses (HCPs). Optical-frequency laser pulses create periodically aligning, rotational wavepackets by driving Raman transitions between rotational states of the same parity. However a unipolar HCP directly drives $\Delta J = \pm 1$ transitions between rotational levels of opposite parity. Thus, simulations predict that in polar molecules, the rotational wavepackets that are produced by HCPs will have mixed parity and exhibit a time-dependent dipole moment [9]. The absence of “up/down” symmetry in these transiently oriented molecules makes them interesting targets for a variety of photo-processes. For example the asymmetry in the strong field ionization and recollision electron recombination rates should make it possible to observe the generation of even as well as odd order harmonics from oriented polar molecules.

Due to its moderate dipole moment (0.82 Debye) and large rotational constant (8.5 cm^{-1}) observable alignment of HBr ($\sim 10\%$ variation in $\langle \cos\theta \rangle$) should be possible with currently achievable HCP field amplitudes ($\sim 100 \text{ kV/cm}$) and moderate rotational cooling ($\sim 10\text{K}$) in a supersonic expansion with He or Ar. In addition, our numerical simulations (and those of others [11]) indicate that significant enhancements in the degree of orientation can be achieved through the use of multiple, time-delayed HCPs or combined HCP and optical fields.

IV. Publications from Last 3 Years of DOE Sponsored Research (July 2002- July 2005)

- 1) E. Wells, K.J. Betsch, C.W.S. Conover, M.J. DeWitt, D. Pinkham, and R.R. Jones, “Closed-Loop Control of Intense-Laser Fragmentation of S_8 ,” *Physical Review A* (submitted).
- 2) D. Pinkham and R.R. Jones, “Intense Laser Ionization of Transiently Aligned CO,” *Physical Review A* (2005, in press).
- 3) E. Wells, I. Ben-Itzhak, and R.R. Jones, “Ionization of Atoms by the Spatial Gradient of the Pondermotive Potential in a Focused Laser Beam,” *Physical Review Letters* **93**, 23001 (2004).
- 4) E. Wells, M.J. DeWitt, and R.R. Jones, “Comparison of Intense Field Ionization of Diatomic Molecules and Rare Gas Atoms,” *Physical Review A* **66**, 013409 (2002).

V. References

1. T. Seideman, *Phys. Rev. Lett.* **83**, 4971 (1999); F. Rosca-Pruna and M.J.J. Vrakking, *Phys. Rev. Lett.* **87**, 163601 (2001).
2. I.V. Litvinyuk et al., *Phys. Rev. Lett.* **90**, 233003 (2003).
3. Alnaser et al.; *Phys. Rev. A* **71**, 031403 (2005).
4. M. Lein et al., *Phys. Rev A* **66**, 023805 (2002); H. Nikura et al., *Nature* **417**, 917 (2002).
5. Itatani et al., *Nature* **432**, 867 (2004); H. Kapteyn (personal communication).
6. A. Rundquist et al., *Science* **280**, 1412 (1998).
7. Leibscher, Averbukh and Rabitz, *Phys. Rev. Lett.* **90**, 213001 (2003).
8. B. Pearson, J.L. White, T.C. Weinacht, and P.H. Bucksbaum, *Phys. Rev. A* **63**, 063412 (2001).
9. M. Machholm and N.E. Henriksen, *Phys. Rev. Lett.* **87**, 193001 (2001).
10. B. Zimmerman, M. Lein, J.M. Rost, *Phys. Rev. A* **71**, 033401 (2005).
11. R. Gordon and I. Averbukh (personal communication).

Atomic and Molecular Physics in Strong Fields

Shih-I Chu

Department of Chemistry, University of Kansas

Lawrence, Kansas 66045

E-mail: sichu@ku.edu

Program Scope

In this research program, we address the fundamental physics of the interaction of atoms and molecules with intense ultrashort laser fields. The main objectives are to develop new theoretical formalisms and accurate computational methods for *ab initio* nonperturbative investigations of multiphoton quantum dynamics and very high-order nonlinear optical processes of one-, two-, and many-electron quantum systems in intense laser fields, taking into account detailed electronic structure information and many-body electron-correlated effects. Particular attention will be paid to the exploration of novel new physical mechanisms, time-frequency spectrum, and coherent control of high-harmonic generation (HHG) processes for the development of table-top x-ray laser light sources. Also to be explored is the ionization mechanisms of molecules in intense laser fields and attosecond physics.

Recent Progress

1. Development of *Self-Interaction-Free* Time-Dependent Density Functional Theory (TDDFT) for Nonperturbative Treatment of Multiphoton Ionization and High-Order Nonlinear Optical Processes in Intense *Pulsed* Laser Fields

To study multiphoton and very-high-order nonlinear optical processes (such as HHG, strong-field ionization and dissociation, Coulomb explosion (CE), etc.) of many-electron quantum systems in intense laser fields using the *ab initio* wave function approach, it is necessary to solve the time-dependent Schrödinger equation of $3N$ spatial dimensions in space and 1D in time (N = the number of electrons). This is well beyond the capability of current supercomputer technology for $N > 2$. Recently we have initiated a series of new developments of *self-interaction-free* time-dependent density functional theory (TDDFT) for probing strong-field physics of many-electron atomic and molecular systems, taking into account electron correlations and detailed electronic structure [1-6]. Given below is a brief summary of the progress in 2003-2005.

- a) *Role of the Electronic Structure and Multi-electron Response in Ionization Mechanisms of Diatomic Molecules in Intense Laser Fields*

The ionization and multiphoton ionization (MPI) of atoms, one of the fundamental processes initiated during the exposure of an atom to an intense laser field, has been extensively studied both experimentally and theoretically in the past decade. Recently, there is also considerable interest in the study of the ionization mechanism of diatomic molecules in intense laser fields. At lower intensities, dissociation may compete with ionization, fragmentation may play an important role, ionization may be sensitive to the alignment of the molecule with the laser field, and multicharged ions formed at higher intensities may be unstable due to Coulomb explosion. The ionization behavior of molecules is thus considerably more complicated than that of the atoms with comparable ionization potentials

Most theoretical studies of strong-field molecular ionization in the recent past are based on approximate models such as the ADK (Ammosov-Delone-Krainov) model, etc. These models usually assume that ionization rates depend only upon laser wavelength and intensity, and the *field-free* ionization potential of the species of interest. Further, most theoretical models considered only the response of the

highest occupied molecular orbital (HOMO). Although these models have some partial success but they cannot provide an overall consistent picture of the ionization behavior of different molecules.

Recently we have extended the self-interaction-free TDDFT [4,5] for nonperturbative investigation of the ionization mechanisms of diatomic molecules (N_2 , O_2 , and F_2) in intense short-pulsed lasers [7]. Our results indicated that the detailed electron structure and correlated multielectron responses are important factors for the determination of the strong-field ionization behavior. Further, we found that it is not adequate to use only the HOMO for the description of the ionization behavior since the inner valence electrons can also make significant or even dominant contributions. Finally, the ionization potential (IP) is laser-intensity and frequency dependent and it is also not the only major factor determining the molecular ionization rates. Further investigation will be continued along this direction.

b) *Very- High-Order Harmonic Generation of Ar Atoms and Ar^+ Ions in Superintense Pulsed Laser Fields: An All-Electron Ab Initio Study*

Recently it has been demonstrated experimentally [8] that the generation of very high-order harmonics (HHG), up to 250 eV, can be obtained by using the Ar gas. Using the ADK model, they inferred that the high harmonic photons arise from the ionized Ar atoms. However there is no full quantum treatment of this process yet. This work shows that HHG from ions may be able to extend laser-based coherent up-conversion into the soft x-ray region of the spectrum.

To explore the underlying quantum dynamics responsible for the production of the very-high-order harmonics, we performed an *all-electron* treatment of the response of Ar and Ar^+ systems to superintense laser fields [9] using the self-interaction-free TDDFT [1-5]. In our study, all the valence electrons are treated explicitly & their partial contributions to the ionization are analyzed. Further, by introducing an effective charge concept, we can study at which laser intensity the contribution to the high-energy HHG from Ar^+ ions precede over the Ar atoms. Comparing the HHG power spectrum from Ar and Ar^+ , we conclude that the high-energy HHG observed in the recent experiment [8] originated from the ionized Ar atoms.

2. Generalized Strong-Field-Approximation Approach to the Study of Molecular Ionization Dynamics

In addition to the TDDFT approach discussed above, we have recently also extended the the *S*-matrix formalism of conventional *strong-field approximation*, supplemented by the LCAO-MO method (utilized for approximate analytical reproduction of the two-centered wave function of initial molecular bound states), for the study of the strong-field ionization behavior of homonuclear diatomic molecules [10]. This approach, while approximate, is a more accurate framework than that of the ADK model. It is also relatively easier to treat than the fully *ab initio* TDDFT approach. We focus on the study of the ionization behavior of several diatomics (such as N_2 , O_2 , and H_2) whose "companion" atoms having nearly identical ionization potential I_p . In this approach, the ionization of a diatomic molecule is described as a quantum-mechanical superposition (*intramolecular interference*) of contributions from ionization amplitudes corresponding to photoelectron emission from two atomic centers. Besides the bonding (or anti-bonding) symmetry of the HOMO, its spatial configuration and predominant orientation with respect to the internuclear axis and polarization of incident laser field are also found to be of substantial importance and, thus, are taken into detailed consideration. Moreover, wherever appropriate, the comparable contributions from other (inner) molecular valence shells are also taken into account. The related results for calculated differential and/or integral molecular ionization rates, molecular photoelectron spectra, and angular distributions are fairly well consistent with available experimental data.

3. *Ab Initio* Nonperturbative Approach Beyond the Born Oppenheimer Approximation for the Exploration of the Coulomb Explosion Dynamics Through Excited Molecular Vibrational States

The study of ionization and molecular fragmentation is a subject of considerable interest in strong-field molecular physics. In particular, the response of the simplest prototype molecular systems H_2^+ (D_2^+) and H_2 (D_2) in intense laser fields have been experimentally studied in the recent past. The major fragmentation mechanisms can arise from several different sources, such as above-threshold dissociation (ATD), dissociation via chemical bond softening, bond hardening, Coulomb explosion (CE) by charge resonance enhanced ionization (CREI), and CE by recollision of electrons, etc. These mechanisms produce direct peaks in the kinetic-energy release (KER) spectrum of H^+ that have been observed experimentally. The KER spectrum reflects the nuclear state(s) at the time when H_2^+ breaks up.

In intense laser fields, the electron of H_2^+ can be excited and/or ionized. If the electron is ionized, the H_2^+ ion breaks up via direct Coulomb explosion (DCE), producing H^+ ions. If the electron is excited to continuum vibrational states, H_2^+ can dissociate via states directly or be further ionized by the laser. The latter process, which will be called *excitation-ionization-dissociation* (EID) is a two-step process, in which H_2^+ in intermediate continuum vibrational states induces CE. Recent experiments of ion-induced molecular fragments showed that the excited states of the transient molecular ions have strong influence on KER spectra. Due to this influence, the KER spectra have fine structures that differ greatly from the DCE spectra. Thus the conventional DCE picture alone is not adequate to describe the molecular fragmentation dynamics.

In a recent work [11], we investigate the fragmentation dynamics of H_2^+ molecular ions in intense laser fields by means of an *ab initio* method beyond the Born-Oppenheimer approximation. Special attention is paid to the exploration of the Coulomb explosion (CE) mechanisms and quantum dynamics through excited vibrational states of H_2^+ . A novel kinetic-energy release (KER) spectrum and CE phenomenon are predicted, in which the kinetic-energy distribution of H^+ ions exhibits a series of peaks separated by one photon energy. A proposed scheme for the experimental observation of the KER spectrum and CE dynamics is presented.

4. Recent Development of Generalized Floquet Formalisms for Nonperturbative Treatment of Multiphoton Processes in Intense One-Color and Multi-Color Laser Fields

a) In the last several years, we have continued the development of generalized Floquet formalisms and complex quasienergy methods for nonperturbative treatment of a broad range of multiphoton and high order nonlinear optical processes in intense monochromatic (periodic) or polychromatic (quasi-periodic) laser fields. An extensive review article on these developments and their applications has been recently published [12].

b) For the treatment of many-electron quantum systems, we have recently initiated the development of the generalized Floquet formulations of time-dependent density functional theory (TDDFT) and time-dependent current density functional theory (TDCDFT) [12-14]. The Floquet-TDDFT approach allows exact transformation of the *periodically* or *quasi-periodically* time-dependent Kohn-Sham equation into an equivalent time-independent generalized Floquet eigenvalue problem. An exterior-complex scaling (ECS)-generalized pseudospectral (GPS) method [15] is developed for accurate solution of the non-Hermitian Floquet-TDDFT Hamiltonian. The ECSGPS technique appears very useful in TDDFT-Floquet calculations where the exchange-correlation potentials may exhibit quite complicated behavior as functions of the electron coordinates and cannot be easily treated by means of the conventional uniform-complex-scaling techniques.

c) Precision Calculation of High-Order Harmonic Generation Spectrum of H_2^+ in Intense Laser Fields: Time-Dependent Non-Hermitian Floquet Approach

The generalized Floquet approaches developed in the past involved the determination of the complex quasienergies from a *time-independent* non-Hermitian Floquet matrix [12]. For more complex many-electron quantum systems, the dimensionality of the Floquet matrix can become very large and the

problem can become intractable. Recently we have introduced an alternative method, the *time-dependent* non-Hermitian Floquet approach [16,17], for overcoming some of the ultralarge complex matrix eigenvalue problems. The procedure involves the complex-scaling generalized pseudospectral spatial discretization of the time-dependent Hamiltonian and non-Hermitian time propagation of the time-evolution operator in the *energy* representation. The approach is designed for effective treatment of multiphoton processes in very intense and/or low-frequency laser fields, which are generally more difficult to treat using the *time-independent* Floquet matrix techniques.

The procedure is applied to the precision calculation of multiphoton ionization (MPI) and HHG calculations of H_2^+ [17] for the wavelength 532 nm at the equilibrium internuclear separation ($R = 2.0$ a.u.) and several laser intensities, as well as at the laser intensity 5×10^{13} W/cm² and various internuclear distances in the range between 3.0 and 17.5 a.u. We found that both the MPI and HHG rates are strongly dependent on R . Further, at some internuclear separations R , the HHG productions are strongly enhanced and this phenomenon can be attributed to the resonantly enhanced MPI at these R . Finally, the enhancement of higher harmonics is found to take place mainly at larger R . Detailed study of the correlation between the behavior of MPI and HHG phenomena is presented. The time-dependent non-Hermitian Floquet approach has been also recently applied to the study of very high-order above-threshold ionization (ATI) of H^- system [16].

Future Research Plans

In addition to continuing the ongoing researches discussed above, we plan to initiate the following several new project directions: (a) Development and extension of the Floquet formulation of TDDFT to the more complex molecular systems. (b) Development and extension of self-interaction-free TDDFT to diatomic molecular systems including the vibrational degrees of freedom for the study of the ionization mechanism and HHG phenomena in strong fields. (c) Development of spin-dependent *localized* Hartree-Fock (LHF)-DFT method for the study of singly, doubly, and triply excited states of Rydberg atoms and ions [18]. (d) Exploration of rescattering and attosecond phenomena in strong fields.

References Cited (* Publications supported by the DOE program in the period of 2004-2005.)

- [1] X. M. Tong and S. I. Chu, Phys. Rev. A **57**, 452 (1998).
- [2] X. M. Tong and S. I. Chu, Int. J. Quantum Chem. **69**, 305 (1998).
- [3] X. M. Tong and S. I. Chu, Phys. Rev. A **64**, 013417 (2001).
- [4] X. Chu and S. I. Chu, Phys. Rev. A **63**, 023411 (2001).
- [5] X. Chu and S. I. Chu, Phys. Rev. A **64**, 063404 (2001).
- [6] A. K. Roy and S. I. Chu, Phys. Rev. A **65**, 043402 (2002).
- *[7] X. Chu and S. I. Chu, Phys. Rev. A **70**, 061402 (R) (2004).
- [8] E. A. Gibson, *et al.*, Phys. Rev. Lett. **92**, 033001 (2004).
- *[9] J. Carrera, X. M. Tong, and S. I. Chu, Phys. Rev. A **71**, 063813 (2005).
- *[10] V. I. Usachenko and S. I. Chu, Phys. Rev. A **71**, 063410 (2005).
- *[11] Z. Y. Zhou and S. I. Chu, Phys. Rev. A **71**, 011402 (R) (2005).
- *[12] S. I. Chu and D. Telnov, Physics Reports **390**, 1-131 (2004).
- [13] D. Telnov and S. I. Chu, Chem. Phys. Lett. **264**, 466 (1997).
- [14] D. Telnov and S. I. Chu, Phys. Rev. A **63**, 012514 (2001).
- [15] D. Telnov and S. I. Chu, Phys. Rev. A **66**, 043417 (2002).
- *[16] D. Telnov and S. I. Chu, J. Phys. B **37**, 1489 (2004).
- *[17] D. Telnov and S. I. Chu, Phys. Rev. A **71**, 013408 (2005).
- *[18] Z. Y. Zhou and S. I. Chu, Phys. Rev. A **71**, 022513 (2005).

Control of Molecular Dynamics: Algorithms for Design and Implementation

Herschel Rabitz and Tak-San Ho, Princeton University
Frick Laboratory, Princeton, NJ 08540, hrabitz@princeton.edu, tsho@princeton.edu

A. Program Scope

This research is concerned with developing the concepts for the systematic study of controlled quantum phenomena. Theoretical studies and simulations continue to play central roles for achieving control over quantum dynamics in conjunction with the realization of closed-loop learning experiments. Recent laboratory control advances have opened up many questions and possibilities for new directions in the fields. The research in this program involves several interrelated components aiming at developing a deeper understanding of the principles of quantum control and providing new algorithms to extend the laboratory control capabilities.

B. Recent Progress

1. **Quantum Optimal Control of Ozone Isomerization**[1] The creation of the theoretically predicted stable ring form of ozone has been a long sought after goal. This work presented a feasibility study for achieving ozone isomerization based on an accurate *ab initio* potential energy surface and a model Hamiltonian constructed by holding the bond lengths constant and using the valence angle as the isomerization coordinate. Optimal control theory was used to find an electric field that drives isomerization with a yield of 95% to the symmetric metastable triangular form of ozone. A frequency filter was applied as an additional spectral constraint limiting the field bandwidth. A *post facto* analysis was performed showing a degree of inherent robustness of the isomerization yield to field noise.
2. **Generalized Monotonically Convergent Algorithms for Solving Quantum Optimal Control**[2] A wide range of cost functionals that describe the criteria for designing optimal pulses can be reduced to two basic functionals by the introduction of product spaces. This work extended previous monotonically convergent algorithms to solve the generalized pulse design equations derived from those basic functionals. The new algorithms were proved to exhibit monotonic convergence. Numerical tests were implemented employing both stationary and non-stationary targets with and without the presence of relaxation.
3. **Efficient Extraction of Quantum Hamiltonians from Optimal Laboratory Data**[3] Optimal identification (OI) is a recently proposed procedure for extracting information about quantum Hamiltonians from experimental data.

It employs techniques from coherent learning control to drive the quantum system such that dynamical measurements provide maximal information about the Hamiltonian. OI is an optimal procedure as initially presented; however, the data inversion component is computationally expensive. Here, we demonstrated that a highly efficient global, nonlinear, map-facilitated inversion procedure can be combined with the OI concept to make it more suitable for laboratory implementation. A simulation of map-facilitated OI illustrated how the input-output maps can greatly accelerate the data inversion process.

4. **Quantum Control of Molecular Motion including Electronic Polarization Effects with a Two Stage Toolkit**[4] A novel method for incorporating strong field polarization effects into optimal control calculations was presented in this work. A Born-Oppenheimer like separation, referred to as the electric-nuclear Born-Oppenheimer (ENBO) approximation, was introduced in which variations of both the nuclear geometry and of the external electric field are assumed to be slow compared with the speed at which the electronic degrees of freedom respond to these changes. This assumption permits the generation of a potential energy surface that depends not only on the relative geometry of the nuclei, but also on the electric field strength and on the orientation of the molecule with respect to the electric field. The range of validity of the ENBO approximation was examined. A two-stage toolkit implementation was presented to incorporate the polarization effects and reduce the cost of the optimal control dynamics calculations. As an illustration of the method, it was applied to optimal control of vibrational excitation in a hydrogen molecule aligned with the field. *Ab initio* configuration interaction calculations with a large orbital basis set were used to compute the H—H interaction potential in the presence of the electric field. A significant computational cost reduction afforded by the toolkit implementation was demonstrated.
5. **Observable Preserving Control of Quantum Dynamics over a Family of Related Systems**[5] An important objective of quantum control is the understanding of dynamical control within a family of related quantum systems. To explore this issue, diffeomorphic changes in the system Hamiltonian are introduced by scanning over a homotopy parameter and then monitoring the control field response needed to maintain the value of a specified target observable. This operation is implemented through a procedure referred to as diffeomorphic modulation under observable response preserving homotopy (D-MORPH). The governing D-MORPH differential equation determining the control laser field is shown to explicitly allow for innumerable solutions, with each characterized by the choice of an arbitrary function of the homotopy parameter and time. The presence of this arbitrary function makes clear the origin of multiple control fields that produce the same observable objective value. A stable algorithm was developed for practical execution of D-MORPH with the only criterion that the Hamiltonian permits reaching the objective over the full homotopy domain being sampled. Both analytic and numerical examples were pursued to illustrate the D-MORPH concept.

C. Future Plans

The research ahead aims to focus on better identifying the principles of quantum control and its future prospects in the laboratory. A key issue is to explain why the experiments work well and why it appears relatively easy to find successful controls in a short laboratory time-scale, despite the involvement of typically hundreds of control phase and amplitude variables in the process. Explaining why quantum control beats the curse of dimensionality should provide insights into the classes of quantum control experiments expected to be most successful in the future. In addition, a host of new questions and issues are now open for study as well, including the general topology of quantum control search landscapes, the effect of spatial and orientation inhomogeneities during control, the relationships between the control of homologous quantum systems, and the feasibility of controlling specific molecular systems. An effort will be undertaken to explore these issues. Finally, new algorithms will be developed to explore the prospects of combining the capabilities of high throughput photonic reagent and chemical reagent machines for optimal performance of controlling molecular dynamics.

D. References

1. Quantum control of ozone isomerization, M. Artamonov, T.-S. Ho, and H. Rabitz, *Chem. Phys.*, **305**, 213-222 (2004).
2. Generalized monotonically convergent algorithms for solving quantum optimal control equations in product spaces, Y. Ohtsuki, G. Turinici, and H. Rabitz, *J. Chem. Phys.*, **120**, 5509 (2004).
3. Efficient extraction of quantum Hamiltonian information from optimal laboratory data, J. M. Geremia and H. Rabitz, *Phys. Rev. A*, **70**, 023804 (2004).
4. Quantum control of molecular motion including electronic polarization effects with two stage toolkit, G. Balint-Kurti, F. Manby, Q. Ren, M. Artamonov, T.-S. Ho, and H. Rabitz, *J. Chem. Phys.*, **122**, 084110 (2005).
5. Observable-preserving control of quantum dynamics and the diffeomorphic exploration of Hamiltonian space, A. Rothman, T.-S. Ho, and H. Rabitz, *Phys. Rev. A*, in press.
6. Efficient algorithms for the laboratory discovery of optimal quantum controls, G. Turinici, C. Le Bris, and H. Rabitz, *Phys. Rev. E*, **70**, 016704 (2004).
7. Mechanism analysis of controlled quantum dynamics in the coordinate representation, R. Sharp and H. Rabitz, *J. Chem. Phys.*, **121**, 4516-4527 (2004).
8. Development of Solution Algorithms for Quantum Optimal Control Equations in Product Spaces, Y. Ohtsuki and H. Rabitz, *Proceedings of CRM*, **33**, (2003).

9. Manipulating bond lengths adiabatically with light, I. R. Sola, B.Y. Chang, and H. Rabitz, *J. Chem. Phys.*, **119**, 10653-10657 (2003).
10. Light-induced trapping of molecular wave packets in the continuum, B.Y. Chang, H. Rabitz, and I. R. Sola, *Phys. Rev. A*, **68**, 031402 (2003).
11. Revealing quantum-control mechanisms through Hamiltonian encoding in different representations, A. Mitra, I. Sol, and H. Rabitz, *Phys. Rev. A*, **67**, 043409-1-9 (2003).
12. Optimal Hamiltonian identification: The synthesis of quantum optimal control and quantum inversion, J.M. Geremia and H. Rabitz, *J. Chem. Phys.*, **118**, 5369-5382 (2003).
13. Quantum Physics Under Control, I. Walmsley and H. Rabitz, *Physics Today*, **56**, 43-49 (2003).
14. Tying the loop tighter around quantum systems, H. Rabitz, *J. Mod. Opt.*, **50**, 2291-2303 (2003).
15. Error bounds for molecular Hamiltonians inverted from experimental data, J.M. Geremia and H. Rabitz, *Phys. Rev. A*, **67**, 022711-1-11, (2003).
16. Reproducing kernel Hilbert space interpolation methods as a paradigm of high dimensional model representations: Application to multidimensional potential energy surface construction, T.-S. Ho and H. Rabitz, *J. Chem. Phys.*, **119**, 6433-6442 (2003).
17. Quasi-classical trajectory calculations on a fast analytic potential energy surface for the reaction, L. Banares, F.J. Aoiz, S.A. Vzquez, T.-S. Ho, and H. Rabitz, *Chem. Phys. Lett.*, **374**, 243-251 (2003).
18. Implementation of a fast analytic ground state potential energy surface for the Reaction, T.-S. Ho, H. Rabitz, F.J. Aoiz, L. Banares, S.A. Vzquez, and L.B. Harding, *J. Chem. Phys.*, **119**, 3063-3070 (2003).
19. Optimal use of time dependent probability density data to extract potential energy surfaces, L. Kurtz, H. Rabitz, and R. de Vivie-Riedle, *Phys. Rev. A*, **65**, 032514-1-11 (2002).
20. A globally smooth ab initio potential surface of the 1 A' State for the reaction, T.-S. Ho, T. Hollebeek, H. Rabitz, S.D. Chao, R.T. Skodje, A.S. Zyubin, and A.M. Mebel, *J. Chem. Phys.*, **116**, 4124-4134 (2002).
21. Multivariate radial basis interpolation for solving quantum fluid dynamical equations, X.-G. Hu, T.-S. Ho, H. Rabitz, and A. Askar, *Comput. Math. Appl.*, **43**, 525-537 (2002).

Coherent Control of Multiphoton Transitions in the Gas and Condensed Phases with Ultrashort Shaped pulses

DOE Grant No. DE-FG02-01ER15143

Marcos Dantus

Department of Chemistry and Department of Physics, Michigan State University, East Lansing MI 48824
dantus@msu.edu

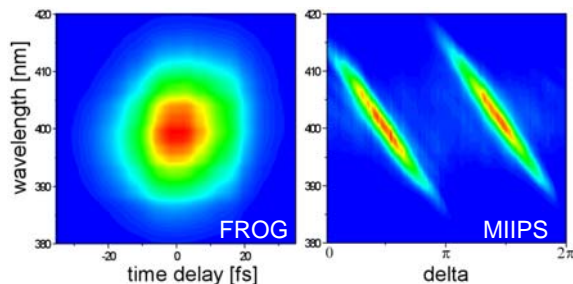
1. Program Scope

Controlling laser-molecule interactions has become an integral part of developing future devices and applications in spectroscopy, microscopy, optical switching, and photochemistry. Coherent control of multiphoton transitions could bring a significant improvement of these methods. In microscopy, multi-photon transitions are used to activate different contrast agents and suppress background fluorescence; coherent control could bring selective probe excitation. In photochemistry, different dissociative states are accessed through two, three, or more photon transitions; coherent control could be used to select the reaction pathway and therefore the yield specific products. There are a number of biomedical applications that range from imaging to photodynamic therapy that could benefit from selective multiphoton excitation. The scope of our research program is to develop the capabilities required for reproducible femtosecond laser pulse shaping, and then to use them as the dreams of coherent control are turned into robust applications.

2. Recent Progress

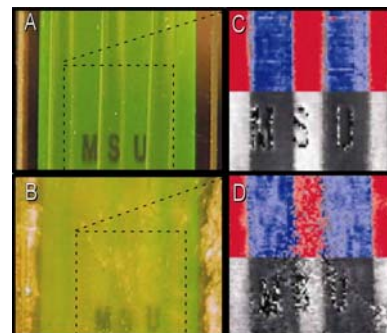
Research on gas phase molecular manipulation focused on photon echo measurements. These measurements were aimed at the manipulation of quantum mechanical states of small isolated molecules. One of the most important impediments for the coherent manipulation of quantum states is decoherence. We measured the femtosecond time-resolved photon echo of electronic coherent relaxation between the $X(^1\Sigma_g^+)$ and $B(^3\Pi_{0u^+})$ states of I_2 in the presence of He, Ar, N_2 , O_2 , C_3H_8 . We found that the cross section for decoherence was greatest between two iodine molecules and it was on the order of 2.2 nm, several times larger than the Van der Waals radius. This finding revealed the very long-range interactions involved in electronic decoherence. We were surprised to find that despite all the degrees of freedom available in propane, its decoherence cross section is similar to that of nitrogen.

Our research on accurate and reproducible pulse shaping led us to the development of multiphoton intrapulse interference phase scan (MIIPS). MIIPS has turned out to be an extremely accurate method for measuring group velocity dispersion introduced by different optics, or the spectral phase of femtosecond pulses. Because MIIPS uses a pulse shaper, it can compensate spectral phase distortions to produce transform limited pulses with time-bandwidth products better than 1.01. We have compared MIIPS to other widely used methods for phase retrieval and MIIPS has been found to be as accurate as SPIDER, much more accurate than FROG, and as accurate as white-light interferometry for measuring group velocity dispersion. MIIPS is now integrated in our laser systems for automatically optimizing the output until it is transform limited, and then carrying out phase shaping projects. The figure on the right shows an SHG FROG trace on the left and a MIIPS scan for the same 18 fs, transform-limited pulses.

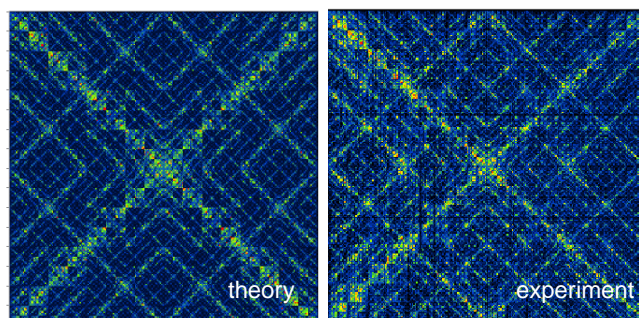


Projects using selective multiphoton excitation on large molecules led us to demonstrate selective two-photon microscopy. In these projects we demonstrated selective excitation of two different chromophores or a single chromophore but in different environments. The latter experiment sparked the idea of using phase shaping for functional imaging. The goal was to use a two-photon active chromophore that was sensitive to a chemical gradient such as pH. We then use phase shaping to control the excitation of the chemically sensitive chromophore. Results from the initial measurements were very encouraging, especially when working with HPTS, a large organic molecule with a pH dependent two-photon cross section spectra that always emits at the same wavelength.

We tested if coherent control methods based on ultrashort pulse phase shaping could be applied when the laser propagates through biological tissue. Our results demonstrated experimentally, for the first time, that the spectral phase properties of shaped laser pulses optimized to achieve selective two-photon excitation survive as the laser pulses propagate through tissue. This observation was used to obtain functional images based on selective two-photon excitation of a pH-sensitive chromophore in a sample that is placed behind a slice of biological tissue. The figure shows two panels on the left with the experimental setup, which consists of three capillary tubes with an acidic solution submerged in an alkaline solution. Both solutions contain HPTS, therefore they are both green. The panels in the bottom have one millimeter of biological tissue in front of the fluorescent sample, and the detector is behind the setup. The panels on the right show functional images displaying the two-photon fluorescent signal obtained with shaped laser pulses. The top half uses false color (red for acidic and blue for alkaline) the bottom half of each panel is in plain black and white. Clearly, the panels on the left show no difference but the panels on the right obtained with shaped pulses show a clear difference based entirely on the response of the pH sensitive chromophore to the differently shaped laser pulses. The observation of coherent control of two-photon excitation through biological tissue made here opens the possibility of selective multiphoton-based biomedical imaging and photodynamic therapy (PDT).



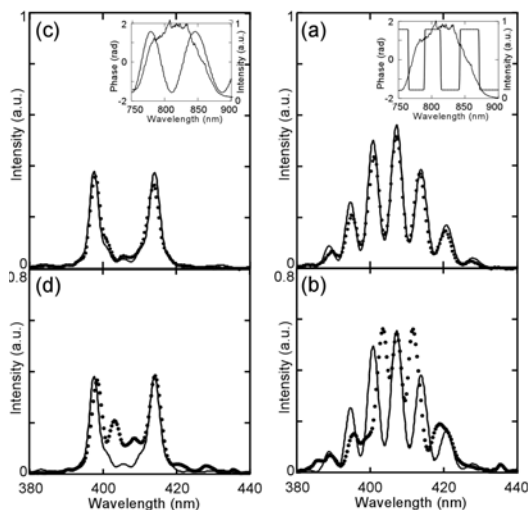
We embarked on a systematic study of the effects of phase shaping on multiphoton transitions. This study primarily focused on selective two-photon excitation, the competition of two- versus three-photon transitions, and on selective CARS excitation. This study (slated to appear shortly in Chem. Phys. Chem.) explores the most efficient methods for controlling multiphoton transitions. Starting from first principles we review a number of different phase functions and conclude with very valuable lessons. The most valuable being that selective excitation requires the pixels of the pulse shaper to take only two phase values, and not a whole range of values as we used to think. Binary phase shaping, when the difference between the two phase values is π , has made a quantum leap in our progress towards controlling multiphoton processes and the design of robust applications using coherent control. Theoretical work in our laboratory has progressed at the same rate as our experiments. We are presently able to calculate optimum phase functions using a computer operating at 3 GHz, and then implement those phase functions in the lab.



We can alternatively make experimental measurements and then simulate them accurately using our theory. To demonstrate our present capabilities we evaluated 2^{16} different 16-bit binary phase functions for their ability to generate SHG intensity at 400 nm within a narrow 0.5 nm spectral width, while keeping the background SHG outside that spectral window to a minimum. The results from that research project are mapped on the left (theoretical prediction on the left and experimental result on the right). The measured figure of merit

ranged from red (factor of 2.5 signal-to-background) to black (factor of 0.5 signal-to-background) in the figures on the left. The systematic evaluation of binary phase functions and mapping the results has now become a standard in our group that we have applied to a number of projects such as the identification of chemical warfare agents.

We subjected the MIIPS method to a number of rigorous tests to determine if it could yield accurately phase shaped pulses in a number of conditions, such as when the beam traverses thick substrates, scattering media, and high numerical aperture microscope objectives. MIIPS performed extremely well in all these tests. For example, the figure on the right shows theoretical prediction (line) and experimental measurement (dots) for two types of phase functions imposed on 12 fs pulses, continuous and binary phase. Notice that we are able to deliver at the sample the



desired phase with remarkable precision (top). When we turn off the MIIPS compensation, the agreement between experiment and theory is lost, demonstrating the importance of being able to deliver accurately shaped pulses at the sample.

3. Future Plans

We are presently setting up a microscope for carrying out selective excitation experiments on single molecules. This project is being carried out in collaboration with Eric Betzig, one of the pioneers in single molecule imaging. The microscope is now ready and we expect to see the first images very soon. The aim of this work is to probe the microchemical environment of these molecules. We hope to explore influences from acidic sites as well as amplification of electric fields by metallic nanoparticles near the chromophore.

We are planning some fundamental work on controlling multiphoton nonlinear optical transitions in the gas phase. The goal is to explore to what extent a single pulse can control the creation of vibronic wave packets with a well defined phase. These experiments will be carried out on iodine, a diatomic molecule with a very well understood spectroscopy in the time and frequency domains.

Finally, we have started experiments that explore the influence of pulse shaping on the interaction between high-intensity laser pulses and bulk matter. These experiments are aimed at enhancing the sensitivity and selectivity of laser-induced breakdown spectroscopy (LIBS). These studies will also provide valuable information about the early dynamic processes. For these experiments we are using amplified and shaped 30 fs pulses. Preliminary results indicate that the LIBS signal has a simple relationship to the total laser intensity; however, the LIBS signal has a very complex relationship to the peak intensity of the shaped pulses. This indicates that the time dependent structure of the binary shaped pulses has a significant effect on the total LIBS signal and in some cases can enhance one atomic emission versus another. The dependence to linear chirp is also interesting and requires further exploration. We will explore the characteristics that enhance or suppress LIBS emission and link the time-dependent features to the early dynamic processes occurring within the first 100 fs of irradiation.

Finally, we have initiated collaboration with the Van Andel Institute to explore the feasibility of selective two-photon excitation PDT. Preliminary experiments have focused on viral neutralization. We have been able to cause 98% viral deactivation while maintaining cell viability. Our goal is to complete the feasibility experiments and then to have this project fully supported by NIH.

Publications Resulting from this Grant 2003-2005:

1. M. Comstock, V. V. Lozovoy and M. Dantus, "Femtosecond photon echo measurements of electronic coherence relaxation between the $X(1\Sigma_g^+)$ and $B(3\Pi_{0u^+})$ states of I_2 in the presence of He, Ar, N_2 , O_2 , C_3H_8 ," J. Chem. Phys. 119, 6546 (2003)

2. V. V. Lozovoy, I. Pastirk, M. Comstock, K. A. Walowicz, and M. Dantus, "Femtosecond four-wave mixing for molecule based computation," Ultrafast Phenomena XIII, Eds. R.J.D. Miller, M. Murnane, N. F. Scherer and A. M. Weiner. Springer-Verlag, Berlin Heidelberg p.97 (2003)

3. V. V. Lozovoy, I. Pastirk, K. A. Walowicz, and M. Dantus, "Multiphoton intrapulse interference II. Control of two- and three-photon laser induced fluorescence with shaped pulses," J. Chem. Phys. 118, 3187, (2003)

4. J. M. Dela Cruz, I. Pastirk, V. V. Lozovoy, K. A. Walowicz and M. Dantus, "Multiphoton Intrapulse Interference 3: probing microscopic chemical environments," J. Phys. Chem. 108, 53 - 58, (2004) Our results were featured in the cover.

5. I. Pastirk, J. M. Dela Cruz, K. A. Walowicz, V. V. Lozovoy, and M. Dantus, "Selective two-photon microscopy with shaped femtosecond pulses", Optics Express, 11, 1695 (2003)



6. V. V. Lozovoy, I. Pastirk, M. Dantus, "Multiphoton intrapulse interference 4; Characterization and compensation of the spectral phase of ultrashort laser pulses", 29, 7, 775-777, *Optics Letters* (2004)
7. M. Dantus, V. V. Lozovoy, I. Pastirk, "Measurement and Repair: The femtosecond Wheatstone Bridge", *OE Magazine* 9 (September) 15, (2003)
8. J. Dela Cruz, I. Pastirk, V.V. Lozovoy, K.A. Walowicz, and M. Dantus, "Control of nonlinear optical excitation with multiphoton intrapulse interference," *Ultrafast Molecular Events in Chemistry and Biology*, M. M. Martin and J.T. Hynes Eds. Elsevier (2004)
9. V.V. Lozovoy, M. Comstock, I. Pastirk, and M. Dantus, "Femtosecond Photon Echo Measurements of Electronic Coherence Relaxation of I₂ in the presence of He, Ar, N₂, O₂, C₃H₈," *Ultrafast Molecular Events in Chemistry and Biology*, M. M. Martin and J.T. Hynes Eds. Elsevier (2004)
10. M. Dantus and V.V. Lozovoy, "Experimental Coherent Laser Control of Physicochemical Processes", *Chem. Reviews*, Special Issue on Femtochemistry, A. H. Zewail and M. Dantus Eds. 104, 1813-1860, (2004)
11. M. Comstock, V. V. Lozovoy, I. Pastirk, and M. Dantus, "Multiphoton intrapulse interference 6; binary phase shaping", 12, 6, 1061-1066, *Optics Express* (2004)
12. V. V. Lozovoy and M. Dantus, "Systematic control of nonlinear optical processes using optimally shaped femtosecond pulses," *Chem. Phys. Chem.* Invited Review, in press (2005)
13. J. M. Dela Cruz, I. Pastirk, M. Comstock, and M. Dantus, "Coherent control through scattering tissue, Multiphoton Intrapulse Interference 8," *Optics Express*, 12, 4144 (2004)
14. J. M. Dela Cruz, I. Pastirk, M. Comstock, V. V. Lozovoy, and M. Dantus, "Use of coherent control methods through scattering biological tissue to achieve functional imaging", *Proceedings of the National Academy of Sciences USA* 101, 16996-17001 (2004)
15. B. Xu, J. M. Gunn, J. M. Dela Cruz, V. V. Lozovoy, M. Dantus, "Quantitative investigation of the MIIPS method for phase measurement and compensation of femtosecond laser pulses," *J. Optical Society B*, (submitted March 2005).

Theory and Simulations of Nonlinear X-Ray Spectroscopy of Molecules

Shaul Mukamel

Department of Chemistry
University of California, Irvine
Irvine, CA 92697-2025
Email: smukamel@uci.edu

A correlation function formalism for computing combined x-ray/optical and all-x-ray nonlinear signals was developed. Time-resolved sum frequency generation(SFG) was calculated for a one-dimensional molecular chain. The second order nonlinear polarization induced by two radiation fields, an optical light pulse with a wave vector \mathbf{k}_1 and a x-ray pulse with a wave vector \mathbf{k}_2 , is predicted with variable time delay between the pulses. By tuning the x-ray frequency to the core excitation of a particular atom, a valence exciton wave packet motion can be launched and probed at the targeted atomic site. The technique provides real-time, real-space snapshots of the valence-exciton motion induced by the first optical light pulse with atomic scale precision.[9]

A code for computing time resolved XANES spectra from photoexcited molecules was developed. The L_3 edge X-ray Absorption Near Edge Spectrum (XANES) of the ground electronic state and the metal to ligand charge transfer state of ruthenium tris-2,2'-bipyridine was calculated. The final valence states and energies in the presence of the photoelectron and core hole, and the corresponding transition intensities were computed using Time Dependent Density Functional Theory (TDDFT)[8]. Calculations show a valence shift of the primary XANES peak and the appearance of the new XANES transition to the hole created by the optical excitation, in agreement with experiment. Simulated excited state XANES (optical pump x-ray probe) of benzonitrile (BCN) (Nitrogen K-edge) give the splitting between the first two resonances to be 1.0 eV, in excellent agreement with experiment and other theories. Ongoing simulations focus on the x-ray emission spectra of optically excited BCN.

Spectral features in the oxygen K-edge XANES spectra of water are at the center of a current controversy.[1] Neutron and x-ray diffraction experiments have measured the mean and deviations of inter-atomic distances in liquid water, but its instantaneous angular structure at room temperature is still unknown. A narrow pre-edge feature present in bulk water and absent in ice has been attributed to the presence of a broken hydrogen bond on the absorbing oxygen. Ratios of edge intensities were taken to imply that a water molecule in the liquid phase is connected to its neighbors by an average of 2.2 hydrogen bonds. This is in marked contrast to the near tetrahedral arrangement of water hydrogen bond networks predicted by almost all force field models used today. Models for XANES line broadening due to hydrogen bonding fluctuations are being developed. The ground state XANES and emission spectra of a water molecule were simulated(Fig. 1). The excited state calculations were performed at the time-dependent Hartree-Fock (TDHF) level. We find a peak splitting of 1.92 eV, in very good agreement with the experimental value of 1.90 eV. Calculations using Stobe and CPMD predict 1.83 eV and 2.04 eV respectively. Our future goal is to simulate how the XANES spectrum of a water molecule changes under the electric field of the neighbouring molecules. A similar molecular dynamics strategy was successfully employed for the OH stretch of water in the infrared. [2]

The development of bright attosecond sources for soft and hard x-rays has triggered considerable interest in all-x-ray nonlinear spectroscopy. In resonant optical techniques in the visible the light is tuned to high frequency ($\sim 2\text{eV}$) electronic transitions. However, a wealth of information is provided on nuclear (vibrational and phonon), degrees of freedom with much lower frequencies

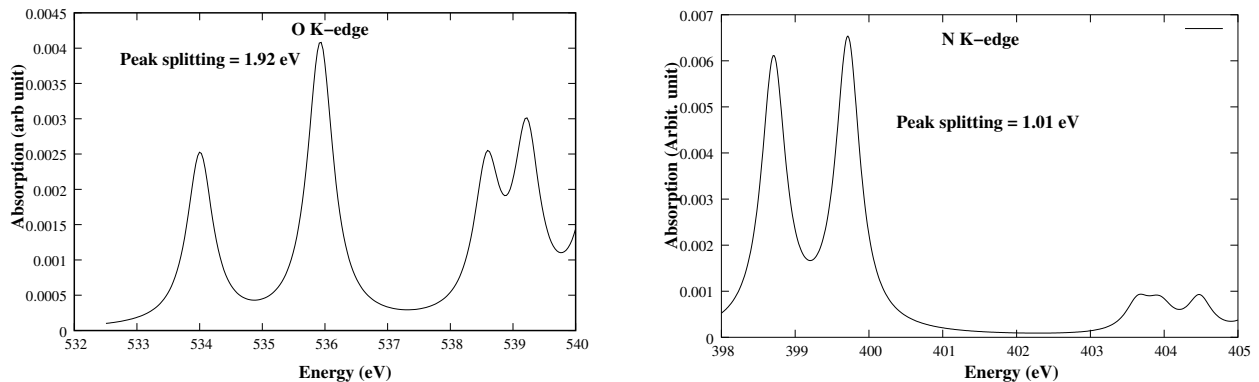


FIG. 1: Calculated X-ray absorption near edge spectrum (XANES) of water(left) and the benzonitrile(right).

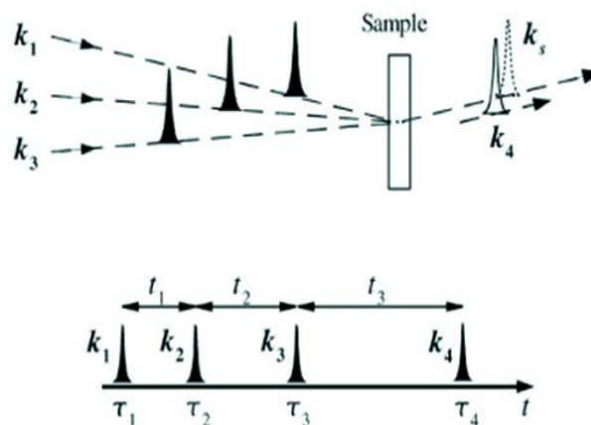


FIG. 2: Pulse sequence corresponding to an X-ray four wave mixing experiment.

(< 0.4eV) which are accessible through *multiphoton* (e.g. Raman-type) resonances with differences (and higher combinations) of visible photons. In a completely analogous manner, combinations of x-ray photons, resonant with high frequency (keV) core transitions can probe the lower frequency (< 50eV) electronic valence excitations. By exploiting this analogy, we can use the theoretical apparatus developed for optical transitions, to predict nonlinear x-ray signals and design new coherent experiments. For example, multidimensional techniques which provide extremely valuable information on optical excitons in molecular aggregates can be extended to probe correlations among multiple core hole states. Displaying the signals as a function of the time delays t_1 , t_2 and t_3 provides correlation plots of valence electron wavepackets related to charge density fluctuations.

Correlation function expressions are derived for the coherent response of molecules to three resonant ultrafast pulses in the x-ray regime (Fig. 2). The ability to create two-core-hole states with controlled attosecond timing provides new windows into the response of valence electrons, which are not available from incoherent x-ray Raman and fluorescence techniques. Multiple core-hole coherence can be probed in x-ray four-wave-mixing spectroscopies.

The multipoint correlation functions may be calculated using several levels of theory. (i) Multiple summations over the many electron states of the valence system with N , $N + 1$, and $N + 2$

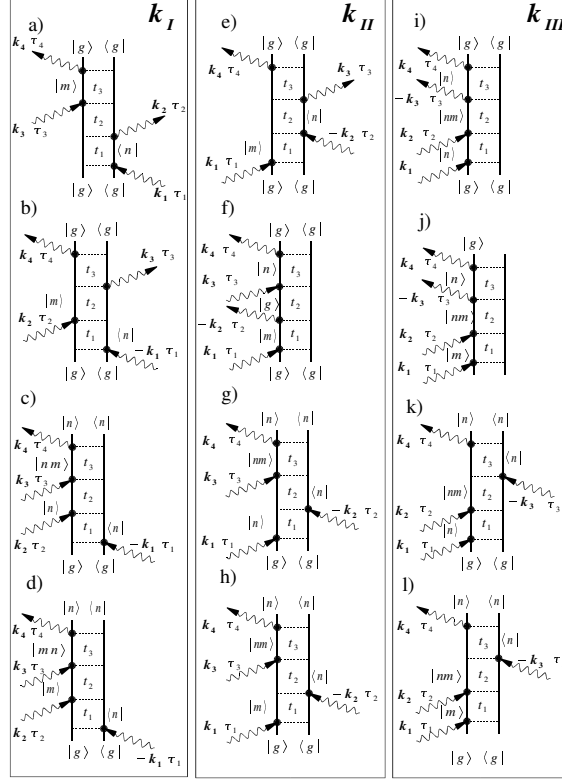


FIG. 3: Double-sided Feynman diagrams representing the Liouville-space pathways contributing to the third-order response in the rotating wave approximation. Shown are the diagrams contributing to the four-wave mixing signal generated along the various possible directions: $\mathbf{k}_I = -\mathbf{k}_1 + \mathbf{k}_2 + \mathbf{k}_3$, $\mathbf{k}_{II} = \mathbf{k}_1 - \mathbf{k}_2 + \mathbf{k}_3$, and $\mathbf{k}_{III} = \mathbf{k}_1 + \mathbf{k}_2 - \mathbf{k}_3$. Diagrams (a), (b), (e), and (f) only include one-exciton states. All other diagrams also involve two-exciton states.

electrons in the presence of zero, one and two core holes respectively. (ii) The transition state potential method which uses a reference system with partially filled orbitals[3]. (iii) Many body Green function perturbative techniques[4]. (iv) Replacing the original model by an Electron Boson Model (EBM) for charge density fluctuations. [5]

Method (i) is the simplest conceptually but the most expensive numerically. The sum over state (SOS) expressions allow us to employ any level of quantum chemistry for computing electronically excited states. TDDFT, for example, provides a relatively efficient way for computing a large number of electronically excited states. The relevant states are determined by the pulse bandwidth. e.g. 375eV for a 10as pulse. Method (ii) Calculates only one set of orbitals and represents systems with different numbers of core holes by different occupation numbers. This approximate method works well for core level spectroscopies of small molecules, and may be extended to nonlinear response. Method (iii) Was used by Nozieres and coworkers to compute XANES and x-ray Raman spectra starting with the deep-core Hamiltonian. It is formally exact, but allows the development of powerful approximations.

The EBM is by far the simplest to implement since it is exactly solvable. The slow response of an active space of valence electrons to an instantly switched core hole, was calculated. Closed expressions for four-wave-mixing, fluorescence and the pump probe signals are derived by starting

with the electron-boson model for the fluctuating potentials. The additional information obtained from the nonlinear response could be used to test the validity of the electron-polaron picture and refine its Hamiltonian. The valence electrons relax in the field of the core-hole in hundreds of attoseconds to femtoseconds. By treating the core hole potential as a switchable perturbation, the time evolution in the interaction picture was calculated by the second order cumulant expansion for the valence electron degrees of freedom. Valence excitations are treated as quasiboson oscillators. This approach has been used successfully in the past for optical excitations; the model is analogous to the response of a nuclear wavepacket to electronic excitations in optical spectra.

Nonlinear core-hole spectroscopy provides new windows into electronic valence excitations. By controlled attosecond switching of external potentials, it could help develop more realistic anharmonic hamiltonians for the core-valence couplings, and test the validity of approximate model Hamiltonians.

-
- [1] Ph. Wernet, et. al., *Science* 304, 995 (2004); J. D. Smith, et. al., *Science* 306, 851 (2004)
 - [2] T. Hayashi, T. Jansen, W. Zhuang, S. Mukamel, *J. Phys. Chem. A*, 109 64-82 (2005).
 - [3] A. R. Williams, R. A. deGroot and C. B. Summers, *J. Chem. Phys.* 63(2) 628 (1975)
 - [4] P. Nozières and C. T. DeDominicis, *Phys. Rev.* 178(3) 1097 (1969)
 - [5] D. C. Langreth, *Phys. Rev.* **182**(3), 973 (1969)
 - [6] Mukamel, S. *Principles of Nonlinear Optical Spectroscopy*; Oxford University Press: New York, (1995)
 - [7] Mukamel, S.; Abramavicius D. *Chem. Rev.* **104**, 2073 2004

Publications Resulting from the Project

- [8] "Simulation of x-ray absorption near edge spectra of electronically excited ruthenium tris-2,2'-bipyridine," S. Mukamel and L. Campbell, *J. Chem. Phys.* 121(24), (2004)
- [9] "Simulation of Optical and X-ray Sum Frequency Generation Spectroscopy of 1-dimensional Molecular Chain," S. Tanaka and S. Mukamel, *J. Electron Spectrosc. Relat. Phenom.* 136,185 (2004)
- [10] S. Mukamel, "Multiple Core-Hole Coherence in X-Ray Four-Wave-Mixing Spectroscopies," (in preparation) (2005)
- [11] "Superoperator Many-body Theory of Molecular Currents:Non-equilibrium Green Functions in Real Time, U. Harbola and S. Mukamel in *Theory and Applications of Computational Chemistry: The First 40 Years*". (Editors) C. E. Dykstra, G. Frenking, K. S. Kim and G. E. Scuseria, Elsevier, (2005) (In Press)
- [12] "Simulation of Optical and X-ray Sum Frequency Generation Spectroscopy of 1-dimensional Molecular Chain," S. Tanaka and S. Mukamel, *J. Electron Spectrosc. Relat. Phenom.* 136, 185 (2004).
- [13] "Simulation of x-ray absorption near edge spectra of electronically excited ruthenium tris-2,2'-bipyridine," S. Mukamel and L. Campbell, *J. Chem. Phys.* 121(24), (2004).
- [14] "Ligand Effects on the X-ray Absorption of a Nickel Porphyrin Complex," L. Campbell, S. Tanaka, and S. Mukamel, *Chem. Phys.* 299, 225-231 (2004).
- [15] "Probing Exciton Dynamics Using Raman Resonances in Femtosecond X-Ray Four Wave Mixing" S. Tanaka and S. Mukamel, *Phys. Rev. A.* 67, 033818 (2003).
- [16] "Nonlinear Response of Classical Dynamical Systems to Short Pulses", C. Dellago and S. Mukamel, *Bull. Kor. Chem. Soc.* 24, 1097-1101 (2003).
- [17] "A Mechanical Force Accompanies FRET" A. Cohen and S. Mukamel, *J. Phys Chem. B.*, 107, 3633-3638 (2003).
- [18] "One-dimensional Transport with Dynamic Disorder" V. Barsegov, Y. Shapir and S. Mukamel, *Phys. Rev. E.* 68, 011101 (2003).
- [19] "Multipoint Fluorescence Quenching Time Statistics for Single Molecules with Anomalous Diffusion", V. Barsegov and S. Mukamel, *J. Phys. Chem.*, 108, 15-24 (2004).

Nonlinear Photoacoustic Spectroscopies Probed by Ultrafast EUV Light

Keith A. Nelson

Department of Chemistry, Massachusetts Institute of Technology
Cambridge, MA 02139
Email: kanelson@mit.edu

Henry C. Kapteyn, Margaret M. Murnane

JILA, University of Colorado and National Institutes of Technology
Boulder, CO 80309-0440
E-mail: kapteyn@jila.colorado.edu, murnane@jila.colorado.edu

Program Scope

This project is aimed at direct spectroscopic access to mesoscopic (nanometer) length scales and ultrafast time scales in condensed matter, with the objective of revealing the length scales associated with dynamical events in condensed matter. The primary effort in the project is directed toward nonlinear time-resolved spectroscopy with coherent soft x-ray, or extreme ultraviolet (EUV), wavelengths. Time-resolved four-wave mixing, or transient grating, measurements are conducted in order to directly define an experimental length scale as the interference fringe spacing formed by two crossed excitation pulses.[1] Dynamics are recorded through measurement of time-resolved coherent scattering, or diffraction, of probe pulses from the induced grating pattern. Measurements of the dynamical responses at various transient grating fringe spacings (i.e. grating wavevectors) provide both correlation length and time scales for the processes under study. For most complex materials, especially those in which dynamical responses span a wide range of time scales (e.g. polymer relaxation dynamics, dipole or spin glass polarization or magnetization dynamics, etc.), we know little about the correlation length scales involved or whether there is a range of correlation lengths with a well defined correspondence to the multiscale correlation times. For example, it is far from clear whether the faster and slower components of polymer relaxation dynamics should be associated with motions on shorter and longer lengths scales (e.g. molecular end groups and segments or whole molecules) respectively. It is tempting to imagine such an association, but the intuitive connection is challenged by the fact that nearly identical multiscale and temperature-dependent dynamics are observed in supercooled liquids composed of small molecules, aqueous solutions, and atomic ions, none of which have extended structural elements but which may still have long correlation lengths. In these and many other complex condensed matter systems, direct experimental measurements of length and time scales are needed for elucidation of the underlying mechanisms of dynamical processes.

Continued progress in high harmonic generation [2] has yielded femtosecond soft x-ray pulses with nanojoule energies and excellent spatial coherence and focusability. The possibility of intensity levels comparable to those used in much of condensed matter nonlinear spectroscopy encourages the effort to extend the spectroscopic methods to EUV wavelengths. EUV transient grating measurements would provide fringe spacings in the range of a few tens of nanometers, permitting direct assessment of condensed matter correlation lengths that are almost all in the mesoscopic range. These correlation lengths have eluded study with optical wavelengths, since the shortest transient grating fringe spacing is on the order of the wavelength.

The initial experiments are aimed at generation and time-resolved detection of acoustic waves whose wavelength and orientation match those of the transient grating pattern. Optical absorption of the crossed excitation pulses gives rise to spatially periodic heating and thermal expansion which launches the acoustic response. [1] Acoustic wave characterization permits direct determination of structural relaxation time scales τ that are a significant fraction of the acoustic oscillation period, i.e. acoustic absorption is maximized when $\omega\tau = 1$ where ω is the acoustic frequency. It also permits assessment of correlation length scales d , i.e. acoustic scattering increases dramatically as $qd \rightarrow 1$ where $q = 2\pi/\Lambda$ is the acoustic wavevector magnitude and Λ the acoustic wavelength. Transient grating measurements with optical wavelengths have permitted study of acoustic waves with wavelengths in the micron range and frequencies in the MHz range. With soft x-ray wavelengths, acoustic waves with wavelengths of a few tens of nanometers and frequencies in the 100-GHz range can be reached. This provides access to picosecond structural relaxation dynamics and nanometer structural correlation lengths in a wide range of complex materials. In polymers and other glass-forming liquids, the full range of relaxation dynamics obtained through EUV and optical experiments permits direct determination of multiscale relaxation dynamics across a very wide range, and the connections between these and nanometer correlation lengths will be tested. High-frequency acoustic wave characterization also offers a wide range of potential practical application including determination of thin film properties such as modulus and thickness.

Strong absorption of EUV wavelengths at bulk material surfaces leads to the generation of surface acoustic waves whose characterization will yield dynamic shear and longitudinal modulus properties at ultrahigh frequencies. A parallel set of experiments has been undertaken to extract a subset of this information, the longitudinal component, for some materials including those that can be deposited as thin films. In these measurements, a thin metal film is irradiated by a sequence of femtosecond optical pulses, and temporally periodic thermal expansion of the film launches an acoustic wave into and through an underlying material layer and a second metal film. The acoustic frequency is given by the repetition rate of the optical pulse sequence. The acoustic wave is detected optically upon reaching the back of the sample. This approach resembles traditional ultrasonics, with photoacoustic rather than piezoelectric transducers. It is not as generally applicable as the EUV transient grating method because of its demands for specialized sample fabrication and the need for acoustic wave propagation through the sample, but for those materials that are amenable, this approach provides a useful segue to the EUV measurements.

Recent Progress

The EUV effort at probing high-frequency acoustic waves has made three advancements to date: 1) we obtained the first experimental data demonstrating transient grating excitation of structured surfaces using EUV high-harmonic radiation as a probe; 2) we demonstrated up to 2 orders of magnitude increased sensitivity in the EUV compared with visible laser probes; and 3) we demonstrated the use of EUV light as a probe of a uniform material excited in a transient grating set-up that measured the acoustic dispersion of thin films. The first two achievements have been reported recently and all three measurements are the first of their kind. [3,4]

The third advance was achieved with a new apparatus that allows optical excitation pulses to be passed through a transparent substrate and crossed at the back of a thin film sample, thereby generating surface acoustic waves that propagate laterally in the film, and allows an EUV probe pulse to be directed to the front of the sample and diffracted by the acoustic waves.

This versatile arrangement allows for excitation with range of optical wavelengths and geometries, i.e. with different angles between the excitation beams to produce different interference fringe spacings and corresponding acoustic wavelengths. The time-dependent diffraction shows acoustic oscillations whose frequencies yield the thin film acoustic waveguide mode dispersion characteristics from which film properties may be extracted. This work is of interest both for basic science and as a potential diagnostic for micro-fabricated structures. It is broadly applicable to a wide range of patterned or unpatterned materials.

The parallel approach to ultrahigh-frequency acoustic wave generation, involving irradiation of the sample with a sequence of femtosecond pulses, required development of a novel femtosecond pulse shaping method involving multiple traversal of an incident laser pulse around a recirculating reflective system, with partial transmission yielding an output pulse each time around. The time interval between successive pulses is adjusted by movement of a single delay stage that carries two of the four 90-degree reflectors in the recirculating system, permitting pulse repetition rates throughout the GHz range. Generation of tunable acoustic waves in thin metal films, with acoustic frequencies up to about 400 GHz, was demonstrated. These results have been reported recently. [5,6]

The first spectroscopic measurements using this approach have been conducted on amorphous silica layers in the 100-1000 nm thickness range. [7] Acoustic waves at frequencies up to 300 GHz, corresponding to wavelengths down to about 20 nm, were generated in a 20-nm aluminum film on one side of the silica sample and detected interferometrically at the back of another 20-nm aluminum layer on the other side of the silica. Note that these were not surface acoustic waves propagating laterally across the sample, as in the case described above, but longitudinal waves propagating through the sample, from front to back. Strong scattering of the acoustic waves due to inherent nanometer-scale structural heterogeneity in the glass was characterized. The wavelength-dependence of the scattering strength permitted comparison of the results to contrasting models of amorphous solid structural correlation lengths.

Future Plans

Transient grating measurements are being conducted with progressively shorter excitation pulse wavelengths and interference fringe spacings, permitting generation of acoustic waves with correspondingly shorter wavelengths and higher frequencies, in regions not accessible using visible wavelength probes. The submicron acoustic wavelengths already being produced will be useful for measurements on phononic bandgap materials which show strongly wavelength-dependent acoustic transmission and filtering. Measurements will be conducted as a function of acoustic wavelength and as a function of acoustic wave orientation relative to the symmetry directions of the periodic structure.

Multiple-pulse photoacoustic measurements on silica glass will be conducted at various sample temperatures to assess whether there are important dynamical contributions to acoustic attenuation in the 100-GHz frequency range, as suggested by some models. Other types of glasses including metallic, polymer, and small-molecule glasses also will be examined to compare the mesoscopic correlation lengths in different amorphous material types. Preliminary results from very thin (~ 40 nm) liquid samples have been recorded, and attempts will be made to conduct temperature-dependent measurements in order to elucidate compressional dynamics of supercooled liquids over a wide frequency range.

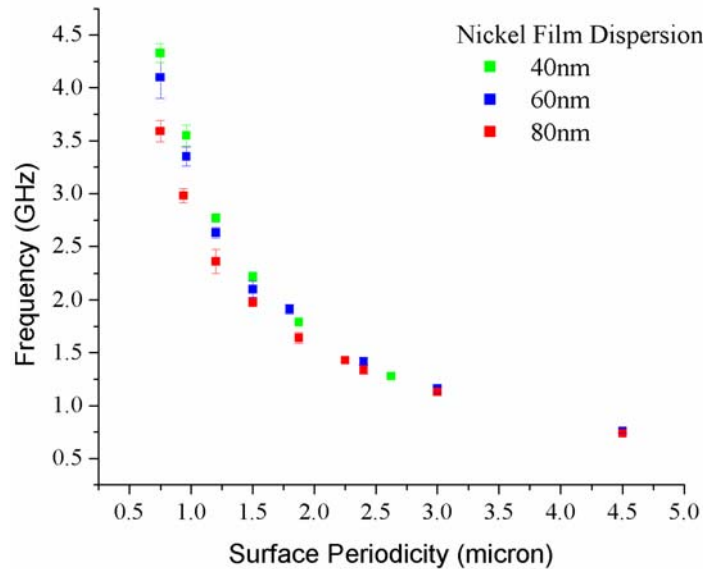


Figure 1: Measurement of the acoustic dispersion for different Ni film thickness of 40nm, 60nm and 80nm using EUV light. Each data point is a 20 minute scan. At large values of the surface periodicity, all the films have similar acoustic dispersion, indicating that the excitation extends deep into substrate, However, for smaller periodicities, the measurements diverge, indicating that the acoustic excitation is increasingly localized in the film.

References

1. "Impulsive stimulated light scattering from glass-forming liquids: I. Generalized hydrodynamics approach; II. Salol relaxation dynamics, nonergodicity parameter, and testing of mode coupling theory," Y. Yang and K.A. Nelson, *J. Chem. Phys.* **103**, 7722-7731; 7732-7739 (1995).
2. "Phase-matched generation of coherent soft-x-rays," A. Rundquist, C. Durfee, Z. Chang, S. Backus, C. Herne, M. M. Murnane and H. C. Kapteyn, *Science* **280**, 1412 – 1415 (1998).
3. "Nanoscale photothermal and photoacoustic transients probed with extreme ultraviolet radiation," R.I. Tobey, E.H. Gershgoren, M.E. Siemens, M.M. Murnane, H.C. Kapteyn, T. Feurer, and K.A. Nelson, *Appl. Phys. Lett.* **85**, 564-566 (2004).
4. "Probing of thermal acoustic transients in materials using EUV radiation," R. I. Tobey E. Gershgoren, M. Siemens, M. Murnane, H. Kapteyn, T. Feurer, K. Nelson, in *Ultrafast Phenomena XIV*, T. Kobayashi, T. Okada, T. Kobayashi, K. A. Nelson, and S. D. Silvestri, Eds. (Springer-Verlag, Berlin 2005), pp. 239-241.
5. "Ultrahigh frequency acoustic phonon generation and spectroscopy with Deathstar pulse shaping," J.D. Beers, M. Yamaguchi, T. Feurer, B.J. Paxton, and K.A. Nelson, in *Ultrafast Phenomena XIV*, T. Kobayashi, T. Okada, T. Kobayashi, K.A. Nelson, and S. De Silvestri, eds. (Springer-Verlag, Berlin 2005), pp. 236-238.
6. "Generation of ultrahigh frequency tunable acoustic waves," J. D. Choi, T. Feurer, M. Yamaguchi, B. Paxton, and K. A. Nelson, *Appl. Phys. Lett.*, in press (2005).
7. "Direct observation of multiple-cycle ultrahigh-frequency acoustic wave propagation through amorphous silica," J.D. Choi, T. Feurer, M. Yamaguchi, B. Paxton, K. Katayama, and K.A. Nelson, in preparation (2005).

Femtosecond X-ray Beamline for Studies of Structural Dynamics

Robert W. Schoenlein

Materials Sciences Division
Lawrence Berkeley National Laboratory
1 Cyclotron Rd. MS: 2-300, Berkeley, CA 94720
rwschoenlein@lbl.gov

Roger W. Falcone (co-PI)

Physics Department, University of California, Berkeley
rwf@physics.berkeley.edu

Background and Program Scope

A fundamental challenge in condensed matter research is to understand the dynamic interplay between electronic structure (energy levels, charge distributions, bonding, spin) and atomic structure (coordination, bond distances, atomic arrangements). X-rays are ideal probes of atomic structure, and they also offer important advantages for probing electronic structure via transitions from element-specific core levels with well-defined symmetry. A new frontier in x-ray research is the application of x-ray structural probes on the fundamental, ultrafast time-scales of atomic vibrational periods, electron-phonon, and electron-electron interactions. Such studies are important for understanding chemical reaction dynamics (formation/dissolution of bonds, conformational changes), phase transitions in solids (involving atomic structure and/or electronic properties), and complex systems in which atomic and electronic degrees of freedom are strongly correlated.

The development of ultrafast x-ray science to date has been limited by the lack of suitable tunable x-ray sources for probing structural dynamics on the femtosecond time scale. This research program is based on a novel technique for generating ~ 100 fs x-ray pulses from a synchrotron storage ring by using femtosecond optical pulses to modulate the energy (and time structure) of a stored electron bunch. The scope of this program includes the development of a simple femtosecond bend-magnet beamline (and associated time-resolved detection and measurement techniques) to serve as a proving ground for time-resolved x-ray science incorporating femtosecond laser systems and end stations suitable for x-ray diffraction, EXAFS, XANES, and photoionization.

An important component of this research program is the development of scientific applications using ultrafast x-rays. Initial research focuses on three main areas: (1) ultrafast atomic and electronic phase transitions in crystalline materials, (2) light-induced structural changes in solvated molecules, and (3) x-ray interactions with atoms in the presence of strong laser fields (see A. Belkacem et al. AMOS abstract). This basic research component of the program will expand significantly with the pending completion of a femtosecond undulator-based beamline at the Advanced Light Source, providing $\sim 10^3$ increase in average femtosecond x-ray flux.

Recent Progress

Ultrafast Soft X-ray Spectroscopy of Correlated Materials

The first femtosecond spectroscopy measurements using synchrotron radiation have been demonstrated this past year. Scientific applications have focused on time-resolved

XANES measurements in the model correlated electron system VO₂. The goal of this research is to understand the relationship between electronic structural changes and atomic structural changes associated with the photo-induced insulator-metal transition. Femtosecond absorption measurements have been made at the V L-edge near 516 eV (probing the correlated *d*-bands from V-2*p* states) and at the O K-edge near 531 eV (probing hybridized *p*-bands from O-1*s* states). At the V L-edge, we observe an ultrafast transient bleach associated with the photo-excitation of electrons into unoccupied *d*-band states. As the carriers thermalize, we observe a long-lived absorption due to the collapse of the band-gap and formation of the metallic state. Complementary behavior is observed at the O K-edge in which a transient absorption indicates the photo-excitation of holes in the *p*-bands. At very early times, we observe evidence of a core-level shift of the O-1*s* level due to a transient increased valency of the O²⁻ anion resulting from photoexcitation.

Time-resolved XAS of Solvated Transition-Metal Complexes

Time-resolved x-ray absorption (XAS) measurements have been made of the spin-crossover reaction in solvated transition-metal complexes. The goal is to quantify the dynamic changes in the ligand bond distance and understand their role in facilitating the ultrafast the spin transition. XAS measurements were made on the spin-crossover complex [Fe(tren(py)₃)](PF₆)₂, dissolved in acetonitrile. Static XAS measurements, at the Fe K-edge, on the low-spin parent compound and a high-spin analog, [Fe(tren(6-Me-py)₃)](PF₆)₂, reveal distinct spectroscopic signatures for the two spin states in the x-ray absorption near edge structure (XANES) and in the x-ray absorption fine structure (XAFS). For the time-resolved studies, 100 fs pulses at 400 nm are used to initiate a charge transfer transition in the low spin complex. The subsequent electronic and geometric changes associated with the formation of the high-spin excited state are probed with 70 ps x-ray pulses tunable near 7.1 keV. Modeling of the transient XAS data reveals that the average Fe–N bond is lengthened by 0.21±0.03 Å in the high-spin excited state relative to the ground state, and that the bond dilation occurs within 70 ps. This structural modification causes a change in the metal-ligand interaction reflected by the altered density of states of the unoccupied metal orbitals. Our results constitute the first direct measurements of the dynamic atomic and electronic structural rearrangements occurring during a photo-induced Fe(II) spin crossover reaction in solution.

Ultrafast X-ray Beamline Development

We have made the first observation of coherent synchrotron radiation in the infrared region, consisting of a single-cycle pulse at ~100 μm. This is a direct result of the ultrafast time structure created in the long electron bunch by the femtosecond optical pulse. Based on this, we have developed a new diagnostic to monitor the interaction between the laser and electron beam.

Significant improvements have been made in the capability for generating femtosecond x-rays during normal user operation of the Advanced Light Source. A modified wiggler was installed in the storage ring and commissioned to provide for efficient femtosecond laser modulation of the stored electron beam, while simultaneously providing x-rays for protein crystallography beamlines. Previously, these two uses of the wiggler were mutually exclusive, significantly limiting the availability of femtosecond x-rays

Finally, significant progress has been made in the design, prototyping, and testing of a gated x-ray detector with nanosecond gating capability and high detection efficiency. This

design incorporates a grazing-incidence photocathode providing near-unity quantum efficiency for both hard and soft x-rays. This is critical in order to isolate a single bunch (for time-resolved measurements) during the common multi-bunch fill pattern at the ALS. This detector will also serve as an ultrafast x-ray streak camera, at somewhat lower quantum efficiency. A camera of similar design has demonstrated single-shot temporal resolution of ~500 fs by illuminating the photocathode with 60 fs pulses at 266 nm. In accumulating mode, a resolution of ~1 ps was observed integrating at 1 kHz for 1 sec.

Future Plans

A new undulator-based ultrafast x-ray beamline is now nearing completion at the ALS. The beamline will consist of a 1.5 T undulator/wiggler providing femtosecond x-rays for two branchlines: a soft x-ray branchline operating in the 0.3-2 keV range, and a hard x-ray branchline operating in the 2-10 keV range. The soft x-ray branchline will include a spectrograph providing <1 eV resolution for single-wavelength experiments, and ~100 eV bandwidth for dispersive spectroscopic measurements. The hard x-ray branchline will include a double-crystal monochromator providing ~2 eV resolution. The beamlines will include a high repetition rate (20 kHz) femtosecond laser system with an average power of ~50 W. The average flux from this beamline is expected to be $\sim 10^7$ ph/sec/0.1% BW (with roughly 100x increase in flux from the insertion device relative to the current bend-magnet, and another 10x increase over the present laser repetition rate). The beamline will provide ~200 fs duration x-ray pulses for a wide range of experiments in ultrafast x-ray science.

Completion of the soft x-ray branchline will enable XANES studies of correlated materials. Initial experiments will focus on complete spectral characterization of VO₂, building on the initial ultrafast x-ray spectroscopy from the bend-magnet beamline. The objective is to understand the dynamic evolution of the electronic bands associated with the insulator-metal transition, and the relative contributions and time scales for *d*-band shifting, band filling, and core-level edge shifts. In the future, these studies will be extended to phase transition dynamics and critical phenomena in more complex correlated systems such as manganites.

Completion of the hard x-ray branchline will enable femtosecond EXAFS measurements to quantify the atomic structural changes in VO₂ (particular V-O bonding) and other correlated materials following non-adiabatic photo-doping. Time-resolved EXAFS of solvated molecules will focus initially on transition-metal spin-crossover complexes. With femtosecond resolution, we can directly probe the dynamic distortion of the ligand bonds and begin to understand how the atomic structural dynamics are correlated with the electronic spin dynamics. EXAFS studies of photodissociation in Co-based metal carbonyls will be used to understand the transient solvent substitution in the intermediate molecular structures.

Two material systems of interest for ultrafast x-ray diffraction studies on the new beamline are ferroelectrics, and transition-metal organic crystals. In the ferroelectric LiTaO₃, the goal is to quantify the atomic displacement and relate this to anharmonicity and mode softening near the ferroelectric transition. In the linear-chain transition-metal molecular complex [Pt(C₂H₈N₂)₂I₂][Pt(CN)₄], the goal is to understand the coherent Pt-I vibration (Peierls distortion) associated with photoexcitation and subsequent formation of the self-trapped exciton.

Publications from DOE Sponsored Research (2002-2005)

- A. Staudte, C.L. Cocke, M.H. Prior, A. Belkacem, C. Ray, H.H.W. Chong, T.E. Glover, R.W. Schoenlein, and U. Saalman, "Observation of a nearly isotropic, high-energy Coulomb explosion group in the fragmentation of D_2 by short laser pulses," *Phys. Rev. A*, **65**, 2002.
- T.E. Glover, G.D. Ackermann, A. Belkacem, P.A. Heimann, Z. Hussain, H.A. Padmore, C. Ray, R.W. Schoenlein, and W.F. Steele, "Kinetics of cluster formation during femtosecond laser ablation," **Ultrafast Phenomena XIII**, R.D. Miller, M.M. Murnane, N.F. Scherer, A.M. Weiner, Eds., Springer-Verlag, p 42, (2002).
- T.E. Glover, G.D. Ackerman, A. Belkacem, P.A. Heimann, Z. Hussain, R.W. Lee, H.A. Padmore, C. Ray, R.W. Schoenlein, W.F. Steele, and D.A. Young, "Metal-insulator transitions in an expanding metallic fluid: particle formation kinetics," *Phys. Rev. Lett.*, **90**, pp.236102/1-4, (2003).
- A.Cavalleri and R.W. Schoenlein, "Femtosecond x-ray studies of lattice dynamics in solids," in **Ultrafast Dynamical Processes in Semiconductors**, ed. by K.T. Tsen, *Topics in Applied Physics* Series No. 92, Springer Verlag, (2004).
- M. Saes, C. Bressler, F. van Mourik, W. Gawelda, M. Kaiser, M. Chergui, D. Grolimund, R. Abela, T.E. Glover, P.A. Heimann, R.W. Schoenlein, S.L. Johnson, A.M. Lindenberg, and R.W. Falcone, "A setup for ultrafast time-resolved x-ray absorption spectroscopy", *Rev. Sci. Inst.*, **75**, pp. 24-30, (2004).
- P. A. Heimann, H. A. Padmore, and R. W. Schoenlein, "ALS Beamline 6.0 For Ultrafast X-ray Absorption Spectroscopy", in **Synchrotron Radiation Instrumentation**, T. Warwick, J. Author, H.A. Padmore, and J. Stohr Eds., AIP Conf. Proc. 705, 1407 (2004).
- R. W. Schoenlein, A. Cavalleri, H. H. W. Chong, T. E. Glover, P. A. Heimann, A. A. Zholents, and M. S. Zolotarev, "Generation of Femtosecond Synchrotron Pulses: Performance and Characterization", in **Synchrotron Radiation Instrumentation**, T. Warwick, J. Author, H.A. Padmore, and J. Stohr Eds., AIP Conf. Proc. 705, 1403 (2004).
- A. Cavalleri, H.H.W. Chong, S. Fourmaux, T.E. Glover, P.A. Heimann, J.C. Kieffer, B.S. Mun, H.A. Padmore, and R.W. Schoenlein, "Picosecond soft x-ray absorption measurement of the photo-induced insulator-to-metal transition in VO_2 ," *Phys. Rev. B*, **69**, 153106 (2004).
- A. Cavalleri, H.H.W. Chong, S. Fourmaux, T.E. Glover, P.A. Heimann, J.C. Kieffer, H.A. Padmore, R.W. Schoenlein, "Femtosecond Near Edge X-ray Absorption Measurement of the VO_2 Phase Transition", in **Ultrafast Phenomena XIV**, Springer Series in Chemical Physics **79**, T. Kobayashi, T. Okada, T. Kobayashi, K.A. Nelson, S. De Silvestri, Eds., Springer-Verlag, p. 343, (2004).
- A.Cavalleri, M. Rini, H.H.W. Chong, S. Fourmaux, T.E. Glover, P.A. Heimann, J.C. Kieffer, M. Rini, R.W. Schoenlein, "Band-Selective Measurements of Electron Dynamics in VO_2 Using Femtosecond Near-Edge X-Ray Absorption", *Phys. Rev. Lett.* (in press).
- M. Khalil, M.A. Marcus, A.L. Smeigh, J.K. McCusker, H.H.W. Chong, and R.W. Schoenlein, "Picosecond x-ray absorption spectroscopy probes the structural dynamics of a photoinduced iron(II) spin crossover reaction in solution", *Proc. Natl. Acad. Sci.*, (submitted).
- A.Cavalleri, M.Rini, R.W. Schoenlein, "Femtosecond Optical and X-ray Measurements of the Photo-induced Phase transition in VO_2 ," *J. Phys. Soc. Jap.*, (submitted).

Electronic Excitations in Carbon Nanotubes Induced by Femtosecond Pump-Probe LASER Pulses

Pat Richard

JR Macdonald Laboratory, Physics Department, Kansas State University
Manhattan, Kansas 66506

richard@phys.ksu.edu

In this presentation I will review work on a new effort in the JR Macdonald Laboratory directed toward the study of Carbon Nanotubes. We use time-of-flight of electrons emitted from carbon nanotubes following femtosecond pump-probe laser pulses generated by the ultra-fast Ti:Sapphire Kansas Light Source to deduce the energy and temporal behavior of the electronic states of carbon nanotubes.

Time-resolved photo imaging of image-potential states in carbon nanotubes

Experimental Group: M. Zamkov, N. Woody, B Shan, Z. Chang, and P. Richard

Theory Group: H.S. Chakraborty and U. Thumm

The experimental exploration of image-potential states, following their first observation, was limited, almost exclusively, to metal surfaces. The whole arsenal of spectroscopic tools for probing metallic image states can, however, be applied to systems which are at the core of nano-material and nano-device research. The observation of image states in a variety of nanoscopic settings including molecular nanowires, and metal nanoclusters is a possibility. In this context, the study of image-potential states in carbon nanotubes is of unique interest. The cylindrical geometry of the nanotube induces a special rotational degree of freedom, which gives rise to a centrifugal force that counters the electron's association with the bulk. Recently, the Harvard group of Granger, Kral and Sadgepour (PRL **89**, 135506 (2002)) predicted that for a strong centrifugal repulsion associated with high values of electron angular momenta, single wall carbon nanotubes, SWNTs, could support *tubular* image states that form in the potential well between the repulsive barrier and the long-range image interaction. In an extension of this work, our recent study suggested that in addition to tubular image states, both single- and multi-walled carbon nanotubes, SWNTs and MWNTs respectively, can support low- and zero-angular momentum image states with weak transverse penetrations into the bulk (publication #1). We argued that in sharp contrast to image states above metal surfaces, where the conduction band-embedded delocalization of a state is also possible, the image-potential state of a nanotube can always be localized, and hence experimentally accessible, due to the electron's reflection from the transverse potential wall inside the carbon cage. This universal availability of nanotube image states for localized excitations and their augmented sensitivity to the surface structure make them strong candidates for surface spectroscopic and STM studies.

We designed an apparatus to search for image-potential states in MWNTs and conducted a successful experiment. Fig. 1 shows the electron spectrum for the case of a 230 fs delayed probe pulse (the pump is the third harmonic, 4.71 eV, of the primary laser beam). The higher energy peaks in the spectrum at ≥ 3.5 eV above the Fermi level are the proposed observed image potential states. We published the first experimental

observation of image-potential states in carbon nanotubes in 2004 in PRL (Publication #2). The observed features constitute a new class of surface image states owing to their quantized centrifugal motion. Measurements of binding energies and the temporal evolution of image electron wave-packets were performed using femtosecond time-resolved photoemission. The associated image electron lifetimes are found to be 220 ± 5 fs as compared with the 40 fs lifetime associated with $n = 1$ image state of graphite, indicating a strong localization of an image-potential state in front of the nanotube surface. The existence of individual nanotubes within a sample plays a key role in the formation of image-potential states. Due to the fact that “image” electrons are spatially extended from the tube’s surface at distances of up to a few nanometers, the nanotubes need to be isolated from any source of interaction, such as the substrate, micelle or other SWNTs. Synthesis of the adequate size SWNT sample with the latter characteristics is

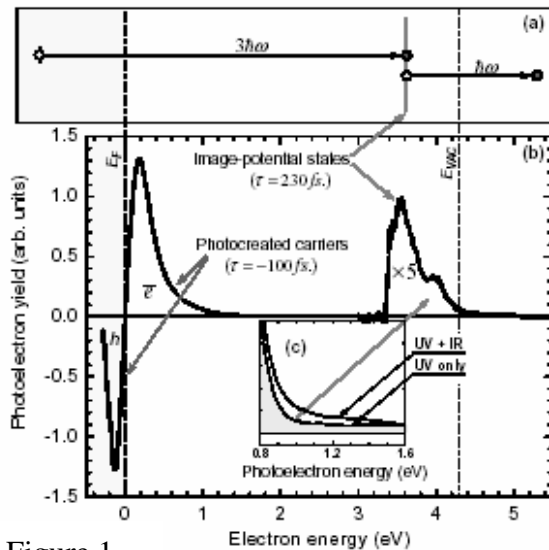


Figure 1

complicated by the tendency of SWNTs to form bundles (ropes). Thus, as a viable alternative, samples of individual MWNTs were used in the present study. The diameter distribution of high-purity (> 95%) MWNTs were within 10-20 nm, as confirmed by STM measurements. The samples used in the photoemission study, consisted of 0.4-mm-thick freestanding MWNTs “buckypaper” (provided by Nanolab, Inc, Boston, MA), which was attached to a Ta substrate and out gassed thoroughly in multiple heating and annealing cycles with a peak temperature of 700 K.

Publication # 1: Image Potential States of single- and multi-walled Carbon Nanotubes, M. Zamkov, N. Woody, B. Shan, H. S. Chakraborty, Z. Chang, U. Thumm, and P. Richard, Phys. Rev. B **70**, 115419 (2004).

Publication # 2: Time-Resolved Photoemission of Image-Potential States in Carbon Nanotubes, M. Zamkov, N. Woody, B. Shan, H. Chakraborty, Z. Chang, U. Thumm, and P. Richard, Phys. Rev. Lett. **93**, 156803 (2004).

Lifetime of Charge Carriers in Multi-walled Nanotubes

M. Zamkov, N. Woody, B. Shan, Z. Chang, and P. Richard

In this study we investigated the nature of the low-energy excitations in MWNTs by means of femtosecond time-resolved photoemission. These excitations are observed in the low energy spectrum in Fig. 1, which corresponds to the case where the pump and probe beams are time reversed from those used in the image-potential state experiment. The energy dependence of electron lifetimes due to e-e scattering in the vicinity of the Fermi level was selectively measured by plotting the temporal behavior of the spectrum

for each electron energy bin (Fig. 2 shows the decay curve for the 0.17 eV electron energy bin). The observed lifetimes were in the range of 200 to 700 fs. We found the lifetime behavior to be inversely proportional to the square of the excitation energy (experimental result $\tau \sim (E-E_F)^{-n}$ with $n \approx 2.07 \pm 0.1$). See publication #3. This result

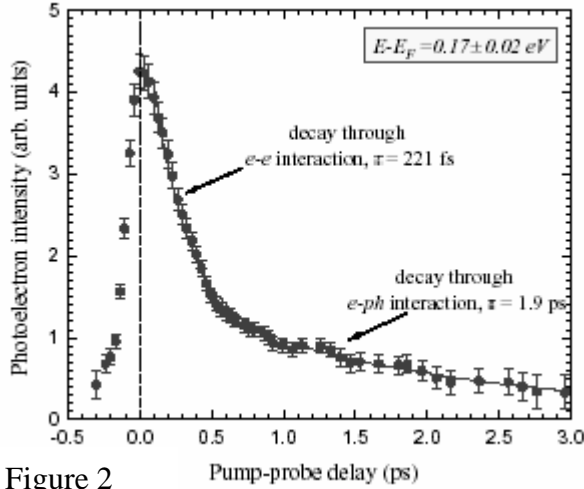


Figure 2

provides strong evidence that electron transport in MWNTs exhibits a Fermi-liquid behavior, indicating that long-range e-e interaction along the tube vanishes due to screening. The corresponding character of the charge propagation is, therefore, consistent with two- or three-dimensional transport. This result is in contrast to observations in single wall nanotubes which show a deviation from the inverse square behavior and is indicative of one-dimensional structures or Luttinger Liquids.

Publication # 3: **Lifetime of Charge Carriers in Multi-walled Nanotubes** M. Zamkov, N. Woody, B. Shan, Z. Chang and P. Richard, Phys. Rev. Lett. **94**, 056803 (2005).

The Determination of the Electron Mean free Path in Carbon Nanotubes through Electron-Phonon Scattering Dynamics

M. Zamkov, A. Alnaser, N. Woody, S. Bing, Z. Chang, and P. Richard

Hertel, Fasel, and Moos (Appl. Phys. A **75** 449 (2002)) recently observed that the decay curves for electron states near the Fermi level in SWNTs consist of two components. We observe the same phenomena in MWNTs as can be seen in Fig. 2. The short decay component is due to e-e interactions as discussed in the previous section and the long decay is due to e-phonon interactions. By measuring the decay time and knowing the excitation energy of the electron we can obtain its mean free path. We obtain mean free paths between approximately 4.0 and 0.8 μm as a function of excitation energy. We can then use this data to test models of the electron interactions leading to this mean free path.

The effect of the laser pump-pulse is to promote the electrons into the conduction band and thus increase the thermal energy of the electronic system. In this case the thermal equilibrium between the unperturbed lattice and the excited carriers will be realized by the energy exchange through e-ph coupling. In the framework of the two-temperature model, TTM (Hertel PRL **84**, 5002 (2002)), the temperature can be related to the e-ph coupling term. We determine the temperature for a given delay time between the pump and probe by fitting the spectra to a difference of the Fermi-Dirac distribution functions for the non equilibrium minus the equilibrium case. The non-equilibrium temperature deduced from the data is then used in the TTM to determine the e-ph energy transfer rate and thusly the corresponding electron mean free path. A very good

agreement is found between the measured mean free path and the e-ph interaction model predicted mean free path (This work is not published but is submitted for publication, see below).

Publications: The Determination of the Electron Mean free Path in Carbon Nanotubes through Electron-Phonon Scattering Dynamics

M. Zamkov, A. Alnaser, N. Woody, S. Bing, Z. Chang, and P. Richard, submitted to Phys. Rev. Lett. June 2005.

Work in Progress and Future Work: Observation of the Excitonic Blockade of Photoemission from Semi-Conductive Single Wall Nanotubes

M. Zamkov, A. Alnaser, Z. Chang, I. Chatzakis, A. Habib, and P. Richard

We have turned our attention to SWNTs which is the subject of greatest interest in the field of carbon nanostructures. Most of the information about nanostructures is obtained from Photo Luminescence which can be performed for nanotubes in dielectric media.

Nanotube sample production is at the forefront in the development of new science and of applications of nanotubes in areas such as electronic devices. Sample production of nanotubes at best isolates single wall, double wall and sets of multi-wall nanotubes. In each of these types of samples a distribution of nanotubes diameters is produced. Furthermore the samples are a mixture of semi-conductive (*S*) and metallic (*M*) nanotubes. In some processes the nanotube samples are free standing, some form bundles of nanotubes, and in some processes they are created in a dielectric environment such as in a micelle-suspension or in an aqueous solution.

The dynamic interplay of e-hole pairs near the Fermi level is solely responsible for many unique properties of SWNTs. Retrieving an accurate time-resolved description of e-h motion, however, is hampered by the fundamental differences in contributions from *M* and *S* nanotubes that are inevitably mixed in the samples.

We are studying the electron emission from SWNTs using a modified version of our pump-probe technique used in the work on MWNTs. We have replaced the normal pump pulse from the Ti:Sapphire with an Optical Parametric Amplifier output of variable frequency. The probe is the third harmonic of the primary Ti:Sapphire pulse.

We have compared our electron emission spectra with photo absorption measurements on an identical sample of SWNTs. The characteristic absorption lines that appear at the first and second band gaps for the *S* nanotubes are not observed in our electron emission spectra; however electron emission is seen for the *M* SWNTs. This is an important result which demonstrates the dominant formation of strongly bound excitons in *S* nanotubes at room temperature. We refer to this observation as excitonic blockade of photo electron emission in *S* nanotubes. The electron emission lines in *M* SWNTs are from unbound e-hole pairs which can be easily ionized. Recent predictions show that weak excitons are also formed in *M* SWNTs. Time permitting I will discuss the most recent results of our experiment and recently calculated and measured electronic structures of *S* SWNTs.

Publications: This is work in progress. First results are being prepared for publication.

Structure and Dynamics of Atoms, Ions, Molecules and Surfaces: Atomic Physics with Ion Beams, Lasers and Synchrotron Radiation

Uwe Thumm, J.R. Macdonald Laboratory, Kansas State University
Manhattan, KS 66506 thumm@phys.ksu.edu

1. Laser-assisted collisions (with Thomas Niederhausen)

Project scope: This project seeks to develop numerical and analytical tools to efficiently predict the effects of a strong laser field on the dynamics of electron capture and emission in ion-atom collisions. In particular, we are interested in calculating and understanding the probabilities for electron transfer, emission, and loss in the elementary three-body laser-assisted collision system of slow protons colliding with atomic hydrogen as a function of both, collision and laser parameters. These investigations may motivate and assist in the planning of future challenging experiments using synchronized crossed laser and particle beams. Laser pulses with lengths of a few nano-seconds and intensities of about 10^{12} W/cm² and higher should allow for the experimental verification of the predicted dichroism in the capture probability. In the long run, our studies may contribute to the improved control of chemical reactions with intense laser light.

Recent progress: We investigated the effects of a strong 1064nm laser field on electron capture and emission in slow (keV) proton-hydrogen collisions within both, a simplified 2D reduced dimensionality model and new full 3D calculations that include all three electronic degrees of freedom (Fig.1). In the 2D model of the scattering system, the motion of the active electron and the laser electric field vector are confined to the scattering plane. We have extended these 2D calculations by propagating the time-dependent 3D Schrödinger equation on a numerical grid. We examined the probabilities for electron capture and ionization as a function of the laser intensity, the projectile impact parameter b , the angle α between the collision plane and the plane in which the circularly polarized laser electric field vector rotates, and the laser phase Φ that determines the orientation of the laser electric field with respect to the internuclear axis at the time of closest approach between target and projectile. Since the laser fields breaks the cylindrical symmetry of the collision system, our new 3D calculations of laser-assisted capture and ionization cross sections require the addition of a large number of projectile trajectories. We have tested the convergence of the cross sections (i.e. of the integration over the impact parameter vector) as a function of the number of included trajectories. We found a relatively weak variation of the laser-phase-resolved capture cross section on the angle α , such that our reduced-dimensionality and full 3D cross section are qualitatively similar functions of Φ (Fig.2 and [1]).

As a test for the accuracy of our 3D numerical wave function propagation, we turned the laser field off and found agreement with known experimental capture cross sections for $p + H$ collisions. Both, laser-assisted ionization and capture probabilities show a strong dependence on Φ and on the helicity of the circularly polarized laser light (Fig.2). For intensities above 2×10^{12} W/cm², we predict a noticeable circular dichroism in the capture probability for slow proton-hydrogen collisions. This dichroism persists after averaging

over Φ . Capture and electron emission probabilities defer significantly from results for laser-unassisted collisions. Ionization probabilities depend less sensitively on Φ , and their phase averages differ much less for co- and counter-rotating collisions than the phase-averaged capture probabilities. For 1.21 keV protons, the difference in the capture cross sections for co- and counter rotating collisions at a laser intensity of 5×10^{13} W/cm² amounts to 40% in our 2D and to 15% in our 3D calculations. Our 3D calculations confirm evidence found in previous 2D calculations for a charge resonance enhanced ionization mechanism that may enable the measurement of the laser phase Φ [1].

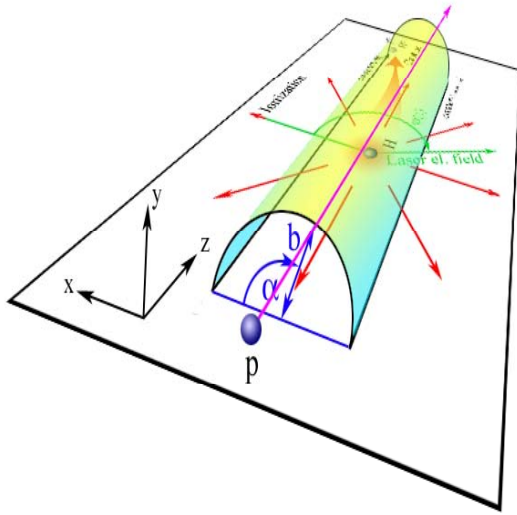


Fig.1. Collision scenario for a proton colliding at impact parameter b with an atomic hydrogen target. For positive impact parameters, the projectile follows the rotating laser field (“co-rotating” case); for negative impact parameters, the projectile moves against the rotating electric field (“counter-rotating” case). α denotes the angle between the collision plane and the plane defined by the rotating laser electric field vector.

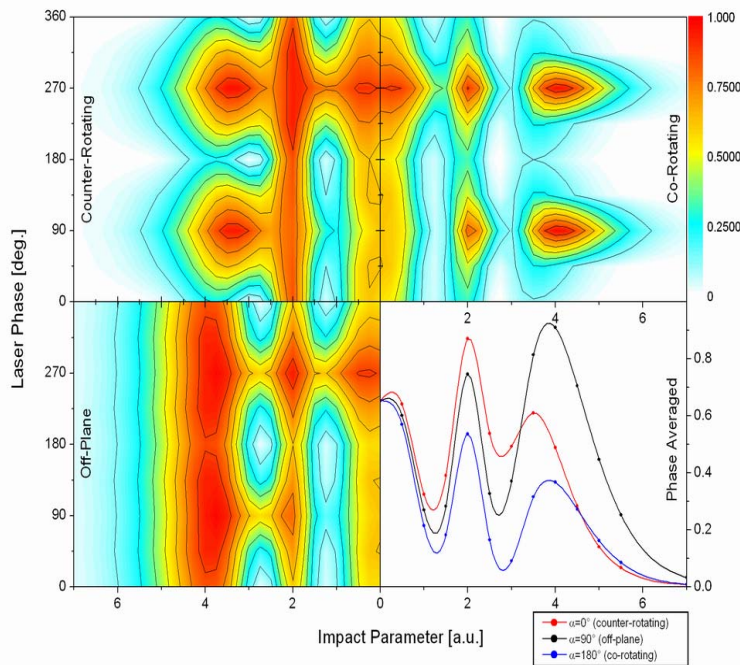


Fig.2. **Top row:** Contributions to counter- and co- rotating capture probabilities from $\alpha = 180$ and 0 degrees, respectively, for 1.21 keV p - H collisions in a 5×10^{13} W/cm² circularly polarized laser field. **Bottom left:** Contribution for $\alpha = 90$ degrees. **Bottom right:** Laser phase-averaged capture cross section for $\alpha = 0, 90,$ and 180 degrees.

Future plans: (i) We are currently completing 3D calculations for capture and ionization in laser assisted $p + H$ collisions. We plan to extend these calculations to the asymmetric collision system $He^{2+} + H$. and to investigate the dependence of capture and ionization on the laser intensity, wave length, and degree of elliptical polarization. (ii) We found evidence for a charge resonant enhanced ionization mechanism in laser-assisted ionization [1] and intend to continue to investigate this effect for various collision and laser parameters. Further, we will attempt to calculate the kinetic energy distribution of the emitted electrons. (iii) We have started to compute perturbatively the scattering amplitude for laser assisted ionization. By comparing numerical results for the S-matrix approach with current 3D grid-propagated cross sections, we plan to evaluate the accuracy of model three-center Coulomb-Volkov wave functions. (iv) We intend to search for optimal collision and laser parameters for the generation of higher harmonics in laser-assisted collisions. In particular, we are interested in isolating contributions to the higher harmonics spectrum that are due to rescattering of the ionizing electron on the projectile.

2. Surface-morphology effects during the neutralization of negative hydrogen ions near metal surfaces (with Himadri Chakraborty, Thomas Niederhausen, and Boyan Obreshkov)

Project scope: The goal of this project is to compute and understand the resonant transfer of a single electron, initially bound to the projectile, during the reflection of a slow ion or atom on a metal surface as a function of the collision parameters and the electronic structure and crystal orientation of the surface. Apart from contributing to the qualitative understanding of the interaction mechanisms through computer animations, this project contributes to the quantitative assessment of charge transfer and wave function hybridization in terms of level shifts, decay widths, and ion-neutralization probabilities. In the long run, it may improve our understanding of surface chemical reactions, catalysis, and diagnostics.

Recent progress: By direct propagation of the time-dependent Schrödinger equation on a 2D numerical grid using the Crank-Nicholson wave-packet propagation method, we investigated resonant charge transfer (RCT) between hydrogen anions and plane Ag [2], Cu [3], and Pd [4] surfaces of (100) and (111) symmetries.

The competitive population of the Shockley surface state and image states during RCT appears to be relevant for the ion survival after specular reflection at the investigated metal surfaces. We found that different H^- neutralization probabilities near Ag(111) and Pd(111) surfaces are mainly due to dissimilar characters of their respective image states: the conduction-band-embedded image states in Ag(111) strongly favor electron recapture, while localized image states in Pd(111) drive the electron away from the ion and hinder recapture. In addition, by comparing these (111) surfaces with Pd(100), we found that the effect of the long-lived Shockley surface state inside the projected L-band

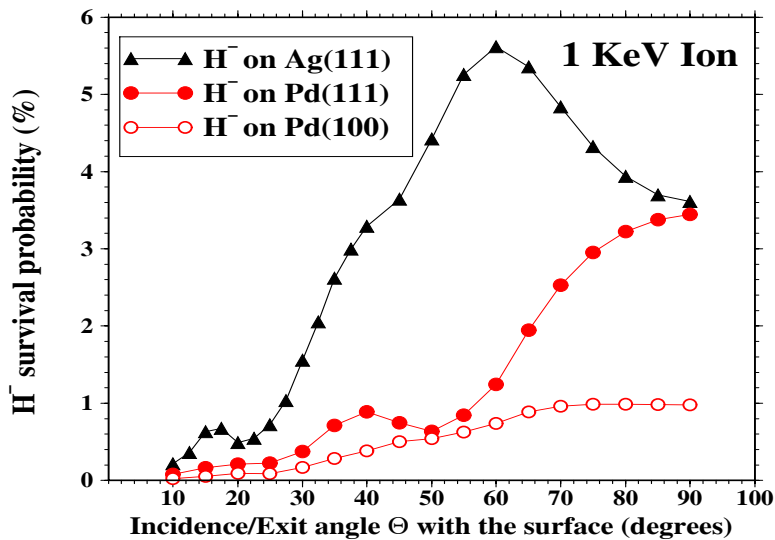


Fig.3: Percentage survival probability of 1keV H⁻ ions scattered from Ag(100), Ag(111), and Pd(100) surfaces as a function of the incident angle (= exit angle) with respect to the surface plane.

gap of Pd(111) can only counter this image state effect over a small range of incidence angles near normal incidence (Fig.3).

Future plans: (i) We plan to extend our calculations for plane Ag/Cu/Pd (111/100) surfaces to three dimensions. (iii) We intend to investigate the neutralization dynamics of H⁻ near the (111) and (100) surfaces of Pt. (ii) We have begun and intend to continue to investigate resonance formation and charge exchange near vicinal surfaces. In particular, we will investigate the importance of lateral confinement effects (evidence for which was found in photo-emission experiments) for RCT. (iv) We plan to provide adiabatic decay rates and ionization probabilities for surface-scattered Rydberg atoms.

- [1] T. Niederhausen, B. Feuerstein, and U. Thumm, "Circular Dichroism in Laser-Assisted Proton - Hydrogen Collisions", *Phys. Rev. A* **70**, 023408 (2004).
- [2] H.S. Chakraborty, T. Niederhausen, and U. Thumm, "Effects of the Surface Miller Index on the Resonant Neutralization of Hydrogen Anions near Ag surfaces", *Phys. Rev. A* **69**, 052901 (2004).
- [3] H.S. Chakraborty, T. Niederhausen, and U. Thumm, "Resonant Neutralization of H⁻ near Cu surfaces", *Phys. Rev. A* **70**, 052903 (2004).
- [4] H.S. Chakraborty, T. Niederhausen, and U. Thumm, "On the Effect of Image States on Resonant Neutralization of Hydrogen Anions near Metal Surfaces", *Nucl. Instrum. Methods Phys. Res. B*, accepted.
- [5] M. Zamkov, H.S. Chakraborty, A. Habib, N. Woody, U. Thumm, and P. Richard, "Image-Potential States of Single- and Multi-Walled Carbon Nanotubes", *Phys. Rev. B* **70**, 115419 (2004).
- [6] A.A. Khuskivadze, I.I. Fabrikant, and U. Thumm, "Static Electric Field Effects in the Photodetachment of Cs⁻", *Phys. Rev. A* **68**, 063405 (2003).
- [7] B. Feuerstein and U. Thumm, "Mapping of Coherent and Decohering Nuclear Wave Packet Dynamics in D₂⁺ with Ultrashort Laser Pulses", *Phys. Rev. A.*, **67**, 063408 (2003).
- [8] B. Feuerstein and U. Thumm, "Fragmentation of H₂⁺ in strong 800nm Laser Pulses: Initial Vibrational State Dependence", *Phys. Rev. A.* **67**, 043405 (2003).
- [9] B. Feuerstein and U. Thumm, "On the Computation of Momentum Distributions in Wave Packet Propagation Calculations", *J. Phys. B* **36**, 707-716(2003).

High- n Rydberg atoms and tailored pulses: a laboratory for wavefunction engineering, non-linear dynamics and decoherence.

C.O. Reinhold

Physics Division, Oak Ridge National Laboratory, Oak Ridge, TN 37831

Mesoscopic objects with a typical size of a few μm provide a bridge between the microscopic quantum world and the macroscopic classical world. A well-established route to mesoscopic quantum coherent entities is the laser excitation of Rydberg atoms with very high principal quantum numbers n . Rydberg atoms with $n \sim 500$ can be routinely produced in several laboratories with narrow-linewidth frequency stabilized lasers [1]. The diameter of such atoms, $d \sim 2n^2 a_0$ can reach $\sim 20 \mu m$. Likewise, the classical Kepler period of such a “planetary” atom, $T_{Kepler} = 2\pi n^3 a.u.$ can be as long as $10 ns$ and can thus be probed with conventional electronics. High- n Rydberg atoms are therefore ideal candidates for exploring fundamental notions such as that of coherent control, decoherence, and the classical limit of quantum mechanics.

One practical limitation for exploiting these unique features was, until recently, the difficulty in controlling and manipulating these extremely fragile objects. The recent availability of half-cycle pulses (HCPs) from conventional pulse generators [2] has opened up novel opportunities to control, shape, and manipulate wavefunctions in Rydberg states. Remarkably, these extremely fragile objects (with binding energies as low as $50 \mu eV$) can be stabilized by tailored pulse sequences. Their susceptibility to random stray fields and collisions with ambient molecules can be profitably explored to study the quantum-to-classical crossover and decoherence at a level of detail difficult to achieve in other systems.

Recent Progress

In the past few years we have extensively exploited these new capabilities in close collaboration with the experimental group of F.B. Dunning at Rice University and we have developed several schemes for manipulating and probing Rydberg electrons [3-13]. Atoms subject to a train of periodic HCPs have provided an experimental realization of the kicked atom, a valuable test bed for the study of non-linear dynamics in Hamiltonian systems. Studies of kicked atoms have furnished new insights into classical-quantum correspondence as well as a variety of phenomena such as dynamical stabilization and quantum localization which illuminate how the classical world emerges from the quantum world. Dynamical stabilization leads to strong transient periodic localization of the excited electron in phase space and creation of periodic non-dispersive wavepackets. In fact, we have shown that the mixed phase space of regular and chaotic dynamics induced by a periodic sequence of HCPs can be used to filter and shape Rydberg wavepackets. Strong transient phase space localization can also be generated using quasi-one-dimensional Rydberg atoms and a single HCP. Such localization provides new opportunities for control of the atomic wavefunction, i.e., for atomic engineering, by application of a carefully tailored sequence of HCPs to steer wavepackets to desired target states. Transiently localized states can be “trapped” for extended periods using a train of HCPs and later “released” simply by turning off the pulses. Trapping results because the combination of the Coulomb interaction and the external periodic driving field gives rise to sizable stable islands in an otherwise chaotic phase space from which the electron cannot escape. Trapping islands can also be used as tweezers capable of picking up the electron in a given region of phase space and moving it to a different region by using a carefully tailored chirped train of HCPs with varying frequency and strength.

In parallel to these studies, we have invested a considerable amount of time in the development of a theoretical framework describing the collisional decoherence of open quantum systems [14-18]. We plan to exploit this capability in the future to study the decoherence of Rydberg wavepackets. As a prototype for collisional decoherence we chose the internal electronic state of a fast ion traversing solids, which is an

example of an open quantum system in contact with a “large reservoir”. The reservoir includes both the radiation field and the degrees of freedom of the solid. One of our ultimate goals was to simulate the decoherence of the internal electronic state of atoms and ions as exactly as possible. Specifically, we studied the dynamics of hydrogenic one-electron ions traversing amorphous carbon foils, for which accurate experimental data have recently become available [19]. We have derived from first principles a general theoretical framework that incorporates the complex array of collisions with electrons and ionic cores. Interactions with the solid environment and the radiation field are treated on the same footing and the quantum master equation for the reduced density matrix of the electronic state of the ion is approximated by a Lindblad equation. The latter allows the solution of this multi-state problem in terms of Monte Carlo sampling of quantum trajectories whose dynamics is governed by a stochastic non-linear Schrödinger equation. This work has been carried out in close collaboration with the theory group of J. Burgdorfer (Vienna).

Future Plans

When a Rydberg wavepacket interacts with an environment (e.g. an ambient gas), the interaction leads to an irreversible dephasing of the wavepacket, referred to as decoherence. Given recent developments, it is possible to envision studies of decoherence of Rydberg wavepackets interacting with “partially controlled” environments. Preliminary work suggests that decoherence rates can be quantified from the dephasing of Rydberg wavepackets [18]. We plan to use as environments a gas of atoms or molecules (whose density can be varied) or well characterized noise produced, for example, using a random sequence of electric field pulses. Clearly, one goal would be to control and modify decoherence with the view to the design and construction of decoherence-free subspaces within which information is embedded. Another goal would be the utilization of decoherent dephasing as a tool to measure cross sections for quasi-elastic electron-atom (or molecule) collisions at energies extending down to micro electron volts.

Present experiments are limited to low scaled frequencies of the trains of pulses. Raising this limit would provide new opportunities for the study of quantum localization and other phenomena at high scaled frequencies. Achieving this goal requires increasing the n -level of the initial stationary quasi-1D atoms, which is currently limited to $n \sim 350$. One of our goals is the design of a tailored sequence of pulses for transporting polarized states to higher n -levels.

In order to probe wavepackets, single pulses have been used at variable time delay after the steering pulses to probe the momentum and/or spatial distributions of the excited electron [22,23]. We plan to develop a scheme for probing the equivalent of the Husimi distribution of Rydberg wavepackets: i.e. the joint position and momentum distribution. The probability to find the electron at a given time with a given position and momentum can be obtained from the survival probability resulting from the application to the wavepacket of a controllable train of pulses featuring a dominant stable island in phase space centered at the desired position and momentum.

Another avenue for future investigation is the study of pulse-driven recombination. Bound-free transitions induced by stochastic sequences of momentum transfers play an important role in atom transport through solids and in plasmas. No systematic investigations of recombination induced by multiple pulses have been reported although recombination driven by a single HCP has been examined in connection with recombination in plasmas [20] and discussed as an efficient means to recombine positrons and antiprotons to form antihydrogen [21].

References

- [1] M. Littman, M. Kash, and D. Kleppner, *Phys. Rev. Lett.* **41**, 103 (1978); T. H. Jeys, G. W. Folz, K. A. Smith, E. J. Beiting, F. G. Kellert, F. B. Dunning and R. F. Stebbings, *Phys. Rev. Lett.* **44**, 390 (1980); T. F. Gallagher, *Rydberg Atoms (Cambridge Univ. Press, Cambridge (1994))*.
- [2] M.T. Frey, X. Ling, B.G. Lindsay, K.A. Smith and F.B. Dunning, *Rev. Sci. Instrum.* **64**, 3649 (1993).
- [3] F.B. Dunning, C.O. Reinhold, and J. Burgdorfer, *Phys. Scripta* **68**, C44 (2003).
- [4] E. Persson, S. Yoshida, X. Tong, C.O. Reinhold, and J. Burgdorfer, *Phys. Rev. A* **68**, 063406 (2003).
- [5] D. G. Arbó, C. O. Reinhold, J. Burgdörfer, A. K. Pattanayak, C. L. Stokely, W. Zhao, J. C. Lancaster and F. B. Dunning, *Phys. Rev. A* **67**, 063401 (2003).
- [6] C. L. Stokely, J. C. Lancaster, F. B. Dunning, D. G. Arbo, C. O. Reinhold, and J. Burgdorfer, *Phys Rev A* **67**, 013403 (2003).
- [7] C.O. Reinhold, W. Zhao, J.C. Lancaster, F.B. Dunning, E. Persson, D.G. Arbo, S. Yoshida, and J. Burgdorfer, *Phys Rev A* **70**, 033402 (2004).
- [8] D.G. Arbo, C.O. Reinhold, and J. Burgdorfer, *Phys Rev A* **69**, 023409 (2004).
- [9] W. Zhao, J.C. Lancaster, F.B. Dunning, C.O. Reinhold, and J. Burgdörfer, *Phys. Rev. A* **69**, 041401 (2004).
- [10] S. Yoshida, C.O. Reinhold, E. Persson, J. Burgdorfer, B. E. Tannian, C. L. Stokely, and F. B. Dunning, *Physica Scripta* **T110**, 424 (2004).
- [11] F.B. Dunning, J. C., Lancaster, C. O. Reinhold, S. Yoshida, and J. Burgdörfer, to be published in *Adv. At. Mol. Phys.* (2005).
- [12] W. Zhao, J.C. Lancaster, F.B. Dunning, C.O. Reinhold, and J. Burgdörfer, *J. Phys. B* **38**, S191 (2005).
- [13] S. Yoshida, C. O. Reinhold, E. Persson, J. Burgdörfer and F. B. Dunning, *J. Phys. B* **38**, S209 (2005).
- [14] T. Minami, C. O. Reinhold, J. Burgdorfer, *Phys. Rev. A* **67**, 022902 (2003).
- [15] T. Minami, C. O. Reinhold, J. Burgdorfer, *Nuc Inst Meth B* **205**, 818 (2003).
- [16] M. Seliger, C.O. Reinhold, T. Minami, and J. Burgdorfer, *Phys. Rev. A* **71**, 062901 (2005).
- [17] M. Seliger, C.O. Reinhold, T. Minami, and J. Burgdorfer, *Nuc. Instr. Meth. B.* **230**, 7 (2005).
- [18] C.O. Reinhold, J. Burgdorfer, and F. B. Dunning, *Nuc Instr Meth B* **233**, 48 (2005).
- [19] J.P. Rozet, D. Vernhet, I. Bailly-Despiney, C. Fourment, L.J. Dube, *J. Phys. B* **32**, 4677 (1999); D. Vernhet, J.P. Rozet, E. Lamour, B. Gervais, C. Fourment, L.J. Dub_e, *Phys. Scr.* **T80A**, 83 (1999). T. Minami, C.O. Reinhold, M. Seliger, J. Burgdorfer, C. Fourment, B. Gervais, E. Lamour, J.-P. Rozet, D. Vernhet, *Phys. Rev. A.* **65**, 032905 (2002).
- [20] T. J. Benschky, M. B. Campbell and R. R. Jones, *Phys. Rev. Lett.* **81**, 3112 (1998).
- [21] C. Wesdorp, F. Robicheaux and L. D. Noordam, *Phys. Rev. Lett.* **84**, 3799 (2000); *Phys. Rev. A* **64**, 033414 (2001).
- [22] R. R. Jones, *Phys. Rev. Lett.* **76**, 3927 (1996).
- [23] C. O. Reinhold, J. Burgdörfer, M. T. Frey and F. B. Dunning, *Phys. Rev. A* **54**, R33 (1996); B. E. Tannian, C. L. Stokely, F. B. Dunning, C. O. Reinhold and J. Burgdörfer, *Phys. Rev. A* **64**, 021404(R) (2001).

Mode-Specific Polyatomic Photoionization[‡]

Robert R. Lucchese
Department of Chemistry, Texas A&M University
College Station, TX, 77843-3255
lucchese@mail.chem.tamu.edu

Program Scope

This program is based on a close collaboration between theory and experiment to study molecular photoionization in systems which have strong energy-dependent mode-specific behavior, primarily through the measurement and computation of vibrational branching ratios. Comparisons between theory and experiment can lead to the identification and characterization of the physical process responsible for a particular feature observed in a mode-specific cross section.

Recent Progress

Vibrational branching ratios are ratios of cross sections for photoionization from the same initial state to two different vibrational states of a given final electronic state of an ion. In the Franck-Condon approximation, branching ratios are just ratios of the square of vibrational overlap integrals. In this simplest approximation, the branching ratios are independent of the photon energy. Non-Franck-Condon contributions to the branching ratios are most prominent when there are resonant processes in the ionization continuum and are therefore usually strongly energy dependent. Thus the study of the energy dependence of mode-specific molecular photoionization cross sections is an approach for investigating such resonant processes and their dependence on molecular geometry.

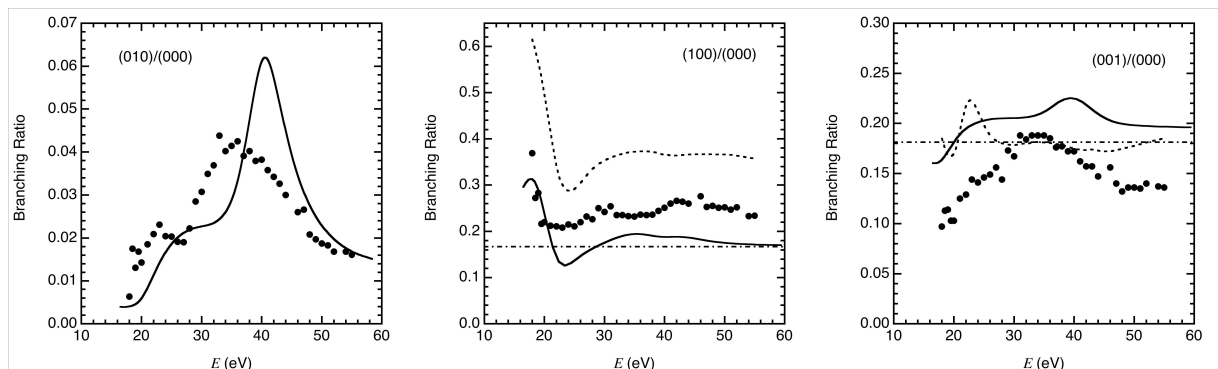
Our theoretical approach has been to study these mode-specific photoionization processes using the adiabatic approximation. Thus we compute the photoionization cross section using the fixed nuclei approximation and then average the geometry dependent dipole matrix elements over appropriate initial and final state vibrational wave functions.

Significant non-Franck-Condon effects can come from two sources. First, the cross sections at energies near to the energy of a resonant state can be very sensitive to the geometry of the molecule, e. g. the position and width of the resonant state changes rapidly with geometry. Second, the excitation of a particular mode can be symmetry forbidden at the equilibrium geometry, leading to an identically zero Franck-Condon intensity. Then if there is a symmetry breaking vibrational mode of the molecule, it is possible that the Franck-Condon forbidden mode may acquire intensity.

We have recently completed a detailed study of the photoionization of N₂O leading to the $(7\sigma)^{-1} A^2\Sigma^+$ state of N₂O⁺. Although the system does not have a center of symmetry, both the vibrational modes and bound and resonant electronic states have been found to have approximate inversion symmetry. From symmetry arguments using the Franck-Condon approximation one would expect that the excitation of the approximately symmetric stretching mode would be strong, the excitation of the approximately antisymmetric stretching mode would be weak, and the excitation of the bending mode would be forbidden. There are three one-electron resonances

[‡] This research is done in collaboration with Erwin Poliakoff (Louisiana State University) and John Bozek (LBNL)

present in this system: a σ resonance that occurs at a photon energy of approximately 20 eV, a second σ resonance that occurs at approximately 40 eV, and a broad π resonance that also occurs at about 40 eV. The effects of the low energy σ resonance on the vibrational branching ratios have been previously studied. At these energies non-Franck-Condon features are seen in the vibrational excitation of the symmetric stretch due to the strong dependence of the energy of the resonance on that mode of the system.



Vibrational branching ratios for N_2O leading to the $(7\sigma)^{-1} A^2\Sigma^+$ state of N_2O^+ . The solid lines are the present results, the dots are the present experimental results, the dotted lines are the results of Braunschweig and McKoy, [J. Chem. Phys. **90**, 1535 (1989)], and the dot-dashed line is the Franck-Condon approximation.

Of more interest are the high-energy resonances which occur at approximately 40 eV. We find that the σ resonance is only weakly excited, whereas the π resonance is somewhat more strongly excited. The weakness of the σ resonance can be understood since both the 7σ orbital and the 40 eV σ resonant state have approximately odd symmetry with respect to inversion. The presence of this resonance leads to a strong feature in the excitation of the bending mode which is forbidden in the Franck-Condon approximation. Additionally there is a corresponding feature seen in the approximately antisymmetric stretching mode.

A careful analysis of the computed results reveals that the cross section in the region of the 40 eV σ resonance behaves differently when the N–O bond is stretched compared to when the N–N bond is stretched. This is in contrast to the lower energy resonance where the position of the resonance is more sensitive to the total length of the molecule rather than to the lengths of the individual bonds.

We have recently extended these studies to non-linear molecular systems. The first system we considered was the photoionization of BF_3 leading to the E^2A_1' of BF_3^+ . In this channel there is a broad shape resonance at approximately 30 eV which is evident in the cross section as well as in the photoelectron asymmetry parameter. Experimentally, what is found is a broad feature in the vibrational branching ratios for excitation of $\nu = 1, 2, 3,$ and 4 of the symmetric stretch. A similar structure is found in the computed results, indicating that this resonant enhancement is due to the shift of the position of the resonance as a function of geometry.

Similar results have been found for the symmetric stretching mode of the SiF_4 molecule for photoionization leading to the \tilde{D}^2A_1 state of SiF_4^+ . In this system there are two prominent shape resonances that occur at 24 and 48 eV. Both of these features appear in the cross sections and in the photoelectron asymmetry parameters. A strong shift of the resonance energies as a

function of the symmetric stretching mode leads to significant non-Franck-Condon branching ratios seen in the experimental and theoretical results.

Future Plans

In the coming year we will investigate other types of vibrational modes in non-linear polyatomic molecules. For example, we will consider bending modes in the SiF_4 molecule. We will also consider even larger systems such as C_6F_6 . For this system the close collaboration between theory and experiment will be important since the multiplicity of possible vibrational modes makes the unambiguous assignment of experimental features difficult without the support of theory.

Our theoretical efforts will also be directed towards the computation of mode-specific cross beyond the adiabatic approximation. It should be possible to implement a vibrational close-coupling approach to compute the vibrationally resolved photoionization cross sections. This approach has characteristics that should allow it to be implemented without the computations becoming unduly lengthy. First, for systems with a significant amount of symmetry, the full symmetry of the system at the equilibrium geometry can be retained even as symmetry-breaking vibrations are being considered. Second, the interaction with the nuclear potential will not have the same cusp behavior near the nuclei as in the fixed nuclei calculations, thus making the single-center expansion approach used in the calculations converge more rapidly.

DOE Sponsored Publications in the Last Three Years

G. J. Rathbone, E. D. Poliakoff, John D. Bozek, R. R. Lucchese, and P. Lin, Mode-specific photoelectron scattering effects on CO_2^+ ($\text{C}^2\Sigma_g^+$) vibrations, *J. Chem. Phys.* **120**, 612-622 (2004).

G. J. Rathbone, E. D. Poliakoff, John D. Bozek, and R. R. Lucchese, Observation of the symmetry-forbidden $5\sigma_u \rightarrow k\sigma_u$ CS_2 transition: A vibrationally driven photoionization resonance, *Phys. Rev. Lett.* **92**, 143002:1-4 (2004).

G. J. Rathbone and E. D. Poliakoff, John D. Bozek, and R. R. Lucchese, Intrachannel vibronic coupling in molecular photoionization, *Canadian J. Chem.* **82**, 1043-1051 (2004).

G. J. Rathbone, E. D. Poliakoff, John D. Bozek, and R. R. Lucchese, Electronically forbidden ($5\sigma_u \rightarrow k\sigma_u$) photoionization of CS_2 : Mode-specific electronic-vibrational coupling, *J. Chem. Phys.* **122**, 064308:1-9 (2005).

G. J. Rathbone, E. D. Poliakoff, John D. Bozek, Daniele Toffoli, and R. R. Lucchese, Photoelectron trapping in N_2O $7\sigma \rightarrow k\sigma$ resonant ionization, *J. Chem. Phys.* - accepted for publication.

An X-ray Microprobe of Laser-Ionized Atoms

E. P. Kanter, R. W. Dunford, D. L. Ederer, C. M. Hoehr, B. Krässig,
E. C. Landahl, E. R. Peterson, J. Rudati, S. H. Southworth, and L. Young
Argonne National Laboratory, Argonne, Illinois 60439

A major research theme with 4th-generation x-ray light sources will be pump/probe experiments using femtosecond lasers. In an effort to understand how x-ray photon-atom interactions will be affected by the presence of the strong electromagnetic fields produced by such lasers, we have begun a program to study such phenomena in isolated atoms and molecules at the Advanced Photon Source (APS) at Argonne National Laboratory. During the past year, considerable progress has been made in this work including: 1) demonstration of an x-ray microprobe of the transient underdense plasma created by 4×10^{14} W/cm² ionization of Kr; 2) molecular dynamics simulations of the time-development of the Coulomb expansion; and 3) an investigation of the alignment produced by tunnel ionization.

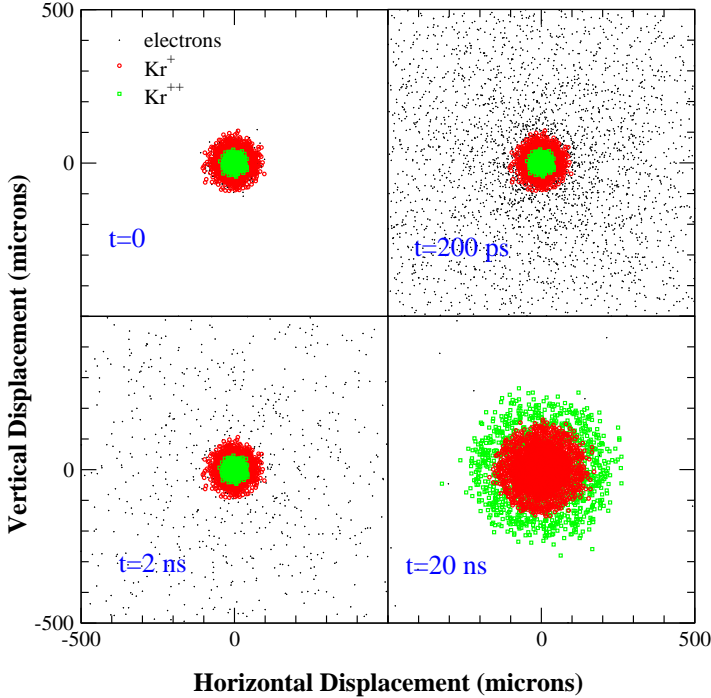


FIG. 1: Simulation results for 10,000 particles including 3335 Kr⁺ ions, 1110 Kr⁺⁺ ions, and 5555 electrons with an initial Kr density of $80/\mu^3$. Plotted are the particle distributions in the transverse plane (perpendicular to both laser and x-ray beams) at $t=0$, 0.2, 2, and 20 nsec after the laser pulse.

calculations (D.R. Beck, L. Pan, and S. O'Malley, these Proceedings and to be published) of the Kr⁺ and Kr⁺⁺ ions. Those calculations have enabled us to fit all of the Rydberg structures observed below the shifted continua. The combination of such spectroscopy combined with the simulations has also demonstrated an important new probe of the complex dynamics that ensues in such laser-produced plasmas.

The most prominent feature in the near edge spectrum is the $1s \rightarrow 4p$ excitation which is absent in the neutral and thus a very clean signal of x-ray/laser overlap. Recently, we investigated the alignment produced in the tunnel ionization creating the $4p$ vacancy by measuring the dependence of this x-ray transition on the polarization direction of the laser. We found a $\sim 2:1$ ratio for this excitation when the laser polarization was parallel to the x-ray polarization compared to when they were transverse. Investigations of the time dependence of such data will help in understanding both the initial alignment and subsequent reorientation following tunnel ionization.

The experiments were carried out at Sector 7 of the Advanced Photon Source. A Ti:sapphire laser (2.5 mJ/pulse, 50 fs at 1 kHz), synched to the x-ray storage ring rf, was focussed on an effusive jet of Kr. The laser intensity in the focal volume ($\sim 4 \times 10^{14}$ W/cm²) exceeded the intensity needed to saturate ionization of the Kr $4p$ shell. Removing an electron from the closed Kr $4p$ shell, produced an underdense ($\sim 10^{14}$ /cm³) neutral plasma. As shown by our simulations, the relatively hot ($U_p = 24$ eV, $T = 12$ eV) electrons produced by tunnel ionization leave the focal volume within a few nanoseconds (see lower left panel in Fig. 1) leaving an ionic target which is well-localized in space by the laser focus. The monochromatized x-rays were focussed with a Kirkpatrick-Baez mirror set to $\sim 10\mu\text{m}$ within the larger $\sim 100\mu\text{m}$ laser focus. By varying the relative positions and delay times of these two beams, we probed both the spatial and temporal evolution of the ionic cloud.

We detected the $K\alpha$ fluorescence produced by x-ray photoabsorption using Si drift detectors. Additional measurements were conducted with various ion spectrometers (electrostatic and TOF) to characterize the ion velocities produced by the Coulomb expansion. The fluorescence measurements offer a distinct advantage in probing the primary excitation/ionization processes since it is prompt (femtosecond timescale) and insensitive to collisional processes. These results have demonstrated a new form of precision ion spectroscopy with isolated atoms and have necessitated new atomic structure

Nondipolar photoelectron angular distributions: A spectroscopic tool to study quadrupole resonances

B. Krässig, E.P. Kanter, S.H. Southworth, L. Young

Chemistry Division, Argonne National Laboratory

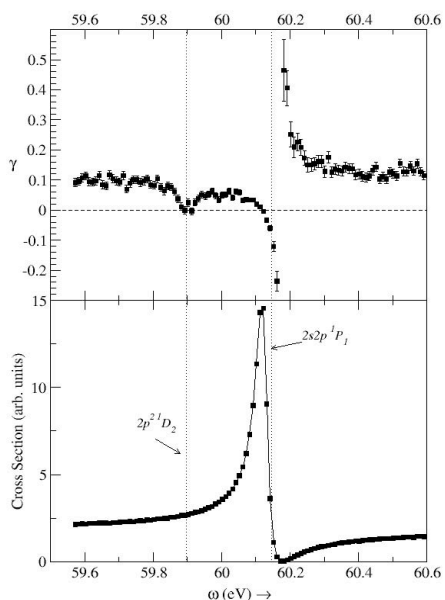
N.L.S. Martin, B.A. de Harak

University of Kentucky, Lexington

R. Wehlitz

Synchrotron Radiation Center, Stoughton, WI

The lowest-order correction to the usual treatment of photoionization processes in dipole approximation manifests itself as a forward-backward asymmetry of the photoelectron angular distribution with respect to the direction of photon propagation. The nondipole effects, albeit generally small in the VUV regime, can be strongly amplified when either the dominant dipole interaction is suppressed or the quadrupole interaction is enhanced. The former situation arises in a Cooper minimum or the minimum of a dipole resonance;



the latter can be the case in a quadrupole resonance and this enables us to study such resonances.

Quadrupole resonances are not directly observable in photoabsorption. They are seen in electron energy loss spectroscopy, however the extractable information is limited because many multipoles contribute to their formation. The figure on the left shows our experimental data in the energy region of the helium $2s2p\ ^1P$ dipole autoionization resonance.

The photo ion yield in the bottom panel reflects the well-studied Fano profile of this resonance. The top panel contains the nondipolar asymmetry parameter γ , which is a measure of the forward-backward asymmetry in the photoelectron emission. Here two resonance features are discernible, one at the location of the dipole resonance and one at the location of the $2p^2\ ^1D$ quadrupole autoionization resonance. For this

quadrupole resonance we do not observe an enhancement but rather nearly a window resonance with vanishing asymmetry at the minimum. At the maximum of the dipole resonance, the forward-backward asymmetry also vanishes because of the strong enhancement of the dipole amplitude; in the minimum the asymmetry nearly diverges because the dipole amplitude vanishes. Off-resonant one can see the typical extent of the observable nondipolar asymmetry in this energy region. We were able to extract the complete set of Fano resonance parameters for this quadrupole resonance. We will be presenting results on a number of such resonances in helium and neon.

Inner-Shell Photoionization of Atoms and Small Molecules

A. Belkacem

Chemical Sciences Division, Lawrence Berkeley National Laboratory, Berkeley, CA 94720

Email: abelkacem@lbl.gov

Objective and Scope

The goal of this part of the LBNL AMOS program is to understand the structure and dynamics of atoms and molecules using photons as probes. The current research carried at the Advanced Light Source is focused on studies of inner-shell photoionization and photo-excitation of atoms and molecules, as well as breaking new ground in the interaction of x-rays with atoms and molecules dressed with femto-second laser fields. The low-field photoionization work seeks new insight into atomic and molecular processes and tests advanced theoretical treatments by achieving new levels of completeness in the description of the distribution of momenta and/or internal states of the products and their correlations. The intense-field two-color research is designed to provide new knowledge of the evolution on a femto-second time scale (ultimately atto-second) of atomic and molecular processes as well as the relaxation of atomic systems in intense transient fields.

Double-photoionization of CO few eV above threshold.

We measured double photoionization of CO molecules at 48 eV photon energy. The double ionization of CO produces mostly $C^+ + O^+$ fragments with non-measurable amounts of CO^{2+} . The formation of $C^+ + O^+$ can proceed through two possible channels: a) Direct ionization of two electron into the continuum – similar to the H₂ double ionization – direct channel. b) Ionization of one electron into the continuum followed by autoionization of a second electron – Indirect channel. The electron distribution measured with a COLTRIMS shows a very clear distinction of the direct and indirect channels. The kinetic energy release spectrum shows a series of peaks corresponding to the transient vibrational states of the various electronic states of $(CO^{2+})^*$. These states are similar to previous measurements at higher energies (K-shell photoionization). $(CO^{2+})^*$ is found to predissociate through a $^3\Sigma^-$ and $^1\Delta$ dissociative states leading to considerably faster dissociation times than natural lifetimes of the electronic bound states. We plan to improve our current measurement by detecting both electrons in coincidence. We will be able to estimate the dissociation time of these states by using an analysis technique similar to that used to estimate the time of the isomerization of acetylene to vinylidene.

Double-slit interference of photoelectrons from hydrogen molecules

Electrons with de Broglie wavelengths λ_e close to the size (0.72 Å) of the H₂ (or D₂) molecule can be expected to show effects similar to Young's double slit diffraction of light. In a naïve view, one thinks of photo-electron emission arising coherently from near two identical centers leading to a far field interference modulation in the molecular frame

angular distribution. In the case of double ionization with photon energies well above the threshold (e.g. 300 eV) the electrons have strongly asymmetric sharing of the excess energy. The higher energy electron (say 250 eV, $\lambda_e = 0.78 \text{ \AA}$) shows interference perturbed by the presence of a slower few eV partner. One can select the inter-nuclear separation within the spread of the $v=0$ vibrational wavefunction by selecting narrow regions of kinetic energy release in the H^+ , H^+ explosion. The electron emission is not from two well localized sites in this case, but is spread over the extent of the initial electron wavefunction, thus the pattern might resemble more the interference from two wide slits...i.e. a combination of interference modulated by diffraction.

Electron correlation during photoionization and relaxation of potassium and argon after K-shell photoexcitation

The dynamics of inner-shell photoionization and the resulting relaxation of the excited atom are complicated by the collective response of all the electrons of the atomic target. Furthermore, this correlated response of the electrons in the atom couples the photoionization and the relaxation processes. In this work we compare the different ion yields and charge state distribution for potassium and argon after K-shell ionization with photon energies from about 100 eV below to about 100 eV above their respective K-shell edge. Though loosely bound, the potassium valence electron plays a major role in the ionization dynamics. Striking differences and surprising similarities are observed between the charge state distributions, which can be traced to the interplay between the various processes (shake-up, correlation between the valence electron and the photoelectron, post collision interaction effects, pre-edge K-shell ionization, and double-excitation with a single photon). We find that the valence electron is rarely a spectator during core relaxation, and its presence enhances loss of the photoelectron excited into Rydberg levels or strongly suppresses recapture of slow photoelectrons through post-collision interaction.

Inner-shell photoionization of laser excited potassium

The goal of this study is to modulate the interaction of hard or soft x-rays with the inner-shells of an atom by controlling the excitation of the atom with a sequence of short laser pulses. The binding energy of a core electron of an atom is influenced by the presence and configuration of other electrons in the atom, due to electron correlation effects such as charge screening and coupling. The fact that core electrons are tightly bound and have high (classical) speed allows them to follow adiabatically valence electron configuration changes. The change of the inner-shell excitation energy is induced by the sudden change of the Coulomb screening when the valence electron population is modified. We performed the preliminary experiments at beamline 5.3.1 at the Advanced Light Source using 70 ps x-ray pulses. Due to its low binding energy (4.3 eV) the excitation and ionization of the potassium 4s valence electron is very accessible to existing femtosecond lasers. We developed a time-of-flight detection system in a rapidly but adiabatically decreasing magnetic field (inverse of a magnetic bottle) to detect KLL Auger electrons following K-shell ionization. We found that the 1s-4p excitation energy and the K-shell edge of potassium are modified when the outer 4s-electron is ionized or excited with a femtosecond laser. We also measured a cross correlation between the femtosecond laser and the ALS x-ray pulse. This cross correlation reflects the pulse length of the ALS x-rays and shows the ability of our set up to synchronize both in space and time the laser and the x-rays. This technique that uses the detection of KLL Auger

electron via time-of-flight can work equally well with femtosecond x-rays at beamline 6, SPPS or LCLS when available.

Development of a COLTRIMS set up to measure DEA of NO and H₂O

The formation of the resonant dissociative negative molecular states typically peak at electron energies below 10 eV. Thus a major technical problem is the production of a controlled, defined low electron beam that can strike the molecular jet within the uniform electric field of the COLTRIMS spectrometer. Our approach uses the uniform field and an orthogonal uniform magnetic field. This ExB field steers the electrons along the directions of the gas jet without (or minimally) affecting the electron energy. The low magnetic field (~10 G) used has a minimal effect on the motion of the slow heavy negative ion. This COLTRIMS configuration allowed us the injection of a usable low electron beam into the interaction region of the spectrometer. Earlier studies of DEA found in the literature measured angular distributions of negative ion products, however the COLTRIMS approach will result in higher sensitivity and simultaneous coverage of a wide range of negative ion final momenta.

Development of a high intensity high harmonic source.

While the strong interaction regime has typically been inaccessible to (low peak power) synchrotron sources, it can be accessed with recently developed and with foreseeable sources. X-ray Free Electron Lasers will offer high flux (~ 10^{12} photons/pulse) while high harmonics sources have recently been demonstrated to achieve focal intensities up to ~ 10^{14} W/cm². We plan to study fundamental high field and nonlinear interactions with simple atomic and molecular systems using a high harmonics source optimized for high peak power. We are constructing a high harmonic source based on a 30 mJ, 10 Hz, 800 nm laser system (10 Hz, 800 nm). The laser will drive high harmonic generation and related work in this area suggests that a photon flux exceeding 10^9 photons/pulse is feasible as are peak intensities in the range 10^{12} - 10^{14} W/cm². The harmonics will be generated in a long (~10 cm) gas cell and directed into an existing experimental chamber. We fabricated a parabolic mirror with multilayer coating to focus the monochratized harmonic to micron size spot. The initial experiment will focus on studying multiphoton ionization of neon atoms and neon dimmers.

Future Plans

We plan to extend the pump-probe experiments at the ALS to the new undulator femtosecond beamline 6. We will continue our studies with potassium and extend the measurements to CO. We plan to finish the construction of the high intensity high harmonic source and start initial measurements of two-photon ionization of Neon using high harmonic VUV photons.

We plan to continue application of the COLTRIMS approach to achieve complete descriptions of the single photon double ionization of CO and its analogs. New measurements will be made close to the double ionization threshold and approaching the regime where the outgoing electrons and the ions have nearly the same velocities. Our earlier observations of the isomerization of acetylene to the vinylidene configuration forms a basis for possible further studies of this phenomena perhaps using deuterated acetylene to alter the relative time scales of molecular rotation and the dissociation dynamics.

Recent Publications

“Electron correlation during photoionization and relaxation of potassium and argon after K-shell photoexcitation”, M. Hertlein, H. Adaniya, K. Cole, B. Feinberg, J. Maddi, M. Prior, R. Schriel and A. Belkacem, *Phys. Rev. A* **71**, 022702 (2005)

“The pair production channel in pair production”, A. Belkacem and A. Sorensen, in print in *Radiation Physics and Chemistry*.

A. Knapp, B. Krassig, A. Kheifets, I. Bray, Th. Weber, A. Landers, S. Schossler, T. Jahnke, J. Nickles, S. Kammer, O. Jagutzki, L. Ph. H. Schmidt, M. Schoffler, T. Osipov, M. Prior, H. Schmidt-Bocking, C.L. Cocke and R. Dorner, *J. Phys. B: At. Mol. Opt. Phys.* **38**, 615 (2005)

A. Knapp, B. Krassig, A. Kheifets, I. Bray, Th. Weber, A. Landers, S. Schossler, T. Jahnke, J. Nickles, S. Kammer, O. Jagutzki, L. Ph. H. Schmidt, M. Schoffler, T. Osipov, M. Prior, H. Schmidt-Bocking, C.L. Cocke and R. Dorner, *J. Phys. B: At. Mol. Opt. Phys.* **38**, 635 (2005)

A. Knapp, B. Krassig, A. Kheifets, I. Bray, Th. Weber, A. Landers, S. Schossler, T. Jahnke, J. Nickles, S. Kammer, O. Jagutzki, L. Ph. H. Schmidt, M. Schoffler, T. Osipov, M. Prior, H. Schmidt-Bocking, C.L. Cocke and R. Dorner, *J. Phys. B: At. Mol. Opt. Phys.* **38**, 645 (2005)

“Vibrationally resolved K_α-shell photoionization of CO with circularly polarized light”, T. Jahnke, L. Foucar, J. Titze, R. Wallauer, T. Osipov, E. P. Benis, A. Alnaser, O. Jagutzki, W. Arnold, S. K. Semenov, N. A. Cherepkov, L. Ph. H. Schmidt, A. Czasch, A. Staudte, M. Schöffler, C. L. Cocke, M. H. Prior, H. Schmidt-Böcking, and R. Dörner, *Phys. Rev. Lett.* **93**, 083002 (2004)

“Complete photo-fragmentation of the deuterium molecule” T. Weber, A. O. Czasch, O. Jagutzki, A. K. Mueller, V. Mergel, A. Kheifets, E. Rotenberg, G. Meigs, M. H. Prior, S. Daveau, A. Landers, C. L. Cocke, T. Osipov, R. Diez Muiño, H. Schmidt-Böcking and R. Dörner, *Nature*, **431**, 437 (2004)

“Fully Differential Cross Sections for Photo-Double-Ionization of D₂”, Th. Weber, A. Czasch, O. Jagutzki, A. Müller, V. Mergel, A. Kheifets, J. Feagin, E. Rotenberg, G. Meigs, M.H. Prior, S. Daveau, A.L. Landers, C.L. Cocke, T. Osipov, H. Schmidt-Böcking and R. Dörner, *Phys. Rev. Lett.* **92**, 163001 (2004).

“Metal-insulator transitions in an expanding metallic fluid: particle formation kinetics”, T.E. Glover, G. D. Ackerman, A. Belkacem, P. A. Heimann, Z. Hussain, R. W. Lee, H. A. Padmore, C. Ray, R. W. Schoenlein, W. F. Steele, and D. A. Young, *Phys. Rev. Lett.* **90**, 23102-1 (2003)

“Measurement of vacuum-assisted photoionization at 1 GeV for Au and Ag targets”, D. Dauvergne, A. Belkacem, F. Barrue, J. P. Bocquet, M. Chevallier, B. Feinberg, R. Kirsch, J. C. Poizat, C. Ray, and D. Rebreyent, *Phys. Rev. Lett.* **90**, 153002 (2003)

“Auger electron emission from fixed-in-space CO”, T. Weber, M. Weckenbrock, M. Balsler, L. Schmidt, O. Jagutzki, W. Arnold, O. Hohn, M. Schoffler, E. Arenholz, T. Young, T. Osipov, L. Foucar, A. de Fanis, R. D. Muino, H. Schmidt-Bocking, C.L. Cocke, M.H. Prior, and R. Dorner, *Phys. Rev. Lett.* **90**, 153003 (2003)

“Photoelectron-photoion momentum spectroscopy as a clock for chemical rearrangements: isomerization of the Di-cation of acetylene to vinylidene configuration”, T. Osipov, C.L. Cocke, M. Prior, A. Landers, T. Weber, O. Jagutzki, L. Schmidt, H. Schmidt-Bocking and R. Dorner, *Phys. Rev. Lett.* **90**, 233002 (2003)

Reaction and Fragmentation Interferometry

Department of Energy 2005-2006

James M Feagin

*Department of Physics
California State University–Fullerton
Fullerton CA 92834
jfeagin@fullerton.edu*

Although much has been achieved experimentally with quantum information and control with photons and quantum optics, there remains fundamental interest in establishing analogous tools with charged particles, especially correlated electrons and ions.¹ Key steps in this direction have been of course the successes with ion traps, for example not only in assembling a data bus with control gates² but in resolving diffraction patterns in differential charge-transfer cross sections³ as well as a recent precision demonstration of Bell's theorem with a trapped ion pair.⁴ Related directions include advances in atom interferometry—even fullerenes⁵ and BEC fragments⁶ can be diffracted with standing waves of light, technology akin to the recent remarkable confirmation of the Kapitza-Dirac effect with electrons.⁷ We are thus motivated to consider few-body fragmentation detection from the more general perspective of reaction interferometry.

Two-Center Interferometry and Decoherence Effects

It is natural to regard the position of a macroscopic object to be sharply defined: if a cat is sleeping in the chair, we don't consider for a moment that she may in fact be out on a bench in the garden. Yet, quantum mechanics encourages us to superpose displaced and narrow wavepackets to describe states of a single 'sleeping cat' that could be either in the chair or on a bench. This quantum reality and the wider notion of entanglement (something bumps the cat and adds bench and chair markers) are profound and continue to generate debate over what the wavefunction actually describes.⁸ Nevertheless, it is now widely recognized that interactions with the environment and their inevitable entanglements can dephase the quantum superpositions. The resulting decoherence eliminates macroscopic interferences and thereby restores a natural sense of reality.⁹

¹ J. Ullrich et al., *Rep. Prog. Phys.* **66**, 1463 (2003); J. Ullrich and V. P. Shevelko, Eds., *Many-Particle Quantum Dynamics in Atomic and Molecular Fragmentation*, Springer, New York (2003).

² D. Bouwmeester, A. Ekert, and A. Zeilinger, Eds., *The Physics of Quantum Information*, Springer, Heidelberg (2001); M. A. Nielsen and I. L. Chuang, *Quantum Computation and Quantum Information*, Cambridge, New York (2000).

³ X. Flechard et al., *Phys. Rev. Lett.* **87**, 123203 (2001); M. van der Poel et al., *Phys. Rev. Lett.* **87**, 123201 (2001).

⁴ M. A. Rowe, D. Klempinski, V. Meyer, C. A. Sackett, W. M. Itano, C. Monroe, and D. J. Wineland, *Nature* **409**, 791 (2001); see also H. J. Metcalf and P. van der Straten, *Laser Cooling and Trapping*, Springer, New York (1999) and references therein.

⁵ Nairz et al., *Phys. Rev. Lett.* **87**, 160401 (2001) and references therein.

⁶ E. W. Hagley, L. Deng, W. D. Phillips, K. Burnett, and C. W. Clark, *Optics & Photonics News*, May (2001), p. 22, and references therein.

⁷ D. L. Freimund, K. Afatoon, H. Batelaan, *Nature* **413**, 142 (13 Sep 2001). See also P. H. Bucksbaum, *Nature* **413**, 117 (13 Sep 2001).

⁸ See for example H. P. Stapp, *Mind, Matter and Quantum Mechanics*, (2nd Ed., Springer Verlag, Heidelberg, 2004) and A. Peres, *Quantum Theory: Concepts and Methods*, (Kluwer Academic Publishers, Dordrecht, 1995).

⁹ E. Joos et al., *Decoherence and the Appearance of a Classical World in Quantum Theory*, (Springer, Berlin, 2003).

Advances in atom interferometry and ion trapping now afford systematic study of quantum interferences in mesoscopic systems with parameters that can be tracked from quantum towards macroscopic limits. For example, Pritchard and coworkers at MIT¹⁰ have observed the interference fringes of a sodium atom passing through a Mach-Zehnder interferometer while scattering a photon. Likewise, Monroe and coworkers¹¹ at NIST in Boulder have engineered the external motion of a linearly trapped ${}^9\text{Be}^+$ ion into a double-humped Schrödinger-cat superposition of two displaced coherent-state wavepackets.

We have thus considered the trapped-ion interferometry of a ‘kicked-cat’ state generated by photon scattering from a Schrödinger-cat state in analogy with scattering from the two arms of a Mach-Zehnder atom interferometer.¹² We consider an incident photon \mathbf{k}_L resonantly scattered by an atom or ion target with center-of-mass (CM) position \mathbf{C} , as depicted in Fig. 1. We assume for simplicity the photon encounter is impulsive and that the target’s external CM motion is described by the initial wavefunction $g_0(\mathbf{C})$ throughout the collision. The asymptotic photon-ion wave is then given by

$$\psi \sim \frac{e^{ikr}}{r} f_\gamma(\mathbf{k}) e^{i\mathbf{q}\cdot\mathbf{C}} g_0(\mathbf{C}),$$

where $\mathbf{k} \equiv k \hat{\mathbf{r}}$ and $f_\gamma(k\hat{\mathbf{r}})$ is the *free-atom* resonance fluorescence amplitude. Here, $\mathbf{q} \equiv \mathbf{k}_L - \mathbf{k}$ so that $\hbar\mathbf{q}$ is a momentum transfer to the target by the scattered photon, and $e^{i\mathbf{q}\cdot\mathbf{C}}$ is the momentum boost of the target external state due to the impulsive encounter once a photon detection direction $\hat{\mathbf{r}}$ is selected. This boost and the resulting nonlocal phase shifts when the initial wavefunction $g_0(\mathbf{C})$ is double humped are key elements of the interference effects we analyze. Consider for example the Schrödinger-cat superposition $g_0(\mathbf{C}) = g_0^{(0)}(\mathbf{C} - \mathbf{C}_0) + g_0^{(1)}(\mathbf{C} - \mathbf{C}_1)$ describing the state of a *single* target atom or ion. If the component wavepackets $g_0^{(n)}$ are relatively narrow compared to their separation $\mathbf{d} \equiv \mathbf{C}_0 - \mathbf{C}_1$, then the asymptotic *kicked-cat* state is approximately

$$\psi \sim f_\gamma(\mathbf{k}) \frac{e^{ik_L r}}{r} \left(e^{i\mathbf{q}\cdot\mathbf{C}_0} g_0^{(0)} + e^{i\mathbf{q}\cdot\mathbf{C}_1} g_0^{(1)} \right),$$

which makes clear the photon-atom or -ion entanglement relative to the approximate photon scattering points \mathbf{C}_n . The scattered-photon states $e^{i\mathbf{q}\cdot\mathbf{C}_n} f_\gamma(\mathbf{k}) e^{ik_L r}/r$ are not orthogonal and

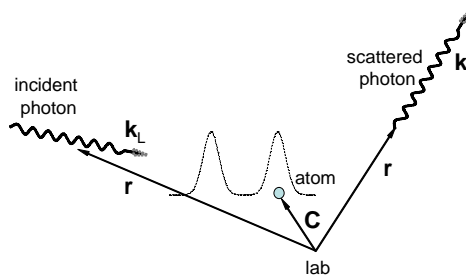


FIG. 1: Incident photon with momentum $\hbar\mathbf{k}_L$ scattered by a two-center target, e.g. two actual trapped ions or a single trapped ion in a double-humped initial state. Here, $\mathbf{k} \equiv k \hat{\mathbf{r}}$ is the scattered-photon asymptotic wavevector.

¹⁰ M. S. Chapman et al., Phys. Rev. Lett. **75**, 3783 (1995); D. A. Kokorowski et al., Phys. Rev. Lett. **86**, 2191 (2001).

¹¹ C. Monroe et al., Science **272**, 1131 (1996).

¹² J. M. Feagin, Phys. Rev. Lett., submitted (2005).

therefore will not fully discriminate which end of the kicked cat, $g_0^{(0)}$ or $g_0^{(1)}$, the atom or ion was in when it scattered the photon. Thus, when allowed to recombine, the two ends of the cat will again interfere but with a visibility reduced by the partial overlap of these photon states.

This work is an outgrowth of general considerations of scattering interferometry and two-center interference effects from extended mesoscopic targets. Within the impulse-approximation, we have developed a simple framework¹³ for describing a variety of experiments including the observation of Young's interference fringes with photons scattered by a *pair* of trapped ions¹⁴ as well as photon two-slit interference with a trapped-ion source and thus a realization of Wootters and Zurek's seminal quantum discussion of Einstein's celebrated recoiling-slit gedanken experiment.^{15,16}

Hardy Nonlocality

In parallel work, we have analyzed the detection of a pair of recoiling reaction fragments, each by its own interferometer,¹⁷ to demonstrate Hardy's contradiction between quantum mechanics and local hidden variables.¹⁸ Hardy's theorem sidesteps Bell's inequality by establishing the contradiction with just four measurement outcomes on two system fragments. Whereas Bell's theorem involves fully statistical violations of the quantum description, the Hardy result is simpler and hinges on essentially perfect correlations to establish nonlocality. Our interferometry is based on the projectile-target momentum entanglement and is independent of the identity and internal state of the fragments. Although no doubt a very difficult experiment, our approach is thus relatively straightforward, at least conceptually.

Dichroism and Nondipolar Effects

Two-slit detection would also provide new probes of photoionization angular distributions. Even with the photo *single* ionization of an unoriented atom, we have demonstrated¹⁹ that one could generate a circular dichroism analogous to the well established effect seen in photo *double* ionization²⁰ and thereby extract phase information on nondipolar amplitudes.

A related dichroism and nondipolar probe is expected in ordinary fluorescence in which a photon takes the role of the photoionized electron and is analyzed by two-port interferometry, as depicted in Fig. 2. Such an experiment is currently in progress by T. Gay and coworkers at the University of Nebraska and interference fringes have been observed with rubidium fluorescence photons. Our preliminary analysis indicates the technique may provide a useful method for extracting electric and magnetic *quadrupole* contributions to dipole allowed transitions.

Collective Coulomb Excitations

The coincident measurement of two continuum electrons^{21,22} has been extended to the photo double ionization of molecular hydrogen in the isotopic form D₂ including coincident detection of the deuterons.²³ We have thus developed a description of the photo double ionization cross

¹³ J. M. Feagin, Phys. Rev. A, submitted (2005).

¹⁴ W. M. Itano et al., Phys. Rev. A **57**, 4176 (1998).

¹⁵ W. K. Wootters and W. H. Zurek, Phys. Rev. D **19**, 473 (1979).

¹⁶ J. M. Feagin and S. Han, Phys. Rev. Lett. **86**, 5039 (2001); Phys. Rev. Lett. **89**, 109302 (2002).

¹⁷ J. M. Feagin, Phys. Rev. A **69**, 062103 (2004).

¹⁸ L. Hardy, Phys. Rev. Lett. **71**, 1665 (1993).

¹⁹ J. M. Feagin, Phys. Rev. Lett. **88**, 043001 (2002).

²⁰ V. Mergel et al., Phys. Rev. Lett. **80**, 5301 (1998) and references therein; A. Knapp et al, J. Phys. B: At. Mol. Opt. Phys. **35**, L521 (2002). (*Feagin is a coauthor on these papers.*)

²¹ A. Knapp et al, J. Phys. B: At. Mol. Opt. Phys. **35**, L521 (2002). (*Feagin is a coauthor.*)

²² M. Walter, J. S. Briggs and J. M. Feagin, J. Phys. B: At. Mol. Opt. Phys. **33**, 2907 (2000).

²³ Th. Weber et al., Phys. Rev. Lett. **92**, 163001 (2004) and references therein. (*Feagin is a coauthor.*)

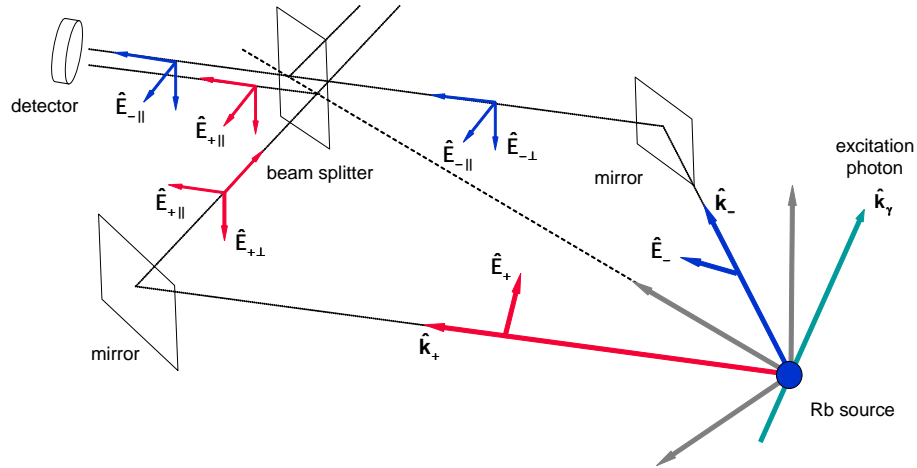


FIG. 2: Fluorescence photon interferometry with a single beam splitter. Here \mathbf{k}_+ and \mathbf{k}_- are photon momentum components towards the two entrance ports (mirrors) of the interferometer with $\hat{\mathbf{E}}_+$ and $\hat{\mathbf{E}}_-$ the corresponding photon polarization directions. The trick is to resolve these polarization vectors into detector-frame components parallel and perpendicular to the plane of the interferometer, which we find must be tilted relative to the excitation photon momentum \mathbf{k}_γ to see an effect.

section for diatomic molecules²⁴ based closely on the cross section for helium. We derive a dependence of molecular excitation amplitudes on electron energy sharing and dynamical quantum numbers labeling internal modes of excitation of the escaping electron pair.

Publications and Recent Submissions

Decoherence of a Trapped Ion in a Split Motional Wavepacket, J. M. Feagin, Phys. Rev. Lett., submitted (2005).

Two-Center Interferometry and Decoherence Effects, J. M. Feagin, Phys. Rev. A, submitted (2005).

Hardy Nonlocality via Few-Body Fragmentation Imaging, J. M. Feagin, Phys. Rev. A **69**, 062103 (2004).

Fully Differential Cross Sections for Photo Double Ionization of Fixed-in-Space D_2 , Th. Weber et al, Phys. Rev. Lett. **92**, 163001 (2004). (*Feagin is a coauthor.*)

Comment on Reaction Imaging with Interferometry, J. M. Feagin and Si-ping Han, Phys. Rev. Lett. **89**, 109302 (2002).

Energy Sharing and Asymmetry Parameters for Photo Double Ionization of Helium 100 eV Above Threshold, A. Knapp et al, J. Phys. B: At. Mol. Opt. Phys. **35**, L521 (2002). (*Feagin is a coauthor.*)

Circular Dichroism in Photo Single Ionization of Unoriented Atoms, J. M. Feagin, Phys. Rev. Lett. **88**, 043001 (2002).

Reaction Imaging with Interferometry, J. M. Feagin and Si-ping Han, Phys. Rev. Lett. **86**, 5039 (2001).

²⁴ J. M. Feagin, J. Phys. B: At. Mol. Opt. Phys. **31**, L729 (1998); T. J. Reddish and J. M. Feagin, J. Phys. B: At. Mol. Opt. Phys. **32**, 2473 (1999).

A Dual Bose-Einstein Condensate: Towards the Formation of Heteronuclear Molecules

Principal Investigator:

Dr. Chandra Raman
Assistant Professor
School of Physics
Georgia Institute of Technology Atlanta, GA 30332-0430
craman@gatech.edu

Program:

This research program explores quantum gases of atoms and molecules. Our goal is the study of superfluidity and correlated quantum effects in low temperature gases. As an experimentalist, one can manipulate the trapping potential (either optically or magnetically) as well as the microscopic interactions to realize a number of low temperature physical systems, from superfluids to superconductors and low temperature magnets.

Our work has a two-fold thrust. Our “atomic” approach explores superfluidity in single component (i.e., atomic) Bose-Einstein condensates (BECs) through the study of quantized vortices and vortex lattices. A related and important goal is to realize persistent superfluid currents in the laboratory. We are also pursuing heteronuclear molecular quantum gases. Our approach is to use sympathetic cooling to form a dual BEC, then to create molecules by magneto-association using a number of recently predicted Feshbach resonances [1]. The eventual goal of the molecular effort is to create a dipolar superfluid, a novel strongly correlated quantum system.

Our experiment centers on the production of large atom-number sodium Bose-Einstein condensates (5-10 million atoms). Our method is naturally suited to efficient sympathetic cooling of Rb and the study of Na-Rb mixtures, through the large Na sample available from a high-flux Zeeman slowed atomic beam. Our apparatus is flexible enough that we eventually hope to explore superfluidity and related quantum effects in any of the systems ^{23}Na , ^{85}Rb , ^{87}Rb , as well as mixtures (and molecules) of Na and Rb. The latter mixture has not been magnetically trapped to date.

Recent Progress:

We have realized a novel implementation of the “optically plugged” quadrupole magnetic trap (OPT), a hybrid of optical and magnetic forces [2]. This trapping method affords a large loading volume while maintaining good optical access to the sample, and thus combines the advantages of both magnetic and optical trapping. The OPT employs the AC Stark shift of a blue-detuned laser beam (in our case, a 2.5 Watt, 532 nm laser focused to a $\sim 40 \mu\text{m}$ beam waist) to create an energy barrier that repels atoms from the vicinity of the magnetic field zero at the center of the coils. Without the plug, the atoms can be lost by Majorana transitions to an untrapped state near the magnetic field zero.

A simple estimate of the AC Stark shift required to suppress Majorana loss suggests that the barrier height U_0 should exceed $3/2 k_B T_i$, where T_i is the temperature of atoms at the start of the evaporation process. While previous work [3] only examined barriers of approximately this height, about $k_B \times 350 \mu\text{K}$, in our work [2] we could produce a BEC using considerably lower barriers of about $60 \mu\text{K}$. One explanation for this is that Majorana loss, which scales with temperature as T^{-2} , becomes significant only at low T , when the cloud size is small and the atoms have a high probability of encountering the “hole”. The small loss at higher temperatures can be overcome by the increase in phase space density due to evaporative cooling. Our results thus point to the versatility of the OPT, and suggest that the AC Stark shift barrier may not need to be as large as what one might expect. Future designs might be able to use a laser whose total power is less than 1 Watt.

Papers submitted or in preparation:

- **Metastable BEC.** We have created a Bose-Einstein condensate whose spin orientation is metastable in an external, inhomogeneous magnetic field. The trapping field can in principle be used to coherently control the coupling between spin and spatial wavefunctions. We realized this metastable BEC by transferring the BEC into a “linear” trap formed by only the quadrupole coils, where the magnetic field is zero at the center. Our work is the first realization of a 3-dimensional linear potential for Bose condensates.

Our goal was to explore how a BEC undergoes Majorana transitions to an untrapped state. We have observed a slow decay of atoms over 100-200 milliseconds due to these Majorana transitions. For a thermally excited atom one may use a semiclassical approach to understand the rate of spin flips by considering the motion of an atom along a trajectory in the presence of the field zero. However, for a BEC one must use a quantum picture, in which the spin-flip transition occurs through a coherent evolution of both spatial and spin wavefunctions. We have developed a microscopic picture that connects the semiclassical and quantum-mechanical models. Our results have been recently submitted for publication.

- **Vortex Matter.** We have used Bragg spectroscopy to study lattices of quantized vortices in a BEC. We created these vortices using the rotating magnetic asymmetry of a TOP, or time-orbiting potential trap. Our Bragg scattering technique directly probes the velocity distribution of the rotating superfluid, which is the gradient of the wavefunction phase (see Figure 1). Moreover, our method allows us to directly sense the rotation through the *spatial structure* of the diffracted atoms, and therefore to construct a complete picture of the two-dimensional velocity flow. It is more general than time-of-flight imaging, which relies on the spatial scaling of the density distribution during expansion. Our results are currently in preparation.

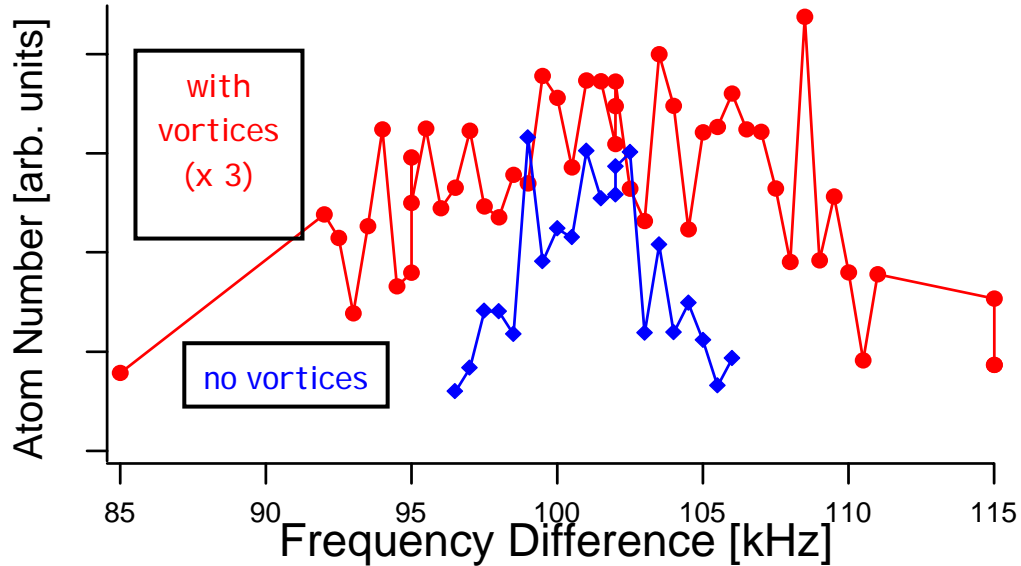


Figure 1: Spectrum of Bragg scattering of atoms from stationary (diamonds) and rotating (circles) condensates. The rotating cloud contains about 35 vortices, and therefore, the spectrum exhibits Doppler broadening compared with the stationary condensate, whose linewidth is mainly limited by mean-field effects.

Future Directions:

- **Dual-species BEC.** We are currently integrating Rb into our BEC apparatus. We are currently implementing a dual atom source, followed by dual-species Zeeman slowing. Our apparatus will feature:
 - a. Mixtures of ^{23}Na with ^{85}Rb or ^{87}Rb . We expect to trap 10^{10} Na atoms and 10^8 Rb atoms, allowing for efficient sympathetic cooling of the latter by the former.
 - b. Feshbach resonances. Using optical traps, we can explore magnetic feshbach resonances in a wide range of magnetic fields up to 1.2 kGauss . A number of resonances below 1 kGauss have been predicted for heteronuclear collisions of ^{23}Na - ^{87}Rb . Calculations of the ^{23}Na - ^{85}Rb system are underway, which would afford additional possibilities.
- **Toroidal BEC.** Most trapping geometries have a harmonic variation about the trap minimum, resulting in a BEC shaped as an ellipsoid. We plan to deploy hollow laser beams to create a rotating BEC in a toroidal trap, where superfluid

flow is predicted to sustain persistent currents (individual quantized vortices which have been observed are not generally stable).

References

1. M. Bhattacharya, et al., "Feshbach resonances in Na-23-Rb-87". *Eur Phys J D*, **31**(2): p. 301-306 (2004).
2. D.S. Naik and C. Raman, "Optically plugged quadrupole trap for Bose-Einstein condensates". *Phys. Rev. A*, **71**(3): p. 033617 (2005).
3. K.B. Davis, et al., "Bose-Einstein Condensation in a Gas of Sodium Atoms". *Phys. Rev. Lett.*, **75**: p. 3969-3973 (1995).
4. J.R. Abo-Shaeer, C. Raman, and W. Ketterle, "Formation and Decay of Vortex Lattices in a Bose-Einstein Condensate". *Phys. Rev. Lett.*, **88**: p. 070409 (2001).
5. P.C. Haljan, et al., "Driving Bose-Einstein-Condensate vorticity with a rotating normal cloud". *Phys. Rev. Lett.*, **87**(21): p. art. no.-210403 (2001).
6. K.W. Madison, et al., "Vortex formation in a stirred Bose-Einstein condensate". *Phys. Rev. Lett.*, **84**: p. 806-809 (2000).
7. E. Hodby, et al., "Vortex Nucleation in Bose-Einstein Condensates in an Oblate, Purely Magnetic Potential". *Phys. Rev. Lett.*, **88**(1): p. 010405-4 (2002).

“Atomic Physics Based Simulations of Ultra-cold Plasmas”

F. Robicheaux

*Auburn University, Department of Physics, 206 Allison Lab, Auburn AL 36849
(robicfj@auburn.edu)*

Program Scope

This theory project focuses on the study of atomic processes that occur in ultra-cold plasmas. We have investigated plasmas in strong magnetic fields and without magnetic fields. The results of our studies of atomic processes in strongly magnetized plasmas are of direct relevance to the two collaborations (ATHENA and ATRAP) that are attempting to create cold anti-hydrogen. The results of our studies of plasmas without magnetic fields were used to interpret the results from several experimental groups.

Typically, the plasmas (without magnetic fields) we study have electron temperatures between 1 and 100 K, sizes of a few 100 μm , and evolve over time scales of several 10 μs . The main interest is the non-linear interplay between atomic and plasma processes. For example, two free electrons can scatter near an ion so that one becomes captured by the ion and the other gains energy. Thus, a Rydberg atom is formed and energy is released to the free electrons. The Rydberg atom can serve as a heat source for the plasma because other electrons can scatter from the Rydberg atom and drive the atom to more deeply bound states.[1] We find that the huge role played by the Rydberg atoms in the plasma is analogous to that played by dust in dusty plasmas: the evolution of the properties of the Rydberg atoms and the plasma are strongly linked.[2] Our goal with this project was to understand some of the basic and peculiar properties of ultra-cold plasmas and demonstrate how they arise from the non-perturbative coupling of atomic and plasma physics. Our simulations correctly described all of the puzzling experimental measurements and also motivated several experimental and theoretical studies.

During the past year, we have begun studies of ultra-cold plasmas in strong magnetic fields. The motivation for this study is the interplay between the atomic and plasma physics in strong magnetic fields. A further motivation is that recent experiments have claimed the formation of anti-Hydrogen by causing anti-protons to traverse ultra-cold positron plasmas; unfortunately, very little is known about the processes that lead to the anti-Hydrogen formation or about the properties of the anti-Hydrogen atoms. We are in the process of developing ideas and computer programs to understand the basic atomic processes in strong magnetic fields. The processes that will need to be understood include: three body recombination, electron-Rydberg atom scattering, photon emission from Rydberg atoms, motion of Rydberg atoms, and electron-proton scattering. Even crude estimates of some of these processes will greatly improve our understanding about the formation and evolution of Rydberg atoms in strong magnetic fields.

Recent Progress 2004-2005

We have recently started simulations of atomic processes in strong magnetic fields. We began with the simulation of three body recombination in a strong

magnetic field. We have completed the first stage of this study which was published in Phys. Rev. A.[3] Glinsky and O'Neil computed the rate for this process in the limit that the magnetic field strength goes to infinity. In this limit, the electrons can only move along the field and the positive ion is fixed in space. They obtained a rate that was roughly a factor of 10 smaller than the $B=0$ rate. We noted that in the recent experiments to make anti-Hydrogen the magnetic fields are very large (3 or 5.4 T) but are not in the limit of Glinsky and O'Neil. We performed classical Monte Carlo simulations of the three body recombination rate including next order effects in $1/B$. Our simulations allowed the proton to have its full motion while the electron motion was found using the guiding center approximation since the cyclotron orbit of the electron was by far the fastest time scale and smallest length scale. We found that the recombination rate was roughly 60% higher than in the $B=\infty$ limit for a proton moving slowly through an electron gas.

A much more ambitious study tried to model the motion of the anti-proton through a realistic representation of the trap. In order to do this, we self-consistently solved for the electric potential with a cold positron plasma using the experimental trap geometries and voltages. The simulation included the slowing of the anti-proton due to interaction with plasma waves in the positron cloud, individual scattering with positrons, and capture of positrons and stripping in the trap electric fields. We identified the short time the anti-proton spends in the positron clouds as a dominant effect in the experiments. Detailed calculations are mostly in agreement with all experimental measurements. We were able to obtain additional information about the velocity distribution of the anti-hydrogen and the binding energy distribution and found that the anti-hydrogen atoms had substantially higher than expected speeds along the B-field. The results are published in Ref. [4]. The results of this study confirmed some of the expectations from Ref. [3]. However, we found that the short time spent in the positron plasma greatly reduced the binding energy compared to expectations. This has major implications for the experiments. These results were verified in two later papers published in PRL.

We have completed or will complete by September 2005 the 4 goals set in last year's report. (1) *Three body recombination (TBR) in strong B-field without the guiding center approximation.* The character of the states formed in TBR will determine whether anti-hydrogen atoms can be trapped. We have written and used a program to compute TBR ($e + e + p$ goes to $H + e$) in a strong B-field using the full Newtonian equations of motion. Because of the short cyclotron period of the electron, the numerical solution of this problem is quite challenging; the computations are performed on a massively parallel computer. We have found that the majority of the atoms formed have high B-field seeking character which precludes trapping in magnetic multipole fields. We are currently trying to find simple rules for how the properties depend on the electron temperature and the magnetic field strength. [Status: paper in preparation] (2) *Radiative decay in strong B-field.* The radiative decay of Rydberg states is qualitatively changed by B-fields of 1 or more Tesla. We have solved for the fully quantum radiative decay of a H atom in strong B-field using a basis set expansion of the eigenstates. We have followed the decay from states with up to $n=40$ to the ground state by directly solving the time dependent rate equations. Also, we examined a semi-classical

approximation to a subset of states. [Status: paper completed, to be submitted soon]

(3) *Double charge exchange*. The ATRAP group succeeded in making anti-hydrogen by a two stage process: (a) highly excited Cs was introduced into a positron plasma where a charge exchange occurred making highly excited Ps, then (b) the highly excited Ps entered a region where anti-protons were trapped and a second charge exchange occurred giving highly excited anti-hydrogen. Previous theoretical treatment ignored the strong B-field. We have solved Newton's equations for this system to obtain the properties of the highly excited Ps and anti-hydrogen as a function of the initial n-quantum number of the Cs atom. We found that, for the ATRAP experiment, the recombination preferentially creates Ps with velocity perpendicular to the B-field and anti-hydrogen atoms that were in high field seeking states. [Status: paper under review at PRA]

(4) *Closer interaction with anti-hydrogen experimental groups*. The competitive nature of the two groups, ATHENA and ATRAP, attempting to make and trap anti-hydrogen put external scientists in an awkward position...not having access to discussions of the interesting physics issues and not being informed of new measurements until after publication. In 2004, the ATHENA group split into 2 groups: ALPHA and AEGIS. The ALPHA group asked me to join that collaboration and I accepted. The atomic physics simulations performed at Auburn University are an important part of the discussions. [Status: formal agreement between institutions to be signed shortly]

We also completed two atomic theory projects in related areas. In Ref. [5], we give the results of calculations of electron impact ionization from excited states of H and H-like ions (Li^{2+} and B^{4+}). We compared fully quantum calculations with distorted wave perturbation theory and a completely classical calculation. This is important because ionization from the ground state is not a one step process in many plasmas; the ionization occurs by electron impact excitation to high n states followed by a subsequent ionization. Not surprisingly, we found that the perturbative calculations improved as the charge increased and n decreased. However, we found that the classical calculations did not approach the quantum calculations quickly with increasing n. Fully quantum calculations are time consuming and can be converged only for $n < 6$. Many plasma modeling programs use simple approximations for ionization out of high n states based on mixed classical/quantum calculations whose validity is now suspect. Our conclusion is that electron impact ionization of highly excited ions is an urgent, open question. In Ref. [6], we computed the charge transfer in collisions of p or He^{2+} with H_2^+ molecular ion. In particular, we investigated the dependence on the angle of the molecular ion relative to the projectile's velocity. The motivation was calculations performed by Cheng and Esry that did not agree with the results of experiments performed at KSU. Our calculations qualitatively agreed with the calculations of Cheng and Esry.

Finally, this program has several projects that are strongly numerical but only require knowledge of classical mechanics. This combination is ideal for starting undergraduates on publication quality research. Since 2004, 5 undergraduates have participated in this program. Daniel Phalen completed the quantum scattering calculation of Ref. [6] during the summer of 2004. Chris Norton and Michael Wall completed the double charge exchange calculation described above during spring of 2005; they are now working on a time dependent quantum problem. Michelle

Zhang and Christine Taylor are working on a project to simulate the motion of an anti-hydrogen atom interacting with the complicated magnetic fields in the proposed anti-hydrogen traps in order to test ideas about measuring whether or not the anti-hydrogen atoms are trapped. In addition to these undergraduates, this grant supports the investigations of Turker Topcu who is a graduate student; he has completed the investigation of radiative cascade in strong B and is now finishing model quantum calculations of electron impact ionization of Rydberg atoms ($n \sim 25$).

Future Plans

Ultra-cold plasmas Recent experiments by S. Bergeson's group at BYU and G. Raithel's group at U. Michigan have uncovered interesting behavior of ultra-cold plasmas with cylindrical symmetry. The BYU experiments have $B \sim 0$ while the UM experiments are in high B. We plan to: (1) simulate the expansion of ultracold plasma in cylindrical symmetry with and without high B and compare to experiment and our previous results for spherical symmetry, (2) simulate TBR in an expanding ultracold plasma in strong B and the properties of the atoms, and (3) simulate plasma stability due to electron-electron collisions in the presence of magnetic multipole fields (under hot debate between several experimental groups).

Anti-hydrogen motivated calculations The next stage of the anti-hydrogen experiments will focus on trapping the atoms. This has raised several interesting questions which we will address. We plan to: (1) investigate the properties of atoms formed through TBR in strong B fields and their properties after collisions, (2) investigate the center of mass motion of highly excited H atoms through spatially varying E- and B-fields focusing on how the electric and magnetic dipole moments couple to the motion, and (3) investigate methods to cool highly excited atoms in strong fields.

Related problems In many plasma simulations, electron scattering from highly excited atoms is treated by a classical approximation but this may be accurate[5]. Also, several of the projects above assume the availability of scattering data which, in some cases, is not available. We plan to: (1) perform model quantum calculations with reduced dimensionality in order to treat very high n and understand how the quantum results approach the classical and (2) investigate collisions between charged particles (e.g. $e + p$, $e + e$, & $p + p$) at low temperatures but in strong B-fields.

DOE Supported Publications (2002-2005)

- [1] F. Robicheaux and J.D. Hanson, Phys. Rev. Lett. **88**, 055002 (2002).
- [2] F. Robicheaux and J.D. Hanson, Phys. Plasmas **10**, 2217 (2003).
- [3] F. Robicheaux and J.D. Hanson, Phys. Rev. A **69**, 010701 (2004).
- [4] F. Robicheaux, Phys. Rev. A **70**, 022510 (2004).
- [5] D.C. Griffin, C.P. Balance, M.S. Pindzola, F. Robicheaux, S.D. Loch, J.A. Ludlow, M.C. Witthoef, J. Colgan, C.J. Fontes, and D.R. Schultz, J. Phys. B **38**, L199 (2005).
- [6] D.J. Phalen, M.S. Pindzola, and F. Robicheaux, Phys. Rev. A **72** (2005) in press.

Laboratory Research Summaries
(by institution)

AMO Physics at Argonne National Laboratory

R. W. Dunford, E. P. Kanter, B. Krässig, S. H. Southworth, L. Young
Argonne National Laboratory, Argonne, IL 60439

dunford@anl.gov, kanter@anl.gov, kraessig@anl.gov, southworth@anl.gov, young@anl.gov

Our central goal is to establish a quantitative understanding of x-ray interactions with free atoms and molecules. With the advent of hard x-ray FELs, exploration of nonlinear and strong-field phenomena in the hard x-ray regime becomes accessible for the first time. For example, strong focusing can lead to a situation where photoabsorption rates exceed Auger rates to create large ensembles of hollow atoms. Understanding and tracking the vacancy cascade process in these hollow atoms is of intrinsic interest and will be of great importance in accessing radiation damage. We have made progress in understanding the hard x-ray formation of hollow atoms (see Double K-Vacancy Production in Heavy Atoms) and in measuring vacancy cascades using x-ray—x-ray coincidence techniques (see Two-Photon Decay and Vacancy Cascades). Techniques for microfocusing of x-rays are being developed for our project aimed at understanding the behavior of atoms and molecules in strong-optical fields (see X-ray Microprobe of Optical Strong-Field Processes). X rays provide a simple window on optical strong-field processes because the optical-fields perturb the outer electron shells, but x-ray absorption starts from an unperturbed inner-core level to yield easily interpretable spectra. The time-resolved x-ray microprobe with spectral sensitivity further allows us to probe ion dynamics in complex plasma environments with ~ 10 -micron spatial and ~ 100 -ps temporal resolution. These studies of atoms and molecules in strong-optical fields will be relevant for pump/probe experiments at next generation sources. Foundational to these new experiments is the detailed understanding of x-ray photoionization (see Nondipole Interactions in Photoelectron Angular Distributions). We have explored a broad energy range where the dominant interaction evolves from photoabsorption to scattering, with careful attention to regions near resonances and thresholds. We have focused on understanding the limitations of *ab initio* theory, in particular the validity of the independent particle approximation and the role of multipole effects in the weak-field regime. Recent progress is described below.

X-ray microprobe of optical strong-field processes

L. Young, R.W. Dunford, C. Hoehr, E.P. Kanter, B. Krässig, E.R. Peterson,
S.H. Southworth, D.L. Ederer¹, E.C. Landahl², J. Rudati², R. Santra³

Understanding the behavior of atoms and molecules in strong external fields is of both intrinsic and topical interest. The manipulation of electron motion by imposing strong laser fields has led to high harmonic generation, strong-field control of molecular dissociation, Coulomb explosion, and x-ray generation in clusters. The unique feature of our studies is the use of microfocused tunable, pulsed x-rays from the Advanced Photon Source to probe within the strong-field environment provided by a focused laser. The controlled microfocusing of x-rays provides many advantages: 1) access to a strong-field environment using standard kHz laser technology, i.e. more efficient use of laser power, 2) micron-level spatial resolution combined with 100-ps temporal resolution to monitor dynamical processes such as Coulomb explosion, 3) ease of sample replenishment. With the x-ray microprobe, we can probe not only isolated atom behavior, but also plasma dynamics with spatial and spectroscopic resolution. This past year we

have completed three distinct studies: 1) isolated atom x-ray spectroscopy of Kr ions produced by the strong field laser, 2) monitoring and simulating Coulomb explosion dynamics in a transient underdense laser-produced plasma, 3) polarization probes of the alignment induced by tunnel ionization.

Our apparatus for x-ray microfocusing into the strong laser-field environment at Sector 7 of the Advanced Photon Source currently yields $\sim 10^6$ monochromatic 14 keV x-rays/pulse into a ~ 10 -micron spot using a Kirkpatrick-Baez mirror pair. An active feedback system was implemented to stabilize the x-ray beam position to ~ 1 micron to enable energy scanning with the double crystal Si(111) monochromator. The x rays were overlapped with the focused output of a new Ti:sapphire regenerative amplifier with 2.5 W average power and repetition rates from 1-5 kHz (e.g. 2.5 mJ/pulse, 50 fs at 1 kHz). The new Ti:sapphire amplifier with its increased reliability and pulse energy, installed in November 2004, was instrumental to the considerable progress that we have made this past year.

A dramatic laser-induced modification of the near-edge spectrum of Kr gas can be achieved via short pulse laser irradiation, as shown in Fig 1. The laser pulse (50 fs) preceded the x-ray pulse (100 ps) by ~ 1 ns and the two were spatially overlapped in an effusive jet of Kr with density $\sim 10^{14}/\text{cm}^3$. The spectra were acquired by monitoring Kr $K\alpha$ fluorescence as a function of x-ray excitation energy. The striking new feature in the x-ray spectrum is the appearance of a strong resonance at 14.314 keV due to the 4p hole created by tunnel ionization at an intensity of $\sim 4 \times 10^{14} \text{ W}/\text{cm}^2$. At this intensity it is impractical to create only a single charge state of Kr. Thus, the laser-on spectrum contains contributions from both Kr^{1+} and Kr^{2+} .

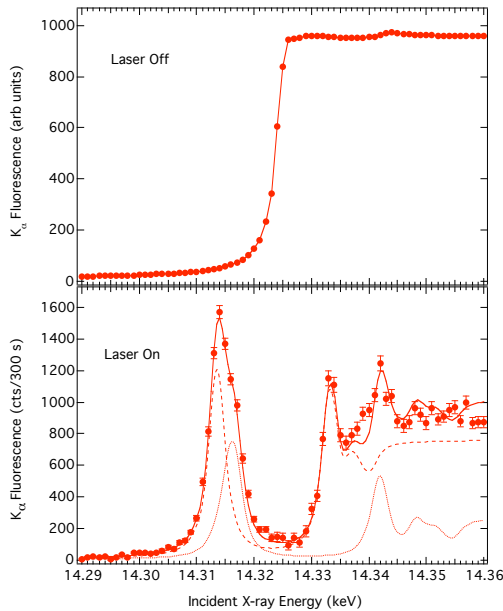


Fig 1. Top: Fluorescence excitation near-edge spectrum of neutral krypton. Bottom: Same for laser-ionized krypton. Dashed (dotted) line is the *ab initio* Kr^+ (Kr^{2+}) spectrum convolved with the instrument function. Solid line is the sum of the Kr^+ and Kr^{2+} components used to fit the data. The $\text{Kr}^+/\text{Kr}^{2+}$ ratio is ~ 3 .

The spectra for the krypton ions were constructed by combining the discrete lines from *ab initio* relativistic configuration interaction calculations by L. Pan, D.R. Beck and S. O'Malley (submitted for publication) with a continuum matching algorithm proposed by Reilman and Manson (1978). The spectra reveal the shifting of the oscillator strength from the continuum to the discrete lines as a function of ionization stage as well as the change in the K-shell oscillator strength sum rule for higher Z -atoms. It is interesting to compare the incipient ion densities of $10^{14}/\text{cm}^3$ over an interaction length of ~ 1 cm, with that in a typical collinear ion beam experiment, densities of $10^7/\text{cm}^3$ and interaction length of 100 cm. This demonstrates that laser-generated transient species, e.g. ions, can easily be generated with sufficient density for x-ray spectroscopy.

Beyond the measurement of isolated atom properties obtained at “zero” time delay and “zero” spatial offset, one can also monitor ion dynamics in the complex plasma environment created by the ultrafast laser by changing the time delay and spatial position of the x-ray microprobe.

Under our conditions (density $\sim 10^{14}/\text{cm}^3$, laser spot size $\sim 100 \mu\text{m}$ FWHM, Rayleigh range ~ 30 mm) we create a transient underdense plasma with a central core of Kr^{2+} imbedded in a broader distribution of Kr^{1+} .

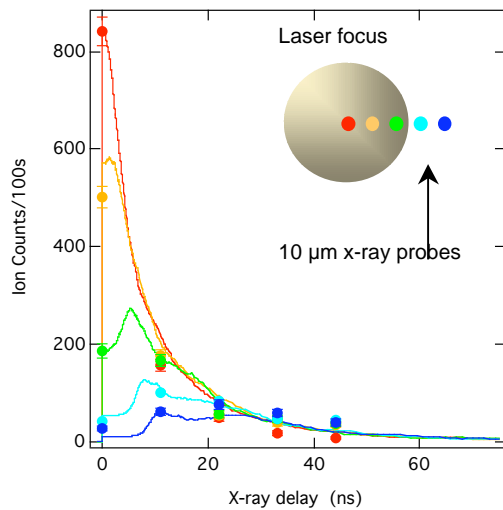


Fig 2. Ion densities as a function of x-ray probe displacement. Probe positions are successively displaced $20 \mu\text{m}$ from central position. The corresponding traces are from MD simulation.

The subsequent Coulomb explosion can be monitored by tuning the x-ray energy to the $1s \rightarrow 4p$ resonance to follow the time development of the ion density at various points in space. Within the laser focus, the ion signal is initially a maximum and then decays due to Coulomb explosion whereas outside the laser-irradiated volume, a later maximum occurs as the ions traverse the probe region (Fig 2). The energetic electrons ($U_p \sim 24\text{eV}$) leave the interaction region within ~ 1 ns and do not appreciably affect the ion dynamics. A molecular dynamics simulation (10000 particles) shows good agreement with the measured temporal development as well as with measured ion kinetic energies. In addition, the simulation reveals a definitive spatial/temporal segregation of the ions that can be useful (see Kanter et al abstract).

A third development has been to probe alignment caused by tunnel ionization using polarized x-rays tuned to the $1s \rightarrow 4p$ resonance. With the quantization axis (z) defined by the laser polarization, the tunnel ionization process preferentially produces a hole in the p_z orbital. As a consequence, the eigenstates of the ion that can be probed by x-ray absorption are $|4p_{3/2}, m\rangle$ and $|4p_{1/2}, m\rangle$ where $m = \pm 1/2$. The $m = \pm 3/2$ states have no overlap with the $4p_z$ orbital. As one rotates the plane of polarization of the tunnel ionization laser relative to that of the x-ray probe, then one expects a modulation of the strength of the $1s \rightarrow 4p$ resonance, as shown in Fig 3. The large modulation $\sim 2:1$ is indicative of significant alignment. The alignment markedly changes the appearance of the absorption spectrum since the $4p$ resonance is suppressed ~ 2 -fold relative to the continuum when the laser and x-ray polarizations are perpendicular. Following the time development of the resonance can probe reorientation of the $4p$ hole. The $4p$ resonance has also been used to measure the x-ray pulse duration through cross-correlation. These data are being prepared for publication.

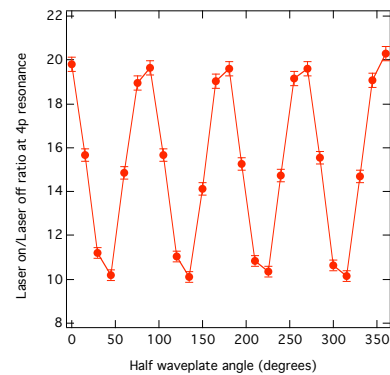


Fig 3. Strength of the $1s \rightarrow 4p$ resonance as a function of angle between laser and x-ray polarization directions. Amplitude for the parallel orientation is ~ 2 times greater than for perpendicular.

A wide variety of phenomena can be probed with time-resolved x-ray spectromicroscopy, such as molecular alignment, energy dependence of x-ray propagation through plasmas, and laser ablation mechanisms. We plan experiments to measure the x-ray spectrum of a dressed atom which will complement theory (R. Santra). Initial tests using the kHz laser to align molecules are underway. Aligned molecules will permit stringent tests of molecular photoionization in addition to being useful for many applications.

Nondipole interactions in photoelectron angular distributions

S. H. Southworth, E. P. Kanter, B. Krässig, R. W. Dunford, L. Young,
L. A. LaJohn⁴, R. H. Pratt⁴, B. A. DeHarak⁵, N. L. S. Martin⁵, R. Wehlitz⁶

In theoretical formulations of photoionization, first-order corrections to the dipole approximation include interference of electric-dipole (E1) amplitudes with electric-quadrupole (E2) and magnetic-dipole (M1) amplitudes. For a linearly-polarized photon beam, the differential cross section can be expressed as [J. W. Cooper, Phys. Rev. A **47**, 1841 (1993)]

$$\frac{d\sigma}{d\Omega}(\theta, \phi) = \frac{\sigma}{4\pi} \left\{ 1 + \beta(3\cos^2\theta - 1)/2 + (\delta + \gamma\cos^2\theta)\sin\theta\cos\phi \right\},$$

where σ is the angle-integrated cross section, β is the dipole anisotropy parameter, and δ and γ characterize the "nondipole asymmetries" resulting from E1-E2 and E1-M1 cross terms. Nondipole asymmetries are sensitive to variations in the magnitudes and phases of E1, E2, and M1 photoionization amplitudes and provide information on photoionization dynamics that complements or extends information from cross sections and dipole anisotropies. We have developed a photoelectron spectrometer with four rotatable analyzers that determines the β , δ , and γ parameters from photoelectron intensities measured at selected angles. Experiments on atomic and molecular inner shells have been made using 13–22 keV x rays at Argonne's Advanced Photon Source and valence electrons were studied using 10–200 eV radiation at Wisconsin's Synchrotron Radiation Center.

We previously reported on an experimental and theoretical study of the nondipole asymmetries of Kr 1s photoelectrons over the 11–8000 eV kinetic energy range [Ref. 1]. In a recent paper [S. H. Southworth *et al.*, submitted to Radiat. Phys. Chem.] we compared nondipole asymmetries of Kr 1s and Br K-shell photoelectrons of Br₂ and BrCF₃ with first-order retardation calculations within the independent-particle approximation (IPA). The point-Coulomb model is inaccurate at lower kinetic energies where screening affects the normalizations and asymptotic phase shifts of the continuum functions. Both full multipole relativistic IPA and nonrelativistic IPA calculations agree well with the measured Kr 1s asymmetries. Two continuum waves are treated in the nonrelativistic model, $1s \rightarrow \epsilon p$ by E1 interaction and $1s \rightarrow \epsilon d$ by E2 interaction. The angular distribution is simplified to the form with $\beta = 2$, $\delta = 0$, and γ can be expressed in atomic units as

$$\gamma = 3\alpha\omega \frac{Q}{D} \cos(\delta_2 - \delta_1),$$

where α is the fine-structure constant, ω is the photon energy, D , Q are the radial dipole and quadrupole matrix elements, and $\delta_{1,2}$ are the asymptotic phase shifts. Inspection of the calculated normalizations and phase shifts indicates the presence of an IPA shape resonance in the ϵd channel that produces rapid variation of the calculated γ parameter over the 1–10 eV kinetic energy region for both Kr 1s and Br 1s. The nondipole asymmetries of Br K-shell photoelectrons of Br₂ and BrCF₃ show energy variations similar to that of Kr 1s. The nondipole asymmetries are negative over the ≈ 5 –800 eV kinetic energy range, i.e., the angular distributions are tilted backwards with respect to the photon propagation vector, contrary to the intuitive idea of the photoelectron being pushed forward by the photon momentum. The molecular Br K-shell asymmetries agree fairly well with IPA calculations for atomic Br 1s, which indicates that the ϵp and ϵd continuum waves of the atomic model are not significantly modified by rescattering in the molecular field produced by neighboring atoms.

While the IPA appears to be adequate to describe the nondipole asymmetries of K-shell photoelectrons, electron-correlation effects are generally important for valence-shell photoionization where discrete and continuum photoexcitations overlap. Discrete-continuum and continuum-continuum interactions in E1 and E2 photoexcitation channels were studied in earlier measurements of He 1s [B. Krässig *et al.*, Phys. Rev. Lett. **88**, 203002 (2002); Ref. 6] and Xe 5s [Ref. 7] nondipole asymmetries. We recently improved the performance of our electron spectrometer by reducing stray electric and magnetic fields and by adding trimming circuits to match the dispersions of the four analyzers. We made more extensive measurements of E1 and E2 autoionizing resonances in He 1s and Ne 2p photoionization and made survey measurements on H₂. Data analysis is in progress.

Double K-photoionization of Heavy Atoms

E. P. Kanter, R. W. Dunford, D. S. Gemmell, B. Krässig, S. H. Southworth, and L. Young

The double K-photoionization of heavy atoms is a rare process which produces a *hollow* atom. The process itself is of fundamental interest as a measure of electron-electron correlations in high-Z systems, but this work has several practical applications as well. For example, planning for future work with the LCLS requires a more complete understanding of the decay paths of such multiply-ionized atoms. We have previously reported on a comprehensive study of double K-photoionization of Ag (Z=47). Measurements were carried out at several photon energies from just below the double K-ionization threshold (51.782 keV) to the region of the expected maximum in the cross-section (~90 keV). The energy-dependence of those data was fitted with a model in which the shakeoff and scattering contributions are calculated independently. Because of extensive previous studies of this atomic system using the electron capture (EC) decay of ¹⁰⁹Cd, the shakeoff contribution is well known experimentally for the single-electron final state produced in EC. Thus, our photoionization measurements served to isolate the effects of the dynamic electron-electron scattering term. Analysis of those results demonstrated a significantly larger scattering contribution than in lighter atoms. Using the scaling properties of electron impact ionization cross sections, we have developed a model which quantitatively describes these observations. In an effort to confirm this model and complete this work, we recently attempted to extend those measurements to 300 keV, well beyond the peak near 100 keV. Such measurements could demonstrate the predicted fall-off toward the EC asymptotic limit. Because of an accident affecting the wiggler beamline used for those high energies we could not obtain sufficient flux during our scheduled period and we will need to repeat those measurements in the near future.

Two Photon Decay and Inner-shell Vacancy Cascades

R. W. Dunford, E. P. Kanter, B. Krässig, S. H. Southworth, L. Young, P. H. Mokler⁷,
and Th. Stöhlker⁷

There are a number of processes initiated by photoionization of the K shell of an atom which involve the coincident emission of two or more photons. One process involves two-photon decay in which an ns or nd electron directly fills the K-hole with the emission of two-photons. This transition proceeds via a complete set of virtual intermediate states. Another process involves a cascade of E1 transitions via real intermediate states. We are studying both of

these processes in heavy atoms using x-rays from the APS. The two-photon decay process provides a unique means of testing atomic theory. Typical measurements result in data on transition probabilities differential in the opening angle distribution and the energy of the individual photons. Together these characteristics provide a wealth of information to test the details of the atomic structure of these heavy atomic systems. The study of cascades is part of a general effort by the group aimed at understanding the complex issue of vacancy cascades following photoionization. In our most recent measurements, a pair of germanium detectors was arranged around a gold target that was irradiated with x-rays from the APS. Some of the K-holes produced in the gold target decayed by emission of two photons or participated in a vacancy cascade. We studied these processes by looking for coincidences between the two detectors. Data analysis is currently in progress. The two-photon data provide a measurement of the differential probability for this process as a function of the energy of the individual photons. Our analysis of the cascade data has shown that we can also measure a three-step process involving emission of two photons accompanied by a Coster-Kronig rearrangement in the intermediate state.

Gerade and ungerade photo-double ionization correlation functions in helium at 100 eV and 450 eV above threshold

Bertold Krässig, Alexandra Knapp⁸, Reinhard Dörner⁸

Using the formalism which we reported in a previous year, we extracted the shapes, magnitudes and relative phase of the two dipole correlation functions in photo-double ionization of helium from experimental data taken at 100 eV and 450 eV above threshold [Ref 18]. The experiment carried out by the Frankfurt group marks the highest excess energy at which differential measurements of this process have been made. At 100 eV above threshold the results are qualitatively similar to those at lower excess energies with a peaking of the correlation functions for opposite emission of the two photoelectrons. At 450 eV this situation is dramatically changed. At an energy sharing ratio of about 1:10 the results show the maximum in the correlation functions to be shifted away from 180 degrees to much smaller angles, indicating a shift in importance of the knock-out and shake-off mechanisms in this process at high versus low excess energies.

Future Plans

We plan to emphasize those aspects of our program related to the ultrafast and ultraintense x-ray sources of the future. This includes studies of strong-field effects on x-ray photoionization and vacancy decay. We plan to exploit the ultrafast x-ray microprobe technique to probe aligned molecules and other phenomena e.g. x-ray propagation in plasmas. The facility at APS Sector 7, x-ray microprobe coupled with the high-power ultrafast laser, is positioned to play a unique role in understanding strong-field processes. We plan active involvement in the project to produce 1ps x-ray bunches at the Advanced Photon Source as originally proposed by Zholents [NIM **A425**, 385 (1999)] and recently simulated for the APS by Borland [(Phys Rev Special Topics - Accelerators and Beams **8**, 074001 (2005))]. Our traditional program studying higher-order x-ray induced photoprocesses serves as a basis for studies in the new ultrafast/ultraintense x-ray regime and some specific plans are outlined in each subsection.

¹ Tulane University

² Advanced Photon Source, Argonne National Laboratory, Argonne, IL 60439

³ ITAMP, Harvard-Smithsonian Institution, Cambridge, MA

⁴ University of Pittsburgh, Pittsburgh, PA 15260

⁵ University of Kentucky, Lexington, KY 40506

⁶ Synchrotron Radiation Center, Stoughton, WI 53589

⁷ GSI, Planckstrasse 1, D64291 Darmstadt, Germany

⁸ University of Frankfurt, Frankfurt, Germany

Selected Publications 2003 – 2005

[1] Nondipole asymmetries of Kr 1s photoelectrons,

B. Krässig, J.-C. Bilheux, R. W. Dunford, D. S. Gemmell, S. Hasegawa, E. P. Kanter, S. H. Southworth, L. Young, L. A. LaJohn and R. H. Pratt., *Phys. Rev. A* **67**, 022707 (2003).

[2] Threshold krypton charge-state distributions coincident with K-shell fluorescence,

G. B. Armen, E. P. Kanter, B. Krässig, J. C. Levin, S. H. Southworth, and L. Young, *Phys. Rev. A* **67**, 054501 (2003).

[3] Two-photon decay in gold atoms following photoionization with synchrotron radiation,

R.W. Dunford, E.P. Kanter, B. Krässig, S.H. Southworth, L. Young, P.H. Mokler, and Th. Stöhlker., *Phys. Rev. A* **67**, 054501 (2003).

[4] Applications of position sensitive germanium detectors for X-ray spectroscopy of highly charged heavy ions, T. Stöhlker, D. Banas, H.F. Beyer, A. Gumberidze, C. Kozhuharov, E.

Kanter, T. Krings, W. Lewoczko, X. Ma, D. Protic, D. Sierpowski, U. Spillmann, S. Tachenov, and A. Warczak., *Nucl. Instrum. Meth. B* **205**, 210-214 (2003).

[5] Double K-shell photoionization of neon,

S. H. Southworth, E. P. Kanter, B. Krässig, L. Young, G. B. Armen, J. C. Levin, D. L. Ederer, and M. H. Chen, *Phys. Rev. A* **67**, 062712 (2003).

[6] E1-E2 interference in the VUV photoionization of He,

E. P. Kanter, B. Krässig, S. H. Southworth, R. Guillemin, O. Hemmers, D. W. Lindle, R. Wehlitz, M. Ya. Amusia, L. V. Chernysheva, and N. L. S. Martin., *Phys. Rev. A* **68**, 012714 (2003).

[7] Dramatic nondipole effects in low-energy photoionization: experimental and theoretical study

of Xe 5s, O. Hemmers, R. Guillemin, E. P. Kanter, B. Krässig, D. W. Lindle, S. H. Southworth, R. Wehlitz and J. Baker, A. Hudson, M. Lotrakul, D. Rolles, W. C. Stolte, I. C. Tran, A. Wolska, S. W. Yu, M. Ya. Amusia, K. T. Cheng, L. V. Chernysheva, W. R. Johnson, and S. T. Manson., *Phys. Rev. Lett.* **91**, 053002 (2003).

[8] Towards ultrahigh sensitivity analysis of ⁴¹Ca

I.D. Moore, K. Bailey, Z.-T. Lu, P. Müller, T.P.O'Connor and L. Young, *Nucl. Instr. Meth. B* **204**, 701-704 (2003).

[9] Triple Ionization of Lithium by Electron Impact

M.-T. Huang, W.W. Wong, M. Inokuti, S.H. Southworth, L. Young *Phys. Rev. Lett.* **90**, 163201:1-4 (2003).

- [10] From the atomic to the femtoscale
L. Young, in From the Atomic to the Nano-Scale (AIP Press NY, C.T. Whelan & J.H. McGuire, Ed., 2003) p204
- [11] Higher-order processes in X-ray photoionization and decay
R.W. Dunford, E.P. Kanter, B. Krässig, S.H. Southworth, and L. Young
Radiation Physics and Chemistry **70**, 149 (2004).
- [12] Inner-shell photoionization in weak and strong radiation fields
S.H. Southworth, R.W. Dunford, D.L. Ederer, E.P. Kanter, B. Krässig, and L. Young
Radiation Physics and Chemistry **70**, 655 (2004).
- [13] Lifetime of the 2^3P_0 state of He-like ^{197}Au
S. Toleikis, B. Manil, E. Berdermann, H. F. Beyer, F. Bosch, M. Czanta, R. W. Dunford, A. Gumberidze, P. Indelicato, C. Kozhuharov, D. Liesen, X. Ma, R. Marrus, P. H. Mokler, D. Schneider, A. Simionovici, Z. Stachura, T. Stöhlker, A. Warczak, and Y. Zou
Phys. Rev. A **69**, 022507 (2004).
- [14] Two-Photon Decay in Heavy Atoms and Ions
P. H. Mokler and R. W. Dunford
Physica Scripta **69**, C1 (2004).
- [15] Counting Individual Ca Atoms with a Magneto-Optical Trap
I. D. Moore, K. Bailey, J. Greene, Z.-T. Lu, P. Muller, T. P. O'Connor, Ch. Geppert, K. D. A. Wendt, and L. Young
Phys. Rev. Lett. **92**, 153002 (2004).
- [16] Spectator electron behavior during cascade decay in krypton
G.B. Armen, E.P. Kanter, B. Krässig, J.C. Levin, S.H. Southworth, and L. Young
Phys. Rev. A **69**, 062710 (2004).
- [17] Nonvanishing $J=1 \leftrightarrow 0$ two-photon decay: $E1M2$ decay of the He-like 2^3S_1 state
R. W. Dunford
Phys. Rev. A **69**, 062502 (2004).
- [18] Photo double ionization of helium 100 eV and 450 eV above threshold: III. Gerade and ungerade amplitudes and their relative phases
A. Knapp, B. Krässig, A. Kheifets, I. Bray, Th. Weber, A. L. Landers, S. Schössler, T. Jahnke, J. Nickles, S. Kammer, O. Jagutzki, L. Ph. H. Schmidt, M. Schöffler, T. Osipov, M. H. Prior, H. Schmidt-Böcking, C. L. Cocke, and R. Dörner
J. Phys. B: At. Mol. Opt. Phys. **38**, 645 (2005).
- [19] Nondipole effects in molecular nitrogen valence shell photoionization
O. Hemmers, R. Guillemin, D. Rolles, A. Wolska, D. W. Lindle, E. P. Kanter, B. Krässig, S. H. Southworth, R. Wehlitz, P. W. Langhoff, V. McKoy, and B. Zimmermann
J. Elec. Spect. and Rel. Phen. **144-147**, 155-156 (2005).

Overview of J. R. Macdonald Laboratory Program for Atomic, Molecular, and Optical Physics

For more than three decades research in the J.R. Macdonald Laboratory has focused on the dynamics of ions (fast and slow, singly and multiply charged) colliding with ions, atoms, molecules, clusters and surfaces. A major strength of the laboratory has been the presence of a large number of both experimentalists and theorists working in this area, often in collaboration with each other. The science is driven by both theory and experiment. Over the past three years the Lab has added an “ultrafast” intense laser facility (the Kansas Light Source, KLS) and hired new faculty to develop and use it. Even though the laser pulses are actually longer than the collision time scales traditionally studied in the JRML and the electric fields generated by the “intense” laser pulses are typically weaker, using the lasers to interrogate the same targets provides one important benefit — control. The time-dependent profile of the laser pulse can be shaped by the experimentalist and addresses all targets within the interaction volume simultaneously. The presence of the KLS has resulted in a shift in the direction of much of the program away from pure collisions toward intense-laser-matter interactions. This change should be viewed as more adiabatic than sudden: the experimental expertise built in the laboratory over many years for providing targets and for imaging their breakup products and the theoretical tools developed for collisions studies have carried over directly to the AMO ultrafast area. Broadly speaking, the theme that unites the JRML current activities is the same as it has always been: studying the dynamical processes involving ions, atoms, molecules, surfaces, nanostructures exposed to short, intense bursts of electromagnetic radiation. The new feature is the thrust to develop ways to follow these processes in real time. Following the time evolution of a system can provide considerable insight into the dynamics in ways that measuring cross sections alone often cannot.

Most of the present and future activities of the laboratory fall into one of the following theme areas (see following abstracts for further explanation of these topics):

-Time-resolved dynamics of heavy-particle motion in single molecules and molecular ions (Litvinyuk, Ben-Itzhak, Esry, Thumm, Lin, Cocke) COLTRIMS, Coulomb imaging, aligned molecules, pump-probe experiments, time-resolved photoelectron spectroscopy.

-Coherent excitation and control in multilevel systems (DePaola, Chang, Cocke) MOTRIMS, COLTRIMS.

-Interaction of KLS radiation and ions with surfaces and nanostructures (Thumm, Richard) Nanotubes, negative ions on surfaces.

-Attosecond science (Chang, Lin, Cocke) Real-time probes of electronic wave function, harmonic generation, pulse shape characterization.

-Collisions with highly charged ions from the EBIS (Ben-Itzhak, Fehrenbach, DePaola) Slow capture from molecules, MOTRIMS .

-Development of “ultrafast” and other facilities (Chang, Fehrenbach, DePaola, Ben-Itzhak, Carnes, Litvinyuk, Cocke) (Phase stabilized few-cycle laser pulses, femtosecond streak camera, hard-photon/soft-photon pump-probe, “picopulsed” beams of high energy ions)

-Use of national DOE facilities such as the ALS and LCLS within the above themes.

**Structure and Dynamics of Atoms, Ions, Molecules, and Surfaces:
Molecular Dynamics with Ion and Laser Beams**

*Itzik Ben-Itzhak, J. R. Macdonald Laboratory, Kansas State University
Manhattan, Ks 66506; ibi@phys.ksu.edu*

The goals of this part of the JRML program are to study the different mechanisms leading to molecular dissociation and charge exchange following fast collisions, slow collisions, or interactions with an intense short-pulse laser.

Dissociation and ionization of molecular ions by ultra-short intense laser pulses, Itzik Ben-Itzhak, Pengqian Wang, A. Max Saylor, Kevin D. Carnes, and Brett D. Esry, – partly in collaboration with Z. Chang’s group and C. Fehrenbach.

Only a handful of experimental studies of intense ultrashort laser interaction with the simplest molecular ions, H_2^+ , have been conducted so far [1-3]. We have experimentally explored the dependence of laser-induced dissociation and ionization of H_2^+ on the pulse duration using the coincidence 3D momentum imaging technique. The vibrationally excited molecular ion beam (~ 4.2 keV), in our case, is crossed by an ultrashort intense laser beam (35-150 fs, 10^{13} - 10^{14} W/cm²). The resulting fragments are recorded in coincidence by a position-sensitive detector (see publication #12). Complete angular distribution and kinetic energy release maps are reconstructed from the measured dissociation-momentum vectors as shown in figure 1 for 135 fs (left) and 45 fs (right) FWHM, respectively.

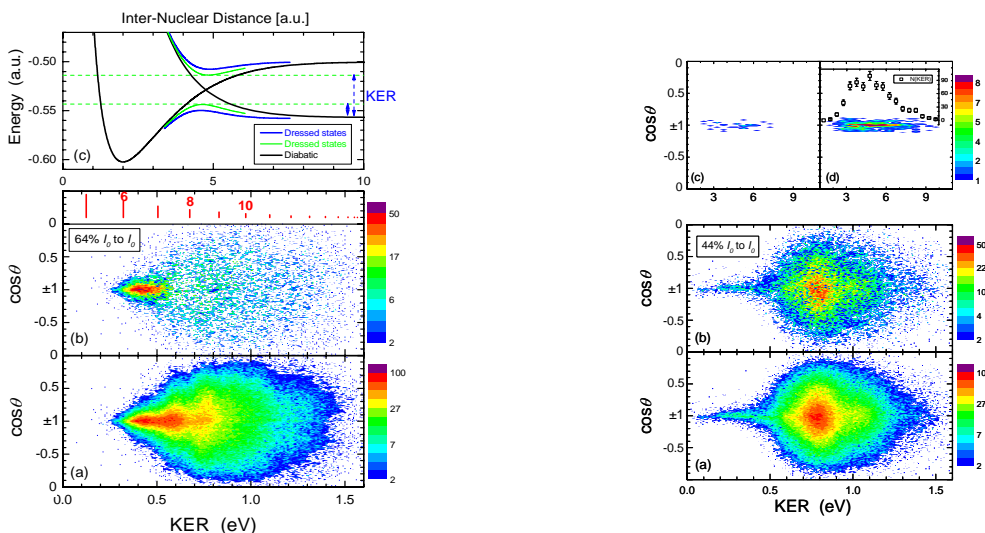


Figure 1. $N(\text{KER}, \cos\theta)$ density plots of H_2^+ exposed to 135 fs (left) and 45 fs (right) FWHM pulses of about 2.5×10^{14} W/cm² peak intensity. The center panel shows the spectra obtained by subtracting two measurements of different peak intensities thus eliminating the contributions from the low intensities caused by the volume effect. In panels c and d we show a similar distribution for the ionization channel.

The data measured with the longer pulse exhibits vibrational structure similar to that observed by Sändig *et al.* [2]. The shorter pulse in contrast leads to a broad peak centered about KER ~ 0.8 eV and a weaker feature at lower KER which is strongly aligned along the laser polarization. Eliminating contributions from low intensities using the IDS method (see panel b, and publication #13) suggest that the broad feature dominates at higher intensities, thus suggesting that it is due to ATD. Calculations performed by Esry indicate that this feature is due to net 2-photon ATD. A similar intensity slice on the longer pulse shows clearly the bond-softening of

the $v=6,7$ states dominates in this case. In addition, we observed ionization only for the shorter pulse at this peak intensity. It is important to note that the observed differences with pulse duration are much larger than one would expect from previous measurements comparing longer pulses, i.e. 135 fs and longer [2,3]. The KER distribution of the ionization channel is broad (see panel d and publication #17) and indicates no double-peak structure, as was suggested in some theoretical treatments of charge resonance enhanced ionization (CREI) (see, for example, Ref. 4), nor vibrational structure reported recently by Pavičić *et al.* [3] for 100 fs at somewhat lower intensities.

Future plans: We are in the process of evaluating the ionization to dissociation branching ratio as a function of peak intensity for the 45 fs pulse. This ratio will be compared with 3D calculations conducted by Esry's group. In addition, we will measure the ionization and dissociation of H_2^+ for a few cycle pulses. Preliminary results for 12 fs FWHM pulse (i.e. 4-5 cycles) are currently being analyzed, and further measurements will be conducted exploring the pulse-duration domain which is comparable to the dissociation time scale. Further in the future we hope to measure the predicted effects of the carrier envelop phase (CEP) on these processes (see publication #9). In addition, we will explore the dissociation and ionization of a few other diatomic molecules, such as O_2^+ and N_2^+ .

1. I.D. Williams, P. McKenna, B. Srigengan, I.M.G. Johnston, W.A. Bryan, J.H. Sanderson, A. El-Zein,, T.R.J. Goodworth, W.R. Newell, P.F. Taday, and A.J. Langley, *J. Phys. B* **33**, 2743 (2000).
2. K. Sändig H. Figger, and T.W. Hänsch, *Phys. Rev. Lett.* **85**, 4876 (2000); C. Wunderlich, H. Figger, and T.W. Hänsch, *Phys. Rev. A* **62**, 023401-1 (2000).
3. D. Pavičić, A. Kiess, T.W. Hänsch, H. Figger, *Phys. Rev. Lett.* **94**, 163002 (2005); and *Eur. Phys. J. D* **26**, 39 (2003).
4. T. Zou and A.D. Bandrauk, *Phys. Rev. A* **52**, R2511 (1995).

Isotopic effects in bond-rearrangement of water ionized by fast proton impact and asymmetric bond cleavage of HDO molecular ions. *M. Leonard, A.M. Saylor, K.D. Carnes, R.C. Trujillo, B.D. Esry, and I. Ben-Itzhak.* Studies of ionization and fragmentation of water molecules by fast protons and highly charged ions have revealed an interesting isotopic preference for H-H bond rearrangement. Specifically, the dissociation of $H_2O^+ \rightarrow H_2^+ + O$ is about twice as likely as $D_2O^+ \rightarrow D_2^+ + O$, with $HDO^+ \rightarrow HD^+ + O$ in between. Further investigations of this isotopic effect lead us to discover that bond rearrangement occurs also when the water molecule is multiply ionized, i.e. $H_2O^{2+} \rightarrow H_2^+ + O^+$, $H_2O^{3+} \rightarrow H_2^+ + O^{2+}$, etc. Furthermore, a similar isotopic preference was measured following double ionization. In addition, we observe a strong preference for cleavage of the O-H bond over the O-D bond, specifically about a factor of 2 and 5 for HDO^+ and HDO^{2+} , respectively (see publication #11). Time evolution calculations of the initial nuclear wave packet projected on the potential energy surface (PES) of the molecular ion are underway in order to determine the relative production rates of this dissociation channels for the different isotopes.

Future plans: We plan to explore if these phenomena also occur following electron capture by a slow highly charged ion. For that case, kinematically complete measurements are possible and are expected to reveal more details about these interesting reaction mechanisms.

Publications:

1. “Dissociation and ionization of H_2^+ by ultrashort intense laser pulses probed by coincidence 3D momentum imaging”, I. Ben-Itzhak, P.Q. Wang, J.F. Xia, A.M. Saylor, M.A. Smith, K.D. Carnes, and B.D. Esry, *Phys. Rev. Lett.* **95**, ##### (2005) – in print.
2. “Proton-Carbon Monoxide Collisions From 10 keV to 14 MeV, I. Ben-Itzhak, E. Wells, Vidhya Krishnamurthi, K.D. Carnes, N.G. Johnson, H.D. Baxter, D. Moore, K.M. Bloom, B.M. Barnes, and H. Tawara, *Phys. Rev. A* (2005) *accepted*.
3. “One- and Two-electron processes in collisions between hydrogen molecules and slow highly charged ions”, E. Wells, K.D. Carnes, H. Tawara R. Ali, E.Y. Sidky, C. Illescas, and I. Ben-Itzhak, *Nucl. Instrum. and Methods B* (2005) *accepted*.
4. “Highlighting the angular dependence of bond softening and bond hardening of H_2^+ in an ultrashort intense laser pulse”, P.Q. Wang, A.M. Saylor, K.D. Carnes, J.F. Xia, M.A. Smith, B.D. Esry and I. Ben-Itzhak, *J. Phys. B* **38**, L251 (2005).
5. “Intensity-selective differential spectrum: Application to laser-induced dissociation of H_2^+ ”, P.Q. Wang, A.M. Saylor, K.D. Carnes, B.D. Esry, and I. Ben-Itzhak, *Opt. Lett.* **30**, 664 (2005).
6. “Dissociation and ionization of molecular ions by ultra-short intense laser pulses probed by coincidence 3D momentum imaging”, I. Ben-Itzhak, P.Q. Wang, J.F. Xia, A.M. Saylor, M.A. Smith, K.D. Carnes, and B.D. Esry, *Nucl. Instrum. and Methods B* **233**, 56 (2005).
7. “Bond rearrangement caused by sudden single and multiple ionization of water molecules”, I. Ben-Itzhak, A.M. Saylor, M. Leonard, J.W. Maseberg, D. Hathiramani, E. Wells, M.A. Smith, J.F. Xia, P.Q. Wang, K.D. Carnes, and B.D. Esry, *Nucl. Instrum. and Methods B* **233**, 284 (2005).
8. “Electrostatic Ion Beam Trap for Electron Collision Studies”, O. Heber, P.D. Witte, A. Diner, K.G. Bhushan, D. Stasser, Y. Toker, M.L. Rappaport, I. Ben-Itzhak, D. Schwalm, A. Wolf, N. Alstein and D. Zajfman, *Rev. Sci. Instrum.* **76**, 013104 (2005).
9. “Controlling HD^+ and H_2^+ dissociation with the carrier-envelope phase difference of an intense ultrashort laser pulse”, V. Roudnev, B.D. Esry, and I. Ben-Itzhak, *Phys. Rev. Lett.* **93**, 163601 (2004).
10. “Ionization of atoms by the spatial gradient of the pondermotive potential in a focused laser beam”, E. Wells, I. Ben-Itzhak, and R.R. Jones, *Phys. Rev. Lett.* **93**, 023001 (2004).
11. “Size dependent electron impact detachment of internally cold C_n^- and Al_n^- clusters”, A. Diner, Y. Toker, D. Stasser, O. Heber, I. Ben-Itzhak, P.D. Witte, A. Wolf, D. Schwalm, M.L. Rappaport, K.G. Bhushan, and D. Zajfman, *Phys. Rev. Lett.* **93**, 063402 (2004).
12. “Electrostatic Ion Beam Trap”, O. Heber, N. Alstein, I. Ben-Itzhak, A. Diner, M.L. Rappaport, D. Strasser, Y. Toker, and D. Zajfman, *Nuclear Science Symposium and Medical Imaging conference, 2004 IEEE*, edited by J.A. Seibert (Piscataway, IEEE 2004) vol. **2**, p-1110.
13. “Electron impact detachment of small negative clusters”, D. Zajfman, O. Heber, A. Diner, P.D. Witte, D. Stasser, Y. Toker, M.L. Rappaport, I. Ben-Itzhak, O. Guliamov, L. Kronik, D. Schwalm, and A. Wolf, “Electron impact detachment of small negative clusters”, *Electron and Photon Impact Ionization and Related Topics 2004*, Institute of Physics conference series **183**, 173 (2005).
14. “Reexamining if long-lived N^- anions are produced in fast dissociative electron-capture collisions” I. Ben-Itzhak, O. Heber, I. Gertner, A. Bar-David, and B. Rosner, *Phys. Rev. A* **69**, 052701 (2004).
15. “Interference effects in double ionization of spatially aligned hydrogen molecules by fast highly charged ions”, A.L. Landers, E. Wells, T. Osipov, K.D. Carnes, A.S. Alnasser, J.A. Tanis, J.H. McGuire, I. Ben-Itzhak, and C.L. Cocke, *Phys. Rev. A* **70**, 042702 (2004).
16. “Probing very slow $H^+ + D(1s)$ collisions using the ground state dissociation of HD^+ ”, E. Wells, K.D. Carnes, and I. Ben-Itzhak, *Phys. Rev. A* **67**, 032708 (2003).
17. “Bond-Rearrangement in Water Ionized by Ion Impact”, A.M. Saylor, J.W. Maseberg, D. Hathiramani, K.D. Carnes, and I. Ben-Itzhak, *Application of Accelerators in Research and Industry*, edited by J.L. Duggan and I.L. Morgan (AIP press, New York 2003), vol. **680**, p. 48.

Structure and Dynamics of Atoms, Ions, Molecules and Surfaces: Atomic Physics with Ion Beams, Lasers and Synchrotron Radiation

C.L.Cocke, Physics Department, J.R. Macdonald Laboratory, Kansas State University,
Manhattan, KS 66506, cocke@phys.ksu.edu

The goals of this aspect of the JRML program are to explore mechanisms of ionization of atoms, ions and small molecules by intense laser pulses and ions and to investigate the dynamics of photoelectron emission from small molecules interacting with x-rays from harmonic generation and synchrotron radiation.

Recent progress and future plans:

1) Two-electron removal from small molecules by short intense laser pulses, *Ali Alnaser, S.Voss, T.Osipov, B.Ulrich, C.M.Maharjan, X.-M.Tong, C.D.Lin, Z.Chang, P.Ranitovic, D.Ray, I.Litvinuyuk, I.Bocharova, C.L.Cocke*

(a) The purpose of this project is to develop methods for following, on the shortest time scale possible, the real-time evolution of small molecules placed in non-stationary states. We have continued our investigation of the real-time evolution of the simplest of all molecules, H_2^+ (D_2^+) using short (down to 8 fs FWHM) intense ($< 10^{16}$ W/cm²) laser pulses. Such short pulses are necessary because the characteristic time scale for heavy particle motion for this (as well as for many other light “real” molecules) is less than 20 fs. We ionize the molecule by a gentle single electron removal which launches a wave packet into the $1s\sigma_g$ ground state potential of the molecular ion. After a determined delay we remove the second electron with a much more intense probe pulse and the remaining two-protons “Coulomb explode”. Fig. 1 shows an example of the results, where we plot the kinetic energy release of the two coincidentally measured protons as a function of the delay time between pump and probe pulses. We observe coherently evolving wave packets which oscillate in the “bound” $1s\sigma_g$ potential curve and which dissociate on the $2p\sigma_u$ potential curve. We are able to observe not only the evolution of the centroid of the two-component wave packet, but, in the case of the $1s\sigma_g$ packet, the structure of the wave packet as well. The general appearance of the oscillating packet is that of outgoing waves whose reflection at the outer turning point is sufficiently “soft” that the reflected packets are hardly observable, but whose reflection at the “hard” inner turning point reforms the wave packet again, resulting in repeated out-going wave packets separated in time by the modified period of the $1s\sigma_g$ potential. On the dissociating $2p\sigma_u$ curve the packet proceeds inexorably outward. For weaker probe pulses the well known enhanced ionization is revealed on this trajectory, allowing us to quantify better the properties of this ionization process. The experimental results are in excellent agreement with model predictions of X.-M.Tong. Similar measurements for molecular oxygen targets show qualitatively similar spectra, with distinguishable oscillatory and dissociative components of the wave packets. Analysis of these data should help us to determine the energy surfaces on which the molecule moves and dissociates and illuminate the mechanisms whereby these surfaces are populated in the first place by the pump pulse. Of particular interest in this case is our ability to analyze the decay from molecules of different total charge in the same experiment. We are continuing the extension of this approach to heavier molecules.

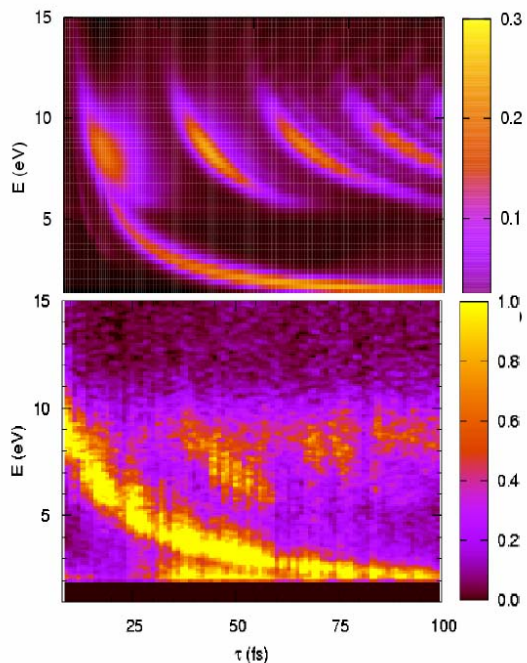


Fig. 1. Plot of Kinetic Energy release versus pump-probe delay time for an 8 fs pulse on D_2 . The pump probe launches a wave packet on the $1s\sigma_g D_2^+$ potential curve and the probe pulse removes the second electron, resulting in a “Coulomb explosion”. Upper panel: Model calculation by X.-M.Tong. Lower panel: experimental result. Both bound and dissociative wave packets are seen.

(b) Using circularly polarized light we have observed that the recoil-momentum spectra from doubly ionized Ar and Ne targets has marked structure in the “sequential ionization” region. We interpret this to result from the emission of the two electrons at different field levels on the rise of the smoothly evolving pulse. The recoil momentum measures the vector sum of the two momenta, each of which is in turn a measure of the vector potential of the electromagnetic pulse at the time of emission. By combining knowledge of the characteristics of the pulse with the measured momentum spectra we are able to deduce the time elapsed between the emission of the two electrons with a precision of less than the optical period of the pulse (2.7 fs). This represents an extremely fast clock for the timing of sequential events in the destruction of an atomic system. In the future, we hope to be able to exploit the angular correlation of the momenta of the electrons using COLTRIMS methods as a “second hand” of the clock to press this time scale into the sub-fs range.

2) Time-resolved photoelectron spectroscopy, P.Ranitovic, A.Hupach, B.Grankow, C.L.Cocke We are developing a system for doing time-resolved photoelectron spectroscopy in a COLTRIMS geometry. The intent is to use soft x rays in the 20-90 eV range from harmonic generation to photoeject electrons from atoms/molecules which have been previously prepared with infrared pulses. We will use a pump-probe approach to measure the evolution of photoelectron spectra as a function of time after preparation. In the first step of this project, we have now succeeded in measuring photoelectron spectra from Ar targets in a COLTRIMS geometry which collects the entire momentum space distribution of the electrons. Fig. 2 shows an example of the resulting electron momentum spectra, sliced in the x-y plane, where the x-ray polarization vector lies along the z direction. The spectrum is dominated by ionization from the 19th through the 23rd harmonics (photon energies 29-36 eV). We are presently trying to increase the harmonic yields before proceeding to pump-probe experiments.

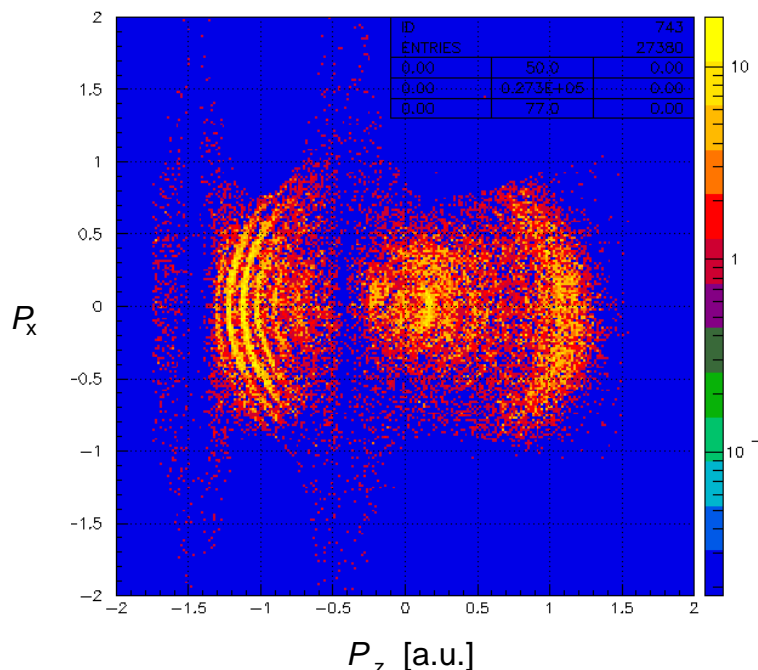


Fig. 2. Momentum spectrum of photoelectrons ejected from Ar in a COLTRIMS geometry using a soft x ray beam obtained from harmonic generation. The most intense rings (to the left, where the resolution is better) correspond to harmonics 19-23 .

3) Picopulsing the Tandem , *K.Carnes,Z.Chang,A.Rankin,M.Wells,C.L.Cocke*

As discussed in our last progress report, we are engaged in a project to try to generate ultrashort pulses (few ps) of very energetic (MeV/nucleon) heavy ions from our Tandem Van de Graaff Accelerator. The ions are generated in the high energy column of the accelerator by 25 fs pulses from the Kansas Light Source (KLS). Time focusing of the pulses is achieved by a judicious choice of the drift distance between acceleration and detection. The transfer line is complete, the focusing mirror has been installed in the terminal of the Tandem and diagnostics of the particle pulses are now underway. We have had to replace the first spiral tube section in the high energy column of our Tandem with a straight-field section to allow the ions to exit the tube. We observe the expected yields of ions (up to several tens of ions per pulse). The next step is to diagnose and optimize the time duration of the pulses.

4) Synchrotron radiation experiments, *T. Osipov, A.Alnaser, P.Ranitovic, C.Marhajan, B.Ulrich,C.L. Cocke (KSU), A. Landers (Auburn Univ.), R. Doerner, Th. Weber, L. Schmidt,A. Staudte, H. Schmidt-Boecking, et al. (U. Frankfurt), M.H. Prior (LBNL)*. At the Advanced Light Source, we have measured the correlated momentum-space distributions of photoelectrons and charged photofragments from energetic photons on small molecules using COLTRIMS. This work is carried out by a large multi-laboratory collaboration involving the University of Frankfurt, LLBL, Auburn Univ. and KSU. During the past year we have focused on the publication of work on Auger emission from fixed-in-space CO, and double ionization of D₂ and He. (publications from this collaboration are listed as 1,3,5,9,14,16-18 below).

Publications appearing in 2004-2005 not previously listed:

1. Auger Electron Emission from Fixed-in-Space CO, Th. Weber, *et al.*, Phys. Rev. Letters **90** 153003 (2003).

2. Laser-peak Intensity Calibration Using Recoil-Ion Momentum Imaging, A.S. Alnaser, X.M. Tong, T. Osipov, *et al.*, Phys. Rev. A **70** 023413 (2004).
3. Vibrationally Resolved K-shell Photoionization of CO with Circularly Polarized Light, T. Jahnke, *et al.*, Phys. Rev. Letters **93** 083002 (2004).
4. Cold-Target Recoil Momentum Spectroscopy Studies of Capture from Atomic and Molecular Hydrogen by O⁸⁺ and Ar⁸⁺, E. Edgu-Fry, *et al.*, Phys. Rev. A **69** 052714 (2004).
5. Multicoincidence Studies of Photo and Auger Electrons from Fixed-in-Space Molecules Using the COLTRIMS Technique, T. Jahnke, *et al.* Journal of Electron Spectroscopy and Related Phenomena **141**, 229 (2004).
6. High Resolution Kinetic Energy Release Spectra and Angular Distributions from Double Ionization of Nitrogen and Oxygen by Short Laser Pulses, S. Voss, A.S. Alnaser, X-M Tong, *et al.*, J. Phys. B: At Mol. Opt. Phys. **37**, 4239 (2004).
7. Interference Effects in Double Ionization of Spatially Aligned Hydrogen Molecules by Fast Highly Charged Ions, A.L. Landers, E. Wells, T. Osipov, K.D. Carnes, A.S. Alnaser, J.A. Tanis, *et al.*, Phys. Rev. A **70**, 042702 (2004).
8. Rescattering Double Ionization of D₂ and H₂ by Intense Laser Pulses, A.S. Alnaser, T. Osipov, E.P. Benis, A. Wech, *et al.*, Phys. Rev. Letters Volume **91** 163002 (2004).
9. Complete Photo-Fragmentation of the Deuterium Molecule, Th. Weber, *et al.*, Nature, Volume **431** (2004).
10. Post ionization alignment of the fragmentation of molecules in an ultrashort intense laser field, X M Tong, Z X Zhao, *et al.*, J. Phys. B: At. Mol. Opt. Phys. **38**, 333 (2004).
11. Effects of orbital symmetries in dissociative ionization of molecules by few-cycle laser pulses, A. S. Alnaser, *et al.*, Phys. Rev. A **71**, 031403 (2005).
12. Routes to Control of H₂ Coulomb Explosion in Few-Cycle Laser Pulses, A. S. Alnaser *et al.*, Phys. Rev. Lett. **93**, 183202 (2004).
13. Effects of Molecular Structure on Ion Disintegration Patterns In Ionization of O₂ and N₂ by Short Laser Pulses, A. S. Alnaser, S. Voss, X. -M. Tong, C. M. Maharjan, P. Ranitovic, B. Ulrich, T. Osipov, B. Shan, Z. Chang, and C. L. Cocke, Phys. Rev. Lett. **93**, 113003 (2004).
14. Vibrationally Resolved K-shell Photoionization of CO with Circularly Polarized Light, T. Jahnke *et al.*, Phys. Rev. Lett. **93**, 083002 (2004).
15. Laser-peak-intensity calibration using recoil-ion momentum imaging, A. S. Alnaser, X. M. Tong, T. Osipov, S. Voss, C. M. Maharjan, B. Shan, Z. Chang, and C. L. Cocke, Phys. Rev. A **70**, 023413 (2004).
16. Photo double ionization of helium 100 eV and 450 eV above threshold: I. Linearly polarized light, A. Knapp, *et al.*, J. Phys. B: At. Mol. Opt. Phys. **38**, 615 (2005).
17. Photo double ionization of helium 100 eV and 450 eV above threshold: II. Circularly polarized light, A. Knapp, *et al.* J. Phys. B: At. Mol. Opt. Phys. **38**, 635 (2005).
18. Photo double ionization of helium 100 eV and 450 eV above threshold: III., Gerade and ungerade amplitudes and their relative phases, A. Knapp, *et al.*, J. Phys. B: At. Mol. Opt. Phys. **38**, 645 (2005).

Population Dynamics in Coherent Excitation of Cold Atoms

B. D. DePaola, Physics Department, J.R. Macdonald Laboratory, Kansas State University, Manhattan, KS 66506, depaola@phys.ksu.edu

The research projects described here have as a unifying theme the measurement of the population dynamics in cold atomic and molecular systems under the influence of coherent light. Through these measurements, all of which are done using the K-State MOTRIMS apparatus, various atomic processes are better understood. The processes include efficient multi-level excitation, and laser-assisted cold collisions. Ancillary measurements of certain charge transfer cross sections have also been made.

Recent Progress and Future Plans

1) Capture cross sections for 7 keV Na^+ + Rb(4d), *M. H. Shah, H. A. Camp, M. L. Trachy, X. Fléchar, M. A. Gearba, H. Nguyen, R. Brédy, S. R. Lundeen, and B. D. DePaola.* The original purpose behind the development of the MOTRIMS methodology was to measure charge transfer cross sections in ion-atom collisions for which some unknown fraction of the target atoms had been prepared into an excited state. Because of the flexibility of the technique, however, once these cross sections have been measured, the same apparatus can be used to measure the relative populations in the target system, using charge transfer with a beam of ions as the probe. Since several processes of interest (described below) involve the $4d_{5/2}$ state of ^{87}Rb , it was necessary to make accurate measurements of charge transfer cross sections from this state. Na^+ was chosen as the projectile because in collisions with Rb, the resulting Q-value spectra have well-resolved peaks. Cross sections for the two major charge transfer channels, resulting in Na(3d) and Na(4s) were measured relative to the previously-measured cross section for the process $\text{Na}^+ + \text{Rb}(5s) \rightarrow \text{Na}(3s) + \text{Rb}^+$. These results have been accepted for publication.

2) Capture cross sections for 7 keV Na^+ + Rb(9f), *M. H. Shah, M. L. Trachy, E. Snow, S. R. Lundeen, and B. D. DePaola.* In one future project, described in section 3, population dynamics for a 4-level ladder system in ^{87}Rb will be measured. In order to carry out these measurements, the relative capture cross sections for all four levels must be known. In collaboration with a group at Colorado State University (ES and SRL) we have therefore made a measurement of the charge capture cross section for 7 keV Na^+ + Rb(9f). This was, essentially, a proof of principle experiment and the cross section obtained is considered preliminary. Nevertheless, based on these results it seems that future experiments on 4-level ladder systems have a good chance of success. However, before the Rb(9f) cross sections can actually be used in population dynamics measurements, values with smaller error bars must be obtained. A new scheme for locking all 3 lasers has been implemented allowing for the extended data acquisition time that will be required to accumulate the necessary statistics.

3) STIRAP for a three level ladder system in ^{87}Rb , *H. A. Camp, H. Nguyen, M. H. Shah, M. L. Trachy, M. A. Gearba, and B. D. DePaola.* STIRAP, or stimulated Raman rapid adiabatic passage, is becoming an increasingly important procedure for the efficient transfer of populations into a desired state. The STIRAP process is being used in fields ranging from quantum information, to quantum chemistry. Until now, however, no measurement has been made of the temporal evolution of the populations being moved *via* the STIRAP process. Now, using the MOTRIMS methodology, the dynamics of the

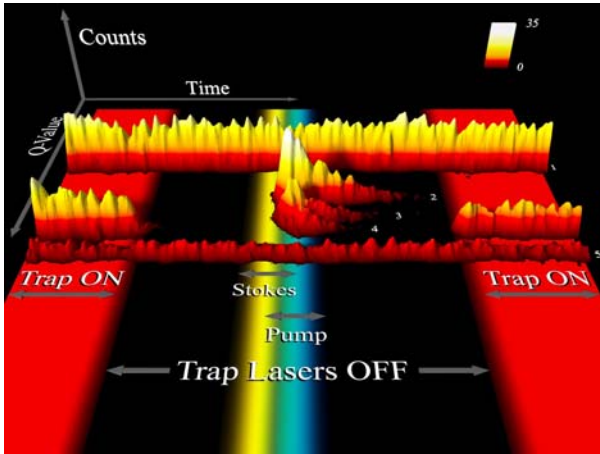


Figure 1: Raw data in 3-level STIRAP experiment.

STIRAP process have been measured. In this study, a beam of 7 keV Na^+ ions was made incident on a target of cooled and trapped ^{87}Rb . Periodically, the trapping lasers were turned off, the Rb was allowed to decay to the ground state, and two pulses of light were used to excite the Rb from the ground state directly to the $4d_{5/2}$ level. From the Q-value spectra, charge transfer from the 5s, 5p, and 4d states could be distinguished. Since the relative charge transfer cross sections from these states have already been measured, the relative populations of these states could be readily deduced from the Q-value

measurements. Furthermore, by sorting these Q-value spectra as a function of time, keyed to the laser pulsing sequence, the relative populations of these states were continuously measured (with 2 ns temporal resolution) as the trap was turned off, the STIRAP lasers were tuned on, then off, and the system was allowed to decay. Figure 1 shows raw data for this experiment. Counts are plotted *versus* Q-value and time referenced from the laser pulse sequence. The temporal locations of the trapping, Stokes, and pump laser pulses are indicated. Each ridge in the figure corresponds to a particular charge transfer channel. The ridges relevant to this population measurement are labeled 5, 4, and 2, corresponding to transfer channels originating from 5s, 5p, and 4d, respectively. The onset of coherent excitation is shown by the appearance of charge transfer from Rb(4d). These represent the very first measurement of the temporal evolution of population during coherent excitation. However, the highest predicted population transfer fraction has still not been realized. In the coming year, the full parameter space of the system (intensities and pulse widths of the two lasers, 1- and 2-photon detunings, and relative timing of the two pulses) will be explored. In order to facilitate this study, control of the lasers will be handled by a computer; the level population data will be fed back into this computer and an optimization algorithm will be used to find the optimal laser values – within the limitations of the apparatus.

Because of the potential application in quantum information devices, there is a re-newed interest in the efficient production of Rydberg atoms. One promising approach is STIRAP. Therefore, with the improved Rb(9f) cross section measurement, and with the improved

locking scheme already in place, the STIRAP process for a 4-level ladder system in ^{87}Rb will be investigated. The excitation scheme is: $5s-5p-4d-9f$.

4) Photo-association, associative ionization, and “Penning” ionization in cold collisions, *M. L. Trachy, M. H. Shah, R. Brédy, and B. D. DePaola.* Three important loss mechanisms in excited cold atoms are photo-association (PA), associative ionization (AI), and “Penning” ionization (PI). In the first process, neutral molecules are formed in photon-assisted collisions between two cold atoms. That is, as two atoms approach, forming a transitory molecule in the electronic ground state, a photon brings the molecule to an excited bound state. In some cases, this electronically excited molecule, generally in a high vibrational state, can then decay to a bound ground state. When this happens, a stable molecule is formed – and is no longer held in the trap. In some variations of PA, additional photons are used to stimulate emission down to the bound ground molecular state. The AI process is similar, but the excitation by more than one laser results in a molecular ion. In true Penning ionization, the internal energies of two excited atoms are pooled, resulting in an ionization event. However, for cold atoms, the collision time is typically much longer than the radiative lifetime, and so this process cannot really occur. In a process related to AI, instead of being excited to a bound molecular ion, the intermediate molecular state can be excited to a repulsive potential in the molecular ion manifold, resulting in the production of a singly charged atom.

For lack of a better term this is being called “Penning” ionization, though this does not reflect the fact that the system must pass through an intermediate molecular state. Building on the work of previous researchers, progress has been made at the JRML in developing an understanding of the complicated processes of PA and AI in cooled and trapped ^{87}Rb . Thus far, most of our attention has been focused on AI. The dc electric fields that already exist in the MOTRIMS apparatus were ideal for the extraction of both molecular and atomic ions. The atoms/molecules were prepared with 50 ns pulses of light slightly red-detuned from the $5s-5p$ resonance (~ 780 nm) and slightly

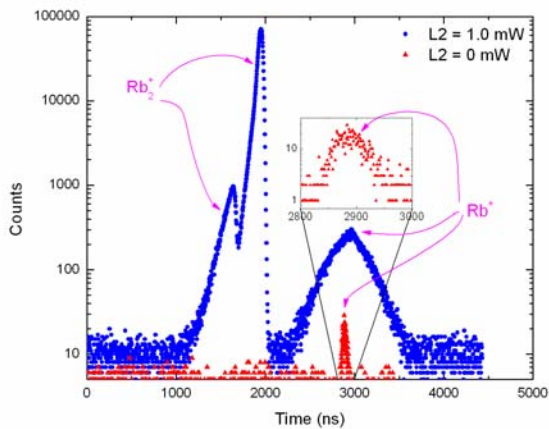


Figure 2: Time-of-flight data. (Time increases to the left.) L2 refers to the laser driving the $5p-4d$ transition.

blue-detuned from the $5p-4d$ resonance (~ 1529 nm). Figure 2 is a time-of-flight spectrum in which one can see two peaks associated with molecular ions, and a single structure associated with atomic ions. The broader atomic structure yields the energy spread of the repulsive potential curve. When compared with theoretical calculations of these curves, this will hopefully give information on the internuclear separation at the time of excitation. In red triangles is shown the atomic ion feature in the absence of the 1529 nm radiation (designated “L2” in the figure). Note that no molecular ions are formed under these conditions. Experiments have already been done in which these

spectra are taken as a function of the intensities of the two lasers. The relative areas under the 2 molecular and 1 atomic peaks vary differently with these intensities, giving some clues as to their excitation paths. In the coming year, more systematic measurements of molecular and atomic ion production will be made as a function of the two lasers' intensity and detuning (measured from atomic resonance). In addition, measurements of PA will be attempted, using the projectile ions of the MOTRIMS apparatus as a probe of neutral molecule formation. An informal collaboration has been established with Prof. Ortiz, of the Kansas State Univ. Chemistry Department. Helped by his expertise in molecular structure calculations, it is hoped that the excitation channels can be determined in PA, PI, and AI.

Publications appearing in 2004-2005 not previously listed:

1. Entropy lowering in ion-atom collisions, H. Nguyen, R. Brédy, T. G. Lee, H. A. Camp, T. Awata, and B. D. DePaola, *Phys. Rev. A* **71**, 062714 (2005).
2. Numerical exploration of coherent excitation in three-level systems, H. A. Camp, M. H. Shah, M. L. Trachy, O. L. Weaver, and B. D. DePaola, *Phys. Rev. A* **71**, 053401 (2005).
3. Three-dimensional spatial imaging in multiphoton ionization rate measurements, R. Brédy, H. A. Camp, T. Awata, B. Shan, Z. Chang, and B. D. DePaola, *J. Opt. Soc. Amer. B* **21**, 2221 (2004).
4. Differential charge-transfer cross sections for systems with energetically degenerate or near-degenerate channels, H. Nguyen, R. Brédy, H. A. Camp, T. Awata, and B. D. DePaola, *Phys. Rev. A* **70**, 032704 (2004).
5. Charge transfer cross sections for Rb(4d), M. H. Shah, H. A. Camp, M. L. Trachy, X. Fléchar, M. A. Gearba, H. Nguyen, R. Brédy, S. R. Lundeen, B. D. DePaola, *Phys. Rev. A* 2005 (accepted).
6. Time evolution of coherent excitation, H. A. Camp, M. H. Shah, M. L. Trachy, H. Nguyen, M. A. Gearba, R. Brédy, X. Fléchar, B. D. DePaola, *Science*, 2005, (submitted).

TIME-DEPENDENT TREATMENT OF THREE-BODY SYSTEMS IN INTENSE LASER FIELDS

B.D. Esry

J. R. Macdonald Laboratory, Kansas State University, Manhattan, KS 66506

esry@phys.ksu.edu

<http://www.phys.ksu.edu/~esry>

Program Scope

The primary goal of this program is to understand the behavior of H_2^+ in an intense laser field. Because the system has more degrees of freedom than can be directly treated, past theoretical descriptions have artificially reduced the dimensionality of the problem or excluded one — or more — important physical processes such as electronic excitation, ionization, vibration, or rotation. One component of this work is thus to systematically include these processes in three dimensions and gauge their importance based on actual calculations. Further, as laser pulses get shorter and more intense, approaches that have proven useful in the past may become less so. A second component of this program is thus to develop novel analytical and numerical tools to describe H_2^+ . The ultimate goal is to understand the dynamics of these strongly coupled systems in quantum mechanical terms.

Recent progress

In the last year, we have worked to develop our ability to solve the time-dependent Schrödinger equation for H_2^+ and its isotopes in an intense laser pulse. We now have computer codes to solve this problem at several levels of approximation, including most standard approximations. In fact, our most sophisticated code matches the state-of-the-art. We have used these codes to study novel effects such as the dependence of dissociation on the carrier-envelope phase difference (Pubs. [5] and [6]) and to support the experimental efforts of I. Ben-Itzhak's group (Pubs. [7,8,10,12]).

Our most sophisticated code solves the time-dependent Schrödinger equation assuming that the nuclei can move only along the direction of the linearly polarized laser. Nuclear rotation is thus ignored, but all other degrees of freedom — both nuclear and electronic — are included exactly. The resulting calculations are three dimensional: nuclear vibration plus two electronic degrees of freedom (the azimuthal angle about the molecular axis can be eliminated by symmetry). These spatial degrees of freedom are discretized using finite differences, and the time evolution is accomplished through a combination of split operator techniques and Crank-Nicolson propagation. Our implementation allows us, however, to treat non-Cartesian coordinates with nonuniform grids while explicitly maintaining the symmetry of the Hamiltonian. We also take advantage of the mass difference between the nuclei and electron by using larger time steps for the nuclear propagation than for the electronic propagation. Finally, we use coordinate scaling to propagate the system to large times, allowing easier extraction of the nuclear momentum distribution. Details of this method are given in Pub. [6].

Probably our most fruitful results (to date) from this code have been in uncovering the influence of the carrier-envelope phase difference (CEPD) on the dissociation of H_2^+ and HD^+ (see Pubs. [5,6]). In particular, our initial calculations showed that the ratio between

dissociation of HD^+ into $p+\text{D}$ and $\text{H}+d$ can vary by as much as a factor of three with the CEPD for 10 fs laser pulses ($\sim 7 \cdot 10^{14}$ W/cm², 790 nm). Similar effects can be seen in the angular distribution of dissociation fragments from H_2^+ . More detailed calculations showed that the kinetic energy release spectrum of the fragments can show an even more marked difference between the two channels — as much as a factor of 100 at some energies.

These calculations showed that the dissociation of HD^+ or H_2^+ could, in principle be controlled by varying the CEPD with laser and detector technologies currently available. The caveat is that in our calculations we considered only the situation in which the molecules started in their ground state. In reality, these molecular ions are produced in an ion source from neutral molecules. The charge stripping is, to a very good approximation, described as a Franck-Condon transition leading to a distribution of vibrational states in the molecular ion. In order to predict whether these CEPD effects can be seen experimentally, then, we should repeat the calculations for each of these initial vibrational states and weight the results with their proper Franck-Condon factor. Moreover, we should include an average over the intensity distribution in the focal volume of the laser. We have recently carried out such calculations and found that while each individual initial vibrational state shows CEPD dependence, the average effectively does not. To see the CEPD dependence, a differential quantity such as the energy distribution must be considered. We are in the process of preparing these results for publication.

We have also used this code to carry out calculations corresponding to the experiments of I. Ben-Itzhak's group (see his abstract for more details). In addition, at lower intensities where ionization is less important or negligible, we have solved the time-dependent Schrödinger equation in the Born-Oppenheimer representation. As seems to be the case generally in the field of intense laser-molecule interactions, both theoretical approaches give general agreement when compared with experiment, but differ in some details. It is not clear whether the discrepancies are the consequence of approximations in the theoretical approaches or in unaccounted for experimental conditions.

Future plans

We will continue to develop the theoretical methods and computer codes described above. In particular, we plan to work closely with I. Ben-Itzhak's group to refine the methods and resolve lingering differences between theory and experiment. For instance, efforts are already underway to include nuclear rotation in the Born-Oppenheimer treatment of dissociation.

Beyond our efforts to perform accurate calculations for these systems, we will spend more time developing simple models with which these systems can be understood in at least a semi-quantitative manner. Although not described above, we have spent time during this past year on such models, and they are beginning to show promise.

Finally, we will continue to search for novel effects — such as the CEPD dependence of dissociation — in these systems.

Publications

12. "Dissociation and ionization of H_2^+ by ultra-short intense laser pulses probed by coincidence 3D momentum imaging," I. Ben-Itzhak, P.Q. Wang, J.F. Xia, A.M. Saylor, M.A. Smith, K.D. Carnes, and B.D. Esry, *Phys. Rev. Lett.* (accepted) (2005).
11. "Lattice approach for $\alpha + \text{H}_2^+$ collisions," S.C. Cheng and B.D. Esry, *Phys. Rev. A* (accepted) (2005).
10. "Highlighting the angular dependence of bond softening and bond hardening of H_2^+ in an ultrashort intense laser pulse," P.Q. Wang, A.M. Saylor, K.D. Carnes, J.F. Xia, M.A. Smith, B.D. Esry, and I. Ben-Itzhak, *J. Phys. B* **38**, L251 (2005).
9. "Bond rearrangement caused by sudden single and multiple ionization of water molecules," I. Ben-Itzhak, A.M. Saylor, M. Leonard, J.W. Maseberg, D. Hathiramani, E. Wells, M.A. Smith, J. Xia, P. Wang, K.D. Carnes, and B.D. Esry, *Nucl. Instrum. Meth. B* **233**, 284 (2005).
8. "Dissociation and ionization of molecular ions by ultra-short intense laser pulses probed by coincidence 3D momentum imaging," I. Ben-Itzhak, P. Wang, J. Xia, A.M. Saylor, M.A. Smith, K.D. Carnes, and B.D. Esry, *Nucl. Instrum. and Meth. B* **233**, 56 (2005).
7. "Disentangling volume effect through intensity-difference spectra: Application to laser-induced dissociation of H_2^+ ," P. Wang, A.M. Saylor, K.D. Carnes, B.D. Esry, and I. Ben-Itzhak, *Optics Letters* **30**, 664 (2005).
6. " HD^+ photodissociation in the scaled coordinate approach," V.R. Roudnev and B.D. Esry, *Phys. Rev. A* **71**, 013411 (2005).
5. "Controlling HD^+ and H_2^+ dissociation with the carrier-envelope phase difference of an intense ultrashort laser pulse," V. Roudnev, B.D. Esry, and I. Ben-Itzhak, *Phys. Rev. Lett.* **93**, 163601 (2004).
4. "Localized component method: application to scattering in a system of three atoms," V. Roudnev, Proceedings of the Seventeenth International IUPAP Conference on Few-Body Problems in Physics, Elsevier (2004), p. S292.
3. "Split diabatic representation," B.D. Esry and H.R. Sadeghpour, *Phys. Rev. A* **68**, 042706 (2003).
2. "Hyperspherical close coupling calculations for charge transfer cross sections in $\text{He}^{2+} + \text{H}(1s)$ collisions at low energies," C.N. Liu, A.T. Le, T. Morishita, B.D. Esry and C.D. Lin, *Phys. Rev. A* **67**, 052705 (2003).
1. "Ultraslow \bar{p} -H collisions in hyperspherical coordinates: Hydrogen and protonium channels," B.D. Esry and H.R. Sadeghpour, *Phys. Rev. A* **67**, 012704 (2003).

Theoretical Studies of Interactions of Atoms, Molecules and Surfaces

C. D. Lin

J. R. Macdonald Laboratory
Kansas State University
Manhattan, KS 66506
e-mail: cdlin@phys.ksu.edu

In this abstract I report recent progress and future plans in the theoretical studies involving atoms and molecules within my group. References to our published papers or preprints (the full list is given at the end of this report) are given in bold letters in the text.

1. Interaction of intense laser fields with molecules and high-order harmonic generation from aligned molecules

Recent Progress:

In collaboration with experimentalists at JRML we continued to explore the double ionization dynamics of molecules. By using sub-10fs pulses with relatively low laser intensity it has been demonstrated that the angular distributions of the atomic ion yields from the breakup of molecules can be explained by the alignment dependence of the tunneling ionization rates of molecules with respect to the laser polarization direction. Experiments performed for N₂, O₂, CO, CO₂, and C₂H₂ molecules have been confirmed from our theoretical calculations. These results have been published with experiments in **A7**, **A10**, **A14**. In the theory paper **A10**, we also showed that further focusing of the atomic ions towards the laser polarization direction is large when longer pulses or higher intensities are used in such experiments. The theory explains why in most of the earlier experiments the ion fragments appear to emerge mostly in the laser polarization direction.

We have also published the detailed paper on sequential double ionization of molecules (**A15**) during this period. The rescattering theory developed earlier has also been used to explain the experimental results, see **A13**. A short review paper on the ionization dynamics of molecules by lasers is given in **A12**, while a longer review has been submitted as a chapter in a monograph (**B3**).

During the last few months, we have undertaken the study of the high-order harmonic generation (HHG) from aligned molecules. Since full *ab initio* calculations are still impractical we adopted the Lewenstein model for the HHG calculation but using accurate molecular wavefunctions. We have illustrated that the angular dependence of HHG also depends critically on the symmetry of the highest occupied molecular orbital (HOMO), see **A4**. This study was motivated by recent HHG measurements in Canada and Japan using the pump-probe method where a pump beam was used to align the molecules while the probe beam was used to generate high-order harmonics at the rotational revival periods where the molecules are best aligned.

Future plans:

We anticipate that additional works on laser-molecule interactions be carried out, especially by few-cycle pulses, to study the dependence of the ionization yields vs the carrier-envelope phase of the pulse. The dependence of HHG on the alignment of molecules will be analyzed further since a recent experiment by Kanai et al [Nature 436, 470 (2005)] indicates that internuclear separation also plays an important role in determining the angular dependence of HHG.

2. Attosecond Physics

Recent Progress:

In the emerging field of attosecond physics, we have made a few relevant theoretical studies. Cross correlations between the attosecond pulse with few-cycle infrared lasers are the standard methods for such experiments. We have analyzed the electron spectra of an autoionizing state which was created by an attosecond XUV pulse and decays in the presence of the IR laser. By analyzing how the electron spectra change with the time delay between the two pulses, we showed how to extract the resonance parameters of the autoionizing state (A2). We have also calculated the angular distributions of the photoelectron spectra by an attosecond pulse in the presence of a circularly polarized IR laser. We showed how to extract the attosecond pulse parameters such as the pulse duration and the chirp from the angular distributions of the electrons (A5). This study was initiated in lieu of the attosecond pulses generated by the polarization gating method at JRML by Dr. Z. H. Chang's group.

In a separate theoretical paper (A8) we showed that the presence of an intense laser can modify the electron spectra produced by an attosecond XUV pulse with the emergence of new resonances that are not produced by the weak attosecond pulse alone. This is analogous to the linear Stark effect where new states can be generated by the electric field.

Future plans:

Attosecond pulses are expected to be used to probe the time evolution of the electronic motion. To study electron-electron interactions, one of the most exciting areas is the probing of the *collective modes* between the electrons in doubly excited states. Under the previous DOE support we had studied these modes theoretically in the 1980's. Now it appears that attosecond pulses can be used to probe these modes experimentally. First we ask how would the electron spectra change with time when coherently populated doubly excited states are probed with attosecond pulses. Preliminary results indicate that the bending vibrational modes of the initial states can indeed be observed directly in the time-domain in the photoelectron spectra.

Another related application of attosecond pulses is to map the vibrational wave packet of a molecular ion when the molecule is first ionized. Theoretically the vibrational wave packet can be calculated, including its spreading and possible interference. Using 8 fs lasers for pump-probe experiment, Cocke's group have shown that it is possible to map out the time evolution of the wave packet (see his abstract). However, the wave packet is only partially mapped at each time in their experiment. We have performed calculations using attosecond pulses as the probe and it was found that the *whole* wave packet can be mapped out directly.

3. **Hyperspherical approach for low-energy rearrangement collisions**

Recent Progress:

We have applied the general hyperspherical close-coupling code to perform a few more calculations. One was for the positronium formation in positron-Li and positron-Na collisions (A6) and another was for muon transfer from muonic hydrogen to atomic oxygen and nitrogen (A9). Both calculations were carried out in view of some controversy in experimental results or in other theoretical calculations. We also studied $C^{6+}+H$ collisions using the hyperspherical method and extended it to below thermal energies. The calculation also resolved the controversy from a recent extended theoretical calculation (B2) based on the semiclassical method. A review paper from a conference talk on this subject (applications of atomic collision data for fusion) was also published (A3) recently.

4. **Doubly excited states of He near the three-body breakup threshold**

Recent Progress:

Based on our recently developed diabaticization technique in hyperspherical close-coupling method, we have applied it to study the level statistics of resonances near the three-body breakup threshold of He. By eliminating channels which belong to different bending modes, we have been able to reduce the number of channels in the close-coupling calculations from many hundreds to a few tens, and the reduced Hilbert space was then used in the calculation and analysis of doubly excited states below the $N=20-40$ thresholds of the He^+ ion. Using the Bredy parameter, we have been able to demonstrate the gradual evolution of level statistics toward the Wigner distribution as the threshold is approached from below. To simplify the calculations we have also employed the so-called s^2 model where the angular momentum of each electron was restricted to zero. This work has been written up recently (**B4**) but much more has to be done and can be done. Future calculations would involve the calculation of cross sections from photoabsorption or from electron scattering and it is hoped that Ericson fluctuation will appear as the three-body breakup threshold is approached.

Publications (A1-15 are new papers since the last DOE meeting)

- A1. X. M. Tong and C. D. Lin, "Empirical formula for static field ionization rates of atoms and molecules by lasers in the barrier-suppression regime", *J. Phys.* **B38**, 2593 (2005).
- A2. Z. X. Zhao and C. D. Lin, "Theory of laser-assisted autoionization by attosecond light pulses", *Phys. Rev.* **A71**, 060702(R) (2005).
- A3. C. D. Lin, A. T. Le, T. G. Lee and C. N. Liu, "New and old theoretical tools for evaluating cross sections for ion-atom collisions", in *Atomic and Molecular Data and their applications*, AIP conference proceedings, **771**, 229 (2005).
- A4. X. X. Zhou, X. M. Tong, Z. X. Zhao and C. D. Lin, "Role of molecular orbital symmetry on the alignment dependence of high-order harmonic generation with molecules", *Phys. Rev.* **A71**, 061801(R) (2005).
- A5. Z. X. Zhao, Z. H. Chang, X. M. Tong and C. D. Lin, "Circularly-polarized laser-assisted photoionization spectra of argon for attosecond pulse measurements", *Optics Express* **13**, 1968 (2005).
- A6. A. T. Le and C. D. Lin, "Positronium formation in positron-Li and positron-Na collisions at low energies", *Phys. Rev.* **A71**, 032713 (2005).
- A7. A. S. Alnaser, C. M. Maharjan, X. M. Tong, B. Ulrich, P. Ranitovic, B. Shan, Z. Chang, C. D. Lin, C. L. Cocke and I. V. Litvinyuk, "Effect of orbital symmetries in dissociative ionization of molecules by few-cycle laser pulses", *Phys. Rev.* **A71**, 031403 (2005).
- A8. X. M. Tong and C. D. Lin, "Double photoexcitation of He atoms by attosecond XUV pulses in the presence of intense few-cycle infrared lasers", *Phys. Rev.* **A71**, 033406 (2005).
- A9. A. T. Le and C. D. Lin, "Muon transfer from muonic hydrogen to atomic oxygen and nitrogen", *Phys. Rev.* **A71**, 022507 (2005).
- A10. X. M. Tong, Z. X. Zhao, A. S. Alnaser, S. Voss, C. L. Cocke and C. D. Lin, "Post Ionization Alignment of fragmentation of molecules in an ultrashort intense laser field", *J. Phys.* **B38**, 333 (2005).

A11. Toru Morishita and C. D. Lin, "Hyperspherical analysis of radial correlations in four-electron atoms", Phys. Rev. **A71**, 012504, (2005).

A12. X. M. Tong, Z. X. Zhao and C. D. Lin, "Molecular Tunneling ionization and rescattering induced double ionization of H₂ and D₂ molecules", J. of Modern Optics, **52**, 185 (2005).

A13. A. S. Alnaser, X. M. Tong, T. Osipov, S. Voss, P. Ranitovic, B. Ulrich, B. Shan, Z. Chang, C. D. Lin and C. L. Cocke, "Routes to control of H₂ Coulomb Explosion in few-cycle laser pulses", Phys. Rev. Lett. **93**, 183202 (2004).

A14. S Voss, A S Alnaser, X-M Tong, C Maharjan, P Ranitovic, B Ulrich, B Shan, Z Chang, C D Lin and C L Cocke, " High resolution kinetic energy release spectra and angular distributions from double ionization of nitrogen and oxygen by short laser pulses", J. Phys. **B37**, 4239 (2004).

A15. X. M. Tong and C. D. Lin, "Time-resolved sequential double ionization of D₂ molecules in an intense few-cycle laser pulse", Phys. Rev. **A70**, 023406 (2004).

Preprints (As of August 1, 2005)

B1. C. D. Lin, X. M. Tong and Z. X. Zhao, "Effects of orbital symmetries on the ionization rates of aligned molecules by short intense laser pulses", J. of Mod. Optics

B2. C. N. Liu, S. C. Cheng, A. T. Le and C. D. Lin, "Charge transfer in slow collisions of C⁶⁺ with H below 1 keV/amu", accepted, PRA.

B3. C. D. Lin and X. M. Tong, "Probing orbital symmetries and ionization dynamics of simple molecules with femtosecond laser pulses," book chapter, edited by S. H. Lin.

B4. A. T. Le, Toru Morishita, X. M. Tong and C. D. Lin, "Signature of chaos in high-lying doubly excited states of helium atoms", submitted to PRA.

Atomic, Molecular and Optical Sciences at LBNL

A. Belkacem, H. Gould, M. Hertlein, C.W. McCurdy, T. Rescigno

Chemical Sciences Division, Lawrence Berkeley National Laboratory, Berkeley, CA 94720

Email: abelkacem@lbl.gov, hagould@lbl.gov, mphertlein@lbl.gov, cwmccurdy@lbl.gov,
tnrescigno@lbl.gov

Objective and Scope

The AMOS program at LBNL is aimed at understanding the structure and dynamics of atoms and molecules using photons and electrons as probes. The experimental and theoretical efforts are strongly linked and are designed to work together to break new ground and provide basic knowledge that is central to the programmatic goals of the Department of Energy. The current emphasis of the program is in three major areas with important connections and overlap: inner-shell photo-ionization and multiple-ionization of atoms and small molecules; low-energy electron impact and dissociative electron attachment of molecules; and time-resolved studies of atomic processes using a combination of femtosecond X-rays and femtosecond laser pulses.

The experimental component at the Advanced Light Source makes use of the Cold Target Recoil Ion Momentum Spectrometer (COLTRIMS) to advance the description of the final states and mechanisms of the production of these final states in collisions among photons, electrons and molecules. Parallel to this experimental effort, the theory component of the program focuses on the development of new methods for solving multiple photo-ionization of atoms and molecules. This dual approach is key to break new ground and solve the problem of photo double-ionization of small molecules and unravel unambiguously electron correlation effects.

The relativistic collisions part of the program has been phased out in favor of branching into dissociative electron attachment measurements using COLTRIMS in support of the theoretical effort in the area of electron driven chemistry. These studies make use of the group's expertise at performing "complete" experiments using COLTRIMS. The theoretical project seeks to develop theoretical and computational methods for treating electron driven processes that are important in electron-driven chemistry and that are beyond the grasp of first principles methods.

The goal of the ultrafast science effort is to probe fundamental atomic and molecular processes involving femtosecond (and ultimately attosecond) x-rays interacting with atoms and molecules in the presence of laser fields and shed light on electron correlation within these systems. LBNL is at the forefront in the development of femtosecond X-ray science and the AMOS group is playing a major role in this development. This effort, ultimately, is aimed at extending the inner-shell photo-ionization and photo-fragmentation studies into the time-domain by using COLTRIMS type detection techniques to perform similar "kinematically complete" experiments. This work uses a combination of femtosecond "sliced" X-rays at the undulator beamline at the ALS and a high harmonic generation source. Major parts of this effort will form a basis of the involvement of the AMOS group in research that will be conducted at LCLS.

Atomic, Molecular, and Optical Science: Fractional-Cycle Excitation of Bound State Transitions

Harvey Gould

Mail Stop 71-259
Lawrence Berkeley National Laboratory, Berkeley, CA 94720
e-mail: hagould@lbl.gov

August 2005

Abstract

Excitation of bound state transitions by fractional-cycle pulses is compared to excitation of the same transitions by single-cycle and multi-cycles pulses. Preliminary results show striking new effects that are also likely to be seen in short-pulse laser experiments.

1 Program Scope and Definition

Subtask

The fractional cycle pulse experiment was a subtask of the LBNL AMOS program.¹

Background

Laser pulses have been shortened to a single cycle at XUV wavelength, less than a single cycle at optical wavelength, and may soon reach one-half cycle. At 780 nm, the time span of a single cycle is about 2.7 fs.

The interaction of fractional-cycle pulses with matter is expected to be different than the interaction of multi-cycle pulses with matter because simplifications such as transitions between isolated states, and the rotating wave approximation are no longer valid. For example, a transition induced by a single-cycle pulse will, because of the uncertainty principal, have a coherent bandwidth equal to the frequency of the radiation (about 1.5 eV for 780 nm) and far greater than natural linewidths.

For many systems, the transition linewidths will be of the order of the variations in level spacings. The system can then respond as if it had equally spaced levels, allowing successive transitions to populate additional levels. For some systems, the transition bandwidth will encompass multiple levels.

¹also funded by NASA and by a NIST Precision Measurements Grant.

2 Preliminary Results

Experiments on Magnetic Hyperfine Levels of Laser-Cooled Cs Atoms in a Fountain

Transitions between cesium ground state m_F (hyperfine) sublevels separated by a weak magnetic field were studied. Two-cycle pulses, single-cycle pulses and half-cycle pulses were applied the fraction of atoms, transferred from the $m_F = 4$ state to one of the other 8 m_F states was measured. For each pulse type the measurement is performed using first a sine wave pulse shape and then using a cosine wave pulse shape. In a cosine wave pulse the initial amplitude is a maximum.

Data

The data were taken by Jason Amini² and by Harvey Gould. Theory support and design assistance are provided by Charles Munger. The data are shown in Fig. 1. Pulse lengths of two cycles, one cycle and one-half cycle were used and for each of these two different starting phases (sine and cosine) were compared. As the frequency was scanned, the pulse length was adjusted to maintain a fixed number of cycles. As the number of cycles was reduced from two cycles to one cycle to one-half cycle, the power was proportionally increased to maintain equivalent transition probability. The power was initially chosen to maximize transitions from the starting level.

Because the nine m_F sublevels levels were equally spaced, successive transitions, $m_F = 4 \rightarrow m_F = 3 \rightarrow m_F = 2 \dots m_F = -4$ are allowed, as are transitions that return the atom to the initial $m_F = 4$ state. This is similar to what may be expected with laser pulses in which the coherent bandwidth is comparable to the differences in level spacings.

In Fig. 1 we see the transition resonance peak shifting from the 190 Hz transition energy, broadening, and distorting, as the number of cycles decreases from two cycles to one-half cycle (a decrease in the number of surviving atoms indicates that transitions are being induced). Structure at low frequencies also develops, especially for the cosine pulse.

The implications are that fractional cycle pulses may not provide reliable spectroscopic measurements. There may be effects due to the carrier-envelope phase, and transitions may appear at frequencies much lower than the presumed transition frequency.

Similar results were seen when comparing 180-degree phase pulses (negative sine wave) with 270-degree (negative cosine) pulses and are also seen at a different transition frequency. In the sine wave data, an attempt was made to observe stronger oscillatory behavior by increasing the power, but only a small effect resulted. Similarly, reducing the power in the cosine data made the amplitudes smaller but did not remove the oscillations or change their basic character.

A time-dependent Schrödinger Equation calculation, which does not use the rotating wave approximation, was performed by C. T. Munger. The calculation reproduces

²J.A. is supported by NASA and by a NIST Precision Measurements Grant

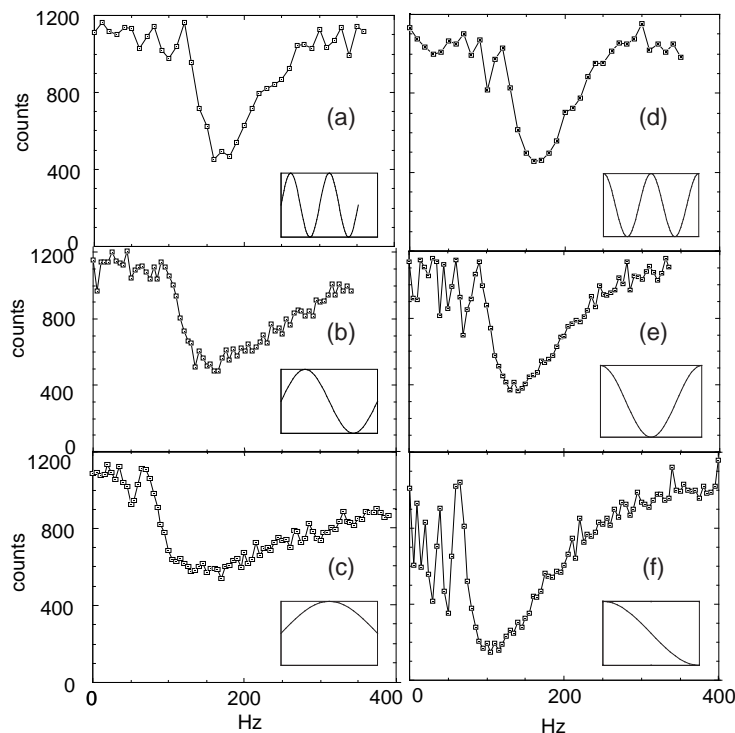


Figure 1: Transitions induced by two-cycle, single-cycle and half-cycle sine and cosine pulses from 10 Hz to 400 Hz. The surviving fraction of the initial $m_F = 4$ state is measured so that transitions appear as a decrease in counts from the nominal 1200 counts. In (a) - (c) the pulse is a sine wave which begins at zero amplitude and in (d) - (f) the the pulse is a cosine wave which begins at its maximum amplitude. In (a) and (d) are shown the results for two cycle pulses, (b) and (e) for one cycle pulses, and (c) and (f) for one-half cycle pulses. The waveform is shown in a box in the lower right of each figure. The nominal transition frequency, measured with a multicycle pulse about 190 Hz.

some of the observed features in Fig. 1. This gives us confidence that the observed effects are not artifacts of the apparatus.

3 Future Work

There are no plans for future work in this area.

4 DOE Sponsored Research Published in the Past Three Years

H. Gould and T.M. Miller, “Recent Advances in the Measurement of Static Electric Dipole Polarizabilities,” to be published in *Advances in Atomic, Molecular, and Optical Physics* (Ben Bederson volume), ed. H.H. Stroke (Academic, Boca Raton, 2005).

J. G. Kalnins, J.A. Amini, and H. Gould, “Focusing a fountain of neutral cesium atoms with an electrostatic lens triplet” to be published in *Phys. Rev. A*.

H. Nishimura, G. Lambertson, J.G. Kalnins and H. Gould, “Feasibility of a storage ring for polar molecules in strong-field-seeking states,” *Europhysics J*, **D31**, 359 (2004).

J. M. Amini and H. Gould, “High Precision measurement of the Static Dipole Polarizability of Cs,” *Phys. Rev. Lett.* **91**, 153001 (2003).

H. Nishimura, G. Lambertson, J.G. Kalnins, and H. Gould, “Feasibility of a synchrotron storage ring for neutral polar molecules,” *Rev. Sci. Instr.* **74**, 3271 (2003).

J. G. Kalnins, G. Lambertson, and H. Gould, “Improved alternating gradient transport and focusing of neutral molecules,” *Rev. Sci. Instr.* **73**, 2557 (2002).

Acknowledgments

Support is gratefully acknowledged: from the Office of Science, Office of Basic Energy Sciences, of the U.S. Department of Energy, from NASA, and from a NIST Precision Measurements Grant. This work was performed at the Lawrence Berkeley National Laboratory which is operated for the U.S. Department of Energy under Contract DE-AC02-05CH11231

Multiparticle Processes and Interfacial Interactions in Nanoscale Systems Built from Nanocrystal Quantum Dots

Victor Klimov

Chemistry Division, C-PCS, MS-J567, Los Alamos National Laboratory
Los Alamos, New Mexico 87545, klimov@lanl.gov, <http://quantumdot.lanl.gov>

1. Program Scope

Controlling functionalities of nanomaterials requires a detailed physical understanding from the level of the individual nanoscale building blocks to the complex interactions in the nanostructures built from them. This project concentrates on electronic properties of semiconductor quantum-confined nanocrystals [nanocrystal quantum dots (NQDs)] and the electronic and photonic interactions in NQD assemblies. Specifically, we study multiparticle processes in individual NQDs and interfacial interactions in NQD-based “homogeneous” and “hybrid” structures. Multiparticle states (e.g., quantum-confined biexcitons) and multiparticle interactions (e.g., Auger recombination) play an important role in both optical gain and band-edge optical nonlinearities in NQDs. Interfacial interactions (e.g., electrostatic coupling) can enable communication between NQDs (homogeneous systems) or between NQDs and other inorganic or organic structures (hybrid systems), leading to such important functionality as energy transfer. The ability to understand and control both multiparticle processes and interfacial interactions developed in this project can potentially lead to such new NQD-based technologies as solid-state optical amplifiers and lasers, nonlinear optical switches, and electrically pumped, tunable light emitters.

2. Recent Progress

The work in this project during the reviewed period has concentrated on experimental and theoretical studies of electronic and optical properties of NQDs with a focus on the dynamical behavior of single- and multi-particle excitations in both isolated and communicating NQD systems. One goal of this project has been the comprehensive investigation of multiparticle interactions as a function of NQD size, shape, and surface conditions. As a result of these studies we have developed methods for controlling the spectra and dynamics of multiparticle states via the manipulation of nanoparticle shape or by utilizing heterostructured NQDs.

Another goal of this project has been the studies of ensembles of NQDs communicating via electrostatic Coulomb interactions. Such interactions can allow communication between nanoparticles via incoherent exciton/energy transfer. Even in NQD assemblies that are not optimized structurally (such as nominally monodispersed NQD solids), exciton transfer has a dramatic effect on NQD optical properties leading, e.g., to a strong red shift of the emission band. While providing strong indication for interactions between NQDs, spectral shifts cannot be used to directly evaluate the strength of these interactions. To obtain more direct information about time scales characteristic of energy transfer in NQD materials, we have performed spectrally selective time-resolved photoluminescence (PL) studies of monodisperse CdSe NQD solids and “energy-gradient” NQD multilayers. As one practical application of high-efficiency energy transfer in NQD systems, we explored the use of electrostatic coupling of quantum-well (QW) excitations to an NQD dipole as a means for “non-contact” pumping of nanocrystals.

Our studies of fundamental interactions in NQD systems have been supported by the development of advanced spectroscopic instrumentation utilizing such methods as near-field, broad-band extinction spectroscopy and single-dot PL excitation (PLE) spectroscopy.

Specific topics/sub-topics under investigation during the reviewed period included:

- *Single-exciton recombination and energy relaxation dynamics in NQDs*
 - Different radiative recombination regimes in CdSe NQDs [1].

- Single-exciton radiative decay in heterostructured ZnSe/CdSe and Co/CdSe NQDs [2, 3].
- Intraband electron and hole relaxation in CdSe NQDs (“phonon bottleneck” problem) [4, 5].
- ***Fundamental physics of exciton-exciton interactions in NQDs***
 - “Visualization” of NQD biexcitons using ultrafast photoluminescence (PL) gating techniques and direct measurements of exciton-exciton interaction energies (biexciton binding energies) [6].
 - “Geometrical” effects (NQD size and shape) in Auger recombination and, specifically, the effect of the 0D-to-1D transformation on Auger recombination rates [7, 8].
 - Exciton-exciton interactions in inverted, core/shell NQDs [9].
 - Carrier multiplication in NQDs and implications for solar energy conversion [10].
- ***Exciton-exciton interactions and optical gain in NQDs***
 - The effect of exciton-exciton interactions (Auger recombination and biexciton effects) on optical gain in NQDs [11 - 14].
 - NQD lasing using nanocrystal solids incorporated into various microcavities [15, 16].
 - Optical gain in shape-controlled nanocrystals (quantum rods) [7, 8].
 - Competition between optical gain and excited state absorption [17].
 - Infra-red optical gain and amplified spontaneous emission using PbSe NQDs [18, 19].
 - NQD/sol-gel nanocomposites for optical gain and nonlinear optical applications [18, 20].
- ***Interfacial energy transfer in NQD assemblies***
 - Energy transfer in “random” and ordered, “energy-gradient” NQD assemblies [21, 22].
 - Energy transfer in hybrid systems comprising colloidal NQDs and epitaxial quantum wells [23, 24].
 - Energy transfer interactions of NQDs with metals [25].
- ***Single-nanoparticle spectroscopy***
 - The structure of excited states in NQDs probed by single-dot PLE spectroscopy (related to ultrafast intraband relaxation) [26, 27].
 - Electronic excitations in single metal nanoparticles and single dimers of metal nanoparticles probed by broad-band, near-field spectroscopy [28, 29].

3. Future Plans

The quantum-size effect has been a powerful tool for controlling spectral responses of NQDs and for enabling such potential applications as multicolor labeling, color conversion in displays, and low-cost lighting. Size control, however, has a limited applicability for tuning dynamical and nonlinear responses of nanostructures. As a continuation of this project, we will explore the use of heterostructured, multicomponent (multishell) nanocrystals for controlling dynamics of electronic excitations and their nonlinear interactions. Specifically, we will use hybrid metal/semiconductor NQDs to further extend the concept of wavefunction engineering and to introduce new functionality beyond that provided by semiconductors alone. For example, we will prepare magnetic-metal/semiconductor core/shell NQDs that will enable multifunctional nano-biotags. Fundamentally, these hybrid NQDs will permit studies of the effect of the magnetic core on the optical properties of the semiconductor shell, control of semiconductor degeneracy by a “local nanomagnet,” and control of the blocking temperature of the magnetic core by an inorganic shell. Alternatively, we will investigate hybrid NQDs comprising a noble metal with a semiconductor. Here, strong exciton-plasmon interactions will be used to enhance the oscillator strength of optical transitions and to increase the rate of the radiative decay and nonlinear optical susceptibilities.

We will also work on hybrid colloidal-epitaxial assemblies to address the problem of electrically interfacing NQDs with external electrical circuits. This work will target applications of NQDs in light-emitting diodes and photovoltaic solar cells. Specifically, we will explore combining NQDs with epitaxial heterostructures for either injecting charge carriers into NQDs electrically or extracting charges from

NQDs for charge collection by an external circuit. In this work, we will combine NQDs with epitaxial quantum wells or will use “soft” deposition techniques (such as neutral-atom beam epitaxy) to directly incorporate NQDs into epitaxial semiconductor layers.

4. Publications

1. S. A. Crooker, T. Barrick, J. A. Hollingsworth, and V. I. Klimov, Multiple temperature regimes of radiative decay in CdSe nanocrystal quantum dots: Intrinsic limits to the dark-exciton time, *Appl. Phys. Lett.* **82**, 2793 (2003)
2. H. Kim, M. Achermann, J. A. Hollingsworth, and V. I. Klimov, Synthesis and Characterization of Co/CdSe Core/Shell Nanocomposites: Bi-functional Magnetic-Optical Nanocrystals, *J. Am. Chem. Soc.* **127**, 544 (2005)
3. L. P. Balet, S. A. Ivanov, A. Piryatinski, M. Achermann, and V. I. Klimov, Inverted core/shell nanocrystals continuously tunable between Type-I and Type-II localization regimes, *Nano Lett.* **4**, 1485 (2004).
4. S. Xu, A. A. Mikhailovsky, J. A. Hollingsworth, and V. I. Klimov, Hole intraband relaxation in strongly confined quantum dots: Revisiting the “phonon bottleneck” problem, *Phys. Rev. B* **65**, 53191 (2002).
5. A. A. Mikhailovsky, S. Xu, and V. I. Klimov, Femtosecond intraband modulation spectroscopy, *Rev. Sci. Instr.* **73**, 136 (2002).
6. M. Achermann, J. A. Hollingsworth, and V. I. Klimov, Multiexcitons confined within a sub-excitonic volume: Spectroscopic and dynamical signatures of neutral and charged biexcitons ultrasmall semiconductor nanocrystals, *Phys. Rev. B* **68**, 245302 (2003).
7. H. Htoon, J. A. Hollingsworth, R. Dickerson, and V. I. Klimov, Zero- to one-dimensional transition and Auger recombination in semiconductor quantum rods, *Phys. Rev. Lett.* **91**, 227401 (2003).
8. H. Htoon, J. A. Hollingsworth, A. V. Malko, R. Dickerson, and V. I. Klimov, Light amplification in semiconductor nanocrystals: Quantum rods vs. quantum dots, *Appl. Phys. Lett.* **82**, 4776 (2003).
9. S. A. Ivanov, J. Nanda, A. Piryatinski, M. Achermann, L. P. Balet, I. V. Bezel, P. O. Anikeeva, S. Tretiak, V. I. Klimov Light Amplification Using Inverted Core/Shell Nanocrystals: Towards Lasing in the Single-Exciton Regime, *J. Phys. Chem. B* **108**, 10625 (2004).
10. R. D. Schaller and V. I. Klimov, High efficiency carrier multiplication in PbSe nanocrystals: Implications for solar-energy conversion, *Phys. Rev. Lett.* **92**, 186601 (2004).
11. V. I. Klimov, Nanocrystal quantum dots: From fundamental photophysics to multicolor lasing, *Los Alamos Science* **28** (LANL 60th anniversary issue), 214 (2003).
12. V. I. Klimov, Charge carrier dynamics and optical gain in nanocrystal quantum dots: From fundamental photophysics to lasing devices, in book *Semiconductor and Metal Nanocrystals: Synthesis and Electronic and Optical Properties*, Ed. V. I. Klimov (Marcel Dekker, New York, 2003), pp. 159 - 214.
13. V. I. Klimov, Carrier dynamics, optical nonlinearities, and optical gain in nanocrystal quantum dots, in book *Semiconductor Nanocrystals: From Basic Principles to Device Applications*, Eds. Al. Efros, D. J. Lockwood, and L. Tsybeskov (Kluwer Academic Publishers, 2003) pp. 73 – 111.
14. A. A. Mikhailovsky, A. V. Malko, J. A. Hollingsworth, M. G. Bawendi, and V. I. Klimov, Multiparticle interactions and stimulated emission in chemically synthesized quantum dots, *Appl. Phys. Lett.* **80**, 2380 (2002).
15. A. V. Malko, A. A. Mikhailovsky, M. A. Petruska, H. Htoon, J. A. Hollingsworth, M. G. Bawendi, and V. I. Klimov, From amplified spontaneous emission to microring lasing using nanocrystal quantum dot solids, *Appl. Phys. Lett.* **81**, 1303 (2002).
16. H.-J. Eisler, V. C. Sundar, M. G. Bawendi, M. Walsh H. I. Smith and V. I. Klimov, Color-selective semiconductor nanocrystal laser, *Appl. Phys. Lett.* **80**, 4614 (2002).

17. A. V. Malko, A. A. Mikhailovsky, M. A. Petruska, J. A. Hollingsworth, and V. I. Klimov, Interplay between optical gain and photoinduced absorption in CdSe nanocrystals, *J. Phys. Chem. B* **108**, 52550 (2004).
18. M. A. Petruska, A. P. Bartko, and V. I. Klimov, An Amphiphilic Approach to Nanocrystal Quantum Dot-Titania Nanocomposites, *J. Am. Chem. Soc.* **126**, 714 (2004).
19. R. D. Schaller, M. A. Petruska, V. I. Klimov, Tunable Near-Infrared Optical Gain and Amplified Spontaneous Emission Using PbSe Nanocrystals, *J. Phys. Chem. B* **107**, 13765 (2003) (cover article).
20. M. A. Petruska, A. V. Malko, P. M. Voyles, and V. I. Klimov, High-performance, quantum-dot nanocomposites for nonlinear-optical and optical-gain applications, *Advanced Materials* **15**, 610–613 (2003).
21. S. A. Crooker, J. A. Hollingsworth, S. Tretiak, and V. I. Klimov, Spectrally-resolved dynamics of energy transfer in quantum-dot solids: Towards engineered energy flows in quantum-dot assemblies, *Phys. Rev. Lett.* **89**, 186802 (2002).
22. M. Achermann, M. A. Petruska, S. A. Crooker, and V. I. Klimov, Picosecond energy transfer in quantum dot Langmuir-Blodgett nanoassemblies, *J. Phys. Chem. B* **107**, 13782 (2003).
23. M. Achermann, M. A. Petruska, S. Kos, D. L. Smith, D. D. Koleske, V. I. Klimov, Energy-transfer pumping of semiconductor nanocrystals using an epitaxial quantum well, *Nature* **429**, 642 (2004).
24. S. Kos, M. Achermann, V. I. Klimov, and D. L. Smith, Different regimes of Forster-type energy transfer between an epitaxial quantum well and a proximal monolayer of semiconductor nanocrystals, *Phys. Rev. B* **71**, 205309 (2005).
25. I. A. Larkin, M. I. Stockman, M. Achermann, and V. I. Klimov, Dipolar emitters at nanoscale proximity of metal surfaces: Giant enhancement of relaxation in microscopic theory, *Phys. Rev. B* **69**, 121403(R) (2004).
26. H. Htoon, P. J. Cox, and V. I. Klimov, The Structure of Excited-State Transitions in Individual Semiconductor Nanocrystals Probed by Photoluminescence Excitation Spectroscopy, *Phys. Rev. Lett.* **93**, 187402 (2004).
27. S. Xu, A. A. Mikhailovsky, J. A. Hollingsworth, and V. I. Klimov, Hole intraband relaxation in strongly confined quantum dots: Revisiting the “phonon bottleneck” problem, *Phys. Rev. B* **65**, 53191 (2002).
28. A. A. Mikhailovsky, M. A. Petruska, M. I. Stockman, and V. I. Klimov, Broadband, near-field, interference spectroscopy of metal nanoparticles using femtosecond white-light continuum, *Opt. Lett.* **28**, 1686 (2003).
29. A. A. Mikhailovsky, M. A. Petruska, Kuiru Li, M. I. Stockman, and V. I. Klimov, Phase-sensitive spectroscopy of surface plasmons in individual metal nanostructures, *Phys. Rev. B* **69**, 85401 (2004).

**ATOMIC AND MOLECULAR PHYSICS RESEARCH
AT
OAK RIDGE NATIONAL LABORATORY**

David R. Schultz, Group Leader, Atomic Physics
ORNL, Physics Division, P.O. Box 2008
Oak Ridge, TN 37831-6372

Principal Investigators

E. Bahati [bahatie@ornl.gov], postdoctoral fellow
M. E. Bannister [bannisterme@ornl.gov]
M. R. Fogle, Jr. [foglem@ornl.gov], postdoctoral fellow
C. C. Havener [havenercc@ornl.gov]
H. F. Krause [krausehf@ornl.gov]
J. H. Macek [macek@utk.edu]
F. W. Meyer [meyerfw@ornl.gov]
C. Reinhold [reinhold@ornl.gov]
D. R. Schultz [schultzd@ornl.gov]
C. R. Vane [vanecr@ornl.gov]
L. I. Vergara [vergarali@ornl.gov], postdoctoral fellow

The ORNL atomic physics program has as its overarching goal the understanding and control of interactions and states of atomic-scale matter. The scientific objective is to enhance progress toward development of detailed understanding of the interactions of multicharged ions, charged and neutral molecules, and atoms with electrons, atoms, ions, surfaces, and solids. Towards this end, a robust experimental program is carried out by our group centered at the ORNL Multicharged Ion Research Facility (MIRF) and as needed at other world-class facilities such as the ORNL Holifield Radioactive Ion Beam Facility (HRIBF) and the CRYRING heavy-ion storage ring in Stockholm. Closely coordinated theoretical activities support this work as well as lead investigations in complementary research. Specific focus areas for the program are broadly classified as particle-surface interactions, atomic processes in plasmas, and manipulation and control of atoms, molecules, and clusters, the latter focus area cross cutting the first two.

The MIRF High Voltage Platform – *F. W. Meyer, M. E. Bannister, J. W. Hale, C. C. Havener, H. F. Krause, and C. R. Vane*

A new 250 kV high voltage platform has been installed at the ORNL Multicharged Ion Research Facility (MIRF) to extend the energy range of multicharged ions available for experimental investigations of their collisional interactions with electrons, atoms, molecules, and solid surfaces¹. In late January of 2005, this first, and most challenging, phase of a major upgrade project at the MIRF was completed, and routine operation started. By end of February, first ion beams had been extracted from the new all permanent magnet ECR ion source on the platform, and transported for initial diagnostics tests to two upgraded, previously installed end stations, the Merged Electron Ion Beam Energy Loss (MEIBEL) experiment, and the Ion-Atom-Merged-Beams Experiment. Ion beams were successfully accelerated from the platform at potentials up to 215 kV, and transported with 100% efficiency through the first section of the new high-energy beamline, verifying proper operation of the installed optics components, and validating the ion optics design.

Initiated in FY 1997 as a capital equipment project to expand the energy capability available at MIRF, a full funding plan was developed in FY2002 with participation of DOE OFES. The present upgrade follows installation of the original ORNL ECR source in 1984, at the time the only ECR worldwide dedicated to atomic physics studies, and its replacement by a new, then state-of-the-art ECR source from Grenoble in 1992. The current upgrade project is the most far-ranging in the facility's history. It involved the new design, fabrication, and installation of a 250 kV high voltage platform and ECR ion source together

with associated beamlines, and major relocations and upgrades of end stations. Concurrent with this effort, an active research program was maintained with the present CAPRICE ECR source. In addition to expanding the capabilities of present on-line experiments, access to higher energy beams makes possible new investigations as well, such as studies of dissociative recombination of molecular ions beyond the mass limit of current magnetic storage rings.

The second part of the facility upgrade entails relocation of the present CAPRICE ECR ion source within MIRF, and installation of a floating beamline, to extend the availability of very low energy multicharged or molecular ion beams. In this new configuration, keV-energy beams will be transported with high efficiency to end stations and then decelerated there to a few eV $\times q$ (where q is the charge state of the ion of interest), using efficient ion optics already developed for the MIRF floating ion-surface interaction experiment. With these two ECR sources, an energy range of almost five orders of magnitude will be available to the various experiments, a significant improvement over the 1-25 keV/ q energy range capability of the present MIRF source configuration.

The new all-permanent magnet ECR ion source, built at CEA Grenoble, operates in the frequency range 12.75 – 14.5 GHz at power levels up to 750W, and is capable of producing up to 0.5 mA of Ar^{8+} . Its magnetic field structure is achieved using compact NdFeB permanent magnet assemblies for both radial hexapolar and axial solenoidal fields, both of which have peak values in the excess of 1 T, and thus requires no high current power supplies. The performance of the new source exceeds that of the MIRF's present 10 GHz CAPRICE source by up to factors of 2 to 3 in the case of the highest charge state Xe ions.

The design energy range of the high voltage platform is 20 – 270 $\times q$ keV. To achieve this wide energy range with maximum beam transmission, a number of specific features were incorporated into the design of the beam transport system². All effective optic element apertures on the platform (including the usable analyzing magnet gap) and up to, and including, the first 65 degree spherical deflector beam switcher were designed for 100% beam transport for beams having an unnormalized emittance of 160 π -mm-mrad at 20 $\times q$ keV. This large acceptance was achieved for the electrostatic beam switcher by the use of two interchangeable sets of deflection electrodes, the first with a 2.5 inch gap to handle beams up to about 150 $\times q$ keV, and the second set with a 1.5 inch gap to handle the lower divergence-angle beams at energies beyond this value. In addition, two einzel lenses were added on either side of the acceleration column to permit refocusing of the beam at the entrance waist of the tandem quadrupole triplet section for low platform voltages where the focusing of the acceleration column itself is weak or non-existent. Finally, large 2-inch-acceptance-aperture quadrupole lenses were used in a tandem configuration before the first beam switcher to achieve both high transmission at low energies and sufficient focusing power with ± 20 kV electrode potentials at high energies.

The 65° spherical sector electrostatic deflector beam switchers, together with the slit assemblies, are mounted on turntables supported by a ceramic ball bearing race. The turntables are externally rotated about a vertical axis to one of three positions: the first two direct beam either into the left or right beamline, by a rotation of 115° that reverses entrance and exit planes of the deflector, and the “straight-thru” position allows the beam to pass undeflected through the chamber past the outside of the “outer” electrode structure, which has a milled slot to accommodate up to 1 in. diameter beams.

Monitoring and control functions on the HV platform³ as well as the beamlines leading to the various end stations are achieved via Allen-Bradley ControlLogix programmable logic controllers (PLC's) in three separate chassis linked by Ethernet-bridge-driven fiber-optic cables and controlled by a single Logix5555 processor in the ground potential chassis. Several devices employ serial protocols over RS-232 or GPIB communication channels. All devices are integrated into a Linux-hosted, EPICS-based distributed control system which provides device independent, uniform access to all hardware via a distributed real-time database. This approach is compatible with that used at the ORNL Spallation Neutron Source, and serves as a testbed for the control system being developed for the HV platform being constructed as part of the new High Power Target Lab (HPTL) at the ORNL Physics Division Holifield Radioactive Ion Beam Facility (HRIBF).

All active cooling of platform components is achieved “on-board”, and is thus independent of the HRIBF cooling tower. The microwave power amplifier for the ECR source is cooled by 250 CFM of forced air flow. Sufficient cooling of the ECR source to permit operation at injected microwave power levels up to 750 W is critical in order to avoid irreversible de-magnetization of the NdFeB permanent magnet structures. It is achieved using a NESLAB recirculating chiller with deionizer, operating at platform potential. The resistive losses in the analyzing magnet coils approach 10 kW when transporting beams with maximum magnetic rigidity. This heat load is dissipated by closed-loop circulation of cooling water

through a finned-coil radiator with forced air flow of 1500 CFM. The water circulation is achieved by a centrifugal water pump capable of providing a 2 GPM flow rate at 80 psi head pressure, and the necessary air flow is achieved using a directly driven ducted fan. For optimum space utilization, the heat exchange/fan assembly was installed above the analyzing magnet.

Electrical power to the platform is supplied by an efficient 250 kV mineral-oil-filled isolation transformer capable of providing up to 30 kW of three-phase 208V power. This power is distributed to the various platform and source potential electrical components via a balanced single and three phase distribution network fed from the isolated transformer Y-connection with loadable midpoint (N) at the end of an oil-filled nylon pylon extending across the 29 inch gap between ground enclosure and HV platform. Total power required by platform components in the present configuration is a little over 20 kW, leaving almost 10 kW available for future expansion.

1. F. W. Meyer, M. E. Bannister, D. Dowling, J. W. Hale, C. C. Havener, J. W. Johnson, R. C. Juras, H. F. Krause, A. J. Mendez, J. Sinclair, A. Tatum, C. R. Vane, E. Bahati Musafiri, M. Fogle, R. Rejoub, and L. Vergara, "The ORNL Multicharged Ion Research Facility Upgrade Project," to be published in Nucl. Instrum. Methods Phys. Res. B (2005).
2. F. W. Meyer, M. E. Bannister, J. W. Hale, J. W. Johnson, and D. Hitz, "The ORNL Multicharged Ion Research Facility (MIRF) High Voltage Platform Project," 2005 Particle Accelerator Conference, Knoxville, TN, May 16 – 20, 2005, to be published, IEEE Conference Proceedings (2005).
3. M. E. Bannister, F. W. Meyer, and J. Sinclair, "Control System for the ORNL Multicharged Ion Research Facility High Voltage Platform", 2005 Particle Accelerator Conference, Knoxville, TN, May 16 – 20, 2005, to be published, IEEE Conference Proceedings (2005).

In-Situ Electron Cyclotron Resonance (ECR) Plasma Potential Determination Using Emissive and Langmuir Probes - F. W. Meyer and Hyun Jong You¹

In order to accurately determine energies of beams decelerated to eV-range energies, and ultra-low relative collision velocities in merged beams configurations, it is important to know the plasma potentials of the ion sources used to produce the ion beams, since they define the birth potential of the extracted ions. To this end, real-time, in-situ, plasma potential measurements² have been carried out for an ECR ion source and correlated with extracted beam characteristics. The local real-time plasma potential of the ORNL MIRF Caprice ECR ion source was measured using both active and passive Langmuir probes, which were inserted perpendicularly from the plasma chamber wall at the mid-plane of the ECR zone between one of the six radial loss cones of the magnetic field structure, where their perturbation of the main ECR plasma is small. Slots machined through the plasma- and puller-electrodes at the plasma chamber wall radius permitted insertion of the probes from the extraction side of the ECR source without perturbation of the coaxial microwave injection, and without affecting ion beam extraction and measurement after charge state analysis. The emissive probe technique permits plasma potential determination independent of plasma conditions and avoids problems related to probe geometry. The probe loop tip was pointed toward the chamber center in a radial plane and was located about 5 mm outside of the ECR zone. In addition to plasma potential information, the measurements permitted estimates to be made of ECR plasma electron density and temperature, and provided insights into the evolution of these plasma parameters as conditions for multicharged ion production were optimized.

1. PhD student, Hanyang University, Seoul, Korea; partial support from the Korean Science and Engineering Foundation (KOSEF).
2. J. You, Y. Liu, and F. W. Meyer, "In-situ Electron Cyclotron Resonance (ECR) Plasma Potential Determination Using an Emissive Probe," 2005 Particle Accelerator Conference, Knoxville, TN, May 16 – 20, 2005, to be published, IEEE Conference Proceedings (2005).

Low-Energy Ion-Surface Interactions – F. W. Meyer, H. F. Krause, and L. I. Vergara

There is significant technological interest in using graphite as a plasma-facing component on present and future fusion devices, and in using different types of graphite or carbon fiber composites (CFC's), together with tungsten, beryllium, or other refractory metals, in the ITER divertor.¹ Motivated in part by this interest, an experimental research program² was recently started at the ORNL Multicharged Ion Research Facility (MIRF) to investigate chemical sputtering of graphite surfaces in the limit of very low

impact energies (i.e. below 10 eV/D), where there is currently no available experimental data, and which is the anticipated regime of operation of the ITER divertor. In addition to the exploration of very low impact energies, this research focuses on comparisons of atomic and molecular ion impact, to better determine the range where atomic and molecular species at the same velocity behave in an equivalent manner with respect to the chemical sputtering yields. In subsequent years the chemical sputtering measurements will be initiated using a time-of-flight approach³ to detect product radicals and greatly reduce or eliminate the need for “wall corrections” presently needed to deduce the chemical sputtering yield.

The experimental approach used a sensitive quadrupole mass spectrometer which monitored the partial pressures of selected mass species in the range 1 – 60 amu present in the scattering chamber. A Macintosh-based data acquisition system was used to measure mass distributions at fixed intervals in time, or alternatively, to follow the intensities of selected mass peaks as function of beam exposure times. The evolution of the detected intensities of hydrocarbon species such as CD, CD₂, CD₃, CD₄, C₂D₂, C₂D₄, and C₂D₆ was followed as a function of accumulated beam dose until saturation in their intensities occurred. Calibrated hydrocarbon leaks were used to determine absolute yields of the sputtering products of interest.

The energies investigated so far⁴ span the range 4 – 130 eV/D. At the lower energies, comparisons have been made of the methane and acetylene production yields for equal velocity incident D⁺, D₂⁺, and D₃⁺. We found factors of two differences below 60 eV/D, with the atomic projectile, i.e. D⁺, having the smallest yields and D₃⁺ projectiles the biggest. At higher energies, where immediate dissociation of incident molecular projectiles is highly probable, the observed yields for equivelocity incident atomic and molecular ions are the same. It is speculated that at the lower energies, dissociation most likely occurs later in the projectile slowing in the bulk. The higher mass of the undissociated molecules may enhance the kinetically assisted desorption of sputter products, thereby increasing the observed yields. Similar mass effects have been observed when comparing yields for equivelocity H⁺ and D⁺ incident projectiles.

To date, measurements at ORNL have focused on ATJ graphite, with the goal of comparing chemical sputtering characteristics of virgin tiles and tiles recently removed from the DIII-D machine after 8 years of exposure to plasma shots. Future measurements will use HOPG and pyrolytic graphite as well. With HOPG, comparative measurements will be performed for surfaces oriented parallel and perpendicular to the graphite basal planes, thereby probing the effect on sputter yields of modifications of sputter product diffusion back to the surface.

1. J. T. Hogan, P. Krstic, and F. W. Meyer, “New Directions for Computer Simulations and Experiments in Plasma-Surface Interactions for Fusion,” accepted for publication, Nucl. Fusion (2005).
2. F. W. Meyer, H. F. Krause, and L. I. Vergara, “Measurements of Chemical Erosion of ATJ Graphite by Low Energy D₂⁺ Impact Proceedings,” International Conference on Plasma Surface Interactions, Portland, Maine, May 24-28, 2004, J. Nucl. Mater. **337-339**, 922 (2004).
3. F. W. Meyer, L. I. Vergara, and H. F. Krause, “Recent ORNL Measurements of Chemical Sputtering of ATJ Graphite by Slow Atomic and Molecular D ions”, [Invited presentation] Workshop on New Directions for Advanced Computer Simulations and Experiments in Plasma Surface Interactions, March 21-23, 2005, accepted for publication in Physics Scripta (2005).
4. L. I. Vergara, F. W. Meyer, and H. F. Krause, “Chemical Sputtering of ATJ Graphite Induced by Low-Energy D₂⁺ Bombardment”, accepted for publication, J. Nucl. Materials (2005).

Angular Distribution Studies of Ions Guided Through a Nanocapillary Array – H. F. Krause, C. R. Vane, and F.W. Meyer

We have expanded investigations begun in FY2004 of the transport, angular scattering, charge exchange, and energy loss of low-energy (5-140 keV) single- and multiply-charged ions in a mesoscopic structure. This work is part of the larger beam-surface effort at the ORNL MIRF which seeks to develop a fundamental understanding of neutralization, energy dissipation, and sputtering processes that occur when slow, highly-charged ions interact with metal, semiconductor, and insulator surfaces.

The consequences of incident 10–20 keV/q ions of Ar⁺, Ar³⁺, Ne³⁺, and Ne⁷⁺ scattered in an Al₂O₃ anodic nanocapillary array have been studied. The array consists of a dense distribution (> 3x10⁹ pores/cm²) of nanopores typically 100 nm dia. and 60 micron length. The commercial array has been extensively characterized previously by other researchers using techniques such as scanning electron microscopy, gas absorption, deuterium based nuclear magnetic resonance, and small angle neutron

scattering. The uniform pores are smooth, straight, and arranged in a hexagonal pattern. The arrays, commonly used in biofiltration and separations applications, have potential electronic and materials applications in memory storage devices, microwave guides, and as a substrate for aligned carbon nanotube arrays. These nanochannels are 6x longer than those used to guide much lower energy ions in insulating PET films.¹ Heretofore, experimental high-resolution angular scattering studies have not been reported for any nanocapillary target.

To reduce charging of the sample, entrance ions passed through a high-transmission grounded grid before entering the array (insulator). Arrays with a 10 nm layer of Au deposited on the entrance and/or exit surfaces were also studied. The target array was mounted in a precision goniometer to allow alignment with the incident beam and to study changes in angular distributions when the alignment of capillaries and the beam was varied. Ions emerging from the array were electrostatically deflected out of plane so that final q-state selected angular distributions (including emerging neutrals) could be obtained. Resultant two-dimensional angular distributions were measured using a rotatable high-resolution 2D position sensitive detector which sampled about ± 0.9 degrees.

The principal transmitted q-state observed is the incident q-state in all cases. The transmitted fraction using wire mesh ($\sim 2 \times 10^{-8}$) is many orders of magnitude smaller than the array's surface porosity ($\sim 30\%$). The transmitted fraction for Au plated targets is about a factor of 10-20 times larger than that obtained using wire mesh, suggesting a reduction in the electrical charging of the sample. No evidence of significant energy loss is observed for the transmitted ions. Yields in lower q-states and neutrals formed by e-capture are typically below 1% of the entrance q-state yield. Observed angular distributions consist of well-resolved two-dimensional structures sitting on a continuum distribution. Angular structure disappears at high incident beam intensity ($I > 3$ nA) for Au plated targets probably because of space charge effects inside the pores.

The angular distribution and sharp angular structures are easily steered in the direction of the nanochannels within about ± 1 degrees by rotating the sample with respect to the incident beam, even for 140 keV Ne^{7+} ions. Structure observed at the highest energies match the effective collimation of individual nanopores (~ 1.6 mrad). The intensity of periodic structure decreases as the angle between the nanochannel direction and the beam is increased. All data suggest that the structure in the scattered ions arises when they bounce at ultra-low grazing angles in very large impact parameter Coulomb collisions with electrically charged nanopore walls. Up to four internal bounces with walls have been identified when the target is tilted. Our results for anodic arrays contrast sharply with those obtained using much lower porosity and thinner PET films at lower energy.¹

Results for these rare projectile charge-conserving ultra-low grazing angle collisions with an insulator surface also contrast sharply with previously obtained results for low-energy grazing collisions on ordered insulator surfaces such as LiF, where charge capture and neutralization processes dominate in much larger angle scattering events. The anodic nanocapillary arrays studied have potential applications for the production and steering of low-intensity micro-beams.

1. N. Stolterfoht et al., "Transmission of 3 keV Ne^{7+} Ions through Nanocapillaries Etched in Polymer Foils: Evidence for Capillary Guiding," *Phys. Rev. Letters* **88**, 133201 (2002); N. Stolterfoht et al., "Transmission of 3 keV Ne^{7+} Ions through Nanocapillaries Etched in Polymer Foils," *Nucl. Instrum. Meth. Phys. Res. B* **203**, 246 (2003).

Electron-Molecular Ion Interactions – *M. E. Bannister, C. R. Vane, E. Bahati, and M. Fogle*

Electron-molecular ion recombination, dissociation, and excitation and ionization processes are important from a fundamental point of view, especially in that they provide a testable platform for investigating and fully developing our understanding of the mechanisms involved in electronic energy redistribution in fragmenting many-body quantum mechanical systems. These processes are also important practically in that electron-ion collisions are in general ubiquitous in plasmas and molecular ions can represent significant populations in low to moderate temperature plasmas. Neutral and charged radicals formed in dissociation of molecules in these plasmas represent some of the most highly reactive components in initiating and driving further chemical reaction pathways. Thus electron-molecular ion collisions are important in determining populations of some of the most reactive species in a wide variety of environments, such as the diverter edge regions in fusion reactors, plasma enhanced chemical vapor deposition reactors, environments where chemistries are driven by secondary electron cascades, for

example in mixed radioactive waste, the upper atmospheres of planets, and cooler regions of the solar or other stellar atmospheres. To correctly model these environments it is absolutely essential to know the strengths (cross sections and rates), branching fractions, and other kinematical parameters of the various possible relevant collision processes.

Dissociative Excitation and Ionization: Measurements of cross sections for electron-impact dissociative excitation (DE) and dissociative ionization (DI) of molecular ions have continued using the MIRF crossed-beams apparatus.¹ The dissociation of N_2H^+ ions forming NH^+ fragments has been investigated in a complementary experiment to dissociative recombination (DR) studies undertaken by our collaborators at CRYRING.² The preliminary cross sections are fairly flat in the 30-100 eV range, but some structure is apparent around 20 eV. In addition, experiments have continued for the CH_3^+ target ion with measurements completed for the CH^+ and C^+ ion fragment channels; cross sections for both channels exhibited a smooth energy dependence over the 3–100 eV range of the measurements with no apparent resonance features. However, a strong resonance-like feature is observed near 15 eV in the dissociation of DCO^+ ions producing CO^+ ions.³ This feature is similar to that measured for the production of CH^+ from the dissociation of CH_2^+ .⁴

The dissociation experiments discussed above used molecular ions produced by the ORNL MIRF Caprice ECR ion source,⁵ but other cooler sources will also be used in order to understand the role of electronic and ro-vibrational excited states. A second ion source, a hot-filament Colutron ion source, is presently online and expected to produce fewer excited molecular ions. An even colder pulsed ion source, very similar to the one used for measurements⁶ on the dissociative recombination of rotationally cold H_3^+ ions at CRYRING, is under development for use at the ORNL MIRF. Additionally, work continues on a similar supersonic source that uses a piezoelectric mechanism for more reliable pulsed valve operation. With this range of ion sources, one can study dissociation with both well-characterized cold sources and with hotter sources that better approximate the excited state populations in plasma environments found in applications such as fusion, plasma processing, and aeronomy.

1. M. E. Bannister, H. F. Krause, C. R. Vane, N. Djuric, D. B. Popovic, M. Stepanovic, G. H. Dunn, Y.-S. Chung, A. C. H. Smith, and B. Wallbank, "Electron-Impact Dissociation of CH^+ Ions: Measurement of C^+ Fragment Ions," *Phys. Rev. A* **68**, 042714 (2003).
2. W.D. Geppert, R. Thomas, J. Semaniak, A. Ehlerding, T.J. Millar, F. Österdahl, M. af Ugglas, N. Djuric, A. Paál, and M. Larsson, "Dissociative Recombination of N_2H^+ : Evidence for Fracture of the N-N Bond," *Astrophys. J.* **609**, 459 (2004).
3. E. M. Bahati, R. D. Thomas, C. R. Vane, and M. E. Bannister, "Electron-impact dissociation of $D^{13}CO^+$ molecular ions to $^{13}CO^+$ ions," *J. Phys. B* **38**, 1645 (2005).
4. C. R. Vane, M. E. Bannister, and R. Thomas, "Electron-Impact Dissociation of CH_2^+ Producing CH^+ Fragments," XXIII ICPEAC Abstracts, Stockholm, Sweden (2003).
5. F. W. Meyer, "ECR-Based Atomic Collision Research at the ORNL MIRF," in *Trapping Highly Charged Ions: Fundamentals and Applications*, edited by J. Gillaspay (Nova Science, Huntington, NY, 1997), p. 117.
6. B. J. McCall et al., "An Enhanced Cosmic-Ray Flux towards Zeta-Persei Inferred from a Laboratory Study of the $H_3^+-e^-$ Recombination Rate," *Nature* **422**, 500 (2003).

Dissociative Recombination: The process of dissociative recombination (DR) of relatively simple three-body molecular ions is being studied in our ongoing collaboration with Prof. Mats Larsson and colleagues at the Manne Siegbahn Laboratory (MSL), Stockholm University. Absolute cross sections, branching fractions, and measurements of the dissociation kinematics, especially of the three-body breakup channel, are being investigated at zero relative energy for a variety of light and heavy vibrationally-cold triatomic di-hydrides and other molecular ions with three-body channels. This research is carried out using the MSL CRYRING heavy ion storage ring facility, which is still expected to continue to be available for our electron-molecular ion measurements at least into calendar year 2007. We have now completed analysis of CH_2^+ , and NH_2^+ three-body DR measurements and the results compared with H_2O^+ are published in *Physical Review A*.¹

In the last year, we have initiated studies of two new systems $D_3O_2^+$ and O_3^+ . These experiments are a continuation of previous measurements concerning the DR of similar molecules, such as H_2O^+ , NH_2^+ , CH_2^+ , and SD_2^+ that have all revealed three-body break-up as the dominant reaction channel.¹⁻⁵ In order to

study the three body break-up dynamics in detail, a high-resolution imaging technique is used to measure the displacement of the fragments from the center of mass of the molecule.⁶ The displacement is related to the kinetic energy of the fragments and therefore information about the dynamics involved in the process can be obtained, i.e., the internal state distribution of the fragments. These event-by-event measurements yield information about how the kinetic energy is distributed between the two light fragments and the angular distribution of the dissociating molecules. In all of the triatomic di-hydride systems previously studied, the branching fractions showed very roughly (7:2:1) ratios for (X + H + H; XH + H: X + H₂), while the observed energy sharing and angular distributions of the three-body breakup product channel could depend heavily on the structure, bonding and charge centre of the parent molecular ion. In contrast to these previously-studied di-hydride systems, D₅O₂⁺ provides an excellent opportunity for investigating the role played by internal states of fragments in the DR process. The preliminary branching results indicate that the D₂O + D + D₂O channel contributes more than 90% of the DR. The energy available to the products is approximately 5 eV; for ground state fragments this would mean 5 eV of kinetic energy, mostly given to the single D atom. Preliminary analysis of our imaging measurements, however, suggests that this is not the case, but instead that a significant portion of the available energy is used in internal excitation of the D₂O molecules. A more detailed analysis of the imaging data is in progress. For the O₃⁺ system, preliminary branching fractions show that more than 60% of DR events lead to three separate O atoms, consistent with the dominance of the three-body channels observed in DR of di-hydride ions. This finding would have a significant impact on models of atmospheric chemistry where DR plays a crucial role by producing excited O atoms. Analysis of the imaging data for the O₃⁺ system has just commenced. Absolute DR cross sections have also been measured in the 0-1 eV range for both D₅O₂⁺ and O₃⁺.

1. R. Thomas et al., "Three-Body Fragmentation Dynamics of Amidogen and Methylene Radicals via Dissociative Recombination," *Phys. Rev. A* **71**, 032711 (2005).
2. L. Viktor et al., "Branching Fractions in the Dissociative Recombination of NH⁺ and NH₂⁺ Molecular Ions," *Astron. Astrophys.* **344**, 1027 (1999).
3. Å. Larson et al., "Branching Fractions in Dissociative Recombination of CH₂⁺," *Astrophys. J.* **505**, 459 (1998).
4. S. Rosén et al., "Recombination of Simple Molecular Ions Studied in a Storage Ring: Dissociative Recombination of H₂O⁺," *Faraday Discussions* **115**, 295 (2000).
5. F. Hellberg et al., "Investigating the Breakup Dynamics of Dihydrogen Sulfide Ions Recombining with Electrons," *J. Chem. Phys.* **122**, 224314 (2005).
6. R. Thomas et al., "Investigating the Three-Body Fragmentation Dynamics of Water via Dissociative Recombination and Theoretical Modeling Calculations," *Phys. Rev. A* **66**, 032715 (2002).

Near-Thermal Collisions of Multicharged Ions with H and Multi-Electron Targets - C. C. Havener R. Rejoub, and D. R. Schultz

Electron capture by multi-charged ions from neutrals is important in many technical plasmas including those used in material processing, lighting, ion-source development, and for spectroscopic diagnostics and modeling of core, edge, and divertor regions of magnetically confined fusion plasmas. At ORNL, the merged-beams technique¹ is being used to explore near-thermal collisions (meV/u – keV/u) of multi-charged ions with neutral atoms and molecules, providing benchmark measurements for comparison with state-of-the-art theories.

Dipole polarization effects are one of the dominant features in electron capture at low (eV/u) collision energies. While the cross section often increases toward lower energies (as in recent measurements^{2,3} for Ne⁴⁺ and Ne³⁺) due to trajectory effects caused by the ion-induced dipole potential, several systems have been found where the cross section "oscillates" toward lower energies due to the quantal nature of the collision dynamics.⁴ For endoergic or accidentally resonant electron capture channels that exhibit an energy threshold, the decreasing cross section is also modified by the collision dynamics. For He²⁺ + H which exhibits an exponentially decreasing cross section, our merged-beams measurements are used to benchmark recent Hidden-Crossing Molecular Orbital Coupled Channel and Hyper-Spherical Coupled Channel calculations (see ref. 5 and references within).

The ion-atom merged-beams apparatus has been upgraded and moved to the HV platform to take advantage of the high velocity multi-charged ion beams. First measurements for N²⁺ + H have been

reported⁴ and together with previous measurements with D, confirm that the cross section increases toward lower energies, in contrast to several recent molecular orbital coupled channel calculations (see Ref. 4) which predicted that the cross section peaked at 0.4 eV/u. Our measurements again confirm that dipole polarization effects dominate electron capture at eV/u energies and below.

The apparatus upgrade and HV platform provide several enhancements to our investigation of near-thermal collisions. The higher velocity beams now available increase the angular collection of the apparatus from 2.3 to 3.3 degrees in the lab frame, eliminating concerns over incomplete collection of the signal in the center-of-mass frame and allow measurements with both H and D to directly observe isotope effects. Measurements with heavy atomic and molecular ions are now possible for the first time. The observed beams were of sufficient intensity that state-selective measurements using photon spectroscopy should now be possible. For the $N^{2+} + H$ measurements discussed above, ion beams were found to have at least a factor of four less divergence, increasing the resolution at low energies by more than a factor of two from 25 meV/u to 10 meV/u. This will allow an investigation of the possible structure in the system below 1 eV/u. The recent addition of a Cs sputter ion source allows merged-beams measurements to be performed with a variety of neutral beams such as Li, B, Na, Cr, Fe, etc., and molecular beams such as O_2 , CH_4 , ... Our goal is to measure $He^{2+} + Li$, Li 36 x more polarizable than H, where strong shape resonances are predicted due to the strong ion-induced dipole between reactants.

We have also continued the development of new theoretical tools to study processes such as charge transfer over a broad range of energies. In particular, we continue exercise of a method to describe charge transfer in ion-atom collisions that hybridizes the lattice, time-dependent Schrödinger equation (LTDSE) approach with the atomic-orbital, coupled-channel technique. This method takes advantage of the completeness of the treatment of the collision problem through the LTDSE approach within a relatively small space around the distance of closest approach during the collision. It then extends the solution into the asymptotic regime through the less computationally intensive continuation of the time evolution of the electronic states under consideration utilizing a small, external coupled-channels expansion. The results show excellent agreement with experimental measurements and constitute improvements over various existing theoretical treatments. We have also applied this approach to treat swift collisions of Ar^{18+} with carbon in support of transport modeling, for $H^+ + H(2s)$, and for He^{2+} and $Be^{4+} + H$ collisions as a new benchmark for certain fusion energy relevant cross sections.

1. C. C. Havener, "Low-Energy Electron Capture Measurements Using Merged Beams," in *The Physics of Multiply Charged Ions*, Vol. 2, Kluwer Academic Publishers, The Netherlands, 2003, pp. 193-21.
2. C. C. Havener, R. Rejoub, C. R. Vane, H. F. Krause, D. W. Savin, M. Schnell, J. G. Wang, and P. C. Stancil, "Electron Capture by Ne^{4+} Ions from Atomic Hydrogen," *Phys. Rev. A* **71**, 034702 (2005).
3. R. Rejoub, M. E. Bannister, C. C. Havener, D. W. Savin, C. J. Verzani, J. G. Wang, and P. C. Stancil, "Electron Capture by Ne^{3+} Ions from Atomic Hydrogen," *Phys. Rev. A* **69**, 052704 (2004).
4. C. C. Havener and R. Rejoub, "Dipole Polarization Effects on Highly-Charged Ion-Atom Electron Capture," to be published in the invited proceedings, *International Conference on Photonic, Electronic, and Atomic Collisions*, Rosario, (World Scientific) 2005.
5. C. C. Havener, R. Rejoub, P. S. Krstic, and A. C. H. Smith, "Charge Transfer in Low-Energy Collisions of He^{2+} with Atomic Hydrogen," *Phys. Rev. A* **71**, 042707 (2005).

High-*n* Rydberg Atoms and Tailored Pulses: A Laboratory for Wavefunction Engineering, Non-Linear Dynamics and Decoherence – C. O. Reinhold

When a Rydberg wavepacket interacts with an environment (e.g., an ambient gas), the interaction leads to an irreversible dephasing of the wavepacket, referred to as decoherence. Given recent developments, it is possible to envision studies of decoherence of Rydberg wavepackets interacting with "partially controlled" environments. Preliminary work suggests that decoherence rates can be quantified from the dephasing of Rydberg wavepackets. We plan to use as environments a gas of atoms or molecules (whose density can be varied) or well characterized noise produced, for example, using a random sequence of electric field pulses. Clearly, one goal would be to control and modify decoherence with the view to the design and construction of decoherence-free subspaces within which information is embedded. Another goal would be the utilization of decoherent dephasing as a tool to measure cross sections for quasi-elastic electron-atom (or molecule) collisions at energies extending down to micro electron volts.

Present experiments for the kicked Rydberg atom are limited to low scaled frequencies of the trains of pulses. Raising this limit would provide new opportunities for the study of quantum localization and other phenomena at high scaled frequencies. Achieving this goal requires increasing the n -level of the initial stationary quasi-1D atoms, which is currently limited to $n \sim 350$. One of our goals is the design of a tailored sequence of pulses for transporting polarized states to higher n -levels.

In order to probe wavepackets, single pulses have been used at variable time delay after the steering pulses to probe the momentum and/or spatial distributions of the excited electron. We plan to develop a scheme for probing the equivalent of the Husimi distribution of Rydberg wavepackets (i.e., the joint position and momentum distribution) using tailored trains of pulses as probes.

Another avenue for future investigation is the study of pulse-driven recombination. Bound-free transitions induced by stochastic sequences of momentum transfers play an important role in atom transport through solids and in plasmas. To our knowledge, no previous systematic investigations of recombination induced by multiple pulses have been reported.

Analysis of Structure in Low-Energy Ion-Atom Collisions – J. H. Macek and S. Yu. Ovchinnikov.

Structure in low-energy ion-atom collisions originates from a variety of effects related to wave motion. Highly accurate, state-of-the art calculations of proton-atomic hydrogen atom collisions has identified structure in total cross sections related to glory scattering, shape resonances, and the newly identified "Regge" oscillations.¹ These latter oscillations have been overlooked until now, however, it appears that they should be present in almost all low energy processes when the atomic masses are sufficiently large that several partial waves contribute to integral cross sections. A systematic study of these structures for potentials, e. g., Thomas-Fermi potentials, will be undertaken to see if the "Regge" oscillations also occur in these widely used potentials.

Rosenthal-Bobashev oscillations are also a notable feature of low-energy ion-atom collisions. These structures are well-understood and can be used to test theoretical models. We will examine such oscillations in processes where double negative ions M^{-} , where M stands for a molecule, are formed by collisions with target atoms. The position and strength of the oscillations will be computed for comparison with measurements.

The hidden crossing theory has provided valuable insights and quantitative results for low-energy inelastic processes. The accuracy of the theory is comparable to the WKB theory for elastic processes, even though the hidden crossing theory employs purely classical trajectories for relative motion of ions and atoms. We will modify the hidden crossing theory to apply to ion-atom interactions in the domain where a common classical trajectory is inadequate. Protonium formation in antiproton-hydrogen atom collisions is an ideal testing ground for the modified theory since the final protonium states are quantized standing waves in the coordinate of relative motion of the proton and antiproton while the electron is ejected as a free particle. This requires a WKB treatment of relative motion. Our theory will be tested by computing the n and l distribution of protonium states for comparison with CTMC-type computer simulations.²

1. J. H. Macek, P. S. Krstic, and S. Yu. Ovchinnikov, "Regge Oscillations in Integral Cross Sections for Proton Impact on Atomic Hydrogen," *Phys. Rev. Lett.* **93**, 183203 (2004).
2. S. Yu. Ovchinnikov and J. H. Macek, "Protonium Formation in Antiproton-Hydrogen-Atom Collisions," *Phys. Rev. A* **71**, 052717 (2005).

References to Publications of DOE Sponsored Research from 2003-2005 (descending order)

Year 2005 publications

"Path Dependence of the Charge-State Distributions of Low-Energy F^{q+} Ions Backscattered from $RbI(100)$," L. I. Vergara, F. W. Meyer, and H. F. Krause, *Nucl. Instrum. Methods Phys. Res.* **B 230**, 379 (2005).

"Charge Transfer in Low-Energy Collisions of He^{2+} with Atomic Hydrogen," C. C. Havener, R. Rejoub, P. S. Krstic, and A. C. H. Smith, *Phys. Rev. A* **71**, 042707 (2005).¹

- “Electron Capture by Ne^{4+} Ions from Atomic Hydrogen,” C. C. Havener, R. Rejoub, C. R. Vane, H. F. Krause, D. W. Savin, M. Schnell, J. G. Wang, and P. C. Stancil, *Phys. Rev. A* **71**, 034702 (2005).
- “Electron-Impact Dissociation of D^{13}CO^+ Molecular Ions to $^{13}\text{CO}^+$ Ions,” E. M. Bahati, R. D. Thomas, C. R. Vane, and M. E. Bannister, *J. Phys. B* **38**, 1645 (2005).
- “Three-Body Fragmentation Dynamics of Amidogen and Methylene Radicals via Dissociative Recombination,” R. Thomas, F. Hellberg, A. Neau, S. Rosen, M. Larsson, C. R. Vane, M. E. Bannister et al., *Phys. Rev. A* **71**, 032711 (2005).
- “Investigating the Breakup Dynamics of Dihydrogen Sulfide Ions Recombining with Electrons,” F. Hellberg, V. Zhaunerchyk, A. Ehlerding, W. D. Geppert, M. Larsson, R. D. Thomas, M. E. Bannister, E. Bahati, C. R. Vane et al., *J. Chem. Phys.* **122**, 224314 (2005).
- “The Effect of Bonding on the Fragmentation of Small Systems,” R. Thomas et al., *J. Phys. Conf. Ser.* **4**, 187 (2005).
- “Target Orientation Dependence of the Charge Fractions Observed for Low-Energy Multicharged Ions Ne^{9+} And F^{9+} Backscattered from $\text{RbI}(100)$,” L. I. Vergara, F. W. Meyer, and H. F. Krause, *Surface and Coatings Technology* **196**, 19 (2005).
- “An All-Permanent Magnet ECR Ion Source for the ORNL MIRF Upgrade Project,” D. Hitz, M. Delaunay, A. Girard, L. Guillemet, J.M. Mathonnet, J. Chartier, and F.W. Meyer, *AIP Conference Proceedings* **749**, 123 (2005).
- “Traveling Wave Vs. Cavity RF Injection for the ORNL HRIBF “Volume-Type” ECR Ion Source”, Y. Liu, F. M. Meyer, and J. M. Cole, *AIP Conference Proceedings* **749**, 187 (2005).
- “Non-Unitary Master Equation for the Internal State of Ions Transversing Solids,” M. Seliger, C. O. Reinhold, T. Minami, and J. Burgdorfer, submitted to *Nucl. Instrum. Methods Phys. Res. B* **230**, 7-11 (2005).
- “Steering Rydberg Wave Packets Using a Chirped Train of Half-Cycle Pulses,” S. Yoshida, C. O. Reinhold, E. Persson, J. Burgdorfer, and F. B. Dunning, *J. Phys. B* **38**, S209-S217 (2005).
- “Performances of Volume versus Surface ECR Ion Sources,” Y. Liu, G. D. Alton, H. Z. Bilheux, and F. M. Meyer, *AIP Conference Proceedings* **749**, 191 (2005).
- “Measurements of Chemical Erosion of ATJ Graphite by Low Energy D_2^+ Impact,” F. W. Meyer, H. F. Krause, and L. I. Vergara, *Proceedings, International Conference on Plasma Surface Interactions*, Portland, Maine, May 24-28, 2004, *J. Nucl. Mater.* **337-339**, 922 (2005).
- “The ORNL Multicharged Ion Research Facility Upgrade Project,” F. W. Meyer, M. E. Bannister, D. Dowling, J. W. Hale, C. C. Havener, J. W. Johnson, R. C. Juras, H. F. Krause, A. J. Mendez, J. Sinclair, A. Tatum, C. R. Vane, E. Bahati Musafiri, M. Fogle, R. Rejoub, L. Vergara, to be published in *Nucl. Instrum. Methods Phys. Res. B.* (2005).
- “The ORNL Multicharged Ion Research Facility (MIRF) High Voltage Platform Project,” F. W. Meyer, M. E. Bannister, J. W. Hale, J. W. Johnson, and D. Hitz, 2005 Particle Accelerator Conference, Knoxville, TN, May 16 – 20, 2005, to be published, *IEEE Conference Proceedings* (2005).
- “Control System for the ORNL Multicharged Ion Research Facility High Voltage Platform,” M. E. Bannister, F. W. Meyer, and J. Sinclair, 2005 Particle Accelerator Conference, Knoxville, TN, May 16 – 20, 2005, to be published, *IEEE Conference Proceedings* (2005).

“Isobar Suppression by Photodetachment in a Gas-filled RF Quadrupole Ion Guide,” Y. Liu, J. R. Beene, C. C. Havener, and J. F. Lang, to be published *Applied Physics Letters* (2005).

“Chemical Sputtering of ATJ Graphite Induced by Low-Energy D_2^+ Bombardment,” L. I. Vergara, F. W. Meyer, and H. F. Krause, accepted for publication in *J. Nucl. Materials* (2005).

“Experiments on Electron-Impact Ionization of Atomic and Molecular Ions,” M. E. Bannister, pp. 172-179, *Proceedings of the 4th ICAMDATA Conference, Oct. 5-8, 2004, Toki, Japan*, AIP Conf. Proceedings 730, Woodbury, NY (2005).

“Recent ORNL Measurements of Chemical Sputtering of ATJ Graphite by Slow Atomic and Molecular D Ions,” F. W. Meyer, L. I. Vergara, and H. F. Krause, [Invited presentation] Workshop on New Directions for Advanced Computer Simulations and Experiments in Plasma Surface Interactions, March 21-23, 2005, accepted for publication in *Physics Scripta* (2005).

“New Directions for Computer Simulations and Experiments in Plasma-Surface Interactions for Fusion,” J. T. Hogan, P. Krstic, and F. W. Meyer, accepted for publication, *Nucl. Fusion* (2005).

“Control System for the ORNL Multicharged Ion Research Facility High Voltage Platform”, M. E. Bannister, F. W. Meyer, J. Sinclair, 2005 Particle Accelerator Conference, Knoxville, TN, May 16 – 20, 2005, to be published, *IEEE Conference Proceedings* (2005).

“The ORNL Multicharged Ion Research Facility (MIRF) High Voltage Platform Project,” F. W. Meyer, M. E. Bannister, J. W. Hale, J. W. Johnson, and D. Hitz, 2005 Particle Accelerator Conference, Knoxville, TN, May 16 – 20, 2005, to be published, *IEEE Conference Proceedings* (2005).

“In-situ Electron Cyclotron Resonance (ECR) Plasma Potential Determination Using An Emissive Probe,” H. J. You, Y. Liu, and F. W. Meyer, 2005 Particle Accelerator Conference, Knoxville, TN, May 16 – 20, 2005, to be published, *IEEE Conference Proceedings* (2005).

“Laser Ion Source Development for ISOL Systems at RIA,” Y. Liu, C. Baktash, J. R. Beene, H. Z. Bilheux, C. C. Havener, H. F. Krause, D. R. Schultz, D. W. Stracener, C. R. Vane, K. Brück, Ch. Geppert, T. Kessler, and K. Wendt, 2005 Particle Accelerator Conference, Knoxville, TN, May 16 – 20, 2005, to be published, *IEEE Conference Proceedings* (2005).

“Dipole Polarization Effects on Highly-Charged Ion-Atom Electron Capture,” C. C. Havener and R. Rejoub, to be published in the invited proceedings, *International Conference on Photonic, Electronic, and Atomic Collisions*, Rosario, (World Scientific), 2005.

Year 2004 publications

“Multi-Electron Dynamics for Neutralization of Highly Charged Ions Near Surfaces,” J. Burgdorfer, L. Wirtz, C. O. Reinhold, and C. Lemell, *Vacuum* **73**, 3 (2004).

“Classical and Quantum Scaling for Localization of Half-Cycle Pulse-Driven Rydberg Wavepackets,” D. G. Arbo, C. O. Reinhold, and J. Burgdorfer, *Phys. Rev. A* **69**, 023409 (2004).

“Characterization of Quasi One-Dimensional Rydberg Atoms Using Half-Cycle Pulse Applied Perpendicular to the Atomic Axis,” W. Zhao, J. C. Lancaster, F. B. Bunning, C. O. Reinhold, J. Burgdorfer, *Phys. Rev A* **69**, 041301 (2004).

“High-Energy Ion Generation by Short Laser Pulses,” A. Maksimchuk, K. Klippo, H. Krause, G. Mourou, K. Nemoto, D. Schultz, D. Umstadter, R. Vane, V. Yu. Bychenkov, G. I. Dudnikova, V. F. Kovalev, K. Mima, V. N. Novikov, Y. Sentoku, and S. V. Tolokonnikov, *Plasma Phys. Rep.* **30**, 473 (2004).

“Dynamics of Ionization in Atomic Collisions,” S. Yu. Ovchinnikov, G. N. Ogurtsov, J. H. Macek, and Yu. S. Gordeev, *Phys. Rep.* **389**, 119 (2004).

“Tailoring and Controlling Wave Packets In Multi-Photon Atom Collisions,” Yoshida, S., E. Persson, C. O. Reinhold, J. Burgdörfer, B. E. Tannian, C. L. Stokely, and F. B. Dunning, [Invited Presentation], Proceedings of XXIII International Conference on Photonic, Electronic, and Atomic Collisions (ICPEAC), Stockholm, Sweden, July 23-29, 2003, *Physica Scripta* **T110**, 424 (2004).

“Electron Capture by Ne^{3+} Ions from Atomic Hydrogen,” Rejoub, R., M. E. Bannister, C. C. Havener, D. W. Savin, C. J. Verzani, J. G. Wang, and P. C. Stancil, *Phys. Rev. A* **69**, 052704 (2004).

“Charge Changing Interactions of Ultrarelativistic Pb Nuclei,” C. Scheidenberger, I. A. Pshenichnov, K. Summerer, A. Ventura, J. P. Bondorf, A. S. Botvina, I. N. Mishustin, D. Boutin, S. Datz, H. Geissel, P. Grafstrom, H. Knudsen, H. F. Krause, B. Lommel, S. P. Moller, G. Munzenberg, R. H. Schuch, E. Uggerhøj, U. Uggerhøj, C. R. Vane, Z. Z. Vilakazi, and H. Weick, *Phys. Rev. C* **70**, 014902 (2004).

“Site-Specific Neutralization of Slow Multicharged Ions Incident on Solid Surfaces,” F. W. Meyer, H. F. Krause, V. A. Morozov, C. R. Vane, and L. I. Vergara, *Physica Scripta* **T110**, 403 (2004).

“Analysis of Structures in the Cross Sections for Elastic Scattering and Spin Exchange in Low Energy $\text{H}^+ + \text{H}$ Collisions,” P. S. Krstic, J. H. Macek, S. Yu. Ovchinnikov, and D. R. Schultz, *Phys. Rev. A* **70**, 042711 (2004).

“Regge Oscillations in Integral Cross Sections for Proton Impact on Atomic Hydrogen,” J. H. Macek, P. S. Krstic, and S. Yu. Ovchinnikov, *Phys. Rev. Lett.* **93**, 183203 (2004).

“Energy and Angular Distributions of Electrons Ejected from Atomic Hydrogen by Low Energy Proton Impact,” J. H. Macek and S. Yu. Ovchinnikov, *Phys. Rev. A* **70**, 052702 (2004).

“Response of Highly Polarized Rydberg States to Trains of Half-Cycle Pulses,” C. O. Reinhold, W. Zhao, J. C. Landcaster, F. B. Dunning, E. Persson, D. G. Arbo, S. Yoshida, and J. Burgdorfer, *Phys. Rev. A* **70**, 035203 (2004).

“Coherence Parameters for Charge Transfer in Collisions of Protons with Helium Calculated Using a Hybrid Numerical Approach,” T. Minami, C. O. Reinhold, D. R. Schultz, and M. S. Pindzola, submitted to *J. Phys. B* **37**, 4025 (2004).

“Energy and Angular Distributions of Electrons Ejected from Atomic Hydrogen by Low Energy Proton Impact,” J. H. Macek and S. Yu. Ovchinnikov, accepted for publication in *Phys. Rev. A* (2004).

“Low Energy Charge Transfer with Multicharged Ions Using Merged Beams,” C. C. Havener, pp. 235-244, Proceedings, American Physical Society Spring Meeting on Atomic Processes in Plasmas, Santa Fe, New Mex., April 19-22, 2004, AIP Conference Proceedings 730, Woodbury, N.Y. (2004).

“Computations of Elastic Scattering and Spin Exchange in $\text{H}^+ + \text{H}$ Collisions for Impact Energies between 10^{-4} and 10 eV,” P. Krstic, J. H. Macek, and S. Yu. Ovchinnikov, accepted for publication, *Phys. Rev. A* (2004).

Year 2003 publications

“Initial testing of the 6 GHz, all-permanent magnet, “Volume-Type” ECR ion source”, H. Billeux, G. D. Alton, Y. Liu, F.W. Meyer, J.M. Cole, C.A. Reed, C. L. Williams, AIP Conference Proceedings **680**, 1058 (2003).

“Absolute Measurements of Cross Sections for Near-Threshold Electron-Impact Excitation of Na-like and Mg-like Multiply Charged Ions,” A.C.H. Smith, M. E. Bannister, Y.-S. Chung, A. M. Derkatch, N. Djuric, H. F. Krause, D. B. Popovic, B. Wallbank, and G. H. Dunn, *Nucl. Instrum. Methods Phys. Res. B* **205**, 421 (2003).

“Electron-Impact Dissociation of CH^+ Ions: Measurements of C^+ Fragment Ions,” M. E. Bannister, H. F. Krause, C. R. Vane, N. Djuric, D. B. Popovic, M. Stepanovic, G. H. Dunn, Y.-S. Chung, A.C.H. Smith, and B. Wallbank, *Phys. Rev. A* **68**, 042714 (2003).

“Observation of Trielectronic Recombination in Be-like Cl Ions,” M. Schnell, G. Gwinner, N. R. Badnell, M. E. Bannister, S. Böhm, J. Colgan, S. Kieslich, S. D. Loch, D. Mitnik, A. Müller, M. S. Pindzola, S. Schippers, D. Schwalm, W. Shi, A. Wolf, and S.-G. Zhou, *Phys. Rev. Lett.* **91**, 043001 (2003).

“Production of Quasi-One-Dimensional Very-High- n Rydberg Atoms,” C. L. Stokely, J. C. Lancaster, F. B. Dunning, D. G. Arbo, C. O. Reinhold, and J. Burgdörfer, *Phys. Rev. A* **67**, 013403 (2003).

“Liouville Master Equation for Multi-Electron Dynamics: Neutralization of Highly Charged Ions Near an LiF Surface,” K. Wirtz, C. O. Reinhold, C. Lemell, and J. Burgdörfer, *Phys. Rev. A* **67**, 012903 (2003).

“Three-body Reaction Dynamics in Dissociative Recombination,” R. Thomas, F. Hellberg, M. Larsson, C. R. Vane, P. Andersson, J. Pattersson, A. Petrigani, and W. J. van der Zande, *AIP Conference Proceedings* **680**, 187-190 (2003).

“Recent Studies of Three-Body Fragmentation Dynamics via Dissociative Recombination in CRYRING,” R. Thomas, S. Datz, M. Larsson, W. J. van der Zande, F. Hellberg, A. Petrigani, S. Rosén, A. M. Derkatch, A. Neau, and C. R. Vane, pp. 95-100, in *Dissociative Recombination of Molecular Ions with Electrons*, ed., S. Guberman, Kluwer Academic Publication (2003).

“Quantum Trajectory Monte Carlo Method for Internal State Evolution of Fast Ions Traversing Amorphous Solids,” T. Minami, C. O. Reinhold, J. Burgdörfer, *Phys. Rev. A* **67**, 022902 (2003).

“Quantum Trajectory Monte Carlo Method Describing the Coherent Dynamics of Highly Charged Ion,” T. Minami, C. O. Reinhold, and J. Burgdörfer, *Nucl. Instrum. Methods Phys. Res. B* **205**, 818 (2003).

“Low-Energy Electron Capture Measurements Using Merged Beams,” pp. 193-218, C. C. Havener, in *The Physics of Multiply and Highly Charged Ions*, Vol. 2 of *Interactions with Matter*, ed. Fred J. Currell, Kluwer Academic Publishers, The Netherlands (2003).

“Ionization of Helium by Antiprotons: Fully Correlated, Four-Dimensional Lattice Approach,” D. R. Schultz, and P. S. Krstic, *Phys. Rev. A* **67**, 022712 (2003).

“Elastic and Transport Cross Sections for Argon in Hydrogen Plasmas,” P. S. Krstic, D. R. Schultz, and T. Chung, *Phys. Plasmas* **10**, 869 (2003).

“Site-Resolved Neutralization of Slow Singly and Multiply Charged Ions during Large-Angle Backscattering Collisions with RbI(100),” F. W. Meyer, H. F. Krause, and C. R. Vane, *Nucl. Instrum. Methods Phys. Res. B* **203**, 231 (2003).

“Laser-Modified Charge Transfer Processes in Proton Collisions with Lithium Atoms,” M. S. Pindzola, T. Minami, and D. R. Schultz, *Phys. Rev. A* **68**, 013404 (2003).

“Excited-State Evolution Probed by Convoy-Electron Emission in Relativistic Heavy-Ion Collisions,” Takabayashi, Y., T. Ito, T. Azuma, K. Komaki, Y. Yamazaki, H. Tawara, E. Takada, T. Murakami, M. Seliger, K. Tökesi, C. O. Reinhold, and J. Burgdörfer, *Phys. Rev. A* **68**, 042703 (2003).

“Electron Capture by Ne^{2+} Ions from Atomic Hydrogen,” T. Mroczkowski, D. W. Savin, R. Rejoub, P. S. Krstic, and C. C. Havener, *Phys. Rev. A* **68**, 032721 (2003).

“Quantum Localization in the Three-Dimensional Kicked Rydberg Atom,” E. Persson, S. Yoshida, X.-M. Tong, C. O. Reinhold, and J. Burgdörfer, *Phys. Rev. A* **68**, 063406 (2003).

“Projectile Neutralization in Large-Angle Back-Scattering of Slow F^{q+} , Ne^{q+} , and Ar^{q+} Incident on RbI(100),” F. W. Meyer, H. F. Krause, and C. R. Vane, *Nucl. Instrum. Methods Phys. Res. B* **205**, 700 (2003).

“Highly Transverse Velocity Distribution of Convoy Electrons Emitted by Highly Charged Ions,” M. Seliger, K. Tokesi, C. O. Reinhold, and J. Burgdörfer, *Nucl. Instrum. Methods Phys. Res. B* **205**, 830 (2003).

“Pulse-Induced Focusing of Rydberg Wavepackets,” D. G. Arbo, C. O. Reinhold, J. Burgdörfer, A. K. Pattanayak, C. L. Stokely, W. Zhao, J. C. Lancaster, and F. B. Denning, *Phys. Rev. A* **67**, 063401 (2003).

“Annihilation of Low Energy Antiprotons in Hydrogen,” S. Yu. Ovchinnikov and J. H. Macek, *CAARI 2002*, AIP Conference Proceedings **680** (2003).

“Quantum Trajectory Monte Carlo Method Describing the Coherent Dynamics of Highly Charged Ions,” T. Minami, C. O. Reinhold, and J. Burgdörfer, *Nucl. Instrum. Methods Phys. Res. B* **205**, 818 (2003).

“Liouville Master Equation for Multi-Electron Dynamics: Neutralization of Highly Charged Ions near a LiF Surface,” L. Wirtz, C. O. Reinhold, C. Lemell, and J. Burgdorfer, *Phys. Rev. A* **67**, 012903 (2003).

“Interaction of Highly Charged Ions with Insulator Surfaces at Low Velocities: Estimates for Auger Rates,” J. Burgdorfer, C. O. Reinhold, and F. Meyer, *Nucl. Instrum. Methods Phys. Res. B* **205**, 690 (2003).

“The Kicked Rydberg Atom: A New Laboratory for Study of Non-Linear Dynamics,” F. B. Dunning, C. O. Reinhold, and J. Burgdörfer, *Physica Scripta* **68**, C44 (2003).

University Research Summaries
(by PI)

Properties of Transition Metal Atoms and Ions

Donald R. Beck
Physics Department
Michigan Technological University
Houghton, MI 49931
e-mail: donald@mtu.edu

Program Scope

Transition metal atoms are technologically important in plasma physics (e.g., as impurities in fusion devices), Atomic Trap Trace Analysis (detection of minute quantities of radioactive species), astrophysical abundance (e.g., Fe II) and atmospheric studies, deep-level traps in semiconductors, hydrogen storage devices, etc. The more complicated rare earths which we are beginning to study are important in lasers, high temperature superconductivity, advanced lighting sources, magnets, etc.

Because of the near degeneracy of nd and $(n+1)s$ electrons in lightly ionized transition metal ions and the differing relativistic effects for d and s electrons [1], any computational methodology must simultaneously include the effects of correlation and relativity from the start. We do this by using a Dirac-Breit Hamiltonian and a Relativistic Configuration Interaction (RCI) formalism to treat correlation. Due to the presence of high- l (d) electrons, computational complications are considerably increased over those in systems with just s and/or p valence electrons. These include the following: (1) larger energy matrices (5-10x larger) because the average configuration can generate many more levels [2]. Multi-root RCI calculations with matrices of order 20,000 are becoming common. With the use of REDUCE [3], these can be equivalent to calculations 10 times (or more) larger, (2) increased importance of interactions with core electrons (d 's tend to be more compact, and there can be more of them), (3) a significant variation of the d radial functions with level (J), which requires the presence of second order effects. Methodological improvements [3] are needed: (i) in the treatment of second order effects (e.g., Fe II), (ii) to include continuum properties such as photoionization cross sections (e.g., Kr II), (iii) to more accurately treat Rydberg series-perturber interactions (e.g., Mo VI). Progress has been made in all these directions, during this last project year.

Recent Progress

[A] Fe II Energy Levels and Oscillator Strengths

Fe II Oscillator Strengths are of great interest to astrophysicists for determination of stellar abundances and Fe II and its homologs are perhaps the most difficult transition metals to deal with. This is because some of the most dominant pair correlation ("first order") effects leaves one with the most complicated "core", viz d^5 . Additionally, same symmetry adjacent levels can be very close together (a few thousand cm^{-1} on average), making the thorough inclusion of both correlation and relativity essential. Successful treatment is only possible through years of development of software, one alternative of which has been developed by the PI [3].

However, the existing software needed further improvement—specifically in the efficient inclusion of magnetic Breit effects, in order to make the Fe II calculations manageable. Speed gains of an order of magnitude were achieved as part of this project. Careful attention to developing well converged radial and angular spaces and minimizing their size impact (through use of REDUCE [3]) was essential to pushing the previous d^5 limit to the most complicated d^7 cases.

A few Fe II levels are so close that (75 cm^{-1} in the worst case), semi-empirical corrections had to be made to a (very) few of the diagonal matrix elements. The Fe II work is now completed [4], and is in good agreement with two large widely used semi-empirical data bases and the few available experimental measurements. Our techniques and results are complimentary and competitive with those of Hibbert (presented at the ASOS8 conference [5]), whose work is part of the FERRUM project. Hibbert uses a semi-relativistic Hamiltonian (low Z Pauli) which should be adequate for Fe II, but will not be adequate for higher Z homologs. This is a Hamiltonian the PI used in his Ph.D. research (1968).

[B] Kr II and Kr III Energy Levels and f -values

Krypton is an important element in controlled fusion experiments, where it is used as a density diagnostic. It is simple enough (all closed shells) to be one of the easier elements to study experimentally or computationally. Yet, until a 1980 experimental study using synchrotron radiation [6] it was difficult to establish a value for the K shell ionization potential to better than $\sim 2.5 \text{ eV}$. This was due in the main to instrumental and final state broadening effects, as well as to the presence of nearby resonances, which need to be deconvoluted from the observed cross sections. Computationally, to achieve accuracies of $\sim 1 \text{ eV}$, effects of relativity, relaxation, QED and correlation [7] must be included. At this time, the treatment of QED effects (for closed shell systems) seems to be the limiting factor in computational accuracy.

Our work on $1s$ excitation or removal in Kr II and Kr III was undertaken in conjunction with on going experimental work at Argonne National Laboratory, and has been used in a poster presentation at the last DAMOP meeting [8]. Our work reporting [9] f -values and transition energies for $1s \rightarrow np$ transitions is quite consistent with observation [8], and our $1s$ ionization potential for Kr I is in very good agreement with an existing theoretical result [7]. As part of this work, we had to extend our codes [3] to permit generation of the lowest 60 (up from 30) energy levels for each symmetry.

[C] Mo V and Mo VI Energy Levels and Oscillator Strengths

Previously, we had completed calculations for the isoelectronic Zr III and Nb IV $J=0 \rightarrow J=1^o$ E1 transitions [10]. Zr III is astrophysically important, semi-empirical f -values were only available for Zr III [11] and there was some doubt [12] of the location of the Nb IV $5s^2 J=0$ state. Computationally, these species were of interest to us because of the near degeneracy of the $4d np$, $4d nf$ and $5s5p J=1$ levels, implying the need of carefully including correlation and relativistic effects.

For Mo V $J=1$ states, these near degeneracies still persist, there are no f -values available, and even the energy level data is sparse and sometimes inconsistent. Our published calculations [13] have average energy errors of 229 cm^{-1} and 368 cm^{-1} ($J=0, 1$) and the length and velocity f -values agree, on average, to 3.1%. Our energy levels agree better with

the newer measurement [13], although the $5s5p\ ^1P$ level remains characteristically high ($\sim 1671\text{ cm}^{-1}$).

An interesting aspect of the Mo v $J=1$ results is the first prediction of “low-lying” $4p^5\ 4d^3$ levels (i.e. lying in the 30 lowest roots). These are somewhat difficult to place accurately ($< 2\text{-}3000\text{ cm}^{-1}$), because of the changing $4p$ and $4d$ occupations which changes a “2” electron problem into an “8” electron problem (some core-core and more core-valence correlation is needed), and the penetration of a perturber ($4p^5\ 4d^3$) into Rydberg series ($4p^6\ 4d\ (np+nf)+5s5p$).

At the suggestion of Joe Reader [12], we extended our work to Mo VI, where these levels have been seen [14,15], but have not been conclusively identified. Here, we are looking at the $J=5/2^o$ levels ($4p^6\ nf$ perturbed by $4p^5\ 4d^2$), and transitions from them to the $4p^6\ nd$ levels. Proper treatment of this problem—which involves allowance for the difference in radial functions (e.g. $4p$) between perturber and series, reduction of cancellation in correlation effects (changing occupancy of the $4p$ subshell, which can necessitate inclusion of correlation effects from $3d$ and $4s$ subshells)—should give us insight into similar problems such as Yb II ($4f^{13}\ 6s^2$ vs $4f^{14}\ 6p$) which is still not well described. Calculations on Mo VI should be completed early in the next project period [16], nearly coincidental with a new experimental analysis of the species [12].

[D] Polarizability of U v and U VII

These two valences are commonly found in nuclear waste products. Although occurring in a molecule or the solid phase, knowledge of atomic (ionic) polarizabilities may be useful for semi-empirically modeling. We are evaluating these, in conjunction with an experimental proposal by Steve Lundeen [17] submitted to DOE, by using an oscillator strength sum formulation. In this, transitions to the continuum are replaced with 1-2 functions localized near the $\langle r \rangle$ of the initial state’s transitioning electron, in the spirit of Hibbert *et al* [18]. We are also evaluating the tensor polarizability [19] of U VII. To test the methodology we are comparing with measurements in Ne II [20] and unpublished RMPBT results for Th IV. This work should be completed early in the next project period [21].

[E] DOE Publications mid 2002-mid 2005

In addition to items 2, 4, 9, 10, 13 in the reference list, we have also published f -values for K II [22], and Magnetic Quadrupole Lifetimes in the rare gases [23], for which there was previously a discrepancy between theory and experiment.

Future Plans

Near future applications include completion and publication of the Mo VI, U^{n+} polarizabilities, and Kr^{n+} photoionization cross-sections.

References

- [1] R. L. Martin and P. J. Hay, *J. Chem. Phys.* **75**, 4539 (1981).
- [2] S. M. O'Malley and D. R. Beck, *Phys. Scr.* **68**, 244 (2003) Drafts of all the PIs recent publications are available from www.phy.mtu.edu (under *faculty*).
- [3] The RCI program suite consists of 3 unpublished programs written by D. R. Beck over a period of years. RCI calculates the bound state wavefunctions, hyperfine structure, and Landé g -values. RFE uses RCI wavefunctions and computes E1, E2, M1 and M2 f -values, including the effects of non-orthonormality. REDUCE minimizes the number of eigenvectors needed for a correlation manifold by rotating the original basis to maximize the number of zero matrix elements involving the reference functions; only rotated vectors having non-zero reference interactions are retained.
- [4] D. R. Beck, *Phys. Scr.* **71**, 447 (2005).
- [5] Atomic Spectra and Atomic Oscillator Strength Conference 8, Madison, Wisconsin (2004). Invited talks to be published as a technical report in *Physica Scripta* (2005).
- [6] M. Breinig *et al*, *Phys. Rev. A* **22**, 520 (1980).
- [7] P. Indelicato and E. Lindroth, *Phys. Rev. A* **46**, 2426 (1991).
- [8] L. Young, R. W. Dunford, D. L. Ederer, E. P. Kanter, B. Kraessig, J. Rudati, S. H. Southworth, E. C. Landahl, D. Arms, and E. M. Dufresne, *Bull. Am. Phys. Soc.* **50**, 87 (2005).
- [9] L. Pan, D. R. Beck and S. M. O'Malley, "Removal or Excitation of a 1s Electron in Kr II and Kr III", *J. Phys. B*, submitted for publication.
- [10] D. R. Beck and L. Pan, *Phys. Scr.* **69**, 91 (2004).
- [11] J. Reader and N. Acquista, *Phys. Scr.* **55**, 310 (1997).
- [12] J. Reader, private communication.
- [13] L. Pan and D. R. Beck, *Phys. Scr.* **70**, 257 (2004).
- [14] A. Tauheed, K. Rahimullah, and M. S. Z. Chaghtai, *Phys. Rev. A* **32**, 237 (1985).
- [15] J. Sugar and A. Musgrove, *J. Phys. Chem. Ref. Data* **17**, 155 (1988).
- [16] L. Pan and D. R. Beck, unpublished.
- [17] S. Lundeen, private communication.
- [18] A. Hibbert, M. Le Dourneuf, and V. K. Lan, *J. Phys. B* **10**, 1015 (1977).
- [19] J. R. P. Angel and P. G. H. Sandars, *Proc. Roy. Soc.* **305**, 125 (1968).
- [20] R. F. Ward, Jr, W. G. Sturru, and S. R. Lundeen, *Phys. Rev. A* **53**, 113 (1996).
- [21] D. R. Beck, unpublished.
- [22] D. R. Beck, *J. Phys. B* **35**, 4155 (2002).
- [23] D. R. Beck, *Phys. Rev. A* **66**, 034502 (2002).

PROBING COMPLEXITY USING THE ADVANCED LIGHT SOURCE

Nora Berrah

Physics Department, Western Michigan University, Kalamazoo, MI 49008
e-mail:Berrah@wmich.edu

Program Scope

The objective of our research program is to carry out science which will further our understanding of *fundamental interactions between vuv/x-ray photons and complex systems* using the Advanced Light Source (ALS). The focus of our program is to pursue emerging research directions in specific photon energy ranges that will probe inner-valence, intermediate shells and core orbitals. In these regimes, the independent particle models sometimes fail dramatically. Our program will take advantage of the combination of highly efficient instrumentation and intense photon fluxes available from ALS, to examine complex photo-processes in selected atomic, molecular, clusters and their negative ions. These studies may lead to a better understanding of the response of matter to photoexcitation. Our measurements will provide accurate experimental data for primary physical processes. These data will be used to test advanced theoretical treatment, further *ab-initio* models of atomic, molecular and cluster dynamic and structure and may advance our understanding of the general many-body problem. We present here results completed and underway this past year and plans for the immediate future.

Recent Progress

1) Inner-shell Photodetachment Thresholds: Unexpected Long-range Validity of the Wigner Law (Ref. 1)

Descriptions of the energy dependence of a reaction yield near a threshold, or threshold laws, are of general interest in many areas of physics. Such threshold laws are independent of the specifics of the reaction or reaction products, and can therefore be equally applicable to, for example, fragmentation at the molecular, atomic, or even subatomic level.

Valence shell photodetachment studies of negative ions have extensively focused in the past 20 years, among many other interesting effects, on threshold laws. In particular, experimental and theoretical studies reviewed by Andersen et al. [a] explored various ionic targets as well as different approaches to extend the range of validity of the Wigner law [b]. This law stipulates that the threshold behaviors are governed by the longest-range interaction between the product fragments resulting from the dissociation of a target into a pair of particles. The photodetachment cross section in negative ions can be written as, $\sigma = \sigma_0 \varepsilon^{l+1/2}$, where σ_0 is the amplitude, $\varepsilon = h\nu - \varepsilon_t$ is the photoelectron energy, ε_t is the threshold energy and $l = |l_0 \pm 1|$ is the angular momentum of the photoelectron, with l_0 being the angular momentum of the detached bound electron. This threshold law, important to determine the electron affinities of valence electrons, has been verified for both single processes [c] as well as for multi-photon processes [d]. The question that arises is what about its validity in the case of inner-shell photodetachment? In this case, the process consists of the ionization of two electrons in two steps; first the photoionization of the core electron and second the ejection of an Auger electron, resulting in the observation of the positive ion.

We have carried out detailed threshold photodetachment measurements for He^- and S^- . In the case of He^- , whose ground state is $1s2s2p^4P$, the ionization of a K-shell electron would need to produce an outgoing p-wave, due to momentum conservation. On the other hand, in the case of a

2p ionization in S^- , an outgoing s-wave will be expected. Our measurements have shown that in both cases the Wigner law is valid, even in the case of He^- where severe post-collision interaction (PCI) occurs. This effect, which leads to the recapture of the photoelectron by the He^+ target, was measured [e] and explained [f]. Furthermore, our measurements demonstrated that the range of validity in the case of the S^- photodetachment experiments exceeds the expected range, based on valence photodetachment work, by at least an order of magnitude [1].

The data was fit to the Wigner law where $\sigma = \sigma_0 \varepsilon^{3/2}$ since in this case $l=1$ for a p-outgoing wave. The fit to the data, uncorrected for PCI, yielded an exponent of 1.47 (7) in excellent agreement with the Wigner p-wave law resulting from detachment of an s-electron and giving an exponent of 1.5. The threshold energy obtained from the fit is found to be $\varepsilon_t = 38.595$ (9) eV. Furthermore, the comparisons of our data with calculations that either include or not include PCI demonstrate clearly that the PCI correction is indeed needed in the calculation. They also reveal a surprisingly excellent agreement with the Wigner p-wave threshold law which does not take PCI into account [1].

2) Imaging Wavepacket Interferences using Auger Resonant Raman Spectroscopy (Ref. 2).

One manifestation of coherence under resonant excitation conditions is the dependence of the electron or photon emission of the decay process upon the incoming photon distribution. First identified in rare gases and later in small molecules as subnatural narrowing and dispersion of the resonant Auger lines with spectral detuning, this effect came to be called the Auger Resonant Raman Effect (ARRE) [e] and found immediate applications in the study of electron correlation and resonant molecular dynamics.

The response of the molecule to the short-lived inner-shell excitation has been successfully treated by theory using either a time-dependent or -independent framework. In the former, the short-lived intermediate state is described as a nuclear wavepacket evolving in time on the potential energy surface. Relaxation of the electronic excitation is governed by the core-hole lifetime $1/\Gamma_d$ and takes place on the femtosecond time-scale of the nuclear motion. This implies that the evolution of the nuclear wavepacket is dominated by concurrent dissipation and dispersion, contrasting with electronic wavepackets in Rydberg atoms that can be tailored to minimize both effects. This competition is evident in the fine structure of the Auger electron bands. For example, lifetime vibrational interference (LVI) due to coherent deexcitation of discrete nuclear states occurs when vibrational period and core-hole lifetime are comparable. Integration of ARRE into the unified theory of inelastic X-ray scattering has led to the design and interpretation of experiments aimed at investigating the decay dynamics of core-excited systems.

We have excited the core dissociative state $1\sigma^{-1}2\sigma^23\sigma^21\pi^44\sigma^*(^1\Sigma^+)$ in HF by linearly polarized light with a bandwidth of 0.2 eV. The Auger electron spectra were recorded at several values of the detuning Ω from the resonant absorption maximum at 687 eV. At negative detunings, the molecular features, albeit enhanced, remain smooth and structureless while at positive detunings, a distinct oscillatory structure appears. These are interpreted as interference effects in the Auger resonant Raman transitions of core-excited HF since pronounced oscillations, controlled by detuning above the resonance maximum, appear in the spectator decay spectra of the dissociating molecule. Using predictions from the time-dependent theory of the resonant inelastic Raman scattering, these observations are explained by a favorable spatial localization of the nuclear wavepacket in the intermediate state during its creation. This phenomenon should occur whenever photoexcitation, electronic decay and nuclear dynamics have comparable time scales [2].

3) Spin and Angle Resolved Spectroscopy of S 2p Photoionization in Hydrogen Sulfide Molecule (Ref. 3, 4, 5)

Spin resolved studies of molecules are rare in the literature unlike the atomic case. In fact, due to weak signal strength, only spin-resolved data for the outer shell photoionization of HI [f] and HBr [g] have been reported. Recently, we have demonstrated how the properties of the inner S2p shell in OCS and H₂S molecules can be investigated by combining spin-resolved and angle-resolved measurements [4, 5].

We have extended the investigation we began in H₂S two years ago by carrying out new angle resolved measurements that allowed the anisotropy parameters to be obtained between 180-260 eV. In addition, we measured the electron spin-polarization of S2p using linearly polarized light. Angle- and spin-resolved photoelectron spectroscopy techniques, using circularly and linearly polarized synchrotron radiation, were then used to probe the electronic structure of hydrogen sulfide molecule. A strong effect of the molecular environment appears in the spin resolved measurements and, although less clearly, in the angular distribution of the sulfur 2p photoelectrons. Furthermore, the anisotropy and spin parameters of the three main spectral components have been obtained. We have also compared our data with a simple theoretical calculation for Ar (close to H₂S) [h] and have found that the simple atomic theory models satisfactorily our data in the case of the angular distribution but doesn't agree as well in the case of the spin-parameters [3].

Future Plans.

The principal areas of investigation planned for the coming year are to: 1) Finish building and testing an ion imaging detector to complement the photoelectron spectroscopic methods we use for our research. 2) Finish building and testing the movable ion beamline which will be used in the collinear and cross geometry with several photon beamlines at the ALS. 3) Finish the analysis of the dissociation mechanism in small negative ions clusters. 4) Finish the analysis of high-resolution measurements of inner-shell photodissociation dynamics in diatomic neutral molecules (HCl, HBr and DBr). 5) Complete and analyze our measurements on angle and spin resolved photoionization experiments in van der Waals Ar and Xe clusters.

Publications from DOE sponsored research.

- [1] R. C. Bilodeau, J. D. Bozek, N. D. Gibson, C. W. Walter, G. D. Ackerman, I. Dumitriu, and N. Berrah, "Inner-shell Photodetachment Thresholds: Unexpected Long-range Validity of the Wigner Law" (Phys. Rev. Lett. in press).
- [2] S. E. Canton, E. Kukk, J. D. Bozek, D. Cubaynes, and N. Berrah "Imaging Wavepacket Interferences using Auger Resonant Raman Spectroscopy", Chem. Phys. Lett, **402**, 143, (2005).
- [3] G. Turri, G. Snell, B. Langer, M. Martins, E. Kukk, S. E. Canton, R. C. Bilodeau, N. Cherepkov, J. D. Bozek, and N. Berrah, "Probing the Molecular Environment using Spin-Resolved Photoelectron Spectroscopy" Phys. Rev. Lett. **92**, 013001 (2004).
- [4] G. Turri, G. Snell, B. Langer, M. Martins, E. Kukk, S.E. Canton, R.C. Bilodeau, N. Cherepkov, J.D. Bozek, A.L. Kilcoyne and N. Berrah "Spin and Angle Resolved Spectroscopy of S 2p Photoionization in Hydrogen Sulfide Molecule", Phys. Rev. A **70**, 022515 (2004).
- [5] G. Turri, G. Snell, B. Langer, M. Martins, E. Kukk, S. E. Canton, R. C. Bilodeau, N. Cherepkov, J. D. Bozek, and N. Berrah, "Probing the Molecular Environment using Spin-Resolved Photoelectron Spectroscopy" AIP (American Institute of Physics) conference proceedings **697**, pp 133, ed: G.F. Hanne, L. Malegat, H. Schmidt-Boecking (2004).
- [6] N. Berrah, J. D. Bozek, R. C. Bilodeau and E. Kukk, "Studies of Complex Systems: From Atoms to Clusters", Radiat. Phys. Chem, **70**, Issue 1, 57 (2004).

- [7] D. Cubaynes, M. Meyer, A. Grum-Grzhimailo, J.-M. Bizau, E. T. Kennedy, J. Bozek, M. Martins, S. Canton, B. Rude, N. Berrah, and F. J. Wuilleumier, "Dynamically and quasiforbidden lines in photoionization of open-shell atoms: a combined two-color experiment and theoretical study", *Phys. Rev. Lett.* **92**, 233002 (2004).
- [8] N. Berrah, R. C. Bilodeau, G. Ackermann, J. D. Bozek, G. Turri, B. Rude, N. D. Gibson, C. W. Walter and A. Aguilar, "Probing Negative Ions from Within", *Physica Scripta* **T110**, 51 (2004).
- [9] R. C. Bilodeau, J. D. Bozek, G. Turri, G. D. Ackerman, and N. Berrah, Simultaneous 3-electron Decay and Triply Excited Quartet States in He⁻, *Phys. Rev. Lett.* **93**, 193001 (2004).
- [10] N. Berrah, R. C. Bilodeau, G. Ackermann, J. D. Bozek, G. Turri, E. Kukk, W. T. Cheng, and G. Snell " Probing atomic and Molecular Dynamics from Within" *Radiat. Phys. Chem.*, **70**, 491 (2004).
- [11] B. Lohmann, B. Langer, G. Snell, U. Kleiman, S. Canton, A. Martins, U. Becker and N. Berrah, "CI-Induced Spin Polarization of the Ar* (2p⁻¹ 4s)_{j=1} Resonant Auger decay", *Phys. Rev. A* **71**, R020701 (2005).
- [12] N. Berrah, R. C. Bilodeau, J. D. Bozek, G. Turri and G.D. Ackerman, "Double photodetachment in He⁻: Feshbach and triply excited resonances, *J. Elect.Spec. and Relat. Phen.* **144-147**, 19 (2005).
- [13] N. D. Gibson, C. W. Walter, O. Zatsarinny, T. W. Gorczyca, G. D. Ackerman, J. D. Bozek, M. Martins, B. M. McLaughlin, and N. Berrah, "K-shell photodetachment of C⁻, *Phys. Rev. A* **67**, R030703 (2003).
- [14] J. D. Bozek, S. E. Canton, E. Kukk and N. Berrah, "Vibrationally resolved resonant Auger spectroscopy of formaldehyde at the C 1s-1* resonance", *Chemical Physics*, **289**, pages 149-161 (2003).
- [15] James R. Harries, James P. Sullivan, James B. Sternberg, Satoshi Obara, Tadayuki Suzuki, Peter Hammond, John Bozek, Nora Berrah, Monica Halka, and Yoshiro Azuma, "Double Photoexcitation of Helium in a Strong dc Electric Field", *Phys. Rev. Lett.* **90**, 133002-1 (2003).
- [16] S E Canton, A A Wills, T W Gorczyca, E Sokell, J D Bozek, G Turri, M Wiedenhoef, X Feng and N Berrah "New Low-Lying Mirroring Singly and Doubly Excited Resonances in Neon", *J. Phys. B. Lett.* **36**, L181 (2003).
- [17] N. Berrah, J. D. Bozek, G. Ackerman, G. Turri, R. C. Bilodeau, S. Canton, and E. Kukk, "Photodetachment and Photoionization Studies: From Atoms to Clusters" Proceeding of the International Workshop, *From the Atomic to the Nano-Scale*, ODU, Edited by C. T. Whelan and J. H. McGuire (2003).
- [18] S. E. Canton, A. J. Yench, E. Kukk, J. D. Bozek, M. C. A. Lopes, G. Snell, and N. Berrah, comment on "Experimental Evidence of a Dynamic Jahn-Teller Effect in C₆₀⁺", *Phys. Rev. Lett.* **90**, 249602 (2003).
- [19] B. Lohmann, B. Langer, G. Snell, U. Kleiman, S. Canton, M. Martins, U. Becker and N. Berrah, "Angle and Spin Resolved Analysis of the Resonantly Excited Ar* (2p⁻¹_{3/2}4s_{1/2})_{j=1} Auger Decay, AIP (American Institute of Physics) conference proceedings **697**, pp 133, ed: G.F. Hanne, L. Malegat, H. Schmidt-Boecking (2004).

References

- [a] T. Andersen, T. et al., *J. Phys. Chem. Ref. Data* **28**, 1511 (1999) and references therein.
- [b] E. P. Wigner, *Phys. Rev.* **73**, 1002 (1948).
- [c] T. Andersen et al., *J. Phys. Chem. Ref. Data* **28**, 1511 (1999) and references therein.
- [d] R. C. Bilodeau, M. Scheer, and H. K. Haugen, *Phys. Rev. Lett.* 143001 (2001).
- [e] N. Berrah, J. D. Bozek, G. Turri, G. Akerman, B. Rude, H. L. Zhou, H and S. T. Manson, *Phys. Rev. Lett.* 88(9), 093001 (2002).
- [f] J.L. Sanz-Vicario et al., *Phys. Rev. A* 66, 052713 (2002); T. W. Gorczyca, O. Zatsarinny, H-L. Zhou, S. T. Manson, Z. Felfi, Z., and A. Msezane, *Phys. Rev. A* **68**, 050703(R) (2003).
- [e] A. Kivimäki, A. Naves de Brito, S. Aksela, H. Aksela, O.-P. Sairanen, A. Ausmees, S. J. Osborne, L. B. Dantas, S. Svensson, *Phys.Rev. Lett.* 71, 4307 (1993).
- [f] N. Böwering, M. Müller, M. Salzmann and U. Heinzmann, *J. Phys. B* **24**, 4793 (1991).
- [g] M. Salzmann, N. Böwering, H.-W. Klausning, R. Kuntze and U. Heinzmann, *J. Phys. B* **27**, 1981 (1994).
- [h] N. A. Cherepkov, *J. Phys. B* **12**, 1279 (1979); N. A. Cherepkov, *J. Phys. B* **14**, 2165 (1981).

Bose-Fermi Mixtures Near an Interspecies Feshbach Resonance

John L. Bohn
JILA, UCB 440
University of Colorado
Boulder, CO 80309
bohn@murphy.clolorado.edu

Program Scope:

The work in this program revolves around the theory of novel few- and many-body systems that are now becoming experimentally feasible. One such system is an ultracold gas of alkali atoms whose interparticle interaction varies resonantly with a magnetic field. A second is an ultracold gas of dipolar molecules, where the strong and anisotropic dipole-dipole interaction will make correlation effects dominant.

Recent Progress:

Perhaps the most notable outcome of the creation of atomic Bose-Einstein condensates (BEC's) in 1995 was the understanding that perturbative many-body theories suddenly had an experimentally realizable system to which they applied. The familiar Gross-Pitaevskii (GP) equation, assuming contact interactions between atomic constituents of the gas, serves to describe quantitatively the many-body ground state, while the Hartree-Fock-Bogoliubov (HFB) extension of this theory has much to say about their collective excitations, at least at zero temperature.

This situation was enriched somewhat in 1998, when experimentalists began to manipulate the effective interaction between atoms using magnetic-field Feshbach resonances. The interaction, formally described by the two-body scattering length, could now rise, in principle, to infinite strength. Moreover, by ramping magnetic fields across these resonances, it became possible to populate molecular states consisting of pairs of atoms. Theoretically, it was found that this seemingly nonperturbative situation could still be handled within the HFB formulation, but with a twist: it was assumed that correlated atom pairs participating in the resonance could be regarded as a separate, "molecular" field described by its own equation of motion [1,2]. This theory works well to describe such things as atom-molecule Rabi oscillations in a BEC, as well as the crossover between Bose-condensed molecules and BCS pairs in a degenerate Fermi gas.

Our main finding in this first year of DOE funded research is that the same theory is *not* adequate to the description of Feshbach resonances in a mixture of bosons and fermions [3]. We have formulated the time-dependent HFB equations

of motion for such a mixture, and have solved them numerically for a ^{40}K - ^{87}Rb mixture, which possesses an interspecies resonance at 511 gauss [4]. As an initial test of the theory, we modeled a sudden change in field strength from far-off-resonance, to a position near resonance that should support a weakly-bound molecular state. We then observed regular oscillations in the molecule number, at a frequency that can be identified with the molecular binding energy. The resulting binding energy versus magnetic field is shown in the figure below. The solid black curve denotes the two-body binding energy. For a comparatively dense Fermi gas, the molecular binding energy is renormalized by its many-body environment, yielding the lower (gray) curves.

In the limit of low density, the renormalized binding energy ought to reduce to the two-body limit; however, this does not happen. Instead, in this limit the binding energy approaches the linear function of magnetic field denoted by the dotted line. This linear dependence is a remnant of the unrenormalized two-body interaction that went into the theory in the first place. This behavior is quite unlike the case of the bose-bose or fermi-fermi cases, where the physical two-body limit is recovered. We have analyzed the inadequacy of the theory using a perturbative, path-integral approach that is guaranteed to reproduce the two-body limit. This analysis shows that the standard HFB approach does not account adequately for the *noncondensed* atomic bosons. Ultimately, this failure lies deep within the theory as an approximation of a three-body (atom-atom-molecule) correlation function in terms of less accurate two-body (atom-atom) correlation functions. We have therefore reformulated the theory, incorporating directly the missing three-body piece [3]. In this sense, the theory has gone “beyond the mean-field level.”

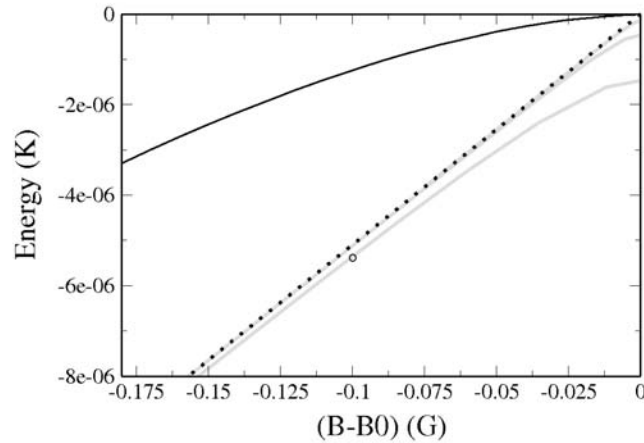


Figure. Binding energy of ultracold ^{40}K - ^{87}Rb molecules as a function of magnetic field detuning. The solid black curve is the two-body binding energy. The gray curves denote renormalized binding energies in the many-body environment, for fermion densities of (low to high curves) 10^{12} , 10^{11} , and 10^{10} cm^{-3} . The dotted curve is the “bare” (i.e., unphysical) binding energy that serves as a raw input parameter to the theory.

Future Plans:

We will continue to explore this system, first by including the additional three-body correlation function into the equations of motion. It should then be possible to address realistic issues such as nascent experimental efforts to study mechanical stability of a resonant Bose-Fermi mixture, to create heteronuclear fermionic molecules, and to address aspects of Bose-mediated fermionic superfluidity in these systems.

In addition, we will return to the subject of dipolar gases. Preliminary (unpublished) results that solve the GP equation for this system have shown serious discrepancies with the quantitatively accurate calculations of D. Blume at the Washington State University. To help resolve this discrepancy, we will focus on two- and three-molecule variants of trapped polar molecules. Here numerically exact solutions to the Shrodinger equation should be possible. In addition, treating these problems in the well-established hyperspherical coordinate formulation should reveal the character of correlations to be expected in this strongly-interacting system.

References:

- [1] S. Kokkelmans and M. Holland, Phys. Rev. Lett. **89**, 180401 (2002); R. Duine and H. Stoof, Phys. Rep. **396**, 115 (2004).
- [2] S. Kokkelmans *et al.*, Phys. Rev. A **65**, 053617 (2002); Y. Ohashii and A. Griffin, Phys. Rev. A **67**, 033603; A. Avdeenkov and J. L. Bohn, Phys. Rev. A **71**, 023609 (2005).
- [3] D. Bortolotti, A. Avdeenkov, C. Ticknor, and J. L. Bohn, cond-mat/0505355 (2005).
- [4] S. Inouye *et al.*, Phys. Rev. Lett. **93**, 183201 (2004).

Exploiting Universality in Atoms with Large Scattering Lengths

Eric Braaten

Contact info

Physics Department
Ohio State University
191 W Woodruff Ave
Columbus OH 43210-1117
(braaten@mps.ohio-state.edu)

Program scope

Atoms whose scattering lengths are large compared to the range set by their interactions exhibit universal behavior at sufficiently low energies. Recent dramatic advances in cooling atoms and in manipulating their scattering lengths have made this phenomenon of practical importance for controlling ultracold atoms and molecules. This research project is aimed at developing a systematically improvable method for calculating few-body observables for atoms with large scattering lengths starting from the universal results as a first approximation. The ultimate goal is to be able to predict and control the behavior of ultracold atoms and molecules near a Feshbach resonance.

Recent publications

- *Universality in Few-body Systems with Large Scattering Length*, Eric Braaten and H.-W. Hammer, arXiv:cond-mat/0410417.
- *Factorization in Break-up and Recombination Processes for Atoms with a Large Scattering Length*, E. Braaten and D. Zhang, arXiv:cond-mat/0501510.

Ultrafast X-Ray Coherent Control

P.H. Bucksbaum and D.A. Reis

*FOCUS Center, Physics Department, University of Michigan,
Ann Arbor, MI 48109-1120 phb@umich.edu Grant DEFG02-00ER15031*

Program Scope

This is a program to develop ultrafast x-ray physics at synchrotrons and linear accelerators. The research is carried out at the Advanced Photon Source sector 7, with the MHATT-XOR collaboration (previously MHATT-CAT); and at the Stanford Linear Accelerator Center, with the SPPS collaboration and the Stanford Ultrafast Science Center. Our research concentrates on ultrafast and coherent dynamical processes in solids and molecular systems. Along with new science, we are developing new ultrafast methodology that will be utilized on future generation ultrafast x-ray sources such as LCLS.

Ultrafast science probes dynamics on the atomic and molecular scale of bond vibration in a molecule or optical phonons in a solid. This is typically on the order of 100 fsec, but can in some cases be as long a few picoseconds. X-rays are ideal probes of motion on these scales because of their short wavelength, and there has been much progress towards producing ultrafast x-ray pulses for transient dynamical studies.

Early efforts in the field concentrated on laser-generated plasmas, which can produce x-ray bursts as short as a few hundred femtoseconds. These sources are quite weak, however, and this has limited their use to a few very high contrast problems, such as crystalline melting. Electron beam-based x-ray sources can be much brighter. The challenge therefore has been to make these accelerator-based x-ray pulses short, so that they can record more than the time-averaged motion of transiently excited materials.

Third generation synchrotron pulses, which are 30-100 psec in duration, are tantalizingly close to the required duration, and so we and others have been working with them to learn about dynamics of transient molecular and solid state processes. Techniques that we and others have developed include picosecond x-ray streak cameras; X-ray switches based on x-ray transmission through or reflection from transiently excited crystals; and methods to shorten the electron bunches in the synchrotron.

We have also been key participants in the Stanford Sub-Picosecond Pulse Source, which produces sub-100fsec x-ray pulses from compressed electrons traversing an undulator in the SLAC Final Focus Test Beam facility. The SPPS team has compressed 30 GeV electrons at SLAC, shortening the bunch length to about 80 fsec. The ultrafast pulses of x-rays produced in the undulator have now been used in two different experiments which we describe below. This physics defines the frontier of ultrafast x-ray science that will be explored at LCLS.

Recent Progress:

SPPS The SPPS collaboration has broken new ground this year in both ultrafast x-ray science and new x-ray techniques. Our first three research papers, one in *Science* and two in *Physical Review Letters* [1-3] concern the synchronization of laser pulses with the x-rays produced at SPPS, and the dynamics of ultrafast disordering in laser-excited solids using the SPPS x-rays. In earlier work we and others have found that there are technical impediments to synchronizing a laser with a linear accelerator-based x-ray source to much better than a picosecond. This poses severe constraints on the time resolution of pump-probe techniques. We have recently

shown that this difficulty can be overcome in several ways. One simple method, takes advantage of the large scale changes in structure that occur during laser melting of crystalline materials. The change in x-ray scattering is so dramatic that merely a single x-ray pulse is sufficient to record the dynamics. We studied the transient disorder in laser-heated crystalline InSb excited by a short pulse laser. The laser and the x-rays impinged the sample at different angles, so that the relative arrival time varied across the irradiated spot. Data recorded on each laser shot showed how the arrival time varied, sometimes by more than a picosecond. When this was corrected and the data from different laser shots was combined, we found that in the first hundreds of femtoseconds following excitation, the x-ray diffraction efficiency decreases at a rate that is limited only by the ballistic motion of atoms away from their lattice sites. This was shown for each of the two x-ray diffraction planes studied. These results are consistent with an isotropic flattening of the interatomic potentials, such that the atoms are "free" to move about essentially with the same momentum set by their thermal motion before the laser excitation [3]. On a longer time scale (picosecond), the atoms begin to collide and the motion transitions from ballistic to diffusive behavior. In this case, however, the disordering occurs faster along the initial tetrahedral bonding directions [1]. On this time scale, the material is still solid in the sense that long range order has not been destroyed, and the full equilibrium liquid dynamics are yet to be realized.

Not all experiments can be done in a single shot, so we need a mechanism to determine relative arrival time between x-rays and the laser on every shot. We have demonstrated that spatially resolved electrooptic sampling (EOS) of the electron bunch field is a non-invasive measurement of the pump-probe delay on every shot (as well as a bunch length diagnostic). In this manner, a series of shots can be taken in a random sampling fashion, and later rearranged according to arrival time. This post-binning makes more traditional, repetitive pump-probe measurements possible. Using the single-shot disordering experiment mentioned above as an independent measurement of the x-ray arrival time, we were able to show that we could correlate the EOS to the arrival time of the x-rays to within 60fs, rms [2]. In these experiments, we use a single pulse from the laser oscillator to probe the relativistically enhanced ($\gamma=60,000$) electric field near the electron bunch just before it radiates x-rays in the undulator. A synchronized oscillator pulse is then amplified and used for the excitation of the InSb crystal. So long as the path lengths remain stable, the pulses should be locked to each other. We believe that on the short-term the measurements are resolution rather than jitter limited.

APS One of the main goals of our experimental progress at APS is to control x-ray diffraction in order to produce a femtosecond switch for x-rays. On the picosecond time-scale we used coherent control of vibrational excitations as a means to exchange energy between two distinct diffracted beams in the anomalous transmission of x-rays. But, we also used this new phenomenon to study the dynamics of the dense electron hole plasma generated in semiconductors following ultrafast laser-excitation. These experiments centered on the zone center coherent acoustic phonons generated through the deformation potential. However, the path to equilibrium is much more complicated, involving processes that occur from tens of femtoseconds to microseconds. We are currently looking at the initial cooling of the electrons through the emission of phonons with wavevectors spanning the entire Brillouin zone, through time-resolved x-ray diffuse scattering.

These new experiments are challenging because the count rates are low and backgrounds can easily exceed the signal. In a recent experiment with the laser running at 5kHz, we used a grazing exit geometry to maximize the spatial overlap between the x-rays and the laser. In this case, the count rate was on order of 0.1Hz. Nonetheless, we have preliminary evidence suggesting that the emission of zone edge phonons (at the L-point) in InSb is dominated by longitudinal and not transverse modes.

This could prove important because it can distinguish between the two main cooling channels for the electrons: the Frohlich interaction where zone center LO phonons are produced and intervalley scattering to the L valley (and back) accompanied by primarily zone edge LA phonon emission. While we are not sensitive to the LO phonons, they will decay into two zone center LA phonons which will subsequently decay into other acoustic modes. As a consequence, we expect a pile up in long lived TA modes near the L point. Little is known about these processes, especially at high excitation densities, except indirectly by optical means. X-ray diffuse scattering provides an important tool in understanding the full phonon dynamics. These experiments are primarily limited by flux and temporal resolution; consequently, and perhaps ultimately single-shot experiments are planned for LCLS.

Finally, we have been actively studying potential science opportunities for ultrafast compressed x-ray pulses at the APS, where, accelerator physicists have been looking at the possibility of generating high brightness picosecond x-rays using an insertion device. We are very encouraged by their work, which suggests that 1ps FWHM pulses can be produced for every bunch in the storage ring. This would indeed be a major development for 3rd generation sources, and would be complementary to 4th generation machines. We have collaborated with APS machine physicists to study this problem. Our contribution is in the demonstration of short pulses. To this end, we have made additional progress in our picosecond streak camera and have recently demonstrated the ability to image on a single-sweep.

Future Plans:

SPPS will continue for another nine months, and we have plans for participation in several experiments. The first experiment is the generation and observation of high amplitude optical phonons in Bi films. This follows on recent experimental (optical) and theoretical work from our group [7,9] and on work by von der Linde *et al.*, in which phonon modes were observed via their modulation of the diffraction of laser plasma-produced ultrafast x-rays. The SPPS beam is more than ten orders of magnitude brighter and about a factor of four shorter than the laser-produced plasma source, and this should make it possible for us to view the dynamics in much greater detail. Other experiments that are planned for SPPS include transient XANES measurements to observed transient sivation of photo-ionized Cu^+ in solution; and time-resolved measurements of Auger spectra of atomic Kr in a strong laser field.

At the APS, we plan to initiate a number of improvements to the diffuse scattering experiments, and to participate in further studies of pulse shortening. Particular improvements in the diffuse scattering include moving to grazing incidence geometry, which when combined with x-ray focusing can yield a factor of 100 in count rate. With these and other improvements we hope to reveal a more detailed picture of the equilibration process for hot electron and nonequilibrium phonons.

Publications, 2004-5

- [1]. "Observation of structural anisotropy and the onset of liquid-like motion during the nonthermal melting of InSb," K..J. Gaffney, A.M. Lindenberg, J. Larsson, K. Sokolowski-Tinten, C. Blome, O. Synnergren, J. Sheppard, C. Caleman, A.G. MacPhee, D. Weinstein, D.P. Lowney, T. Allison, T. Matthews, R.W. Falcone, A.L. Cavalieri, D.M. Fritz, S.H. Lee, P.H. Bucksbaum, D.A. Reis, J. Rudati, A.T. Macrander, P.H. Fuoss, C.C. Kao, D.P. Siddons, R. Pahl, K. Moffat, J. Als-Nielsen, S. Duesterer, R. Ischebeck, H. Schlarb, H. Schulte-Schrepping, Th. Tschentscher, J. Schneider, D. von der Linde, O. Hignette, F. Sette, H.N. Chapman, R.W. Lee, T.N. Hansen, S. Techert, J.S. Wark, M. Bergh, G. Huldt, D. van der Spoel, N. Timneanu, J. Hajdu, R.A. Akre, E. Bong, P. Krejčík, J. Arthur, S. Brennan, K. Luening, J.B. Hastings, *Phys. Rev. Lett.* accepted for publication (2005).
- [2]. "Clocking Femtosecond X-Rays," A. L. Cavalieri, D. M. Fritz, S. H. Lee, P. H. Bucksbaum, D. A. Reis, D. M. Mills, R. Pahl, J. Rudati, P. H. Fuoss, G. B. Stephenson, D. P. Lowney, A. G. MacPhee, D. Weinstein, R. W. Falcone, R. Pahl, J. Als-Nielsen, C. Blome, R. Ischebeck, H. Schlarb, Th. Tschentscher, J. Schneider, K. Sokolowski-Tinten, H. N. Chapman, R. W. Lee, T. N. Hansen, O. Synnergren, J. Larsson, S. Techert, J. Sheppard, J. S. Wark, M. Bergh, C. Caleman, G. Huldt, D. van der Spoel, N. Timneanu, J. Hajdu, E. Bong, P. Emma, P. Krejčík, J. Arthur, S. Brennan, K. J. Gaffney, A. M. Lindenberg, and J. B. Hastings, *Phys. Rev. Lett.* **94**, 114801 (2005).
- [3]. "Atomic-scale visualization of inertial dynamics," A.M. Lindenberg, J. Larsson, K. Sokolowski-Tinten, K. Gaffney, C. Blome, O. Synnergren, J. Sheppard, C. Caleman, A.G. MacPhee, D. Weinstein, D.P. Lowney, T. Allison, T. Matthews, R.W. Falcone, A.L. Cavalieri, D.M. Fritz, S.H. Lee, P.H. Bucksbaum, D.A. Reis, J. Rudati, D.M. Mills, P.H. Fuoss, G.B. Stephenson, C.C. Kao, D.P. Siddons, R. Pahl, J. Als-Nielsen, S. Dusterer, R. Ischebeck, H. Schlarb, H. Shulte-Schrepping, Th. Tschentscher, J. Schneider, O. Hignette, F. Sette, H.N. Chapman, R.W. Lee, T.N. Hansen, S. Techert, J.S. Wark, M. Bergh, G. Huldt, D. van der Spoel, M. Timneanu, J. Hajdu, D. von der Linde, R.A. Akre, E. Bong, P. Emma, P. Krejčík, J. Arthur, S. Brennan, K. Luening, and J.B. Hastings, *Science* **308**, 392-395 (2005).
- [4]. "X-ray movies of wiggling crystals", P.H. Bucksbaum, *Science* **306**, 1691-2 (2004).
- [5]. "Ultrafast X-ray physics," D.A. Reis, P.H. Bucksbaum, M.F. DeCamp, *Radiation Physics and Chemistry* **70**,605–609 (2004).
- [6] S. H. Lee, A. L. Cavalieri, D. M. Fritz, M. Myaing, and D. A. Reis. Adaptive dispersion compensation for remote fiber delivery of near-infrared femtosecond pulses. *Opt. Lett.*, **29**(22):2602-2604, 2004.
- [7] S. Fahy and D. A. Reis. Coherent phonons: Electronic softening or anharmonicity? *Phys. Rev. Lett.*, **93**:109701, 2004.
- [8] M. F. DeCamp, D. A. Reis, D. M. Fritz, P. H. Bucksbaum, E. M. Dufresne, and R. Clarke. X-ray synchrotron studies of ultrafast crystalline dynamics. *J. Synch. Rad.*, **12**:177-192, 2004.
- [9] E. D. Murray, D. M. Fritz, J. K. Wahlstrand, S. Fahy, and D. A. Reis. Transient phonon softening in photoexcited bismuth. to be published, *PRB rapid communications*, 2005.
- [10]. "Spectrally Resolved Transient Alignment of Molecular Iodine, " Doug Broege, Emily Peterson, Philip Bucksbaum, DAMOP 2005.
- [11]. "Ultrafast coherent control in x-ray scattering," P. H. Bucksbaum and D. A. Reis, *ACS Symposium on Emerging Ultrafast Spectroscopies: From Chemistry to Biophysics* (2004).
- [12]. "Single shot characterization of subpicosecond and ultra-relativistic compressed electron bunches at the SLAC SPPS experiment," Adrian Cavalieri, David M. Fritz, Soo-Heyong Lee, Philip H. Bucksbaum, David A. Reis, Holger Schlarb, Jerome Hastings, DAMOP 2004.
- [13] F. Van den Berghe, Durster S., J. Feldhaus, R. Ischebeck, K. Ludwig, J. Hauschildt, H. Schlarb, B. Schmidt, P. Schm user, S. Simrock, B. Steffen, A. Winter, P. H. Bucksbaum, A. L. Cavalieri, D. M. Fritz, S. H. Lee, D. A. Reis, and F. Ludwig. Proposal for a sub-100 fs electron bunch arrival-time monitor for the VUV-FEL at DESY. In *Proceedings of EPAC 2004*, pages 345-347, Lucerne, Switzerland, 2004.

Formation of Ultracold Molecules

Robin Côté

Department of Physics, U-3046
University of Connecticut
2152 Hillside Road
Storrs, Connecticut 06269

Phone: (860) 486-4912
Fax: (860) 486-3346
e-mail: rcote@phys.uconn.edu
URL: <http://www.physics.uconn.edu/~rcote>

Program Scope

Current experimental efforts to obtain ultracold molecules (*e.g.*, photoassociation (PA), buffer gas cooling, or Stark deceleration) raise a number of important issues that require theoretical investigations and explicit calculations.

This Research Program covers interconnected topics related to the formation of ultracold molecules. We propose to investigate schemes to form ultracold molecules, such as homonuclear alkali metal dimers using stimulated and spontaneous processes. We will also study heteronuclear molecules, in particular alkali hydrides; these polar molecules have very large dipole moments. In addition, we will investigate the enhancement of the formation rate via Feshbach resonances, paying special attention to quantum degenerate atomic gases. Finally, we will explore the possible formation of a new and exotic type of molecules, namely ultralong-range Rydberg molecules.

Recent Progress

Since the start of this Program (August 1st 2005), we have worked on the formation of alkali hydrides from one- and two-photon photoassociative processes. We found that the one-photon formation rate for LiH and NaH in their $X^1\Sigma^+$ ground electronic state is sizable in the upper ro-vibrational states $|v'', J = 1\rangle$; assuming conservative values for the atom densities (10^{11} cm^{-3}), temperature (1 mK), laser intensity (1000 W/cm^2), and the volume illuminated by it (10^{-6} cm^3), the rate coefficients are of the order $3 \times 10^{-13} \text{ cm}^3/\text{s}$, leading to about 3,000 molecules per second [1]. We also found that all of those molecules would populate a narrow distribution of J -states in the $v'' = 0$ vibrational level by spontaneous emission cascading; the momentum transfer due to the photon emission is not large enough for remove the molecules from traps deeper than $10 \mu\text{K}$ or so. In the two-photon case, we found rate coefficients about 1000 times larger.

We also began working on the Rydberg-Rydberg interactions to explain some spectral features observed in ^{85}Rb experiments. This work is underway, but preliminary results reproduce the lineshapes observed within the experimental uncertainties [2].

Future Plans

In the coming year, we plan to continue the alkali hydride work by exploring the formation of molecules in the $a^3\Sigma^+$ electronic state. It is predicted to support one ro-vibrational level, leading to a sample in a pure single ro-vibrational state. We will carry more calculations on Rydberg-Rydberg interactions and explore the possibility of forming metastable long-range doubly-excited Rydberg molecules as well as the experimental signature to be expected. Finally, we will also work on the spectroscopic signature of Cooper pairs in a degenerate Fermi gas, namely ^6Li .

Publications sponsored by DOE

- [1] E. Juarros, K. Kirby, and R. Côté, *One-photon Assisted Formation of Ultracold Polar Molecules*. In preparation.
- [2] J. Stanojevic, R. Côté, D. Tong, S.M. Farooqi, E.E. Eyler, and P.L. Gould, *Long-range Rydberg-Rydberg interactions and molecular resonances*. In preparation.

Optical Two-Dimensional Fourier-Transform Spectroscopy of Semiconductors

Steven T. Cundiff

JILA, University of Colorado and National Institute of Standards and Technology

Boulder, CO, 80309-0440

cundiffs@jila.colorado.edu

Program Scope: The goal of this program is to implement optical 2-dimensional Fourier transform spectroscopy and apply it to semiconductors. Specifically of interest are quantum wells that exhibit disorder due to well width fluctuations and quantum dots. In both cases, 2-D spectroscopy will provide information regarding coupling among excitonic localization sites.

Progress: During the past year, we have perfected the two-dimensional Fourier-transform spectrometer [1], used it to obtain magnitude spectra of the exciton resonances in a semiconductor multiple quantum well [2] and made further improvements to phase resolve the signal to obtain the real and imaginary spectra [3].

Many-body interactions in solids are a topic of long-standing and continuing interest. Optical excitations in direct-gap semiconductors are a convenient system for the study of many-body interactions. The primary tool for these studies has been transient-four-wave-mixing (TFWM) using ultrashort (~100 fs) laser pulses, which has also proven to be powerful for studying molecular dynamics. The strong similarities between coherent optical excitation of resonant systems (including TFWM) and nuclear magnetic resonance (NMR) has meant the NMR concepts and language are often used in optics. This similarity means that NMR advances suggest improvements to optical spectroscopy. Indeed, the concepts of multidimensional NMR spectroscopy have recently been adapted to the infrared and optical regimes to study vibrational and electronic excitations in molecules.

Significant progress has been made in understanding how many-body interactions are manifest in the TFWM signal from exciton resonances in semiconductors. Early experiments were interpreted in terms of a two-level model. The observation of signals for “negative” delay in a two-pulse experiment indicated that such a simple picture was insufficient. Negative delay signals have also been observed in experiments on molecular iodine and atomic potassium. A phenomenological description of these observations was obtained by adding biexcitonic effects, the local field correction (LFC), excitation induced dephasing (EID) or excitation induced shift (EIS) to the two-level model. A fundamental theoretical description also reproduces these observations, although correlation terms beyond Hartree-Fock must be included. Coupling between optically induced excitations was also addressed, starting with beats in the TFWM signal due to excitons localized by well-width fluctuations. To determine if the beats were due to electromagnetic or quantum interference, time-resolved TFWM and spectrally-resolved TFWM were used. Interference between the exciton resonance and unbound electron-hole continuum states was also observed. The fact that the exciton and continuum states are coupled by many-body interactions was discovered using partially-non-degenerate TFWM and in 3-pulse TFWM. These results explained the earlier observation that the TFWM signal from the exciton decays anomalously fast when the excitation spectrum overlapped continuum states.

A single two-dimensional Fourier transform spectrum (2DFTS) exemplifies virtually the entire body of work on TFWM spectroscopy of excitons in semiconductors. Furthermore, significant insight can be obtained directly from qualitative descriptions of two-dimensional

spectra and detailed calculations are not required. We address coupling between excitonic resonances, particularly the heavy-hole and light-hole excitons in quantum wells, and coupling between continuum states (unbound electron-hole pairs) and excitons. The power of Fourier-transform spectroscopy to address these issues does not come from use of a Fourier transform *per se*, but rather it comes from the fact that the *phase* of the TFWM signal is coherently tracked as a function of the *phase-delay* between the first two excitation pulses. Consequently, it is significantly more powerful than previous experiments that characterized the emitted TFWM signal without considering how its phase dependence on the delay between input pulse.

We have implemented 2DFTS at near visible wavelengths (~ 800 nm) to study optical excitations in semiconductors, particularly excitons. The timing and geometry are shown schematically in Fig. 1. The requirement of stabilizing the phase between excitation pulses and measuring the signal coherently is more demanding for shorter wavelengths compared to IR, since the fluctuations of the path length and beam direction cause larger phase errors. One approach to 2D experiments in the visible is to maximize the stability of the apparatus passively and simply measure the phase delays, however this requires resampling the data, which must be done with great care. Another approach relies on either a pulse shaper and/or diffractive optics to generate inherently phase-stable excitation pulses. There are certain limitations for each implementation. For example, spurious pulses often overlap with main peaks from an acousto-optic pulse shaper in time domain and cause harmful amplitude modulation. Furthermore, the range of delay between pulse pairs is constrained by the frequency resolution to about tens of picoseconds, making studies, for example, of the population relaxation process in semiconductors infeasible. In the case of diffractive optics approach, the reference pulse also passes through the sample, possibly introducing undesirable dynamical modifications in systems with strong excitation induced effects, such as semiconductors. In our experiments, active interferometric stabilization based on feedback electronics is used to maintain the phase stability of the excitation pulse pairs and the reference pulse. The experimental apparatus is shown in Fig. 2. The active stabilization achieves $\lambda/200$ stability between the first two excitation pulses and $\lambda/20$ stability between the third pulse and the reference pulse used for spectral interferometry. The overall phase fluctuations of the entire apparatus are on the order of 0.06π radians with a maximum fluctuation approximately 10

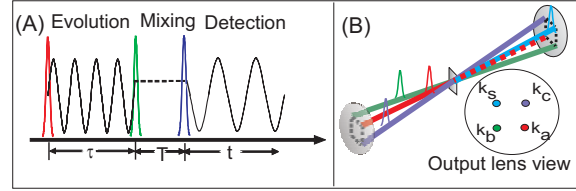


Fig. 1. (A) Schematic of the excitation sequence showing the relevant time intervals. Note the dashed line indicating that the phase during time period t is determined by the phase evolution during time. (B) Diagram showing geometry of excitation pulses and generated signal.

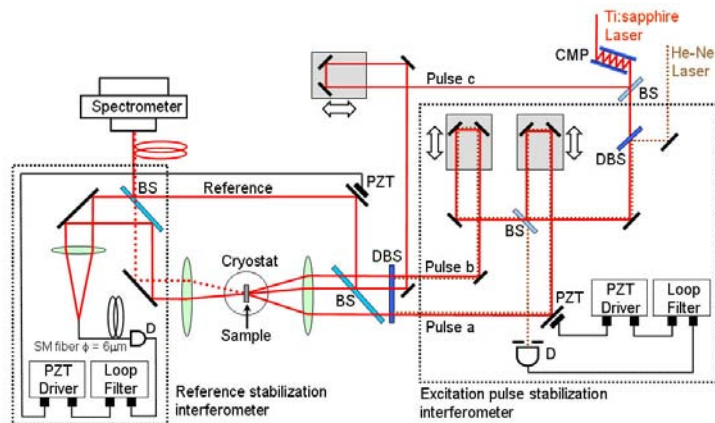


Fig. 2. Experimental setup for 2DFTS. The delay between the first two pulses is stabilized and scanned by the interferometer enclosed in the right hand box. The reference phase is locked by the second interferometer enclosed in the left hand box. CMP: chirped mirror; D: photodiode; BS: beamsplitter; DBS: dichroic BS; PZT: piezoelectric transducer.

times larger. A full description of the apparatus and characterization of its performance can be found in Ref. 1.

Using this actively stabilized apparatus, we have obtained a two-dimensional Fourier transform spectrum of the optical excitations in a GaAs multiple quantum well. The sample consists of 10 periods of a 10 nm GaAs well and 10 nm AlGaAs barrier and is held at 8K in an optical cryostat. Due to confinement, the heavy-hole and light-hole valence bands are energetically split by approximately 6 meV, resulting in two corresponding exciton resonances. Coincidentally, the exciton binding energy is also approximately 6 meV, which results in the light-hole exciton being degenerate with the edge of the heavy-hole continuum states. The linear absorption spectrum, shown in Fig. 2 gives a heavy hole linewidth of about 1.5 meV, which is due in part to inhomogeneous broadening from well width fluctuations. At the excitation densities used in these experiments of $\sim 10^{10}$ excitons/well/cm², the homogeneous linewidth is ~ 0.8 meV. The incident laser pulses are approximately 100 fs in duration. They are tuned above the light hole exciton in order to compensate for the oscillator strengths and get comparable excitation density of heavy-hole excitons, light-hole excitons and unbound electron-hole pairs.

The magnitude of the 2DFTS is shown in Fig. 3. Several features are apparent, including diagonal peaks corresponding to the heavy-hole and light-hole excitons, off-diagonal peaks corresponding to absorption by the light-hole exciton but emission by the heavy-hole exciton and vice-versa and a vertical stripe at the heavy hole emission energy due to absorption by continuum states. Two features are qualitatively striking and due to the strong many-body interactions. The first is that the off-diagonal peak is the strongest and that the off diagonal peaks are unequal in strength. The second is that the continuum shows up as a vertical stripe at the heavy-hole exciton emission energy. Simulations show that these features can only be reproduced by including many-body effects in phenomenological calculations [2].

Based on the time ordering of the conjugated field, \mathbf{k}_a , both rephasing and nonrephasing experiments can be performed. For rephasing (or photon echo) measurements, \mathbf{k}_a arrives first and the system evolves in conjugate frequencies during the time periods τ and t . For nonrephasing (or virtual echo) measurements, \mathbf{k}_a arrives second and the system has the same phase evolution direction during τ and t , i.e.. The real parts of the spectra for the nonrephasing and rephasing measurements are displayed in Fig 3. The phase evolution during the detection time, t , is used to define the sign of the frequencies. Thus rephasing processes produce signals with negative ω_τ (Fig. 4A), whereas non rephasing processes correspond to positive ω_τ (Fig. 4B). Experimentally, the reference pulse has an arbitrary phase with respect to the third pulse. Thus a phase rotation must be applied to the as-measured signal to obtain the correct decomposition into real and imaginary parts.

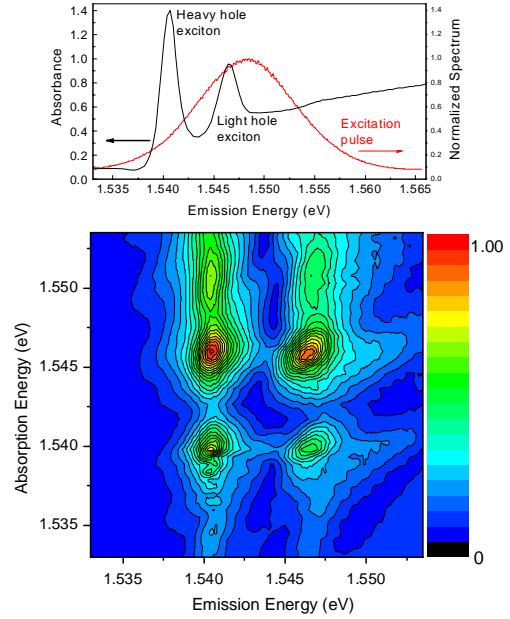


Fig. 3 (upper) Linear absorption spectrum of the sample and spectrum of the excitation pulses. (lower) Normalized magnitude of the two-dimensional Fourier-transform spectrum.

The line shapes of the real spectra reveal the dominant microscopic mechanism responsible for the coherent optical response. In general, the real part of a two-dimensional spectrum is not perfectly absorptive but “phase-twisted” with inherently mixed absorptive and dispersive characteristic. A slice taken exactly along the resonance in either the absorption or emission dimension yields a familiar absorptive feature. For simple two-level systems, a purely absorptive two-dimensional line shape may be obtained by summing the rephasing and nonrephasing measurements.

The dominance of “dispersive” line shapes (the derivative of a peak) of both the diagonal and cross peaks shown in Fig. 4A and 4B, however, qualitatively contradicts the prediction of a simple theory. Particular types of many-body coupling can reproduce the observed spectra [3]. We note that there is almost no negative delay τ signal observed in time-integrated FWM experiments performed under the same conditions as the Fourier transform spectroscopy measurements. We attribute the lack of a negative delay signal to suppression by disorder-induced inhomogeneous broadening. Therefore, two-dimensional Fourier transform spectroscopy provides evidence for many-body interactions even when the classic signature in FWM experiments is suppressed.

Future Plans: Currently the 2D spectrometer is working in a nearly routine fashion. In the near future, we plan to do two experiments. The first is to explore the polarization dependence of the 2D spectra. Polarization is known to be a means of influencing the many-body interactions. Furthermore, the interplay between disorder and many-body effects has resulted in curious TFWM signals. Preliminary data shows that the 2D spectra are polarization sensitive. The second is to look at a series of heterostructures that contains pairs of quantum wells with varying barrier thickness between them. This will allow their coupling to be systematically varied. In the past, there have been signatures of anomalously large coupling, but the origin was not clear. 2D spectroscopy is an ideal tool for unraveling this mystery. On the technical front, we are looking at means of improving the locking, and locking T, using diffractive optics. This would allow us to prove 2-photon coherences due to biexcitons. In the longer term, we plan to look at strongly localized excitons in “natural quantum dots.” To do so, we first need to improve the sensitivity and reach lower excitation densities.

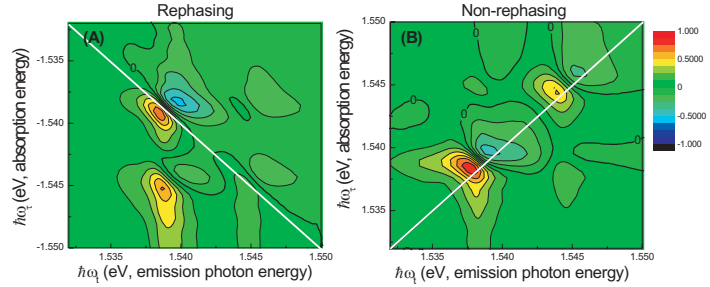


Fig. 4. Real spectra of the rephasing (A) and non-rephasing (B) pulse sequences. Both are normalized to the most intense peak

- [1] T. Zhang, C.N. Borca, X. Li and S.T. Cundiff, “Optical two-dimensional Fourier transform spectroscopy with active interferometric stabilization,” submitted to Optics Express (2005).
- [2] C.N. Borca, T. Zhang, X. Li and S.T. Cundiff, “Optical Two-dimensional Fourier Transform Spectroscopy of Semiconductors,” submitted to Chemical Physics Letters (2005).
- [3] X. Li, T. Zhang, C.N. Borca and S.T. Cundiff, “Many-body Interactions in Semiconductors Probed by Optical Two-Dimensional Fourier Transform Spectroscopy,” submitted to Physical Review Letters (2005).
- [4] C. N. Borca, T. Zhang, and S. T. Cundiff, Two-dimensional fourier transform optical spectroscopy of GaAs quantum wells in *Ultrafast Phenomena in Semiconductors and Nanostructure Materials VIII* ed., (SPIE - The International Society for Optical Engineering, Bellingham, WA, 2004), Vol. 5352, p. 257-265.
- [5] C. N. Borca, A. G. V. Spivey, and S. T. Cundiff, "Anomalously fast decay of the LH-HH exciton Raman coherence," *Physica Status Solidi B-Basic Research* **238**, 521-524 (2003).

Theoretical Investigations of Atomic Collision Physics

A. Dalgarno

Harvard-Smithsonian Center for Astrophysics
Cambridge, MA 02138
adalgarno@cfa.harvard.edu

The research develops and applies theoretical methods for the interpretation of atomic, molecular and optical phenomena and for the quantitative prediction of the parameters that characterize them. The program is responsive to experimental advances and influences them. A particular emphasis has been the study of collisions in ultracold atomic and molecular gases.

Long range forces play a controlling role in the physics of atomic and molecular collisions at cold and ultracold temperatures. We have continued our studies of them and the determination of the leading van der Waals coefficient for interactions with excited atoms. The coefficient of the R^{-6} term, where R is the internuclear distance, may be expressed in terms of the product of the dynamic polarizabilities of the interacting atoms at imaginary frequencies.

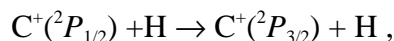
For atoms in states of non-zero orbital angular momentum, the scalar and tensor polarizabilities are needed in order to obtain the dependence on orientation and to distinguish between the different molecular states that can be populated by the approach of the atoms. We have completed calculations for helium interacting with the first excited states of the alkali metal atoms Li, Na, K and Rb for which the dynamic polarizabilities were calculated to high precision using many body perturbation theory. In collaboration with Xi Chu, a postdoctoral fellow supported by DoE, who is an expert on density functional theory, we obtained values of the isotropic polarizability of a broad range of complex atoms. We have extended a time-dependent version of density functional theory (TDDFT) to the determination of tensor polarizabilities. We also clarified the basic theory of the response of non-spherical atoms to electric fields. We have applied TDDFT to the specific cases of He interacting with $Sc(^2D)$ and $Ti(^3F)$. We obtained very small values for the long-range anisotropies which suggest that the cross sections for inelastic collisions at low temperatures will be small. The small anisotropies at long range are consistent with the ab initio calculations of the interaction potentials in which we participated. The anisotropies are small because of the shielding effects of the outer $4s^2$ shell. Calculations for other complex atoms are in progress.

In separate investigations, Xi Chu continued her collaboration with Shih-I Chu and explored the influence of electronic structure and correlation on ionization mechanisms of diatomic molecules responding to intense short-pulse lasers.

In collaboration with Roman Krems and others we continued our studies of scattering theory of atoms and molecules in the presence of magnetic fields. We computed the potential energy surface for the HeNH molecular system and assessed its accuracy by calculating the bound states of the molecular complex. We made estimates of the rate coefficients for collisionally induced Zeeman relaxation. We found that minute variations in the fitting of the potential energy surface altered the relaxation rate coefficient by as much as 50%.

A still more extreme sensitivity was found in our study of the inelastic scattering of helium with hydrogen molecules in which we explored the differences caused by two versions, each of apparently high accuracy, of the potential energy surface of HeH₂. Cross sections for elastic scattering and for pure rotational excitation differed typically by a factor of less than two but exceptions occurred for specific transitions because of the presence of zero energy resonances in one of the surfaces and not in the other.

Few studies have been reported of inelastic collisions of positive ions with neutral atomic and molecular systems at ultralow temperatures. We carried out complete quantum mechanical calculations of the cross sections for the fine-structure transition



The cross sections obey Wigner's law at energies less than 10^{-3} cm^{-1} and yield a large rate coefficient of $2.6 \times 10^{-10} \text{ cm}^3 \text{ s}^{-1}$ at zero temperature.

Publications

- B. Zygelman, A. Dalgarno, M. J. Jamieson, and P.C. Stancil, Multichannel Study of Spin-Exchange and Hyperfine-Induced Frequency Shift and Line Broadening in Cold Collisions of Hydrogen Atoms, *Phys. Rev. A* 67, 042715, 2003.
- R.C. Forrey, S. Jonsell, P. Froelich and A. Dalgarno, Cold Collisions of Spin-Polarized Metastable Hydrogen Atoms, *Phys. Rev. A* 67 040701(R), 2003.
- R. Krems and A. Dalgarno, Threshold Laws for Collisional Reorientation of Electronic Angular Momentum, *Phys. Rev. A* 67, 050704-1, 2003.
- N. Balakrishnan, G.C. Groenenboom, R.V. Krems and A. Dalgarno, The He-CaH($^2\Sigma^+$) Interaction: II. Collisions at Cold and Ultracold Temperatures, *J. Chem. Phys.* 118, 7386, 2003.
- R. V. Krems, A. Dalgarno, N. Balakrishnan, and G. C. Groenenboom, Spin-flipping Transitions in $^2\Sigma$ Molecules Induced by Collisions with Structureless Atoms, *Phys. Rev. A* 67,060703 (R) (2003).

- N. Balakrishnan and A. Dalgarno, On The Isotope Effect in F+HD Reaction at Ultracold Temperatures, *J. Phys. Chem.* 107, 7101, 2003.
- R. V. Krems and A. Dalgarno, Disalignment Transitions in Cold Collisions of ^3P Atoms with Structureless Targets in a Magnetic Field, *Phys. Rev. A* 68, 013406, 2003.
- R. V. Krems, H.R. Sadeghpour, A. Dalgarno, D. Zgid, and G. Chalasinski, Low-temperature Collisions of $\text{NH}(X^3\Sigma^-)$ Molecules with He Atoms in a Magnetic Field: an Ab initio Study, *Phys. Rev. A* 68, 051401, 2003.
- X. Chu, M. J. Jamieson and A. Dalgarno, Scattering Lengths for Collisions of Hydrogen and Deuterium Atoms, *J. Phys. B* 36, L415, 2003.
- P. Froelich, B. Zygelman, A. Saenz, S. Jonsell, S. Eriksson and A. Dalgarno, Hydrogen-antihydrogen Molecule and Its Properties, *Few-Body Systems* 34, 63, 2004.
- S. Jonsell, A. Saenz, P. Froelich, B. Zygelman and A. Dalgarno, Hydrogen-Antihydrogen Scattering in the Born-Oppenheimer Approximation, *J. Phys. B.* 37, 1195, 2004.
- R. V. Krems and A. Dalgarno, Quantum Mechanical Theory of Atom Molecule and Molecular Collisions in a Magnetic Field: Spin Polarization, *J. Chem. Phys.* 120, 2296, 2004.
- E. Bodo, F. A. Gianturco, N. Balakrishnan, and A. Dalgarno, Chemical Reactions In The Limit Of Zero Kinetic Energy: Virtual States And Ramsauer Minima in $\text{F} + \text{H}_2 \rightarrow \text{HF} + \text{H}$, *J Phys. B* 37 3641, 2004.
- X. Chu and A. Dalgarno, Linear Response Time-Dependent Density Functional Theory for Van Der Waals Coefficients, *J. Chem. Phys.* 121, 4083, 2004.
- C. Zhu, A. Dalgarno, A., S. Porsev, and A. Derevianko, Dipole Polarizabilities of Excited Alkali-Metal Atoms and Long Range Interactions with Helium Atoms, *Phys. Rev. A* 70, 03722, 2004.
- X. Chu and Shih-I Chu, Role of the electronic structure and multielectron responses in ionization mechanisms of diatomic molecules in intense short-pulse lasers: An all-electron *ab initio* study, *Phys. Rev. A*, 70, 061402 (R), 2004.
- R. Krems, G. Groenenboom, and A. Dalgarno, Electronic Interaction Anisotropy between Atoms in Arbitrary Angular Momentum States, *J. Phys Chem A*, 108, 8941, 2004.
- R. V. Krems, J. Klos, M.F.Rode, M.M.Szczesniak, G.Chalasinski and A. Dalgarno., Suppression of Angular Forces in Collisions of Non-S-State Transition Metal Atoms, *Phys. Rev.Lett.* 94, 013202 2005.
- Teck-Ghee Lee, C. Rochow, R. Martin, T. K. Clark, R. C. Forrey, N. Balakrishnan, P. C. Stancil, D. R. Schultz, A. Dalgarno and Gary J. Ferland, Close-coupling calculations

- of low-energy inelastic and elastic processes in ^4He collisions with H_2 : A comparative study of two potential energy surfaces, *J. Chem. Phys.* 122, 024307, 2005.
- G. Barinovs, M.C. van Hemert, R. Krems and A. Dalgarno, Fine-structure Excitation of C^+ And Si^+ by Atomic Hydrogen, *ApJ* 620, 537, 2005.
- M. Bouledroua, A. Dalgarno and R. Côté, Viscosity and Thermal Conductivity of Li, Na, and K Gases, *Physica Scripta*, 71, 519, 2005 .
- H. Cybulski, R. V. Krems, H.R. Sadeghpour, A. Dalgarno, J. Klos, G.C. Groenenboom, A. van der Avoird, D. Zgid and G. Chalasinski, Interaction of $\text{NH X}^3\Sigma^-$ with He: Potential Energy Surface, Bound States and Collisional Zeeman Relaxation, *J. Chem. Phys.* 122, 094307, 2005.
- C. Zhu, J. F. Babb and A. Dalgarno, Theoretical Study of Pressure Broadening of Lithium Resonance Lines by Helium Atoms. *J. Phys B. Phys. Rev. A*, 71, 052710, 2005.
- X. Chu, and A. Dalgarno, Polarizabilities of ^3P atoms and van der Waals coefficients for their interaction with helium atoms, *Adv. Atom. Mol. Opt. Physics*, in press, 2005
- X. Chu, A. Dalgarno, and G. C. Groenenboom, Polarizabilities of Sc and Ti Atoms and Dispersion Coefficients for their Interaction with Helium Atoms, *Phys. Rev. A* in press, 2005
- C.M. Dutta, C. Oubre, P. Nordlander, M. Kimura and A. Dalgarno, Charge Transfer Cross Sections in Collisions of Ground State Ca and H^+ , *Phys. Rev. A* in press, 2005

Interactions of ultracold molecules: collisions, reactions, and dipolar effects

D. DeMille

Physics Department, Yale University, P.O. Box 208120, New Haven, CT 06520

e-mail: david.demille@yale.edu

Program scope: The goal of our project is to study the reactive, inelastic, and elastic collisions of polar molecules (specifically, RbCs) in the ultracold regime. A variety of physical effects associated with the low temperatures and/or the polar nature of the molecules should be observable for the first time. These include phenomena such as chemical reactions at vanishing temperature,¹ ultra-long range “field-linked” states of polar molecules in an external electric field,² extraordinarily large ($\sim 10^8 \text{ \AA}^2$) elastic collision rates in the presence of a polarizing electric field,^{3,4} etc. In addition, the study of inelastic (e.g., vibrationally or rotationally quenching) collisions will make it possible to produce optimized sources of ultracold polar molecules for a variety of applications.

Recent progress: Our group has recently demonstrated the novel ability to produce and state-selectively detect ultracold heteronuclear molecules. These techniques yield RbCs molecules at translational temperatures $T < 100 \text{ \mu K}$, in any of several desired rovibronic states—including the absolute ground state, where RbCs has a substantial electric dipole moment. Our method for producing ultracold, ground state RbCs consists of several steps. In the first step, laser-cooled and trapped Rb and Cs atoms are bound together into an electronically excited state, via the process known as photoassociation.⁵ These initially-created molecules decay rapidly into a few, weakly bound vibrational levels in the ground electronic state manifold.⁶ Specifically, by proper choice of the photoassociation resonance, we form metastable molecules exclusively in the $a \text{ } ^3\Sigma^+$ level. This sample has significant population in only a small number of rotational levels.

We state-selectively detect these long-lived molecules with a two-step, resonantly-enhanced multiphoton ionization process (1+1 REMPI) followed by time-of-flight mass spectroscopy.⁷ This unique detection capability (for ultracold molecules) was enabled by our spectroscopic characterization of RbCs in a previously inaccessible range of energy levels. Our method makes it possible to determine the distribution of population among vibrational levels; under typical conditions, the $a(v=37)$ level (bound by $\sim 5 \text{ cm}^{-1}$) is most highly populated, although this distribution can be changed considerably (towards higher or lower vibrational levels) by the choice of photoassociation resonance.

In our most recent work, we have demonstrated the long-sought ability to transfer population from these high vibrational levels, into the lowest vibronic states $X \text{ } ^1\Sigma^+(v=0,1)$ of RbCs.⁸ The technique is based on a laser “pump-dump” scheme. Two sequential laser pulses (each $\sim 5 \text{ ns}$ in duration, $\sim 100 \text{ \mu J}$ pulse energy) drive population first “upward” into an electronically excited level, then “downward” into the vibronic ground state. At present, the vibronic ground-state molecules are spread over a small number (2-4) of the lowest rotational levels, determined by the finite spectral resolution of the pump/dump lasers. These ground-state molecules are also detected with 1+1 REMPI.

Future plans: We are currently implementing the improvements needed to optically trap dense samples of RbCs molecules with a single, low-lying rovibronic state populated. A new vacuum system will allow us to trap both the precursor Rb and Cs atoms and the resulting molecules

(regardless of internal state) in a CO₂ laser trap. Our present plan is to begin by trapping Rb and Cs in the CO₂ trap, and cooling them to T~10 μK. Next we will apply the photoassociation laser beam to form and accumulate vibrationally-excited RbCs. The initial goal is to observe simple processes such as vibrational quenching by collisions with precursor atoms.

The next phase of our work will focus on transferring population to the rovibronic ground state $X^1\Sigma^+(v=0, J=0)$ in the trapped RbCs sample, and then “distilling” the sample so that only these ground-state molecules remain. Using a new laser system with transform-limited pulses, we expect to have high efficiency and excellent state selectivity for the transfer process. In addition, we have worked out a plausible protocol for the distillation which takes advantage of the large polarizability characteristic of the rovibronic ground state (and of no other states or species present in the trap.) The pure sample of dense, ultracold, strongly polar molecules we anticipate producing will represent a near-ideal starting point for studying the new phenomena mentioned above.

References

- ¹E. Bodo, F. A. Gianturco, N. Balakrishnan, and A. Dalgarno, *J. Phys. B: At. Mol. Opt. Phys.* **37**, 3641 (2004), and references therein.; R.V. Krems, in *Recent Research Developments in Chemical Physics*, vol. 3 pt. II, p. 485 (2002).
- ²A.V. Avdeenkov and J. L. Bohn, *Phys. Rev. Lett.* **90**, 043006 (2003); A.V. Avdeenkov, D.C.E. Bortolotti and J.L. Bohn, *Phys. Rev. A* **69**, 012710 (2004).
- ³D. DeMille, D.R. Glenn, and J. Petricka, *Eur. Phys. J. D* **31**, 275 (2004).
- ⁴M. Kajita, *Eur. Phys. J. D* **20**, 55 (2002).
- ⁵A.J. Kerman *et al.*, *Phys. Rev. Lett.* **92**, 033004 (2004).
- ⁶T. Bergeman *et al.*, *Eur. Phys. J. D* **31**, 179 (2004).
- ⁷A.J. Kerman *et al.*, *Phys. Rev. Lett* **92**, 153001 (2004).
- ⁸J.M. Sage, S. Sainis, T. Bergeman, and D. DeMille, *Phys. Rev. Lett.* **94**, 203001 (2005).

Ultracold Molecules: Physics in the Quantum Regime

John Doyle

Harvard University

17 Oxford Street

Cambridge MA 02138

doyle@physics.harvard.edu

1. Program Scope

Our research encompasses a unified approach to the trapping of both atoms and molecules. Our goal is to extend our very successful work with CaH to NH and approach the ultracold regime. We plan to trap and cool 10^{11} NH molecules loaded directly from a molecular beam. Elastic and inelastic collisional cross sections will be measured and cooling to the ultracold regime will be attempted. To date, no collisional cross sections have been measured for ultracold heteronuclear molecules. Theory has now begun to offer predictions for NH. We note that as part of this work, we are continuing to develop an important trapping technique, buffer-gas loading. This method was invented in our lab and its significant advantages (large numbers of trapped atoms and molecules as well as general applicability) indicate that further development is warranted.

2. Recent Progress

The milestones for this project are:

- x-spectroscopic detection of ground-state NH molecules via LIF
- x-production of NH in a pulsed beam
- x-spectroscopic detection of ground-state NH molecules via absorption
- x-injection of NH beam into cryogenic buffer gas (including LIF and absorption detection)
- x-realization of 4 T deep trap run in vacuum
- x-injection of NH molecules into cryogenic trapping region
- x-loading of NH molecules into cryogenic buffer gas with 4 T deep trap
- x-trapping of NH
- o-measurement of spin-relaxation rate of NH with He
- o-removal of buffer gas after trapping of NH
- o-measurement of elastic and inelastic cross sections
- o-attempt evaporative cooling

NH, like many of the diatomic hydrides, has several advantages for molecular trapping including large rotational constant and relatively simple energy level structure. There were several key questions before us when this project began. Could we produce enough NH using a pulsed beam? Is it possible to introduce a large number of NH molecules into a buffer gas? Would the light collection efficiency be enough for us to adequately detect fluorescence from NH? Could we get absorption spectroscopy to work so that absolute number measurements could be performed? Could we achieve initial loading of NH into the magnetic trap? We have now answered these questions, all to the positive.

There are key questions left. Will the spin relaxation rates with helium be low enough for us to remove the buffer gas? Will the NH-NH collision rates be adequate for evaporative cooling or will another method (like sympathetic or laser cooling) be necessary to cool NH into the ultracold regime. There is strong indication that the answer to the first is “yes.” Recent theoretical calculations by Krems and coworkers (motivated by our experiment) indicate that NH will survive in the low-field-seeking state for several hundred thermalization times before it spin relaxes. The final question is still open and, indeed, answering this question is the key stated goal of this work.

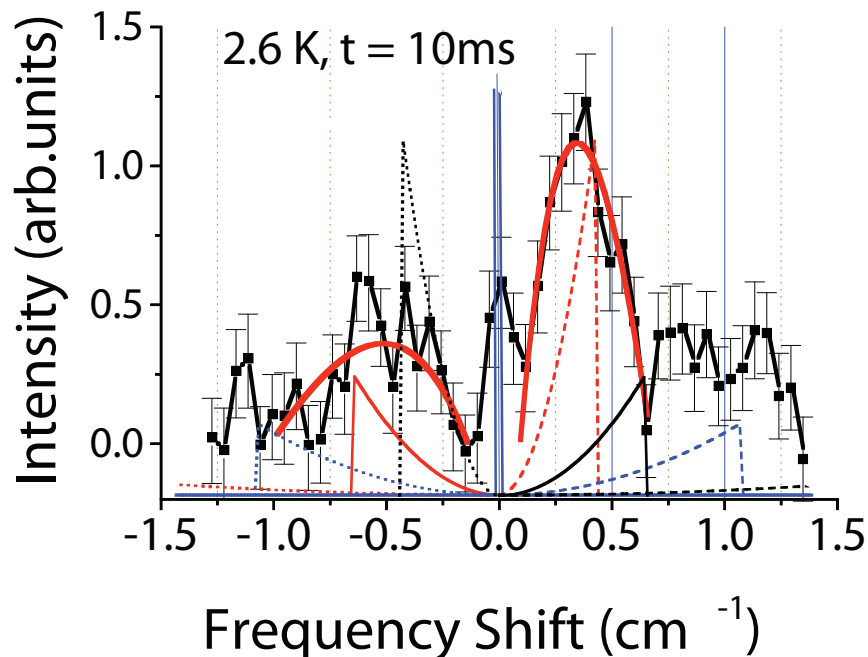


Figure 1: Spectra of trapped NH molecules at 2.6 K. Thick lines are guides to the eye. Thin lines are 0-th order simulated spectra for various transitions. Data is consistent with a trapped distribution of NH low-field seekers.

Summary of Status of Project

The heart of the apparatus is a beam machine that we use to produce pulsed NH in a supersonic beam (see figure 2). (We are in the supersonic regime only to maximize NH flux; 3 dimensional translational cooling and rotational cooling are provide by the buffer gas.) The design of the pulsed source is based on the production of OH via DC discharge as executed by Nesbitt. In short, we have a pulsed valve and a slit plate with a layer of BN in between. A voltage between the plates and the nozzle of the pulsed valve produces a discharge whenever we allow gas into the nozzle. This is done by opening the pulsed valve, with a solenoid, for times about 1 ms.

This beam is directed toward our trapping magnet, the bore of which forms a cryogenic buffer-gas cell. This was constructed with a small entrance orifice of a few mm in diameter to allow the beam of NH to enter, thus buffer-gas cooling the NH. Several windows exist for the the introduction and collection of light. In this initial setup the magnet (and, therefore, the buffer gas) can be cooled to as low as around 2.5 K.

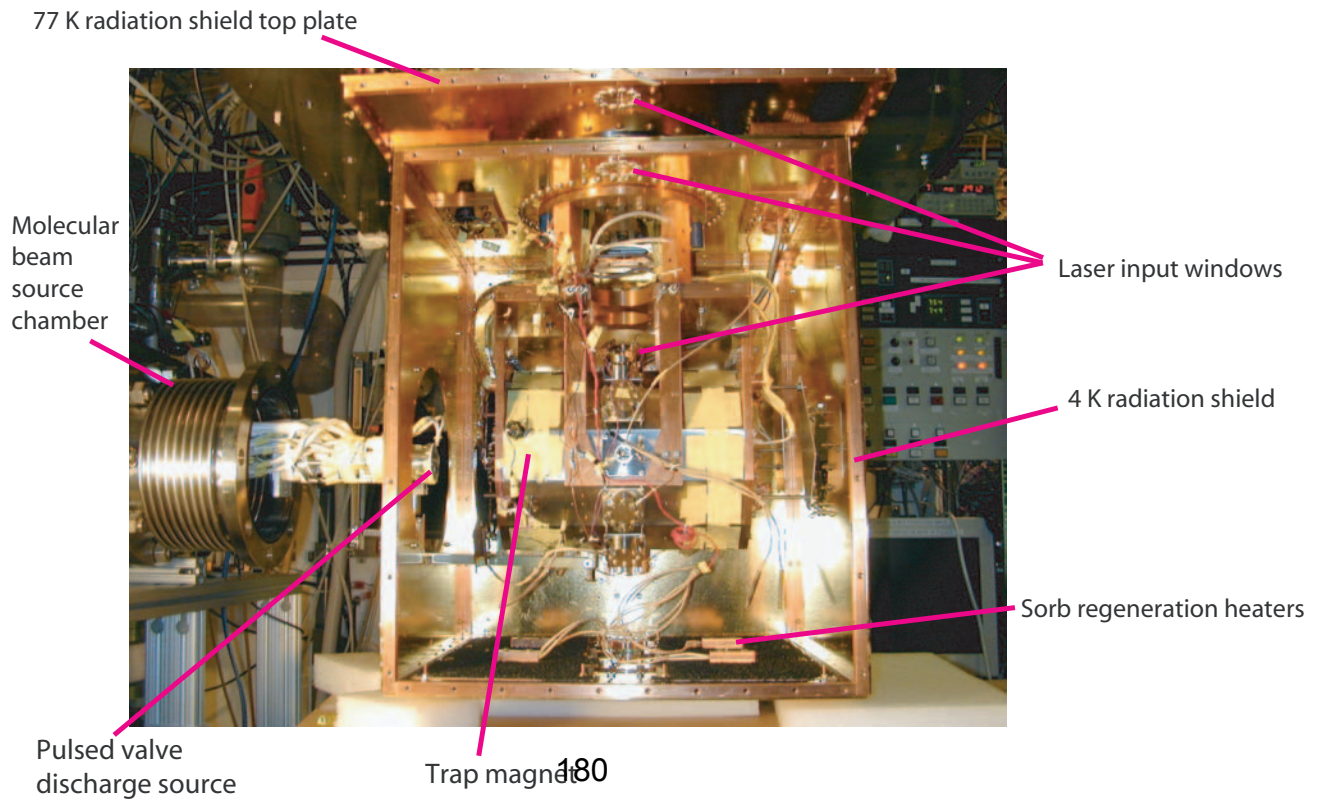
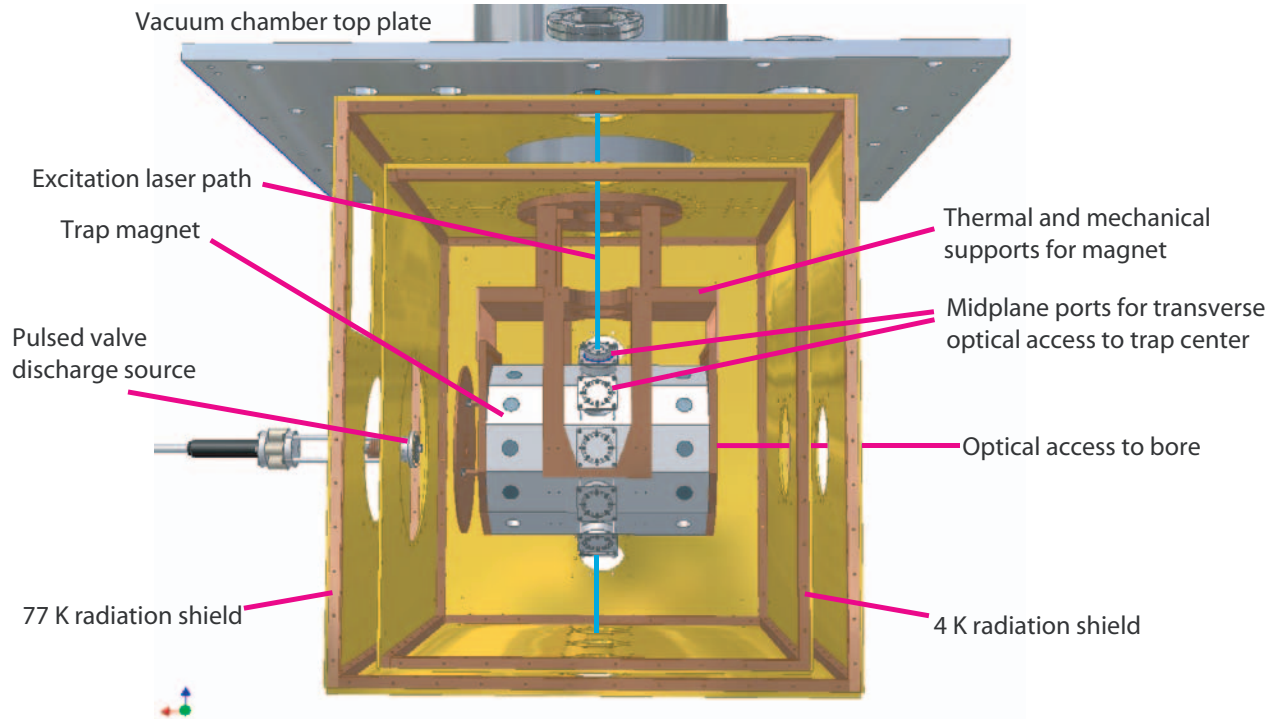
The basic experimental procedure is as follows. The pulse valve of our NH source is opened for about one millisecond. During this time a jet of ammonia exits the valve, entering the discharge region near the jaws, creating a beam of ammonia, NH and other species. This long pulse beam travels about 10 cm to the face of the cell where approximately all of the molecules heading toward the entrance orifice enter the cell. The NH are then cooled by the buffer gas in the cell. In our latest experiments we have been using fluorescence spectroscopy to detect the NH in the trapping region. We have been able to observe the NH molecules fall into the trap and our data is consistent with only low field seekers being present. In these test runs at high temperature (around 2.5 K), the lifetime of the trapped sample is short, only around 10 ms. This is consistent with our evaporation

model for these low ratios of trap depth to temperature. We see no evidence of spin relaxation of NH, consistent with recent theory.

3. Future Plans

We continue on our program of trapping of NH. The next step is to buffer-gas load NH into the buffer-gas cell while the cell is inside the energized trap with the cell at lower temperatures, around 400 mK (instead of 2.5 K). In this way we should be able to spectroscopically determine the helium-NH spin relaxation rates. This will require installation of our He3 refrigerator as well and a new cell that is thermally isolated from the magnet.

Figure 2:



Atomic Electrons in Strong Radiation Fields

J. H. Eberly

Department of Physics and Astronomy
University of Rochester, Rochester, NY 14627
eberly@pas.rochester.edu

Program Scope: Large Classical Ensemble Dynamics

We are integrating Newtonian equations for large ensembles ($10^5 - 10^6$ members) of nonlinearly coupled pairs of charges in a combination of their mutually repulsive coulomb field, a time-dependent external laser field and the internal atomic field of a nucleus to study very strongly correlated electron behavior analogous to that seen experimentally in non-sequential double ionization (NSDI) of atoms and molecules. Here we report preliminary results on the average temporal dynamics of two electrons in a classical “atom” in pulses as short as a single cycle, under peak pulse intensities between 10^{14} and 10^{16} watts/cm². Our classical two-electron system is designed to have single and double ionization thresholds of 13 and 39 photons of 780 nm laser radiation, similar to several noble gas atoms for which experimental results are available. For this two-electron system a typical double ionization event [1, 2] follows several or many recollisions back into the nuclear region by the first-liberated electron, but our current extension of previous work is showing [3] that the probability of correlated double ionization is greatest in the first recollision.

Background

Radiation fields that act like fields and not just collections of photons can induce coherent responses in atomic electrons. Such coherence, induced by very strong phase-coherent laser pulses, has opened a frontier in atomic physics where sub-cycle features of electron motion can be reliably predicted and controlled. One counter-intuitive element of this new domain is that the coherence resides in what are nominally strongly ionizing bound-free transitions. In such strong and coherent fields photoionization loses its one-way character and during the pulse becomes a multi-cycle periodic process for an electron.

This is a breakdown of standard radiative perturbation theory and it is already reached in the “low intensity” vicinity of 10^{12} watts/cm². The accepted alternative theory is a systematic extension [4] of the Keldysh theory [5] of photoemission via tunneling. Multi-site experimental study

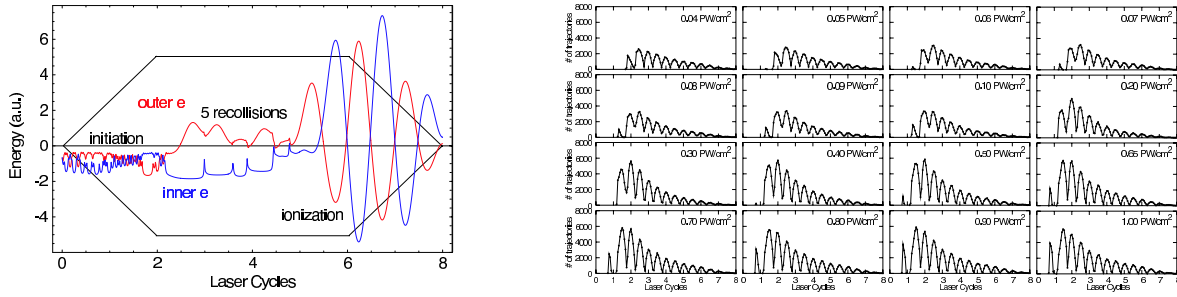


Figure 1: Left frame: Energy trajectories for a single electron pair, showing the four episodes in a typical NSDI event – initiation, recollision, ionization, free-electron jitter motion. The trapezoidal overlay indicates the turn-on and turn-off of the laser field envelope. Right frame: Evolution showing the distribution in time of recollision events during a single 8-cycle pulse for 16 intensities in the range 10^{14} - 10^{15} watts/cm² under the trapezoidal field envelope shown in the left frame.

of double ionization (for early reports, see [6, 7]) in the strong-field tunneling regime shows that modifications of existing theory are needed for intensities that are two to four orders of magnitude greater than 10^{12} watts/cm².

Two-Electron Theory

For helium double ionization the exact numerical solution of the time-dependent Schrödinger equation (TDSE) in the NSDI experimental regime by the Taylor group [8] is generally accepted as the most that will be feasible for the foreseeable future. Very large basis sets are needed for 2-e wave function expansion in a full-dimensional approach. Even approximation by well-designed truncations of these basis sets stretch computer resources to the current limit. However, the physics behind the computational challenge can be used to suggest different categories of approximation, one of which is the so-called aligned electron approximation. Here one tries to extract an advantage from the strong linearly polarized laser fields used in experiments, by introducing the ansatz of linear motion for the electrons, basically entraining their motion along the polarization direction.

Under the aligned electron ansatz a variety of solutions of the TDSE for two coupled atomic electrons have been calculated and compared with experimental reports. The calculations can be done much more rapidly because of the dimensional restriction. Aligned-electron TDSE wave functions for two electrons are consistent with the NSDI “knee” in the ion-count data, a result not yet duplicated with full-dimensional calculations because not enough full-dimensional throughput has been generated to make the required curve.

In a parallel development, evidence has been accumulating that the origin of the non-sequential nature of NSDI lies to a large degree in strong but purely classical correlation. Classical evolution of NSDI, illustrated in the left frame of Fig. 1, shares the interpretive framework of the well-known two-step “rescattering” scenario first proposed for NSDI by Corkum [9]. A number of partially or entirely quantum mechanical versions of NSDI theory strongly guided by this picture have been advanced [10].

It has been repeatedly demonstrated that a fully classical theory gives many similar results as quantum theory (see, e.g., [11, 12]). In addition, the outcome of fully classical calculations is

surprisingly satisfactory for prediction of the major elements of NSDI [1, 2], including aspects of COLTRIMS longitudinal momentum distributions still not fully understood, and recent full-dimensional classical calculations in collaboration with Panfili and Haan corroborate the reduced dimensional results.

Recent Progress: Short-Pulse Predictions

As the left frame of Fig. 1 shows, a typical classical double-ionization event is preceded by several or even many recollisions. This picture stands in contrast to the two-step quantum picture in which double ionization is deemed to occur in the very first recollision cycle. Experiments using shorter pulses (e.g. [13]) which eliminate recollision effects requiring more than one or two cycles, now show that double ionization does not require multiple recollisions.

An open question has been whether the classical theory can agree with this, and we summarize here some recent results obtained in examining this question [3]. We have confirmed that the famous “knee” signature is still obtained for pulses as short as 1 cycle, establishing that fully classical NSDI can still occur without multiple recollisions. This positive answer prompts another question: how does the classical picture incorporate both long and short pulse NSDI schemes?

In the right frame of Fig. 1 we show a new form of time record for ionizing pulses [3]. When the intensities are in the “knee” region the entire recollision sub-ensemble is smoothly depleted during the double ionization over 8 cycles. Clearly the most likely double-ionization event occurs at the first recollision, even though many recollisions typically occur. One can predict that each recollision will remove a fraction of the participating bound electrons, making an exponential decrease in number of recollisions per half cycle. This is an example of classical features not available in a quantum calculation. Subsequent analysis shows that the exponential prediction is well-confirmed in the data [3].

In summary, to emphasize the main question, one sees in the right frame of Fig. 1 that in a classical analysis the highest number of recollisions, each of which is a gateway to NSDI, occurs in the half cycle that is the very first one after the pulse reaches full strength. This confirms that the classical picture requires only one recollision in order to generate NSDI electrons, even though the most typical double-ionization event may be preceded by several recollisions.

Future Plans

We expect to explore the effects of electron correlation in very high-field environments by further adapting large ensemble solutions of Newtonian equations of motion. These should provide access to the dynamical behavior of more than two atomic or molecular electrons in strong and coherent fields, where no quantum TDSE approach is expected to be feasible, whether fully dimensioned or not. We expect to benefit from experimental input, as laboratory results on non-sequential multi-ionization (NSMI) have already begun to be reported [14].

Acknowledgement We have appreciated extended discussions with S.L. Haan, R. Panfili, and Phay J. Ho. This work was partially supported by DOE Grant DE-FG02-05ER15713.

References

- [1] Phay J. Ho, R. Panfili, S. L. Haan and J. H. Eberly, *Phys. Rev. Lett.* **94**, 093002 (2005)
- [2] Phay J. Ho, arXiv:physics/0504037 (*Phys. Rev. A*, in press).
- [3] Phay J. Ho and J.H. Eberly, arXiv: physics/0507175.
- [4] See F.H.M. Faisal, *J. Phys. B* **6**, L89 (1973) and H.R. Reiss, *Phys. Rev. A* **22**, 1786 (1980).
- [5] L.V. Keldysh, *Zh. Eksp. Teor. Fiz.* **47**, 1945 (1964) [*Sov. Phys. JETP* **20**, 1307 (1965)].
- [6] D. N. Fittinghoff, P. R. Bolton, B. Chang and K. C. Kulander, *Phys. Rev. Lett.* **69**, 2642 (1992); B. Walker *et al.*, *Phys. Rev. Lett.* **73**, 1227 (1994); S. Augst, A. Talebpour, S.L. Chin, Y. Beaudoin, and M. Chaker, *Phys. Rev. A* **52**, 917(R) (1995); A. Talebpour *et al.*, *J. Phys. B* **30**, 1721 (1997); S. Laroche, A. Talebpour and S. L. Chin, *J. Phys. B* **31**, 1201 (1998).
- [7] C. Guo, and G. N. Gibson, *Phys. Rev. A* **63**, R040701 (2001); M. J. DeWitt, E. Wells, and R. R. Jones, *Phys. Rev. Lett.* **87**, 153001 (2001); E. Wells, M. J. DeWitt, and R. R. Jones, *Phys. Rev. A* **66**, 013409 (2002).
- [8] See, for example, the report on helium in J. S. Parker *et al.*, *J. Phys. B* **36**, L393 (2003).
- [9] P. B. Corkum, *Phys. Rev. Lett.* **71**, 1994 (1993).
- [10] See, for example, T. Brabec, M. Yu. Ivanov and P. B. Corkum, *Phys. Rev. A* **54**, R2551 (1996), A. Becker and F. H. M. Faisal, *Phys. Rev. A* **59**, R1742 (1999); A. Becker and F. H. M. Faisal, *Phys. Rev. Lett.* **84**, 3546 (2000); S.P. Goreslavskii, S.V. Popruzhenko, R. Kopold, and W. Becker, *Phys. Rev. A* **64**, 053402 (2001), G. L. Yudin and M. Yu. Ivanov, *Phys. Rev. A* **63**, 033404 (2001), L.-B. Fu, J. Liu and S.-G. Chen, *Phys. Rev. A* **65**, 021406(R) (2002), and G. Lagmago Kamta and A.J. Starace, *Phys. Rev. A* **68**, 043413 (2003).
- [11] R. Panfili, J. H. Eberly and S. L. Haan, *Opt. Express* **8**, 431 (2001); and R. Panfili, S. L. Haan, and J. H. Eberly, *Phys. Rev. Lett.* **89**, 113001 (2002).
- [12] S. L. Haan, P. S. Wheeler, R. Panfili and J. H. Eberly, *Phys. Rev. A* **66**, 061402(R) (2002).
- [13] See, for example, A. Rudenko, et al., *Phys. Rev. Lett.* **93**, 253001 (2004)
- [14] See L.F. DiMauro and P. Agostini, in *Adv. At. Mol. Opt. Phys.* **35**, edited by B. Bederson and H. Walther (Academic, 1995), and recent reports in A. Rudenko, et al., *Phys. Rev. Lett.* **93**, 253001 (2004), and S. Palaniyappan, et al., *Phys. Rev. Lett.* **94**, 243003 (2005).

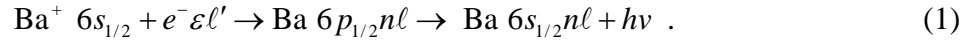
Studies of Autoionizing States Relevant to Dielectronic Recombination

T.F. Gallagher
Department of Physics
University of Virginia
P.O. Box 400714
Charlottesville, VA 22904-4714
 tfg@virginia.edu

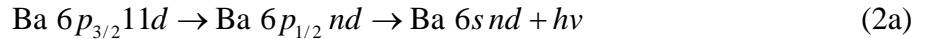
This program is centered on the study of doubly excited autoionizing states of atoms. The practical motivation is that a systematic study of autoionization allows us to understand the reverse process dielectronic recombination (DR), i.e., recombination of ions and electrons via intermediate autoionizing states. While radiative recombination (RR) provides an efficient recombination mechanism for low temperature electrons, at high temperatures DR is much more efficient, and it is important in high temperature laboratory and astrophysical plasmas.^{1,2}

During the past year we have worked on three projects. First, to mimic the effects of electron collisions on DR we have examined the effects of high frequency microwave fields on DR. Second, we are presently examining the relative effects of the microwave field on incoming electrons in different entrance channels for DR and comparing the effects of broadband noise to those due to monochromatic fields. Finally, we have made microwave resonance measurements of the spacings between autoionizing Ba $5d_{3/2} ng$ and $5d_{3/2} nh$ states, where n is the principal quantum number.

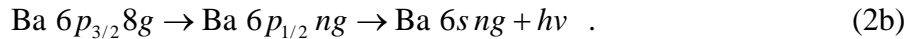
In Ba, the atom we have studied, DR is the recombination of a continuum (free) electron with a Ba ion via an intermediate autoionizing state. For example,



In this case the incoming $\varepsilon \ell'$ electron excites Ba^+ from the $6s_{1/2}$ to $6p_{1/2}$ state and is itself captured in the $n\ell$ orbit. Then, if radiative decay to the bound $6s_{1/2} n\ell$ state occurs, recombination has taken place. In our experiments we do not really study DR but a process which we term DR from a continuum of finite bandwidth. In DR from a continuum of finite bandwidth we replace the true continuum with a continuum of finite bandwidth, either the broad $6p_{3/2} 11d$ or $6p_{3/2} 8g$ ionizing state straddling the $\text{Ba}^+ 6p_{1/2}$ limit.³ We have examined the two processes



and



An atom in the $6p_{3/2} 11d$ or $6p_{3/2} 8g$ state makes the interchannel transition to the degenerate $6p_{1/2} nd$ or $6p_{1/2} ng$ state ($40 < n < \infty$). If it decays radiatively to the bound $6s_{1/2} nd$ or $6s_{1/2} ng$ state, DR has occurred. The primary attractions of this technique are the energy resolution of $\sim 0.5 \text{ cm}^{-1}$ ($< 0.1 \text{ meV}$), the fact that the experiments can be done in zero electric and magnetic field,

and that the partial wave of the entrance channel is well defined. In the continuum of finite bandwidth experiments the $11d$ or $8g$ electron makes about twenty orbits and collides with the Ba^+ core twenty times before it autoionizes. State of the art DR experiments are now done in storage rings.⁴ Our ring, the $11d$ or $8g$ orbit, is just smaller than most.

We have examined the process of Eq. (2a) in high frequency microwave fields as a way to mimic long range electron collisions in a plasma.⁵⁻⁸ In our previous work using microwave frequencies of 4 – 12 GHz we observed resonant enhancement of DR when the microwave frequency nearly matched the $\Delta n = 1, 2,$ or 3 transition frequencies.^{7,8} In the present work we have used frequencies up to 40 GHz and are able to observe enhancement resonances up to $\Delta n = 10$.⁹ A very interesting aspect of the measurements is the observation that roughly the same field strength is required to see the $\Delta n = 4$ enhancement as the $\Delta n = 10$ enhancement. This somewhat surprising observation can be rationalized in the following way. For $\Delta n > 1$ the dipole matrix elements fall off as $1/n^3$. The detuning of the nd states and np states from the nearest manifold of high ℓ states also scales as $1/n^3$. Equating the Rabi frequencies for the transition, $\propto E/n^3$, to the detuning, also $\propto 1/n^3$, gives an n independent microwave field E . A further interesting aspect of this work is that for large $|\Delta n|$ there is a clear difference in the frequency intervals for positive and negative Δn . For example at $n = 100$ the $\Delta n = +6$ resonance, to $n = 106$, occurs at 36.3 GHz while the $\Delta n = -6$ resonance, to $n = 94$, occurs at 43.1 GHz. By tracking all the observed resonances it is clear that the enhancement is due to the $\Delta n = +6$ resonance, not the $\Delta n = -6$ resonance. The propensity for $\Delta n > 0$ is reasonable since the probability of autoionizing, as opposed to radiating, scales as $1/n^3$.

We have recently been examining the relative effect of microwave fields on DR with incoming electrons with different angular momenta. Specifically, we have been studying the relative effects of 18-26 GHz fields on the processes of Eqs. (2a) and (2b). Although this work is in progress, several features are apparent. First, lower microwave fields are required to enhance DR when the incoming electrons are g electrons (Eq. (2b)). This observation is consistent with the fact that in Ba the ng energies are almost hydrogenic, with quantum defects of 0.05, whereas the nd electrons have quantum defects of 0.25. Second, for the ng states a broad range of microwave fields produces enhancement. At the lowest fields the enhancement occurs at exactly the right binding energy to match the $\omega = 1/n^3$ resonance requirement, i.e., at the energy $W = -1/2\omega^{2/3}$, but at higher fields the enhancement shifts quadratically with microwave field to lower energy. At the high microwave field required for enhancement of the nd states enhancement of both the ng and nd states occurs at the same energy. We are presently investigating the source of the energy shift.

Finally, we have examined the enhancement of DR by broadband 18-26 GHz noise. Our preliminary measurements indicate that it is approximately a factor of two less effective in producing the enhancement than monochromatic microwave field in this frequency band for the ng states and roughly the same for the nd states. This observation implies that using a monochromatic microwave field to mimic electron collisions is, in fact, reasonable.

The third project we have undertaken is to conduct microwave spectroscopy of autoionizing states.¹⁰ To our knowledge these are the first measurements of this type, although

efforts along this line are underway elsewhere as well.¹¹ Specifically, we have examined the Ba $5d_{3/2} ng (J = 2) \rightarrow 5d_{3/2} (n \pm 1)h (J = 3)$ transitions for $45 \leq n \leq 49$. These transitions fall in the 50 – 75 GHz frequency range, and the technique we used is delayed field ionization.¹² We chose to begin with these transitions primarily because these ng states are relatively long lived, making it possible to use the field ionization approach even at relatively low n . A drawback to these transitions is that we are not able to separate the contributions to the observed intervals. The differences from the hydrogenic intervals are due to the first order quadrupole interaction and the second order dipole and quadrupole interactions between the ion core and the Rydberg electron. For ionic states such as these with anisotropic cores the first order quadrupole term is usually dominant.¹³⁻¹⁵ To separate these contributions will require that more intervals be measured. Nonetheless, it is possible to compare our measurements with calculated intervals, and we have done so. One of the more interesting results of this process is that we have realized that the commonly used core polarization representation of the second order dipole and quadrupole interactions breaks down for anisotropic cores.¹⁶ In particular, the second order quadrupole interaction cannot be represented by a quadrupole core polarization.

In the coming year we plan to finish the ongoing work on the relative enhancement of DR from ng and nd states and return to the question of DR in combined E and B fields. According to simple models of this process, for a given E, as B is increased DR should just be enhanced, reach a maximum, and finally decline to a value equal to the $E = 0$ value. To date there have been no measurements to demonstrate that this picture is correct.

References

1. A. Burgess, *Astrophys. J.* **139**, 776 (1964).
2. A.L. Merts, R.D. Cowan, and N.H. Magee, Jr., Los Alamos Report No. LA-62200-MS (1976).
3. J.P. Connerade, *Proc. R. Soc. London, Ser. A*, **362**, 361 (1978).
4. T. Bartsch, S. Schippers, A. Muller, C. Brandau, G. Gwinner, A.A. Saghiri, M. Beutelspachier, M. Grieser, D. Schwalm, A. Wolf, H. Danared, and G.H. Dunn, *Phys. Rev. Lett.* **82**, 3779 (1999).
5. A. Burgess and H.P. Summers, *Astrophys. J.* **157**, 1009 (1969).
6. V.L. Jacobs, J. Davis, and P.C. Kepple, *Phys. Rev. Lett.* **37**, 486 (1976).
7. V. Klimenko and T.F. Gallagher, *Phys. Rev. Lett.* **85**, 3357 (2000).
8. V. Klimenko and T.F. Gallagher, *Phys. Rev. A* **66**, 023401 (2002).
9. E.S. Shuman and T.F. Gallagher, *Phys. Rev. A* **71**, 033425 (2995).
10. E.S. Shuman and T.F. Gallagher (submitted for publication).
11. Ch. Jungen (private communication).
12. T.F. Gallagher, R. Kachru, and N.H. Tran, *Phys. Rev. A* **26**, 2611 (1982).
13. R.F. Ward, Jr., W.E. Sturru and S.R. Lundeen, *Phys. Rev. A* **53**, 113 (1996).
14. W. Clark, C.H. Greene, and G. Miecznik, *Phys. Rev. A* **53**, 2248 (1996).
15. W.H. Clark and C.H. Greene, *Rev. Mod. Phys.* **71**, 821 (1999).
16. B. Edlen, in *Spectroscopy I*, edited by S. Flugge, *Handbuch der Physik*, Vol. 27 (Springer, Berlin, 1964).

Publications 2003-2005

1. C.M. Evans, E.S. Shuman, and T.F. Gallagher, "Microwave-induced dielectronic recombination above the classical ionization limit in a static field," Phys. Rev. A 67, 043410 (2003).
2. V. Klimenko, L. Ko, and T.F. Gallagher, "Enhancement of dielectronic recombination in crossed electric and magnetic fields," Phys. Rev. A 68, 012723 (2003).
3. E.S. Shuman, C.M. Evans, and T.F. Gallagher, " ℓ dependence of dielectronic recombination from a continuum of finite bandwidth in an electric field" Phys. Rev. A 69, 063402 (2004).
4. E.S. Shuman and T.F. Gallagher, "Resonant Enhancement of dielectronic recombination by a high frequency microwave field," Phys. Rev. A 71, 033415 (2005).

Experiments in Ultracold Collisions

Phillip L. Gould
Department of Physics U-3046
University of Connecticut
2152 Hillside Road
Storrs, CT 06269-3046
<phillip.gould@uconn.edu>

Program Scope:

Ultracold atoms and molecules have played a leading role in many of the rapidly advancing research areas in atomic, molecular, and optical (AMO) physics. Examples include: Bose-Einstein condensation (BEC) and atom lasers; degenerate Fermi gases (and their connection to superconductivity); photoassociative spectroscopy; ultracold molecule production; ultracold chemistry; ultracold Rydberg gases and plasmas; optical lattices; quantum optics and quantum computing; precision spectroscopy and improved atomic clocks; studies of photoionization, electron scattering, and ion-atom collisions; and fundamental atomic and nuclear physics experiments with radioactive isotopes. Most of these applications require high densities (e.g., $n > 10^{11} \text{ cm}^{-3}$) and low temperatures (e.g., $T < 100 \text{ } \mu\text{K}$), conditions under which collisions between the ultracold atoms become important. In many cases, these collisional processes can be undesirable. For example, inelastic collisions can cause atoms to be heated or ejected from the trap which confines them. On the other hand, ultracold collisions can also be beneficial. For example, evaporative cooling, the final stage of BEC production, requires elastic collisions for thermalization. Also, many of the proposed schemes for quantum computation with ultracold atoms require some type of collisional interaction in order to produce the desired entanglement. The main motivation of our experimental program is two-fold: (1) improve our understanding of ultracold collisions, and (2) devise ways to control these collisional processes to our benefit.

In addition to the relevance of our studies to applications of ultracold atoms, as discussed above, atomic collisions at these extremely low energy (e.g., $\sim 10^{-8} \text{ eV}$) are of significant fundamental interest. Since the colliding partners are barely moving, their motion can be dramatically altered by the long-range dipole-dipole interactions involving excited atoms. This allows the collision dynamics to be controlled with laser light – both enhancement and suppression have been demonstrated. Furthermore, the combination of low velocities (e.g., $v \sim 20 \text{ cm/s}$) and large distance scales (e.g., $R \sim 100 \text{ nm}$) results in the dynamics occurring on a slow time scale. This not only allows the collisions to be probed and manipulated in real time, but also means that spontaneous decay of excited states can occur during the course of a collision, a situation unique to the ultracold domain.

Our ultracold samples of rubidium are produced using a diode-laser-based dual magneto-optical trap (MOT) system. Rb is the ideal atom for our experiments for several reasons: 1) its resonance lines (780 nm and 795 nm) are well-matched to readily available diode lasers; 2) there are two stable and abundant isotopes (^{85}Rb and ^{87}Rb), enabling isotopic differences in collisional properties to be investigated; and 3) ^{87}Rb , because of its favorable collisional properties, has emerged as the most popular atom for BEC studies. Our apparatus uses a “source” MOT to generate a slow atomic beam. These atoms are then loaded into a second MOT which is operated in the phase-stable configuration. The density-dependent atomic loss rates from this MOT, coupled with absolute density measurements, yield the inelastic collisional rate constants.

Recent Progress:

Our recent efforts have focused mainly on ultracold collisions induced by frequency-chirped laser light. The ability to control the temporal variation of both the frequency and amplitude of the light opens up new possibilities in manipulating ultracold collisions. Prior to our recent work, ultracold collision experiments involving excited atoms have used fixed-frequency light applied either continuously (cw) or pulsed (e.g., pulse widths ~ 100 ns). In this case, a given detuning of the light below the atomic resonance excites an atom pair to the attractive molecular potential at a particular internuclear separation R . If the excited pair subsequently gains sufficient kinetic energy (e.g., ~ 1 K) to leave the trap before decaying to the ground state, an inelastic trap-loss collision results. By “chirping” the light, i.e., changing its frequency as a function of time, atom pairs spanning a wide range of R can be excited and caused to collide. A significant advantage of the chirp is that if the laser intensity is sufficiently high, the population is transferred adiabatically to the excited state, making the process efficient and robust. We have investigated the dependence of the collisional loss rate on various parameters of the chirped light: intensity, chirp rate, and chirp direction. We observe that the rate of collisions does indeed saturate with intensity, as expected for an adiabatic process. This saturated rate is consistent with all collision pairs which are accessed by the chirp (and whose excitation survives to short range) undergoing an inelastic trap loss collision. This verifies that the chirped excitation is indeed efficient. The dependence on chirp rate, while maintaining a fixed chirp range, is an important test of the dynamics. At a chirp rate of 10 GHz/ μ s, the collision rate is at least an order of magnitude larger than when the chirp is slow enough to be considered quasi-cw. This verifies that the efficient excitation provided by the chirp is important, and that simply having a range of frequencies present is not sufficient. We have compared the collision rates induced by positive (red-to-blue) and negative (blue-to-red) chirps and find no significant difference under our current conditions. However, we expect differences to emerge at larger detunings. The positive chirp should be more robust and efficient because the excitation proceeds from smaller to larger R , while the motion of the atom pair on the attractive potential proceeds oppositely. Therefore, an atom pair, once excited, is unlikely to further interact with the chirped field, minimizing the possibility of stimulated emission back to the ground state.

We have developed a novel system to produce the frequency-chirped light required for these collision experiments. The injection current of an external-cavity diode laser is rapidly modulated to yield the initial chirp. Unfortunately, the desired frequency modulation is accompanied by significant amplitude modulation. This is reduced by injecting a small amount of light from the chirped “master” laser into a separate free-running “slave” diode laser. The frequency of the injection-locked slave laser tracks the chirp of the master, while its output power remains almost constant. We use various heterodyne diagnostics in order to characterize the chirp. Chirp rates up to 15 GHz/ μ s, with power modulations $<1\%$, have been produced in this manner. The master-slave arrangement also has the advantage of providing significantly higher laser power to the experiment. Our work so far has utilized a linear chirp, but controlling the injection current with an arbitrary waveform generator looks to be a promising method for producing more general chirps.

Future Plans:

In the coming year, we will extend our work on frequency-chirped collisions. We will first vary the frequency range covered by the chirp. This will change the range of R over which atom pairs are excited, as well as the time scale for their motion. At larger detunings, we expect to see significant differences between positive and negative chirp directions. We will also vary

the delay between successive chirps and look for cooperative effects. For sufficiently short delays, we expect that the atom pairs available for a given chirp will be depleted by the preceding chirp. On the other hand, under some conditions, we expect enhancement of one chirp's collision rate by its predecessor. This will occur if long-range collisional flux is excited by the first chirp, but the excitation decays before an inelastic trap-loss collision occurs. This enhanced flux is then available to be re-excited by the second chirp. Besides varying the delay between successive chirps, we will also vary the shape of the chirp itself. So far, we have used linear current ramps to produce simple linear chirps, but with an arbitrary waveform generator, we can produce more sophisticated chirps and vary these chirps to optimize collision rates. All of our measurements to date have used chirped light tuned below the $5P_{3/2}$ level (780 nm). However, the complicating aspects of hyperfine structure are considerably simpler below the $5P_{1/2}$ level (795 nm), so we will adapt our chirped-laser system to this wavelength. Finally, we will apply a separate fixed-frequency laser, tuned to a photoassociative resonance, and use the frequency chirp to transiently enhance the flux available for photoassociation.

Recent Publications:

“Landau-Zener Problem for Trilinear Systems”, A. Ishkhanyan, M. Mackie, A. Carmichael, P.L. Gould, and J. Javanainen, *Phys. Rev. A* **69**, 043612 (2004).

“Frequency-Chirped Light from an Injection-Locked Diode Laser”, M.J. Wright, P.L. Gould, and S.D. Gensemer, *Rev. Sci. Instrum.* **75**, 4718 (2004).

“Control of Ultracold Collisions with Frequency-Chirped Light”, M.J. Wright, S.D. Gensemer, J. Vala, R. Kosloff, and P.L. Gould, *Phys. Rev. Lett.* **95**, 063001 (2005).

Physics of Correlated Systems
Chris H. Greene
Department of Physics and JILA
University of Colorado, Boulder, CO 80309-0440
chris.greene@colorado.edu

1. Program scope and overview

This research effort aims at developing an understanding of how energy is coupled and redirected among the various degrees of freedom in an atom, molecule, or cluster. Because most systems of interest are too complicated to solve exactly, we focus on developing approximation methods that incorporate the most important quantum physics beyond the scope of perturbation theory. While we have tended to concentrate on species that are microscopic, the last few years have begun to see an increasing emphasis on larger systems, such as clusters subjected to intense laser radiation, and most recently, electron scattering from biological molecules.

2. Electron scattering from polyatomic molecules

A growing interest of this research project in recent years has been the study of mechanisms for energy interconversion between the kinetic energy of an incident electron and the dissociative energy sufficient to break a chemical bond. The initial step needed for most photoionization and electron-molecule collision calculations is a solid calculation of the clamped-nuclei electron scattering amplitudes. A graduate student supported by this project, Stefano Tonzani, has continued to develop the capability to carry out such calculations. The first results from his new computer code, along with a detailed description of his three-dimensional finite-element methodology, were presented in a recent publication.[1] That study showed how this method can predict shape resonances in electron scattering from polyatomic molecules as complicated as ethylene (C_2H_4). More recently, this method has been pushed to treat molecules as large as the DNA and RNA bases, the two purines adenine ($C_5H_5N_5$), guanine ($C_5H_5N_5O$), and the pyrimidines thymine ($C_5H_6N_2O_2$), cytosine ($C_4H_5N_3O$), and uracil ($C_4H_4N_2O_2$).[2] The shape resonances in these bases are of importance for understanding single and double strand breaks that are caused by collisions with low energy secondary electrons; this has become realized through the important work of the Sanche group. In the coming year, Tonzani should complete his PhD research with some additional studies of electron collisions with polyatomic molecules, including a description of bond-breaking dissociation dynamics at some level of approximation.

A continuing long-term goal of this project is the description of dissociative recombination that occurs when a low-energy electron (0-10 eV) collides with a polyatomic molecule of atmospheric relevance. Before embarking on production calculations of the reaction rates for such processes, however, we are involved in a phase of algorithm development, which focuses on formulating efficient and broadly applicable theoretical tools. An early success of this line of research was our demonstration that a

Jahn-Teller coupling mechanism is responsible for the unexpectedly high dissociative recombination rate when a low energy electron collides with the simplest polyatomic ion, H_3^+ . While this ion is not directly important for atmospheric applications, it has been a key prototype molecule to understand in detail, because many polyatomics are increasingly understood to have conical intersections in their Born-Oppenheimer potential energy surfaces, which can play a controlling role in the fragmentation dynamics. A second step of progress was the development of a new theoretical technique that combined disparate theoretical elements to quantitatively calculate the H_3^+ recombination rate, treating all degrees of freedom quantum mechanically.

The approach uses hyperspherical coordinate techniques to treat the nuclear motion, multichannel quantum defect ideas combined with a rovibrational frame transformation to handle the electronic-vibrational coupling, and Siegert states in the hyperradius to allow dissociative flux to escape. The resulting recombination rates, when corrected for important details such as experimental resolution and a toroidal correction associated with the merging of the electron and ion beams, are in generally good agreement with experiment except for a few energy ranges of discrepancy. Photoionization of the H_3^+ metastable state was also calculated, and shows very close agreement with the experiments of Helm in some energy ranges, while discrepancies remain at higher energies.[3-8] Our first application to a molecule heavier than H_3^+ was a study of dissociative recombination by HCO^+ .[9] This calculation did not show agreement with experimental recombination rate measurements of Le Padellec et al., nor with the spectroscopic experiments of Grant and coworkers, at the level that has been achieved for H_3^+ . Studies are underway to ascertain whether some of the approximations require further optimization and improvement.

3. Description of decay and fragmentation using Siegert states

Some of our recent studies of molecular dissociation have utilized an adaptation of Siegert pseudostates to describe the vibrational degrees of freedom in diatomic and polyatomic molecules. These states were introduced originally by Siegert in 1939 to describe outgoing scattering waves. One reason they are finding new applications in recent years derives from a new and efficient method for calculating them that was proposed by Tolstikhin and coworkers. We have found that their use as a vibrational basis set is an effective and natural way to deal with dissociation, in problems where the electronic degrees of freedom are handled by multichannel quantum defect techniques. At the same time, Siegert pseudostates obey an unusual “overcompleteness” relation that makes some of their properties complicated to deal with. In a study involving undergraduate student Jeffrey Sha inline and postdoctoral associate Robin Santra, we have studied the overcompleteness and found that it poses no key difficulties.[10] That study went on to derive the time-dependent propagation of wavepackets using these states, which results in a somewhat surprising nonexponential time evolution. This may pave the way to future applications of Siegert states in time-dependent problems.

4. Atoms, ions, and clusters in an intense VUV laser field

During his postdoctoral work in Boulder, Robin Santra spearheaded a project to develop a theoretical description of xenon clusters exposed to intense VUV radiation, of the type provided by the free-electron laser at the TESLA Test Facility (TTF) in Hamburg. This is a new regime of strong photon-cluster interactions, very different from the physics of infrared lasers that are directed at such clusters. Our first theoretical treatment [11] showed that linear physics is able to explain why approximately 30 photons per atom are absorbed, in a 100 femtosecond pulse of intensity 7.3×10^{13} W/cm². [The experimental research was published by H. Wabnitz *et al.*, Nature **420**, 482 (2002).] Our calculations suggest that this absorption of this many VUV photons, one at a time, can be understood once realistic screened potentials are used to describe the behavior of the electrons, in addition to plasma screening effects. Another experimental study by the same group measured multiphoton ionization processes. Robin Santra also was instrumental in developing a detailed theoretical calculation of the multiphoton ionization rates of single ions by these VUV photons. [12] During the past year, graduate student Zachary Walters has made a number of improvements to the initial model calculations reported in [11], which are providing a more complete and quantitative description of this new regime of laser-cluster interaction dynamics. This theoretical project will continue during the coming year, and it should result in a publication being submitted in the near future.

5. Other miscellaneous projects completed since 2003

Papers [13-17] below discuss other results published during the past three years, which were described in detail in past abstracts submitted for this project.

Papers published since 2003 that were supported at least in part by this grant

[1] *Electron-molecule scattering calculations in a 3D finite element R-matrix approach*, S. Tonzani and C. H. Greene, J. Chem. Phys **122**, 014111-1 to -8 (2005).

[2] *Low energy electron scattering from DNA and RNA bases: shape resonances and radiation damage*, S. Tonzani and C. H. Greene, submitted to J. Chem. Phys. (preprint available online at arXiv:physics/0507128).

[3] *Photofragmentation of the H₃ molecule, including Jahn-Teller coupling effects*, V. Kokoouline and C. H. Greene, Phys. Rev. A **69**, 032711-1 to -16 (2004).

[4] *Dissociative recombination of polyatomic molecules: A new mechanism*, C. H. Greene and V. Kokoouline, Phys. Scr. **T110**, 178-182 (2004).

[5] *Triatomic dissociative recombination theory: Jahn-Teller coupling among infinitely many Born-Oppenheimer surfaces*, V. Kokoouline and C. H. Greene, Faraday Discuss. **127**, 413-423 (2004).

- [6] *Theory of dissociative recombination of D_{3h} triatomic ions applied to H_3^+* , V. Kokoouline and C. H. Greene, Phys. Rev. Lett. **90**, 133201-1 to -4 (2003).
- [7] *Unified theoretical treatment of dissociative recombination of D_{3h} triatomic ions: Application to H_3^+ and D_3^+* , Phys. Rev. A **68**, 012703-1 to -23 (2003).
- [8] *Theoretical study of the H_3^+ ion dissociative recombination process*, V. Kokoouline and C. H. Greene, J. Phys. Conf. Series **4**, 74-82 (2005).
- [9] *Dissociative recombination of HCO^+* , A. Larson, S. Tonzani, R. Santra, and C. H. Greene, J. Phys. Conf. Series **4**, 148-154 (2005).
- [10] *Siegert pseudostates: Completeness and time evolution*, R. Santra, J. M. Shainline, and C. H. Greene, Phys. Rev. A **71**, 032703-1 to -12 (2005).
- [11] *Xenon clusters in intense VUV laser fields*, R. Santra, and C. H. Greene, Phys. Rev. Lett. **91**, 233401-1 to -4 (2003).
- [12] *Multiphoton ionization of xenon in the vuv regime*, R. Santra, and C. H. Greene, Phys. Rev. A **70**, 053401-1 to -8 (2003).
- [13] *Properties of metastable alkaline-earth-metal atoms calculated using an accurate effective core potential*, R. Santra, K. V. Christ, and C. H. Greene, Phys. Rev. A **69**, 042510-1 to -10 (2004).
- [14] *Tensorial analysis of the long-range interaction between metastable alkaline-earth-metal atoms*, R. Santra and C. H. Greene, Phys. Rev. A **67**, 067213-1 to -15 (2003).
- [15] *Multichannel cold collisions between metastable Sr atoms*, V. Kokoouline, R. Santra, and C. H. Greene, Phys. Rev. Lett. **90**, 253201-1 to -4 (2003).
- [16] *Nonclassical paths in the recurrence spectrum of diamagnetic atoms*, B. E. Granger and C. H. Greene, Phys. Rev. Lett. **90**, 043002-1 to -4 (2003). [See also our Comment Reply in Phys. Rev. Lett. **91**, 269302-1 (2003).]
- [17] *Phase matching conditions for nonlinear frequency conversion by use of aligned molecular gases*, R.A. Bartels, N.L. Wagner, M.D. Baertschy, J. Wyss, M.M. Murnane, and H.C. Kapteyn, Optics Letters **28**, 346-348 (2003).

Chemistry with Ultracold Molecules

Dudley Herschbach

Department of Chemistry and Chemical Biology

Harvard University, 12 Oxford St., Cambridge, MA 02138

herschbach@chemistry.harvard.edu

This project aims to develop a simple and versatile means to generate slow and cold molecules and manipulate their trajectories. Our approach employs a supersonic nozzle near the tip of a hollow high speed rotor, into which a permanent gas is fed continuously. Spinning the rotor with peripheral velocities of several hundred meters/sec, contrary to the direction of gas flow from the nozzle, markedly reduces the velocity of the emerging molecular beam in the laboratory frame. As compared with other techniques, this method requires far simpler apparatus (no cryogenics at all) and has far wider scope (applicable whether or not a molecule is polar or magnetic).

During the past year, significant progress has been achieved through the efforts of two postdoctoral fellows, Tim McCarthy and Mike Timko. They developed means to overcome a major handicap that resulted from the background produced as the spinning rotor sprays gas over its full orbit. The nozzle is aligned with the detector during less than 5% of each orbit, so only that small fraction of the beam molecules is “harvested.” The yield of slow molecules had been strongly attenuated by collisions with the background gas. With the rotor spinning at 45,000 RPM, it seemed unlikely that a practical way could be found to turn on and off flow from the nozzle. Yet, McCarthy and Timko achieved marked improvement by pulsing the gas fed into the rotor by means of a solenoid valve coupled with two additional pump-out valves, timed to open just as the feed valve closes. This “push-

pull” technique enabled the spinning rotor to be rapidly evacuated. Thereby the background pressure was lowered 20-fold, hugely reducing the scattering problem, which goes exponentially with pressure.

We have also nearly completed another chief component of our program, devoted to developing hardware and software for an “E-H balance.” This device, employing congruent electric and magnetic Stern-Gerlach deflecting fields, can be applied to analyze beams of virtually any slow and cold atomic or molecular species. As the deflecting forces are inversely proportional to the translational kinetic energy of the molecules, for very slow beams sizable deflections can be attained by interaction with the electronic polarizability and the rotational or nuclear magnetic moments. Electronic electric or magnetic dipoles are welcome too, but not needed.

Our next steps focus on demonstrating three ways to exploit our ability to use E and/or H deflecting fields to manipulate trajectories of slow beams. (1) Analyze a Xe beam (used to slow and cool lighter species such as oxygen via inverse seeding). This will provide a much better characterization of the velocity distribution than can be obtained from time-of-flight data (for slow beams, bedeviled by the “wrap-around” problem). We expect to be able to illustrate the E-H resolution capability by resolving the nuclear spin states of two xenon isotopes. (2) Analyze molecular oxygen seeded in xenon, to demonstrate virtually complete separation, and thereby the feasibility of cumulative trapping of the oxygen from many pulses without disruption by further pulses of the xenon carrier gas. (3) Complete a theoretical study showing that microwave spectroscopy of nonpolar molecules such as nitrogen, chlorine, or benzene is feasible. This involves sending a slow molecular beam through an A-C-B Rabi array of static electric fields. When the kinetic energy is very low, even the very weak

induced dipole moments resulting from the molecular polarizability enables the rotational M-states to be separated in the inhomogeneous A and B fields, and therefore transitions induced by microwaves between J,M states in the homogenous C field to be detected with great sensitivity and resolution.

Papers in preparation describe the development of the pulsed rotor source, with data illustrating its performance, and an extensive analysis of manipulation of slow molecule trajectories by E-H deflecting fields.

Resonant Interactions in Quantum Degenerate Bose and Fermi Gases

Principal Investigator: Murray Holland

murray.holland@colorado.edu

440 UCB, JILA, University of Colorado, Boulder, CO 80309-0440

Program Scope

In our program of research, we have been pursuing the development of an effective quantum field theory which describes superfluidity in dilute atomic gases in the presence of resonant interactions. Some time ago, we produced a theoretical proposal pointing out the potential in dilute atomic gases to explore the crossover physics between Bose-Einstein condensation (BEC) and Bardeen-Cooper-Schrieffer (BCS) superfluidity. This has recently developed into a very active field of study in terms of both experiments and theory.

From a theoretical perspective, the rapid developments have led to a major shift in terms of research challenges going forward. Initial theoretical studies in the field of Bose-Einstein condensation in atomic physics were centered around the static and dynamic solutions of simple mean-field theories such as the Gross-Pitaevskii approach. The demonstrations of the BEC to BCS crossover for fermions, as well as the Mott-Insulator to superfluid transition in optical lattices for bosons, were two complementary recent results which both require nonperturbative theoretical studies. The need for a nonperturbative approach is a characteristic of strongly-correlated quantum systems. For this reason, most of our current and future research plans involve the study of strong interaction effects, some of which we now expound on in greater detail.

Effects of a pseudogap on the BEC/BCS crossover physics

We recently improved our previous approaches to the mean field theory of the BEC/BCS crossover to include the effects of the pseudogapped region above the critical temperature T_C . The strong resonant interactions that are possible in atomic physics in presence of Feshbach resonances cause a modification of the nature of the normal Fermi gas, as well as the superfluid crossover which had been previously studied. Understanding this effect was necessary to overcome the limitations of the simple mean-field approaches based on the Leggett and Eagles formalism which treated the fermions in the normal phase as free fermions.

We compared the results of the pseudogap theory to our earlier work for the case of ^{40}K . Figure 1 shows a direct comparison between the critical temperature prediction

of the resonant mean-field approach and the pseudogap theory. With the inclusion of these higher order corrections we still retained a pronounced maximum in the critical temperature T_C near the resonance at about $0.26T_F$, where T_F is the Fermi energy. These results are in general agreement with recent experiments.

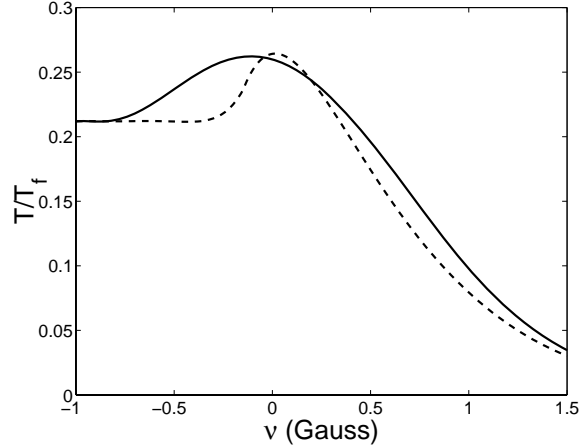


Figure 1. Comparison between the mean-field approach (dashed line) and the pseudogap theory (solid line) for the critical temperature T_C/T_F of ^{40}K as a function of magnetic field.

Fermi-Bose Hubbard model

We also proposed a novel Fermi-Bose Hubbard Hamiltonian to model the system of fermions resonantly coupled in optical lattices. We solved this model in the limit of up to two fermions per site in three dimensions. This is a relevant experimental case, as there are typically $\sim 10^6$ fermions in a cubic lattice with 100^3 sites. Very recently, experimentalists have succeeded in confining ultracold fermions in lattice traps and many groups are developing experiments in this direction. We obtained the phase diagram through the entire crossover for weak tunneling, i.e., a strongly confining lattice. Our model recovered the known BCS and BEC endpoints in the limits of large positive and negative detuning, respectively.

We solved this problem via a variational two-state approximation in the limit of from zero to two fermions per site in the lowest band and zero temperature. Here the fermions always pair and the eigenstates are superpositions of bosons and Fermi-pairs. In fact, we demonstrated that the Hamiltonian can be mapped onto a system of coupled Heisenberg spin magnets.

Swallowtails in nonlinear band theory

We recently formulated a picture of the mechanism for the formation of what are known as “swallowtails” in the nonlinear band structure of interacting Bose Einstein

condensates in optical lattices. In the case of linear band theory, one always has a unique solution for the band energy at given band index and quasimomentum value. However, the solution of the nonlinear Schrödinger equation, rather than the linear Schrödinger equation, can have quite nonintuitive behavior and the most striking example of this is the swallowtail structures. These represent loops in the band patterns giving non-unique band energies at a given quasimomentum.

We studied the band structure of a Bose-Einstein condensate for lattice traps of sinusoidal, Jacobi elliptic, and Kronig-Penney form (series of delta-functions). We showed that swallowtails in a lattice of period $2d$ were adiabatically connected to the non-trivial period-doubled solutions of a lattice of period d . By non-trivial we mean solutions not immediately obvious from the fact that a solution with period d is also a solution of period $2d$. A key point was that most previous explanations were formulated exclusively for the case of repulsive condensates; our way of understanding swallowtails was valid for both repulsive and attractive condensates.

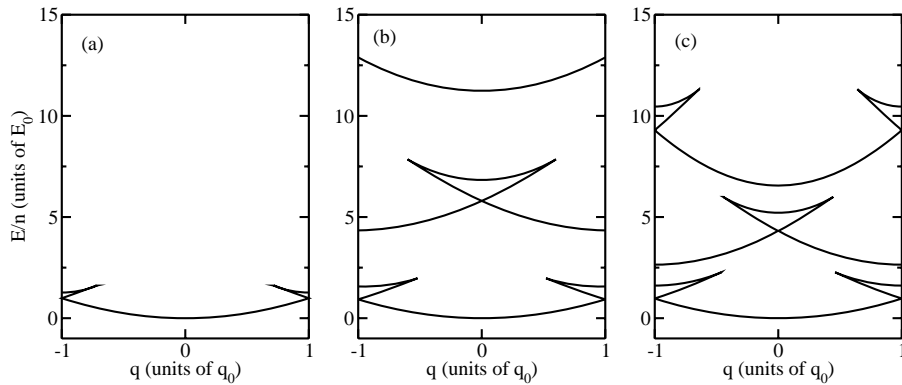


Figure 2. Band structure for a strongly repulsive condensate in a periodic potential, where the quasimomentum q is normalized to the reciprocal lattice spacing q_0 . Shown are results obtained via the analytical methods with (a) a Jacobi elliptic potential, (b) a sinusoidal potential, and (c) a Kronig-Penney potential.

Future work

In future work, we plan to focus our efforts on the description of strong-correlations which emerge between atoms in these complex phases. In particular, the role of correlations which go beyond pairs is important and needs to be incorporated in a consistent manner in the crossover from bosonic to fermionic superfluidity. The theory which has been developed to date is almost entirely for the simplest cases of uniform systems, with no rotation and time-independent potentials, and a major goal is to relax these restrictions in future work.

Publications in peer-reviewed journals on DOE supported research

- [1] B. T. Seaman, L. D. Carr, M. J. Holland *Nonlinear Band Structure in Bose Einstein Condensates: The Nonlinear Schrödinger Equation with a Kronig-Penney Potential*, Phys. Rev. A **71**, 033622 (2005).
- [2] B. T. Seaman, L. D. Carr, M. J. Holland *Effect of a potential step or impurity on the Bose-Einstein condensate mean field*, Phys. Rev. A **71**, 033609 (2005).
- [3] M. Holland *Atomic Beads on Strings of Light*, News and Views section, Nature **429**, 251 (2004).
- [4] L. D. Carr, R. Chiamonte, and M. J. Holland *End-point thermodynamics of an atomic Fermi gas subject to a Feshbach resonance*, Phys. Rev. A **70**, 043609 (2004).
- [5] Jelena Stajic, J. N. Milstein, Qijin Chen, M. L. Chiofalo, M. J. Holland, and K. Levin *Nature of superfluidity in ultracold Fermi gases near Feshbach resonances*, Phys. Rev. A **69**, 063610 (2004).
- [6] L. D. Carr and J. Brand *Pulsed atomic soliton laser*, Phys. Rev. A **70**, 033607 (2004).
- [7] S. G. Bhongale, J. N. Milstein, and M. J. Holland *Resonant formation of strongly correlated paired states in rotating Bose gases*, Phys. Rev. A **69**, 053603 (2004).
- [8] L.D. Carr and J. Brand *Spontaneous soliton formation and modulational instability in Bose-Einstein condensates*, Phys. Rev. Lett. **92**, 040401 (2004).
- [9] J. N. Milstein, C. Menotti, M. J. Holland *Feshbach resonances and collapsing Bose-Einstein condensates*, New Journal of Physics, Focus Issue on Quantum Gases **5**, 52 (2003).
- [10] S. J. J. M. F. Kokkelmans and M. J. Holland *Ramsey Fringes in a Bose-Einstein Condensate between Atoms and Molecules*, Phys. Rev. Lett. **89**, 180401 (2002).
- [11] S. G. Bhongale, R. Walser, and M. J. Holland *Memory effects and conservation laws in the quantum kinetic evolution of a dilute Bose gas*, Phys. Rev. A **66**, 043618 (2002).
- [12] J. N. Milstein, S. J. J. M. F. Kokkelmans, and M. J. Holland *Resonance theory of the crossover from Bardeen-Cooper-Schrieffer superfluidity to Bose-Einstein condensation in a dilute Fermi gas*, Phys. Rev. A **66**, 043604 (2002).
- [13] M. L. Chiofalo, S. J. J. M. F. Kokkelmans, J. N. Milstein, and M. J. Holland *Signatures of Resonance Superfluidity in a Quantum Fermi Gas*, Phys. Rev. Lett. **88**, 090402 (2002).
- [14] S. J. J. M. F. Kokkelmans, J. N. Milstein, M. L. Chiofalo, R. Walser, and M. J. Holland *Resonance superfluidity: Renormalization of resonance scattering theory*, Phys. Rev. A **65**, 053617 (2002).
- [15] M. Holland *Condensates on crest of a wave*, Physics World **15**, 19 (2002).

Exploring Quantum Degenerate Bose-Fermi Mixtures

Deborah Jin
JILA, UCB440
University of Colorado
Boulder, CO 80309
jin@jilau1.colorado.edu

Program Scope

In this project we are exploring interaction dynamics in an ultracold, trapped gas of bosonic and fermionic atoms. Investigation of this new class of quantum degenerate gases concentrates on interaction dominated phenomena such as sympathetic cooling, phase separation, excitations, Feshbach resonances, and the effects of quantum degeneracy. In addition to exploring these new phenomena we seek to understand and ultimately control the interactions in the gas. In particular, effective interactions between the fermionic atoms will be explored in the context of the longer term goal of realizing Cooper pairing of atoms.

Recent Progress and Future Plans

In the recent three year funding period we achieved a quantum degenerate Bose-Fermi mixture using evaporative cooling of the bosonic ^{87}Rb atoms and sympathetic cooling of the fermionic ^{40}K atoms. We characterized the interactions between bosons and fermions in this mixture by measuring the magnitude of the interspecies s-wave scattering length.¹ We then implemented a far off resonance optical dipole trap to confine the ultracold gas mixture with atoms in spin states that cannot be magnetically confined. This allowed us to observe interspecies Feshbach resonances in the ultracold $^{87}\text{Rb}/^{40}\text{K}$ mixture^{2,3}. This work, along with similar results reported by the MIT group using a ^{23}Na and ^6Li mixture⁴, represents the first observation of interspecies Feshbach resonances. The magnetic-field values for four observed Feshbach resonances for ^{87}Rb and ^{40}K allowed us to further refine the value of the interspecies s-wave scattering length. In addition, these resonances open up exciting new possibilities for controlled exploration of interaction effects in ultracold Bose-Fermi gas mixtures. Our results are discussed in more detail below.

Quantum degeneracy and sympathetic cooling

With direct evaporation of the bosonic ^{87}Rb atoms and sympathetic cooling of the ^{40}K atoms we reached quantum degeneracy with the Bose-Fermi mixture. For the Bose gas we can create a nearly pure Bose-Einstein condensate (BEC) while the Fermi gas reaches a T/T_F of about 0.25. The final part of our evaporation trajectory is shown in Fig. 1. This provides an excellent starting point for future experiments that will use the control over interactions afforded by a Feshbach resonance to explore the Bose/Fermi mixture.

In exploring the limits of our sympathetic cooling, we encountered two difficulties that occur at relatively high temperatures well before the gas is quantum degenerate. We propose to address both of these cooling issues in future work. First we

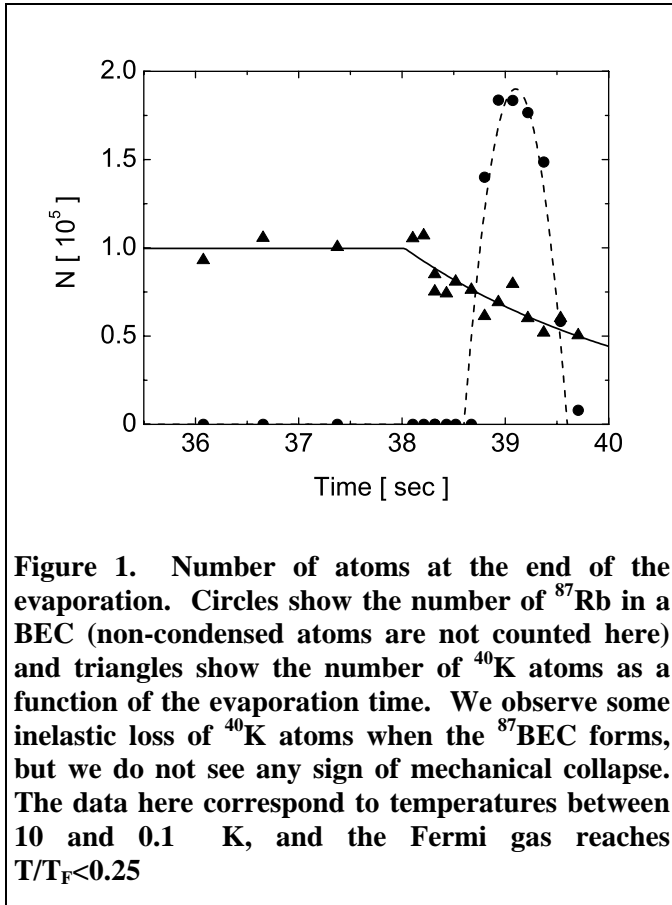


Figure 1. Number of atoms at the end of the evaporation. Circles show the number of ^{87}Rb in a BEC (non-condensed atoms are not counted here) and triangles show the number of ^{40}K atoms as a function of the evaporation time. We observe some inelastic loss of ^{40}K atoms when the ^{87}Rb BEC forms, but we do not see any sign of mechanical collapse. The data here correspond to temperatures between 10 and 0.1 K, and the Fermi gas reaches $T/T_F < 0.25$

This was true with or without a simultaneous ^{87}Rb MOT. While a higher MOT number for the fermionic atoms is not necessary for reaching quantum degeneracy with sympathetic cooling, it would be very helpful in optimizing and diagnosing sympathetic cooling. We have recently opened up our vacuum chamber and put in new homemade potassium sources. Initial measurements have seen about a factor of 10 improvement in the ^{40}K MOT number.

Interaction effects in the Bose-Fermi mixture

One goal of this project is to experimentally investigate interaction effects in the Bose-Fermi mixture, including looking for dramatic, interaction driven phenomena such as phase separation or mechanical collapse. Early on in the previous funding period the LENS group reported the observation of collapse a Bose-Fermi mixture of ^{40}K and ^{87}Rb atoms.⁵ The collapse was presumed to be due to a mechanical instability predicted for Bose-Fermi mixtures with large, attractive interactions between the bosons and fermions. The experimental observation was that of a large, sudden loss of potassium atoms just when the evaporative cooling produced a large BEC. We, of course, immediately set out to look for this phenomenon in our experiment. Even though we were using the same bosonic and fermionic species, a very similar trap strength, and slightly larger numbers of atoms, we did not observe any signature of interaction-driven collapse (see Fig. 1).¹ Furthermore, our measurements of the cloud density profiles also did not reveal strong interaction effects.

observe that the number of ^{40}K atoms at the end of evaporation was only a few percent of the initial number loaded into a magnetic trap. We believe that the observed number loss occurs very early in the cooling. JILA theorist John Bohn predicts that the elastic collision cross section for $^{40}\text{K} + ^{87}\text{Rb}$ collisions has a dramatic temperature dependence, with a relatively small elastic collision cross section for temperatures in the 100's of μK range. The low elastic collision rate here could cause the ^{40}K gas to remain much hotter than the directly cooled Bose gas and lead to losses early in the evaporative cooling.

The second difficulty we encountered is of a technical nature. We found that we had a fairly low number of potassium atoms in the MOT, which we attribute to a problem with our homemade potassium sources (enriched in ^{40}K).

Collapse phenomena, as well as other interaction driven effects, are expected to be strongly dependent on the interaction strength between the Bose and Fermi gases. The interspecies scattering length, which characterizing collisions between ^{40}K and ^{87}Rb atoms, is a key parameter that determines the equilibrium properties of the mixture. We used cross-dimensional rethermalization measurements to determine the elastic collision cross section, which is proportional to the square of the scattering length. We measured $|a_{\text{RbK}}| = 250 \pm 30 a_0$, where a_0 is the Bohr radius;¹ this value is lower than what was expected from the reported collapse of a ^{87}Rb and ^{40}K mixture.

Heteronuclear Feshbach resonances

In the last funding period we added a far-off resonance optical dipole trap (FORT) for the ultracold atoms. This additional technical capability increases the possible spin mixtures available for study and allows us to look for predicted interspecies Feshbach resonances⁶. We formed the FORT with a single 1030 nm Yb:YAG laser beam focused to a 20 μm waist and overlapped with our magnetic trap. The ultracold gas mixture was transferred from the magnetic trap into the FORT, and then rf adiabatic rapid passage was used to move the atoms in both species into their lowest energy spin-state. We then applied a uniform magnetic field and looked for trap loss as a signature of Feshbach resonances. Specifically, we looked for any loss of ^{40}K atoms in a mixture that had a much higher number (and density) of ^{87}Rb atoms. Data was also taken without the ^{87}Rb atoms present to test if the loss was dependent on interspecies interactions.

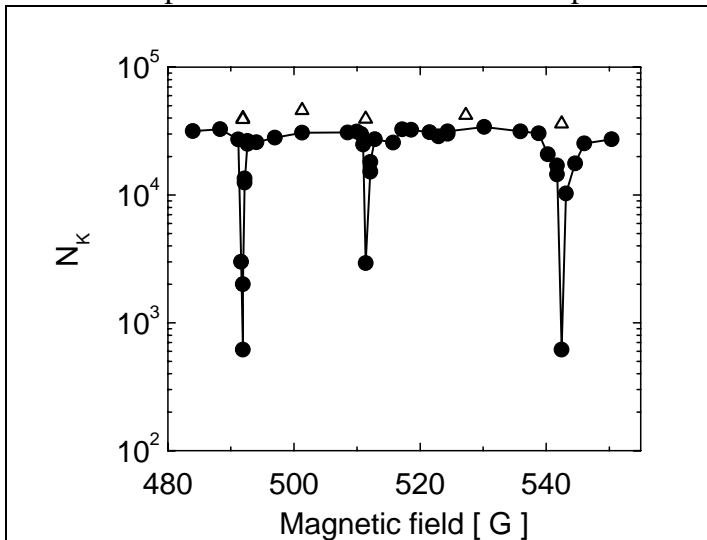


Figure 2. Heteronuclear magnetic-field Feshbach resonances² seen in ^{40}K trap loss. The ^{40}K number N_K is measured after holding at a fixed value of the magnetic field for 1 sec. Circles correspond to data taken in the presence of ^{87}Rb atoms and triangles correspond to a single-species ^{40}K gas. The sharp loss features correspond to enhanced three-body inelastic collision rate near the resonances.

We observed several sharp trap loss features as a function of the strength of the applied magnetic field (see Fig. 3). With theoretical help from John Bohn's group at JILA we identified these features as two s-wave resonances as well as one p-wave resonance. At the same time that we reported these results, the MIT group independently reported observations of Feshbach resonances between ^{23}Na and ^6Li atoms.⁴ These represent the first observation of Feshbach resonances between two different atomic species. Magnetic-field Feshbach resonances have become a powerful tool for many exciting ultracold atom experiments; these include, for example, the realization of Fermi superfluids⁷

and controlled collapse experiments with BEC's^{8,9}. These first observations of interspecies Feshbach resonance open up exciting new possibilities for Bose-Fermi

mixture experiments by allowing precise experimental control over the interactions between bosonic and fermionic atoms.

The best fit between theoretical calculations (John Bohn) and the measured magnetic-field locations of our three observed Feshbach resonances yielded a more precise value of $-281 \pm 15 a_0$ for the triplet scattering length.² This value is in good agreement with the result from our collisional relaxation measurement. The theoretical fit also suggested that another s-wave interspecies Feshbach resonance should be seen a slightly lower magnetic field strength, near 450 Gauss. Recently we observed this fourth resonance.

Future work will explore these Feshbach resonances as a tool for controlling interactions in the Bose/Fermi mixture. It will also be interesting to look for the creation of heteronuclear Feshbach molecules near the resonances.

DOE-supported Publications

1. J. Goldwin, S. Inouye, M. L. Olsen, B. Newman, B. D. DePaola & D. S. Jin, Measurement of the interaction strength in a Bose-Fermi mixture with Rb-87 and K-40, *Phys. Rev. A* **70**, 021601(R) (2004).
2. S. Inouye, J. Goldwin, M. L. Olsen, C. Ticknor, J. L. Bohn & D. S. Jin, Observation of heteronuclear Feshbach resonances in a mixture of bosons and fermions, *Phys. Rev. Lett.* **93**, 183201 (2004).
3. J. Goldwin, S. Inouye, M. L. Olsen & D. S. Jin, Cross-dimensional relaxation in Bose-Fermi mixtures, *Phys. Rev. A* **71**, 043408 (2005).

Bibliography

4. C. A. Stan, M. W. Zwierlein, C. H. Schunck, S. M. F. Raupach & W. Ketterle, Observation of Feshbach resonances between two different atomic species, *Phys. Rev. Lett.* **93**, 143001 (2004).
5. G. Modugno, G. Roati, F. Riboli, F. Ferlaino, R. J. Brecha & M. Inguscio, Collapse of a degenerate Fermi gas, *Science* **297**, 2240-2243 (2002).
6. A. Simoni, F. Ferlaino, G. Roati, G. Modugno & M. Inguscio, Magnetic control of the interaction in ultracold K-Rb mixtures, *Phys. Rev. Lett.* **90**, 163202 (2003).
7. C. A. Regal, M. Greiner & D. S. Jin, Observation of resonance condensation of fermionic atom pairs, *Phys. Rev. Lett.* **92**, 040403 (2004).
8. J. L. Roberts, N. R. Claussen, S. L. Cornish, E. A. Donley, E. A. Cornell & C. E. Wieman, Controlled collapse of a Bose-Einstein condensate, *Phys. Rev. Lett.* **86**, 4211-4214 (2001).
9. E. A. Donley, N. R. Claussen, S. L. Cornish, J. L. Roberts, E. A. Cornell & C. E. Wieman, Dynamics of collapsing and exploding Bose-Einstein condensates, *Nature* **412**, 295-299 (2001).

Ultrafast Atomic and Molecular Optics at Short Wavelengths

P.I.s: Henry C. Kapteyn and Margaret M. Murnane
Department of Physics and JILA
University of Colorado at Boulder, Boulder, CO 80309-0440
Phone: (303) 492-8198; FAX: (303) 492-5235; E-mail: kapteyn@jila.colorado.edu

PROGRAM SCOPE

The goal of this work is to study of the interaction of atoms and molecules with intense and very short (<20 femtosecond) laser pulses, with the purpose of developing new short-wavelength light sources, particularly at short wavelengths. We are also developing novel optical pulse shaping techniques to enable this work. There were five major highlights as a result of prior work –

- The first conclusive demonstration of very high-order harmonic generation from ions.
- Demonstration of a new mechanism for pulse compression at high intensities, that operates without the need for dispersion compensation.
- Demonstration of high harmonic emission from molecules, and UV pulse compression and phase matching of low-order harmonics from aligned molecules.
- Demonstration of the use of learning algorithms to understand and control electron dynamics on attosecond timescales.
- The first experimental demonstration of the use of quasi phase matching techniques for high-harmonic generation, resulting in the generation of coherent light in the “water window” region of the soft x-ray spectrum.

RECENT PROGRESS

In very recent work shown below, we observed high-harmonic (HHG) emission from molecules that are impulsively aligned using an ultrashort laser pulse. The alignment pulse creates a rotational wavepacket that subsequently evolves in time. The molecules periodically align (field-free) as the wavepacket evolves. We then probe the wavepacket by using a second more-intense laser pulse to generate high harmonics. HHG can be described by a “three-step model,” where the atom is first ionized in the optical field through tunnel ionization, followed by electron wavepacket propagation and recollision with the parent ion within a half-cycle of the driving optical field. In this picture, the energy of the high-harmonic emission can be directly related to the recolliding electron energy, and therefore to its de Broglie wavelength. Thus, observing high-harmonic radiation at any particular photon energy provides information on the recollision of an energy-selected, “monochromatic” low-energy electron. The wavelengths of the recolliding electrons-- ~0.1-1 nm for electrons in the energy range of 50-100 eV-- are well matched to interaction dimensions in molecules. By observing high-harmonic emission at varying times during the rotational revival, one can obtain the orientation dependence of HHG emission.

A number of recent experimental and theoretical studies have demonstrated that HHG can be enhanced by aligning the target molecules, and that structural information can be obtained from the spectral characteristics of the high-harmonic emission. It has been suggested by Paul Corkum and others that the electron recollision cross-section responsible for HHG relates directly to the projection of the valence orbitals with respect to the direction of propagation of the recolliding electron, making possible a new type of molecular tomography. Other studies have suggested that quantum interference effects can come into play when the wavelength of the recolliding electron is comparable to interatomic separations in the molecule. In particular, the symmetry, shape and relative orientation of the molecular orbital to the propagation direction of the

returning electron determine the probability of recombination. Thus, by monitoring the HHG yield as a function of the orientation of the molecule with respect to the propagation of the recolliding electron, which is parallel to the polarization of the optical electric field vector, one can map out the molecular orbital.

In initial studies in our lab, we studied the effect of field-free molecular alignment on high-harmonic generation (HHG) in O_2 , CO_2 and other gases. Most importantly, these data include simultaneous detection over a broad range of harmonic orders, allowing for comparison of the relative enhancement (or suppression) of high harmonic emission with alignment, as a function of the energy of the recolliding electron. In these experiments, the molecules align parallel to the polarization ~ 100 fs after the pump pulse. The upper graphs in Figure 1 depict the normalized high harmonic signal, i.e. the ratio of the high harmonic signal with and without pump pulse, from CO_2 as a function of the time delay Δt for harmonic orders 21, 25, 29, 33 and 37. The high harmonic signal was obtained by integrating over the corresponding peak in the harmonic spectrum. At each time-delay step of 25 fs, the signal was accumulated over 10 s. The high harmonic signals are strongly modulated at the time delays corresponding to the $\frac{1}{4}$, $\frac{1}{2}$, $\frac{3}{4}$ and full revival times ($T_{rot} = 42.70$ ps, $B_e = 0.3906$ cm^{-1}). Between these time delays very small modulations are observable. We observe very different behavior in O_2 to CO_2 .

Figure 2 plots the ratios of the integrated spectral lines from aligned and anti-aligned CO_2 molecules to the isotropically distributed samples, for harmonic orders 19 to 47 at three time-delays when the molecules are aligned, and also when they are anti-aligned. The observed modulations in enhancement as a function of harmonic order cannot be explain using simple models based on internuclear separation to calculate the expected quantum interferences, and do not agree with other published work. Therefore, we are working with more general theory in collaboration with Tamar Seideman to explain these results. In the future, we will expand on this work to study the dynamics of structural changes in molecules through monitoring the HHG yield from excited molecules.

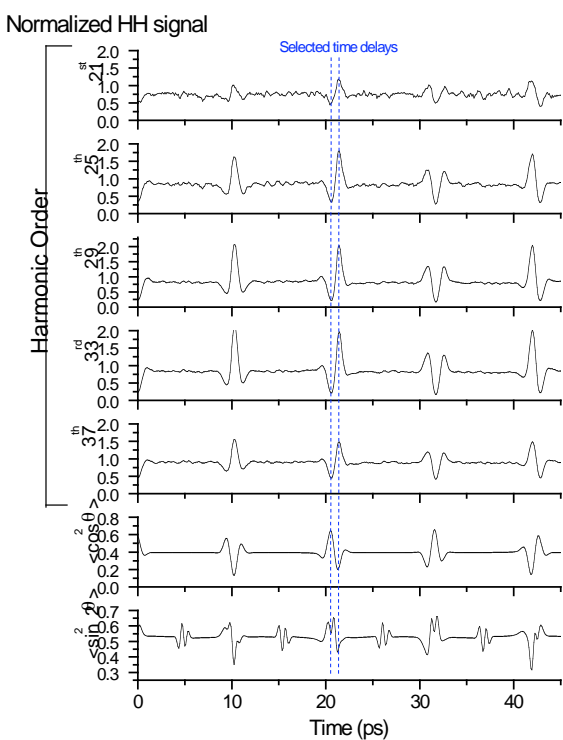
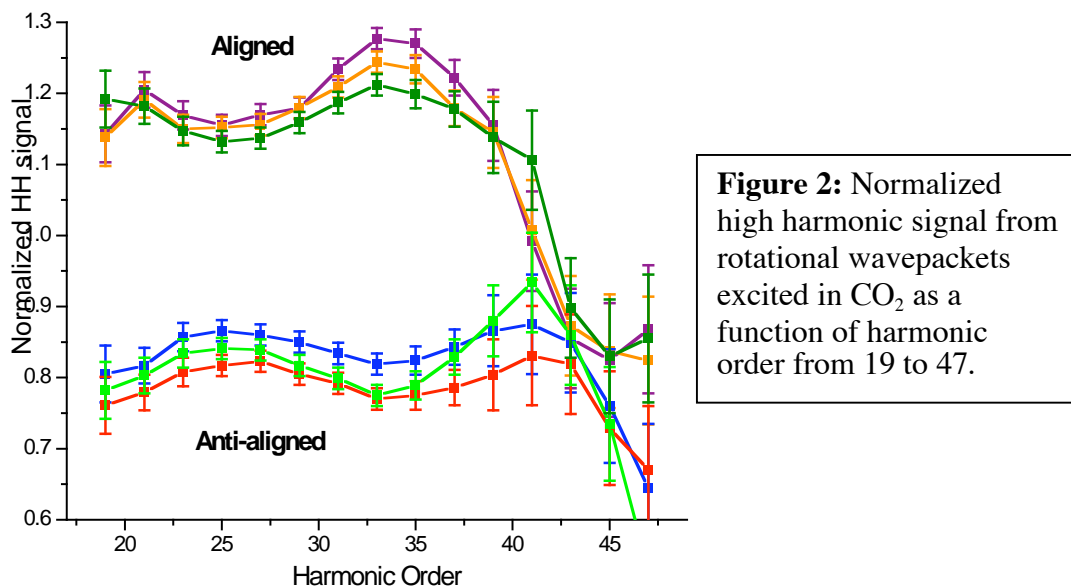


Figure 1: Normalized high harmonic signal from rotational wavepackets excited in CO_2 as a function of time delay between the alignment pulse and the probe pulse that generates the harmonics. The signal from several harmonic orders between 21 and 37 is given.



FUTURE PLANS

During 2005-6, we plan further data analysis with the objective of evaluating HHG as a method for probing molecular dynamics. The goal is to develop a novel probe of molecular systems that combines atomic-scale spatial resolution with femtosecond time resolution. We are implementing a VUV generation setup to resonantly excite transitions in small molecules, to implement an “align-pump-probe” scheme.

Publications (refereed) as a result of DOE support since 2002

1. R. Bartels, T. Weinacht, N. Wagner, M. Baertschy, C. Greene, M. Murnane, H. Kapteyn, “Phase Modulation of Ultrashort Light Pulses using Molecular Rotational Wavepackets”, *Phys. Rev. Lett.* **88**, 019303 (2002).
2. C. Durfee, L. Misoguti, S. Backus, R. Bartels, M. Murnane and H. Kapteyn, “Phase Matching in Cascaded Third-Order Processes, *JOSA B* **19** (4): 822-831 (2002).
3. S. Christensen, H.C. Kapteyn, M.M. Murnane, S. Backus, "Simple, high power, compact, intracavity frequency-doubled Q-switched Nd:YAG laser," *Rev. Sci. Instrum.* **73** (5): 1994-1997 (2002).
4. R. Bartels, N. Wagner, M. Baertschy, J. Wyss, M. Murnane, H. Kapteyn, "Phase-matching conditions for nonlinear frequency conversion by use of aligned molecular gases," *Opt. Lett.* **28**, 346 (2003).
5. Ariel Paul, Randy Bartels, Ivan Christov, Henry Kapteyn, Margaret Murnane, Sterling Backus, “Multiphoton photonics: quasi phase matching in the EUV”, *Nature* **421**, 51 (2003).
6. E. Gibson, A. Paul, N. Wagner, R. Tobey, I. Christov, D. Attwood, E. Gullikson, A. Aquila, M. Murnane, H. Kapteyn, “Generation of coherent soft x-rays in the water window using quasi phase-matched harmonic generation”, *Science* **302**, 95 (2003).
7. E. Gibson, A. Paul, N. Wagner, R. Tobey, I. Christov, M. Murnane, H. Kapteyn, “Very High Order Harmonic Generation in Highly Ionized Argon”, *Physical Review Letters* **92**, 033001 (2004).
8. R. Tobey, E. Gershgoren, M. Siemens, M.M. Murnane, H.C. Kapteyn, T. Feuerer, K. Nelson, “Photothermal and Photoacoustic Transients probed with Extreme Ultraviolet Radiation”, *Appl. Phys. Lett.* **85**, 564 (2004).
9. David M. Gaudiosi, Amy Lytle, Pat Kohl, Margaret M. Murnane, Henry C. Kapteyn, Sterling Backus, “Downchirped Pulse Amplification”, *Optics Letters* **29**, 2665-2667 (2004).
10. Randy A. Bartels, Margaret M. Murnane, Herschel Rabitz, Ivan P. Christov, and Henry C. Kapteyn, “Using learning algorithms to study attosecond dynamics”, *Phys. Rev. A* **70**, 112409 (2004).
11. N. Wagner, E. Gibson, T. Popmintchev, I. Christov, M. Murnane, H. Kapteyn, “Self-compression of ultrashort pulses through ionization-induced spatio-temporal reshaping”, *PRL* **93**, 173902 (2004).

12. E. A. Gibson, I. P. Christov, M. M. Murnane, and H. C. Kapteyn, "Quantum Control of High Harmonic Generation: Applied Attosecond Science," in *Femtosecond Optical Frequency Comb: Principle, Operation, and Applications*, J. Ye, Ed.: Kluwer Publishing Company, 2004.
13. E. Gibson, X. Zhang, T. Popmintchev, A. Paul, N. Wagner, A. Lytle, I. Christov, M. Murnane, H. Kapteyn, "Extreme Nonlinear Optics: Attosecond Photonics at Short Wavelengths", **invited**, *JSTQE* **10**, 1339 (2004).
14. Henry C. Kapteyn, Margaret M. Murnane and Ivan P. Christov, "Coherent X-Rays from Lasers: Applied Attosecond Science", **invited article**, *Physics Today*, page 39 (March 2005).
15. A. Paul, E.A. Gibson, X. Zhang, A. Lytle, T. Popmintchev, X. Zhou, M.M. Murnane, I.P. Christov, H.C. Kapteyn "Phase matching techniques for coherent soft-x-ray generation", **invited paper**, *JSTQE* (to be published 2005)

Physics of Low-Dimensional Bose-Einstein Condensates, Grant No. DE-FG02-01ER15203

Eugene B. Kolomeisky (PI)
Department of Physics
University of Virginia
382 McCormick Road
P.O. Box 400714
Charlottesville, Virginia 22904-4714
ek6n@virginia.edu

The project consists in investigating fundamental properties of low-dimensional superfluids (Bose-condensed alkali gases in strongly anisotropic traps, for example) and related systems within a wider scope of the DOE Nanoscale Science, Engineering, and Technology Initiative.

Recent Progress

During the period of September 2004 - September 2005 we have been working on several projects described below in some detail:

- E.B. Kolomeisky and M. Timmins, **The Zel'dovich effect and evolution of atomic Rydberg spectra along the Periodic Table**, Phys. Rev. A, to be published (2005), <http://arxiv.org/abs/physics/0504154>. In 1959 Ya. B. Zel'dovich predicted that the bound-state spectrum of the non-relativistic Coulomb problem distorted at small distances by a short-range potential undergoes a peculiar reconstruction whenever this potential alone supports a low-energy scattering resonance. However documented experimental evidence of this effect has been lacking. Previous theoretical studies of this phenomenon were confined to the regime where the range of the short-ranged potential is much smaller than Bohr's radius of the Coulomb field. We went beyond this limitation by restricting ourselves to highly-excited s states. This allowed us to demonstrate that along the Periodic Table of elements the Zel'dovich effect manifests itself as systematic variations of the Rydberg spectra having their origin in the binding properties of the ionic core of the atom. Specifically we modeled the residual atomic ion by the Thomas-Fermi-Latter model and computed the corresponding *systematic* quantum defect μ . After subtracting from the outcome the semiclassical background μ_{sc} we observed that the variation of the quantum defect which is due to the Zel'dovich effect, is nearly periodic function of the cubic root of the atomic number $Z^{1/3}$. In order to single out the Zel'dovich effect in experimental and numerical spectra we conducted Fourier analysis of the quantum defect variation

$$\delta\mu(Z^{1/3}) = \mu - \mu_{sc} = \sum_k \mu_k \exp(ikZ^{1/3}) \quad (1)$$

The result for the magnitude of the Fourier coefficients $|\mu_k|$ as a function of k is displayed in Fig. 1 as a series of solid dots which for convenience are connected by straight line segments. The finite values of μ_0 correspond to the presence of nonzero background in experimental and numerical $\delta\mu(Z^{1/3})$ dependences and are of no interest.

For comparison in Fig. 1 we also show the Fourier spectrum of our systematic calculation which, as expected, has only one peak corresponding to the Zel'dovich effect.

Both the experimental and numerical spectra in Fig. 1 have peaks at the same value of $k \simeq 11$ which we argue are the signatures of the Zel'dovich effect (a compilation of experimental data with pertinent references can be found in our paper; the numerical data are due to Manson (1969) and Fano, Theodosiou and Dehmer (1976)).

- Xiao Yang and Chetan Nayak, **Ferromagnetism of Weakly-Interacting Electrons in Disordered Systems**, submitted to Phys. Rev. B (2005), <http://arxiv.org/abs/cond-mat/0501431>. It was realized two decades ago that the two-dimensional diffusive Fermi liquid phase is unstable against arbitrarily weak electron-electron interactions. Recently, using the nonlinear sigma model developed by Finkelstein, several authors have shown that the instability leads to a ferromagnetic state. This paper considers diffusing electrons interacting through a ferromagnetic exchange interaction. Using the Hartree-Fock approximation to directly calculate the electron self-energy, it is found that the total energy is minimized by a finite ferromagnetic moment for arbitrarily weak interactions in two dimensions and for interaction strengths exceeding a critical

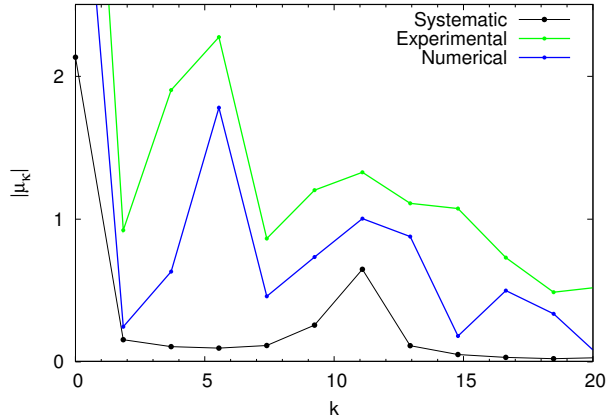


Figure 1: Systematic, experimental and numerical amplitudes of the Fourier coefficients of the quantum defect variation (arbitrary units, same normalization) $|\mu_k|$ as functions of k for $k \geq 0$. The peaks at $k \simeq 11$ correspond to the Zel'dovich effect.

value proportional to the conductivity in three dimensions. The relation between these and previous results is discussed.

- E. B. Kolomeisky and M. Timmins, **Quantum dissociation of an edge of a Luttinger liquid**, submitted to Phys. Rev. Lett. (2005), <http://arxiv.org/abs/cond-mat/0506375>. In a Luttinger liquid phase of one-dimensional molecular matter the strength of zero-point motion can be characterized by the dimensionless De Boer's number quantifying the interplay of quantum fluctuations and two-body interactions. Selecting the latter in the Morse form we show that dissociation of the Luttinger liquid is a process initiated at the system edge. The latter becomes unstable against quantum fluctuations at a value of De Boer's number which is smaller than that of the bulk instability which parallels the classical phenomenon of surface melting.

Future Plans

The demonstration of the Zel'dovich effect in zero angular momentum Rydberg spectra required rather involved analysis which would be impossible to conduct without a guide coming from theoretical understanding of the problem. Therefore we generally plan to carry out calculations pertinent to the physics of the Zel'dovich effect for a series of experimental systems with the goal to compare experimental data with theoretical calculations.

•**Spectral periodicity due to the effects of the shell structure.** An inspection of Fig. 1 reveals that both experimental and numerical spectra have another peak in common located at $k \simeq 5.5$. This peak which is about twice as high as that due to the Zel'dovich effect is natural to relate to the effects of the shell structure. The existence of this peak translates into the $(2\pi/5.5)Z^{1/3} = 1.14Z^{1/3}$ periodicity of the quantum defect variation due to the effects of the shell structure. This conclusion resembles the $Z^{1/3}$ periodic oscillation of the ground-state energy of an atom away from the systematic trend first found by Englert and Schwinger (1985). The numerical difference between the Englert-Schwinger periodicity and our finding in Fig. 1 is within our uncertainty of the peak location. So one explanation might be that our result is a manifestation of the same effect for highly-excited states. We plan to conduct calculations necessary to bring understanding to this issue. It appears that the Englert-Schwinger calculation can be generalized to go beyond the ground-state properties.

•**Zel'dovich effect in other Rydberg systems.** Our analysis can be extended and adopted in several directions for a series of Rydberg systems:

First, there is an abundance of experimental and numerical data for atomic Rydberg states of finite angular momenta which are likely to contain signatures of the Zel'dovich effect. However, in the limit of a very short-ranged inner potential the way the effect manifests itself is somewhat different from its s state

counterpart. This observation makes it pertinent to generalize our analysis to the case of finite angular momentum.

It has been known for some time that the Rydberg formula is superior to the Wannier (Bohr) formula quoted in solid state textbooks in representing excitonic spectra in condensed matter systems. Experimental examples here include clean and doped rare-gas solids and rare-gas impurities in solid hydrogen. Although this is a context in which the Zel'dovich effect has been originally discovered, to the best of our knowledge there were no attempts to relate it to excitonic quantum defects. Because of the dielectric screening of the Coulomb interaction, the Zel'dovich effect in these systems is expected to be more pronounced than in atomic Rydberg spectra. Only minor changes to our analysis are needed to understand the excitonic Rydberg spectra.

Other examples of systems where the Zel'dovich effect should have experimental signatures include Rydberg ions and electronic image states. Here the models of the inner potential will have to be reworked.

Finally we plan to generalize our results to the case of strong magnetic fields which would be pertinent to the properties of matter in the exterior of a neutron star.

•**Interplay between the Zel'dovich and Efimov effects in a three-boson problem.** The Efimov effect occurring in a system of three attractive bosons consists in the formation of arbitrarily large number of loosely bound three-body levels whenever two-body forces are resonant. Exactly at the two-body resonance the effect can be understood as due to the presence of an effective universal attraction decaying as an inverse square of distance. Sufficiently strong attraction of such form is known to lead to the phenomenon of “fall to the center” and the formation of infinitely large number of bound states.

At short distances, however, the infinite range inverse-square attraction gives its way to other forces whose nature depends on the details of direct interparticle interactions. Thus we have a problem where the Zel'dovich effect will take place, and we plan to study how the three-body spectrum evolves in response to changes of the short-range part of the potential. The results might have features in common with those found by Popov (1971) in his analysis of the Dirac equation for an electron in a field of the bare nucleus of charge Ze with $Z > 137$: here the phenomenon of fall to the center also played a crucial role.

•**Universality class of the Coulomb blockade problem.** The goal of this project is to understand how quantum fluctuations arising from the coupling of a quantum dot and a reservoir of electrons modify the classical picture of the Coulomb blockade. This is one of the outstanding problems of mesoscopic physics.

Quantum mechanical tunneling of charge between connecting leads and the dot has been argued to smear the Coulomb staircase even at zero temperature. Although originally treated perturbatively, the smearing finds its strongest support in a connection of the quantum dot problem to a highly anisotropic Kondo problem (Matveev, 1991). In the limit of low transparency, i.e. a small tunneling matrix element, and of large Coulomb repulsion, the charge dynamics on the dot can be approximated by that of a two-level system, with the levels corresponding to charge states of the dot differing by unit charge. Changing the charge on the dot then becomes akin to flipping an impurity spin-1/2. In Kondo language the net charge on the dot parallels the magnetization of the impurity spin while the deviation of the gate voltage from the half-integer value is akin to a Zeeman field applied to the Kondo spin. For a single-channel Kondo problem, the spin susceptibility is well-known to be finite at zero applied field. This correspondingly necessitates the smearing of any discrete charge jump with the variation of the gate voltage.

The connection to a Kondo problem applies in the weak-tunneling limit. The opposite high-transparency limit was treated by Matveev (1995). On the basis of this work it was possible to conjecture that the smeared Coulomb staircase of the weak-tunneling limit smoothly evolves as tunneling is increased into a strictly linear function of the gate voltage. These predictions found partial confirmation in experimental work. The agreement between theory and experiment was limited by finite temperature effects, with the temperature of the quantum dot being far in excess of the putative Kondo temperature.

In DOE supported work the role of quantum fluctuations was re-examined for a large quantum dot - the dot whose charging energy $e^2/(2C)$ is substantially larger than the distance between the energy levels on the dot. We demonstrated that as the strength of the tunneling is tuned, changing the dot from open to closed, a modified Coulomb staircase reappears under certain circumstances with non-zero tunneling. In particular we find that quantum fluctuations need not destroy the Coulomb blockade. We in part arrived at this general conclusion by relating the zero-temperature dynamics of interacting spinless electrons to the classical statistical mechanics of a one-dimensional Ising model with ferromagnetic interactions decaying as

the inverse-square of distance. Within the Ising universality class, we found that all experimental systems must be either of the Kondo subclass (to which the connection to the Kondo system applies) or of a novel tricritical type.

Analyzing the problem by the methods borrowed from classical statistical mechanics our work went beyond the existing treatments questioning universality of the connection to the Kondo problem. Specifically for non-interacting electrons our results are in variance with those based on the Kondo analogy. At the same time we could not state decisively that earlier results are incorrect as we used a variational analysis which is only as good as the ansatz for the wave function.

In this project we will re-examine the whole problem taking into account the electron spin. This is important because this is where the strongest argument in favor of the Kondo connection has been given: Matveev (1995) demonstrated exactly that in the limit of high transparency the capacitance of the dot has a logarithmic singularity whenever the average population of the dot is half-integer. The low-transparency treatment of this problem which used the analogy to the *two-channel* Kondo problem also found a logarithmic divergence which allowed Matveev to argue that the connection to the Kondo problem is universally applicable.

The logarithmic divergence of the high-transparency limit has its origin in the presence of a corresponding logarithmic term in the energy of the dot as a function of the gate voltage. In the theory of critical phenomena this is usually a sign of a marginal situation which we argue presently is due to the assumption of noninteracting electrons in the leads. If this is the case, for *interacting* electrons the logarithmic correction will be replaced by a power law thus having very little to do with the Kondo problem. We claim that this is what is going on, and intend to demonstrate it as follows:

A very similar situation occurs in the context of the Peierls instability (1955) where the electronic energy gain as a function of lattice distortion has a logarithmic correction. Using a renormalization-group method J. P. Straley and the PI (1996) demonstrated that for interacting electrons this correction is replaced by a power law. It appears that a similar treatment can be conducted for the quantum dot problem. If successful, it will allow us to make a reliable statement about the universality class of the Coulomb blockade problem.

The next step would be to analyze the problem again for arbitrary transparency using the variational method of our work, and assess its accuracy via comparison with high-transparency renormalization-group results.

DOE Sponsored Publications during 2002-2005

- E. B. Kolomeisky and M. Timmins, *The Zel'dovich effect and evolution of atomic Rydberg spectra along the Periodic Table*, Phys. Rev. A, to be published (2005), <http://arxiv.org/abs/physics/0504154>.
- J. P. Straley, E. B. Kolomeisky, and S. C. Milne, *The Bose molecule in one dimension*, Journal of Statistical Physics, **116**, 1579 (2004)
- T.J. Newman, E.B. Kolomeisky, and J. Antonovics, *Population dynamics with global regulation: The conserved Fisher equation*, Phys. Rev. Lett. **92**, 228103 (2004).
- E. B. Kolomeisky, J. P. Straley, and R. M. Kalas, *Ground-state properties of artificial bosonic atoms, Bose interaction blockade and the single-atom pipette*, Phys. Rev. A **69**, 063401 (2004).
- E. B. Kolomeisky, X. Qi, and M. Timmins, *Ground-state properties of one-dimensional matter and quantum dissociation of a Luttinger liquid*, Phys. Rev. B **67**, 165407 (2003).
- E. B. Kolomeisky, R. M. Konik, and X. Qi *Quantum fluctuations of charge and phase transitions of a large Coulomb-blockaded quantum dot*, Phys. Rev. B **66**, 075318 (2002).

Program Title:

"Ion/Excited-Atom Collision Studies with a Rydberg Target and a CO₂ Laser"

Principal Investigator:

Stephen R. Lundeen,
Dept. of Physics
Colorado State University
Ft. Collins, CO 80523
Lundeen@Lamar.colostate.edu

Program Scope:

The program involves three projects, two involving the interaction of multiply-charged ion beams with a Rydberg target, and one involving multiply-excited Rb atoms in a MOTRIMS target.

- 1) Studies of the fine structure of high-L Rydberg ions, in order to extract measurements of polarizabilities and electric moments of their positive ion cores.
- 2) Studies of X-rays emitted from the highly-excited Rydberg ions formed in charge capture collisions by highly-charged ions on Rydberg atoms.
- 3) Stepwise excitation of a Rb MOT to high Rydberg states within a MOTRIMS apparatus in order to study the n-dependence of charge capture cross sections.

Recent Progress and Immediate Plans:

Project 1) The eventual goal of this project is to measure polarizabilities and electric moments of high ionization states of actinide ions using the RESIS/microwave technique. Ions like U⁶⁺, U⁴⁺, and Th⁴⁺ often appear in actinide chemistry as nearly free ions, and measurement of the properties that control their long-range interactions, such as polarizabilities and electric moments, can provide new input to chemical models while also checking *a-priori* descriptions of these important ions. A renewal proposal, submitted this year, aims to achieve this, building on the progress already achieved demonstrating the use of the RESIS/microwave technique to measure properties of multiply-charged ions [1,2]. A review paper, submitted this year, discusses the previous work, both experimental and theoretical, which supports this application of Rydberg spectroscopy [3].

An important complement to the new studies of Rydberg ion fine structure[1,2] is the study of Rydberg fine structure in heavy neutral atoms. These studies promise to strengthen the theoretical foundation needed for the actinide ion studies. Over the past two years, we have extensively studied the fine structure in Rydberg states of the Barium atom [4,5], extending measurements to much higher L than studied previously [6]. This year, initial results of a RESIS/microwave study were reported [5] measuring $6 \leq L \leq 11$ fine structure intervals in n=17 and n=20 of Barium. The scaled results of these measurements, illustrated in Fig. 1, result in an improved determination of the dipole and quadrupole polarizabilities of Ba⁺, which are expected to be related to the intercept and initial slope of the scaled plot. Table I summarizes the comparison with previous measurements and with theory [7]. Additional measurements, needed to complete this Barium study, are now in progress.

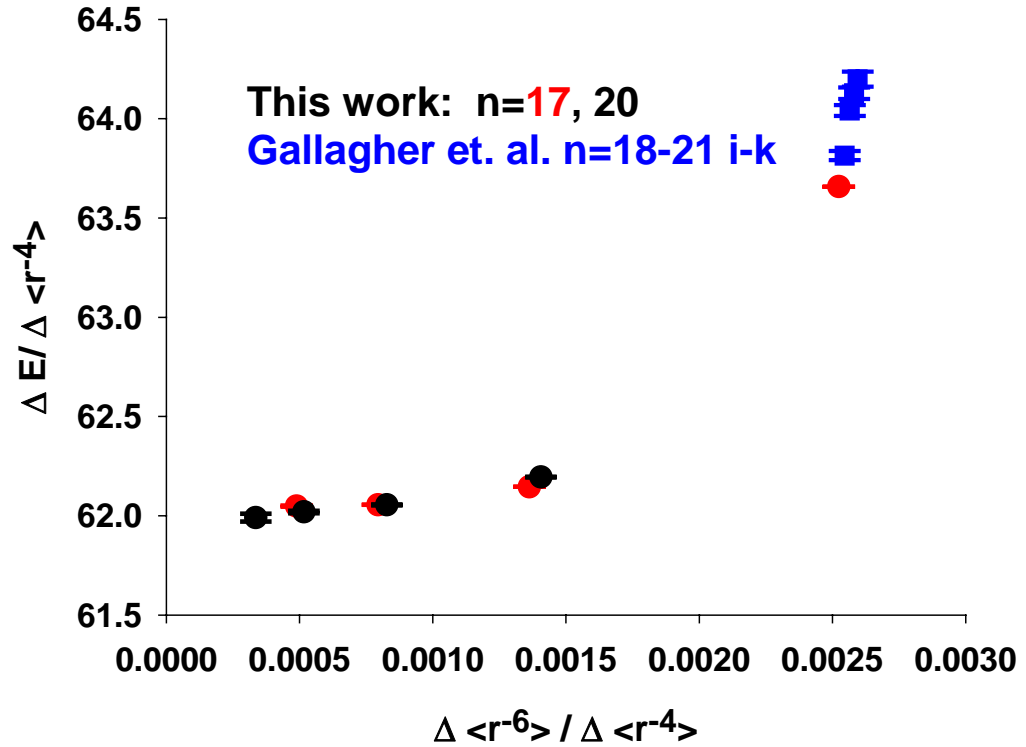


Fig. 1. Scaled plot showing measured fine structure intervals in $6 \leq L \leq 11$ Rydberg levels of $n=17$ and $n=20$ states of Barium (Red and Black points)[5], along with similarly scaled measurements of $L=6$ to $L=7$ intervals in $n=18-21$ (Blue points) [6]. The intercept and slope of this scaled plot are related to the dipole and quadrupole polarizabilities of Ba^+ .

Table I. Comparison of measured dipole and quadrupole polarizabilities of Ba^+ with previous measurements and with theory.

	$\alpha_d(a_0^3)$	$\alpha_Q(a_0^5)$
Theory[7]	124	4240
RESIS/microwave[5]	124.01(5)	3712(232)
RESIS/optical[4]	124.30(16)	2462(361))
Previous Expt.[6]	125.5(1.0)	2050(100)

Project 2) This project has studied the effect of small electric fields on the X-rays emitted after charge capture by highly charged bare and hydrogenic ions from Rydberg atoms. Because the products of such charge transfer are very high Rydberg states of hydrogenic and helium-like ions, the spectrum of x-rays they emit and the rate at which they emit them may be altered by small electric fields, $\leq 10V/cm$, which are nevertheless large enough to Stark-mix the emitting Rydberg manifold. Our measurements confirmed

the details of this process [8]. Often the X-ray emission rate from such states is modeled as either 1) free radiative decay or 2) collisionally mixed decay. In 2), it is assumed that collisional mixing is rapid enough to maintain a fully statistical distribution of states throughout the emission process. Our results point to a third regime, 3) Stark-mixed decay, which obtains in modest external electric fields if collisional mixing is weak. In this case, the rate and spectral distribution of X-ray emission depends on the m-distribution of the Rydberg population with respect to the electric field and can be substantially different from free radiative decay.

Project 3) Our interest in applying the MOTRIMS technique to study of ion-Rydberg collisions stems from the unique ability of the MOTRIMS to measure relative cross sections of capture from different n-levels without needing to establish the relative target thickness of each n[8]. As of this date, we have not yet excited Rydberg levels within the MOTRIMS apparatus, but we expect to do so in late summer, 2005. We have excited $4D_{5/2}$ levels in the Rb MOT and measured the relative capture cross section of 5S, 5P, and 4D levels, a necessary preliminary step to measuring the capture cross section from Rydberg levels [9].

References

- [1] “Determination of the polarizability of Na-like Silicon by study of the fine structure of high-L Rydberg states of Si^{2+} ”, R.A. Komara, M.A. Gearba, S.R. Lundeen, and C.W. Fehrenbach, *Phys. Rev A* 67, 062502 (2003)
- [2] “Ion Properties from High-L Rydberg Fine Structure: Dipole Polarizability of Si^{2+} ” R.A. Komara, M.A. Gearba, C.W. Fehrenbach, and S.R. Lundeen, *J. Phys. B. At. Mol. Opt. Phys.* 38, S87 (2005)
- [3] “Fine Structure in High-L Rydberg states: A Path to Properties of Positive Ions”, S.R. Lundeen, in *Advances in Atomic, Molecular, and Optical Physics, Vol. 52* edited by Chun C. Lin and Paul Berman (Academic Press, 2005)
- [4] “Determination of dipole and quadrupole polarizabilities of Ba^+ by measurement of the fine structure of high-L, n=9 and 10 Rydberg states of Barium” E.L. Snow, M.A. Gearba, W.G. Sturru, and S.R. Lundeen, *Phys. Rev A* 71, 022510 (2005)
- [5] “Fine structure measurements in high-L, n=17 and 20 Rydberg states of Barium: A re-determination of the dipole and quadrupole polarizabilities of Ba^+ ”, E.L. Snow and S.R. Lundeen, *Bull. Am Phys. Soc.* 50(3) 72 (2005)
- [6] “Radio frequency resonance measurements of the Ba $6sng-6snh-6sni-6snk$ intervals: An investigation of the nonadiabatic effects in core polarization”, T.F. Gallagher, R. Kachru, and N.H. Tran, *Phys. Rev. A* 26, 2611 (1982)
- [7] Andrei Derevianko, private communication
- [8] “Stark-induced X-ray emission from H-like and He-like Rydberg ions”, M.A. Gearba, R.A. Komara, S.R. Lundeen, C.W. Fehrenbach, and B.D. DePaola, *Phys. Rev A* 71, 013424 (2005)
- [9] “State Selective charge transfer cross sections for Na^+ with multiply excited rubidium: A unique diagnostic of MOT dynamics”, X. Flechard, H. Nguyen, R. Bredy, S.R. Lundeen, M. Stauffer, H.A. Camp, C.W. Fehrenbach, and B.D. DePaola, *Phys. Rev. Letters* 91, 243005 (2003)

Publications appearing or accepted during this grant period:

- 1) “Ion Properties from High-L Rydberg Fine Structure: Dipole Polarizability of Si^{2+} ”
R.A. Komara, M.A. Gearba, C.W. Fehrenbach, and S.R. Lundeen, *J. Phys. B. At. Mol. Opt. Phys.* 38, S87 (2005)
- 2) “Stark-induced X-ray emission from H-like and He-like Rydberg ions”, M.A. Gearba, R.A. Komara, S.R. Lundeen, C.W. Fehrenbach, and B.D. DePaola, *Phys. Rev A* 71, 013424 (2005)
- 3) “Determination of dipole and quadrupole polarizabilities of Ba^+ by measurement of the fine structure of high-L, $n=9$ and 10 Rydberg states of Barium” E.L. Snow, M.A. Gearba, W.G. Sturru, and S.R. Lundeen, *Phys. Rev A* 71, 022510 (2005)
- 4) “Fine Structure in High-L Rydberg states: A Path to Properties of Positive Ions”, S.R. Lundeen, in *Advances in Atomic, Molecular, and Optical Physics, Vol. 52* edited by P.R. Berman and C.C. Lin (Academic Press, 2005)

Photoabsorption by Atoms and Ions

Steven T. Manson, Principal Investigator

Department of Physics and Astronomy, Georgia State University, Atlanta, Georgia 30303
(smanson@gsu.edu)

Program Scope

The goal of this research program is provide a theoretical adjunct to, and collaboration with, the various atomic and molecular experimental programs that employ third generation light sources, particularly ALS and APS. Calculations are performed employing cutting-edge methodologies with two major aims in mind: providing deeper insight into the physics of the experimental results; and providing guidance for future experimental investigations. The general areas of programmatic focus are: manifestations of nondipole effects in atomic and molecular photoionization; photodetachment of inner and outer shells of negative ions; photoionization of positive ions in ground and excited states; and many-body effects in high-energy photoionization.

Recent Progress

1. Nondipole Effects in Atoms

Up until relatively recently, the conventional wisdom was that nondipole effects in photoionization were of importance only at photon energies of tens of keV or higher, despite indications to the contrary 35 years ago [1]. The last decade has seen an upsurge in experimental and theoretical results [2] showing that nondipole effects in photoelectron angular distributions could be important down to hundreds [3] and even tens [4] of eV. Our recent work has been involved in trying to delineate situations where the nondipole effects are competitive with the dipole effects at low energy. One such situation has been found in the $3p$ photoionization of atomic Ca, along with Ca^+ and Ca^{++} [5]. In the neighborhood of photon energy of 53 eV is the $3s \rightarrow 3d$ *quadrupole* resonance. This resonance shows up very strongly, enhancing the nondipole photoelectron angular distribution parameter γ in the $3p$ channel by more than an order of magnitude to a value of about 1.2, making the nondipole contribution quite competitive with the dipole in this energy region. It is to be emphasized that the relative strength of the nondipole contribution is not due to a weakening of the dipole amplitude (such as in the vicinity of a Cooper minimum), but rather to the strength of the quadrupole resonance itself. Furthermore, significant nondipole effects mean that significant momentum is transferred to the atom from the photon; this results in a net velocity of the photoelectrons in the direction of the incident photons producing a current known as the “drag current” [6]. Both the nondipole photoionization parameters and the drag current predicted appear to be excellent cases for experimental studies.

2. Photodetachment of the C^- Negative Ion

Negative ion photodetachment serves as a “laboratory” for the study of electron-electron correlation since many-electron interactions generally dominate both the structure and dynamics of negative ions. In connection with our recent studies of inner-shell photoabsorption by He^- [7,8] and Li^- [9,10], the R-Matrix code was enhanced to deal with photodetachment—particularly the final-state wave function which was beyond

the then-extant R-Matrix code. Using this experience we have moved on to the C^- ion which is of interest for a number of reasons: there was significant theoretical disagreement for the photodetachment cross section of the ground state of C^- ; C^- is one of the few negative ions to have a bound excited state; and there is experimental data on the cross section for K-shell photodetachment of C^- . Previously, we have looked at the valence photodetachment of the ground 4S state [11]. More recently, the photodetachment of the excited 2D state was considered [12]. In this calculation, which agrees well with experiment for both σ and β (unfortunately only at a single energy) a more limited previous R-Matrix calculation is corrected and the disagreements are reconciled. In addition, many examples of the Auger decay of shape resonances are found, and a detailed exposition of the photodetachment process leading to the lowest 13 states of neutral C is presented.

3. Photoionization of Positive Ions of Be Isoelectronic Sequence

Experimental studies of the photoionization of positive ions have seen a recent upsurge owing to the availability of facilities such as ALS and APS [13]. The Be isoelectronic sequence offers an attractive area of theoretical investigation for a number of reasons: the ions are four-electron systems so the possibility exists of treating them with high accuracy; the four-electron system is quite stable and, therefore, they are ubiquitous in many laboratory and astrophysical plasmas; and there have been recent experimental investigations of several members of the sequence. Employing the eigenchannel R-Matrix methodology [14] that we previously used to study the photoionization of neutral Be in its ground [15] and excited [16] states, and ground-state B^+ [17], our program to study the photoionization of the ions of Be sequence has been continued. Both excited-state B^+ [18] and ground-state C^{+2} [19] have been completed. Of particular interest in these investigations is that the resonance series converging to the various states of the residual ion overlap more and more, with increasing Z , leading to very strongly perturbed resonance series and almost chaotic-looking behavior. Despite the complexity, however, for each resonance we have been able to provide its identification, the resonance energy and the resonance width. Experimental cross sections have been measured in the region below the $2p$ thresholds for B^+ [20] and C^{+2} [21], and we find excellent agreement with the experimental results.

4. Many-Body Effects in High-Energy Dipole Photoionization

The asymptotic high-energy form of the dipole photoionization cross section is a classic problem in atomic physics that was thought to have been solved years ago [22,23]. Recent work has shown that electron-electron correlation, in the form of interchannel coupling, changes the asymptotic form for non- s initial states [24]. We have recently investigated further and surprising new results were found as a consequence of the inclusion of initial-state configuration interaction [25]: The asymptotic form for almost all non- s subshells, of all atoms becomes $E^{-7/2}$ just like s -subshells; and the dominant transition at high energy is photoionization plus excitation, a two-electron satellite transition. This has important implications for double photoionization out of non- s subshells where the ratio of double to single ionization might not approach an asymptotic limit.

Future Plans

Fundamentally our future plans are to continue on the paths set out above. In the area of nondipole effects Xe $5p$ will be investigated to try to unravel the difficulties in two experimental results that disagree quantitatively. In addition, the search for cases where nondipole effects are likely to be significant, as a guide for experiment, will continue. The study of the photodetachment of C^- shall move on to the photoabsorption in the vicinity of the K-shell edge of both the ground 4S and excited 2D states in order to understand how the slight excitation of the outer shell affects the inner-shell photoabsorption and to pave the way for experiment. Finally, the study of the photoionization of the Be sequence shall continue with consideration of the first two excited states of C^{+2} and the ground and excited states of N^{+3} and O^{+4} .

Publications Citing DOE Support Since September, 2003

"Nondipole Effects in the Photoionization of Xe $4d_{5/2}$ and $4d_{3/2}$: Evidence for Quadrupole Satellites," O. Hemmers, R. Guillemin, D. Rolles, A. Wolska, D. W. Lindle, K. T. Cheng, W. R. Johnson, H. L. Zhou and S. T. Manson, *Phys. Rev. Letters* **93**, 113001-1-4 (2004).

"Photodetachment of the Outer Shell of C^- in the Ground State," H.-L. Zhou, S. T. Manson, A. Hibbert, L. Vo Ky, N. Feautrier and J. C. Chang, *Phys. Rev. A* **70**, 022713-1-7 (2004).

"Experimental Investigation of Nondipole Effects in Photoemission at the Advanced Light Source," R. Guillemin, O. Hemmers, D. W. Lindle and S. T. Manson, *Radiation Phys. Chem.* **73** 311-327 (2005).

"Nondipole Effects in the Photoabsorption of Electrons in Two-Center Zero-Range Potentials," A. S. Baltentkov, V. K. Dolmatov, S. T. Manson and A. Z. Msezane, *J. Phys. B* **37**, 3837-3846 (2004).

"Photoionization of the Ground-State Be-Like B^+ Ion Leading to the $n=2$ and $n=3$ States of B^{2+} ," D.-S. Kim and S. T. Manson, *J. Phys. B* **37**, 4013-4024 (2004).

"Nondipole Effects in Xe $4d$ Photoemission," O. Hemmers, R. Guillemin, D. Rolles, A. Wolska, D. W. Lindle, K. T. Cheng, W. R. Johnson, H. L. Zhou and S. T. Manson, *J. Electron Spectrosc.* **144-147**, 51-52 (2005).

"Photoionization of the Excited $1s^2 2s 2p^1$ 3P States of Be-like B^+ ," D.-S. Kim and S. T. Manson, *Phys Rev. A* **71**, 032701-1-12 (2005).

"Photoabsorption By Atoms and Ions," S. T. Manson, in *The Physics of Ionized Gases* in, eds. L. Hadzievski, T. Grozdanov and N. Bibic (AIP, Melville, New York, 2004), pp. 49-58.

"Photoionization of the Ground-State Be-Like C^{+2} Ion Leading to the $n=2$ and $n=3$ States

of C^{3+} ," D.-S. Kim and S. T. Manson, *J. Phys. B* **37**, 4707-4718 (2004).

“Gigantic Enhancement of Atomic Nondipole Effects: the $3s \rightarrow 3d$ Resonance in Ca,” V. K. Dolmatov, D. Bailey and S. T. Manson, *Phys. Rev A* (in press).

References

- [1] M. O. Krause, *Phys. Rev.* **177**, 151 (1969).
- [2] O. Hemmers, R. Guillemin and D. W. Lindle, *Radiation Phys. and Chem.* **70**, 123-148 (2004) and references therein.
- [3] O. Hemmers, R. Guillemin, E. P. Kanter, B. Kraessig, D. W. Lindle, S. H. Southworth, R. Wehlitz, J. Baker, A. Hudson, M. Lotrakul, D. Rolles, W. C. Stolte, I. C. Tran, A. Wolska, S. W. Yu, M. Ya. Amusia, K. T. Cheng, L. V. Chernysheva, W. R. Johnson and S. T. Manson, *Phys. Rev. Letters* **91**, 053002 (2003).
- [4] V. K. Dolmatov and S. T. Manson, *Phys. Rev. Letters* **83**, 939 (1999).
- [5] V. K. Dolmatov, D. Bailey and S. T. Manson, *Phys. Rev A* (in press).
- [6] M. Ya. Amusia, A. S. Baltenkov, L. V. Cernycheva, Z. Felfli, A. Z. Msezane and J. Nordgren, *Phys. Rev. A* **63**, 052511 (2001) and references therein.
- [7] H. L. Zhou, S. T. Manson, L. VoKy, A. Hibbert and N. Feautrier, *Phys. Rev. A* **64**, 012714 (2001).
- [8] N. Berrah, J. Bozek, G. Turri, G. Ackerman, B. Rude, H.-L. Zhou and S. T. Manson, *Phys. Rev. Letters* **88**, 093001 (2002).
- [9] H. L. Zhou, S. T. Manson, L. VoKy, N. Feautrier and A. Hibbert, *Phys. Rev. Letters* **87**, 023001 (2001).
- [10] N. Berrah, J. D. Bozek, A. A. Wills, H.-L. Zhou, S. T. Manson, G. Akerman, B. Rude, N. D. Gibson, C. W. Walter, L. VoKy, A. Hibbert and S. Fergusson, *Phys. Rev. Letters* **87**, 253002 (2001).
- [11] H.-L. Zhou, S. T. Manson, A. Hibbert, L. Vo Ky, N. Feautrier and J. C. Chang, *Phys. Rev. A* **70**, 022713 (2004).
- [12] H.-L. Zhou, S. T. Manson, A. Hibbert, L. Vo Ky and N. Feautrier, *Phys. Rev. A* (submitted).
- [13] J. B. West, *J. Phys. B* **34**, R45 (2001) and references therein.
- [14] F. Robicheaux and C. H. Greene, *Phys. Rev. A* **48** 4429 (1993) and references therein.
- [15] D.-S. Kim, S. S. Tayal, H.-L. Zhou and S. T. Manson, S. T., *Phys. Rev. A* **61**, 062701 (2000).
- [16] D.-S. Kim, H.-L. Zhou, S. T. Manson and S. S. Tayal, *Phys. Rev. A* **64**, 042713 (2001).
- [17] D.-S. Kim and S. T. Manson, *J. Phys. B* **37**, 4013-4024 (2004).
- [18] D.-S. Kim and S. T. Manson, *Phys. Rev. A* **71**, 032701-1-12 (2005).
- [19] D.-S. Kim and S. T. Manson, *J. Phys. B* **37**, 4707-4718 (2004).
- [20] S. Schippers, A. Müller, B. M. McLaughlin, A. Aguilar, C. Cisneros, E. D. Emmons, M. F. Gharaibeh and R. A. Phaneuf, *J. Phys. B* **36**, 3371 (2003).
- [21] A. Müller, R. A. Phaneuf, A. Aguilar, M. F. Gharaibeh, A. S. Schlachter, I. Alvarez, C. Cisneros, G. Hinojosa and B. M. McLaughlin, *J. Phys. B* **35**, L137 (2002).
- [22] H. A. Bethe and E. E. Salpeter, *Quantum Mechanics of One- and Two-Electron Atoms* (Springer-Verlag, Berlin, 1958), Sec. 71.
- [23] U. Fano and A. R. P. Rau, *Phys. Rev.* **162**, 68 (1967).
- [24] M. Ya. Amusia, N. B. Avdonina, E. Drukarev, S. T. Manson and R. H. Pratt, *Phys. Rev. Letters* **85**, 4703 (2000).
- [25] A. M. Sossah, C. Yang, H.-L. Zhou, M. Ya. Amusia, A. Z. Msezane and S. T. Manson, *Phys. Rev. Letters* (submitted).

PROGRESS REPORT

ELECTRON-DRIVEN PROCESSES IN POLYATOMIC MOLECULES

Investigator: Vincent McKoy

A. A. Noyes Laboratory of Chemical Physics

California Institute of Technology

Pasadena, California 91125

email: mckoy@caltech.edu

PROJECT DESCRIPTION

The focus of this project is the application and development of accurate, scalable methods for the computational study of low-energy electron–molecule collisions, with emphasis on larger polyatomics relevant to materials-processing and biological systems. Because the calculations required are highly numerically intensive, efficient use of large-scale parallel computers is essential, and the computer codes developed for the project are designed to run both on tightly-coupled parallel supercomputers and on workstation clusters.

HIGHLIGHTS

We have continued to focus on electron interactions with larger polyatomic molecules, especially those relevant to biological systems and to technological applications. Principal accomplishments in the past year are:

- Completed study of C_{60} elastic scattering
- Completed re-examination of C_2F_4 elastic scattering
- Joint experimental/theoretical study of C_2F_6 electron-impact dissociation
- New approach to polarization devised and tested successfully on C_2H_4
- Elastic scattering calculations for nucleotide bases, deoxyribose, and thymidine
- Electron-impact excitation calculations on uracil
- Continued development of computational methods

ACCOMPLISHMENTS

During 2005, we continued to focus on applications to biological systems and on methodological developments in support of those applications. In one line of work, a graduate student, Sergio Sanchez, carried out studies of elastic scattering by the DNA constituents thymine and deoxyribose as well as by thymidine, which is the combination of thymine plus deoxyribose. These calculations are an initial step in determining how gas-phase electron collision results for subunits such as thymine will correlate with properties of the full macromolecular system. In particular, we are interested in how results from high-level calculations on small subsystems may be extrapolated using guidance from lower-level calculations. Accordingly, calculations on thymine and deoxyribose have been carried out at both the static–exchange level and static–exchange plus polarization levels of approximation, while calculations on thymidine were carried out at the static–exchange level. Further calculations and analysis of the results are continuing.

We also continued calculations on uracil, a constituent base of RNA. Early in the year we concluded that a more extensive treatment of polarization than originally planned would be

necessary, and we have been making methodological improvements to facilitate such a treatment. Specifically, we developed new code for the final phase of the calculation, which involves the solution of a system of linear equations. The new code replaces a system of N equations with complex coefficients by a system of N equations with real coefficients, plus a small auxiliary problem. The new code requires a factor of 2 less memory, runs faster, and can be executed in parallel, all of which facilitate solving larger systems.

A second methodological development involves a new approach to building a “particle orbital” space that represents non-resonant polarization effects efficiently and thereby improves the scaling of the calculation. In the past, we have used the “polarized orbital” approach [1], which can be quite successful but which has two drawbacks: it is based on the long-range form of the polarization interaction, and so does not necessarily represent short-range interactions well, and it generates exactly 3 particle orbitals per hole orbital, with no obvious way to extend the particle space should those prove insufficient. We devised a very simple and readily extensible alternative using so-called modified virtual orbitals [2] and tested it successfully on ethylene, C_2H_4 [3]. Using this particle space, we resolved a long-standing problem by obtaining a minimum observed in the small-angle differential cross section between about 3 and 5 eV that previous high-level calculations had failed to reproduce (Fig. 1).

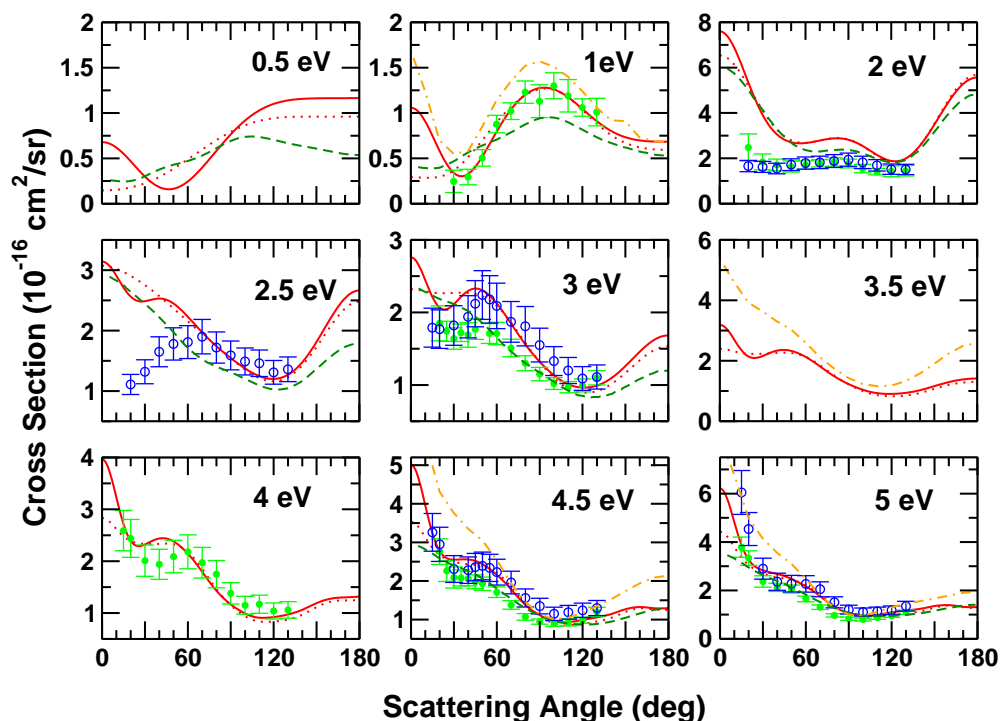


Fig. 1 Elastic electron scattering by C_2H_4 at various collision energies. The solid red line is the present computed result; the blue and green circles are measured values. Figure taken from Ref. [3].

We are in the process of applying both of the above developments to elastic scattering by uracil. It appears that more extensive basis sets than we heretofore expected will also be required to obtain well-converged, numerically stable results, and calculations using such extended bases are under way. We have also carried out preliminary electron-impact excitation calculations on uracil and plan several further excitation calculations that will encompass both $\pi \rightarrow \pi$ and $\pi \rightarrow \sigma$ transitions.

Other work completed during the year included a study of elastic electron scattering by gas-phase C_{60} [4] at the static-exchange level, in which we focused on analysis of the resonance structure in comparison with experimental results, previous calculations, and the predictions of a simple model. We also submitted for publication a joint experimental-theoretical paper [5] on electron-impact dissociation of the plasma etchant C_2F_6 , in which we found that our computed cross section, obtained by summing the excitation cross sections for eight low-lying, dissociative states, gave a reasonably good approximation to the neutral-dissociation cross section derived from experiment (Fig. 2). Our re-examination of the elastic cross section for another etchant, C_2F_4 , appeared during 2005 as well [6]. In that work, we conclude that there is no obvious source of computational error that can explain the large discrepancy between the experimental elastic cross section [7] and our calculations at high collision energies, and we note that the experimental values are also inconsistent with the reported total collision cross section [8]. Conversations with Profs. Buckman and Tanaka at the recent International Symposium on Electron-Molecule Collisions and Swarms indicate that both intend to re-examine this system.

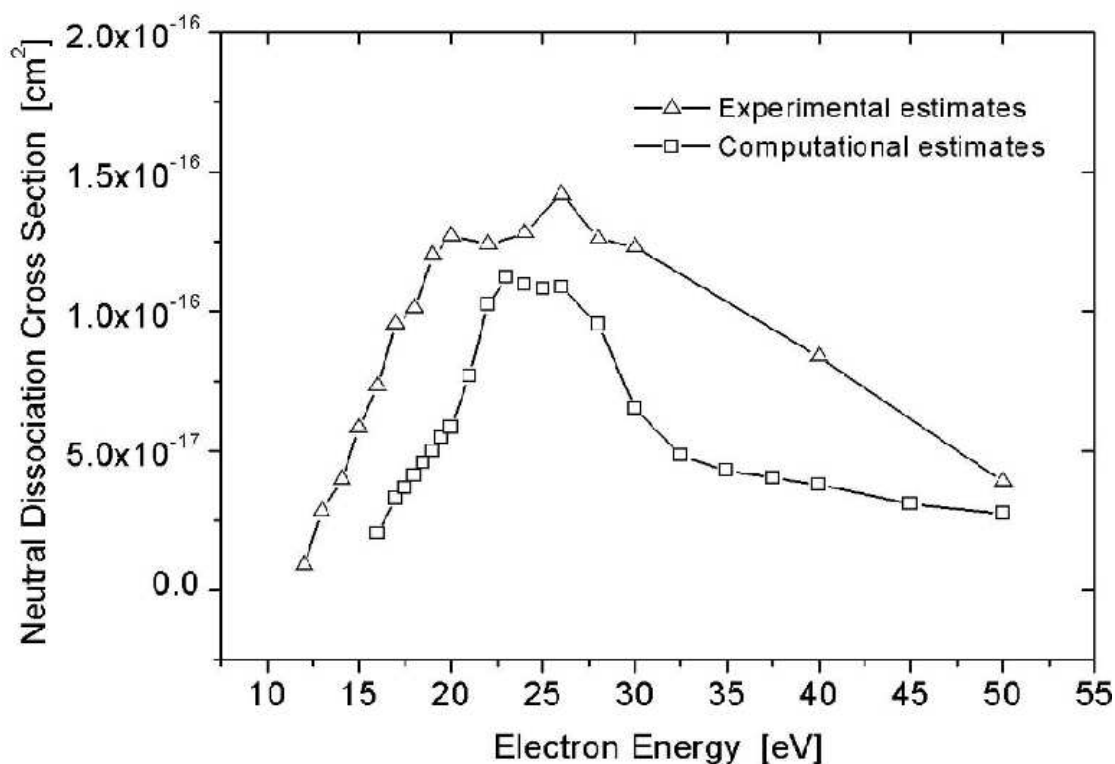


Fig. 2 Experimentally-derived neutral dissociation cross section for C_2F_6 compared to prediction obtained by summing eight computed dissociative-excitation cross sections, from Ref. [5].

PLANS FOR COMING YEAR

We plan to continue work on the DNA and RNA bases as well as on larger subunits such as thymidine or sugar-phosphate moieties. While continuing to work on elastic scattering, we will be increasingly focused on electron-impact excitation, where collision calculations and complementary electronic structure calculations may provide information on neutral dissociation processes that is very hard to obtain from experiment. Code development efforts will be concentrated on modifications to improve the scaling and remove bottlenecks, with a view to facilitating accurate calculations on larger molecules. In particular, we plan to implement a new, parallelized integral transformation procedure in the early stage of the calculation and a new linear solver that distributes not only the computation but also the data structures over multiple processors.

REFERENCES

- [1] B. H. Lengsfeld III, T. N. Rescigno, and C. W. McCurdy, *Phys. Rev. A* **44**, 4296 (1991); T. N. Rescigno, D. A. Byrum, W. A. Isaacs, and C. W. McCurdy, *Phys. Rev. A* **60**, 2186 (1999).
- [2] C. W. Bauschlicher, *J. Chem. Phys.* **72**, 880 (1980).
- [3] C. Winstead, V. McKoy, and M. H. F. Bettega, submitted to *Phys. Rev. A*.
- [4] C. Winstead and V. McKoy, submitted to *Phys. Rev. A*.
- [5] D. W. Flaherty, M. A. Kasper, J. E. Baio, D. B. Graves, H. F. Winters, C. Winstead, and V. McKoy, submitted to *J. Chem. Phys.*
- [6] C. Winstead and V. McKoy, *J. Chem. Phys.* **122**, 234304 (2005).
- [7] R. Panajotovic, M. Jelisavcic, R. Kajita, T. Tanaka, M. Kitajima, H. Cho, H. Tanaka, and S. J. Buckman, *J. Chem. Phys.* **121**, 4559 (2004).
- [8] C. Szmytkowski, S. Kwitnewski, and E. Ptasínska-Denga, *Phys. Rev. A* **68**, 032715 (2003).

PROJECT PUBLICATIONS AND PRESENTATIONS, 2002–2005

1. “Low-Energy Electron Scattering by CH_3F , CH_2F_2 , CHF_3 , and CF_4 ,” M. T. do N. Varella, C. Winstead, V. McKoy, M. Kitajima, and H. Tanaka, *Phys. Rev. A* **65**, 022702 (2002).
2. “Electron Collisions with Tetrafluoroethene, C_2F_4 ,” C. Winstead and V. McKoy, *J. Chem. Phys.* **116**, 1380 (2002).
3. “Electron Transport Properties and Collision Cross Sections in C_2F_4 ,” K. Yoshida, S. Goto, H. Tagashira, C. Winstead, V. McKoy, and W. L. Morgan, *J. Appl. Phys.* **91**, 2637 (2002).
4. “Electron Collision Cross Sections for Tetraethoxysilane (TEOS),” W. L. Morgan, C. Winstead, and V. McKoy, *J. Appl. Phys.* **92**, 1663 (2002).
5. “Developing Cross Section Sets for Fluorocarbon Etchants,” C. Winstead and V. McKoy, *Proceedings of the Third International Conference on Atomic and Molecular Data and Their Applications, Gatlinburg, Tennessee, 24–27 April, 2002*, AIP Conf. Proc. **636**, 241 (2002) (*invited talk*).

6. "Quickly Generating Databases," C. Winstead, Third International Conference on Atomic and Molecular Data and Their Applications, Gatlinburg, Tennessee, 24–27 April, 2002 (*panelist*).
7. "Electron Collisions with SF₆ (Sulfur Hexafluoride)," C. Winstead and V. McKoy, Fifty-Fifth Gaseous Electronics Conference, Minneapolis, Minnesota, 15–18 October, 2002.
8. "Parallel Computations of Electron–Molecule Collisions in Processing Plasmas," V. McKoy, Ninth International Conference on High-Performance Computing, Bangalore, India, 18–21 December, 2002 (*Keynote Lecture*).
9. "Electron–Molecule Collisions in Processing Plasmas," V. McKoy, Applied Materials, Santa Clara, California, 7 February, 2003 (*invited talk*).
10. "Electron–Molecule Collisions in Processing Plasmas," V. McKoy, Colloquium, Departments of Physics and Materials Science, University of Southern California, 28 April, 2003.
11. "Electron–Molecule Collision Calculations on Vector and MPP Systems," C. Winstead and V. McKoy, Cray Users' Group Conference, Columbus, Ohio, 12–16 May, 2003.
12. "Low-Energy Electron Scattering by Methylsilane," M. H. F. Bettega, C. Winstead, and V. McKoy, *J. Chem. Phys.* **119**, 859 (2003).
13. "Low-Energy Electron Collisions with Sulfur Hexafluoride, SF₆," C. Winstead and V. McKoy, *J. Chem. Phys.* **121**, 5828 (2004).
14. "Elastic Electron Scattering by C₂F₄," C. Winstead and V. McKoy, *J. Chem. Phys.* **122**, 234304 (2005).
15. "Low Energy Electron Scattering by DNA Bases," S. d'A. Sanchez, C. Winstead, and V. McKoy, XXIV International Conference on Photonic, Electronic, and Atomic Collisions, Rosario, Argentina, 20–26 July, 2005.
16. "Recent Progress with the Schwinger Multichannel Method," C. Winstead, V. McKoy, and S. d'A. Sanchez, Fourteenth International Symposium on Electron–Molecule Collisions and Swarms, Campinas, Brazil, 27–30 July, 2005 (*invited talk*).
17. "Low-Energy Electron Scattering by N₂O and C₂H₄," M. H. F. Bettega, C. Winstead, and V. McKoy, Fourteenth International Symposium on Electron–Molecule Collisions and Swarms, Campinas, Brazil, 27–30 July, 2005.
18. "Low-Energy Electron Collisions with Buckminsterfullerene, C₆₀," C. Winstead and V. McKoy, submitted to *Phys. Rev. A*.
19. "Elastic Electron Scattering by Ethylene, C₂H₄," C. Winstead and V. McKoy, submitted to *Phys. Rev. A*.
20. "Total Dissociation Electron Impact Cross Sections for C₂F₆," D. W. Flaherty, M. A. Kasper, J. E. Baio, D. B. Graves, H. F. Winters, C. Winstead, and V. McKoy, submitted to *J. Chem. Phys.*

ELECTRON/PHOTON INTERACTIONS WITH ATOMS/IONS

Alfred Z. Msezane (email: amsezane@ctsps.cau.edu)

Clark Atlanta University, Department of Physics and CTSPS
Atlanta, Georgia 30314

Program Scope

We develop methodologies for calculating Regge pole trajectories and residues for both singular and nonsingular potentials, important in heavy particle collisions, chemical reactions and atom-diatom systems. Methods are developed for calculating the GOS, useful in probing the intricate nature of the valence- and open-shell as well as inner-shell electron transitions. Standard codes are used to generate sophisticated wave functions for investigating CI mixing and relativistic effects in atomic ions. The wave functions are utilized in exploring correlation effects in dipole and non-dipole photoionization studies.

A. Complex Angular Momentum Methods for Regge-Poles Calculation

Recently, the complex angular momentum (CAM) theory for integral cross sections has been introduced and used to demonstrate the oscillations, a general feature of potential scattering, in the integral elastic scattering cross sections for proton impact on atomic hydrogen [1]. Thylwe [2] has developed a useful method for discontinuous scattering potentials, particularly for analysis of Regge-poles far out in the CAM plane. The method avoids the details of Stokes' and anti-Stokes' lines, a draw-back of the semi-classical methods. The Padé-Regge approach has been illustrated with several one-particle potential problems [3]. We continue to develop methods that avoid the explicit use of Stokes' and anti-Stokes' lines [4].

We have also considered the Regge pole trajectories corresponding to the Thomas-Fermi potential [5], following essentially the method of Ref. [5]. We found that the anti-Stokes lines for Thomas-Fermi type potentials have a more complicated structure than those for singular potentials and require careful application of complex analysis. For large energies three of the five turning points are close to the poles of the effective potential, thus allowing the decomposition into a series the action integral (Bohr-Sommerfeld quantization condition). We exploit the topology of the anti-Stokes' lines to determine the region of applicability of the semi-classical methods.

B.1 Generalized Oscillator Strengths for 3d Electrons of Cs and Ba

We have investigated for the first time ever the use of the leveraging effect of the spin-orbit interaction to probe correlation effects in the generalized oscillator strength (GOS) of the 3d subshells of Cs and Ba, *viz.* we study how the GOS's of the Cs and Ba $3d_{5/2}$ and $3d_{3/2}$ levels are affected by the intradoublet correlations [6]. We expect new features to appear as has been found elsewhere [7]. The calculations are carried out using the Hartree-Fock (HF) approximation and within the framework of a modified version of the Spin-Polarized Random Phase Approximation within Exchange (SPRPAE) which takes into account of multi-electron

correlation effects. The effects of relaxation of the excited electrons due to the creation of the 3d-vacancy are also accounted for.

Our GOS results for both Cs and Ba, obtained for values of the momentum transfer q from 0 to 4 *a.u.* and energy transfer $\omega = 0.001$ to 8 Ry, demonstrate the “leveraging” role of the spin-orbit interaction, viz. the strong interaction between components of the spin-orbit doublet of the 3d electrons in Cs and Ba. This leads to the appearance of an additional maximum in the GOS for the $3d_{5/2}$ subshell, due to the action of the $3d_{3/2}$ electrons. The inter-doublet correlations are very important in the dipole, monopole and quadrupole transitions.

B.2 Generalized Oscillator Strengths of Atomic Transitions and the Approach to the High-Energy Limit

Minima in the GOS and the convergence of the GOS to the first Born Approximation (FBA) limit for the Ba $6s\ ^1S \rightarrow 6p\ ^1P$ optically allowed transition have been investigated [8]. The RPAE, which takes into account of correlation effects among the atomic electrons themselves, and the convergent close-coupling (CCC) approximation are used for the calculations. We find that: 1) The GOS as a function of the momentum transfer squared q^2 is characterized by a complex structure of multiple minima, significantly different in the two approximations and approaches the high-energy FBA limit only at small q^2 values (less than about 0.5 a.u.). 2) The number of minima calculated in the CCC approximation increases with increase in energy, but does not correspond to the number obtained in the FBA, even at high energy ~ 1 keV. The CCC and FBA first minima are in general not directly related. Only the FBA minima correspond to physical observables at these energies. 3) At high energy the interaction between the incident electron and the target remains significant, resulting in slowing down the convergence of the CCC GOS to the corresponding nonrelativistic FBA results.

B.3 Generalized Oscillator Strengths for Inner-Shell Electron Transitions

A second-quantization formalism has been used to obtain a general expression for the GOS for inner-shell electron transitions between two open shells of any atom [9]. The derived formula together with the spin polarized technique of the RPAE are then employed to investigate correlation effects in the GOS for the Na $2p^6 3s(^2S) \rightarrow 2p^5 3s(^2P)$ transition. Results are compared with the measured ones [10]. The present formula has also been used with Hatree-Fock wave functions to calculate the GOS's for the carbon $2s^2 2p^2(^3P) \rightarrow 2s 2p^3(^3P)$ and $2s^2 2p^2(^3P) \rightarrow 2s 2p^3(^3D)$ transitions. The calculated multiplet oscillator strengths for the two transitions have been compared with the experimental values.

B.4 Giant Resonances in Xe^+ , I and I^+

We have utilized the recently developed RPAE method [9], which can be used to study the inner-shell electron transition of an open shell atom, to calculate the photoionization cross section of the Xe^+ $4d - \epsilon f$, so called giant resonance. We first create the ground state of Xe^+ $4d^{10} 5s^2 5p^5(^2P)$ and core wave functions of $4d^9 5s^2 5p^5(^1P, ^1D, ^1F, ^3P, ^3D, ^3F)$ through self-consistent HF calculations. Then radial functions of the continuum electron are obtained by solving the linear HF equations without self-consistency using those core wave functions. The reduced dipole matrix elements for the relevant transitions are evaluated using the operator [11]. After evaluating the Coulomb matrix elements, the RPAE equation was solved in the same way as in [12] and we obtained the $^2S, ^2P$, and 2D partial cross sections. The maximum of the total

cross section, 24.4 MB at the photon energy of 96.3 eV from our RPAE calculation agrees very well with the experimental maximum of (27 ± 3) MB at the photon energy of 95eV [13].

The 4d giant resonances of I and I^+ have been calculated using our recently developed RPAE program [9]. The results for I^+ agree quite well with the recent experimental data [14]. However, for the I atom the RPAE results for the 4d giant resonance yields maxima at 102 eV of 23.8 MB (length) and 19.6 MB (velocity), which are still much higher than the experimental maximum of 6.5 MB at 91 eV [15].

C. Probing Correlations through Spin-Orbit Interaction

Recently, a new aspect of interchannel coupling has been found [7], known as spin-orbit activated interchannel coupling, stimulated by an experimental study on photoionization of Xe in the vicinity of the 3d threshold [16]. This effect results only through the spin-orbit splitting of inner-shell thresholds. Effects of spin-orbit activated interchannel coupling on dipole [17] and nondipole [18] photoelectron angular distribution asymmetry parameters have been discussed, including the spin-polarization of photoelectrons from 3d electrons of Xe, Cs and Ba, concluding that through spin-orbit interaction polarization can be achieved and correlation probed.

D. Dramatic Distortion of the 4d Giant Resonance by the C_{60} Fullerene Shell

The recent encapsulation of molecular hydrogen in fullerene C_{60} using a molecular surgical method and the possibility of preparing a series of C_{60} fullerenes, encapsulating either small atoms or molecules [19], has prompted this study. The photoionization cross section for the endohedral $Xe@C_{60}$ atom is investigated [20] within the framework of representing the C_{60} by a delta-type potential. Results demonstrate that in $Xe@C_{60}$, the 4d giant resonance is distorted significantly when compared with that of the isolated Xe atom. The reflection of the photoelectron waves by the C_{60} causes strong oscillations in the photoionization cross section resulting in the replacement of the Xe 4d giant resonance by four prominent peaks. The approximation of C_{60} by an infinitely thin real potential preserves reasonably well the sum rule for the 4d electrons but modifies the dipole polarizability of the 4d shell.

Continuing Investigations

We have now forged collaborations with the Oakridge/University of Tennessee group under Dr. Macek and the Queen's University of Belfast group of Dr. Sokolovski on the development and application of the CAM theory, particularly in chemical reactions and heavy particle collisions. Other research activities continue, such as GOS investigations and inner-shell studies as well as probing correlations.

References and Some Publications 2003 – 2005

- [1] J.H. Macek, P.S. Krstic and S. Yu. Ovchinnikov, Phys. Rev. Lett. **93**, 183203 (2004)
- [2] K.-E. Thylwe, J. Phys. A, In Press (2005)
- [3] "A Semiclassical CAM Theory and PADÉ Reconstruction for Resonances, Rainbows and Reaction Thresholds", D. Sokolovski and A.Z. Msezane, Phys. Rev. **A70**, 032710 (2004)

- [4] N.B. Avdonina, S. Belov, Z. Felfli, A.Z. Msezane and S.N. Naboko, *Phys. Rev.* **A66**, 022713 (2002)
- [5] “Regge Poles Trajectories for Nonsingular Potentials: The Thomas-Fermi Potentials”, S.M. Belov, N.B. Avdonina, Z. Felfli, M. Marletta, A.Z. Msezane and S.N. Naboko, *J. Phys.* **A37**, 6943 (2004)
- [6] “Generalized Oscillator Strengths for 3d Electrons of Cs and Ba”, M. Ya. Amusia, L.V. Chernysheva, Z. Felfli and A.Z. Msezane, *Proc. ICPEAC 2005*, Eds. F.D. Colavecchia *et al.*, Vol. 1, p. 26
- [7] M. Ya. Amusia, L.V. Chernysheva, S.T. Manson, A.Z. Msezane and V. Radojevic, *Phys. Rev. Lett.* **88**, 093002 (2002)
- [8] “Minima in Generalized Oscillator Strengths of Atomic Transitions and the Approach to the High-Energy Limit”, N.B. Avdonina, D. Fursa, A.Z. Msezane and R.H. Pratt, *Phys. Rev.* **A71**, 062711(2005)
- [9] Zhifan Chen and A.Z. Msezane, *Phys. Rev. A*, submitted (2005)
- [10] C.E. Bielschowsky *et al.*, *Phys. Rev.* **A43**, 5975 (1991)
- [11] “Generalized Oscillator Strengths for Inner-Shell Electron Transitions”, Zhifan Chen and A.Z. Msezane, *Phys. Rev.* **A70**, 032714 (2004)
- [12] G.A. Vesnicheva, *et al.*, *Sov. Phys. Tech. Phys.* **31**, 402 (1986)
- [13] P. Andersen, *et al.*, *J. Phys.* **B34**, 2009 (2001)
- [14] H. Kjeldsen, *et al.*, *Phys. Rev.* **A62**, 020702 (2000)
- [15] G. O’Sullivan, *et al.*, *Phys. Rev.* **A53**, 3211 (1996)
- [16] A. Kivimäki, *et al.*, *Phys. Rev.* **A63**, 012716 (2001)
- [17] “Spin Polarization of photoelectrons from 3d electrons of Xe, Cs and Ba”, M. Ya. Amusia, N. Chernysheva, Z. Felfli and A.Z. Msezane, *Phys. Rev.* **A70**, 062709 (2004)
- [18] “Non-dipole Effects in Spin-Polarization of Photoelectrons from 3d electrons of Xe, Cs and Ba”, M. Ya. Amusia, N.A. Cherepkov, L.V. Chernysheva, Z. Felfli and A.Z. Msezane, *J. Phys.* **B38**, 1133 (2005)
- [19] K. Komatsu, M. Murata and Y. Murata, *Science* **307**, 238 (2005)
- [20] “Dramatic Distortion of 4d Giant Resonance by the C₆₀ Fullerene Shell”, M. Ya. Amusia, A.S. Baltenkov, L.V. Chernysheva, Z. Felfli and A.Z. Msezane, *J. Phys.* **B38**, L169 (2005)
- [21] “Post-Collision Recapture in the K-shell Photodetachment of Li⁺”, T.W. Gorczyca, O. Zatsarinny, H.-L. Zhou, S.T. Manson, Z. Felfli and A.Z. Msezane, *Phys. Rev.* **A68**, 054701 (R) (2003)
- [22] “From Bose-Einstein to Fermion Condensation”, M. Ya. Amusia, A.Z. Msezane and V.R. Shaginyan, *Physics of Atomic Nuclei* **66**, 1802 (2003)
- [23] “Comment on Relativistic Many-Body Calculations of Energies of n=3 States in Aluminum Like Ions”, G.P. Gupta, K.M. Aggarwal and A.Z. Msezane, *Phys. Rev.* **A70**, 036501(2004)
- [24] “Excitation Energies, Oscillator Strengths and Lifetimes in Ca IX”, V. Tayal, G.P. Gupta and A.Z. Msezane, *Physica Scripta*, In Press (2005)
- [25] “Large Scale CIV3 Calculations of Fine-Structure Energy Levels, Oscillation Strengths and Lifetimes in Fe XIV and Ni XVI”, G.P. Gupta and A.Z. Msezane, *Atomic Data Nuclear Data Tables* **89**, 1 (2005)

Single Molecule Absorption and Fluorescence in Inhomogeneous Environments

Lukas Novotny (*novotny@optics.rochester.edu*)

University of Rochester, The Institute of Optics, Rochester, NY, 14627.

1 Program Scope

This project aims at understanding the excitation and emission process of a single molecule near laser-irradiated nanostructures. In the weak-coupling regime, the interaction with the environment influences the molecule's fluorescence rate and its excited-state lifetime. Our goal is to control these interactions using carefully designed metal nanostructures that can be positioned relative to a single molecule by means of piezoceramic transducers. This mechanical control will allow us to understand and control the competition between fluorescence enhancement and nonradiative decay. It also gives us the opportunity to observe and study new selection rules originating from the highly confined interaction.

2 Recent Progress

In the past project period we set up two different, but related experiments. In one of them we are working towards positioning a single gold nanoparticle near a single fluorescent molecule. The fluorescence lifetime and the fluorescence rate will be monitored as a function of molecule-particle distance as well as nanoparticle size and shape. In the second experiment we irradiate a sharply pointed gold tip with femtosecond laser pulses to locally generate various nonlinear signals such as second-harmonic generation, sum-frequency generation or four-wave mixing. The nonlinear signal is then used as a secondary light source for the interaction with an absorbing sample. We study the extinct radiation as a function of frequency and sample position. The goal is to acquire absorption spectra of larger molecules such as single proteins or semiconductor nanostructures. In this report we will predominantly concentrate on the first project, i.e. the control of fluorescence rate and lifetime using a metal nanoparticle.

Since the pioneering work of Purcell it is known that the lifetime of an excited atomic state is not only a function of the atom but also of its environment. One can design environments (at least theoretically) where the density of states goes to zero forcing the atom to reside in its excited state forever. Different theoretical models have been developed to understand fluorescent decay near metal nanostructures but experimental results are not always consistent. Based on Fermi's Golden Rule, the spontaneous decay rate of a molecule located at \mathbf{r}_m with transition dipole \mathbf{p} pointing in direction \mathbf{n}_p can be expressed as (SI units)

$$\gamma = \frac{2\omega_o}{3\hbar\epsilon_o} |\mathbf{p}|^2 \rho_\mu(\mathbf{r}_m, \omega_o), \quad (1)$$

where ω_o is the transition frequency and ρ_μ the electromagnetic density of states. The latter can be expressed in terms of the system's dyadic Green's function $\overleftrightarrow{\mathbf{G}}$ as

$$\rho_\mu(\mathbf{r}_m, \omega_o) = \frac{6\omega_o}{\pi c^2} \left[\mathbf{n}_p \cdot \text{Im} \left\{ \overleftrightarrow{\mathbf{G}}(\mathbf{r}_m, \mathbf{r}_m; \omega_o) \right\} \cdot \mathbf{n}_p \right]. \quad (2)$$

Unfortunately, calculating the fluorescence rate is not such an easy task as calculating γ . The problem is related to the fact that not all transitions produce a photon that can be recorded with a detector. In other words, a molecule located near a metal structure (such as a particle) will relax to its ground-state through radiative decay (γ_r) and nonradiative decay (γ_{nr}). Both decay rates can be significantly increased over the free-space decay rate γ_o . However, as long as γ_{nr} is much larger than γ_r there will be no observable fluorescence. γ_{nr} accounts for energy transfer to electrons, and ultimately phonons, in the metal nanostructure (dissipation to heat). The emitted fluorescence rate (below saturation) can be written as

$$\gamma_{em}(\omega_o) = \gamma_{exc} [1 - \gamma_{nr}/\gamma] \quad (3)$$

where $\gamma_{exc} \propto |\mathbf{p} \cdot \mathbf{E}|^2$ is the excitation rate depending on the local (enhanced) field \mathbf{E} . The expression in the brackets corresponds to the so-called apparent quantum yield $q_a = \gamma_r/\gamma$. The individual rates γ_i depend on the shape, material, molecular orientation and distance from the metal nanostructure.

To understand the trade-off between fluorescence enhancement and quenching let us consider an emitting molecule represented by a dipole \mathbf{p} and located at \mathbf{r}_m . Following Fig. 1b, we represent the nanostructure by a spheroid with center at \mathbf{r}_o . The field at an arbitrary point \mathbf{r} is then described by the following Green's function

$$\vec{\mathbf{G}}(\mathbf{r}, \mathbf{r}_m) = \vec{\mathbf{G}}^o(\mathbf{r}, \mathbf{r}_m) + \frac{k^2}{\varepsilon_o} \vec{\mathbf{G}}^o(\mathbf{r}, \mathbf{r}_o) \vec{\alpha}_{eff} \vec{\mathbf{G}}^o(\mathbf{r}_o, \mathbf{r}_m), \quad (4)$$

where $k = \omega_o/c$ and $\vec{\mathbf{G}}^o$ is the free-space Green's dyadic. The effective polarizability $\vec{\alpha}_{eff}$ is defined as

$$\vec{\alpha}_{eff} = \vec{\alpha}(\omega) \left[\vec{\mathbf{I}} - i \frac{k^3}{6\pi\varepsilon_o} \vec{\alpha}(\omega) \right]^{-1} \quad (5)$$

Here, the polarizability $\vec{\alpha}$ is simply the quasi-static polarizability tensor of the spheroid. The second term in the expression of $\vec{\alpha}_{eff}$ arises from radiation reaction, i.e. the action of the particle on itself. Notice that $\vec{\mathbf{G}}^o$ and $\vec{\alpha}_{eff}$ are to be evaluated at the transition frequency ω_o . Introducing Eqs. 4 and 5 into Eq. 2 allows us to represent the decay rate as

$$\frac{\gamma}{\gamma_o} = 1 + \frac{6\pi k}{\varepsilon_o} \left[\mathbf{n}_p \cdot \text{Im} \left\{ \vec{\mathbf{G}}^o(\mathbf{r}_m, \mathbf{r}_o) \vec{\alpha}_{eff} \vec{\mathbf{G}}^o(\mathbf{r}_o, \mathbf{r}_m) \right\} \cdot \mathbf{n}_p \right], \quad (6)$$

where γ_o is the decay rate in free-space, i.e. in the absence of the nanostructure. Using the expression for the free-space Green's dyadic we can calculate the decay rate as a function of molecule position and orientation relative to the coordinates of the nanostructure.

To determine the emitted fluorescence rate we also need to calculate the non-radiative decay rate. This can be accomplished by evaluating the rate of energy dissipation in the metal nanostructure. Although it is possible to account for radiation reaction it turns out that P_{abs} is not significantly affected by the self-field and, according to Poynting's theorem, we can express the absorbed power as

$$P_{abs} = \frac{\omega_o}{2} \text{Im} \{ \mathbf{p}_{particle} \cdot \mathbf{E}_m^* \} = \frac{\omega_o}{2} \text{Im} \left\{ \left[\vec{\alpha} \mathbf{E}_m \right] \cdot \mathbf{E}_m^* \right\}, \quad (7)$$

where $\mathbf{p}_{particle}$ is the induced dipole in the nanostructure (at \mathbf{r}_o) and \mathbf{E}_m is the *external* field emitted by the molecule at \mathbf{r}_m (c.f. Fig. 1). Expressing \mathbf{E}_m in terms of the free-space Green's dyadic and making use

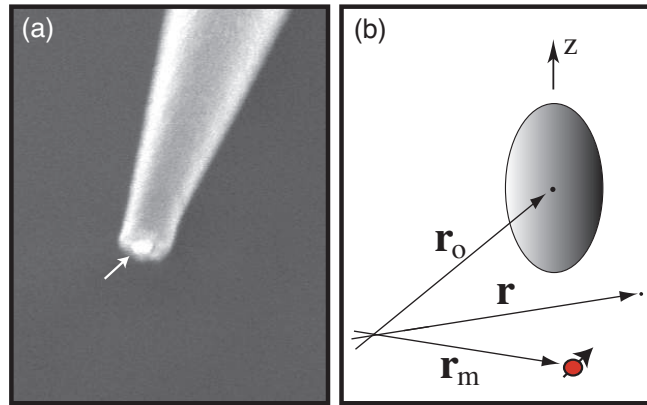


Figure 1: (a) SEM image of a 80nm Au particle trapped at the end of a pulled glass capillary. (b) Coordinates used for the theoretical model.

of energy conservation allows us to express the non-radiative decay rate as

$$\frac{\gamma_{nr}}{\gamma_o} = \frac{P_{abs}}{P_o} = \frac{6\pi k}{\varepsilon_o} \text{Im} \left\{ \left[\overleftrightarrow{\alpha} \overleftrightarrow{\mathbf{G}}(\mathbf{r}_o, \mathbf{r}_m) \mathbf{n}_p \right] \cdot \left[\overleftrightarrow{\mathbf{G}}(\mathbf{r}_o, \mathbf{r}_m) \mathbf{n}_p \right]^* \right\}. \quad (8)$$

Here, P_o is the power radiated by a dipole in free-space. Eq. 8 and Eq. 6 allow us to calculate both the total decay rate and the non-radiative decay rate in presence of the metal tip. The radiative decay rate is simply the difference between the two.

To determine the fluorescence rate expressed in Eq. (3) we also need to calculate the excitation rate γ_{exc} and hence the local field \mathbf{E} at the position of the molecule (\mathbf{r}_m) generated by the incident field \mathbf{E}_o . This field is determined by the induced dipole $\mathbf{p}_{particle}$ according to

$$\mathbf{E}(\mathbf{r}_m) = \mathbf{E}_o(\mathbf{r}_m) + \frac{k^2}{\varepsilon_o} \overleftrightarrow{\mathbf{G}}(\mathbf{r}_m, \mathbf{r}_o) \mathbf{p}_{particle} = \left[\overleftrightarrow{\mathbf{I}} + \frac{k^2}{\varepsilon_o} \overleftrightarrow{\mathbf{G}}(\mathbf{r}_m, \mathbf{r}_o) \overleftrightarrow{\alpha}_{eff} \right] \mathbf{E}_o(\mathbf{r}_m). \quad (9)$$

The excitation rate is now determined by $\gamma_{exc} \propto |\mathbf{p} \cdot \mathbf{E}(\mathbf{r}_m)|^2$, with \mathbf{p} being the molecule's dipole moment.

We have evaluated the decay rates and the fluorescence rate for gold particles with different diameters and for ellipsoidal particles with different aspect ratios. The results have been compared with numerical calculations based on the multiple multipole (MMP) method. For small particles, the dipole model is in satisfactory agreement with the numerical results with the exception of the fluorescence rate at small molecule-particle separations. As an example, Fig. 2a shows the numerically computed decay rates for a molecule with its transition dipole oriented in direction of a spherical gold particle with a diameter of 100nm. The molecule emits at $\lambda = 650\text{nm}$ and its distance from the particle surface is denoted by z . We find that all rates (total, non-radiative, and radiative) increase as the molecule comes closer to the particle surface. The same trend is found for the excitation rate.

Fig. 2b shows, for different particle diameters, the fluorescence rate as a function of molecule-particle separation (z). It is evident that a much higher fluorescence enhancement is observed for large particle diameters. This finding is consistent with the known result that the ratio of the cross-sections of scattering and absorption increases with particle size. The curves in Fig. 2b also show that the fluorescence rate decreases for small distances z , a phenomenon referred to as *fluorescence quenching*. Interestingly, the dipole model developed above *does not* reproduce this quenching phenomenon. In fact, fluorescence quenching is sensitively dependent on the quantum yield $q_a = \gamma_r/\gamma$ and a rigorous calculation is needed to achieve sufficient accuracy for the ratio of the two rates involved.

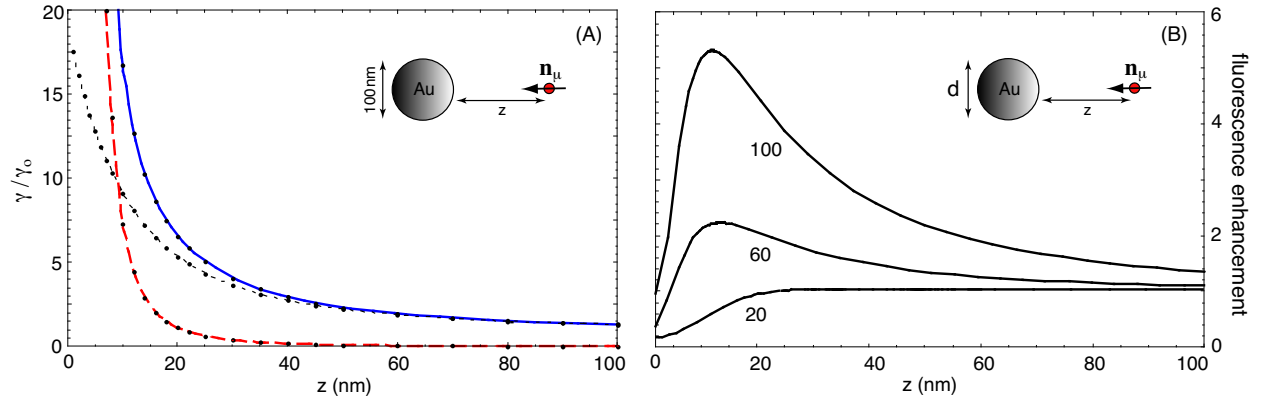


Figure 2: (A) Normalized spontaneous decay rates of a molecule placed at a distance z from the surface of a gold nanoparticle. The transition wavelength is $\lambda = 650\text{ nm}$. The figure shows the total decay rate (blue-solid), the non-radiative decay rate (red-dashed), and the radiative decay rate (black-dotted). (B) Fluorescence enhancement as a function of molecule-particle separation for gold particles with three different diameters.

Prolate spheroidal particles yield fluorescence rates that are much larger than those calculated for spherical particles. We are therefore in the process of developing an experimental strategy for the controlled attachment of ellipsoidal particles to the end of pointed probes. So far, we were successful with spherical particles as shown in Fig. 1a.

3 Future Plans

We are working on an experiment to prove the here outlined theory. Our goal is to understand and control the different parameters involved in fluorescence enhancement. This understanding will help us to develop novel spectroscopic tools providing ultrahigh spatial resolution. We will first use gold particles with different diameters to test the theoretical predictions and then develop strategies for the attachment of ellipsoidal particles. Our theoretical studies predict fluorescence enhancements as large as 20. In a parallel effort we are investigating the possibility of performing absorption spectroscopy on a single molecule. Using the highly localized emission from a metal tip combined with nonlinear optical techniques our preliminary results demonstrate sufficient signal-to-noise to detect a single protein molecule.

DOE sponsored publications (2003-2005)

- [1] A. Bouhelier, M. Beversluis, A. Hartschuh, and L. Novotny, "Near-field second-harmonic generation induced by local field enhancement," *Phys. Rev. Lett.* **90**, 13903 (2003).
- [2] M. R. Beversluis, A. Bouhelier, and L. Novotny, "Continuum generation from single gold nanostructures through near-field mediated intraband transitions," *Phys. Rev. B* **68**, 115433 (2003).
- [3] A. Bouhelier, M. R. Beversluis, and L. Novotny, "Characterization of nanoplasmonic structures by locally excited photoluminescence," *Appl. Phys. Lett.* **83**, 5041 (2003).
- [4] A. Bouhelier, M. R. Beversluis, and L. Novotny, "Near-field scattering of longitudinal fields," *Appl. Phys. Lett.* **82**, 4596 (2003).
- [5] A. Bouhelier, J. Renger, M. Beversluis, and L. Novotny, "Plasmon coupled tip-enhanced near-field microscopy," *J. Microsc.* **210**, 220 (2003).
- [6] A. Hartschuh, H. N. Pedrosa, L. Novotny, and T. D. Krauss, "Simultaneous fluorescence and Raman scattering from single carbon nanotubes," *Science* **301**, 1354 (2003).
- [7] A. Hartschuh, M. R. Beversluis, A. Bouhelier, and L. Novotny, "Tip-enhanced optical spectroscopy," *Phil. Trans. R. Soc. Lond. A* **362**, 807 (2004).
- [8] J. R. Zurita-Sanchez, J.-J. Greffet, and L. Novotny, "Near-field friction due to fluctuating fields," *Phys. Rev. A* **69**, 022902 (2004).
- [9] A. Bouhelier, A. Hartschuh, M. R. Beversluis, and L. Novotny, "Near-field optical microscopy in the nanosciences," in *Microscopy for Nanotechnology*, N. Yao and Z. L. Wang (eds.), Springer Verlag (2005).
- [10] A. Hartschuh, H. N. Pedrosa, J. Peterson, L. Huang, P. Anger, H. Qian, A. J. Meixner, M. Steiner, L. Novotny, and T. D. Krauss, "Single carbon nanotube optical spectroscopy," *ChemPhysChem* **6**, 1–6 (2005).
- [11] L. Novotny and S. J. Stranick, "Near-field optical microscopy and spectroscopy with pointed probes," *Ann. Rev. Phys. Chem.* submitted (2005).
- [12] L. Novotny and A. Bouhelier, "Near-field optical excitation and detection of surface plasmons," in *Surface Plasmon Nanophotonics*, M. Brongersma (ed.), Kluwer Academic Press, in press (2005).
- [13] P. Anger, P. Bharadwaj, and L. Novotny, "Enhancement and quenching of single molecule fluorescence near nanoscale structures," *Phys. Rev. Lett.* in preparation, 2005.

Electron-Driven Excitation and Dissociation of Molecules

A. E. Orel
Department of Applied Science
University of California, Davis
Davis, CA 95616
aeorel@ucdavis.edu

Program Scope

This program uses modern *ab initio* techniques, both for the electron scattering and the subsequent nuclear dynamics studies, to study collisions of electrons. Specifically, this program addresses vibrational excitation, dissociative attachment, and dissociative recombination problems in which a full multi-dimensional treatment of the nuclear dynamics is essential and where non-adiabatic effects are expected to be important.

Recent Progress

We have carried out a number of calculations studying low-energy electron scattering from polyatomic systems, and vibrational excitation and dissociative attachment in a diatomic system. Much of this work has been done in collaboration with the AMO theory group at Lawrence Berkeley Laboratory headed by T. N. Rescigno and C. W. McCurdy. As a result of this collaboration, one of my students has begun work on experiments with the AMO experimental group headed by A. Belcamen. He will carry out experiments on dissociative attachment of NO, while we carry out the calculations to support this work.

Non-local effects in the vibrational excitation of NO by low-energy electrons

Previously we have carried out calculations on low-energy collisions of electron with NO using the local approximation for the interaction potential (see Publication 2). In order to derive this approximation the assumption is made that the anion can autoionize into all vibrational states of the neutral, that is, that the sum of open vibrational states is complete. This is not true in the NO system. We have removed this approximation, using a non-local energy dependent potential that correctly accounts for the autoionization loss. We have computed elastic and vibrationally inelastic cross sections to compare the results from the local complex potential (or “boomerang”) model, the local complex potential model modified by the introduction of “barrier penetration factors” and the nonlocal form for the potential. The nonlocal model was used both for the calculation of the vibrational excitation as well as the dissociative attachment. The present results obtained with more accurate resonance curves and the nonlocal model represent a considerable improvement over the boomerang model used in our previous calculations and are in reasonably good agreement with the most recent experimental measurements.

The results of the calculation are described in a paper published in Physical Review A (Publication 4).

Dissociative attachment of vibrational excited NO

NO is believed to have an extremely small dissociative attachment cross section at low energy from its ground vibrational state. However, consideration of the potential energy curves for the neutral and the resonant states indicate that as the vibrational state is increased the cross section will increase dramatically. This led to a joint theoretical/experimental project, linking the experimental AMO group, with the theory AMO group and UC Davis. Experiments have been proposed to measure the dissociative attachment in this system as a function of initial vibrational state. These experiments will be performed at LBL and will be part of the thesis for H. Adaniya, a UC Davis graduate student. We have carried out calculations on the dissociative attachment of NO as a function of initial vibrational state to guide the experiment and predict the cross section. We have used the potential curves and couplings from our previous calculations, as well as the non-local code described previously.

The results of the calculation are described in a paper published in Physical Review A (Publication 4).

Electron interactions with the CF radical

In collaboration with T.N. Rescigno, LBL, we have studied electron interactions with the CF radical. CF is isoelectronic with NO. Using a simple molecular orbital picture of the relevant wave functions neutral CF has an open-shell $^2\Pi$ ground state; its electronic configuration is $(\text{core})^8 (5\sigma)^2 (1\pi)^4 (2\pi)^1$. The quasi-bound (resonance) anion states have the configuration $(\text{core})^8 (5\sigma)^2 (1\pi)^4 (2\pi)^2$. The two open-shell 2π electrons can be coupled to form three states with symmetries $^3\Sigma^-$, $^1\Delta$ and $^1\Sigma^+$, which, by analogy with NO and O₂, are expected to be separated by only a few electron volts. There have been calculations of the elastic scattering differential cross sections [1,2]. The R-matrix calculations [2] were carried out as a function of the C--F internuclear separation, but no dynamics calculations were performed to obtain dissociative attachment or vibrational excitation cross sections.

We computed complex potential curves (positions and widths) for all resonant anion states. We performed fixed-nuclei scattering calculations using the Complex Kohn variational method and extracted the resonance parameters as a function of geometry by analyzing the energy dependence of the eigenphase sums. As in NO, we used a non-local treatment of the nuclear dynamics to evaluate the vibrational excitation and dissociative attachment cross sections. The calculations revealed a rich series of overlapping resonance structures. As in NO, the dissociative attachment cross sections were found to be small at low energy for low initial vibrational states and increased dramatically as a function of the initial vibrational state.

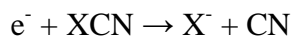
The results of the calculation are described in a paper to be submitted to Physical Review A (Publication 5).

FUTURE PLANS

Dissociative attachment of ClCN and BrCN

We have made significant progress in our studies of the dissociative attachment of

ClCN and BrCN. These systems (and the analogous pseudohalogens, such as HCN) have the interesting property that since both fragments have positive electron affinities, two fragmentation channels are open. These are:



or



where X is Cl or Br. The channel producing X^- was suggested to proceed through the negative ion $^2\Sigma$ resonance state, formed by the addition of an electron to a σ^* antibonding orbital. The second channel, producing CN^- , had been explained as a two-step mechanism. The first step is the transition to the $^2\Pi$ resonance, which is the addition of the electron to a π^* antibonding orbital with energy transfer from the C-N stretching mode into the dissociative X-CN mode[3].

The calculations reveal a much more complicated situation. Although the path to X^- is direct, proceeding as described through the $^2\Sigma$ anion resonance, the path to CN^- has a more interesting structure. The lowest lying $^2\Pi$ anion resonance correlated diabatically to an excited state of the negative ion fragments and does not cross the neutral. Therefore, this state can not directly lead to product. There is a second $^2\Pi$ resonance that dissociates to CN^- . Coupling between these two resonances allow the dissociative attachment to CN^- to occur. We have calculated the resonance curves, autoionization widths and couplings between the two $^2\Pi$ resonances as a function of the X-CN internuclear distance, and used this information dynamics to predict a dissociative attachment cross section. Since the $^2\Sigma$ resonance crosses the neutral near its equilibrium separation it was necessary to use a non-local treatment to correctly describe the dynamics.

We have also investigated the behavior of the neutral and resonance curves as a function of the C-N stretch. For all states, as the C-N distance is increased or decreased (keeping the X-CN distance constant) the energy of the state increases, which can be fit to a harmonic oscillator function. This will not change the dynamics of the dissociation. We are now studying the effect of bending on the resonance curves and autoionization widths. Bending reduces the symmetry from $C_{\infty v}$ to C_s . This allows coupling between channels arising from σ^* and π^* antibonding orbitals, the Σ and one component of the degenerate Π resonance states. Such coupling will affect the cross section by allowing the $^2\Sigma$ and the $^2\Pi$ pathways to mix.

Dissociative Attachment in Halogenated Molecules

There have been no theoretical systematic studies of dissociative attachment in organic molecules. There have been some such experimental studies, but these have been limited[4,5,6]. We have begun a series of calculations on mono-substituted organic compounds to look for general trends and to better understand what controls the energy flow leading to dissociation in these systems. We have chosen the systems, HCCCl, H₃CCCl, H₅CCCl, showing a series from triple, double to single bond respectively.

We will begin with ClCCH, chloroacetylene. This can be studied as a pseudo-diatom, varying the Cl-C internuclear separation and keeping all other bond distances fixed. We can then investigate an intriguing possibility with this system. There has been

some experimental evidence of dramatic effects in the DA cross section due to coupling between channels arising from σ^* and π^* antibonding orbitals[7]. Of course, for ClCCH in its linear configuration, these channels can not mix. However, mixing can occur if the molecule is bent. We are investigating this effect by carrying out the scattering for the bent structure. We are also looking at variations as other bonds are modified. This can be combined into a multi-dimensional study of the dissociation dynamics. If the dynamics are only studied in one-dimension, that is, as a function of the C-Cl bond distance, the physics of the energy transfer process is lost. The effect of the double vs. the triple C--C bond is combined with the effect of the increased symmetry in the linear HCCCl system which does not allow the Σ/Π mixing to occur. However, if the system is studied in multiple dimensions, such that this mixing can occur, a more direct comparison is possible. This is a case where it is critical to go beyond the usual one-dimensional picture to truly understand the dissociation dynamics and energy flow within the modes of the system. We then plan to consider H₃CCCl, the double-bond case and H₅CCCl, the single bond case.

PUBLICATIONS

1. *Ab initio* study of low-energy electron collisions with ethylene
C. S. Trevisan, A. E. Orel, and T. N. Rescigno
Phys. Rev. A, **68**, 062707 (2003).
2. Low-energy electron scattering of NO : *Ab initio* analysis of the $^3\Sigma^-$, $^1\Delta$ and $^1\Sigma^+$ shape resonances in the local complex potential model, Z. Zhang, W. Vanroose, C. W. McCurdy, A. E. Orel, and T. N. Rescigno
Phys. Rev. A, **69**, 062711 (2004).
3. *Ab initio* study of low-energy electron collisions with tetrafluoroethene C₂F₄,
C. S. Trevisan, A. E. Orel, and T. N. Rescigno,
Phys. Rev. A, **70**, 012704 (2004).
4. A nonlocal *ab initio* model of dissociative electron attachment and vibrational excitation of NO, C. S. Trevisan, Karel Houfek, Zhiyong Zhang, A. E. Orel, C. W. McCurdy, and T. N. Rescigno, Phys. Rev. A, **xx**, xxxxx (2005).
5. Resonant electron-CF collision processes, C. S. Trevisan, A. E. Orel, and T. N. Rescigno, to be submitted Phys. Rev. A

REFERENCES

1. M. T. Lee, L. M. Brescansin, L. E. Machado and F. B. C. Machado, *Phys. Rev. A*, **66**, 012720 (2002).
2. I. Rozum, N. J. Mason and J. Tennyson, *J. Phys. B*, **36**, 2419 (2003).
3. F. Bruning, I. Hahndorf, A. Stamatovic, and E. Illenberger, *J. Phys. Chem.*, **100**, 19740 (1996), *Phys. Rev. A*, **11**, 1314 (1975).
4. D. M. Pearl and P. D. Burrow, *J. Chem. Phys.*, **101**, 2940 (1994).
5. K. Aflatooni and P. D. Burrow, *J. Chem. Phys.*, **113**, 1455 (2000).
6. G. A. Gallup, K. Aflatooni and P. D. Burrow, *J. Chem. Phys.*, **118**, 2562 (2003).
7. M. Allan and L. Andric, *J. Chem. Phys.*, **105**, 3559 (1996).

“Low-Energy Electron Interactions with Complex Targets”

Thomas M. Orlando, *School of Chemistry and Biochemistry and School of Physics,*
Georgia Institute of Technology, Atlanta, GA 30332-0400

Thomas.Orlando@chemistry.gatech.edu

Objectives: The primary objectives of this program are to investigate the fundamental physics and chemistry involved in low-energy (1-100 eV) electron scattering with molecular solids, surfaces and interfaces. The program is primarily experimental and concentrates on the important questions concerning how gas-phase concepts have to be modified when trying to understand electron collisions with complex condensed-phase targets such as pure and adsorbate covered water ice thin-films, DNA interfaces and Cl-passivated Si(111) surfaces.

Progress: This is the third year of the program which began in July 2002. We have focused on three main tasks that are being carried out in the Electron- and Photon-Induced Chemistry on Surfaces (EPICS) Laboratory at the Georgia Institute of Technology (GIT).

Project 1. Low-energy (5 –250 eV) electron stimulated desorption of H^+ , H_2^+ , and $H^+(H_2O)_n$ from pure and acid covered low-temperature water ice. Low-energy (5 - 250 eV) electron stimulated desorption (ESD) has been used to study the production and removal of H^+ , H_2^+ and protonated water clusters $H^+(H_2O)_{n=1-8}$ from porous amorphous solid water (PASW), amorphous solid water (ASW), and crystalline (CI) water ice films. The threshold energy for ESD of H_2^+ from CI and H_3O^+ from PASW and ASW is $\sim 22 \pm 3$ eV. There is also a H_2^+ yield increase at $\sim 40 \pm 3$ eV and a $\sim 70 \pm 3$ eV threshold for ESD of $H^+(H_2O)_{n=2-8}$ from PASW and ASW. H_2^+ production and desorption involves direct molecular elimination and reactive scattering of an energetic proton. Both of these channels likely involve localized two-hole one-electron and/or two-hole final states containing $4a_1$, $3a_1$ and/or $2a_1$ character. The 70 eV cluster ion threshold implicates either an initial ($2a_1^{-2}$) state localized on a monomer or the presence of at least two neighboring water molecules each containing a single hole. The resulting correlated two-hole or two-hole, one-electron configurations are localized within a complex and result in an intermolecular Coulomb repulsion and cluster ion ejection. The $H^+(H_2O)_n$ yields are highest from PASW relative to ASW and CI and decrease with temperature, whereas the H_2^+ yields are highest for CI and increase with temperature. The temperature effects and cluster ion distributions are accounted for by distance and temperature dependent hole screening. Changes in screening, hole lifetimes and hopping probabilities are greatest for a_1 levels. This is supported by valence band photoemission studies of ice as a function of temperature.

We have modeled the cluster ion yields with a simple screened hole-hole interaction which leads to an intermolecular Coulomb repulsion effect. If the two neighboring ions remain localized (within 1 - 2 nm of each other) for approximately 100 fs, a cluster ion, whose kinetic energy is determined by the potential of the localized charges, can be produced. Cluster growth is then dominated by formation of ion-dipole bonds as a result of dielectric hole screening. These intensities can be modeled approximately $I(n) \propto A \exp[-E_h \times n / E_n]$. A is a scale factor representing the overall surface area, $E_h = 0.25$ eV is the average binding energy per hydrogen bond in ice and E_n

is the hydration enthalpy of the n^{th} water molecule in the cluster of size n . The fit to the data shown in Figure 1 is very good and is applicable to each phase of ice.

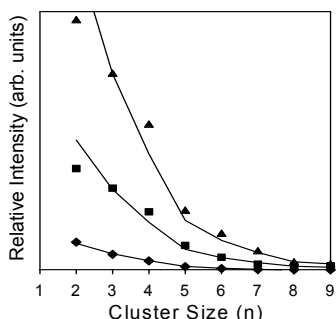


Figure 1. Protonated water cluster yield as a function of the number of water molecules for (\blacktriangle) PASW, (\blacksquare) ASW, and (\blacklozenge) CI. The solid and dashed lines represent the fit to the data using $I(n) \propto A \exp[-E_h \times n / E_n]$. Orlando et. al, Phys. Rev. B. 72, 035431 (2005).

Project 2. A theoretical description and experimental demonstration of diffraction in electron stimulated desorption (DESD). The role of diffraction in electron-stimulated desorption (DESD) has been re-examined and described theoretically. *Specifically, initial state effects in DESD of Cl^+ from $\text{Si}(111)-(1 \times 1):\text{Cl}$ and $\text{Si}(7 \times 7):\text{Cl}$ are examined and the theory is expanded to encompass spherical-wave and multiple scattering effects of low-energy incident electrons by introducing a separable propagator method.*

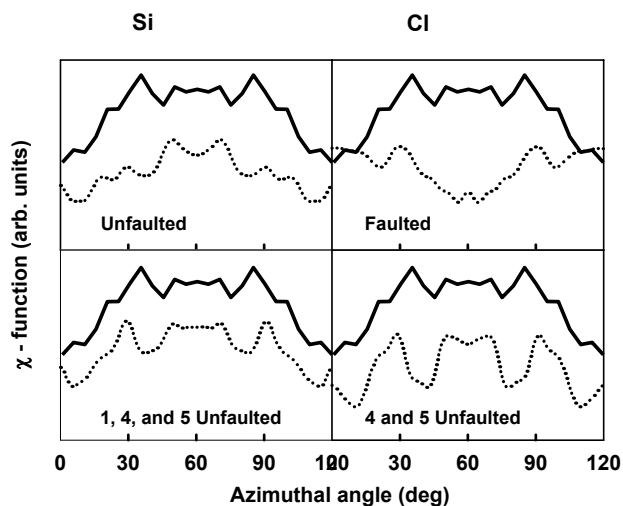


Figure 2. Experimental DESD data (solid line) compared to theoretical model (dashed line) for the ESD of Cl^+ signal from the faulted and unfaulted domains on a Cl terminated $\text{Si}(111)-(7 \times 7):\text{B}$ surface.

Qualitative analysis of Cl^+ desorption shows that the initial excitation occurring on the $\text{Si}(111)-(1 \times 1):\text{Cl}$ surface primarily involves the Si. Desorption involves ionization of the Si(3s) level followed by Auger cascading from the σ -bonding surface state and shake-up of an electron in the non-bonding π -level and/or direct ionization of the Si-Cl σ -bonding state. *For the case of $\text{Si}(111)-(7 \times 7)$ surface, a propensity for the removal of Cl^+ from the unfaulted region has been observed. This offers the possibility of nanoscale pre-patterning using DESD. Finally, temperature effects on DESD rates are also analyzed and modeled.*

Project 3. Low-energy electron-induced damage of DNA: Neutral fragments yields.

We have utilized a vacuum ultraviolet (VUV) laser source using third-harmonic

generation in rare gases to detect the neutral fragments produced during the low-energy electron beam induced damage of DNA plasmids physisorbed on graphite substrates. We are also monitoring the DNA damage using *in situ* Fourier transform infrared spectroscopy and post-irradiation gel-electrophoresis. In addition, we have modified the code used to describe DESD on single crystal surfaces, to model diffraction effects during electron scattering with DNA.

Future Plans: The white peaks in Figure 3 are the cluster ion signal from 10 ML of water adsorbed on graphite. This signal is actually very small relative to the same coverage on many other substrates such as Pt(111), ZrO₂, and Si(111). However, an enormous increase in yield is found when water is adsorbed onto a few ML thick Xe overlayer pre-deposited on the graphite. We have submitted a renewal proposal which plans to examine the roles of hole transfer, Auger decay and ICD in the stimulated production and desorption of cluster ions. Specifically, we propose to carry out studies of water adsorbed on graphite and graphite containing rare gas (Xe and Ar) spacer layers.

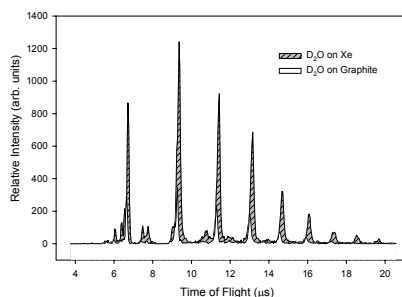


Figure 3. Cluster ion distribution observed during 100 eV pulsed electron beam bombardment of 10 ML of water on clean graphite (white peaks) and of submonolayer coverages of water on 3 ML of a Xe spacer layer adsorbed on the graphite.

We will continue to emphasize experimental and theoretical studies of electron scattering with DNA and constituents of DNA. Figure 4 shows the *preliminary* results of our calculation. The left plot shows the partial wave sum and resonance structure which is reminiscent to that observed experimentally. In the right-hand plot of Figure 3, we also show some *preliminary* results which allows comparison of the scattering in the presence of an initial core-hole. There are some observable differences indicating that the core hole may be relevant to accurately describing interactions of low-energy electrons with DNA.

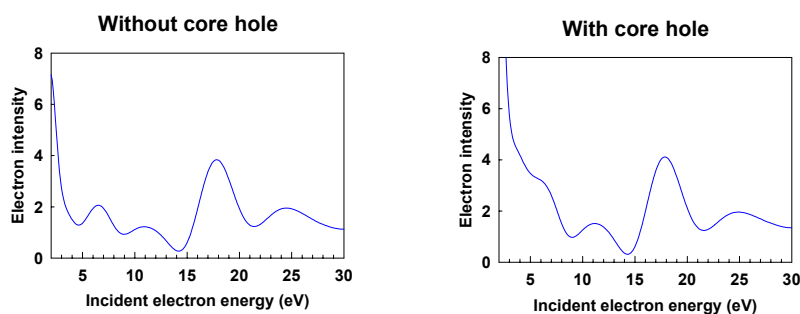


Figure 4 Calculation of the incident electron intensity at the center of the ring of a DNA target molecule as a function of incident electron energy. The phase shift data for each scatter were calculated by using the FEFF 8.2 code. The phase shift for the right hand plot was obtained by assuming that there is core hole.

Publications from this program:

- 1.) T. M. Orlando and M. T. Sieger, "The Role of Electron-stimulated production of O₂ from water ice and the radiation processing outer solar system surfaces" *Surf. Sci.* **528**, 1-7 (2003).

- 2.) J. Herring, A. Alexandrov, and T. M. Orlando, “The stimulated desorption of cations from pristine and acidic low-temperature ice surfaces” *Phys. Rev. Lett.* **92**, 187602-1 (2004).
- 3.) T. M. Orlando, D. Oh, M. T. Sieger, and C. Lane, “Electron collisions with complex targets: diffraction effects in stimulated desorption”, *Physica Scripta*, **T110**, 256 (2004).
- 4.) J. Herring-Captain, G. A. Grieves, M. T. Sieger, A. Alexandrov, H. Chen and T. M. Orlando “Electron-stimulated desorption of H^+ , H_2^+ , and $H^+(H_2O)_n$ from nanoscale water thin-films” *Phys. Rev. B.* **72**, 035431 (2005).
- 5.) C. Lane, K. Shepherd, A. Alexandrov and T. M. Orlando, “Low-energy electron-stimulated desorption of $SiCl_4$ multilayers adsorbed on Si(111)” (*in press*) *Surf. Sci.*
- 6.) D. Oh, M. T. Sieger and T. M. Orlando, “A theoretical description and experimental demonstration of diffraction effects in electron-stimulated desorption” (*Feature article*, *J. Phys. Chem.*)
- 7.) J. Herring-Captain, A. Alexandrov, and T. M. Orlando “Probing the interaction of hydrogen chloride on low-temperature water ice surfaces using electron stimulated desorption”, (*submitted*), *J. Chem. Phys.*
- 8.) J. Herring-Captain, N. G. Petrik, G. A. Kimmel, A. Alexandrov and T. M. Orlando, “Photoionization of liquid jets containing aqueous salts”, (*submitted*), *J. Phys. Chem.*

The program funded four full-time graduate students:

Janine Herring, Chris Lane, Doogie Oh, and Yangfen Chen

Energetic Photon and Electron Interactions with Positive Ions

Ronald A. Phaneuf,
Department of Physics /220
University of Nevada
Reno NV 89557-0058
phaneuf@physics.unr.edu

Program Scope

This experimental program investigates processes leading to ionization of positive ions by photons and electrons. The objective is a deeper understanding of both ionization mechanisms and electron-electron interactions in ions of atoms, molecules and nanoparticles. Monenergetic beams of photons and electrons are crossed or merged with ion beams to selectively probe their internal electronic structure and the interaction dynamics. In addition to precision spectroscopic data for ionic structure, measurements of absolute cross sections for photoionization and electron-impact ionization provide critical benchmarks for the theoretical calculations that generate opacity databases. The latter are critical to models of astrophysical, fusion-energy and laboratory plasmas. Examples of particular relevance to DOE include the Z pulsed-power facility at Sandia National Laboratories, the world's brightest and most efficient x-ray source, and the National Ignition Facility at Lawrence Livermore National Laboratory, the world's most powerful laser. Both facilities are dedicated to high-energy-density science, fusion energy and defense-related research.

Recent Progress

The major thrust of this research program has been the application of an ion-photon-beam (IPB) research endstation to experimental studies of photoexcitation and photoionization of singly and multiply charged positive ions using synchrotron radiation. The high photon beam intensity and energy resolution available at ALS undulator beamline 10.0.1 make photoion spectroscopy a powerful probe of the internal electronic structure of atomic and molecular ions, permitting tests of sophisticated structure and dynamics codes at unprecedented levels of detail and precision. Photon-ion measurements using the IPB endstation at ALS define the state of the art with respect to energy resolution in studies of photon-ion interactions by at least an order of magnitude. Specific accomplishments of the past year are highlighted below.

- Fullerene ions are of special interest because they bridge the gap between molecules and solids. Absolute cross sections for photoionization of C_{60}^+ were measured over the energy range 17-310 eV. A detailed investigation was made of the relative roles of localized and collective electron excitations in the photoionization and photofragmentation of C_{60} and C_{70} ions. As has been observed in photoionization of neutral C_{60} , a giant dipole resonance at a photon energy near 20 eV was found in photoionization of C_{60}^+ , C_{60}^{2+} and C_{60}^{3+} ions. This resonance feature is attributed to a surface plasmon excitation of the delocalized valence electrons, representing a periodic motion of the spherical shell of valence electrons with

respect to the positive ionic core. A second broad resonance was identified near 40 eV in each case. On the basis of theoretical calculations using the time-dependent local-density approximation performed by collaborators at the Max Planck Institute for Complex Systems in Dresden, this feature was identified as a volume plasmon excitation of the valence electrons, analogous to a breathing mode in which the electron density in the spherical shell oscillates. This work was published by Physical Review Letters [13] featured as a *Physics News Update* by the American Institute of Physics [14]. At photon energies above 280 eV, the photoionization cross sections for fullerenes ions become distinctly molecular in character, and are dominated by narrower resonances due to localized K-shell excitation of carbon atoms.

- A systematic study of photoionization of ions of the nitrogen isoelectronic sequence was completed and published [15]. Absolute cross-section measurements and their analysis were reported for photoionization of metastable and ground-state F^{2+} and Ne^{3+} . Based on the Ph.D. thesis research of Alejandro Aguilar, this paper includes a quantum-defect analysis of four Rydberg series of resonances observed in photoionization of N, O^+ , F^{2+} and Ne^{3+} .
- An investigation of photoionization of ions of the iron isonuclear sequence, Fe^{3+} , Fe^{5+} and Fe^{7+} was completed, resulting in the Ph.D. thesis of Mohammad Gharaibeh in January, 2005. Interpretation of the results for these ions with open d-shells is complicated by a multitude of metastable levels that are populated in the primary ion beam. Comparison of the Fe^{3+} results with new R-matrix theoretical calculations indicates the inadequacy of theory for ions with such complex electronic structure, and has motivated additional theoretical work.
- An investigation of photoionization of ions of the xenon isonuclear sequence was conducted with a focus on applications in 13.5 nm light sources for EUV lithography. The results for Xe^{3+} were compared with complementary results for electron-impact ionization, constituting the M.S. thesis of Erik Emmons [12] and a paper published by Physical Review A [16]. In collaboration with the NIST EBIT group, this work was extended to measurements on Xe^{4+} , Xe^{5+} and Xe^{6+} , and a manuscript on this work is being prepared for publication.
- Complementary measurements were initiated of photoionization and electron-impact ionization of ions of the krypton isonuclear sequence, which will constitute the Ph.D. thesis research of Miao Lu. Absolute measurements for photoionization of Kr^{3+} , Kr^{4+} and Kr^{5+} were completed and are being analyzed.
- Measurements of photoionization of ions of the chlorine isoelectronic sequence were initiated as part of the Ph.D. thesis research of Ghassan Alna'Washi. Measurements for photoionization of Ca^{3+} were completed and are currently being analyzed.

Future Plans

Future studies will concentrate on collective electron excitations in atomic and molecular ions, as well as on studies of electron-impact ionization of atomic ions that complement photoionization studies at ALS.

- The energy range and high spectral resolution of ALS beamline 10.0 are optimally suited to studies of photoionization and photofragmentation of macro-molecular ions, which have physical properties intermediate between those of molecules and solids. Studies to date have

concentrated mainly on decay of the photo-excited plasmon resonances in C_{60}^{q+} and C_{70}^{q+} molecular ions by ejection of an electron. Exploratory measurements indicate that these giant plasmon resonances may also decay by fragmentation, with ejection of a pair of carbon atoms being most probable. The ion-photon-beam endstation at ALS is well-suited to investigation of photofragmentation channels that yield charged fragments. A systematic investigation is planned of the relative importance of fragmentation versus ionization as the initial charge state of the fullerene ion is increased. Measurements are planned for C_{60}^{q+} , C_{70}^{q+} and C_{84}^{q+} ions in initial charge states $q = 1, 2, 3$.

- A number of studies have demonstrated that single atoms (e.g. of metals) may be stably trapped inside the hollow cage of a fullerene molecule. The technology to produce so-called endohedral fullerenes in macroscopic quantities has advanced to the stage that it may now become feasible to produce charged endohedral fullerene ions in a discharge and to accelerate them. This would enable photoionization studies with mass-analyzed beams of endohedral fullerene ions. Concurrently, the electronic properties of such “caged” atoms has attracted theoretical attention. Of particular interest is the behavior of a giant resonance in photoionization of an atom that is caged within the charged spherical shell of a fullerene molecule. An example is the 4d giant resonance of Xe, which is predicted to be split into four prominent peaks. Another fundamental question to be addressed is the effect of a caged atom on the collective electron motions associated with the surface and volume plasmon resonances in fullerene molecules.
- Complementary studies of electron-impact ionization of ions of the Kr isoelectronic sequence are planned to compare to recent photoionization measurements. The selectivity and energy resolution of the latter should facilitate the identification of indirect ionization contributions to electron-impact ionization.

References to Publications of DOE-Sponsored Research (2003-2005)

1. *Photoionization of isoelectronic ions: Mg^+ and Al^{2+}* , A. Aguilar, J.B. West, R.A. Phaneuf, R.L. Brooks, F. Folkmann, H. Kjeldsen, J.D. Bozek, A.S. Schlachter and C. Cisneros, Phys. Rev. A 67 012701 (2003).
2. *Absolute photoionization cross section measurements of OII ions from 29.7 eV to 46.2 eV*, A. Aguilar, A.M. Covington, G. Hinojosa, R.A. Phaneuf, I. Álvarez, C. Cisneros, J.D. Bozek, I. Dominguez, M.M. Sant’Anna, A.S. Schlachter, S.N. Nahar and B.M. McLaughlin, Astrophys. J (Supplement Series) 146, 467 (2003).
3. *Photoionization of Sc^{2+} ions by synchrotron radiation: high-resolution measurements and absolute cross sections in the photon energy range 23-68 eV*, S. Schippers, A. Müller, S. Riez, M.E. Bannister, G.H. Dunn, A.S. Schlachter, G. Hinojosa, C. Cisneros, A. Aguilar, A.M. Covington, M.F. Gharaibeh and R.A. Phaneuf, Phys. Rev A 67, 032702 (2003).
4. *Photoionization studies of the B^+ valence shell: experiment and theory*, S. Schippers, A. Müller, B.M. McLaughlin, A. Aguilar, C. Cisneros, E.D. Emmons, M.F. Gharaibeh and R.A. Phaneuf, J. Phys. B: At. Mol. Opt. Phys. 26, 3371 (2003).

5. *Photoionization of C^{2+} ions*, A. Müller, R.A. Phaneuf, A. Aguilar, M.F. Gharaibeh, A.S. Schlachter, I. Álvarez, C. Cisneros, G. Hinojosa and B.M. McLaughlin, Nucl. Instrum. Methods Phys. Res. B 205, 301 (2003).
6. *Photoionization of Sc^{2+} : experimental link with photorecombination of Sc^{3+} by application of detailed balance*, S. Schippers, A. Müller, S. Ricz, M.E. Bannister, G.H. Dunn, J. Bozek, A.S. Schlachter, G. Hinojosa, C. Cisneros, A. Aguilar, A.M. Covington, M.F. Gharaibeh and R.A. Phaneuf, Nucl. Instrum. Methods Phys. Res. B 205, 297 (2003).
7. *Photoionization of positive ions: the nitrogen isoelectronic sequence*, A. Aguilar, Ph.D. Dissertation, University of Nevada, Reno (2003).
8. *Lifetime of a K-shell vacancy in atomic carbon created by 1s-2p photoexcitation of C^+* , A.S. Schlachter, M.M. Sant'Anna, A.M. Covington, A. Aguilar, M.F. Gharaibeh, E.D. Emmons, S.W.J. Scully, R.A. Phaneuf, G. Hinojosa, I. Álvarez, C. Cisneros, A. Müller and B.M. McLaughlin, J. Phys. B 37, L103 (2004).
9. *Threshold truncation of a 'giant' dipole resonance in photoionization of Ti^{3+}* , S. Schippers, A. Müller, R.A. Phaneuf, T. van Zoest, I. Álvarez, C. Cisneros, E.D. Emmons, M.F. Gharaibeh, G. Hinojosa, A.S. Schlachter and S.W.J. Scully, J. Phys. B 37, L209 (2004).
10. *Threshold truncation of a 'giant' dipole resonance in photoionization of Ti^{3+}* , S. Schippers, A. Müller, R.A. Phaneuf, T. van Zoest, I. Álvarez, C. Cisneros, E.D. Emmons, M.F. Gharaibeh, G. Hinojosa, A.S. Schlachter and S.W.J. Scully, J. Phys. B 37, L209 (2004).
11. *Electron-impact ionization of Ti^{3+} ions*, T. van Zoest, H. Knopp, J. Jacobi, S. Schippers, R.A. Phaneuf and A. Müller, J. Phys. B 37, 4387 (2004).
12. *A complementary study of photoionization and electron-impact ionization of an atomic ion: Xe^{3+}* , E. Emmons, M.S. Thesis, University of Nevada, Reno (May 2004).
13. *Photoexcitation of a volume plasmon in C_{60} ions*, S.W.J. Scully, E.D. Emmons, M.F. Gharaibeh, R. A. Phaneuf, A.L.D. Kilcoyne, A.S. Schlachter S. Schippers, A. Müller, H.S. Chakraborty, M.E. Madjet and J.-M. Rost, Phys. Rev. Lett. 94, 065503 (2005).
14. *240 Electrons Set in Motion*, Physics News Update 722 #1 American Institute of Physics, (March 17, 2005).
15. *Photoionization of ions of the nitrogen isoelectronic sequence: experiment and theory for F^{2+} and Ne^{3+}* , A. Aguilar, E.D. Emmons, M.F. Gharaibeh, A.M. Covington, J.D. Bozek, G. Ackerman, S. Canton, B. Rude, A.S. Schlachter, G. Hinojosa, I. Alvarez, C. Cisneros, B.M. McLaughlin and R.A. Phaneuf, J. Phys. B At. Mol. Opt. Phys. 38, 343 (2005).
16. *Photoionization and electron-impact ionization of Xe^{3+}* , E.D. Emmons, A. Aguilar, M.F. Gharaibeh, S.W. J. Scully, R.A. Phaneuf, A.L.D. Kilcoyne, A.S. Schlachter, I. Alvarez, C. Cisneros and G. Hinojosa, Phys. Rev. A 71, 042704 (2005).
17. *Photofragmentation of ionic carbon monoxide*, G. Hinojosa, M.M. Sant'Anna, A.M. Covington, R.A. Phaneuf, I.R. Covington, I. Domínguez, A.S. Schlachter, I. Alvarez and C. Cisneros, J. Phys. B. 38, 2701 (2005).
18. *Systematic photoionization study along the iron isonuclear sequence*, M. F. Gharaibeh, Ph.D. Dissertation, University of Nevada, Reno (2005).

Cold Rydberg Atom Gases and Plasmas in Strong Magnetic Fields

G. Raithel, FOCUS Center, Physics Department, University of Michigan
 450 Church St., Ann Arbor, MI 48109-1120, graithel@umich.edu
<http://quaser.physics.lsa.umich.edu/projects/highb/>

1 Goals and main methods

The main objective of this project is to investigate interactions in highly magnetized, cold Rydberg-atom gases and magnetized plasmas. The dynamics of highly excited Rydberg atoms and cold plasmas in strong magnetic (B) fields exhibits an extraordinary richness, which is shared by related systems such as positronium, excitons, gases of electrons and positrons, and - in solids - electron-hole plasmas. The system Hamiltonian typically is dominated by the diamagnetic term, and the Coulomb interaction presents only a weak perturbation, giving rise to unusual forms of atom-like diamagnetic matter. The largest fraction of phase space of these atoms corresponds to large values of the magnetic quantum number $|m|$, where the dynamics is regular and characterized by drift-orbit solutions, also known as guiding-center solutions. These drift-orbit states have large densities of states and lifetimes. Therefore, in low-temperature collision-rich environments in strong magnetic fields, such as cold Rydberg atom gases and cold plasmas, they can be quite abundant and may even represent the main portion of Rydberg-atom population. The importance of drift-state Rydberg atoms has become clear in recent anti-hydrogen experiments elsewhere, in which drift-state anti-hydrogen has been formed by recombination in a modified Penning trap and detected by field ionization.

To study cold plasmas and gases of cold Rydberg atoms in a high- B environment, in the last couple of years we have constructed an atom trap that operates at magnetic fields up to 6 Tesla. The trap can be loaded with rubidium ground-state atoms cooled to $\approx 150 \mu\text{K}$. If desired, these atoms can be magnetically trapped. The atoms can also be excited into Rydberg states, which can be promoted into long-lived high-angular-momentum drift-state atoms and subsequently magnetically trapped for times in excess of 100 ms. This atom trap can be combined and spatially overlapped with a Penning charged-particle trap.

2 Electric-field ionization of strongly magnetized Rydberg atoms in low- m states

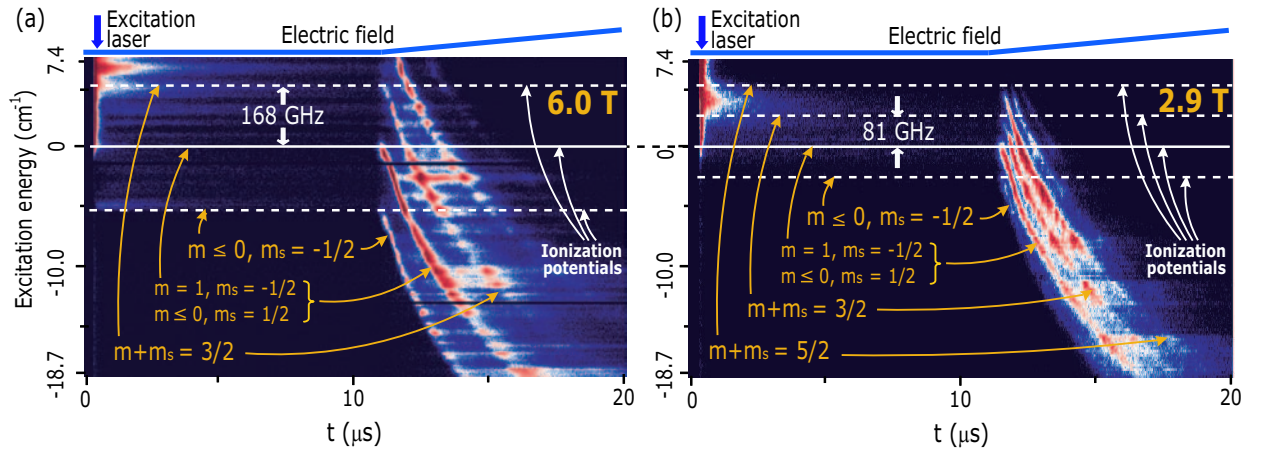


Figure 1: 2D representation of the field ionization behavior at 6 T (left panel) and 2.9 T (right panel) as a function of laser wavelength and ionization electric field. The latter is applied in form of a time-dependent field ionization pulse, as displayed in the top portions of the panels. Optical selection rules allow the excitation of states with spin quantum number $m_s = +1/2$ and orbital quantum numbers $m = 0, 1, 2$. States with other quantum numbers can become populated due to m -mixing and spin-orbit coupling. In the figure, four field ionization (FI) bands are identified by quantum-number assignments. The lowest FI band, labeled $m \leq 0, m_s = -1/2$, becomes populated due to a combination of spin-orbit coupling with m -mixing.

The electric-field and auto-ionization behavior of cold Rydberg atoms of ^{85}Rb in magnetic fields up to 6 T has been investigated. Multiple ionization potentials and field-ionization bands reflecting the Landau energy quantization of the quasi-free Rydberg electron are observed. The study of time-resolved and state-selective

field ionization spectra provides evidence of m -mixing and spin flips of the Rydberg electron. Spin-orbit coupling combined with m -mixing gives rise to a Feshbach-type auto-ionization of metastable positive-energy atoms.

The mentioned processes manifest themselves in experimental field ionization spectra such as the ones displayed in Fig. 1. There, cold atoms collected in the high- B atom trap are excited into Rydberg states at time $t = 0$ (horizontal axis in Fig. 1). The density is kept low enough that the effect of collisions between Rydberg atoms and / or electrons is deemed negligible. In the time interval $0 < t \leq 12 \mu\text{s}$ the atoms evolve in an electric-field-free environment. At later times, an approximately linear electric-field ionization ramp is applied. The observed features in the field-ionization spectra indicate m -mixing, spin-orbit coupling, and auto-ionization. Using the displayed data, the coupling strengths of m -mixing and spin-orbit coupling can be estimated. A paper describing these results in detail has been submitted.

2 Trapping of Rydberg atoms

Using Rydberg-atom excitation at high densities and at energies slightly below the photo-ionization threshold, the excited Rydberg atoms undergo state-changing collisions. Using this mechanism, we have been able to prepare and to magnetically trap long-lived drift-state Rydberg atoms, thereby extending the trapping frontier to include highly-excited atomic species. In our experiment, ^{85}Rb atoms are collected and laser-cooled in the high- B atom trap at a magnetic field of 3 T, excited into highly magnetized Rydberg states, and probed using time-delayed, position-sensitive detection. Due to m -mixing collisions, upon laser excitation a fraction of the atoms evolves into long-lived $\mathbf{E} \times \mathbf{B}$ -drift atoms. We observe magnetic trapping of these drift Rydberg atoms for times up to 200 ms. Employing measurements of oscillations of the atoms in the trap, we have determined an average magnetic moment of the trapped atoms of about $8 \mu_B$ (for the conditions used). A paper describing these results has been submitted.

The magnetic-moment measurements represent the first instance in which we have used observations of the center-of-mass motion of trapped Rydberg atoms in order to determine an atomic parameter. In the case studied, the magnetic moment of the trapped drift-state Rydberg atoms is found to exceed that of the trapped ground-state atoms by about an order of magnitude.

3 Expansion of quasi-neutral plasmas in strong magnetic fields

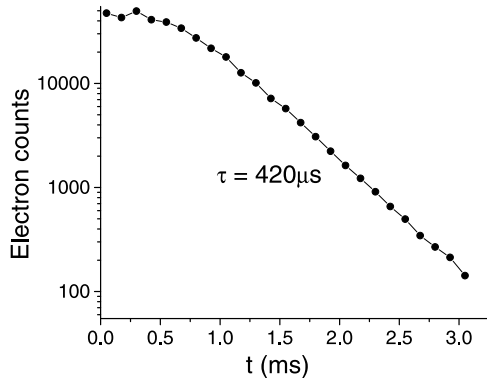


Figure 2: Number of electrons emitted from a highly magnetized, expanding cold plasma vs the time t after plasma excitation.

We have become interested in the expansion dynamics of cold, quasi-neutral plasmas in strong magnetic fields. There are arguably two features that distinguish the case of vanishing B -field, which is intensely studied elsewhere, from the high- B case we are interested in. First, the expansion in the high- B case is one-dimensional. As a result, the lifetimes of meta-stable cold plasmas in high- B are expected to be longer than the lifetimes in low- B . Further, multiple authors have, in the past, reported cross sections for three-body recombination that are much smaller in high- B cold plasmas than in low- B ones. As a result, it is expected that in the high- B case electron heating may be suppressed relative to the case of low- B . It is thus possible that two-component strongly coupled plasmas exist in the environment of a strong magnetic field.

Figure 2 shows recent data in which we measure the number of electrons emitted from a highly magnetized, expanding cold plasma vs the time after plasma excitation. At times larger than about 1 ms, we observe an exponentially decaying signal with a time constant of about four hundred microseconds, which is much longer than the time constants we typically observe in cases of low B . As expected, the expansion dynamics is found to be very sensitive to any bias electric fields in the excitation region. Presently, expansion curves such as the one displayed in Fig. 2 are being taken as a function of initial photo-excitation energy, plasma density and plasma volume.

4 Recombination experiments

In context with anti-hydrogen experiments conducted elsewhere, it is of particular interest how many drift-state Rydberg atoms are formed in a cold, strongly magnetized positron-anti-proton plasma, and how quickly these atoms percolate from high-lying Rydberg states down into the ground state. In our effort to answer some of these questions in our “model case” of a cold, magnetized plasma of electrons and rubidium ions, we have obtained state-selective field ionization spectra of Rydberg atoms formed under various conditions of the initial density, the electron temperature, and the cold-plasma evolution time after photo-excitation. We have observed that Rydberg atoms primarily form, initially, in very high-lying levels, while at later times of the cold-plasma evolution the total number of detected Rydberg atoms declines and the state-distribution shifts to lower states. One may speculate that we witness the percolation of high-lying Rydberg states into states too low to be detected by state-selective electric-field ionization. Efforts are currently underway to directly detect the atoms that have percolated all the way into the ground state via direct ground-state atom counting experiments.

5 Plans

In ongoing studies of non-interacting low-angular-momentum atoms in strong magnetic fields, we are interested in coherent spin oscillations of the Rydberg electron induced by spin-orbit coupling. We believe that we can both excite and detect these oscillations.

The continued work on Rydberg atom trapping evolves towards using the trapping as an analytic tool to measure single-atom properties (electric polarizabilities, magnetic moments, cyclotron transition behavior).

We further intend to study the expansion of cold, strongly magnetized plasmas and to illuminate the fate of Rydberg atoms that form via recombination in such plasmas. Exploiting our capability to trap both atoms and electrons at the same spatial location, we also consider to study collisions between cold-electron clouds and Rydberg atoms implanted into these clouds.

6 Recent publications which acknowledge DoE support:

“Coulomb expansion of laser-excited ion plasmas,” D. Feldbaum, N. V. Morrow, S. K. Dutta, G. Raithel, Phys. Rev. Lett. **89**, 173004 (2002).

“Decay rates of high- m Rydberg states in strong magnetic fields,” J. R. Guest, J.-H. Choi, G. Raithel, Phys. Rev. **A 68**, 022509 (2003).

“High- m Rydberg states in strong magnetic fields,” J. R. Guest, G. Raithel, Phys. Rev. **A 68**, 052502 (2003).

“Cold Rydberg Gas Dynamics,” A. Walz-Flannigan, J. R. Guest, J.-H. Choi, and G. Raithel, Phys. Rev. **A 69**, 063405 (2004).

“Time Averaging of Multi-mode Optical Fiber Output for a Magneto-Optical Trap,” A. P. Povilus, J. R. Guest, S. E. Olson, R. R. Mhaskar, B. K. Teo, G. Raithel, JOSA B **22**, 311 (2005).

“A simple pressure-tuned Fabry-Perot interferometer,” E. Hansis, T. Cubel, J.-H. Choi, J. R. Guest, and G. Raithel, Rev. Sci. Instrum. **76**, 033105 (2005).

“Laser cooling and magnetic trapping at several Tesla,” J. R. Guest, J.-H. Choi, E. Hansis, A. P. Povilus and G. Raithel, Phys. Rev. Lett. **94**, 073003 (2005).

“Magnetic trapping of long-lived cold Rydberg atoms,” J.-H. Choi, J. R. Guest, A. P. Povilus, E. Hansis, and G. Raithel, submitted (2005).

“Landau quantization effects in the ionization of cold, strongly magnetized Rydberg atoms,” J.-H. Choi, J. R. Guest, E. Hansis, A. P. Povilus, and G. Raithel, submitted (2005).

Development and Characterization of Replicable Tabletop Ultrashort Pulse X-ray Sources for Chemical Dynamics Research

Christian Reich,^{*} Taewoo Lee,^{*} Frank Benesch,^{**} and Christoph G. Rose-Petruck^{*}

^{*} Department of Chemistry, Box H, Brown University, Providence, RI 02912

^{**} Division of Engineering, Box D, Brown University, Providence, RI 02912

phone: (401) 863-1533, fax: (401) 863-2594, Christoph_Rose-Petruck@brown.edu

1 Program Scope

Advanced x-ray sources based on accelerator technology and sources based on laser technology form a symbiotic community with each source type addressing specific needs of the scientific community, for instance, average and peak x-ray flux, x-ray pulse lengths, or available beam time. This work focuses on the development and characterization of laser-driven tabletop, ultrashort pulse, hard-x-ray sources with high brightness for x-ray absorption spectroscopy and x-ray diffraction. Primary applications are the measurements of the structural dynamics of molecules during chemical and physical transformations. The sources will operate maintenance-free over long periods at kilohertz repetition rates with x-ray wavelengths selectable in the range from 1 to 7 Å and x-ray pulse durations in the range from about hundred femtoseconds to picoseconds. The sources use high power, femtosecond laser pulses with kilohertz repetition rate to generate x-ray emitting plasmas from solid and liquid metal targets. This research focuses entirely on the sources' optimization and characterization and relies on an existing laser system that has been upgraded to 40-fs laser pulse with an average power of 20-W on target at 4-kHz repetition rate. It is the specific goal of this project, to develop a source that is modular, compact, and robust enough to be replicable by many scientists with diverse experimental backgrounds.

The x-ray brightness and the average x-ray flux of synchrotrons will always be larger than that of the currently developed laser-driven x-ray source. Nevertheless, the x-ray flux per pulse on sample will be comparable to that of 3rd generation synchrotron x-ray sources, consequently providing substantial performance for time-resolved measurements of sample structures. Thus, while these laser-driven sources are valuable in their own right, they will also serve as training environments for ultrafast experiments at 3rd and 4th generation sources.

Integral parts of the project are experiments that serve multiple purposes: First, the data allow the measurements of the sources' pulse lengths over a large spectral range with sub-hundred femtosecond temporal resolution. Second, performance parameters of the entire x-ray spectroscopic system, consisting of source, x-ray imaging optics, spectrometer, and detector, can be determined for representative chemical dynamics experiments in the gas and liquid phases. Simultaneously, the experiments address important topics in gas and condensed phase structural dynamics related to laser-atoms interactions, reorganization motions during electron transfer reactions and structural motions during photo induced ligand substitutions of transition metal coordination complexes.

2 Recent Progress

The x-ray flux from a wire-based ultrafast x-ray source was substantially improved. A second design based on a liquid-mercury target jet has been assembled. Tests of the jet have been successfully completed. Simulations of the x-ray pulse emission of various metal targets after laser-pulse irradiation have been done.

2.1 X-ray source

The construction of the new laser-driven plasma x-ray source has been completed and the source module has been constructed as proposed. It is based on a liquid mercury jet that is irradiated by the ultrafast laser pulses. A picture of the interior part of the x-ray source is shown in Figure 1. The entire system is flange-mounted. The position of the interaction chamber relative to the pump laser beam adjustable from the top of the flange. The target jet is produced

by pumping liquid mercury at a pressure of 7MPa through a 25- μm nozzle. Supporting infrastructure, such as an integrated debris remover, will enable maintenance free operation over long periods of time. Liquid mercury as the target material has the advantages that it can be circulated by a pump yielding a very stable target. The plasma debris is liquid and can be automatically wiped off the chamber window. Furthermore, the plasma-physical properties of mercury make it very well suited for sub-100-fs hard x-ray pulse generation as discussed in the next section.

2.2 Simulation of sub-100-fs x-ray pulse emission from metal targets

The x-ray pulses that will be emitted from the target have been theoretically investigated by a combination of particle-in-cell (PIC) and Monte-Carlo (MC) simulations of the laser target interaction and the resulting electron dynamics. A two-step approach was applied to determine the x-ray emission. First, 1D, oblique incidence PIC simulations¹ of the laser-plasma interaction were performed to obtain the energy distribution of the hot electrons generated during the laser-plasma interaction. All calculations were performed for p-polarized, 100-fs, 800-nm laser pulses with an incidence angle of 45 degrees. An exponential plasma density profile with a scale length $L/\lambda = 0.2$ for a laser wavelength $\lambda = 800$ nm was used. This scale length corresponds approximately to an interaction where a laser pre-pulse or pedestal generates a small amount of preformed plasma. Second, a Monte-Carlo electron-photon transport code² was used to compute the electron trajectories in the mercury target. The generated relativistically corrected continuum intensity for an energy interval around the iron K edge (7.1 to 7.2 keV) was calculated using the Kirkpatrick and Wiedmann evaluation of Sommerfeld's cross section. Mass absorption coefficients for this radiation were taken from NIST tables. Temporal information on electrons and photons was calculated taking into account the electron entry time into the solid as obtained from the PIC calculations, the photon generation time, and the time of flight of the photons to the detector calculated with the MC code. The x-radiation was observed normal to the target front side.

For calibration purposes, we calculated the x-ray emission properties for the wire-target used for the measurements briefly discussed in 2.3. This target consists of a 200- μm steel wire, coated with 10- μm brass. The emitted Fe-K α , Cu-K α , and continuum flux around the Fe-K edge is shown in Figure 2 for a laser pulse intensity



Figure 1: Interior of the new x-ray source

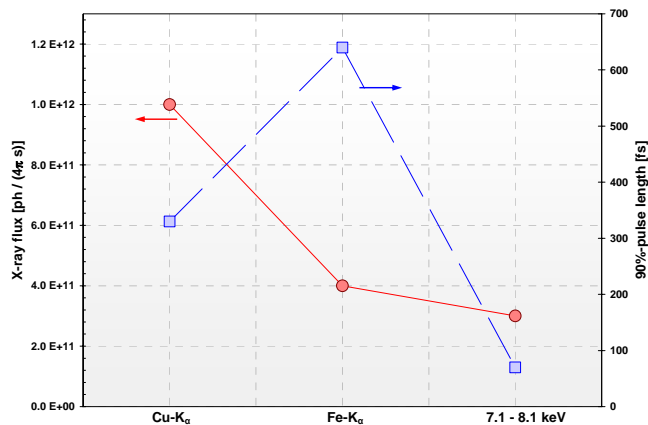


Figure 2: Simulated x-ray flux and pulse length emitted from a copper-coated steel wire target at 10^{17} W/cm², 5 mJ / pulse, 4 kHz repetition rate.

¹ P. Gibbon and A. R. Bell, Physical Review Letters **68** (10), 1535 (1992)

² C. Reich, Ph.D. thesis, Ph.D., Friedrich Schiller Universität Jena, 2002

of 10^{17} W/cm². The calculated flux is larger than that used for the measurements in section 2.3 because these experiments have been performed at 2 kHz and at laser pulse intensities around 10^{16} W/cm². The calculated x-ray pulse length that contains 90% of the pulse energy depends greatly on the x-ray wavelength and the depth in the target at which the radiation is generated. For instance, the Cu-K_α radiation is generated in a volume between the target surface and 10 μm depth and the pulse length is several hundred femtoseconds. In contrast, the Fe-K_α radiation is generated at much greater depth and the diffusion time of the electrons into the target and of the x-radiation out of the target substantially broadens the pulse length. This effect demonstrates that a target with a larger electron stopping cross section and a larger x-ray absorption cross section could potentially substantially reduce the x-ray pulse length. This was evaluated for mercury, the target material for which the x-ray source shown in Figure 1 was designed. Figure 3 shows a simulated x-ray pulse emitted from a mercury target illuminated with a 800-nm, 100-fs laser pulse with an intensity of 10^{17} W/cm² and 5 mJ pulse energy.

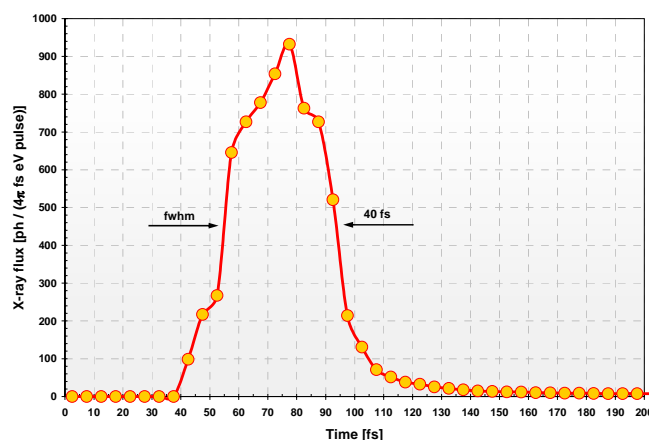


Figure 3: Simulated x-ray pulse in the spectral range from 7.1 to 7.2 keV emitted from a mercury target illuminated with a 800-nm, 100-fs laser pulse with an intensity of 10^{17} W/cm² and 5 mJ pulse energy.

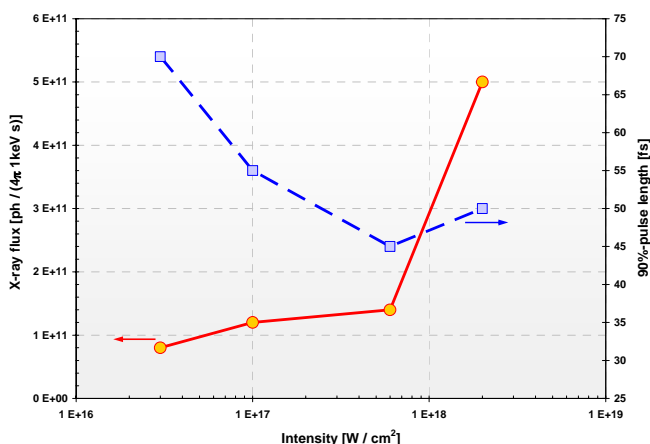


Figure 4: Simulated x-ray flux and pulse length emitted from a mercury target at illuminated with 800-nm, 100-fs laser pulses with 5-mJ pulse energy and a repetition rate of 4 kHz.

section of mercury largely suppresses contributions of “deep” x-ray photons to the overall pulse. Such a trend can not be expected for fluorescence radiation. However, our x-ray applications are mostly in the area of chemical dynamics in solutions, which is best investigated using the continuum radiation for ultrafast x-ray absorption fine structure spectroscopy.

2.3 Study of ultrafast chemical dynamics using the ultrafast table-top x-ray source

The X-ray Absorption Fine Structure (XAFS) spectra of $Fe(CN)_6^{4-}$ solvated in water have been measured before photoexcitation and tens of picoseconds after photoexcitation with ultrashort UV laser pulses. The XAFS spectra after photoexcitation exhibits a chemical shift as well as indications for the increase of the iron-ligand distances. Reference spectra measured at a synchrotron source yield structural data that show bond length changes of

the metal complex due to solvation. The pump-probe delay times are not indicative of the temporal resolution of the experimental setup. The most likely temporal resolution is in the sub-picosecond regime.

2.4 Study of ultrafast chemical dynamics using SPPS

In collaboration with the SPPS-team, but specifically Kelly Gaffney, x-ray absorption measurements of chemical process



the reorganization during charge transfer to solvent (CTTS) and the subsequent solvation of the photoproducts will be measured. The systems Test measurements are planned for end of August 2005.

2.5 Future Plans

The next experiment to be performed will be the measurement of the pulse length of hard x-ray pulses generated from the mercury x-ray source. Simultaneously, these measurements will lay the spectroscopic "foundation" for subsequent experiments focusing on chemical dynamics with sub-picosecond resolution. Xenon gas will be ionized in a gas cell or jet and the change of the x-ray absorption L-edge spectra will be measured as a function of the pump-probe delay. The measurements will provide a cross-correlation between laser and x-ray pulses.

3 References

1. "Ultrafast table-top laser pump - x-ray probe measurement of solvated $\text{Fe}(\text{CN})_6^{4-}$," T. Lee, Y. Jiang, C. Rose-Petruck and F. Benesch, *J. Chem. Phys.* 122 (8), 084506/1 - 084506/8 (2005).
2. Ultrafast table-top laser pump - x-ray probe measurement of solvated $\text{Fe}(\text{CN})_6^{4-}$, T. Lee, Y. Jiang, C. Rose-Petruck and F. Benesch, Selected for re-publication by: *Virtual Journal of Ultrafast Science*, Vol. 4 (3), <http://www.vjultrafast.org/ultrafast/>, edited by P. H. Bucksbaum (American Institute of Physics, American Physical Society, 2005), ISSN: 1553-9601, Original Publication: *J. Chem. Phys.* (2005), 122(8), 084506/1 - 084506/8.
3. Ultrafast table-top laser pump - x-ray probe measurement of solvated $\text{Fe}(\text{CN})_6^{4-}$, T. Lee, Y. Jiang, C. Rose-Petruck and F. Benesch, Selected for re-publication by: *Virtual Journal of Biological Physics Research*, Vol. 9 (5), <http://www.vjbio.org/bio/>, edited by R. H. Austin (American Institute of Physics, American Physical Society, 2005), ISSN: 1553-9628, Original Publication: *J. Chem. Phys.* (2005), 122(8), 084506/1 - 084506/8.
4. "Acoustically Modulated X-ray Phase Contrast and Vibration Potential Imaging," A. C. Beveridge, C. J. Bailat, T. J. Hamilton, S. Wang, C. Rose-Petruck, V. E. Gusev and G. J. Diebold, in *Photons Plus Ultrasound: Imaging and Sensing 2005*, edited by A.A. Oraevsky and L.V. Wang (SPIE Publishing, Bellingham, WA, 2005), Vol. 5697, p. in press.
5. "Acoustic radiation pressure: a "phase contrast" agent for x-ray phase contrast imaging," C. J. Bailat, T. Hamilton, C. Rose-Petruck and G. J. Diebold, *Applied Physics Letters* 85 (19), 4517-4519 (2004).
6. "Acoustically Modulated X-ray Phase Contrast Imaging," T. Hamilton, C. J. Bailat, C. Rose-Petruck and G. J. Diebold, *Physics in Medicine and Biology* 49, 4985-4996 (2004).

New Directions in Intense-Laser Alignment

Tamar Seideman

Department of Chemistry, Northwestern University

2145 Sheridan Road, Evanston, IL 60208-3113

seideman@chem.northwestern.edu

1. Program Scope

Nonadiabatic molecular alignment by short intense pulses has been the topic of rapidly growing activity during the past few years. This activity owes both to the fascinating fundamental physics associated with rotational wavepacket dynamics and to a variety of already demonstrated and projected applications in fields ranging from molecular spectroscopy and laser optics through reaction dynamics and stereochemistry, to quantum storage and information processing.¹ In this approach, a moderately intense laser pulse of duration short with respect to the rotational periods aligns a given molecular axis (axes) to the field polarization vector(s). Nonadiabaticity (rapid turn-off as compared to the system time scales) guarantees that the alignment will survive subsequent to the pulse turn-off, under field-free conditions. Whereas a linearly polarized pulse induces 1D order, leaving the rotation about the field and molecular axes free, an elliptically polarized pulse aligns the three axes of the molecule to three axes defined in space.

Our DOE-sponsored research introduces two new directions in the area of nonadiabatic intense laser alignment and explores them theoretically and numerically. One part of the research extends the concepts of alignment and three-dimensional alignment from the isolated molecule limit to condensed phase environments. Applications of the extended scheme that have been explored during the past year include the development of an approach to control charge transfer reactions in solutions and the introduction of a new approach for probing the properties of dissipative environments.²

The second part of the research extends the theory of rotational revivals from linear systems to molecules of arbitrary symmetry and explores practical and experimental implications. Recent work in this area develops and applies the theoretical framework^{1,3-5} and contrasts different modes of achieving 3D alignment so as to guide ongoing and future experiments.

2. Recent Progress

Since the beginning of our DOE-sponsored research in September 2004, we have focused on two projects (Secs. 2.1 and 2.2) within the first part of the program, addressing alignment in dissipative media, and several related projects within the second part, addressing alignment of isolated complex polyatomic systems (Secs. 2.3-2.5). This research is carried out by a DOE-supported postdoctoral fellow, Edward Hamilton, and a partially DOE supported first year graduate student, Adam Pelzer.

2.1 Intense laser alignment in dissipative media as a route to solvent dynamics

In Ref. 2 we extend the concept of alignment by short intense pulses to dissipative envi-

ronments within a density matrix formalism and illustrate the application of this method as a probe of the dissipative properties of dense media. In particular, we propose a means of disentangling rotational population relaxation from decoherence effects via strong laser alignment. We illustrate also the possibility of suppressing rotational relaxation, so as to prolong the alignment lifetime, through choice of the field parameters.

2.2 Control of torsional motions. Application to the design of a molecular switch

In recent research we extend three-dimensional alignment from a means of controlling solely the overall rotations of molecules with respect to the space-fixed axes, to a means of simultaneously controlling also their torsional motions. In particular, we illustrate numerically the application of circularly and elliptically polarized pulses to eliminate the torsional motions of polyatomic systems while hindering their overall rotations in space. The approach is applied to control of charge transfer reactions in solution. Using a semiclassical 3-state, 3-mode model of a donor-acceptor biphenyl, we find extensive control over the charge transfer rate and explore its physical origin and dependence on the solvent and solute properties.

2.3 Nonperturbative quantum theory of alignment and 3D alignment of complex systems

Much of our effort in the domain of alignment of isolated polyatomic molecules has been devoted to the development of an efficient and accurate theoretical framework to predict the alignment and 3D alignment characteristics of asymmetric tops. Both the theory and its numerical implementation are challenging, quite in contrast to the extensively studied case of linear molecules subject to linearly polarized fields, due to the rich angular momentum algebra and the large number of states involved. At the same time, the rapidly growing interest in nonadiabatic alignment of polyatomic systems, the advance of the experimental technology,³⁻⁵ the qualitative questions posed by experiments and the variety of anticipated applications,¹ motivate an investment on the part of theory. Our methods are summarized in Ref. 3 and discussed in detail in a recent review article.¹ In brief, we solve the time-dependent Schrödinger equation nonperturbatively, transforming between basis sets of symmetric and asymmetric tops to maximize the code efficiency.

2.4 Applications to isolated polyatomic molecules

The formalism has been applied in several collaborative studies with the experimental group of H. Stapelfeldt, which uses femtosecond time-resolved photofragment imaging to probe the time-evolving alignment. In Ref. 3 we explore the nonadiabatic alignment of symmetric top molecules induced by linearly polarized, moderately intense picosecond laser pulse. Using methyl iodide and *tert*-butyl iodide as examples, we calculate and measure the alignment dynamics, focusing on the temporal structure and intensity of the revival patterns, including their dependence on the pulse duration, and their behavior at long times, where centrifugal distortion effects become important. Very good agreement is found between the experimental and numerical results, allowing us to use the theory to provide insight into the origin of the experimental findings.

In Refs. 4 and 5 we apply similar experimental and theoretical methods to study the nonadiabatic alignment of asymmetric top molecules. Numerically, we solve the time dependent Schrödinger equation for a general asymmetric top molecule subject to an intense laser field,

and analyze the dependence of the alignment dynamics on the field strength and on the rotational temperature. Experimentally, we measure the alignment of two molecules with different asymmetry, iodobenzene and iodopentafluorobenzene. Our numerical results explain several counter-intuitive experimental observations and generalize them to other molecules. We show that the rotational revival patterns of asymmetric tops differs qualitatively from the linear and symmetric top cases and explore the information content of these patterns.

An ongoing study studies theoretically, numerically and experimentally a new approach of enhancing the alignment of polyatomic molecules through a combination of short- and long-pulse fields. Our approach is based on the realization that the non-resonant ionization of molecules, which upper bounds the intensity that can be applied, scales differently from alignment in the laser fluence and intensity.

A related theoretical project, to be completed shortly, applies nonadiabatic orientation of a triatomic molecular ion as the first step in a coherent control scheme for selective bond-breaking in polyatomic molecules. Orientation is achieved by application of half-cycle pulses in the low frequency limit to drive sequential $\Delta J = \pm 1$ transitions between rotational levels of opposite parity.

2.5 Time-resolved photoelectron imaging as a probe of rotational coherences

Closely related to the interests of several members of the BES AMOS community, as well as to the topic of strong-field induced rotational revival structures, is the rapidly progressing technique of time-resolved photoelectron imaging (PEI), a pump probe approach, typically applied under nonperturbative conditions, where the probe ionizes a pump-driven ro-vibrational wavepacket. Time-resolved PEI measures the photoionization differential cross section, energy-resolved to within the probe band-width. It thus provides both the energy and the angular distribution of the photoelectron as well as their correlation as a function of time.

The structure of this observable and its relation to the underlying system properties have been exposed in our previous research. In particular, the photoelectron angular distribution is sensitive to the time-evolving rotational composition of wavepackets, reflecting both the relative magnitudes and the relative phases of the rotational components. In the context of alignment of complex systems, where the development of a general and objective probe of the time-evolving alignment remains a challenge, PEI is an interesting opportunity. In Ref. 6 we explore qualitatively the information content of time-resolved PEI regarding the composition of rotational wavepacket and the coherences underlying their spatial properties. We identify a mapping of the alignment properties of time-evolving wavepackets onto the moments of the photoelectron image and investigate its origin and consequences theoretically and numerically.

3. Future Plans

- One of our goals in future research will be to develop a coherent control approach to the design of rotational wavepackets with desired functionality subject to dissipation. To that end we will combine our solution of the quantum Liouville equation, discussed in Ref. 2, with optimal control theory to trigger rotational wavepackets via controlled $\Delta J = \pm 1$ dipole transitions at low frequency. One of our targets will be a rotational superposition that will be immune to rotational relaxation and rotational decoherence on time scales relevant to quantum

storage applications.

- Another goal of future work will be the extension of 3D alignment and torsional control (Sec. 2.2) to guided molecular assembly. We are motivated by the recognition that the performance of molecule-based electronic and photonic devices often depends crucially on the alignment of the molecular layer(s). One example is field-effect transistors, where alignment of the organic molecules constituting the active component of the transistor has been shown to significantly enhance the utility of the device. Another example is solar energy harvesting systems, where assembly that would mimic the light harvesting and charge separation processes in photosynthesis, and/or convert light into current were found to require a handle over the component alignment. A third example is a newly introduced approach to the fabrication of affinity-based molecular sensor devices, where the sensing probe includes an organic conductive wire whose alignment properties affect the performance of the device. Other applications that rely on electron transfer through molecular monolayers, and where alignment of the layer constituents plays an essential role, are found in the expanding field of molecular junctions. Although impressive progress in this area is due to conductance measurements in break junctions and STM environments, most of the research to date has used molecular monolayer-based devices. While one-dimensional laser alignment is expected to be effective in many systems, three-dimensional alignment combined with control over the torsion angles may lead to greater performance enhancement.

Our numerical approach will apply classical molecular dynamics to describe the assembly subject to the combination of the molecular Hamiltonian and the external field. Relevant examples are the phenylacetylene oligomer and the phenylene ethynylene oligomers that have been studied in several recent molecular electronics experiments.

- Our work on torsional control in general, and its application to control charge transfer reactions in solution (Sec. 2.2) in particular, will be continued, as current experimental interest in realizing this scheme offer new questions for theoretical research.

- In related research we are initiating a collaborative study with the group of Murnane and Kapteyn to explore the information content of high harmonic spectra from aligned molecules, both with respect to the electronic wavefunction and with respect to the rotational wavepacket.

4. Published and accepted articles from DOE sponsored research: 09/04–07/05

1. T. Seideman and E. Hamilton, *Nonadiabatic Alignment by Intense Pulses. Concepts, Theory, and Directions*, Ad.At.Mol.Opt.Phys. **52**, in press.
2. S. Ramakrishna and T. Seideman, *Intense Laser Alignment in Dissipative Media as a Route to Solvent Properties*, Phys. Rev. Lett. in press.
3. E. Hamilton, T. Seideman, T. Ejdrup, M.D. Poulsen, C.Z. Bisgaard, S.S. Viftrup and H. Stapelfeldt, *Alignment of Symmetric Top Molecules by Short Laser Pulses*, Phys. Rev. A.
4. M.D. Poulsen, E. Peronne, C.Z. Bisgaard, H. Stapelfeldt E. Hamilton and T. Seideman, *Revivals of Nonadiabatic Alignment of Asymmetric Top Molecules*, J. Chem. Phys. **121**, 783 (2004).
5. E. Péronne, M.D. Poulsen, H. Stapelfeldt, C.Z. Bisgaard, E. Hamilton, and T. Seideman, *Nonadiabatic Laser Induced Alignment of Iodobenzene Molecules*, Phys. Rev. A **70**, 063410 (2004).
6. Y. Suzuki and T. Seideman, *Mapping Rotational Coherences onto Time-Resolved Photoelectron Imaging Observables*, J. Chem. Phys. **122**, 234302 (2005).

Measurement of Electron Impact Excitation Cross Sections of Highly Ionized Ions

A. J. Smith

D. L. Robbins, Postdoctoral Associate

Morehouse College, 830 Westview Dr SW, Atlanta, GA 30314

email:asmith@morehouse.edu

Unfunded Liaison/Collaborator: P. Beiersdorfer

Lawrence Livermore National Laboratory, Livermore, California USA

Scope of work: During the current project year, the main focus has been on measurements of cross sections for electron impact excitation of highly ionized ions. We have used the LLNL electron beam ion trap, EBIT-I to ionize, trap and excite these ions. We use electron beam excitation energies that lie just above threshold to some excitation energies that are several kV's above threshold values for the levels of interest. We also use several types of high-resolution spectrometers to record x-ray spectra. The electron beam imposes a directionality on the emitted x-rays. Measurement of the degree of polarizations of these x-ray emission lines provide a direct measure of the electron impact excitation cross section of the lines. We have therefore continued to make polarization measurements, which test atomic structure calculations of electron impact excitation cross sections. Below are summaries of some of the measurements we have carried out.

1 Cross Sections for Electron Impact Excitation in heliumlike Ar¹⁶⁺, and heliumlike Kr³⁴⁺

In a previous year we measured cross sections for direct excitation of $n = 3-1$ resonance line, $K\beta_1$ and intercombination line, $K\beta_2$, in heliumlike argon at various excitation energies (4.9 kV - 20.0 kV). We have extended these measurements to relativistic energies, and to a much higher Z in heliumlike Kr³⁴⁺. For the Krypton measurements we have used a high-resolution microcalorimeter. We use radiative recombination to normalized our intensity measurements.

2 Polarization of Iron L-shell lines on EBIT-1

We have extended our polarization measurements to include polarization of neonlike and fluorinelike iron using the LLNL EBIT-1, and a two crystal technique. These results are important for the diagnostics of astrophysical as well as of laser-produced plasmas. The observed data is compared with calculations done using the flexible atomic code (FAC). The measurements are presented at the fourth US-Japan plasma spectroscopy conference. In earlier measurements we looked at the polarization of heliumlike V²¹⁺

3 Measurement of the Polarization of Heliumlike and Lithiumlike sulfur

We have continued to work on polarization measurements for heliumlike and lithiumlike sulfur. We have used a two-crystal technique to measure the polarization of the heliumlike sulfur resonance line $1s2p\ ^1P_1 - 1s^2\ ^1S_0$, and of the blend of the lithiumlike sulfur resonance lines $1s2s2p\ ^2P_{3/2} - 1s^22s\ ^2S_{1/2}$ and $1s2s2p\ ^2P_{1/2} - 1s^22s\ ^2S_{1/2}$. We have looked at the polarization of these lines for electron beam energies from near threshold to 144 keV. These observations should test polarization predictions in an energy regime where few empirical results have been reported.

The crystals used in the two crystal technique included a PET crystal (in flat geometry) set at Bragg angle of $\theta_B = 35.2^\circ$, which corresponds to an integrating crystal reflectivity ratio of $R_{PET} \approx 0.28$. The second was a mica (002) crystal which was spherically bent into a Johann type spectrometer. This spectrometer was set at an initial Bragg angle close to 45° , corresponding to a ratio of $R_{Mica} \approx 0.04$. For normalization we have used the forbidden line (z) ($1s2s\ ^3S_1 - 1s^2\ ^1S_0$) in heliumlike sulfur. The line z is intrinsically unpolarized, but can be slightly polarized due to cascades. Our observations agree well with predictions made with the Flexible Atomic Code and the relativistic distorted-wave code.

4 A high-resolution compact Johann crystal spectrometer with the Livermore electron beam ion trap

A compact high-resolution $\lambda/\Delta\lambda = 10,000$ spherically bent crystal spectrometer in the Johann geometry was recently installed and tested on the Lawrence Livermore National Laboratory SuperEBIT electron beam ion trap. The curvature of the mica (002) crystal grating allows for higher collection efficiency compared to the flat and cylindrically bent crystal spectrometers commonly used on the Livermore EBIT. The spectrometers Johann configuration enables us to orient its dispersion plane parallel to the electron beam propagation. Used in concert with a flat crystal spectrometer, whose dispersion plane is perpendicular to the electron beam propagation, the polarization of x-ray emission lines can be measured (sulfur studies above).

5 Level specific DR resonance strengths in He-like Ti^{20+} and Cr^{22+}

We have continued to analyze dielectronic satellite spectra for heliumlike Ti XXI and Cr XXIII, measured in separate earlier experiments using the LLNL EBIT-II and the EBIT high-resolution Bragg crystal spectrometers. We sweep the electron beam energy across individual DR resonances, and thus we have deduced level specific resonance strengths for the strongest DR resonances in doubly excited lithiumlike Ti XX and CrXXII. We have used the MCDF code to calculate the resonance strength, excitation energy, as well as the x-ray energies of these transition. We have wavelength-calibrated the observed spectra, and normalized the intensities to theoretical radiative recombination cross sections. See typical spectra in Fig. 2.

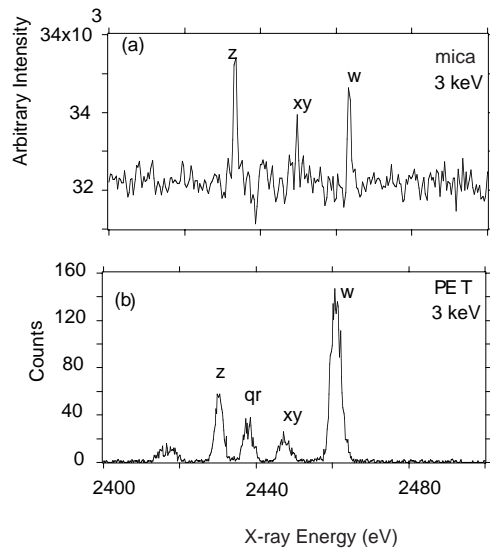


Figure 1. K-shell spectra of sulfur recorded with the spherically bent crystal (a) and with the flat crystal spectrometer (b) at 3 keV beam energy.

6 Future Work

We plan to extend our measurements to higher electron beam energies, and to higher Z-values. Measurements on highly charged, high-Z ions are still few.

7 Acknowledgments

We gratefully acknowledge support by the Office of Basic Energy Science, Chemical Sciences Division. This work was performed under the auspices of the Department of Energy by Lawrence Livermore National Laboratory under contract No. W-7405-ENG-48 and by Morehouse College under contract No. DE-FG02-98ER14877.

Publications List

[1] "Measurement of the Polarization of the $K\beta_2$ line of V^{21+} ", A. J. Smith, P. Beiersdorfer, K. L. Wong, and K. J. Reed, proceedings of 3rd US-Japan Plasma Polarization Spectroscopy workshop, June 18-21, 2000, LLNL, Livermore, ED P. Beiersdorfer and T Fujimoto, LLNL report no. UCRL-ID-146907, Livermore, CA 2002, p299-306.

2) Measurement of the polarization of the K-shell resonance line emission of S^{13+} and S^{14+} a relativistic electron beam energies, D. L. Robbins, A. Ya Faenov, T. A. Pikuz, H. Chen, P. Beiersdorfer, M. J. May, J. Dunn, K. j. Reed, and A. J. Smith, PRA **70** 1(2004).

3) A high-resolution compact Johann crystal spectrometer with the Livermore EBIT, D. L. Robbins, H. Chen, P. Beiersdorfer, a. Ya Faenov, T. A. Pikuz, M. J. May, J. Dunn, A. J. Smith, RSI, 75 Oct(2004) 524410RSI 1.

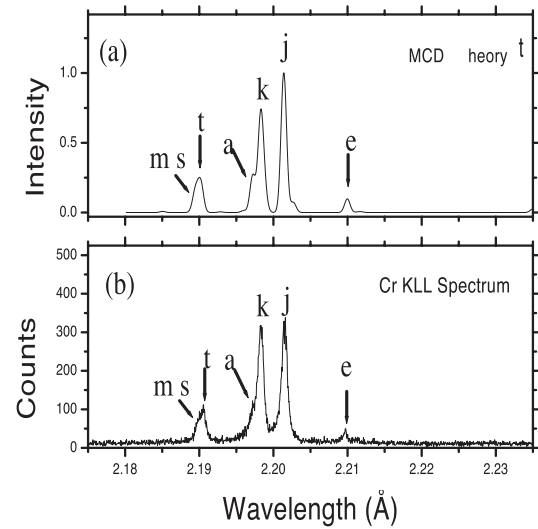


Figure 2. Dielectronic satellite spectra of heliumlike Cr^{22+} ; theory (a), experiment (b).

4) "X-Ray Line Polarization of the K-shell Resonance Line Emission of Heliumlike and Lithiumlike Sulfur at Relativistic Electron Impact Energies," D.L. Robbins, H. Chen, P. Beiersdorfer, A. Ya. Faenov, T.A. Pikuz, M.J. May, J. Dunn, K.J. Reed, and A.J. Smith, Proceedings of 4th International Plasma Polarization Symposium, Kyoto, Japan February 3 - February 6 2004, LLNL Rep. UCRL-PROC-202750.

5) "Polarization measurement of Iron L-shell lines on EBIT-I," H. Chen, P. Beiersdorfer, D.L. Robbins, A.J. Smith, and M.F. Gu, Proceedings of 4th International Plasma Polarization Symposium, Kyoto, Japan February 3 - February 6 2004, LLNL Rep. UCRL-PROC-202745.

DYNAMICS OF FEW-BODY ATOMIC PROCESSES

Anthony F. Starace

*The University of Nebraska
Department of Physics and Astronomy
116 Brace Laboratory
Lincoln, NE 68588-0111
Email: astarace1@unl.edu*

PROGRAM SCOPE

The goals of this project are to understand and describe processes involving energy transfers from electromagnetic radiation to matter as well as the dynamics of interacting few-body, quantum systems. Investigations of current interest are in the areas of high energy density physics, attosecond physics, strong field physics, and double photoionization processes. In some cases our studies are supportive of and/or have been stimulated by experimental work carried out by other investigators funded by the DOE AMO physics program.

RECENT PROGRESS

A. Non-Dipole Effects in Double Photoionization of He

In recent years two major themes in both experimental and theoretical studies of atomic photoionization have been the analysis of nondipole (or retardation) effects in single-electron photoionization (both in the soft x-ray and the vuv regions) and the analysis of double photoionization (especially in the vuv energy region). Surprisingly, there have not been as yet any analyses of nondipole effects on double photoionization. In part this is because nearly all experimental measurements have been carried out with linear polarization in the orthogonal plane geometry (i.e., photoelectrons are detected in the plane perpendicular to the photon wave vector). For this case, non-dipole effects vanish. We have recently completed an analysis of nondipole effects in double photoionization of He (see publications [6] and [9]). Specifically, we have derived a general parameterization for the double photoionization amplitude of He taking into account both dipole (E1) and quadrupole (E2) components of the electron-photon interaction operator. Nondipole effects originate from the interference of the E1 and E2 amplitudes. Our numerical results show that these effects are significant in double photoionization of He even for excess energies as low as 80 eV and that they should be observable in experiments with current state-of-the-art capabilities.

For the case of linearly polarized light, we have analyzed [6, 9] our parameterized formulas for the TDCS and proposed two experimental geometries for which the nondipole effects are maximal, one for equal energy sharing and one for unequal energy sharing. Both are coplanar geometries, in which the momenta, \mathbf{p}_1 and \mathbf{p}_2 , of the two ionized electrons lie in the plane defined by the photon wave vector, \mathbf{k} , and the linear polarization direction. In each case, the TDCS should be measured for two directions of the photon beam propagation: in the directions \mathbf{k} and $-\mathbf{k}$ (with the direction of the linear polarization vector unchanged). Differences in the TDCSs of the order of 15%-20% of the maximum of the TDCS are predicted.

For the case of circularly polarized light, we have recently analyzed [7, 9] the influence of nondipole interactions on the circular dichroism (CD) effect in double photoionization of He. It is well known that the CD effect vanishes ordinarily in the case that the two ionized electrons share the total available energy equally. We have shown analytically that there exists a nonzero CD effect for this case of equal energy sharing when one takes into account the interference of E1 and E2 transition amplitudes. We have also shown that this interference leads to unusual asymmetries of the TDCS for the case of elliptically polarized light. We have proposed two experimental arrangements for measuring each of these effects, which together provide a polarization sensitive means of measuring nondipole effects in double photoionization. Our numerical estimates indicate that CD effects are significant for electron energies as low as 40 eV.

B. GeV Electrons from Ultra Intense Laser Interactions with Highly Charged Ions

We have investigated in great detail the interaction of intense laser radiation with highly charged hydrogenic ions using a three-dimensional relativistic Monte Carlo simulation. This work extended an earlier investigation [S.X. Hu and A.F. Starace, *Phys. Rev. Lett.* **88**, 245003 (2002)] in which it was demonstrated that free electrons cannot be accelerated to GeV energies by the highest intensity lasers because they are quickly expelled from the laser pulse before it reaches peak intensity. We showed that highly charged ions exist that (1) have deep enough potential wells that tunneling ionization is insignificant over the duration of an intense, short laser pulse, and (2) have potentials that are not too deep, so that the laser pulse is still able to ionize the bound electron when the laser field reaches its peak intensity. We showed that when the ionized electron experiences the peak intensity of the laser field, then it is accelerated to relativistic velocity along the laser propagation direction (by the Lorentz force) within a tiny fraction of a laser cycle. Within its rest frame it then “rides” on the peak laser amplitude and is accelerated to GeV energies before being expelled from the laser pulse. Our recent work [S.X. Hu and A.F. Starace, *Phys. Rev. E* (submitted)] includes an extensive set of calculations to examine the dependence of the ionized electron energy spectrum on the experimentally controllable parameters. These include the target ion and the laser intensity, frequency, duration, and, especially, the focal properties.

C. Circularly Polarized Laser-Induced Rescattering Plateaus in Laser-Assisted, Electron-Atom Scattering

Plateau structures in intense laser-atom interactions (i.e., a nearly constant dependence of multiphoton cross sections on photon number n over a wide interval of n up to a cutoff at n_{\max}) are among the most interesting and intensively studied nonlinear phenomena in laser-atom physics. These structures have a one-electron origin and are well-studied both experimentally

and theoretically for the processes of above-threshold ionization (ATI) and high harmonic generation (HHG). Plateau features have also been found in laser-assisted, electron atom scattering processes (LAES).

For the case of an elliptically polarized laser field, we have recently carried out the first analysis of rescattering effects in LAES spectra and found, surprisingly, that plateau effects persist even for the case of circularly polarized laser light [8]. The reason why this result is unexpected stems from existing results for ATI and HHG processes. The high-energy (rescattering) plateaus in ATI and HHG spectra are known to gradually disappear with increasing degree of circular polarization. Indeed, for the case of pure circular polarization, the process of HHG by free atoms is strictly forbidden, whereas plateau structures in ATI simply disappear. Thus it has been generally assumed that rescattering effects vanish for the case of circular polarization owing to the impossibility for the active electron to return to its parent ion. However, for free-free transitions (such as LAES), rescattering effects can take place even for the case of circular polarization, as follows from quite general arguments. For the case of bound-bound or bound-free transitions (i.e., HHG or ATI), the angular momentum l of the bound electron is fixed, so that dipole selection rules for the angular momentum projection m in a circularly polarized field, $|\Delta m| = 1$, forbid HHG and suppress (owing to angular momentum barriers) rescattering effects in ATI. For the case of LAES, however, both incoming and scattered electron waves are superpositions of continuum states with different l and m . Hence, for LAES the selection rules should not lead to such drastic differences in the physics of strong field phenomena for the cases of linear and circular polarizations as they do for ATI and HHG.

In our analysis [8] of rescattering effects for free-free electron transitions in the presence of a circularly polarized laser field we have predicted significant plateau features. In contrast to ATI and HHG, where the height of plateau structures decreases rapidly with increasing ellipticity, we find that for the case of LAES the plateau height is almost insensitive to the degree of circular polarization, whose magnitude and sign determine only the extent of the high-energy plateau region. These features of plateau structures in LAES are shown to follow from an exact quantum solution of the problem, which allows also for a simple classical interpretation in terms of the well-known rescattering picture.

D. FUTURE PLANS

Our group is currently carrying out research on the following projects: (1) Calculation of two-photon, double ionization cross sections for He using an LOPT approach; (2) Development of an effective range theory approach for laser-assisted electron-atom scattering; (3) Analysis of attosecond pulse interactions with atomic systems; (4) Analysis of radiative energy losses in intense laser ionization of highly charged ions.

PUBLICATIONS STEMMING FROM DOE-SPONSORED RESEARCH

(August 2002 – July 2005)

- [1] A.Y. Istomin, N.L. Manakov, and A.F. Starace, “Perturbative Calculation of the Triply Differential Cross Section for Photo-Double-Ionization of He,” *J. Phys. B* **35**, L543 (2002).
- [2] G. Lagmago Kamta and A.F. Starace, “Two-Active Electron Approach to Multielectron Systems in Intense Ultrashort Laser Pulses: Application to Li^- ,” *J. Mod. Optics* **50**, 597 (2003).
- [3] M. Masili and A.F. Starace, “Static and Dynamic Dipole Polarizability of the He Atom Using Wave Functions Involving Logarithmic Terms,” *Phys. Rev. A* **68**, 012508 (2003).
- [4] G. Lagmago Kamta and A.F. Starace, “Elucidating the Mechanisms of Double Ionization Using Intense Half-Cycle, Single-Cycle, and Double Half-Cycle Pulses,” *Phys. Rev. A* **68**, 043413 (2003).
- [5] A.Y. Istomin, N.L. Manakov, and A.F. Starace, “Perturbative Analysis of the Triply Differential Cross Section and Circular Dichroism in Photo Double Ionization of He,” *Phys. Rev. A* **69**, 032713 (2004).
- [6] A.Y. Istomin, N.L. Manakov, A.V. Meremianin, and A.F. Starace, “Non-Dipole Effects in Photo Double Ionization of He by a VUV Photon,” *Phys. Rev. Lett.* **92**, 063002 (2004).
- [7] A.Y. Istomin, N.L. Manakov, A.V. Meremianin, and A.F. Starace, “Circular Dichroism at Equal Energy Sharing in Photo Double Ionization of He,” *Phys. Rev. A* **70**, 010702(R) (2004).
- [8] A.V. Flegel, M.V. Frolov, N.L. Manakov, and A.F. Starace, “Circularly Polarized Laser Field-Induced Rescattering Plateaus in Electro-Atom Scattering,” *Phys. Lett. A* **334**, 197 (2005).
- [9] A.Y. Istomin, N.L. Manakov, A.V. Meremianin, and A.F. Starace, “Nondipole Effects in the Triply-Differential Cross Section for Double Photoionization of He,” *Phys. Rev. A* **71**, 052702 (2005).

FEMTOSECOND AND ATTOSECOND LASER-PULSE ENERGY TRANSFORMATION AND CONCENTRATION IN NANOSTRUCTURED SYSTEMS

DOE Grant No. DE-FG02-01ER15213

Mark I. Stockman, Pi

Department of Physics and Astronomy, Georgia State University, Atlanta, GA 30303

E-mail: mstockman@gsu.edu, URL: <http://www.phy-astr.gsu.edu/stockman>

1 Program Scope

The program is aimed at theoretical investigations of a wide range of phenomena induced by ultrafast laser-light excitation of nanostructured or nanosize systems, in particular, metal/semiconductor/dielectric nanocomposites and nanoclusters. Among the primary phenomena are processes of energy transformation, generation, transfer, and localization on the nanoscale and coherent control of such phenomena.

2 Recent Progress

2.1 SPASER: Effect, and Prospective Devices [1-4]

The known effects and applications in nanooptics are passive, i.e., based on the excitation of the nanosystem by external laser radiation. This mode of excitation has obvious drawbacks: most of the radiation is lost and only a small fraction of photons interact with the nanosystem; it is difficult or impossible to concentrate the excitation in space and time on nanometer-femtosecond scale; the exciting radiation creates a significant background to the relatively weak emissions by the nanosystem. We have introduced a principally different concept of SPASER (Surface Plasmon Amplification by Stimulated Emission of Radiation). The spaser radiation consists of surface plasmons that are bosons just like photons and undergo stimulated emission, but in contrast to photons can be localized on the nanoscale. Spaser as a system will incorporate an active medium formed by two-level emitters, excited in the same way as a laser active medium: optically, or electrically, or chemically, etc. One promising type of such emitters are quantum dots (QDs). These emitters transfer their excitation energy by radiationless transitions to a resonant nanosystem that plays the role of a laser cavity. These transitions are stimulated by the surface plasmons already in the nanosystem, causing buildup of a macroscopic number of the surface plasmons in a single mode. Spaser is predicted to generate ultrashort (10-100 fs) ultraintense (optical electric field $\sim 10^8$ V/cm or greater) pulses of local optical fields at nanoscale. When realized experimentally spaser may completely change the nanooptics.

Recently, we have shown theoretically that the efficient nanolens, which is a self-similar aggregate of a few metal nanosphere, in an active medium of semiconductor quantum dots is an efficient spaser [4]. This spaser possesses a sharp hot spot of local fields in its nanofocus between the minimum-radius nanospheres. Another related recent development has been an experiment by a group of Dr. Eng of Technical University of Dresden (Germany) where the principles of spaser have been confirmed [5].

2.2 Nanofocusing of Optical Energy in Tapered Plasmonic Waveguides [6, 7]

We have predicted theoretically that surface plasmon polaritons propagating toward the tip of a tapered plasmonic waveguide are slowed down and asymptotically stopped when they tend to the tip, never actually reaching it (the travel time to the tip is logarithmically divergent). This phenomenon causes accumulation of energy and giant local fields at the tip. There are various prospective applications of this proposed effect in nanooptics and nanotechnology. Because there is transfer from micro- to nanoscale of not only energy, but also coherence (phase), these results allow for full coherent control on the nanoscale.

2.3 Coherent Control of Ultrafast Energy Localization on Nanoscale [8-14]

Our research has significantly focused on problem of controlling localization of the energy of ultrafast (femtosecond) optical excitation on the nanoscale. This is a formidable problem since it is impossible to achieve such concentration by optical focusing due to the nanosize of the system, or by near-field excitation, because the energy of such excitation is transferred across the entire nanosystem during ultrashort periods on order of the light-wave oscillation. We have proposed and theoretically developed a distinct approach to solving this fundamental problem. This approach, based on the using the relative phase of the light pulse as a functional degree of freedom, allows one to control the spatial-temporal distribution of the excitation energy on the nanometer-femtosecond scale. We have shown that using even the simplest phase modulation, the linear chirp, it is possible to shift in time and spatially concentrate the linear local optical fields, but the integral local energy does not depend on the phase modulation. In contrast, for nonlinear responses, the integral local energy efficiently can be coherently controlled. It is difficult to overestimate possible applications of this effect, including nano-chip computing, nanomodification (nanolithography), and ultrafast nano-sensing.

This effect of the coherent control of local fields on the nanoscale has recently been observed experimentally by H. Petek and collaborators[15, 16]. This key development along with the recently proposed adiabatic transfer of energy and coherence to nanoscale [6, 7] will allow one in perspective to fully control in time and space the ultrafast dynamics of optical energy distribution on the nanoscale.

2.4 Efficient Nanolens [4, 17, 18]

As an efficient nanolens, we have proposed a self-similar linear chain of several metal nanospheres with progressively decreasing sizes and separations. To describe such systems, we have developed the multipole spectral expansion method. Optically excited, such a nanolens develops the nanofocus (“hottest spot”) in the gap between the smallest nanospheres, where the local fields are enhanced by orders of magnitude due to multiplicative, cascade effect of its geometry and high Q -factor of surface plasmon resonance. The spectral maximum of the enhancement is in the near ultraviolet, shifting toward the red as the separation between the spheres decreases. The proposed system can be used for nanooptical detection, Raman characterization, nonlinear spectroscopy, nano-manipulation of single molecules or nanoparticles, and other applications. Recently, we have shown [4] that this nanolens surrounded by an active medium of nanocrystal quantum dots can be an efficient spaser.

2.5 Second Harmonic Generation on Nanostructured Surfaces [19, 20]

This research resulted from an international collaboration with the group of Prof. Joseph Zyss (France). Based on the spectral-expansion Green’s function theory, we theoretically describe the topography, polarization, and spatial-coherence properties of the second-harmonic (SH) local fields at rough metal surfaces. The spatial distributions of the fundamental-frequency and SH local fields are very different, with highly enhanced hot spots of the SH. The spatial correlation functions of the amplitude, phase, and direction of the SH polarization all show spatial decay on the nanoscale in the wide range of the metal fill factors. This implies that SH radiation collected from even nanometer-scale areas is strongly depolarized and dephased, i.e., has the nature of hyper-Rayleigh scattering, in agreement with recent experiments. The present theory is applicable to nanometer-scale nonlinear-optical illumination, probing, and modification. We have recently further investigated this class of phenomena to predict and describe giant fluctuations of local SH fields in random nanostructures [21].

2.6 Strong Field Effects in Nanostructures: Forest Fire Mechanism of Dielectric Breakdown [22]

This research is a result of an extensive international collaboration (UK, Germany, Canada, and the USA). We have described the interaction of ultrashort infrared laser pulses with clusters and dielectrics. Rapid ionization occurs on a sub-laser wavelength scale below the conventional breakdown threshold. It starts with the formation of nanodroplets of plasma that grow like forest fires, without any need for heating of the electrons promoted to the conduction band. This effect is very important for the physics of laser damage of semiconductors and dielectrics by a moderate-intensity radiation.

2.7 Theory of Coherent Near-Field Optical Microscopy [23, 24]

We have developed theory of phase-sensitive near-field scanning optical microscopy (in collaboration with the group of Dr. Victor Klimov, LANL). The developed theory takes into account interference of secondary electromagnetic waves emitted by the metal nanoparticles and the radiation of the near-field optical microscope (NSOM) tip. The latter radiation contains both magnetic-dipole and electric dipole parts. The interference of these radiations of the tip and the metal nanosystem in the far zone depends on their relative phase that in turn is determined by the detuning from the surface plasmon resonance in the metal nanosystem. Owing to this interference, it is possible to determine the spectral phase of the surface plasmon resonances in metal nanoparticles. In turn, this allows us to determine the positions of these resonances with unprecedented resolution. Recently the interference near-field spectroscopy that we proposed and developed was used [25] for further studies of plasmonic nanosystems with proper reference to our work.

2.8 Nanoplasmonics at Metal Surface: Enhanced Relaxation and Superlensing [26, 27]

We have considered a nanoscale dipolar emitter (quantum dot, atom, fluorescent molecule, or rare earth ion) in a nanometer proximity to a flat metal surface. There is strong interaction of this emitter with unscreened metal electrons in the surface nanolayer that causes enhanced relaxation due to surface plasmon excitation and Landau damping. To describe these phenomena, we developed analytical theory based on local random-phase approximation. For the system considered, conventional theory based on metal as continuous dielectric fails both qualitatively and quantitatively.

In a recent development [27], we have considered a principal limitations on the spatial resolution on the nanoscale of the “Perfect Lens” introduced by Pendry, also known as the superlens. In the conventional local electrodynamics, the superlens builds a 3d image in the near zone without principal s on the spatial resolution. We have shown that there is a principal limitation on this resolution, ~5 nm in practical terms, that originates from the spatial dispersion and Landau damping of dielectric responses of the interacting electron fluid in metals.

3 Future Plans

We will develop both the theory in the directions specified above and the collaborations with the experimental and theoretical groups that we have developed. Among the future projects, we will consider attosecond effects of the carrier-envelope phase. The coherent control on nanoscale under conditions of adiabatic energy concentrations will be proposed and studied, which potentially will allow full spatio-temporal control on the nanoscale.

References (2003-2005)

1. D. J. Bergman and M. I. Stockman, *Surface Plasmon Amplification by Stimulated Emission of Radiation: Quantum Generation of Coherent Surface Plasmons in Nanosystems*, Phys. Rev. Lett. **90**, 027402-1-4 (2003).
2. M. I. Stockman and D. J. Bergman, in Proceedings of SPIE: Complex Mediums IV: Beyond Linear Isotropic Dielectrics, edited by M. W. McCall and G. Dewar, *Surface Plasmon Amplification through Stimulated Emission of Radiation (Spaser)* (SPIE, San Diego, California, 2003), Vol. 5221, p. 93-102.
3. D. J. Bergman and M. I. Stockman, *Can We Make a Nanoscopic Laser?*, Laser Phys **14**, 409-411 (2004).
4. K. Li, X. Li, M. I. Stockman, and D. J. Bergman, *Surface Plasmon Amplification by Stimulated Emission in Nanolenses*, Phys. Rev. B **71**, 115409-1-4 (2005).
5. J. Seidel, S. Grafstroem, and L. Eng, *Stimulated Emission of Surface Plasmons at the Interface between a Silver Film and an Optically Pumped Dye Solution*, Phys. Rev. Lett. **94**, 177401-1-4 (2005).
6. M. I. Stockman, in Plasmonics: Metallic Nanostructures and Their Optical Properties II, edited by N. J. Halas and T. R. Huser, *Delivering Energy to Nanoscale: Rapid Adiabatic Transformation, Concentration, and Stopping of Radiation in Nano-Optics* (SPIE, Denver, Colorado, 2004), Vol. 5512, p. 38-49.

7. M. I. Stockman, *Nanofocusing of Optical Energy in Tapered Plasmonic Waveguides*, Phys. Rev. Lett. **93**, 137404-1-4 (2004).
8. M. I. Stockman, S. V. Faleev, and D. J. Bergman, *Coherently Controlled Femtosecond Energy Localization on Nanoscale*, Appl. Phys. B **74**, S63-S67 (2002).
9. M. I. Stockman, S. V. Faleev, and D. J. Bergman, *Coherent Control of Femtosecond Energy Localization in Nanosystems*, Phys. Rev. Lett. **88**, 67402-1-4 (2002).
10. M. I. Stockman, S. V. Faleev, and D. J. Bergman, *Coherently-Controlled Femtosecond Energy Localization on Nanoscale*, Appl. Phys. B **74**, 63-67 (2002).
11. M. I. Stockman, D. J. Bergman, and T. Kobayashi, in Proceedings of SPIE: Plasmonics: Metallic Nanostructures and Their Optical Properties, edited by N. J. Halas, *Coherent Control of Ultrafast Nanoscale Localization of Optical Excitation Energy* (SPIE, San Diego, California, 2003), Vol. 5221, p. 182-196.
12. M. I. Stockman, S. V. Faleev, and D. J. Bergman, *Femtosecond Energy Concentration in Nanosystems: Coherent Control*, Physica B: Physics of Condensed Matter **338**, 361-365 (2003).
13. M. I. Stockman, S. V. Faleev, and D. J. Bergman, in Ultrafast Phenomena XIII, *Coherently-Controlled Femtosecond Energy Localization on Nanoscale* (Springer, Berlin, Heidelberg, New York, 2003).
14. M. I. Stockman, D. J. Bergman, and T. Kobayashi, *Coherent Control of Nanoscale Localization of Ultrafast Optical Excitation in Nanosystems*, Phys. Rev. B **69**, 054202-10 (2004).
15. A. Kubo, K. Onda, H. Petek, Z. Sun, Y. S. Jung, and H. K. Kim, in Ultrafast Phenomena XIV, edited by T. Kobayashi, T. Okada, T. Kobayashi, K. A. Nelson and S. D. Silvestri, *Imaging of Localized Silver Plasmon Dynamics with Sub-Fs Time and Nano-Meter Spatial Resolution* (Springer, Niigata, Japan, 2004), Vol. 79, p. 645-649.
16. A. Kubo, K. Onda, H. Petek, Z. Sun, Y. S. Jung, and H. K. Kim, *Femtosecond Imaging of Surface Plasmon Dynamics in a Nanostructured Silver Film*, Nano Lett. **5**, 1123-1127 (2005).
17. K. Li, M. I. Stockman, and D. J. Bergman, *Self-Similar Chain of Metal Nanospheres as an Efficient Nanolens*, Phys. Rev. Lett. **91**, 227402-1-4 (2003).
18. M. I. Stockman, K. Li, X. Li, and D. J. Bergman, in Plasmonics: Metallic Nanostructures and Their Optical Properties II, edited by N. J. Halas and T. R. Huser, *An Efficient Nanolens: Self-Similar Chain of Metal Nanospheres* (SPIE, 2004), Vol. 5512, p. 87-99.
19. M. I. Stockman, D. J. Bergman, C. Anceau, S. Brasselet, and J. Zyss, *Enhanced Second-Harmonic Generation by Metal Surfaces with Nanoscale Roughness: Nanoscale Dephasing, Depolarization, and Correlations*, Phys. Rev. Lett. **92**, 057402-1-4 (2004).
20. M. I. Stockman, D. J. Bergman, C. Anceau, S. Brasselet, and J. Zyss, in Complex Mediums V: Light and Complexity, edited by M. W. McCall and G. Dewar, *Enhanced Second Harmonic Generation by Nanorough Surfaces: Nanoscale Depolarization, Dephasing, Correlations, and Giant Fluctuations* (SPIE, 2004), Vol. 5508.
21. M. I. Stockman, *Giant Fluctuations of Second Harmonic Generation on Nanostructured Surfaces*, Chem Phys (**In Press**), (2005).
22. L. N. Gaier, M. Lein, M. I. Stockman, P. L. Knight, P. B. Corkum, M. Y. Ivanov, and G. L. Yudin, *Ultrafast Multiphoton Forest Fires and Fractals in Clusters and Dielectrics*, J. Phys. B: At. Mol. Opt. Phys. **37**, L57-L67 (2004).
23. A. A. Mikhailovsky, M. A. Petruska, M. I. Stockman, and V. I. Klimov, *Broadband near-Field Interference Spectroscopy of Metal Nanoparticles Using a Femtosecond White-Light Continuum*, Opt. Lett. **28**, 1686-1688 (2003).
24. A. A. Mikhailovsky, M. A. Petruska, K. Li, M. I. Stockman, and V. I. Klimov, *Phase-Sensitive Spectroscopy of Surface Plasmons in Individual Metal Nanostructures*, Phys. Rev. B **69**, 085401-1-6 (2004).
25. K. Lindfors, T. Kalkbrenner, P. Stoller, and V. Sandoghdar, *Detection and Spectroscopy of Gold Nanoparticles Using Supercontinuum White Light Confocal Microscopy*, Phys. Rev. Lett. **93**, 037401-1-4 (2004).
26. I. A. Larkin, M. I. Stockman, M. Achermann, and V. I. Klimov, *Dipolar Emitters at Nanoscale Proximity of Metal Surfaces: Giant Enhancement of Relaxation in Microscopic Theory*, Phys. Rev. B **69**, 121403(R)-1-4 (2004).
27. I. A. Larkin and M. I. Stockman, *Imperfect Perfect Lens*, Nano Lett. **5**, 339-343 (2005).

Quantum Dynamics of Optically-Trapped Fermi Gases

Grant #DE-FG02-01ER15205
Report for the Period: 11/1/04-10/31/05

John E. Thomas
Physics Department, Duke University
Durham, NC 27708-0305
e-mail: jet@phy.duke.edu

1. Scope

The purpose of this program is to study the many-body quantum dynamics of a very general fermionic system: An optically trapped, strongly-interacting 50-50 mixture of spin-up and spin-down ${}^6\text{Li}$ fermions, in the regime of quantum degeneracy. Strongly-interacting, highly degenerate samples are directly produced in an ultrastable CO_2 laser trap by forced evaporation at a magnetic field tuned near a Feshbach resonance. The resonance permits wide tunability of the s-wave scattering length which determines the interaction strength.

Strongly-interacting mixtures of spin-up and spin-down atomic Fermi gases provide unique systems for stringent tests of competing quantum theories of superfluidity and high temperature superconductivity. In the controlled environment of an optical trap, such mixtures permit wide variation of temperature, density, spin composition and interaction strength. Indeed, strongly-interacting Fermi gases provide scale models of a variety of exotic systems in nature, not only high temperature superconductors, but neutron stars, strongly-interacting matter in general, and even a quark-gluon plasma. The scale is set by the Fermi temperature, which is a few μK in a quantum gas and about an electron volt in a metal or 10^4 K. Near a Feshbach resonance, spin-up and spin-down mixtures of atomic Fermi gases exhibit super-strong pairing interactions and are predicted to achieve superfluid transition temperatures which are a significant fraction of the Fermi temperature. Such high transition temperatures are consistent with recent experiments and correspond to achieving superconductivity in a metal at thousands of degrees, far above room temperature.

2. Recent Progress

During the past year, we achieved two major breakthroughs in the study of strongly-interacting Fermi gases. We made the first thermodynamic measurements, and observed a phase transition in the heat capacity of the gas [1]. We also observed a

transition in the damping rate of the radial breathing mode, measured as a function of temperature [2]. In addition, we made comprehensive measurements of the magnetic field dependence of the damping rate and frequency of the radial breathing mode, and observed a breakdown of hydrodynamics [3]. The primary results are described briefly below.

Heat Capacity of Strongly-Interacting Fermi Gas [1]

Strongly-interacting Fermi gases provide a paradigm for strong interactions in nature. For this reason, measurements of the thermodynamic properties of this unique system are of paramount importance. In studies of superfluidity and superconductivity, measurements of the heat capacity have played an important role in determining phase transitions and in characterizing the nature of the bosonic and fermionic excitations.

Heat capacity measurement requires two ingredients: Precise input of a known energy followed by temperature measurement. The heat capacity is the amount of energy needed to change the temperature by one °K. In a solid, this program is readily implemented. In a strongly-interacting Fermi gas, new methods are needed both for energy input and temperature measurement.

Energy input is readily accomplished by abruptly releasing the gas from the optical trap for a short time and then abruptly reinstating the trapping potential. The gas expands during the release time, which is denoted as t_{heat} . Since the trapping potential is approximately harmonic, the increase in energy scales as the square of the expansion factor of the cloud. The gas is first cooled to the lowest possible temperatures, where the total energy is very close (within a 1 or 2 %) of the ground state value. The cold gas expands hydrodynamically by a known expansion factor, which then determines the total energy $E(t_{heat})$ for a given release time t_{heat} . The gas is allowed to equilibrate after recapture, and then the temperature is measured.

Temperature measurement in a noninteracting Fermi gas is readily accomplished from the shape of the cloud, either in the trap, or after ballistic expansion. The one dimensional (x) transverse density distribution is first obtained by integrating the column density in the axial direction. This distribution has a Thomas-Fermi shape, $n_{TF}(x)$ which is a function of two parameters, the Fermi radius, σ_F and the reduced temperature T/T_F . These parameters are determined from the fits to the measured spatial distributions. To obtain a one-parameter characterization of the temperature, the Fermi radius is held fixed in all of the fits, after it is determined from the data at the lowest temperature. In this way, the shape of the cloud is uniquely correlated with a value of T/T_F .

In a strongly-interacting Fermi gas, the precise shape of the cloud as a function of temperature is still subject to debate. However, our experiments and recent theory show that the shape is very close to that of a noninteracting gas at all temperatures. One can show using model-independent arguments that the shapes precisely agree at

$T = 0$ and at high temperatures, where the gas is classical. Hence, in temperature measurements, we employ an empirical temperature scale: We simply use the best fit to the density, assuming a noninteracting gas Thomas-Fermi shape, $n_{TF}(x)$, and determine two parameters, the interacting gas Fermi radius, σ'_F and the empirical reduced temperature, which is denoted by \tilde{T} . This empirical scale is later calibrated to the true reduced temperature T/T_F using theoretically generated spatial profiles which are functions of a known value of T/T_F .

By measuring the empirical temperature as a function of the input energy, we observe a transition in behavior at an empirical temperature $\tilde{T} = 0.33$: Above this temperature, the energy as a function empirical temperature exhibits ideal gas scaling, while below this temperature, the behavior is different, and is better fit by a power law. Calibrating the temperature reveals that $\tilde{T} = 0.33$ corresponds to $T/T_F = 0.27$. This is quite close to the superfluid transition temperature, near $T/T_F = 0.3$, which predicted by several theory groups.

Transition in the Damping Rate of the Radial Breathing Mode [2]

With our precision energy input and empirical temperature measurement methods, we realized that we could search for transitions in other properties of the gas, and compare the behavior with our observations for the heat capacity.

The frequency and damping rate of the radial breathing mode are two mechanical properties of the gas which can be studied using these new methods. In the experiments, we heat the gas by adding a known energy, let it equilibrate, and measure the empirical temperature. Then the same amount of energy is added, but this time we excite the radial breathing mode as in our previous experiments: The gas is released for a very short time, it expands slightly, and is then recaptured, producing a radial oscillation. The frequency and damping rate are measured as a function of empirical temperature.

The frequency shows no evidence of a phase transition. This is consistent with our expectations: The gas is always strongly hydrodynamic, and oscillates at the hydrodynamic frequency. Only the mechanism changes in the transition region from superfluid hydrodynamics to collisional hydrodynamics.

In contrast to the frequency, the damping rate reveals an abrupt transition in behavior: At low temperatures, the damping rate scales linearly with empirical temperature (linear correlation coefficient 0.998). However, the behavior abruptly changes at $\tilde{T} = 0.5$, where the damping rate deviates strongly from linear scaling. After calibration, we find that $\tilde{T} = 0.5$, corresponds to $T/T_F = 0.35$, not far above that obtained in the heat capacity measurements and consistent with predictions of the superfluid transition temperature.

Nearly 6300 repetitions of the experiment were required to obtain the published data, which was accumulated over several months. At present, there is no theory of damping in a strongly-interacting Fermi gas.

In addition to our temperature dependence measurements, we also made comprehensive, precision measurements of the frequency and damping rate as a function of magnetic field, which required a similar effort to the temperature dependence.

These measurements test predictions for the equation of state of the gas. We find that the data are in quantitative agreement with predictions at resonance. The measured frequency at the Feshbach resonance is in extremely good quantitative agreement with predictions based on universal hydrodynamics. However, we obtain only reasonable qualitative agreement as the magnetic field is tuned above or below resonance. Current theories incorporate superfluid condensed pairs and a mean field approximation, which captures the essence of the data, but does not yield very good quantitative agreement. Hence, further theoretical effort is needed.

The data also reveal a breakdown of hydrodynamics at sufficiently high magnetic field above the Feshbach resonance at 834 G. At 1080 G, the frequency and damping abruptly increase. A similar transition has been observed by the Innsbruck group at a lower magnetic field. These transitions appear to arise when the pairing gap is comparable to the collective mode energy quantum and pairs are broken, as first suggested by the Innsbruck group.

3. Future Plans

Our plans include measurements of the singlet molecular contribution to the pairing wave function, as a function of total energy. We started this experiment last summer, and did not finish, due to a dye laser failure. This work is analogous to that recently published by the Rice group, but our technique employs stabilized lasers. In addition, we are working on methods to perform entropy measurement, as a function of energy, by using magnetic field sweeps from the strongly-interacting regime to the weakly interacting regime. This will provide a model-independent test of the theory, and absolute temperature calibration.

4. References to Publications of DOE Sponsored Research

- 1) J. Kinast, A. Turlapov, and J. E. Thomas (with theory support from Q. Chen, J. Stajic, and K. Levin), “Heat Capacity of a Strongly-Interacting Fermi Gas,” *Science* **307**, 1296 (2005).
- 2) J. Kinast, A. Turlapov, and J. E. Thomas, “Damping in a Unitary Fermi Gas,” *Phys. Rev. Lett.* **94**, 170404 (2005).
- 3) J. Kinast, A. Turlapov, and J. E. Thomas, “Breakdown of Hydrodynamics in the Radial Breathing Mode of a Strongly-Interacting Fermi Gas,” *Phys. Rev. A* **70**, 051401(R) (2004).

Inner-shell electron spectroscopy and chemical properties of atoms and small molecules

T. Darrah Thomas, Principal Investigator
T.Darrah.Thomas@oregonstate.edu

Department of Chemistry
153 Gilbert Hall
Oregon State University
Corvallis, OR 97331-4003

Program scope

Many chemical phenomena depend on the ability of a molecule to accept charge at a particular site in the molecule. Examples are acidity, basicity (proton affinity), rates and regioselectivity of electrophilic reactions, hydrogen bonding, and ionization. Among these, inner-shell ionization spectroscopy (ESCA or x-ray photoelectron spectroscopy) has proven to be a useful tool for investigating how a molecule responds to added or diminished charge at a particular site. The technique is element specific and is applicable to all elements except hydrogen. It is, in many cases site specific. As a result, x-ray photoelectron spectroscopy (XPS) can probe all of the sites in a molecule and identify the features that cause one site to have different chemical properties from another. In addition, the inner-shell ionization energies, as measured by XPS, provide insight into the charge distribution in the molecule – a property of fundamental chemical importance.

During the last 35 years, XPS has been a source of useful chemical information. Until recently, however, the investigation of the carbon 1s photoelectron spectra of the hydrocarbon portion of molecules has been hampered by lack of resolution. Carbon atoms with quite distinct properties may have carbon 1s ionization energies that differ by less than 1 eV, whereas historically the available resolution has been only slightly better than this. In addition, the vibrational excitation accompanying core ionization adds complexity to the spectra that has made analysis difficult.

The availability of third-generation synchrotrons coupled with high-resolution electron spectrometers has made a striking difference in this situation. It is now possible to measure carbon 1s photoelectron spectra with a resolution of about half the natural line width (~100 meV), with the result that recently measured carbon 1s spectra in hydrocarbons show a richness of chemical effects and vibronic structure.

During the last eight years this program has endeavored to exploit this capability in order to investigate systems where new insights can be gained from high-resolution carbon 1s photoelectron spectroscopy. The primary experimental goal has been to determine carbon 1s ionization energies not previously accessible and to use relationships between these energies and other chemical properties to elucidate the chemistry of a variety of systems. Early work focused on understanding the features of the spectra: line shape, line width, vibrational structure, and vibronic coupling, since understanding these features is essential to unraveling the complex spectra that are found for molecules having several carbon atoms. Now that these features are (more or less) understood, emphasis has shifted to investigation of chemically significant systems and to gaining further insights into the relationships between core-ionization energies and chemical properties.

Recent progress (2004-2005)

During the last 18 months, we have had 46 shifts of synchrotron time – 18 at MAX II in May 2004, 10 at the ALS in September 2004, and 18 at MAX II in May 2005. This time was devoted to acquiring primarily carbon 1s photoelectron spectra for a number of compounds of interest. In addition, where appropriate, measurements were made of oxygen and nitrogen photoelectron spectra. Some of the results of these and earlier measurements are summarized below. An additional 10 shifts is scheduled at the ALS in October 2005.

This work has been carried out in collaboration with colleagues from the Universities of Bergen, Turku, and Uppsala.

Conformational effects in inner-shell photoelectron spectroscopy of ethanol. In general, there has been little reason to expect that different conformers of a molecule would give different photoelectron spectra, and, until recently, where this possibility has been investigated no conformational effects on the spectra have been observed. We have, however, found that ethanol proves to be an exception to this expectation. Ethanol exists in two conformers in about equal abundance. In the *anti* form the hydroxyl group is pointed away from the methyl group, with an HOCC dihedral angle of 180° . By contrast, in the *gauche* form this angle is about 60° , with the result that the hydroxyl group can interact strongly with the methyl group. Carbon 1s ionization at the methyl group leaves a localized positive charge at the methyl group, and this positive charge interacts repulsively with the positive charge on the hydroxyl group. In the *anti* form, these charges are far apart, and the interaction is weak. By contrast, in the *gauche* form, the interaction is strong and the *gauche* form is strongly destabilized. As a consequence, core ionization of the methyl group in *gauche* ethanol leads to considerable excitation of torsional motion, but ionization of the *anti* form leads to no excitation of this motion.

This torsional excitation is apparent if we compare the carbon 1s photoelectron spectrum of ethanol with that of chloroethane, where no torsional excitation is possible. In ethanol the peak in the spectrum corresponding to ionization of the methyl group is broad and nearly featureless, while in chloroethane it is sharp and shows only excitation of stretching and bending modes. Theoretical calculations that take into account the possibility of this torsional excitation give good agreement with the experimentally observed features of the spectrum.

It is expected that such conformational effects will be fairly common in core-level spectra of small molecules that exhibit conformational equilibria, and that studies of this type may be of use in resolving questions about molecular conformations.

A paper on this work has been accepted for publication in Physical Review Letters.

Reactivity and core-ionization energies in conjugated dienes. Carbon 1s photoelectron spectroscopy of 1,3-pentadiene. Unsaturated compounds (that is, compounds with double or triple bonds) are of interest in chemistry because of the high reactivity of the multiple bond. This reactivity makes these substances ideal starting materials for the synthesis of other molecules. The addition of a substituent to such a molecule affects the reactivity; for instance, propene, $\text{CH}_2=\text{CHCH}_3$, is more reactive than ethene, $\text{CH}_2=\text{CH}_2$. Moreover, the effect of the methyl group, CH_3 , in propene is to activate the terminal CH_2 group much more than it does the CH group. These features are reflected in the carbon 1s ionization energies of these molecules, where the carbon of the CH_2 group is found to have a very low ionization energy, indicating a high availability of electrons.¹

Analogous to ethene and propene are 1,3-butadiene, $\text{CH}_2=\text{CHCH}=\text{CH}_2$, and 1,3-pentadiene, $\text{CH}_2=\text{CHCH}=\text{CHCH}_3$, where we have the additional complexity of a conjugated chain of double bonds. Measurements of the carbon 1s ionization energies of these compounds at the Advanced Light Source show the similarities and differences between butadiene and pentadiene, on the one hand, and propene and ethene, on the other. First, the larger size of butadiene and pentadiene lead to higher polarizability, lower ionization energies, and greater reactivity. Second, the conjugated bond system in 1,3-pentadiene transmits the effect of the additional methyl group (C5) efficiently to the other end of the molecule, so that the reactivity of the terminal CH_2 carbon (C1) is enhanced almost as much as is that of C3 (which is in a position comparable to the reactive CH_2 group in propene). Finally, the conjugated system of double bonds in 1,3-butadiene and 1,3-pentadiene provides an efficient mechanism for delocalizing charge from one end of the molecule to the other. This effect leads to lower ionization energies and higher reactivities for 1,3-butadiene relative to ethene and for 1,3-pentadiene relative to propene.

A paper on this work has recently appeared in the Journal of Physical Chemistry.²

Fluorine as a π donor. Carbon 1s photoelectron spectroscopy of fluoroethenes, fluorobenzenes, and methylbenzenes. A methyl group attached to a benzene ring donates electrons to the ring, making it more reactive. Fluorine, by contrast, because of its high electronegativity, withdraws electrons, making the ring less reactive. At the same time, however, fluorine is capable of donating electrons into the π system of the ring, adding negative charge back to the carbon atoms that are *ortho* and *para* to the fluorine substituent. Inner-shell electron spectroscopy can, in principle, probe these effects; in practice, the high-resolution electron spectroscopic facilities at third-generation synchrotrons are essential for this purpose.

We have recently measured the carbon 1s photoelectron spectra of a number of fluoroethenes, fluorobenzenes, and methylbenzenes. With the aid of electronic structure theory to predict the vibrational structure in these spectra, we have been able to resolve them into contributions from each of the inequivalent carbon atoms and to assign carbon 1s ionization energies to each chemically unique carbon atom.

In keeping with expectations, the results show that the carbon 1s ionization energies in methylbenzenes are lower than those in benzene, whereas those in fluorobenzenes are higher. Moreover, in both kinds of molecules, the carbon atoms that are *ortho* or *para* to the substituent are found to be relatively electron rich compared with those that are *meta* to the substituent. In addition, it is found that all of the core-ionization energy shifts follow a simple additivity relationship, such that a small number of parameters provides an accurate description of a large number of shifts.

Additional insight is obtained by comparing the core-ionization energies with proton affinities. For molecules in which the proton is attached *meta* to the substituents, there is an excellent linear correlation between proton affinity and carbon 1s ionization energy. However, if we expand the correlation to include protons added at sites that are *ortho* or *para* to a fluorine substituent, we find that these have proton affinities that are significantly higher than would be expected from their carbon 1s ionization energies. We believe that this result reflects the electron acceptor capability of the two hydrogens that are attached to the protonated carbon. Thus, although fluorine is capable of donating electrons to the *ortho* and *para* positions, it is capable of donating even more if there is suitable electron acceptor present. Hence, fluorine can affect the energy of protonation more than the energy of ionization.

Group electronegativities. Carbon 1s photoelectron spectra were measured for a number of molecules that were chosen to shed light on group electronegativities. These include $C(CH_3)$, $HC\equiv CCH_2CH=CH_2$, $CH_2=CHCH_2I$, $CH_3CH_2CH_2I$, CH_3CHICH_3 , $(CH_3)_3CCl$, $CH_3CF_2CH_3$, $CH_3CHBrCH_3$, CF_3Br , CF_2Br_2 , CF_2I_2 , Cl_4 , $CF_3CH_2CF_3$, and 1,2,4,5-tetramethylbenzene. Analysis of these results is in progress.

1. L. J. Sæthre, O. Svaæren, S. Svensson, S. Osborne, T. D. Thomas, J. Jauhiainen, S. Aksela, *Phys. Rev. A*, 2748 (1997).

2. T. D. Thomas, L. J. Sæthre, K. J. Børve, M. Gundersen, and E. Kukk, *J. Phys. Chem. A*, 109, 5085 (2005).

Future plans

We have been allotted 10 shifts of beam time at the Advanced Light Source in October, 2005, and 18 shifts at MAX II in May, 2006. Focus during these periods will be on measurements of carbon 1s photoelectron spectra that will give further insights into chemistry, with emphasis on group electronegativity, interaction of one substituent with another, transmission of substituent effects, and substituent effects in benzene. Some typical compounds that will be of interest are indicated below.

Interaction of halogens with alkyl groups and transmission of substituent effects: $CH_3CH_2CH_2F$, $CH_3CH_2CH_2CH_2F$, $CH_3CHFCH_2CH_3$, $(CH_3)_3CF$. **Substituents effects in benzene:** methoxybenzene, 1,2-, 1,3-, and 1,4-dimethoxybenzene, 1,3,5-trimethoxybenzene, aniline, 1,2-, 1,3-, and 1,4-phenylenediamine, chlorobenzene, 1,2-, 1,3-, and 1,4-dichlorobenzene, nitrobenzene, benzaldehyde, benzenethiol, methylbenzoate, and phenol.

Publications involving DOE support, 2003-2005

Carbon 1s photoelectron spectroscopy of halomethanes. Effects of electronegativity, hardness, charge distribution, and relaxation, T. D. Thomas, L. J. Sæthre, K. J. Børve, J. D. Bozek, M. Huttula, and E. Kukk, *J. Phys. Chem. A* **108**, 4983 (2004).

Carbon 1s photoelectron spectroscopy of six-membered cyclic hydrocarbons, V. M. Oltedal, K. J. Børve, L. J. Sæthre, T. D. Thomas, J. D. Bozek, and E. Kukk, *Physical Chemistry Chemical Physics PCCP*, **6**, 4254 (2004).

Reactivity and core-ionization energies in conjugated dienes. Carbon 1s photoelectron spectroscopy of 1,3-pentadiene, T. D. Thomas, L. J. Sæthre, K. J. Børve, M. Gundersen, and E. Kukk, *J. Phys. Chem. A*, **109**, 5085 (2005).

Conformational effects in inner-shell photoelectron spectroscopy: Ethanol, M. Abu Samha, K. J. Børve, L. J. Sæthre, and T. D. Thomas, *Phys. Rev. Lett.*, in press, 2005.

Laser-Produced Coherent X-Ray Sources

Donald Umstadter

212 Ferguson Hall, University of Nebraska, Lincoln, NE 68588

dpu@unlserve.unl.edu

1 Program Scope:

We study the physics underlying the generation of x-rays from the interaction of relativistic electrons with an ultra-intense laser pulse. The laser pulse acts as the accelerator and wiggler leading to an all-optical synchrotron-like x-ray source. The mm-sized accelerator and micron-sized wiggler (produced either directly by the laser field or via laser-generated ion channels) leads to a compact source of high brightness, ultrafast x-rays with applications in relativistic nonlinear optics, ultrafast chemistry, biology, inner-shell electronic processes and phase transitions.

2 Recent Progress:

We have investigated these sources both experimentally as well as theoretically. Two types of sources were demonstrated: one based on Thomson scattering [11, 8, 4], in which the laser light pulse acts directly as the wiggler, and another based on betatron oscillations, in which an ion channel—produced in the wake of the laser pulse—acts as the wiggler[6]. We have also demonstrated that it is possible to condition a MeV electron beam optically which would enable the generation of attosecond, hard x-ray pulses [3].

2.1 Experiment

The geometry used for these experiments involved either one or two laser pulses. In the former case the scattering pulse was co-propagating with the laser-produced electron beam while in the latter case it was obliquely incident on it (see Fig. 1).

2.1.1 Laser based synchrotron radiation

Beams of x rays in the kiloelectronvolt energy range have been produced from laser-matter interaction. Here, energetic electrons are accelerated by a laser wakefield, and experience betatron oscillations in an ion channel formed in the wake of the intense femtosecond laser pulse. The experiment was performed at the Laboratoire dOptique Applique using a titanium-doped sapphire (Ti:Sa) laser operating at 10 Hz with a wavelength λ_0 of 820 nm in chirped-pulse amplification mode.¹³ The laser delivers energies up to 1 J on target in 30 fs (FWHM) pulses, with a linear horizontal polarization. The laser beam was focused with an $f/18$ off-axis parabolic mirror onto the edge of a supersonic helium gas jet (diameter 3 mm). The vacuum-focused intensity $I_L = 3 \times 10^{18} W cm^2$ for which the corresponding normalized vector potential $a_0 = 1.2$.

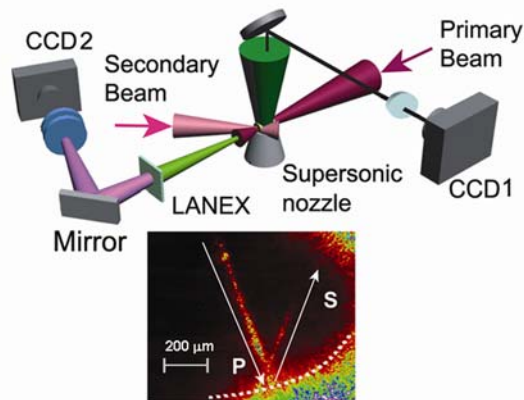


Figure 1: Schematic diagram of experimental setup to study x-ray generation with one and two laser pulses.

The x-ray radiation produced in the plasma was measured using a cooled x-ray charge-coupled device (CCD) camera placed directly on the laser axis. We have characterized the x-ray emission by measuring its spectral and spatial distribution, the x-ray intensity and the spatial distribution as a function of the electron density of the plasma, the variation of the flux with the laser energy. We have observed a beam of x-ray radiation. The radiation is intense, broadband in the keV spectral range, and confined in the forward direction within a 50 mrad cone (FWHM). The spectral distribution of the radiation was measured from 1 keV to 10 keV by placing a set of Be, Al, Cu, and Ni filters in front of the detector. The spectrum depicted decreases exponentially from 1 to 10 keV. The total number of photons (integrated over the bandwidths of the filters and over the divergence of the x-ray beam) is found to be more than 10^8 photons (per shot/solid angle at 0.1% BW).

The most important feature of the observed x-ray emission is its collimation in a low divergence beam centered onto the laser axis. As shown on the beam profile in Fig. 2, recorded for x-ray energies above 1 keV and for $n_e = 8 \times 10^{18} \text{ cm}^{-3}$, the beam divergence is found to be 20 mrad (FWHM).

2.1.2 Optical conditioning of electron beams

The interaction of a laser-produced electron beam with an ultraintense laser pulse in free space is studied. We show that the optical pulse with $a_0 = 0.5$ imparts momentum to the electron beam, causing it to deflect along the laser propagation direction. The observed 3-degree angular deflection is found to be independent of polarization and in good agreement with a theoretical model for the interaction of free electrons with a tightly focused Gaussian pulse, but only when longitudinal fields are taken into account. This technique is used to temporally characterize a subpicosecond laser-wakefield-driven electron bunch.

Optical manipulation of the electron trajectories can be applied to conditioning laser-produced electron beams. Since the magnitude of the deflection depends on the electron energy for a fixed laser intensity, a monochromatic, low-emittance, attosecond electron beam can be obtained by using a suitable aperture downstream of the interaction region. Ponderomotive scattering of electrons traveling at an oblique angle to the laser pulse can therefore select a narrow, tunable energy range of electrons with ultrashort bunch duration and physically separate them for use in other applications such as ultrafast EUV/X-ray sources, fast igniter fusion, high temporal resolution electron diffraction, shock and laboratory astrophysics, and electron beam injection for accelerators.

2.2 Theory

The theoretical research supported has focused on the Thomson scattering of electrons trapped in a 1-dimensional optical lattice [1]. Two counter propagating laser pulses of equal frequency set up a standing wave. Low energy electrons are trapped near the bottom of the resulting ponderomotive potential well and oscillate with a characteristic bounce frequency proportional to $I^{1/2}$. The orbits of these electrons and the subsequent Thomson scattering spectra have been computed. Each particle radiates harmonics of both the laser and bounce frequencies as well as intermodulation products of

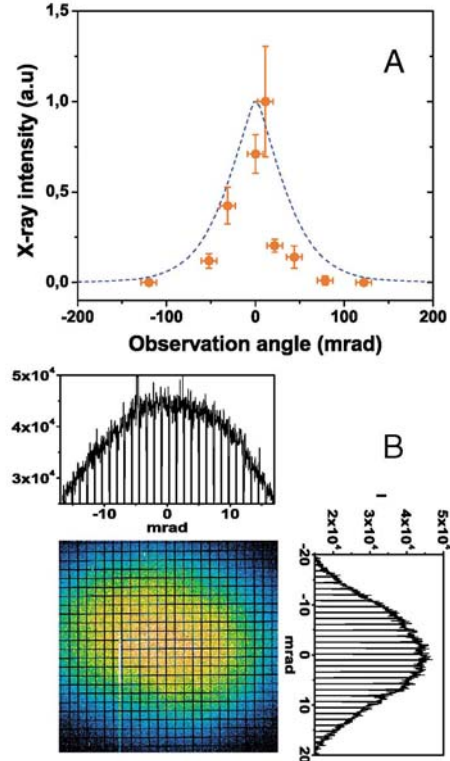


Figure 2: Angular distribution of the radiation for x-ray energies beyond 1 keV. (a) The measurement is made for $n_e = 10^{19} \text{ cm}^{-3}$ in the horizontal plane. The dotted line represents the result obtained from the 3-D PIC simulation. (b) Spatial profile of the x-ray beam at $n_e = 8 \times 10^{19} \text{ cm}^{-3}$. The corresponding lineout graphics, where the shadow of a nickel grid placed in the beam appears, provides the radiation source size in the transverse directions. We obtain a source size of $20 \mu\text{m} \times 20 \mu\text{m}$.

these lines. This process generates infrared light directed along the laser polarization. As this line is physically separated from the laser pulse, the problem of filtering the laser light while allowing the IR radiation to pass is eliminated. Also, as the intermodulation product spectral separation from the laser fundamental mode is directly related to the laser intensity, this is a possible diagnostic for the laser intensity near critical surfaces: for example, in ICF hohlraums. Intermodulation can lead to anomalous spectral broadening as intermodulation products can merge with the laser fundamental spectral mode.

Detailed theoretical calculations have also been performed in support of experiments particularly with regard to the electron motion at relativistic intensities in tightly focused laser beams. It has been shown that current models are inadequate and it is necessary to properly account for the longitudinal fields in order to obtain accurate electron trajectories. These calculations are now being extended to obtain detailed information on the scattered radiation.

3 Future Plans

We are currently engaged in setting up a new laser laboratory at the University of Nebraska, Lincoln. When completed later this year, this will be equipped with a state of the art 100 TW laser system and all experimental equipment required to perform cutting edge research on high-field science and the applications thereof. We will particularly focus on developing the next generation of x-ray sources with a brightness sufficient to enable real-world applications. To this end we propose to implement single and multiple pulse experimental geometries to obtain x-rays via Thomson scattering and/or betatron motion. Recent results on the generation of quasi-monoenergetic electrons from laser-plasma sources will serve to produce intense monochromatic beams of x-rays. Over the next year we propose to investigate in detail the properties of laser produced electron beams, improvement in the beam quality and apply this to x-ray generation. With a 10-Hz laser and 100-TW peak power, tight focusing will not be required to obtain relativistic intensities, leading to a larger interaction volume, and therefore a higher x-ray yield, at high average power. Unlike the low repetition rate lasers used in the past it will also be possible to optimize the performance of these sources even in complex experimental geometries. At this time, detailed calculations are being performed to obtain the x-ray source brightness in order to benchmark these calculations against experiments.

The proposed theoretical work is divided into two key areas. First is ultrafast electromagnetic radiation generation through both Thomson and betatron scattering. Second, using the massively parallel hybrid fluid/particle-in-cell code LSP, we will investigate the parametric dependence of self-injection and the generation of so-called mono-energetic electron beams and using the resulting electron energy spectra, calculate the Thomson scattered X-ray spectra. This is an attractive source for ultrafast X-rays since, for example, as the scattered frequency scales as $4\gamma^2$ in a counter propagating geometry where γ is the Lorentz factor, a 100 Mev electron can produce 150 keV X-rays. Another potential source of ultrafast X-rays is betatron scattering in which energetic electrons oscillate through a plasma channel. Currently, most betatron models simply assume that the electron oscillations are purely circular producing generic synchrotron light. We have begun developing a more realistic plasma channel analytical model in conjunction with LSP simulations of channel formation. With this, the particle orbits can be computed and the betatron spectra calculated directly from these orbits instead of appealing to other models. Also, electron orbits can be tracked directly within LSP and these orbits used to compute the betatron light scattered into the IR, visible, and UV with the plasma channel, electron beam emittance, and laser fields included self-consistently.

References

- [1] S. Sepke, Y.Y. Lau, J.P. Holloway, and, D. Umstadter, "Thomson Scattering and Ponderomotive Intermodulation within Standing Laser Beat Waves in Plasma," Phys. Rev. E 2005 (in press).
- [2] D. Umstadter, S. Sepke, S.Y. Chen, "Relativistic Nonlinear Optics," Advances in Atomic and Molecular Physics, Chap. 7, 152 (2005).
- [3] Sudeep Banerjee, Scott Sepke, Rahul Shah, Anthony Valenzuela, Anatoly Maksimchuk, and Donald Umstadter, "Optical Deflection and Temporal Characterization of an Ultrafast Laser-Produced Electron Beam," Phys. Rev. Lett. 95, 035004 (2005).

- [4] Kim Ta Phuoc, Frderic Burgy, Jean-Philippe Rousseau, Victor Malka, Antoine Rouse, Rahul Shah, Donald Umstadter, Alexander Pukhov and Sergei Kiselev, "Laser based synchrotron radiation," *Phys. Plasmas* 12, 023101 (2005).
- [5] E. S. Dodd, J. K. Kim, and D. Umstadter, "Simulation of ultrashort electron pulse generation from optical injection into wake-field plasma waves," *Phys. Rev. E* 70, 056410 (2004).
- [6] Antoine Rouse, Kim Ta Phuoc, Rahul Shah, Alexander Pukhov, Eric Lefebvre, Victor Malka, Sergey Kiselev, Frderic Burgy, Jean-Philippe Rousseau, Donald Umstadter, and Danile Hulin, "Production of a keV X-Ray Beam from Synchrotron Radiation in Relativistic Laser-Plasma Interaction," *Phys. Rev. Lett.* 93, 135005 (2004).
- [7] D. Umstadter, "Relativistic Nonlinear Optics," *Encyclopedia of Modern Optics*, edited by Robert D. Guenther, Duncan G. Steel and Leopold Bayvel, Elsevier, Oxford, (2004), p. 289.
- [8] K. Ta Phuoc, A. Rouse, M. Pittman, J. P. Rousseau, V. Malka, S. Fritzler, D. Umstadter, and D. Hulin, "X-Ray Radiation from Nonlinear Thomson Scattering of an Intense Femtosecond Laser on Relativistic Electrons in a Helium Plasma," *Phys. Rev. Lett.* 91, 195001 (2003).
- [9] Y. Y. Lau, Fei He, Donald P. Umstadter, and Richard Kowalczyk, "Nonlinear Thomson scattering: A tutorial," *Phys. Plasmas* 10, 2155 (2003).
- [10] Fei He, Y. Y. Lau, Donald P. Umstadter, and Richard Kowalczyk, "Backscattering of an Intense Laser Beam by an Electron," *Phys. Rev. Lett.* 90, 055002 (2003).
- [11] S. Banerjee, A. R. Valenzuela, R. C. Shah, A. Maksimchuk, and D. Umstadter, "High-harmonic generation in plasmas from relativistic laser-electron scattering," *J. Opt. Soc. Am. B* 20, 182 (2003).
- [12] D. Umstadter, "Topical Review: Relativistic Laser-Plasma Interactions," *J. Phys. D: Appl. Phys* 36, R151-R165 (2003).
- [13] D. Umstadter, "Laser-driven x-ray sources," 2003 Yearbook in Science and Technology (McGraw-Hill, New York, 2003), p. 215.

Towards Ultra-cold Molecules – Laser cooling and magnetic trapping of neutral, ground-state, polar molecules for collision studies

Jun Ye

JILA and Department of Physics, National Institute of Standards and Technology and
University of Colorado, Boulder, CO 80309-0440
Email: Ye@jila.colorado.edu

Program Scope

One of the main scientific goals of this work is to achieve a significant improvement in the phase space density of cold, ground-state, polar molecules, opening the door for an external control by applied fields of dipolar interactions important for ultra-cold collisions, certain chemical reactions, and coherent control concepts. We will build upon our current successes in production, detection, and manipulation of cold, stable molecules (hydroxyl radicals OH and formaldehyde H₂CO) in a molecular decelerating apparatus based on the principle of time-dependent Stark shift. We will carry out research on laser cooling of these already cold samples of molecules. The specific approach is based on enhanced scattering via a high finesse optical cavity in the 300 nm region for cavity-assisted laser cooling. Cold OH molecules will be loaded into a magnetic trap after emerging from the Stark decelerator. We expect to lower the OH temperature from 15 mK to 100 μ K and below, leading to an improvement in the phase space density by at least a hundredfold. The low-temperature and high phase-space density cold molecular sample will enable a new class of studies on collisions and inter-molecular dynamics. We are particularly interested in the properties of elastic vs. inelastic collisions among the cold polar molecules under various electromagnetic field configurations. An experiment that will also be undertaken is to study the Hydrogen abstraction channel in the reaction dynamics between OH and H₂CO under the presence of a controlled electric field and with an exquisite control of the collision energy resolution.

Recent Progress

We have proposed a method for controlling a class of low temperature chemical reactions. Specifically, we show the hydrogen abstraction channel in the reaction of formaldehyde (H₂CO) and the hydroxyl radical (OH) can be controlled through either the molecular state or an external electric field. We have also outlined an experiment for investigating and demonstrating control over this important reaction. We have recently demonstrated the first Stark deceleration of the H₂CO molecule, creating a molecular beam of H₂CO to near rest, producing cold molecule packets at a temperature of 100 mK with a few million molecules in the packet at a density of $\sim 10^5$ cm⁻³.

We specifically consider the H-abstraction channel in the reaction of H₂CO and OH: $\text{H}_2\text{CO} + \text{OH} \rightarrow \text{CHO} + \text{H}_2\text{O}$. This reaction not only represents a key component in

the combustion of hydrocarbons, but also plays an important role in atmospheric chemistry where it is the primary process responsible for the removal of the pollutant, H₂CO. Near room temperature the rate of this reaction is weakly dependent on temperature, suggesting the barrier to the process (if any) is very low. Measurements of the thermal activation energy, E , are inconclusive, ranging from $E/R = 750$ K to -931 K, with the most recent measurement giving a value of -320 ± 57 K. Here R is the universal gas constant. The most accurate calculations predict the energy of the transition state for the abstraction to lie between $E/k_B = -700$ K and $+60$ K relative to the reactants, where k_B is the Boltzmann constant. Experimentally so far, both OH and H₂CO molecules have been produced at low temperatures via Stark deceleration in our laboratory. In the case of spontaneous reaction, by magnetically trapping OH in the presence of a tunable bias electric field and “bombarding” the trap with decelerated H₂CO packets the OH - H₂CO total scattering and reaction rates can be mapped as a function of collision energy and applied electric field. Thus the activation energy can be measured. If the activation energy is positive, as some measurements and theory suggest, the collision energy tuning afforded by the Stark decelerator provides a direct way to measure the energy barrier to reaction. Unlike thermal kinetics studies, which rely on fitting the Arrhenius formula to reaction rates, the Stark decelerator can be used to tune the collision energy above and below the threshold energy.

The sensitive dependence of cold molecules on internal states and external electric fields engenders new prospects for probing and controlling the chemical reaction itself. The calculations suggest for the first time that chemical reactions, as well as collision cross sections, can be altered orders of magnitude by simply varying either the molecular state, or external electric field strength. At some low collision energies such as 1 mK, the applied external field has a profound influence on the reaction cross-section, mostly by accessing a very large number of resonant states. Different internal states of OH and H₂CO molecules involved in the reaction exhibit qualitative differences in dynamics, a direct consequence of the dipole-dipole interaction. For polar molecules in weak-field-seeking states, the dipole-dipole interaction can “shield” these molecules from getting close enough together to react chemically. Thus the cross section is strongly suppressed relative to that for strong-field-seekers. However, as the field is increased, the inner turning point of the relevant potential curve moves to smaller values, making the shielding less effective, and hence, the reaction more likely.

Another important capability for current experiments is the direct control of the H-abstraction reaction barrier height through an external electric field. During the H-abstraction process, the energy required to rotate one dipole moment (OH) versus the other (H₂CO) enables our proposed control of reaction dynamics using an external electric field. The important characteristic to note is that the hydrogen-bonded complex (HBC) forms along an attractive direction of the two electric dipoles, but in the transition state (TS) the OH dipole has essentially flipped its orientation relative to the H₂CO dipole. While an external electric field, which orients the molecules would allow (and perhaps even encourage) the formation of the HBC; it would add an energy barrier to the formation of the TS, and thus the H-abstraction channel through the OH dipole-field interaction. The addition to the energy barrier in going from the HBC to the TS would be 10 K under a high, yet attainable, electric field of 250 kV/cm. Thus, assuming a reaction barrier at a H₂CO collision speed of 223 m/s (60 K) the applied electric field would shift

the required collision velocity to 234 m/s, well within the resolution of the Stark decelerator.

The decelerator used for H₂CO is similar to the decelerator in our OH experiments. Molecules in a skimmed, pulsed supersonic beam are focused by an electrostatic hexapole field to provide transverse coupling into the Stark decelerator. The Stark decelerator is constructed of 143 slowing stages spaced 5.461 mm apart with each stage comprised of two cylindrical electrodes of diameter 3.175 mm separated axially by 5.175 mm and oppositely biased at high voltage (± 12.5 kV). Successive stages are oriented at 90° to each other to provide transverse guiding of the molecular beam. The geometry of the slowing stages provides an electric field maximum between the electrodes with the field decreasing away from the electrode center. We have produced cold molecule packets with a translational speed tunable from 350 m/s to 20 m/s, with a minimal thermal temperature of ~ 100 mK.

The H₂CO molecules are produced from the cracking of the formaldehyde polymer to produce the monomer, which is passed through a double u-tube apparatus. Xenon at 2 bar pressure is flowed over the collected H₂CO, held at 196 K where H₂CO has ~ 2.7 kPa (20 Torr) vapor pressure. This Xe/H₂CO mixture is expanded through a solenoid type supersonic valve producing a beam with a mean speed of 350 m/s with approximately a 10% velocity spread. H₂CO is detected using laser-induced fluorescence. The molecules are excited from the $|1_1 1\rangle$ ground state by photons at 353 nm generated from a frequency-doubled, pulsed-dye laser pumped by Nd:YAG laser to the \tilde{A}^1A_2 electronically excited state with one quantum in the ν_4 out-of-plane bending vibrational mode. Approximately 40% of the excited H₂CO decays nonradiatively, while the remaining molecules emit distributed fluorescence from 353 nm to 610 nm.

Future Plans

Our immediate plan is to start a magnetic trapping experiment with OH and test the idea of multiple loading of the magnetic trap to enhance the phase space density. With ultra-sensitive detection capabilities, we will be able to explore dynamics of cold molecular samples located inside electro-magnetic traps. It is possible to create OH magnetic traps with depths comparable to those in alkali atomic systems. Trapping OH molecules in a magnetic trap will be very interesting. The most important advantage is the gained freedom in controlling an external electric field without having to impacting strongly the trap dynamics. This would allow one to perform experiments that utilize an external electric field to influence and control the trapped dipolar gas sample. The second reason that a magnetic trap is favored over an electro-static trap is the possibility of accumulation of decelerated molecular packets emerging from Stark-decelerator. Thirdly, magnetic trapping would accommodate the possibility of spatially collocating both ultra-cold atoms and cold molecules, thus enabling interesting experiments on atom-molecule interactions, with the possibility of using the much colder atomic cloud to sympathetically cool molecules.

We are also making detailed feasibility studies on cavity based laser cooling of OH molecules. Experimental design of the high finesse cavity is in progress and will be quickly implemented once the cooling limitations are clearly understood.

References

E. R. Hudson, C. Ticknor, B. C. Sawyer, C. A. Taatjes, H. J. Lewandowski, J. R. Bochinski, J. L. Bohn, and J. Ye, "Production of cold formaldehyde molecules for study and control of chemical reaction dynamics with hydroxyl radicals," *Phys. Rev. Lett.*, submitted (2005).

Author Index

Alnaser, Ali	112, 114
Bahati, E.....	136, 140
Bannister, M.E.	30, 136, 140
Beck, Donald.....	150
Becker, Kurt H.....	22
Belkacem, Ali	84, 127
Benesch, Frank.....	251
Ben-Itzhak, Itzik	109, 110
Berrah, Nora.....	154
Bocharova, I.....	112
Bohn, John L.....	158
Braaten, Eric	161
Brédy, R.	116, 118
Bucksbaum, Philip.....	162
Camp, H.A.	116, 117
Carnes, Kevin D.....	109, 110, 114
Chang, Zenghu.....	10, 112, 114
Chu, Shi-I.....	44
Cocke, C. L.	112, 113, 114
Côté, Robin	166
Cundiff, Steve	167
Dalgarno, Alexander.....	171
Dantus, Marcos	52
DeMille, David.....	175
DePaola, Brett.....	116, 117, 118
DiMauro, Louis.....	2
Ditmire, Todd.....	18
Doerner, R.....	114
Dörner, Reinhard.....	105
Doyle, John	177
Dunford, Robert.....	82, 100, 103, 104
Ederer, D. L.	82, 100
Eberly, Joseph.....	181
Esry, Brett	109, 110, 120
Falcone, Roger W.	64
Feagin, Jim.....	88
Fléchar, X.....	116
Fogle, Jr., M.R.	136, 140
Gallagher, Thomas.....	185
Gearba, M.A.....	116, 117
Gemmell, D.S.....	104
Gould, Harvey.....	127, 128
Gould, Phillip.....	189
Grankow, B.....	113

Greene, Chris	192
Hale, J. W.	30, 136
Havener, C.C.....	136, 142
Herschbach, Dudley.....	196
Hertlein, M.	127
Ho, Tak-San	70
Hoehr, C.M.	82, 100
Holland, Murray.....	199
Hupach, A.	113
Jin, Deborah.....	203
Jones, Robert.....	40
Kanter, Elliot.....	82, 83, 100, 103, 104
Kapteyn, Henry	6, 207
Klimov, Victor	132
Knapp, Alexandra	105
Kolomeisky, Eugene	211
Kraessig, Bertold.....	82, 83, 100, 103, 104, 105
Krause, H.F.	136, 138, 139
Landahl, E.C.	82, 100
Landers, A.....	114
LaJohn, L.A.	103
Lee, Taewoo.....	251
Leonard, M.....	14, 110
Lin, Chii Dong	123
Litvinyuk, Igor	14, 112
Lucchese, Robert.....	79
Lundeen, Stephen.....	116, 215
Macek, Joseph.....	35, 136, 144
Manson, Steven.....	219
Marhajan, C.....	114
Martin, N.L.S	103
McCurdy, William	26, 127
McKoy, Vincent.....	223
Meyer, Fred.....	30, 136, 138, 139
Mokler, P.H.....	104
Mukamel, Shaul	56
Msezane, Alfred.....	228
Murnane, Margaret	207
Nelson, Keith	60
Nguyen, H.	116, 117
Novotny, Lukas.....	232
Ovchinnikov, S.Yu.....	144
Orel, Ann.....	236
Orlando, Thomas.....	240
Osipov, T.....	114
Peterson, E.R.....	82, 100

Phaneuf, Ronald.....	244
Pratt, R.H.	103
Prior, Michael	114
Rabitz, Herschel.....	48
Raithel, Georg.....	248
Raman, Chandra.....	92
Rankin, A.	114
Ranitovic, P.....	112, 113, 114
Ray, D.	112
Reich, Christian.....	251
Reinhold, Carlos	76, 136, 143
Reis, David.....	162
Rejoub, R.	142
Rescigno, Thomas.....	26, 127
Richard, Pat.....	68
Robbins, D.L.....	259
Robicheaux, Francis.....	96
Rocca, Jorge.....	6
Rose-Petruck, Christoph	251
Rudati, J.	82, 100
Santra, Robin.....	100
Sayler, A.Max	109, 110
Schoenlein, Robert.....	64
Schmidt, L.....	114
Schmidt-Boecking, H.....	114
Schultz, David.....	136, 142
Seideman, Tamar	255
Shah, M.H.	116, 117, 118
Smith, Augustine.....	259
Snow, E.	116
Southworth, Steve	82, 83, 103, 104
Starace, Anthony.....	262
Staudte, A.....	114
Stöhlker, Th.....	104
Stockman, Mark I.....	266
Tarnovsky, Vladimir	22
Thomas, John E.....	270
Thomas, T.Darraha	274
Thumm, Uwe	72
Tong, S.-M.....	112
Trachy, M.L.	116, 117, 118
Trujillo, R.C.	110
Ulrich, B.....	112, 114
Umstadter, Donald.....	278
Vane, Randy.....	32, 136, 139, 140
Vergara, L.I.....	136, 138

Voss, S.	112
Wang, Pengqian	109
Weber, Peter.....	1
Weber, Th.	114
Wehlitz, R	103
Wells, M.....	114
Ye, Jun	282
You, H.J.	30, 138
Young, Linda	82, 83, 100, 103, 104

Participants

Beck, Donald
Michigan Technological University
Physics Department
Houghton, MI 49931
E-Mail: donald@mtu.edu
Phone:906-487-2019

Belkacem, Ali
Lawrence Berkeley National Laboratory
Mail Stop: 2R0300
Berkeley, California 94720
E-Mail: abelkacem@lbl.gov
Phone:510 - 486 7778

Berrah, Nora
Western Michigan University
Physics Department, Everett Tower
Kalamazoo, MI 49008
E-Mail: nora.berrah@wmich.edu
Phone:269-387-4955

Bucksbaum, Philip
FOCUS Center, University of Michigan
Randall Lab
Ann Arbor, MI 48109-1120
E-Mail: phb@umich.edu
Phone:734-764-4348

Chang, Zenghu
Kansas State University
116 Cardwell Hall
Manhattan, Kansas 66509
E-Mail: chang@phys.ksu.edu
Phone:(785)5321621

Cocke, C.L.
Kansas State University
Physics Department, Cardwell Hall,
Manhattan, KS 66506
E-Mail: cocke@phys.ksu.edu
Phone:785 532 1609

Crisp, Michael
Office of Fusion Energy Sciences,
U.S. Department of Energy
1000 Independence Ave, SW
Washington, DC 20585
E-Mail: Michael.Crisp@Science.doe.gov
Phone:301 903 4883

Becker, Kurt
Stevens Institute of Technology
Dept. of Physics
Hoboken, NJ 7030
E-Mail: kbecker@stevens.edu
Phone:2012165671

Ben-Itzhak, Itzhak
J.R. Macdonald Laboratory,
Kansas State University
Physics Department, Cardwell Hall
Manhattan, KS 66506
E-Mail: ibi@phy.ksu.edu
Phone:785-532-1636

Braaten, Eric
Ohio State University
191 W Woodruff Ave
Columbus, OH 43210
E-Mail: braaten@mps.ohio-state.edu
Phone:614-688-4228

Casassa, Michael
BES SC-22, Germantown Building
Department of Energy
1000 Independence Avenue, SW
Washington, DC 20585-1290
E-Mail: michael.casassa@science.doe.gov
Phone:301-903-0448

Chu, Shih-I
University of Kansas
Department of Chemistry, Malott Hall
Lawrence, Kansas 66044
E-Mail: sichu@ku.edu
Phone:785-864-4094

Cote, Robin
University of Connecticut
Physics Dpt U-3046, 2152 Hillside Road
Storrs, CT 06269-3046
E-Mail: rcote@phys.uconn.edu
Phone:(860) 486-4912

Cundiff, Steve
Univ. of Colorado
JILA, UCB 440,
Boulder, CO 80309-0440
E-Mail: cundiffs@jila.colorado.edu
Phone:303-492-6807

Dalgarno, Alexander
Harvard-Smithsonian Center for Astrophysics
60 Garden St
Cambridge, MA 2138
E-Mail: adalgarno@cfa.harvard.edu
Phone:617-495-4403

DePaola, Brett
J. R. Macdonald Lab,
Kansas State University
116 Cardwell Hall
Manhattan, KS 66506
E-Mail: depaola@phys.ksu.edu
Phone:785-532-6777

Ditmire, Todd
University of Texas
Department of Physics
Austin, TX 78712
E-Mail: tditmire@physics.utexas.edu
Phone:512-471-3296

Dunford, Robert
Argonne National Laboratory
9700 S. Cass Ave
Argonne, IL 60439
E-Mail: dunford@anl.gov
Phone:630-252-4052

Esry, Brett
JR Macdonald Lab
Dept. of Physics, 116 Cardwell Hall,
Kansas State Univ.
Manhattan, KS 66506
E-Mail: esry@phys.ksu.edu
Phone:785-532-1620

Gallagher, Thomas
Univ of Virginia
Dept of Physics
Charlottesville, VA 22904
E-Mail: tfg@virginia.edu
Phone:434 924 6817

Gould, Phillip
Univ. of Connecticut
Physics Dept., U-3046, 2152 Hillside Rd.
Storrs, CT 06269-3046
E-Mail: phillip.gould@uconn.edu
Phone:860-486-2950

Dantus, Marcos
Michigan State University
58 Chemistry Building
East Lansing, MI 48864
E-Mail: dantus@msu.edu
Phone:517-355-9715 x314

DiMauro, Louis
The Ohio State University
Department of Physics
Columbus, OH 43210
E-Mail: dimauro@mps.ohio-state.edu
Phone:614-688-5726

Doyle, John
Harvard University
17 Oxford Street
Cambridge, MA 2138
E-Mail: doyle@physics.harvard.edu
Phone:617-495-3201

Eberly, Joseph
University of Rochester
Wilson Blvd.
Rochester, NY 14627
E-Mail: eberly@pas.rochester.edu
Phone:585-275-4351

Feagin, Jim
Cal State University Fullerton
800 North State College Blvd
Fullerton, CA 92834
E-Mail: jfeagin@fullerton.edu
Phone:714-278-3366

Gould, Harvey
LBNL
MS 71-259 LBNL
Berkeley, CA 94720
E-Mail: HAGould@lbl.gov
Phone:510 486-7777

Greene, Chris
University of Colorado
JILA
Boulder, CO 80309-0440
E-Mail: chris.greene@colorado.edu
Phone:303-492-4770

Herschbach, Dudley
Dept. Chemistry,
Harvard University
12 Oxford Street
Cambridge, MA 2138
E-Mail: herschbach@chemistry.harvard.edu
Phone:617 495-3218

Holland, Murray
University of Colorado
440 UCB JILA,
Boulder, CO 80309-0440
E-Mail: murray.holland@colorado.edu
Phone:(303)492-4172

Kanter, Elliot
Argonne National Laboratory
9700 S. Cass Avenue
Argonne, IL 60439
E-Mail: kanter@anl.gov
Phone:(630)252-4050

Klimov, Victor
Los Alamos National Laboratory
MS J567
Los Alamos, NM 87545
E-Mail: klimov@lanl.gov
Phone:505-665-8284

Kraessig, Bertold
Argonne National Laboratory
9700 S. Cass Ave
Argonne, IL 60525
E-Mail: kraessig@anl.gov
Phone:630 252-9230

Litvinyuk, Igor
Kansas State University
116 Cardwell Hall,
Manhattan, Kansas 66506
E-Mail: ivl@phys.ksu.edu
Phone:785-532-1615

Lundeen, Stephen
Colorado State University
Dept. of Physics,
Fort Collins, CO 80523
E-Mail: lundeen@lamar.colostate.edu
Phone:970-491-6647

Hilderbrandt, Richard
BES SC-22, Germantown Building
Department of Energy
1000 Independence Avenue, SW
Washington, DC 20585-1290
E-Mail: richard.hilderbrandt@science.doe.gov
Phone:301-903-0035

Jones, Robert
University of Virginia
Physics Department, Box 400714
Charlottesville, VA 22904-4714
E-Mail: rrj3c@virginia.edu
Phone:(434)924-3088

Kapteyn, Henry
University of Colorado
JILA 440 UCB
Boulder, CO 80309
E-Mail: kapteyn@colorado.edu
Phone:303 492 6763

Kolomeisky, Eugene
University of Virginia
Jesse Beams Lab, 382 McCormick Road,
P.O.Box 400714
Charlottesville, VA 22904-4714
E-Mail: ek6n@virginia.edu
Phone:(434) 924-6809

Lin, Chii Dong
Kansas State University
Department of Physics
Manhattan, KS 66506
E-Mail: cdlin@phys.ksu.edu
Phone:7855321617

Lucchese, Robert
Texas A&M University
Department of Chemistry
College Station, TX 77843-3255
E-Mail: lucchese@mail.chem.tamu.edu
Phone:(979) 845-0187

Macek, Joseph
Univ. Tennessee and Oak Ridge Nat'l Laboratory
401 Nielsen Physics Bldg,
Knoxville, TN 37996-1501
E-Mail: jmacek@utk.edu
Phone:865-974-0770

Manson, Steven
Georgia State University
Dept. of Physics and Astronomy
Atlanta, GA 30303
E-Mail: smanson@gsu.edu
Phone:404-651-3082

Marceau, Diane
DOE Office of Basic Energy Sciences
19901 Germantown Road
Germantown, MD 20874
E-Mail: diane.marceau@science.doe.gov
Phone:301-903-0235

McCurdy, William
U. C. Davis & LBNL
One Cyclotron Rd.
Berkeley, CA 94720
E-Mail: cwmccurdy@lbl.gov
Phone:510 486 4283

McKoy, Vincent
California Institute of Technology
1200 E. California Blvd.
Pasadena, CA 91125
E-Mail: mckoy@caltech.edu
Phone:626.395.6545

Meyer, Fred W.
Oak Ridge National Laboratory
P.O. Box 2008
Oak Ridge, TN 37831-6372
E-Mail: meyerfw@ornl.gov
Phone:865-57404705

Miller, John
BES SC-22, Germantown Building
Department of Energy
1000 Independence Avenue, SW
Washington, DC 20585-1290
E-Mail: John.Miller@science.doe.gov
Phone:301-903-5806

Msezane, Alfred
Clark Atlanta University
223 James P Brawley Drive, SW (Box 92)
Atlanta, GA 30314
E-Mail: amsezane@ctsps.cau.edu
Phone:404-880-8663

Mukamel, Shaul
University of California, Irvine
516 Rowland Hall #433A
Irvine, CA 92697-2025
E-Mail: smukamel@uci.edu
Phone:949-824-7600

Murnane, Margaret
University of Colorado
JILA 440 UCB
Boulder, CO 80309
E-Mail: murnane@colorado.edu
Phone:303 492 6763

Nelson, Keith
Massachusetts Institute of Technology
77 Massachusetts Avenue, Rm. 6-235
Cambridge, Massachusetts 2139
E-Mail: kanelson@mit.edu
Phone:617-253-1423

Novotny, Lukas
University of Rochester
The Institute of Optics
Rochester, NY 14627
E-Mail: novotny@optics.rochester.edu
Phone:585 2755767

Orel, Ann
Department of Applied Science: UC Davis
One Shields Ave.
Davis, CA 95616
E-Mail: aeorel@ucdavis.edu
Phone:(530)752-6025

Orlando, Thomas
Georgia Institute of Technology
1160 Bramlett Forest Trail
Lawrenceville, GA 30045
E-Mail: thomas.orlando@chemistry.gatech.edu
Phone:404-894-822

Phaneuf, Ronald
University of Nevada
Department of Physics /220
Reno, NV 89557-0058
E-Mail: phaneuf@physics.unr.edu
Phone:775-784-6818

Pindzola, Mitch
Auburn University
Department of Physics,
Auburn, AL 36849
E-Mail: pindzola@physics.auburn.edu
Phone:(334) 844-4127

Poliakoff, Erwin
Louisiana State University
Department of Chemistry
Baton Rouge, LA 70803
E-Mail: epoliak@lsu.edu
Phone:225-578-2933

Prior, Michael
Lawrence Berkeley National Laboratory
MS88R0192
Berkeley, California 94720
E-Mail: mhprior@lbl.gov
Phone:510-486-7838

Rabitz, Herschel
Princeton University
Frick Laboratory
Princeton, NJ 8544
E-Mail: jmcclend@princeton.edu
Phone:609 258-4180

Raithel, Georg
University of Michigan
450 Church St.
Ann Arbor, MI 48109-1120
E-Mail: graithel@umich.edu
Phone:734 647 9031

Raman, Chandra
Georgia Tech
837 State St.
Atlanta, GA 30332-0430
E-Mail: craman@gatech.edu
Phone:404-894-9062

Reinhold, Carlos
Oak Ridge National Laboratory
Physics Division
P.O. Box 2008, MS 6372, Bldg 6010
Oak Ridge, TN 37831
E-Mail: reinhold@ornl.gov
Phone:865-574-4579

Reis, David
University of Michigan
450 Church Street
Ann Arbor,, MI 48109-1040
E-Mail: dreis@umich.edu
Phone:734-763-9649

Rescigno, Thomas
LBNL
1 Cyclotron Rd. MS-50F
Berkeley, CA 94720
E-Mail: tnrescigno@lbl.gov
Phone:510 486 8652

Richard, Patrick
Kansas State University
Cardwell Hall
Manhattan, KS 66506
E-Mail: richard@phys.ksu.edu
Phone:7855395670

Robicheaux, Francis
Auburn University
206 Allison Lab
Auburn University, AL 36849
E-Mail: robicfj@auburn.edu
Phone:334-844-4366

Rocca, Jorge
Colorado State University
ERC, 1320 Campus Delivery
Fort Collins, CO 80523-1320
E-Mail: rocca@engr.colostate.edu
Phone:970-491-8371

Rohlfing, Eric
BES SC-22, Germantown Building
Department of Energy
1000 Independence Avenue, SW
Washington, DC 20585-1290
E-Mail: eric.rohlfing@science.doe.gov
Phone:301-903-8165

Rose-Petruck, Christoph
Brown University
324 Brook Str, Box H
Providence, RI 2912
E-Mail: Christoph_Rose-Petruck@brown.edu
Phone:401 863 1533

Schoenlein, Robert
Lawrence Berkeley National Laboratory
1 Cyclotron Rd. MS: 2-300
Berkeley, CA 94720
E-Mail: rwschoenlein@lbl.gov
Phone:(510) 486-6557

Schultz, David
Physics Division, Oak Ridge National Laboratory
MS 6372, Bldg. 6010
Oak Ridge, TN 37831-6372
E-Mail: schultzd@ornl.gov
Phone:(865) 576-9461

Seideman, Tamar
Northwestern University
2145 Sheridan Road
Evanston, IL 60208
E-Mail: seideman@chem.northwestern.edu
Phone:847-467-4979

Smith, Augustine
Morehouse College
830 Westview Dr SW
Atlanta, GA 30314
E-Mail: asmith@morehouse.edu
Phone:404-215-2615

Southworth, Steve
Argonne National Laboratory
Bldg. 203, 9700 S. Cass Ave.
Argonne, IL 60439
E-Mail: southworth@anl.gov
Phone:630-252-3894

Starace, Anthony
The University of Nebraska
Dept of Physics & Astronomy, 116 Brace Lab
Lincoln, NE 68588-0111
E-Mail: astarace1@unl.edu
Phone:(402) 472-2795

Thomas, Darrah
Oregon State University
153 Gilbert Hall
Corvallis, OR 97331-4003
E-Mail: T.Darrah.Thomas@oregonstate.edu
Phone:541-737-6711

Thumm, Uwe
Kansas State University
Physics Dept., Cardwell Hall
Manhattan, KS 66506
E-Mail: thumm@phys.ksu.edu
Phone:785-532-1613

Umstadter, Donald
University of Nebraska, Lincoln
212 Ferguson Hall
Lincoln, NE 68522-0111
E-Mail: dpu@unlserve.unl.edu
Phone:402 472 8115

Vane, Randy
Oak Ridge National Laboratory
P.O. Box 2008, Bldg. 6010, MS-6372
Oak Ridge, TN 37831
E-Mail: vanecr@ornl.gov
Phone:865-574-4497

Weber, Peter
Brown University
324 Brook St., Box H
Providence, RI 02912
E-Mail: Peter_Weber@brown.edu
Phone:401-863-3767

Young, Linda
Argonne National Laboratory
9700 S. Cass Ave.
Argonne, IL 60439
E-Mail: young@anl.gov
Phone:630-252-8878